

Alcator C-Mod
National Tokamak Facility Five Year Research Plan
November, 2008 – October, 2013

Co-Operative Agreement: DE-FC02-99ER54512

Applicant Institution: Massachusetts Institute of Technology
77 Massachusetts Avenue
Cambridge, MA 02139

Principal Investigators:

Earl S. Marmor, Miklos Porkolab, Ian H. Hutchinson
175 Albany Street, NW17-186B
Cambridge, MA 02139
617-253-5455

Email: marmor@psfc.mit.edu

DOE Program Office: Office of Fusion Energy Sciences
DOE Technical Program Manager: Rostom Y. Dagazian

Prepared by Alcator Staff
March 27, 2008

Submitted to:
Office of Fusion Energy Sciences
Office of Science
U.S. Department of Energy
Germantown, MD 20874

Plasma Science and Fusion Center
Massachusetts Institute of Technology
Cambridge, MA 02139

Alcator C-Mod
National Tokamak Facility Five Year Research Plan
November, 2008 – October, 2013

Table of Contents

1. Executive Summary
2. C-Mod's Role in the National and International Programs
3. Transport Research
4. Plasma Boundary
5. Wave Plasma Interactions
 - 5.1. ICRF
 - 5.2. LHRF
 - 5.3. ICRF and LHRF Interactions
6. Macroscopic Stability
7. Pedestal Physics
8. H-mode Integrated Scenarios – ITER Baseline
9. Integrated Scenarios – Advanced Regimes
10. Theory and Simulation
11. Facilities
12. Collaborations
 - 12.1 Princeton Plasma Physics Laboratory
 - 12.2 University of Texas, Austin.
 - 12.3 MDSPlus
13. Key Personnel and Publications
 - 13.1 Resumes
 - 13.2 Publications
14. Management Capability
15. National Budget Summary

1 Executive Summary

1.1 Vision

Alcator C-Mod is the only high-field, high-density divertor tokamak in the world fusion program. The overall theme of the Alcator program is

Compact high-performance divertor tokamak research to establish the plasma physics and plasma engineering necessary for a burning plasma tokamak experiment and for attractive fusion reactors.

Organization of the program is through a combination of topical science areas supporting integrated thrusts. The topics relate to the generic fusion-plasma science, while the thrusts focus this science on integrated scenarios, particularly in support of ITER design and operation. The project is also aggressively investigating important issues on the MFE development path from ITER to DEMO. The program has five topical science areas: core transport; pedestal physics; plasma boundary; wave-plasma interactions; and macrostability. Integrated scenarios encompass the ITER baseline inductive H-modes, and Advanced Scenario operation including partially inductive hybrid modes and fully non-inductive weak and reverse shear operation with active profile control. Advanced operation takes advantage of the unique long-pulse capability of the facility (relative to skin and L/R times), at $B \leq 5$ Tesla, combined with new current drive and density control tools, to investigate the approach to steady-state in fully non-inductive regimes; this is particularly relevant to the prospects for quasi-steady operation on ITER. All aspects of the research are intimately connected to a broad program of theory and modeling. The connections among the topical science areas and the integrated scenarios are illustrated in Figure 1.1.

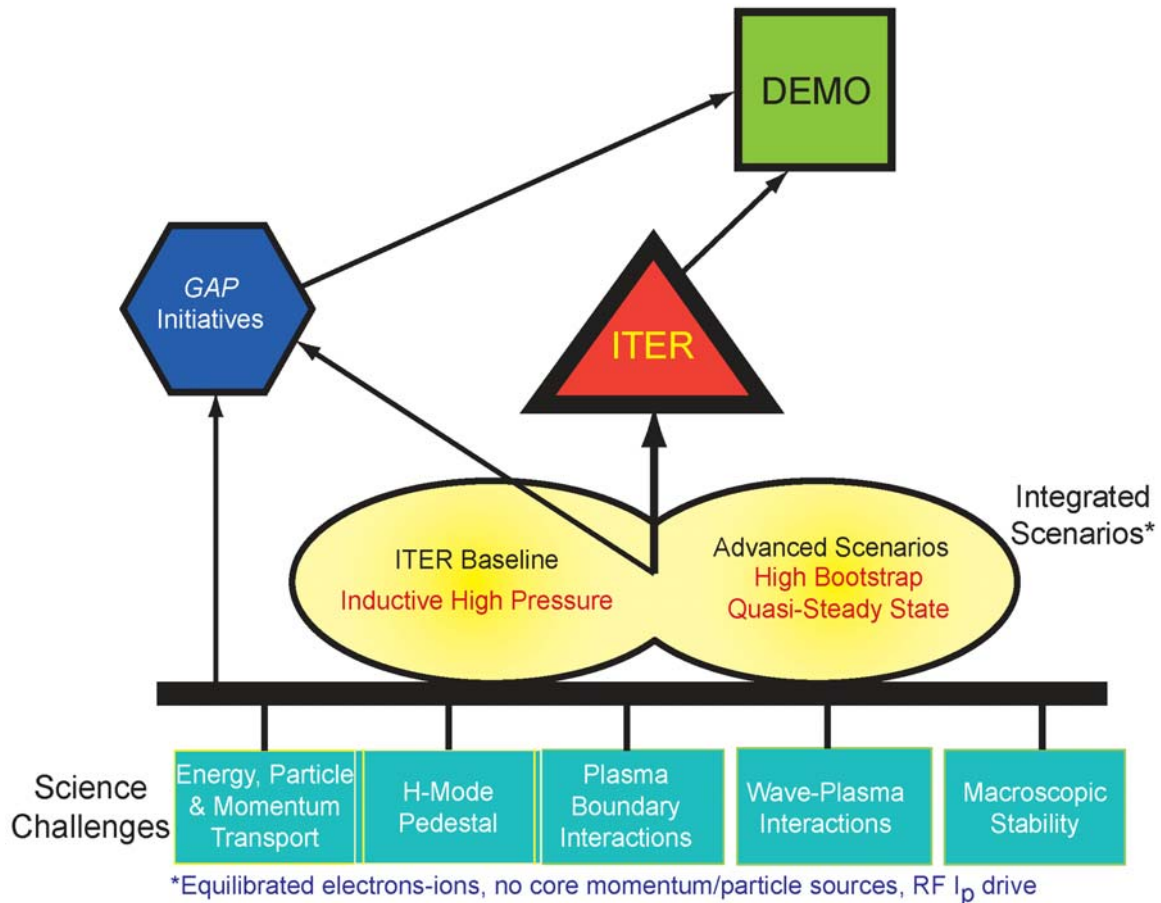


Figure 1.1 Integrated scenarios and topical science areas.

Unique aspects of the Alcator C-Mod facility provide the logical foundations for the scientific areas of emphasis in our research endeavors, which are aimed at answering key outstanding questions in the development of practical fusion energy:

- **Long pulse capability** — C-Mod has the unique ability among highly-shaped, diverted tokamaks, to run high pressure plasmas with pulse length equal to the L/R relaxation time, at $B_T > 4$ Tesla. Combined with Lower Hybrid Current Drive for current density profile control, this provides an outstanding opportunity to investigate the extent to which enhanced confinement and stability of Advanced Tokamak configurations can be maintained in steady-state, using active profile control.
- **High magnetic field** — With capability to operate at very high absolute plasma densities (to 10^{21} m^{-3}) and pressures (approaching 10 atmospheres), and with magnetic field spanning the ITER field (5.3 Tesla) and beyond (to 8 Tesla), C-Mod offers a unique test-bed for exploring the physics and engineering which is prototypical of ITER.
- **Exclusively RF driven** — C-Mod does not use beams for heating, fueling or momentum drive. As a result, the heating is decoupled from particle sources

and there are no external momentum sources to drive plasma rotation. It is likely that the same constraints will exist in a fusion power plant; the studies of transport, macro-stability and Advanced Scenario physics in C-Mod are thus highly relevant to reactor regimes.

- **Unique dimensional parameters** — C-Mod plasmas are dimensionally unique, but can be dimensionlessly comparable to those studied in larger tokamaks, which allows us to provide key points on scaling curves for confinement, H-mode threshold, pressure limits, etc. At the same time, joint experiments with other facilities allow for important tests of the influence of non-similar processes, including radiation and neutral dynamics. Many of these experiments are coordinated through the International Tokamak Physics Activity (ITPA).
- **Very high power density scrape-off layer plasma** — With parallel SOL power flows approaching 1 GW/m^2 (as expected in ITER), C-Mod accesses unique divertor regimes which are prototypical of burning plasma conditions. The issues of edge transport and power handling which are explored go beyond those specific to the tokamak, being relevant to essentially all magnetic confinement configurations.
- **High Z metal plasma facing components** — The solid molybdenum and tungsten plasma facing components on C-Mod are unique among the world's major facilities. The use of high Z PFCs is also reactor prototypical, and leads to unique recycling properties, and wall conditioning, density and impurity control challenges. Because of the tritium retention issues, ITER must consider high Z plasma facing components as one option, and studies of hydrogenic retention in C-Mod, both with molybdenum and tungsten, will contribute significantly to this decision.

The C-Mod facility already has an impressive set of facility capabilities, control tools and diagnostics. During the next five year period, significant facility upgrades, particularly for ICRF and LHRF systems, a new DEMO-like actively heated ($600 \text{ }^\circ\text{C}$) divertor, and upgraded and new diagnostics will be implemented.

The C-Mod program is fully collaborative (see Chapter 12). In addition to MIT, which hosts the facility, major collaborations are ongoing with the Princeton Plasma Physics Laboratory and the University of Texas at Austin. Many smaller groups of collaborators at Universities and Laboratories, both domestic and international, are integral participants in the research.

Education is a very important aspect of the Alcator project mission, and the project has a large contingent of graduate students working toward their PhD degrees. They are drawn from four departments at MIT, as well as from collaborating Universities. At any time, about 30 graduate students are doing their PhD thesis research on Alcator C-Mod.

1.2 High Priority ITER R&D

C-Mod is positioned to investigate many of the key outstanding issues that need resolution to support successful operation of ITER. Research has begun on most of these, and all will be studied in the coming five year period. Many of the experiments are carried out jointly with other tokamak facilities, both in the US and around the world, with coordination through the ITPA. Major C-Mod contributions are as follows.

Integrated Scenarios, Baseline H-mode and Advanced Scenarios:

- Breakdown and current rise in ITER
- Reference set of ITER scenarios for baseline H-mode, steady-state and hybrid operation, for databases and modeling
- ITER hybrid scenarios: experimental development and understanding mechanisms for maintaining $q_0 > 1$
- Profile control methods: especially $j(r)$ with combined LHCD and bootstrap

Transport

- Core transport regimes with equilibrated electrons/ions, no momentum input, dominant electron heating: regime for majority of C-Mod operation.
- Collisionality dependence of density peaking: addition of C-Mod data breaks the covariance between collisionality and n/n_G seen in other experiments; heating decoupled from core fueling.
- Develop and demonstrate turbulence stabilization mechanisms compatible with reactor conditions, such as magnetic shear stabilization, shear flow generation and q profile; compare these mechanisms to theory.
- Develop common technologies for integrated modeling (frameworks, code interfaces, data structures): MDSplus is a model.

Pedestal Physics

- Understand L-H power threshold at low density: C-Mod provides data at unique (ITER value) magnetic field; effects of neutrals/opacity.
- Role of rotation in the H-mode transition.
- Improve predictive and design capability for small ELM and quiescent H-mode regimes: small ELM regimes for $\beta_N > 1.3$; effects of shaping.
- ELM control techniques: stochastic fields with external coils.

Plasma-Boundary Interactions

- Tritium retention and tritium removal: solid high Z PFCs; disruption cleaning; plasma and nuclear damage; erosion.
- Scaling present-day conditioning and operational techniques to future devices: boronization with high Z walls; ICRF induced impurity generation.
- Power handling and impurity control: SOL transport, radiative/detached divertor.

Macro-stability

- Disruption database (energy loss, halo current): excellent diagnostics for radiated power, surface heating, halo currents.
- ITER applicable disruption mitigation, validate 2 and 3-D MHD codes with radiation: pioneering studies with NIMROD/NIMRAD of C-Mod experiments; LHCD for controlling seed population of non-thermal electrons to study runaway amplification/suppression.
- Develop reliable disruption prediction methods: work started on robust algorithms; real-time automatic mitigation using Digital Plasma Control System planned.
- NTM physics: effects of rotation; LHCD control/stabilization
- Understand intermediate n Alfvén Eigenmodes (AE's); Damping and stability of AE's: active MHD antennas couple to intermediate n modes.
- Redistribution of fast particles from AE's: ICRF ion tails drive AE's unstable, Compact Neutral Particle Analyzers (passive and active with Diagnostic Neutral Beam), plus new scintillator lost ion detector to measure effects of AE's on fast particles.

1.3 Fusion Science Priorities

1.3.1 Priorities from the April 2005 FESAC Priorities Report

In April 2005, FESAC identified six research campaigns covering 15 topical scientific questions. C-Mod plays an integral role in addressing all of the magnetic fusion relevant topical questions:

- T1. How does magnetic field structure impact fusion plasma confinement?
- T2. What limits the maximum pressure that can be achieved in laboratory plasmas?
- T3. How can external control and plasma self-organization be used to improve fusion performance?
- T4. How does turbulence cause heat, particles, and momentum to escape from plasmas?
- T5. How are electromagnetic fields and mass flows generated in plasmas?
- T6. How do magnetic fields in plasmas reconnect and dissipate their energy?
- T7. How can high energy density plasmas be assembled and ignited in the laboratory?
- T8. How do hydrodynamic instabilities affect implosions to high energy density?
- T9. How can heavy ion beams be compressed to the high intensities required to create high energy density matter and fusion conditions?
- T10. How can a 100-million-degree-C burning plasma be interfaced to its room temperature surroundings?
- T11. How do electromagnetic waves interact with plasma?
- T12. How do high-energy particles interact with plasma?

- T13. How does the challenging fusion environment affect plasma chamber systems?
- T14. What are the operating limits for materials in the harsh fusion environment?
- T15. How can systems be engineered to heat, fuel, pump, and confine steady-state or repetitively-pulsed burning plasma?

The C-Mod program makes key, unique contributions to most of the recommended areas of US “opportunities for enhanced progress”:

- Carry out additional science and technology activities supporting ITER including diagnostic development, integrated predictive modeling and enabling technologies.
- Predict the formation, structure, and transient evolution of edge transport barriers.
- Mount a focused enhanced effort to understand electron transport.
- Pursue an integrated understanding of plasma self-organization and external control, enabling high-pressure sustained plasmas.
- Study relativistic electron transport and laser-plasma interaction for fast ignition high energy density physics.
- Extend understanding and capability to control and manipulate plasmas with external waves.
- Increase energy ion pulse compression in plasma for high energy density physics experiments.
- Simulate through experiment and modeling the synergistic behavior of alpha-particle dominated burning plasmas.
- Conduct enhanced modeling and laboratory experiments for ITER test blankets.
- Pursue optimization of magnetic confinement configurations.
- Resolve the key plasma-material interactions, which govern material selection and tritium retention for high-power fusion experiments.
- Extend the understanding of reconnection processes and their influence on plasma instabilities.
- Carry out experiments and simulation of multi-kilo-electron-volt megabar plasmas.
- Expand the effort to understand the transport of particles and momentum.

Detailed discussions of how C-Mod’s specific topical science and integrating thrust plans address the programmatic objectives are given in the respective Chapters of this Proposal.

1.3.2 “Gap” issues on the path from ITER to DEMO

In its October, 2007 report, “Priorities, Gaps and Opportunities: Towards A Long-Range Strategic Plan For Magnetic Fusion Energy”, FESAC identified 15 science and technology gaps that need to be filled on the path to designing and building a successful MFE DEMO reactor. Complete resolution of most of these issues requires both a successful ITER program, and additional initiatives, including new facilities, primarily studying D-T burning fusion plasmas. However, many of the issues related to the gaps are amenable to research on existing experiments, coupled with advances in theory and modeling. Alcator C-Mod is working on a significant number of these issues, and

substantial progress is expected in the next five years, which in turn will help to inform the design of new facilities that will be needed. The areas where C-Mod makes the strongest contributions are:

- Plasma facing components: high Z metals, ultra-high SOL power densities.
- Off-normal events: disruption avoidance, prediction and mitigation.
- Plasma-wall interactions: SOL and divertor transport, erosion and redeposition, hydrogen isotope retention.
- Integrated, high performance burning plasmas: focus of the Integrated H-Mode and Advanced Scenarios thrusts.
- Theory and predictive modeling: code benchmarking, discovery of new phenomena, iteration of theory and comparison with experiment.
- Measurements: new and improved diagnostic techniques.
- RF antennas, launchers and other internal components: Advancing the understanding of coupler-edge plasma interactions, improvement of related theories and modeling.
- Plasma modification by auxiliary systems: RF systems (ICRF and LHRF) for current drive, flow drive, instability control; ELM control.
- Control: maintaining high performance advanced scenarios.

1.4 Summary of Achievements

Some of the key research achievements and discoveries of the Alcator program during the prior contractual period (2003-2008) are summarized in bullet form here. Much more detail and explanation of these achievements is given in each topical chapter (3 through 10); a comprehensive list of publications can be found in section 13.2.

- Transport Science
 - Pioneering studies of spontaneous core toroidal rotation in the absence of externally imposed momentum input.
 - Formation of ITB's on C-Mod with off-axis ICRF directly linked to reduction of ITG turbulence drive through gyrokinetic simulations using detailed experimental density and temperature profiles.
 - Identification of increased TEM drive as the controlling mechanism which limits pressure peaking in ITB discharges with the addition of stronger central heating.
 - Validation of gyrokinetic modeling through comparison with core fluctuation measurements.
 - Density peaking clearly linked to collisionality, not distance from the density limit.
- Pedestal Physics
 - Characterization of L-H threshold in terms of more detailed measurements of local variables, including potential explanation of ∇B asymmetry in L-H threshold based on topology dependent flows.

- Extensive database developed mapping the dependence of pedestal characteristics on dimensional and dimensionless plasma parameters. Measurements of density, electron and ion temperature, rotation and radial electric field profiles are now routinely available with ~mm spatial resolution in the pedestal region.
- Dimensionless matched experiments comparing C-Mod with DIII-D indicate that plasma physics plays the dominant role in determining pedestal width. Comparisons with JET show a similar result, but with hints that the density pedestal does broaden for very low densities, when the neutral mean free path is larger than the width (note: reactor regime has a neutral mean free path smaller than pedestal width).
- Pedestal pressure appears to be regulated by a critical gradient mechanism, similar to the dynamics seen in core transport.
- The quasi-coherent (QC) mode, which regulates pedestal density, and impurity outflow in the EDA regime, is consistent with a resistive ballooning drive. Detailed measurements of the QC mode characteristics have been made, and a theoretical picture is emerging. At the highest pedestal pressures on C-Mod, small ELMs appear on top of the QC mode.
- Access to the type I ELM regime on C-Mod has been achieved through modified shaping (in particular, high triangularity at the active X-point); good agreement is found between the threshold conditions for the type I ELMs, due to intermediate n peeling-ballooning modes, and modeling using the M3D resistive 3-D MHD code.
- Plasma Boundary Science
 - Evidence that electromagnetic turbulence sets the observed pressure gradients near the last-closed flux surface.
 - Identification of radial transport-driven edge plasma flows arising from ballooning-like transport asymmetries, which impact the toroidal rotation of the confined plasma and potentially explain the X-point dependence of the L-H power threshold.
 - Unprecedented detailed information on turbulent structures in the scrape-off layer, using a unique set of gas-puff turbulence imaging systems.
 - An enlightening dimensionless scaling study of cross-field particle convection in the far scrape-off layers of DIII-D, C-Mod and JET.
 - Increased understanding of the role of boronization with high-Z metallic plasma facing components.
 - Pioneering measurements of deuterium retention in bulk molybdenum PFCs, and an emerging explanation in terms of the plasma production and subsequent diffusion of defects in the metal which traps hydrogen isotopes.
- Wave-Plasma Interactions
 - World-record power flux levels ($>10 \text{ MW/m}^2$) for plasma heating applied with C-Mod ICRF antennas.
 - Identification of ICRF sheaths as a primary mechanism for impurity generation.

- Development and application of state-of-the-art antenna-plasma simulation code (TOPICA), and validation through detailed comparisons with experimental loading measurements across a range of edge plasma parameters.
 - Successful implementation of a Fast Ferrite Tuner active matching system, which keeps the ICRF system matched over a very wide range of plasma conditions; transient changes as fast as 1 msec can be tracked and accommodated, including L-H transitions and pellet injection.
 - Physics mechanism responsible for antenna breakdown at high neutral pressure has been identified.
 - For the first time, details of ICRF mode conversion processes have been directly observed, using the Phase Contrast Imaging diagnostic. All three plasma waves (fast, ion-Bernstein, and ion-cyclotron) are identified, and simulations with the TORIC code are in excellent agreement with the experiments.
 - ICRF Mode Conversion Current drive used for sawtooth pacing.
 - Greater than 800 kA of current driven non-inductively using Lower Hybrid Current Drive (LHCD), corresponding to 80% of the total current.
 - Off-axis LHCD successfully used to broaden the current density profile.
 - Variable phase control has been used to modify the radial deposition of Lower Hybrid wave, and change internal inductance.
 - Sawtooth stabilization has been accomplished using LHCD.
 - The Motional Stark Effect diagnostic is operational, and first measurements of changes in $j(r)$ due to LHCD have been made.
 - First studies of core plasma rotation changes induced by LHCD have started, and there is evidence for the formation of Internal Transport Barriers in these reduced shear discharges.
- Macrostability
 - Detailed studies of disruption mitigation with massive gas puffing, using combinations of noble gases, including significant reduction of halo currents and nearly 100% conversion of stored kinetic plus magnetic energy into radiation.
 - Advanced 3-D MHD modeling of mitigation dynamics, including radiated power.
 - Demonstrated real-time detection and mitigation of impending Vertical Disruption Events.
 - Important scalings of critical error field thresholds for mode-locking, including coordinated studies with JET and DIII-D for size and field scalings to allow extrapolation to ITER.
 - Radial structure of Reverse Shear Alfvén Eigenmodes, driven unstable by ICRF heating during the current ramp, measured with the PCI diagnostic; detailed comparisons with synthetic diagnostic developed for the NOVA code show excellent agreement for code verification.
 - Integrated Scenarios – ITER H-mode Baseline

- Development of demonstration discharges at world record tokamak plasma pressure ($\langle P \rangle = 1.8$ atmosphere), with $B_T = 5.4$ T and $\beta_N = 1.7$, as planned for the ITER baseline.
 - Scaling to ITER of locked mode threshold, through ITPA coordinated joint experiments.
 - Showed that the low density limit for H-mode access does not scale with $n/n_{\text{Greenwald}}$.
- Integrated Scenarios – Advanced Scenarios
 - Implementation of LHCD system and MSE diagnostic.
 - Successful application of LHCD to modify $j(r)$, including demonstration of nearly 100% non-inductive operation at 1 MA plasma current.
 - Implementation of divertor cryopumping for particle/density control.
 - Successfully combined LHRF and ICRF, and mapped out regimes of operation where good LH coupling can be maintained in the presence of high power ICRF.
 - Coupling of LHRF into H-mode discharges demonstrated.
 - Extension of pulse lengths to 4 seconds, with high power ICRF (>6 MJ total input energy).
 - Significant advances in integrated scenario modeling, using state-of-the-art codes.
 - Control of core transport via ICRF heating profile modifications, and extension of the power and parameter ranges for this regime.

1.5 Outline of Research Proposal

1.5.1 Transport

Self Generated Rotation and Momentum Transport Self-generated rotation, and the closely related issues of momentum transport, are particularly important looking ahead to ITER (where core momentum drive will be weak) and to reactors (where it is likely to be absent). Flows, and flow-shear, are key to many aspects of confinement and mode stabilization. The overall goal is improved understanding so that we can extrapolate to future devices with low input torque. Emphasis will be placed on: the role of electron heating and current drive in modifying self-generated rotation profiles; comparison of measured self generated flows and cross-field fluxes with emerging theories and models; comparisons of fluctuation characteristics with predictions of emerging models; testing the feasibility of IC and IBW flow drive. New and upgraded profile diagnostics are key to much of the progress, particularly the high spatial and spectral resolution imaging x-ray crystal spectrometer.

Particle Transport Particle transport is historically less studied than energy transport, and as a result, less well understood. It impacts fusion power, stability, bootstrap current,

divertor operation and impurity dynamics, and opens another window of the transport physics. The 5 year goal is to perform detailed comparisons of experimental particle transport measurements with models. Emphasis will be on: comparisons of measured profiles, fluxes and fluctuation levels with numerical results from existing gyrokinetic codes; studies of particle transport in regimes without neoclassical pinch (non-inductive current drive); quantitative assessments of the role of magnetic shear in setting density profiles; correlations of particle transport and ion thermal transport across confinement regimes. The addition of a multi-pulse laser blow-off impurity injection system, combined with new and upgraded spectroscopic diagnostics, including CXRS, will aid progress in this area.

Electron Energy Transport Electron energy transport can be an important contributor to overall confinement, especially in cases where the ion channel has been suppressed. The 5 year goal is to gain a better understanding of electron transport in decoupled regimes. Emphasis will be on: identifying the portion of k space most important for anomalous electron heat transport in low density ohmic plasmas; extending the studies to strongly lower hybrid heated low density plasmas; testing models for mixed scale (ion-electron) turbulence.

Internal Transport Barriers ITB regimes are potentially attractive for advanced confinement operation. The 5 year goal is to attain a better understanding of access conditions, transition dynamics and control of ITBs. Emphases will be: validating modeling predictions for the role of ITG in ITB onset; testing predictions for the nature of density fluctuations, particularly for ITB discharges with the addition of central ICRF heating; assessing the roles of magnetic and flow shear in ITB evolution on C-Mod, using both LHCD and ICRF tools; measuring impurity diffusion and heat-pulse propagation across the ITB.

Ion Thermal Transport This is the best studied core transport channel, and within the next 5 years we will make detailed comparisons of ion thermal transport with advanced gyrokinetic numerical models. Emphasis will be on: quantitative assessment of the role of magnetic shear in setting critical temperature gradients; comparisons of the fluctuation spectra and correlations, and their relation to ion, particle and momentum channels.

1.5.2 Pedestal Physics

H-mode Transition Trigger On the path to understanding the physics of the H-mode transition, examining the details of local parameters just at the transition is likely to be very fruitful. The 5 year goal is to identify the critical local parameters and understand their relationship to global threshold conditions. Emphasis will be on: diagnosing edge flow and pressure profiles with improved time resolution; investigating the evolution of radial electric field shear across both fast and slow transitions; identifying the scaling of the low-density limit for H-mode access with dimensional and dimensionless parameters.

Pedestal Structure and Scaling Scaling of results from current experiments to conditions expected on ITER and other future experiments will require improved physics-based understanding of edge plasma and neutral transport. The research will emphasize: investigations of the edge transport barrier flux-gradient relationships for various configurations and operational regimes; studies of the impact of neutral fueling on the pedestal, particularly at reduced density/collisionality; relationships between edge magnetic shear and pedestal width; momentum transport across the pedestal.

Edge Relaxation Mechanism Understanding Large ELMs are probably incompatible with ITER and reactor operation, and ELM-free H-mode has poses severe impurity confinement problems. Finding appropriate relaxation mechanisms, particularly for particle transport, which are still compatible with high pressure pedestals, will be key. The 5 year goal is to understand the physical processes determining the operational space of pedestal relaxation mechanisms. Emphasis will be on: refining the experimental boundaries for ELMs and other pedestal transport-regulating modes; extending the use of MHD codes for identification of relaxation mechanisms; comparing Quasi-Coherent Mode characteristics with theoretical predictions.

Edge Relaxation Mechanism Control Active control of the relaxation mechanism(s) is strongly preferred over relying on finding regimes where the natural mechanisms have the most desirable properties. The 5 year goal is to develop methods for controlling the pedestal and edge relaxation, while maintaining good confinement. Explorations will include: pedestal regulation through shaping and topology; possible application of externally applied non-axisymmetric applied fields to relax the pedestal and/or regulate ELMs; use of LHCD for pedestal/ELM modification; investigation of ICRF beat-wave drive of continuous edge relaxation modes .

Numerical Code Validation The 5 year goal is to validate edge simulation tools that are currently being developed against experimental data. Comparisons should be made of pedestal structure and scalings with transport code predictions, and simulations of dynamic events, including ELMs, will be tested.

1.5.3 Plasma Boundary Interactions

Time-Averaged Edge Transport The goal is to characterize time-averaged SOL density and temperature profiles, radial fluxes and toroidal flows. Topology dependence, including proximity to the X-point, and connections to the pedestal on closed surfaces will be investigated. Detailed edge/SOL diagnostics, including the upgraded SOL Thomson scattering system, will be key to progress.

Edge Turbulence The goal is to characterize edge turbulence at multiple poloidal and toroidal locations, including k spectrum and 3-D structure, develop scalings with plasma parameters, and correlate with plasma fluxes. Existing and upgraded Gas Puff Imaging (GPI) diagnostics will be among the most important measurement techniques. A second goal is to validate first-principles numerical edge turbulence models against the

experimental data. A third goal is to characterize turbulence in the divertor, using an additional dedicated GPI view.

SOL Power and Particle Flows C-Mod accesses ultra-high power flows through the SOL toward the divertor, at reactor level densities. The 5 year goal is to better characterize the parallel power and particle flows from the confined plasma to the divertor targets. Emphases will: measure heat flux profiles on the divertor target; investigate sheath transmission factors; measure upstream ion temperature profiles in the SOL.

Plasma-Surface Physics Impurity sources and sinks, and erosion and redeposition are important for C-Mod and for future experiments. We plan to characterize and control sputtering of plasma facing surfaces, particularly for high-power ICRF heated discharges. A second goal is to measure and understand net erosion on plasma-facing surfaces. These studies rely on in-situ spectroscopic imaging of low and high-Z impurity influx, emissive probe measurements of sheath potentials, and surface analysis using the new accelerator based in-situ ion beam system along with the recently installed Surface Science Station.

DEMO-Like Divertor Tungsten is a candidate material for PFCs in ITER and DEMO. Because of issues with nuclear and plasma damage, tritium retention may be a problem. One possible solution is to operate at elevated ambient bulk temperature (~600 C), which is probably required in any event in a DEMO. We will install a new tungsten outer divertor in C-Mod, which will incorporate active heating to test compatibility with high heat flux, low core tungsten contamination, and low hydrogen isotope retention. The design incorporates the tungsten lamella tiles similar to those being considered for ITER, and which have already been prototype-tested in the current C-Mod divertor.

1.5.4 Wave-Plasma Interactions

ICRF Current Drive ICRF power can be applied in several ways to provide modest current drive, with primary application on C-Mod to provide central seed current for non-inductive scenarios, and sawtooth pacing to minimize the effects of large sawteeth on the ITER baseline H-mode scenario plasmas and to reduce or eliminate sawtooth induced islands which can seed NTMs. The 5 year goals are to investigate three approaches, and to develop the best tools for these applications. Studies will include: using Mode Conversion Current Drive for sawtooth pacing; investigating Fast Wave Current Drive for central seed current, which may be required for our fully non-inductive Advanced scenarios; characterizing Ion Cyclotron Current Drive for sawtooth pacing.

Flow Drive Plasma flows, and flow shear, strongly influence stability and turbulence. Developing a reliable tool to actively control flow would be a significant advance. Our goal is to evaluate the feasibility of flow control with mode conversion drive by investigating low field side launch. Our new high spatial and spectral resolution x-ray crystal spectrographs, combined with CXRS, will enable us to look for even small changes in flow anywhere across the plasma profile.

Validation of Numerical Wave-Plasma Simulations Modeling of waves in plasmas is making dramatic progress, particularly through the SCIDAC initiative. C-Mod has the tools and diagnostics to allow detailed tests of the code predictions, and is active in code development both at MIT and through our collaborations. Validation will be carried out in at least 5 areas: measured ICRF antenna characteristics will be compared with TOPICA simulations; PCI measurements of mode conversion physics will be compared with TORIC simulations; fast ions created with ICRF minority absorption will be measured with the Compact Neutral Particle Analyzer and CXRS-Fast-Ion diagnostics, for comparison with simulations; direct fast-wave absorption will be compared with TORIC simulations; 2nd harmonic minority ion absorption will be compared with simulation.

ICRF Antenna Technology One of the most important technology issues in the RF area for ITER, as well as for C-Mod, is attaining reliable high power density operation of ICRF antennas in the tokamak edge-plasma environment, maximizing coupled power while minimizing negative effects on the plasma, including impurity generation. C-Mod is planning to design, install and test a new 4-strap ICRF antenna with all of these goals in mind. The first new antenna will be commissioned in the first year of the plan. Research will include characterizing RF sheaths as a function of power, phasing and single-pass absorption fraction, utilizing upgraded plasma potential probes and spectroscopic/bolometric diagnostics. This will be followed by research into approaches designed to implement sheath mitigation techniques.

Lower Hybrid Physics at ITER-relevant parameters The C-Mod LHRF system operates very close to that envisioned for ITER in terms of frequency, and uniquely explores the physics of LH wave propagation, damping and current drive at the same plasma frequency and field as ITER. The 5 year goal is to develop a comprehensive set of validated simulations that can be used to predict the performance of LHCD on ITER. Emphases will be to establish a detailed understanding and modeling of: plasma-grill interactions; long-distance coupling from grill to separatrix, including utilization of local gas-puffing tools; propagation of LH waves across the SOL and through H-mode barriers; interactions of LH waves with the electron distribution function and validation of Focker-Planck and Quasi-Linear models, including trapping. Our close connections to the code development efforts are particularly important here.

LHRF Coupler Technology As part of the plan to increase total LHRF power coupled into C-Mod for the Advanced Scenario program, we are developing and will install an advanced coupler, with a novel 4-way power splitter. This approach should be simpler (and cheaper) to construct than more conventional couplers, and should have direct relevance to the design of an efficient, high power-density LH launcher for ITER.

1.5.5 Macroscopic Stability

Disruption Mitigation Mitigation of major disruptions is likely to be needed as a routine tool for ITER operation. Research for the coming 5 years on C-Mod will concentrate on: optimization of the gas mixture, pressure and injection quantities; continued development of real-time disruption prediction and automatic mitigation; modeling with NIMROD/KPRAD of the experimental results, and use of the validated code for ITER predictions; study of runaway electron production during disruptions and mitigation, making use of unique C-Mod tools (LHCD, hard x-ray and synchrotron diagnostics, error-field coils).

Non-Axisymmetric fields Areas of investigation on the effects of non-axisymmetric fields, for both intrinsic and applied error fields, will include: magnetic braking of rotation and tests of the related neoclassical toroidal viscosity theory; exploration of the application of resonant magnetic perturbations to affect/control the edge pedestal and ELMs; investigating the influence on Neoclassical Tearing Mode seed islands.

Stability of ITER-like Equilibria C-Mod is a nearly 1/9 scale model of ITER, with the capability to run the same plasma shapes, using a similar set of poloidal field control coils. Research in the next 5 years will concentrate on: development of advanced controllers for stability at high elongation; investigation of noise effects on feedback control, and development of noise suppression/rejection algorithms.

Neoclassical Tearing Modes With additional plasma heating and current drive, we expect to access higher b regimes on C-Mod, and are likely to pass the NTM threshold. Plans to study NTMs include: investigation of NTM stabilization with LHCD through Δ' modification.

Fast Particle Instabilities, including Toroidal Alfvén Eigenmodes Fast ion distributions, produced with ICRF minority heating on C-Mod, drive a broad range of alfvénic modes. Important diagnostics for studying these include Phase Contrast Imaging, Compact Neutral Particle Analyzers and magnetic pickups. Upgrades are planned for the latter two systems. In addition, we have active MHD antennas to study stable modes in the ITER-relevant intermediate toroidal mode number range. Benchmarking of the NOVA-K and AORSA/CQL3D codes will be a significant part of the planned research.

1.5.6 Integrated Scenarios: ITER H-mode Baseline

ITER Operational Scenarios The 5 year goal is to develop, demonstrate and validate ITER scenarios, including: diverted full bore current ramp-up; ramp-down; approach to and control of the nominal ITER operating point (shape, β , I_i , n_e). With ICRF as the proxy for alpha heating, we also plan to carry out simulated burn control experiments, utilizing the non-linear capabilities of our Digital Plasma Control System.

H-mode Pedestal Relaxation ELM control, small ELM regimes and ELM pacing are all proposed for ITER. The overall goal on C-Mod is to optimize the pedestal relaxation mechanism while maintaining core confinement, with acceptable particle control and heat

exhaust. Experiments will concentrate on: characterizing shape and pedestal parameters resulting in small ELM regimes; testing low n/m Resonant Magnetic Perturbation ELM control using our non-axisymmetric coils (A-coils); exploration of ELM pacing using edge heating and current drive, with both ICRF and LHCD.

High Performance H-mode Scenarios We will operate at ITER-scaled physics parameters (q , β and collisionality), shaping and geometry with the goal of developing and testing high performance H-mode scenarios. Evaluations will include: the influence of pedestal parameters and relaxation mechanisms on core performance; evolution of impurities and core radiation for extended pulse lengths.

ITER-Relevant Plasma Control With its similar configuration and coil-set, and an advanced control system, C-Mod is well positioned to test control algorithms for ITER. These will include: development of robust fault sensing and mitigation techniques for off-normal events, including real-time adaptive control for safe shutdown; real-time stability boundary estimation and response strategies; trial implementation of elements of ITER CODAC algorithms.

1.5.7 Integrated Scenarios: Advanced Scenarios

RF Current Profile Control Most advanced non-inductive scenarios require off-axis current profile drive, with the possible addition of some on-axis seed current. On C-Mod these are provided by a combination of bootstrap and RF. LHCD is aimed at efficient far off-axis drive, and ICRF Fast Wave CD can provide the central seed. Research objectives are: assess LH accessibility and efficiency in H-modes; combine LHCD with high power ICRF/FWCD and compare with modeling from CQL3D and TORIC; test real-time control of current profiles.

Hybrid Scenarios The hybrid scenario is characterized by weak central shear having central q at or slightly above 1 to suppress sawteeth, and with a fraction of the current driven inductively. On C-Mod, we plan to assess the feasibility of these scenarios for plasmas with coupled electrons/ions, no core fueling and no core momentum input, using LHCD to establish and maintain the requisite q profile. Steps along this path will include: demonstration of core shear reduction in H-mode using LHCD; assessment of confinement, including relative roles of the core and pedestal; studies of MHD stability and β scaling; contributions to multi-machine comparisons and model benchmarking, and to predictions and scenario development for the ITER hybrid scenario.

Current-Relaxed Non-Inductive Scenarios One of the primary long term goals for the C-Mod Advanced Scenarios program is the demonstration and assessment of fully non-inductive scenarios, with varying contributions of external and bootstrap current drive, maintained for multiple current diffusion times (τ_{CR}). A multi-pronged approach will include: studies of majority LHCD scenarios; extension to higher confinement regimes with majority bootstrap current; contributions to intermachine comparisons and model benchmarking for the ITER steady state scenario; extending pulse duration to >3 secs;

assessment of feasibility of double-barrier regimes with high bootstrap fraction and improved core confinement and β_N .

Internal Transport Barriers Using our RF tools, especially LHCD, our goal is to demonstrate and understand the control of core transport in regimes with coupled ions/electrons and no core momentum or particle sources. Studies will include: effects of shear modification by LHCD on core barriers formed with off-axis ICRF; barrier formation in L-mode plasmas with off-axis LHCD; exploration of techniques to control particle and energy transport using ICRF and/or LHCD actuators. If successful, we expect to demonstrate real-time control of core transport, temperature and/or density using RF actuators.

Pedestal, SOL and Divertor Long-pulse high-power advanced scenarios will stress particle control and power handling systems, and our goal is to document and optimize edge barrier, SOL and divertor properties in these scenarios. This will involve: evaluation and optimization of active pumping to access low density pedestals compatible with LHCD; study of pedestal and ELM properties in advanced scenarios, and contribution to related international studies; assessment of SOL and divertor heat fluxes in high power non-inductive scenarios; implementation of control techniques and the PFC upgrades (DEMO-like Divertor) needed to enable extension of these regimes for long pulse.

1.5.8 Facility and Diagnostics

An integral part of our proposed plan is to upgrade key components of the C-Mod facility, and add critical new diagnostic capability. The details can be found in Chapter 11. Major hardware upgrades planned for the five year period are summarized here. The schedule for upgrade implementation is detailed in table 11-2.

Lower Hybrid: Increase to 4 MW source power (from the current 3); add a second, advanced launcher, providing higher efficiency, lower power density, and, in conjunction with the first launcher, the capability to explore compound spectra; build a third advanced launcher to replace the first launcher, with a goal of coupling at least 2.5 MW net into plasma from the two launchers.

Ion Cyclotron RF: Replace all current antennas with two advanced high power density 4-strap antennas (with an integral reflectometer density profile diagnostic), to maintain 8 MW source power (~6 MW into plasma), while freeing port space for the second LH launcher; implement 4 Fast Ferrite Tuner systems for active real-time matching to changing plasma conditions.

Divertor: Install DEMO-like solid tungsten outer divertor, with active heating, designed to operated at ambient temperature of 600 C, for high power/energy handling.

Diagnostics are key to increased understanding. Major enhancements in the next five years will include:

Polarimeter system (ITER prototypical) for $j(r)$ profiles, as an adjunct to MSE, especially for high density operation and in the core of the plasma.

SOL Thomson scattering upgrade, to provide T_e and n_e profiles from the bottom of the pedestal well out into the scrape-off layer.

In-situ first wall analysis accelerator, enabling for the first time between-shot surface evaluations over a complete poloidal cross-section of the limiter, divertor and walls.

Infrared Imaging upgrades for diagnosis of power fluxes, especially to the new outer divertor.

MSE upgrades for improved spatial resolution.

Gas Puff Imaging upgrades for improved edge fluctuation characterization.

Charged Neutral Particle Analyzer upgrades for improved spatial resolution.

Reflectometry upgrades to expand the system capability to measure density fluctuations at 4.6 GHz driven by the Lower Hybrid RF.

High harmonic vertically viewing ECE for detection of non-thermal emission associated with LH-driven fast electrons.

Following the Fiscal Year 2008 experimental campaign, we plan a complete inspection of the tokamak core to ensure reliable operation through the next 5 year period.

Within the guidance budgets, run time is very constrained, and many important initiatives cannot be funded. Assuming the proposed budgets, run time will be increased substantially (2010 through 2013), major items to increase capability, reliability and productivity will be accommodated, and associated increases in required personnel are included.

Alcator C-Mod is operated as a National Facility, and includes contributions from major collaborations at PPPL and the University of Texas (Austin), as well as from a large number of smaller national and international collaborations. While this proposal is formally only for the portion of the work funded through the Cooperative Agreement with MIT, all of the planned research assumes an integrated effort involving all of the collaborators. Specific plans from Princeton and Texas are detailed in sections 12.1 and 12.2 respectively.

2 C-Mod's Role in the National and International Programs

The C-Mod research program is not carried out in isolation but rather must be placed into the context of the national and international programs. As one part of that overall effort, C-Mod naturally stresses areas where the unique characteristics of the machine enable especially important contributions and where its program is unique or complementary to others. By extending the range and regimes of tokamak experiments, C-Mod provides critical data for extrapolation to next-step devices and for validation tests of theory and modeling. Many aspects of its operation are particularly relevant to burning plasma and reactor regimes, for example the tight coupling of electrons and ions, the lack of strong core particle or momentum sources and reactor-level power densities. This property allows C-Mod to address crucial questions which face the world fusion program as it moves to the next phases in its development, first to ITER and ultimately to a DEMO reactor.

2.1 Unique Character of C-Mod

As the only compact high-field diverted tokamak in the world, C-Mod can run high performance plasmas at higher density and collisionality than machines of standard design (typically by about an order of magnitude). Note that while the neoclassical collisionality, ν^* , in C-Mod is higher than would be found in a reactor, the collision frequency relative to confinement is much more prototypical than in other devices in that, in most regimes, $\tau_{ei} \ll \tau_E$, resulting in close coupling of electrons and ions. Both aspects of its collisionality regime allow C-Mod to fill important and relevant niches especially for studies of turbulence and transport. The values of normalized gyro-radius, ρ^* , and pressure, β are closer to those in other devices. While high-field operation makes C-Mod far from an ideal platform for studying β limits, it does allow the device to operate in regimes of enhanced confinement or strong heating without confusing β limiting phenomena with other effects. As a compact high-field device, C-Mod can also be paired with larger lower-field devices to perform dimensionless identity and dimensionless scaling experiments. These continue to yield important insights into core, pedestal and SOL physics.

The uniqueness of the C-Mod research program derives from the basic design of the machine itself, as well as from the choices made for auxiliary heating and current drive, plasma facing components and so forth. Unlike most devices, C-Mod uses RF rather than neutral beams as its principal auxiliary heating method. Non-inductive current drive is entirely from the combination of bootstrap plus RF, with no contribution from beams. This scenario has important impacts on operating regimes by decoupling source terms, while in most other devices these are strongly coupled. In particular, in C-Mod the heating source is not associated with strong particle, momentum, or current sources as it is with NBI. In this sense, the ICRH is far more like alpha heating, which will dominate in a reactor. The choice of lower hybrid for current drive allows for flexible control over current deposition profiles at large normalized radius and with high efficiency. With ICRF, again in contrast to NBI, the heating source can be decoupled from the density profile, which allows for additional flexibility when designing experiments. These effects all increase the direct burning plasma and reactor relevance of the advanced scenario physics studied on C-Mod. Research into intrinsic rotation, observed in the absence of

externally applied torques, has been largely pioneered on C-Mod, a direct result of the decoupling between heating and momentum sources.

The C-Mod plasma facing components are made of bulk high-Z metals, unlike most machines which employ various forms of graphite. Current thinking suggests that metals will be needed for a reactor because of their potentially superior properties relative to erosion, tritium retention and power handling. However, with the world database so sparse in this area, C-Mod continues to provide critical data on these issues. ITER is currently weighing options for plasma facing components, and tungsten is one of the few options being considered. ASDEX-U has recently converted to tungsten-coated graphite, while C-Mod is transitioning from solid molybdenum to solid tungsten. Coordinated experiments between the two facilities, and with JET when it converts to tungsten-coated graphite (~2011), will provide the critical information required for informed decisions on ITER. In particular, tritium retention is expected to be quite different in solid tungsten as compared to tungsten-coated graphite.

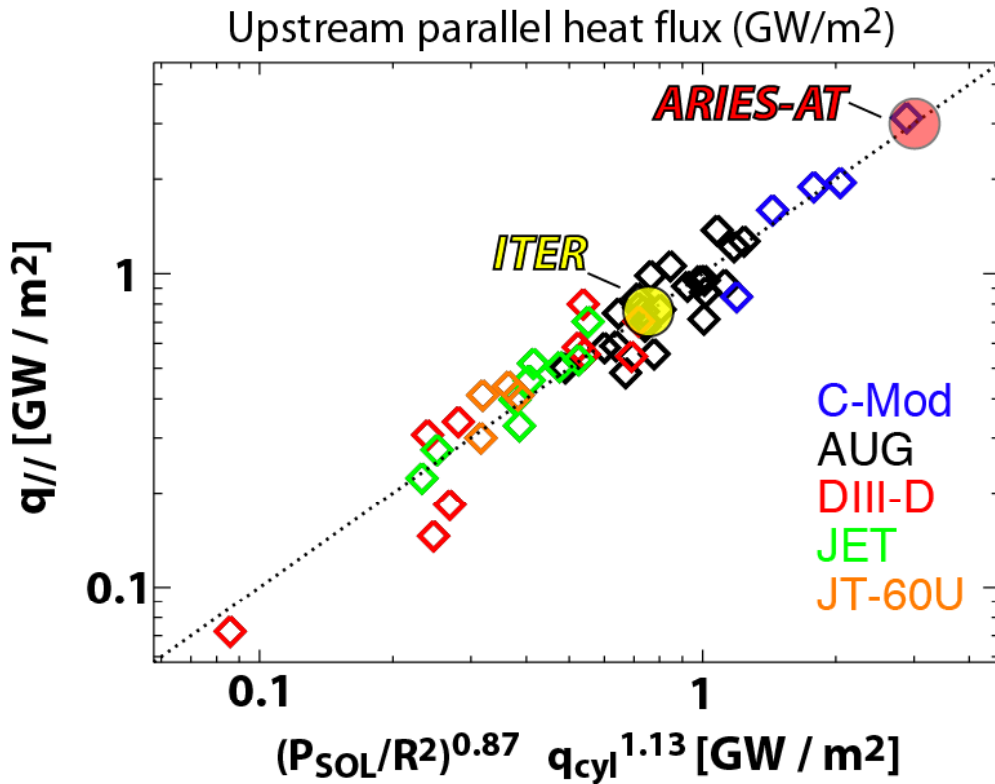


Figure 2.1: Comparisons of upstream parallel heat flux among present-day divertor tokamaks. C-Mod data span the range between ITER and ARIES-AT.

C-Mod also runs at very high divertor power densities, $P_{\text{exh}} / A_{\text{div}} \sim 7\text{-}10 \text{ MW/m}^2$, exceeding that of other machines or even ITER, and typical of those in a reactor. As shown in figure 2.1, upstream parallel Scrape-Off-Layer (SOL) power densities in C-Mod can exceed 1 GW/m^2 , and spans the expected range from ITER to reactors. C-Mod's compact size and high field increase its ability to run pulses which approach steady state relative to plasma current diffusion skin times. The high B/R ratio tends to partition

plasma pressure (which for C-Mod is the world's highest in a tokamak, $\langle P \rangle = 1.8$ Atmosphere) toward higher density rather than temperature. Since current relaxation times scale as $T_e^{3/2} a^2$. C-Mod's relatively compact size means that it has a relaxation time which is typically substantially smaller than discharge times. Even at the reduced densities and higher temperatures characteristic of advanced regimes, C-Mod can run discharges of up to two L/R times. Solid metallic walls have altered hydrogen retention properties relative to graphite (both bare and metal-coated), with the result that C-Mod is currently a unique tokamak test-bed for hydrogenic retention studies. An added benefit in this regard is that because high performance is achieved on C-Mod without neutral beams (and their associated cryopumping) we can perform extremely accurate particle balance measurements on individual pulses.

2.2 C-Mod's Role in Next Step Programs

2.2.1 ITER

ITER, under construction in France, will be the first magnetic confinement experiment to access the burning plasma regime, where fusion-produced alpha particles provide the dominant plasma heating source. ITER is expected to start operation in about a decade, and a great deal of research must be done in the world-wide fusion program during that period to inform design decisions for ITER, and to provide guidance for operational scenarios on ITER. Alcator C-Mod is in many ways prototypical of ITER, capable of operating with the same plasma geometry and magnetic topology, at the same magnetic field strength, and absolute plasma pressure (and therefore also β), the same divertor density, and the same or even higher scrape-off layer power fluxes. C-Mod most closely approaches ITER in terms of edge neutral opacity and radiation trapping, both important for divertor dynamics.

Key C-Mod contributions in many critical areas of ITER research, which will continue in the coming five year period include:

- Integrated Scenarios
 - Breakdown and current rise, including internal inductance, flux consumption and vertical stability
 - Reference ITER scenarios for databases and modeling
 - ITER hybrid scenarios
 - Experimental development
 - Understanding mechanisms for maintaining $q_0 > 1$ in the absence of core fueling, momentum drive
 - Profile control methods, especially $j(r)$ with Lower Hybrid current drive plus bootstrap
- Core Transport
 - Regimes with equilibrated electrons/ions, low momentum input, dominant electron heating
 - Collisionality dependence of density peaking
 - Developing common technologies for integrated modeling (frameworks, code interfaces, data structures)

- MDSplus, developed and maintained at Alcator, is a model
- Pedestal Physics
 - L to H-mode power threshold at low density (uniquely at the ITER magnetic field, with high neutral opacity)
 - Improved predictive capability of small ELM and quiescent H-mode regimes
 - ELM control using stochastic fields with external coils (outside the TF)
- Wave-Plasma Interactions
 - LHCD physics and coupler technology
 - ICRF heating, current and flow drive
 - RF induced sheaths and plasma-wall interactions
- Plasma-Boundary Interactions
 - Tritium retention and removal with solid metallic plasma facing components
 - Plasma and nuclear effects
 - Surface modification
 - Surface effects: impurity generation, wall conditioning
 - Power handling and impurity control
 - Scrape-off layer transport
 - Radiative/detached divertor
- Magneto-Hydrodynamics Macro-stability
 - Disruption database
 - Disruption mitigation
 - Validate 2 and 3-D MHD codes with radiation
 - Runaway electron amplification (lower hybrid RF for controlled seeding of non-thermal electron population)
 - Optimization of massive gas mitigation for speed and reduced particle load
 - Experimental data is uniquely available at the same absolute pressure (in addition to field and β) as anticipated in ITER, one of the critical parameters for penetration of the high pressure gases
 - The combination of high power density and short quench time makes C-Mod closer to ITER than any other operating or planned tokamak with respect to dissipated energy density ($\sim 150 \text{ MW/m}^2$ through the plasma surface) during disruptions.
 - Reliable disruption prediction methods
 - Develop robust algorithms
 - Real-time automatic mitigation
 - Alven Eigenmodes
 - Intermediate toroidal mode number AEs (expected to be most important on ITER)
 - studied with active antennas optimized for this spectrum
 - Fast-particle redistribution by AEs
 - ICRF ion tails drive AEs unstable on C-Mod

Many of these studies require the participation of multiple facilities around the world, to take advantage of differences in dimensional parameters, and to compare different heating and current drive tools. These joint experiments are coordinated through the International Tokamak Physics activity. C-Mod is an extremely active participant in the ITPA joint experiments, and we will continue this strong participation throughout the next five year period.

2.2.2 Contributions to FESAC Gap Issues

Critical gap issues on the fusion development path from ITER to DEMO were identified in the October 2007 FESAC *Report on Priorities, Gaps, and Opportunities: Towards a Long Range Strategic Plan for Magnetic Fusion Energy*. The report assumed that many other issues would be successfully resolved on existing facilities and on ITER. C-Mod will make important contributions to helping resolve many of these issues in the next five years, including:

- B.9 Plasma facing components
 - High Z metals, ultra-high scrape-off layer power densities
- A.5 Off-normal events
 - Disruption avoidance, prediction and mitigation
- B.8 Plasma-wall interactions
 - SOL and divertor transport
 - Erosion/redeposition
 - Hydrogen isotope retention
- A.2 Integrated, high performance plasmas
- A.3 Validated theory and predictive modeling
 - Code benchmarking
 - Discovery of new phenomena
 - Iteration of theory and comparison with experiment
- A.1 Measurement
 - New and improved tokamak diagnostic techniques
- B.10 RF antennas, launchers and other internal components
 - Advancing the understanding of coupler-edge plasma interactions
 - Improvement of theory and modeling
- A.6 Plasma modification by auxiliary systems
 - RF (ICRF and LHRF) for current drive, flow drive, instability control
 - ELM control
- A.4 Plasma control
 - Maintaining high performance advanced scenarios with fully relaxed current profiles

In addition to these important contributions to the “gap” issues, C-Mod is poised to make major contributions to filling a significant piece of one of the actual gaps. With the implementation of the DEMO-like divertor (see chapter 4 of this proposal), C-Mod will be the first tokamak to investigate operation with controlled hot tungsten walls ($T > 600$

⁰C), directly addressing important aspects of gap G-9: *Sufficient understanding of all plasma-wall interactions necessary to predict the environment for, and behavior of, plasma facing and other internal components for Demo conditions. The science underlying the interaction of plasma and material needs to be significantly strengthened to allow prediction of erosion and re-deposition rates, tritium retention, dust production and damage to the first wall.*

2.3 Education

The Alcator C-Mod experiment is unique world-wide among major tokamak facilities in being sited on the main campus of a major university. The close academic connection provides an outstanding environment for education. In the Alcator group, MIT graduate students outnumber MIT physicists. During the past five years, on average at any one

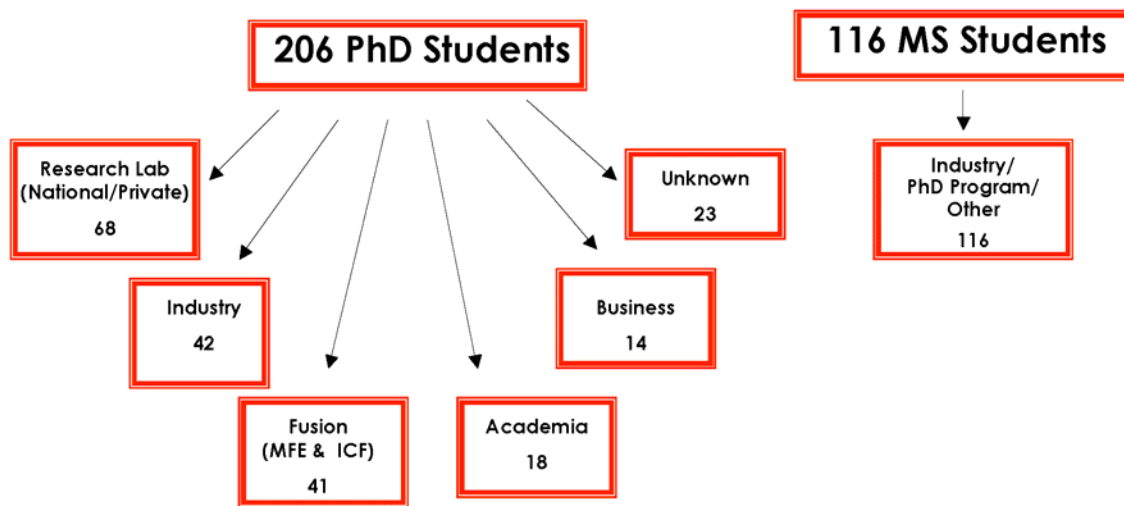


Figure 2.2 Approximate statistics of the employment of graduate students after leaving the MIT Plasma Science and Fusion Center (1980-2006).

time about 30 graduate students were carrying out their thesis research in the Alcator program. These students form a vital part of the research team, without which the effort could not be nearly so cost effective. Looking at statistics for 2007 and 2008, about 40% of all research runs have had student session leaders. Since the start of the C-Mod project, over 70 students have graduated. Former MIT students hold many positions of responsibility within the US (and international) fusion research community. This predominance is testimony to the long tradition of educational excellence at MIT, which proceeds from outstanding teaching and research opportunities in experiment, theory, and engineering. Many students graduating from Alcator can find employment in fusion or plasma research. Recent graduates have gone on to research labs such as General Atomics, LLNL, LANL, PPPL, to University positions, and some overseas. A significant fraction of our graduates have decided to move into other fields of endeavor. The statistics of the MIT Plasma Science and Fusion Center as a whole, which is a fair indication of the Alcator demographics, is illustrated in figure 2.2. Education is essential to the fusion program both as a source of future professionals in our own field and as a contribution to the nation's need for accomplished technical leaders in related fields that

are important economically and to society. Alcator C-Mod takes as a major element of its mission the education of this new generation of fusion plasma physicists and engineers.

3 Transport Research

Progress in understanding transport is essential for the extrapolation to next-generation experiments and for exploitation of fusion for practical energy production. Given sources and boundary conditions, transport determines the profiles of plasma temperature, density and rotation. At the same time, the study of plasma turbulence and transport is among the grand challenges of science with impact across a broad range of physical systems. The long-term goals of transport research on C-Mod are to:

- 1) Contribute toward the development of first-principles understanding of transport in confined toroidal plasmas
- 2) Validate the evolving set of nonlinear turbulence codes
- 3) Discover and exploit new and unexpected results

The C-Mod program seeks to leverage the unique characteristics of the experiment as part of the coordinated national and international efforts in which it is embedded. And while the plan summarized here does describe a large number of critical and unique contributions to that effort, these clearly gain greater value from the context of the world program.

For the proposed five year research period, we have organized transport research into four sub-topics – each with a particular emphasis. We have also identified an overarching theme of model testing and code validation. This is consistent with an increasing awareness, within the national transport community, of the importance and challenges of code validation activities [3.1]. The choices of which areas to emphasize are driven by new experimental capabilities, the need to support the emerging ITER research program and timeliness with respect to advances in theory and modeling. The sub-topical areas to be stressed are a) core transport, with an emphasis on particle and impurity transport and the effects of magnetic shear, b) momentum transport and self-generated flows and c) the creation and control of transport barriers, especially the role of magnetic shear and d) the physics of edge barriers, the L-H transition, pedestals and relaxation mechanisms. While clearly part of the transport program, threshold and pedestal work is described separately in chapter 7. The work on transport barriers, in particular, provides the underpinnings for the research into baseline and advanced scenarios discussed in chapters 8 and 9. The strong connections to studies of turbulent transport in the plasma edge and SOL, summarized in chapter 4, are a noteworthy part of our research as well. In all these areas, experimental progress is linked to the development and deployment of advanced diagnostics and close comparison with theory and modeling.

3.1 Highlights of Recent Research

3.1.1 Highlights: Model Testing and Code Validation

As noted above, critical elements in the development of predictive models of plasma transport are careful, quantitative comparisons between experiments and simulations. It is only by direct confrontation with the data that the accuracy and usefulness of models can be assessed. These comparisons can point out areas or regimes where models fail, and point to additional physics or new theory that needs to be incorporated. Recent work on C-Mod has begun addressing validation issues for the latest generation of gyrokinetic codes. This work includes deployment of capable fluctuation diagnostics and development of synthetic diagnostic post-processors for the new codes [3.2]. Figure 3.1 demonstrates the importance of these efforts by comparing a simple prediction of PCI data with a much more sophisticated synthetic diagnostic [3.3].

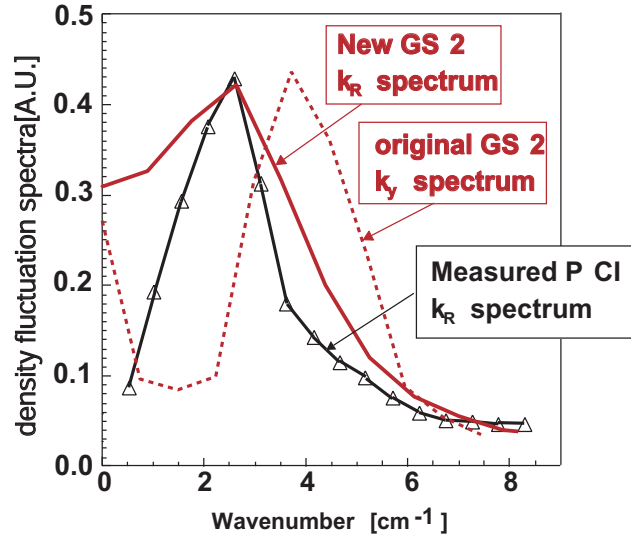


Fig 3.1 The value of sophisticated synthetic diagnostics is illustrated by this comparison of a simplified (original) k spectrum. Only the synthetic PCI spectrum (new) provides a match to the experimental data.

The consistency in the latter case with experimental results, suggests that further tests of the model, which seeks to explain particle transport in C-Mod ITB discharges, are worth pursuing. Other work on ITBs included testing of a hypothesis that formation of these type of discharges could be explained by reduction in ITG drive for plasmas with off-axis ICRF heating. In this case a drop in temperature gradients observed as the ICRF resonance location (via B_T) was scanned (fig 3.2a), led to a stabilization of ITG modes (fig 3.2b) in parameter ranges which corresponded to experimental observations of barrier formation [3.4-5].

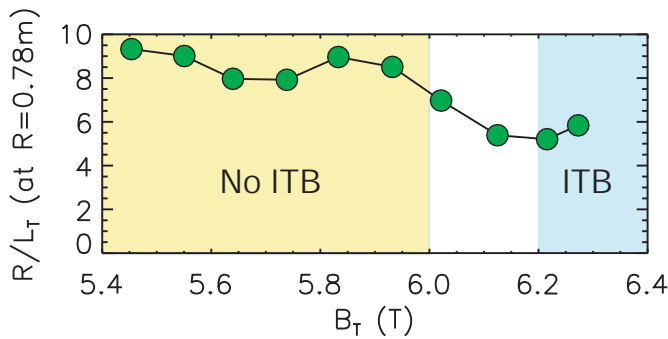


Fig. 3.2a The ITB threshold can be correlated with a decrease in the normalized temperature gradient

Quantitative comparisons of flux-gradient relationships were carried out in well-characterized, standard H-modes [3.6]. In these studies, the role of collisionality in modifying the nonlinear upshift in the normalized temperature gradient (R/L_T) was investigated by comparison of gyrokinetic simulations and experimental data.

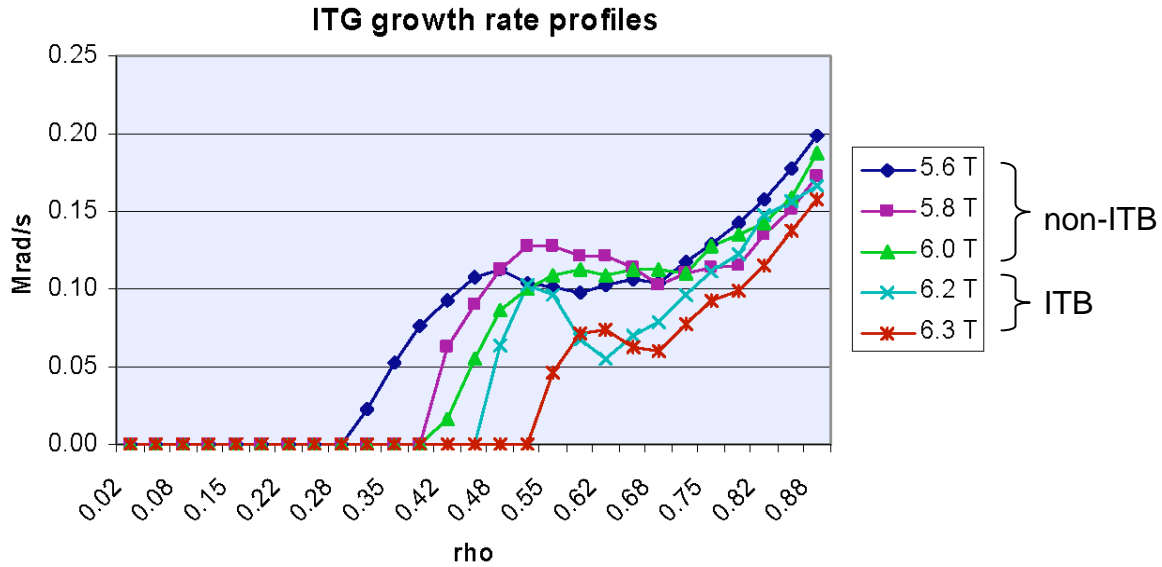


Fig. 3.2b Linear growth rates calculate by gs2 for the same set of shots shown in figure 3.2a. The ITB threshold is seen to correspond to an expansion of the region of ITG stability

Work has also begun on particle transport and density peaking which are observed at low collisionality. More details on these comparisons and others can be found in the following sections and in chapter 10 (Theory and Simulation).

3.1.2 Highlights: Core Particle and Energy Transport

The density profile realized on ITER will have a significant impact on its operation including the overall fusion gain achieved, MHD stability, bootstrap current and divertor operation. At the present time, *ab initio* models are not sufficiently developed to predict that profile so we must rely on extrapolation from current experiments. Data from ASDEX-Upgrade (AUG) [3.7] and JET [3.8] are strong evidence for density peaking at low collisionality and have been used to derive scaling relations which identified the most important parametric dependences [3.9]. However, in the data set that was available, collisionality was strongly correlated to n_e/n_G , the ratio of the experimental density, n_e , to n_G , the density limit calculated empirically [3.10]. This led to divergent predictions for the density profile on ITER, which uniquely will run at low collisionality and at a high fraction of the density limit. Observations on Alcator C-Mod, confirm and extend previous measurements allowing the correlation to be broken and strengthening the case for collisionality as the controlling

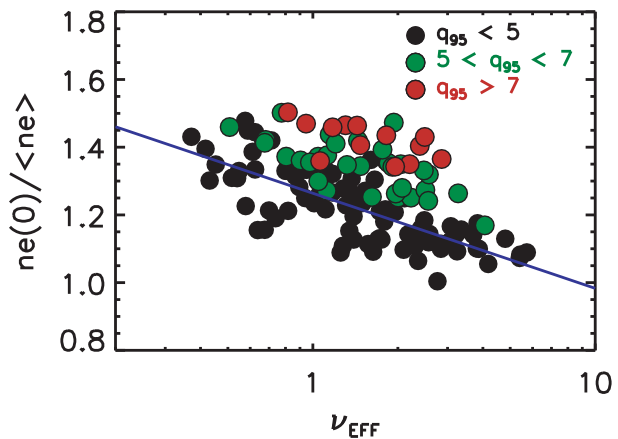


Fig 3.3 Density peaking is found to be well correlated with collisionality and q_{95} .

parameter [3.11]. At the lowest collisionalities, C-Mod attained peaking factors $n_e(0)/\langle n_e \rangle$ approaching 1.5 with $T_i \sim T_e$, high edge neutral opacity and no core fueling. Taken together, data from the three devices strongly suggest that the density peaking factor on ITER in ELMy H-modes will be in the range 1.4-1.6. In scans of plasma current at constant toroidal field, recent experiments have shown a secondary dependence on the edge q or magnetic shear. Both dependencies can easily be seen in figure 3.3. The particle pinch which causes the peaking would appear to be anomalous. Earlier measurements of particle transport on C-Mod via modulated gas puffs found $D \sim \chi$ which implies a pinch velocity, V , much greater than the neoclassical pinch, V_W [3.12]. We also note that the time to establish peaked density profiles in the experiments reported here is much faster than a/V_W . This contrasts markedly with ITB formation in C-Mod where the profile evolution is much slower, consistent with the time scale for the Ware pinch [3.13].

Global nonlinear GYRO simulations of turbulent transport in C-Mod low-density H-mode plasmas with peaked density profiles suggest a possible mechanism for understanding this phenomenon. Preliminary measurements of the ion temperature profile made in 2007 with the new imaging x-ray spectrometer reveal that the ion temperature is not as well coupled to the electron temperature in these lower density plasmas, and that the ion temperature gradient scale length can be significantly longer than L_{Te} for $r/a \sim 0.5$. Such reductions weaken the ITG drive relative to standard high-density H-modes in C-Mod, and the simulations show that modes with $k_\theta \rho_s > 0.6$ produce an inward particle flux that cancels an outward flux at lower $k_\theta \rho_s$ and results in a null net flux at about the density gradient seen in the experiments. Artificially raising the collisionality does not change the null flux result, but using an ion temperature profile that is close to the electron temperature leads to an outward particle flux. The empirically deduced collisionality dependence of H-mode density peaking in C-Mod plasmas may arise through the collisionality dependence of ion-electron temperature equilibration that enables the relaxation of the ion temperature profile in lower collisionality plasmas. This process may also operate in RF heated AUG and JET plasmas, but it probably is not occurring in NBI heated AUG and JET plasmas because the strong central ion heating would not permit relaxation of the ion temperature profile. In ITER and other reactor scale plasmas, the temperatures will be well equilibrated so there could be no relaxation of the ion temperature profile and this mechanism could not produce a pinch. It is therefore imperative to establish more firmly whether the relaxation of the ion temperature profile is real and to understand how this leads to a particle pinch.

Quantitative studies comparing measured and predicted temperature gradients were carried out with the aim of investigating whether the nonlinear upshift [3.14] of the critical gradient threshold for ITG turbulence was operative in highly collisional C-Mod plasmas. In the standard picture, nonlinearly driven zonal flows limit turbulent eddy size, so that just above the *linear* critical gradient, transport increases only slowly with increased drive. If this picture is correct, experimental measurements should correspond to higher gradients, where zonal flows themselves go nonlinearly unstable and transport increases rapidly above an ‘effective’ critical gradient (producing the ‘Dimitis shift’ [3.14]). Our simulations extended the original model by including a nonadiabatic

electron response and collisions, which enter the problem in two competing ways. First, by reducing the kinetic electron response, high collisionality can weaken the drive. Second, by damping zonal flows, which are predicted to be the main nonlinear damping mechanism for the turbulence, collisions could lead to higher transport. For the C-Mod parameters studied, simulations showed that the first effect dominated, leaving the Dimits shift intact and explaining past results where measured temperature gradients in C-Mod were found to be significantly higher than those predicted by widely used models [3.15].

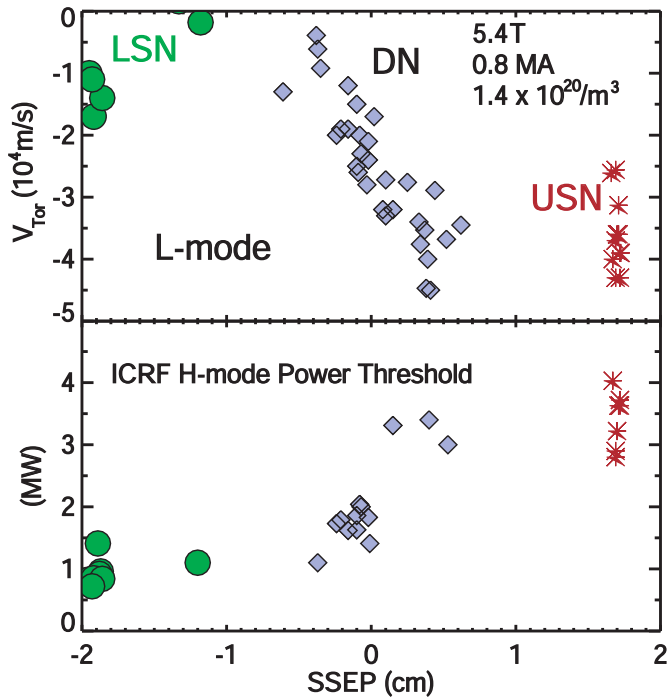


Fig. 3.4 The core L-mode rotation velocity (top) and the H-mode power threshold (bottom) as a function of SSEP.

Electron transport in confined plasmas is only poorly understood, however it is crucial for overall confinement in reactor-like plasmas with coupled electrons and ions. Experiments have begun to characterize turbulence and electron transport in the oldest and simplest tokamak regime, the low-density linear phase of Ohmic confinement. This regime can be accessed on C-Mod at densities below 0.8×10^{20} , where the electrons and ions are clearly decoupled and virtually all input power flows out through the electrons. The basic observation in this case is that confinement scales with density, i.e. electron transport increases markedly as the density drops. The difference in global confinement scaling for this electron transport

dominated regime, namely $\tau_E \sim n^1$ and ion dominated regimes with $\tau_E \sim I_p n^0$ at higher densities is suggestive of a distinct mechanism as well, providing a good case study for electron transport. Turbulence was characterized by use of a 32 channel, phase-contrast imaging diagnostic (PCI) with wavenumber resolution $0.5\text{-}55 \text{ cm}^{-1}$ and frequency resolution up to 5 MHz.

In studies carried out so far, the lower ω , k range, $100 < f < 250 \text{ kHz}$, was probed. Fluctuation levels, $(\tilde{n}/n)^2$, in the linear confinement regime scale with χ_e and rotate in the electron diamagnetic direction. The peak $k\rho_s$ for these fluctuations was on the order 0.3. Touching base with earlier work [3.16-17], fluctuations in the ion direction pick up at higher densities where χ_i is higher as well. Overall this suggests a changeover from TEM to ITG dominated transport as the confinement regime shifts from the neo-Alcator to L-mode regimes. Comparisons with linear and nonlinear gyrokinetic codes are underway.

3.1.3 Highlights: Self-Generated Rotation and Momentum Transport

Spontaneous rotation, in the absence of externally applied torque, has been studied extensively on C-Mod over the last 5 year period, mainly using single chord tangentially viewing x-ray spectrometers. Based on an empirical observational approach, the following picture has emerged [3.18]. In H-mode and other enhanced confinement regimes, substantial co-current rotation has been associated with assorted measures of good energy confinement, for example

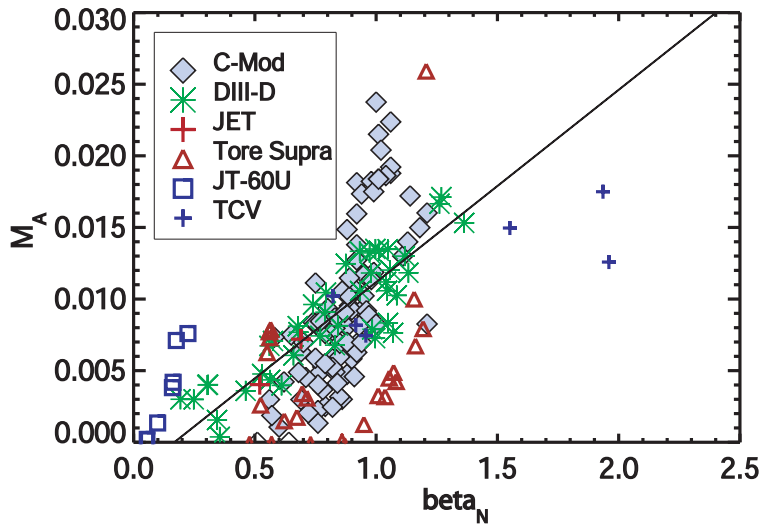


Fig. 3.5 The spontaneous rotation Alfvén Mach number as a function normalized pressure for six devices.

stored energy or plasma pressure. A relatively simple scaling with the change in the rotation between Ohmic L-mode and H-mode proportional to the increase in the plasma stored energy normalized to the plasma current has been documented. The energy confinement H-factor has been found to be proportional to the rotation velocity. This effect holds for both ICRF and Ohmic H-modes which suggests that the self-generated rotation is not due to wave or energetic ion mechanisms [3.19]. In contrast, Ohmic L-mode plasmas typically rotate in the counter-current direction, with a velocity that is a complicated function of electron density, plasma current and magnetic configuration [3.20]. The rotation velocity has been found to depend very sensitively on the distance between the primary and secondary separatrices in near double null configurations, and the magnitude of the velocity seems to be closely related to the H-mode power threshold [3.20-21], as seen in Fig. 3.4. There is evidence that the core rotation is driven by, and responds to changes in, the edge region coupled through momentum transport mechanisms. Using a crude three point velocity profile measurement, momentum transport coefficients have been estimated [3.22-23]. Momentum confinement times are similar in magnitude to energy confinement times, and in ELM-free H-mode discharges there is evidence for an inward momentum pinch. It is worth noting that in these same conditions, impurity particle pinches are also observed [24]

Very similar spontaneous rotation observations have been made subsequently on other tokamaks in H-mode and other enhanced confinement regimes. These are produced by a variety of methods (Ohmic, ICRF, ECH and NBI) indicating the universality of this phenomenon. In order to unify the observations made on various devices, a dimensionless scaling analysis has been performed [3.25]. The Alfvén Mach number has been found to

scale as β_N , as shown in Fig. 3.5. Extrapolation to ITER, operating at $\beta_N = 2.6$, suggests M_A in excess of 2%, possibly high enough for RWM suppression without external momentum input. More rigorous dimensional and dimensionless parameter scaling analysis has been performed, but the extrapolation to ITER remains the same.

3.1.4 Highlights: Internal Transport Barriers

The development of internal transport barriers (ITBs) in C-Mod occurs in plasmas with monotonic q profiles (normal magnetic shear) and small Shafranov shift with relatively low values of rotational shear. The density profiles are flat at the time of onset. The appearance of these barriers in the absence of the stabilizing mechanisms encountered in other devices has inspired careful study of the barrier formation trigger dynamics. Recent work has focused on the marginal stability in off-axis heated ICRF generated ITBs [3.4]. Analysis of the T_e profiles shows a decrease of R/L_{Te} in the ITB region as the RF resonance is moved off axis. Experimental evidence that T_i profiles broaden as the ICRF power deposition changes from on-axis to off-axis has also been obtained, consistent with power balance calculations of the T_i profiles. Linear gyrokinetic stability simulations using *gs2* show that the region of stability to ion temperature gradient driven modes (ITG) widens as the ICRF resonance is moved outward. Non-linear simulations show that the outward turbulent particle flux exceeds the Ware pinch by factor of 2 in the outer plasma region. Reducing the temperature gradient significantly decreases the diffusive flux and allows the Ware pinch to peak the density profile.

Enhancement of several key core diagnostics has resulted in increased understanding of C-Mod ITBs. Ion temperature profile measurements have been obtained using an innovative design for x-ray crystal spectrometry. They clearly show a barrier forming in the ion temperature (Fig. 3.6). Increased spatial resolution in the electron density profiles obtained from Thomson scattering complement those obtained from visible bremsstrahlung to show clearly the particle barrier which develops in these plasmas. Enhanced spatial resolution in the electron temperature measurements

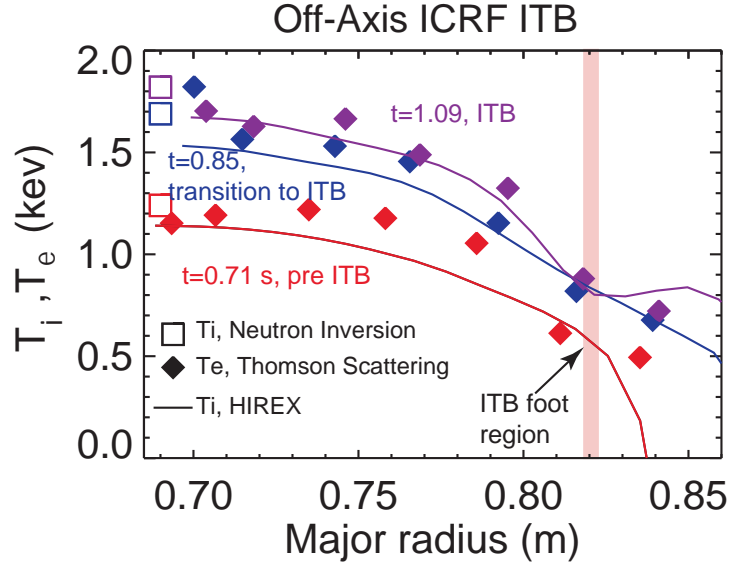


Figure 3.6 Impurity ion temperature profiles obtained from x-ray crystal spectrometry (solid lines) compare well with measurements of electron temperature from Thomson scattering (diamonds) and with central ion temperature from inversion of the global neutron rate (squares). A clear barrier in the temperature profile forms as the ITB develops.

obtained from Thomson scattering as well as from radiometric measurement of electron cyclotron emission provide values of R/L_{Te} which directly contribute critical information for the modeling program. Spatially resolved measurements of low wave number fluctuations in the plasma core have been used to benchmark the gyrokinetic stability modeling by providing evidence that the predicted trapped electron modes driven by the increasing density gradient are developing as the density peaks up in ITB plasmas. Using a new synthetic Phase Contrast Imaging diagnostic in gs2 [3.28], nonlinear gyrokinetic simulations were shown to reproduce the measured k spectrum of density fluctuations during on-axis heating of the C-Mod ITB (see fig. 3.1). Stability analysis shows the fluctuation spectrum is dominated by a strong pure density gradient driven trapped electron mode in the ITB during on-axis heating. Accordingly, the ITB effectively localizes the chord-integrated PCI density fluctuation measurement.

A trend of increasing radius for the ITB foot location with increasing current and decreasing toroidal magnetic field suggests that the size of the region of improved confinement scales inversely with q_{95} [3.27]. These observations motivate further studies of the role of magnetic shear in the formation and control of barriers. Studies of the hysteresis of the ITB formation obtained when the background magnetic field is ramped up or down indicate that an ITB forms in these experiments when the power inside the ITB radius is roughly less than 40% of the total input and that the ITB terminates when the power inside the ITB radius exceeds 60% of the total [3.27-28].

It has been demonstrated that the addition of central ICRF power into an established ITB plasma will control the further rise of the central particle and impurity accumulation, likely through amplifying the trapped electron mode (TEM) driven turbulent transport [3.28]. A bonus of this process is the increase in the central temperature, pressure and fusion rate in the core. Doubling of the central temperature and pressure and 10-fold increase in the fusion rate have been achieved [29].

3.2 Proposed Transport Research

The transport community has made a substantial effort in recent years to identify and articulate the outstanding research questions. The C-Mod plan is designed to address and contribute toward the resolution of most of these. In particular:

1. Particle Transport:
 - a. What is the interplay of the various forms of drift-wave turbulence in determining particle transport?
 - b. What are the connections between the energy and particle transport mechanisms? Are the same mechanisms responsible for both?
 - c. What plasma conditions lead to a significant inward pinch and density peaking?
 - d. What are the conditions where impurity transport might lead to concentration of impurities and unacceptable radiation levels.
2. Momentum Transport:
 - a. What is the origin of self-generated rotation and momentum transport?
 - b. How does it extrapolate into reactor regimes?
 - c. Will it be sufficient to affect micro- or macro-instabilities?
 - d. Can we drive significant flows with RF waves?
3. Ion Energy Transport:
 - a. Can we validate, in detail, the predictions of drift wave models for ion energy transport – especially the role of magnetic shear?
 - b. Can we confirm, at the level of fluctuations, mechanisms for regulating turbulence and transport?
 - c. What options are available for controlling transport barriers?
4. Electron Energy Transport:
 - a. What type and what scale are the fluctuations that cause electron energy transport?
 - b. How do these interact with the ion-gyro scale turbulence?
 - c. Is there an important magnetic component in the turbulence or transport?

C-Mod plasmas are unique and bring a different perspective to these questions in several important ways. Thus experiments on this device can be crucial for validation of physics models. As a compact, high-field device, it typically operates at higher densities (by about an order of magnitude) than low-field machines. By consideration of the coupling collisionality, τ_E/τ_{ei} , it can be seen that C-Mod runs in the reactor-relevant regime with ions and electrons well equilibrated. This is likely more significant than simply having $T_i \sim T_e$. In plasmas close to marginal stability, which may be most plasmas of interest, details of profiles are critical and reactor-like conditions are not necessarily met by forcing weakly coupled electrons and ions to similar temperatures through external heating – that is, the two temperature profiles, self-consistent with strongly coupled transport may be significantly different in the two cases. The high field of the machine tends to systematically reduce β when compared to low-field experiments. While this makes exploration of the β limit itself more difficult, it does allow enhanced regimes to be thoroughly explored without necessarily involving β limiting physics. The exclusive use of RF power for auxiliary heating and current drive has a significant impact when

compared to neutral beam heated experiments, which are typically employed on other devices. There are no core particle sources and no direct momentum source associated with the ICRF or LHCD. Thus the effects of heating, fueling, flow drive and current drive can be decoupled. Further, with ICRF, unlike NBI, the heating profile is decoupled from the density profile. These characteristics will be exploited to create regimes and carry out experiments that can complement results from machines with lower fields and NBI heating.

3.2.1 Proposed Research: Model Testing and Code Validation

Careful, quantitative comparisons between simulations and experiments will be an important activity in the proposed 5 year research plan. While the current C-Mod diagnostic set is quite powerful [3.30], new and upgraded diagnostics, along with developments of corresponding synthetic diagnostics for turbulence codes will be the key to progress [3.31]. For example, the synthetic diagnostic codes for PCI will be extended to include new features of the measurement for both the gs2 and gyro codes and analogous work for reflectometry will be carried out. It should be possible to compare experimental data to predictions of fluctuation amplitudes, k spectra, correlation lengths, correlation times and direction of propagation. An area of focus will be particle transport where models should now have sufficient physics to make meaningful tests. Initial work on the density peaking observed at low collisionality suggested that a reduction in ITG drive was a critical element [3.32]. These studies will be augmented by the availability of additional profile measurements for T_i , E_r and $q(r)$. Work on ion energy transport will continue as well, with quantitative comparisons of gradients and fluctuations taken as a function of magnetic shear. These topics cover areas of theory and simulation which are relatively mature, though not thoroughly validated. In a less mature area, studies of barrier formation and control will test the ability of codes to model transport bifurcations and dynamics. Understanding of electron transport is also rather incomplete, without even an identification of the types of instabilities responsible. Experimental measurements of electron transport will include observations of high-k (up to 55 cm^{-1}), high frequency density fluctuations with PCI. The first objective is to identify the spectral region, and therefore the class of instabilities, responsible for electron heat transport. Models for momentum transport are perhaps in the least developed state. Experimental observations of self-generated flows and transport of intrinsic rotation must first be understood qualitatively. The new imaging x-ray spectrometer will provide unprecedented measurement of rotation profile evolution in torque free plasmas. Transient transport experiments are planned which will probe momentum transport using this diagnostic and a number of rotation perturbations, including mode locking, topology modification and transport bifurcations. As more complete models for momentum transport emerge, it will be possible to identify critical validation measurements. All of these studies will be aided by new local computing capabilities, partially funded by the C-Mod project. Though the overall objective of predictive understanding is certainly many years away, we believe the understanding gained through the research outlined in this chapter will represent important progress toward that goal.

3.2.2 Proposed Research: Core Particle and Energy Transport

In a tokamak reactor, few of the parameters which are predicted to set the level of drift-wave transport are under external control. The ions and electrons will be tightly coupled, with $T_e = T_i$ and neither transport channel negligible; impurity levels must be low with $Z_{\text{EFF}} \ll Z_{\text{IMPURITY}}$ and without core particle sources, density profiles will be set self-consistently by transport and are generally expected to be flatter than temperature profiles with $R/L_n < R/L_T$. Rotation drive from neutral beams is likely to be very small or entirely absent, though shear from self-generated rotation or RF driven rotation may provide some stabilizing effect. (These issues are addressed below.) This leaves magnetic shear as perhaps the only “free” parameter with significant impact on turbulence and transport levels. Steady-state reactor schemes require some level of external current drive, opening up possibilities for controlling transport via control of the current profile. This state of affairs leads to investigation of three areas 1. the role of magnetic shear, 2. particle and impurity transport, 3. electron energy transport.

Magnetic shear is coupled to the other topics as it is predicted to have an impact on ion-energy, electron-energy and particle transport. An idea of the magnitude of these effects can be appreciated from figure 3.7, which shows the results of relatively early models of ITG turbulence. Simulations which include more physics also show strong effects, though the dependences on local gradients and collisionality can be complicated. On C-Mod, the magnetic shear can be modified by changing the plasma current or shape and systematic scans of these parameters will be carried out. However, the LHCD system provides the best opportunity to modify the shear independently of the plasma shape and total current. This capability will be exploited as LH power levels are increased. Careful documentation of T_i and T_e profiles and their gradient scale lengths will be made to permit comparison with theoretical expectations based on temperature-gradient-driven microturbulence. C-Mod experiments will emphasize the study of transport near marginal stability where turbulence, particularly its non-linear saturation mechanisms, may be quite different than in regimes far above the stability boundaries. It is also planned to measure density fluctuation amplitudes and radial correlation lengths to enable a broader comparison with theory. Sufficient modification of the shear may allow formation of internal transport barriers in both electron and ion

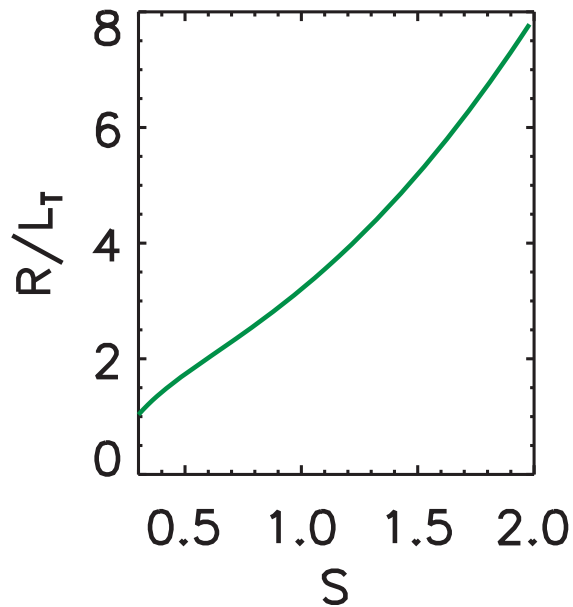


Fig. 3.7 The effects of shear on turbulence and transport are clearly visible in this plot of equation ? from reference []

channels and may provide a means for controlling the strength and position of barriers. This research feeds directly into the AT scenarios thrust.

The ability to predict the density profiles in reactor-like devices is critical for assessing fusion yield, MHD stability and bootstrap current. With its exclusive use of RF for auxiliary heating and current drive coupled with high opacity to neutrals, C-Mod provides a useful test-bed for studies of particle transport with very low levels of core fueling throughout. Thus data from experiments on C-Mod will be particularly useful in extrapolating to ITER and are the subject of strong interest within the ITPA. Recent experiments, which showed the effects of collisionality and shear on particle transport will be extended in the range of parameters and in diagnostic coverage. A key near-term goal will be amassing complete data sets for careful comparison with emerging models of particle transport. It is generally believed that modern gyrokinetic codes like gyro and gs2 now contain all the required physics to characterize particle transport, but general agreement with experimental results has not yet been demonstrated. Experimental data will also be compared to two simplified theoretical models for particle transport: thermodiffusion, which is based on drift-wave turbulence and predicts $L_n \propto L_r$ [3.33] and turbulent equipartition which is based on conservation of the adiabatic invariants during transport and predicts $L_n \propto L_S$, where L_S is the scale length for magnetic shear [3.34-35]. Differences in density peaking in L-mode and H-mode regimes, which are commonly observed, may provide important clues to the underlying mechanisms.

With lower hybrid heating, C-Mod will have access to electron heated regimes with decoupled electrons and ions. Significant changes in self-generated rotation profiles have already been observed in such cases, further motivating studies of particle transport. Comparison with ion-heated regimes, should be illuminating. LHCD will also allow experiments with $V_{\text{LOOP}} = 0$, eliminating the neoclassical pinch. AT and hybrid regimes, which should be enabled by LHCD on C-Mod, typically show anomalous density peaking and will be investigated in the course of the integrated scenarios research. Previous work suggests that changes in particle transport are due to the interplay of ITG and TEM turbulence. In all cases, improved measurement of core fluctuations will be critical for comparison with theory and simulations. It has already been demonstrated that the C-Mod PCI diagnostic is capable of unambiguously determining the direction of propagation of fluctuations in the plasma frame.

Impurity transport is an important issue in itself and provides, through the study of multiple transport channels, important constraints on theoretical predictions. A key question to be addressed is the relation between energy, particle, impurity and momentum transport and their connection to underlying turbulence. To carry out these studies a new impurity injection system is under construction. This approach uses the laser blow-off technique [3.36] in which small, non-perturbing quantities of non-intrinsic, non-recycling impurities are injected at precisely determined times during a discharge. The new system will use a modern, multi-pulse YAG laser, which will allow multiple injections into a single plasma, allowing direct comparison of different confinement regimes. The injected impurities will be observed with UV and x-ray spectrometers already in place. The aim is to provide a robust and reliable tool which will allow routine analysis of

impurity transport. One set of experiments planned will investigate the strength of neoclassical impurity pinching compared to anomalous diffusion. This is particularly important in cases where the background density profile is peaked. Varying the Z of the injected impurity should allow for rigorous tests of these effects. As in the case with background particle transport, observed differences between L-mode and various H-mode regimes will also be studied and compared with gyrokinetic simulations which should be capable of calculating impurity transport.

In reactors, with their strongly coupled electrons and ions, energy will be transported through whichever channel has the poorer confinement, thus both channels must be taken into account. Ion-scale turbulence, though dominant in some regimes, apparently cannot explain all the transport phenomenology which has been observed experimentally - hence the need for better understanding of the electron channel. For example, regimes have been produced in which ion-energy and particle transport have been reduced to neoclassical levels but where no change was seen in the electron thermal confinement [3.37-39], a clear sign of independent dynamics for electron transport. The relative scarcity of electron thermal barriers has been attributed to the difficulty of affecting shorter wavelength turbulence (on scales from c/ω_{pe} to ρ_e) by sheared $E \times B$ flows, however this has not been verified. The difference in global confinement scaling for electron transport dominated regimes, namely $\tau_E \sim n^1$ and ion dominated regimes with $\tau_E \sim I_p n^0$ is suggestive of a distinct mechanism as well. Currently, there are relatively little data on which mechanisms are responsible for electron transport. Discussions with the NSTX and DIII-D teams on joint experiments to be carried out in this area are ongoing.

The experiments, described above, aimed at understanding electron transport in the linear Ohmic regime will be extended to include fluctuations measurements of the full k range accessible by the PCI diagnostic. By exploiting the change in total field angle as the probe beam traverses the plasma to provide spatial localization for what is ordinarily a line-averaged measurement, it will be possible to observe both radial and poloidal components of the short-scale high frequency fluctuations that may be associated with electron transport. This may help to resolve a critical theoretical issue - while electron gyro-radius scale modes are expected to be unstable, they are ordinarily incapable of causing much transport. In order to be effective, the turbulence must develop extended radial structures (streamers) or inverse cascade to larger spatial scales [3.40]. Hence simultaneous measurement of k_r and k_θ spectra is important. Improved profile measurements, particularly for the current profile, ion temperature and velocity will allow more direct comparison with simulations. There are plans to document changes in R/L_{Ti} and R/L_{Te} with an ohmic density scan, and correlate these with density fluctuation amplitude changes. Other experiments will measure how R/L_{Ti} changes with magnetic shear via q scans and by using LHCD to modify the q profile. LH heating will allow extension of these studies to cases with strong auxiliary electron heating in plasmas with decoupled ions and electrons. In all cases, quantitative comparison with emerging models for electron heat transport will be stressed.

Alternate theories for electron transport involve generation of medium scale fluctuations through MHD-like mechanisms - for example by micro-tearing modes or through larger

scale magnetic turbulence. It may be possible to observe such modes in the plasma edge by the use of fast scanning probes with magnetic pick-up coils or in the core via polarimetry.

3.2.3 Proposed Research: Self-Generated Rotation and Momentum Transport

Near term research will be well aligned with the FES Joule Milestone on rotation.

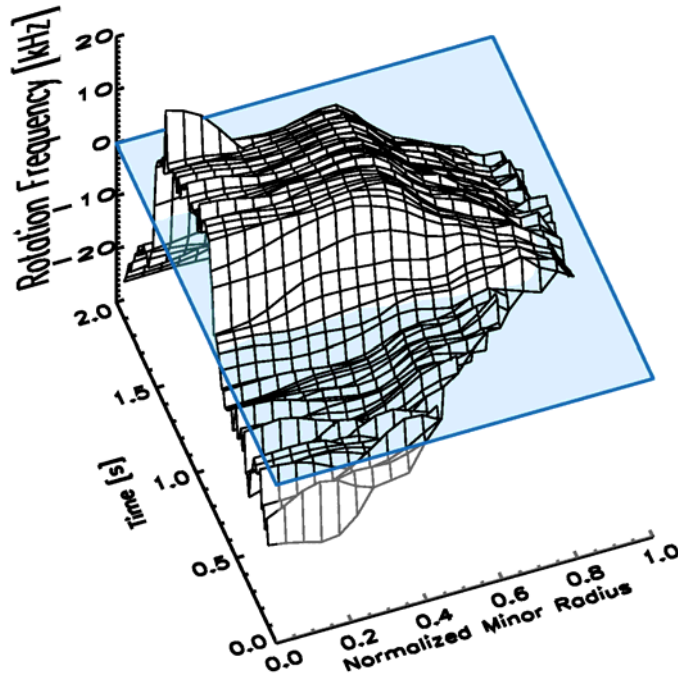


Fig 3.8 Velocity profiles taken with the new high-resolution x-ray spectrometer.

The bulk of the research in the area of core rotation during the next 5 year period will rely on results from the new imaging x-ray spectrometer system [3.41]. This consists of two spherically bent crystals and four 2-D x-ray arrays, which allows for full profile coverage (~ 1 cm spatial resolution) with good (~ 2 ms) time resolution. An example of a preliminary rotation velocity profile temporal evolution is shown in Fig.3.8. For momentum transport studies, the ultimate goal is to characterize the full momentum diffusivity, momentum pinch and/or residual stress profiles under a wide range of operating conditions and to compare these results with recent theoretical predictions. Potential

sources of momentum modulation will be the transition to H-mode and fast changes in SSEP, which have their origins at the plasma edge (Fig.3.9), and the use of A coils for inducing locked modes. This should allow determination of momentum transport coefficients over a wide parameter range, and a detailed comparison with energy, particle and impurity transport.

The new spectrometer system will also provide much more detailed information on the nature/mechanism(s) of spontaneous rotation. Together with results from the CXRS system, the complete E_r profile evolution will be investigated. Scaling studies of intrinsic rotation in H-mode will continue towards higher β_N so that extrapolation to ITER is a smaller step than what is shown in Fig. 3.5. Also of interest to ITER is the possibility of rotation velocity profile control, so variation of profile shapes in ICRF heated plasmas will be documented. Recent results have shown that application of LHCD power causes counter-current rotation, in contrast to co-current rotation with ICRF, providing a potential method for velocity shear profile control. Rotation studies with different LHCD

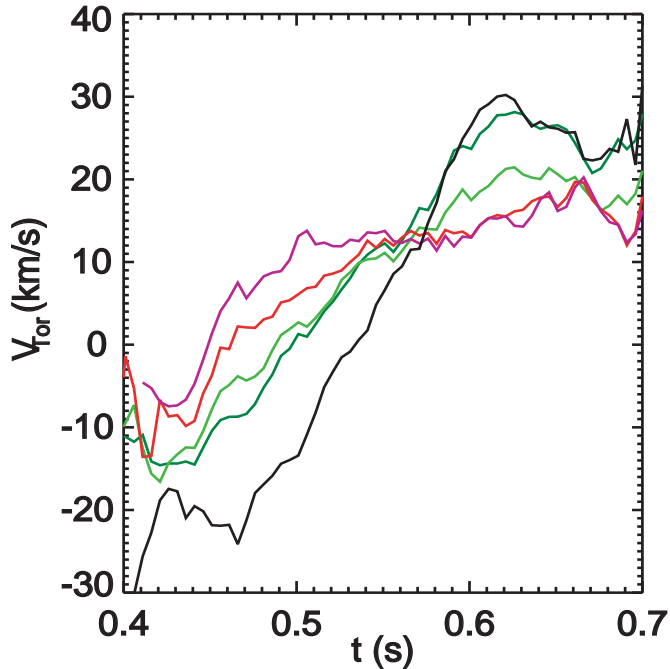


Fig 3.9 The time histories of the rotation velocity at different radial locations, with colored lines from the outer regions and black in the core. The co-current rotation clearly propagates in from the edge.

Bernstein waves [3.42], but little experimental evidence. Because of the limited spatial coverage available on C-Mod in the past, and the sensitivity of the mode conversion layer to the precise mix of ion species, it was not possible to guarantee a measurement at the appropriate point in the plasma. The improved core rotation diagnostic will also enable a more definitive study of ICRF rotation drive.

3.2.4 Proposed Research: Internal Transport Barriers

ITB onset conditions: The present understanding of internal transport barrier formation in Alcator C-Mod is that moving the ICRF resonance off axis slightly broadens the temperature profiles increasing the size of the core region stable to ion temperature gradient driven modes. Gyrokinetic stability simulations show that the fluctuation driven particle flux is reduced to below the level of that caused by the neoclassical pinch allowing the core density to rise. New diagnostic capabilities will allow enhanced study of these onset conditions. In particular, the new spatially resolved x-ray crystal spectrometer measurements of the ion temperature profiles will allow direct verification that the ion temperature gradient is reduced at the ITB onset. At the same time, detailed rotation measurements will be obtained so that the role of flow shear and radial electric field in the C-Mod ITB formation can be determined. gs2 simulations project that the shear is not sufficient in these plasmas to stabilize the drift wave instabilities, but direct

phasing will be performed. Preliminary results of rotation velocity profile modulation with sawtooth oscillations, a topic which has had very little research, show very fast evolution. These findings will be pursued. Also of interest is the rotation velocity profile evolution during mode locking, which will be made possible through use of the A coils. In conjunction with the H-mode intrinsic rotation studies will be investigations of the rotation in L-mode, which is considerably more complicated. This will also provide important information on the underlying mechanism(s) which drives rotation in the absence of external momentum input.

There are theoretical predictions of significant drive by mode-converted ion-cyclotron or ion-

measurement of the rotational shear will confirm or reject this hypothesis. Additionally, neutral beam diagnostics will complement the x-ray crystal measurements and also provide motional stark effect measurements of the q profile. This will allow examination of the role of the magnetic shear in ITB onset. Since the ITBs form spontaneously in Ohmic plasmas as well as with off-axis ICRF heating, understanding the role of temperature gradients, magnetic and flow shear in the barrier onset will further illuminate this process. Simulations will be carried to determine if the previous observations of hysteresis in the ITB transitions can be recovered from ITG/TEM modeling.

Impurity Transport in ITBs: In addition to ion temperature and rotation profiles from the diagnostic neutral beam experiment, the measured density profile of a fully stripped impurity (B+5) can be obtained. This can be used to estimate diffusion relative to pinch (D/v) in the transport. Initial measurements were made for ICRF ITBs during the last campaign. This work will continue to examine the transport during the onset and lifetime of the ITBs for both Ohmic and off-axis heated ITBs, and will be used to study correlations with flow shear and fluctuation levels. The new impurity injection system will also be used in conjunction with x-ray and UV diagnostics to study particle transport in ITBs.

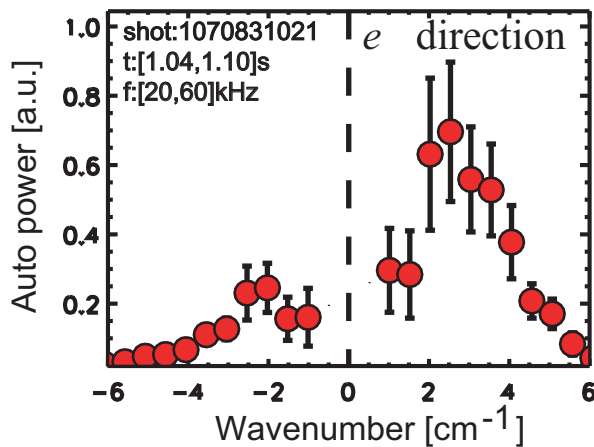


Figure 3.10
Fluctuation measurements obtained from Phase Contrast Imaging that arise during the ITB phase of the plasma in the 20 kHz region have been demonstrated to propagate in the electron diamagnetic direction.

Fluctuation Measurements: The phase contrast imaging (PCI) diagnostic on Alcator C-Mod has been upgraded with the ability to partially mask the phase plate to provide localization of the measured fluctuations. Recently, this allowed determination that a particular fluctuation which grows in intensity as the density rises during the ITB development propagates in the electron diamagnetic direction (Fig 3.10). This is consistent with predictions for the development of trapped electron modes near the ITB foot. Further study of these fluctuations during off-axis ICRF generated ITB plasmas when central ICRF is added in order to halt the density and impurity accumulation is crucial to confirming the theoretical understanding of ITB control. Study of these fluctuations during Ohmic H-mode ITBs will also be important to understanding the ITB physics. The availability of higher frequency reflectometry channels will allow study of the stability of the ITB foot region, especially during low density ITB production.

Heat pulse propagation: An issue that remains to be resolved and requires further study is the apparent discrepancy between steady-state power balance transport analysis which shows a broad region of reduced thermal diffusivity ranging from the axis to $r/a \sim 0.4$ and results of heat-pulse propagation experiments which show a very narrow region of improved transport located near the barrier foot. The resolution may lie in the magnitude of the temperature gradient relative to the nonlinear critical gradient. The barrier foot may represent a region where instabilities have been completely suppressed and both average and incremental diffusivities are low. The core region may be in a region of instability, just above the critical gradient and have high incremental and low average diffusivity. Increasing the number of channels in the soft x-ray measurements in the barrier foot region and taking advantage of high resolution electron cyclotron emission measurements during the ITB phase of the plasma will facilitate resolution and understanding of this issue.

Lower hybrid current drive and advanced scenarios: Lower hybrid current drive provides an opportunity to explore several key issues in the physics of low density ITBs on C-Mod. Since the density peaking is believed to be due to the neoclassical Ware pinch, reducing or eliminating the loop voltage through current drive should allow production of a thermal barrier without the level of impurity accumulation that currently leads to radiative collapse and the termination of the ITB. It will also allow confirmation of results obtained in the gyrokinetic simulations. Various experiments are also planned to investigate effects of heating and current profile on the barrier foot location. Reversed shear ITB formation which has not been possible in the past on C-Mod will now be accessible and modification of the current profile with LHCD may allow the creation of an electron thermal barrier. Experiments to maximize the bootstrap fraction of the plasma have been proposed for low current ITB plasmas, both with and without LHCD. TSC simulation shows significant enhancement of the bootstrap current in H+ITB plasmas over H-mode alone. (See figure 9.7 in Integrated Scenarios: Advanced Regimes, chapter 9.)

3.2.5 Diagnostic Plans Relevant to Transport Research

Improvements in diagnostic coverage are a key element of the transport program. A number of upgrades are planned for measurements of plasma fluctuations. The reflectometry systems will be extended to higher frequencies, allowing measurement at higher density, typically farther into the plasma (available 2009 with proposal budget). This diagnostic will also be configured to measure spatial correlations. A Doppler reflectometry system is planned (available 2009). This diagnostic works by introducing a small tilt angle of the beam with respect to the normal to the cut-off layer, allowing the velocity of perturbations to be directly obtained. Applications include measurement of the radial electric shear and zonal flows. An FIR polarimetry system may provide measurements of magnetic field fluctuations in addition to current profiles, density profiles and density gradients (available 2009). With incremental funding, a CO₂ scattering diagnostic is also under consideration (available 2010 on proposal budget). Other upgrades in profile coverage include improvements in resolution ECE for beam diagnostics, measuring T_i , V_i and n_i and a better view for the heterodyne ECE system

which will improve spatial resolution for the T_e profile (available 2012). Further details on these systems can be found in the facilities write-up, chapter 11.

3.2.6 Summary of Transport Work for ITER/ITPA (Pedestal covered in chapter 7)

Description	JOINT Experiments	Notes on C-Mod Contributions
Confinement scaling, ν^* scans at fixed n/n_G	CDB-4	Initial experiments performed, higher β operation required
ρ^* scaling along ITER relevant path at both low and high β	CDB-8	Will require further development of low density H-modes at high current.
Density profiles at low collisionality	CDB-9	Initial data sets provided, parameter extension required
Impurity transport in peaked density H-modes	Under discussion	Joint experiments under discussion by working group
Scaling of spontaneous rotation with no momentum input	TP-6.1	Exploit improved profile measurements

The C-Mod transport program will also address the following “high-priority research topics identified by the ITPA.

- Utilize upgraded machine capabilities to obtain and test understanding of improved core transport regimes with reactor relevant conditions, specifically electron heating, T_e - T_i and low momentum input, and provide extrapolation methodology
- Develop and demonstrate turbulence stabilization mechanisms compatible with reactor conditions, e.g. magnetic shear stabilization, shear flow generation, q-profile. Compare these mechanisms to theory.
- Study and characterize rotation sources, transport mechanisms and effects on confinement and barrier formation
- Quantitative tests of fundamental features of turbulent transport theory via comparisons to measurements of turbulence characteristics, code-to-code comparisons and comparisons to transport scalings
- Understand the collisionality dependence of density peaking

3.2.7 Support for Fusion Long-Term Goals

C-Mod transport research supports the OFES long-term goal of “progress toward developing a predictive capability for key aspects of burning plasmas using advances in theory and simulation benchmarked against a comprehensive experimental database of stability, transport, wave-particle interaction, and edge effects”. This work will also contribute toward filling the FESAC planning panel reports Gap 1 “Sufficient understanding of all areas of the underlying plasmas physics to predict the performance

and optimize the design and operation of future devices.” The report identified turbulent transport as a particular challenge.

3.2.8 Transport Research Objectives

Research Goal	Intermediate Objectives
Improved understanding of self-generated rotation and momentum transport and extrapolation to future devices with low input torque	Role of electron heating and current drive in modifying self-generated rotation profiles
	Compare measured self-generated flows, and cross-field fluxes with emerging theories and models
	Compare fluctuation levels, spectra and correlations with emerging models
	Test feasibility of IC and IBW flow drive
Detailed comparisons of models with experimental measurements of particle transport	Compare profiles, fluxes, fluctuation levels and correlations with existing gyrokinetic simulation codes
	Study of particle transport in regimes without neoclassical pinch
	Quantitative assessment of the role of magnetic shear in setting density profiles
	Correlation of particle transport and ion thermal transport in a variety of confinement regimes
Better Understanding of electron transport in decoupled regimes	Identify the portion of k space important for anomalous electron heat transport in low density OH plasmas
	Extend studies to strongly heated (LHH) plasmas at low densities
	Test models for mixed scale (ion-electron) turbulence
Characterize anomalous and neoclassical impurity transport.	Install impurity injection system and begin experiments
	Characterize impurity fluxes and their correlation with particle, energy and momentum transport in a variety of confinement regimes.
	Compare anomalous and neoclassical impurity fluxes
	Scaling of impurity fluxes with Z of impurity
Better understanding of access conditions, transition dynamics and control of internal transport barriers	Validate modeling predictions for role of ion temperature gradient in ITB onset
	Test predictions for nature of density fluctuations during ITB, especially after addition of central ICRF
	Assess roles of magnetic and flow shear in C-Mod ITB
	Measure ITB transport behavior with respect to impurity diffusion and electron heat pulse propagation
Detailed comparisons of ion thermal transport with gyrokinetic models	Quantitative assessment of the role of magnetic shear in setting critical temperature gradients
	Comparison with particle and momentum transport channels

3.2.9 Approach and Required Tools for Proposed Transport Research

Objective/Goal	Approach	Key New Diagnostics/Facilities	Modeling Codes
Validation experiment: Role of magnetic shear in drift wave turbulence and transport	Modify magnetic shear with LHCD, compare simulations to Te, Ti, ne profiles and fluctuation amplitudes, spectra and correlations	P _{LHCD} ~2-3 MW, MSE/Polarimetry measurements of q profile; HIREX and CXRS measurements of Ti and velocity profiles,	GS2, GYRO
Validation experiment: electron transport in low-density, electron dominated regimes	Measure k spectrum for low-density Ohmic plasmas in neo-Alcator regime. Follow up with experiments at low density with LHH	Thomson Scattering, PCI, HIREX, CXRS, MSE/Polarimetry, LH systems	GS2, GYRO
Understand origin of self-generated flows and momentum transport	Compare time evolving rotation profiles and cross-field fluxes with emerging theories. Use topology shift (USN-LSN), magnetic braking, H-mode transitions and LHCD as perturbations	HIREX, CXRS	GYRO + emerging theories (TEP for example)
Test feasibility of IC and IBW flow drive with mode converted ICRF	Measure modification in rotation profile during strong ICRF heating in Mode-Conversion scenario.	HIREX, CXRS	TORIC, AORSA
Look for correlations of momentum, particle and energy transport	Compare cross-field fluxes and gradients for all three quantities.	HIREX, Polarimeter/interferometer, MSE, impurity blow-off system.	GS2, GYRO

Objective/Goal	Approach	Key New Diagnostics/Facilities	Modeling Codes
Test models of particle transport	Compare density profiles, fluxes, fluctuation levels and correlations with gyrokinetic simulation codes. Include perturbations from gas puffing, pellet injection and regime transition	Polarimeter/Interferometer	GS2, GYRO
Make quantitative assessment of the role of magnetic shear in setting density profiles	Use LHCD to control shear at constant current and constant q95.	LHCD > 2 MW, MSE/Polarimeter	GS2, GYRO
Study of particle and impurity transport in regimes without neoclassical pinch	Use LHCD to replace all Ohmically driven current.	LHCD > 2 MW, impurity injector	GS2, GYRO
Characterize impurity fluxes and their correlation with particle, energy and momentum transport in a variety of confinement	Install impurity injection system and compare anomalous and neoclassical impurity fluxes	Impurity Injector	GS2, GYRO
Scaling of impurity fluxes with Z of impurity	Inject elements with a wide range in Z	Impurity Injector	

Objective/Goal	Approach	Key New Diagnostics/Facilities	Modeling Codes
Identify the portion of k space important for anomalous electron heat transport in low density electron transport	PCI measurements up to $k \sim 55 \text{ cm}^{-1}$ with spatial localization. Begin with low-density OH plasmas then extend to strongly heated (LHH) discharges	PCI, Polarimeter (B fluctuations), LH	GS2, GYRO
Validate modeling predictions for role of ion temperature gradient, magnetic and flow shear in ITB onset	Measure profile gradients including magnetic and flow shear at transition point. Compare with gk simulations.	HIREX, CXRES, MSE/Polarimetry	GS2, GYRO
Test predictions for nature of transport control during ITB, after addition of central ICRF	Measure density fluctuations with PCI and reflectometry in developed ITB discharges	PCI, Reflectometry	GS2, GYRO
Measure local transport in ITBs with respect to impurity diffusion and electron heat pulse propagation	Measure transient propagation of heat, particles and impurities using laser blow-off and sawtooth perturbations.	Impurity injector, Polarimeter/interferometer	

3.2.10 Transport Research Schedule

	2008	2009	2010	2011	2012	2013
Self-Generated Rotation and Momentum Transport						
	Role of electron heating and current drive – modify self flows					
	Compare flow profiles and cross-field fluxes with theory and models Compare fluctuations with theory and models Test RF Flow Drive Scenarios Exploit if successful					
Particle Transport						
	Correlation of particle and ion thermal transport in variety of regimes					
	Compare profiles, fluxes, fluctuations with gk codes Study of particle transport in regimes without neoclassical pinch Quantitative assessment of role of magnetic shear					
Impurity Transport						
	Install impurity injection system Scaling of impurity fluxes with Z					
	Compare anomalous and neoclassical fluxes Correlate impurity fluxes with particle, energy and momentum					
Ion Transport						
	Comparison with particle and momentum transport Origin and role of zonal/GAM flows Assessment of role of magnetic shear using LHCD					
Electron Transport						
	Identify portion of k space responsible for electron transport in low density plasmas					
	Extend studies to LHH regimes Test models for mixed scale (electron, ion) turbulence					
Internal Transport Barriers						
	Validate gk models for role of LTI in ITB onset					
	Transients : Impurity transport, Heat Pulse Propagation Studies Bifurcation dynamics Assess role of magnetic shear in barrier onset, transport and position Comparison of fluctuations and fluxes with gyro kinetic models					
	2008	2009	2010	2011	2012	2013

3.3. References

- [3.1] P. Terry, M. Greenwald, J-N. Leboeuf, et al., “Validation in Fusion Research: Towards Guidelines and Best Practices”, to be submitted to Physics of Plasmas.
- [3.2] N. Basse, et al., Phys. Plasmas **12**, 052512, 2005.
- [3.3] D. R. Ernst, N. P. Basse, W. Dorland, C. L. Fiore, L. Lin, A. Long, E. S. Marmor, M. Porkolab, and K. Zhurovich, “Observation of trapped electron mode turbulence in tokamak plasmas through direct comparison of nonlinear gyrokinetic simulations with density fluctuation measurements,” submitted to Physical Review Letters Nov. 16, 2007.
- [3.4] K. Zhurovich, C.L. Fiore, D.R. Ernst, et al., Nucl. Fusion **47** (9) (September 2007) 1220-1231.
- [3.5] M. Redi, W. Dorland, C. Fiore, et al, Phys. Plasmas, **12**, 072519, 2005.
- [3.6] D. Mikkelsen, W. Dorland, The role of kinetic electron effects in gyrokinetic turbulence simulations at high and low collisionality, Bulletin of the American Physical Soc. 47th annual DPP meeting, Vol. **50**, No. 9, pg 198, 2005
- [3.7] C. Angioni, A.G. Peeters, G. V. Pereverzev, F. Ryter, G. Tardini and ASDEX-Upgrade Team, Phys. Rev. Lett. **90**, 205003 (2003).
- [3.8] H. Weisen, A. Zabolotsky, C. Angioni et al, Nucl. Fusion **45**, L1 (2005).
- [3.9] C. Angioni, H. Weisen, O.J.W.F. Kardaun, Nucl. Fusion **47**, 1326, 2007.
- [3.10] M. Greenwald, J.L. Terry, S.M. Wolfe, S. Ejima, M.G. Bell, S.M. Kaye, G.H. Neilsen, Nucl. Fusion **28** 2199 (1988)
- [3.11] M. Greenwald, C. Angioni, J.W. Hughes, et al, Nucl. Fusion **47**, L26, (2007).
- [3.12] M. Greenwald, et al., Fusion Sci. and Tech. **51**, 266, (2007)
- [3.13] C. Fiore, et al., Phys. Plasmas **8**, 2023 (2001)
- [3.14] A. Dimits, et al., Phys. Plasmas **7**, 969, 2000
- [3.15] D. Mikkelsen et al., “Nonlinear simulations of Drift-wave turbulence in Alcator C-Mod”, proceedings of 19th IAEA Conference on Fusion Energy, Lyon, 2002.
- [3.16] M. Redi, W. Tang, D. Owens, M. Greenwald, O. Gruber, M. Kaufmann, Fusion Technology **18**, p 223, 1980
- [3.17] C. Rettig et al., PPCF, **43**, 1273, 2001.

- [3.18] J.E.Rice et al., Fusion Sci. Technol. **51** (2007) 288.
- [3.19] J.E.Rice et al., Phys. Plasmas **11** (2004) 2427.
- [3.20] J.E.Rice et al., Nucl. Fusion **45** (2005) 251.
- [3.21] B.LaBombard et al., Nucl. Fusion **44** (2004) 1047.
- [3.22] W.D.Lee et al., Phys. Rev. Lett. **91** (2003) 205003.
- [3.23] J.E.Rice et al., Nucl. Fusion **44** (2004) 379.
- [3.24] J.E. Rice et al., Fusion Science and Technology, **51** 357, 2007
- [3.25] J.E.Rice et al., Nucl. Fusion **47** (2007) 1618.
- [3.26] C. L. Fiore et al, Plasma Phys. Control. Fusion **46** B281, 2004
- [3.27] C. Fiore et al., Phys. Plasmas, 11, 2480, 2004.
- [3.28] D. R. Ernst et al., proc. 21st Int'l. Atomic Energy Agency Fusion Energy Conference, Chengdu, China, 16-21 October 2006, paper IAEA-CN-149/TH/1-3. Available as <http://www-naweb.iaea.org/napc/physics/FEC/FEC2006/html/node43.htm#12707>.
- [3.29] C. L. Fiore, et al., 2007 Fusion Science and Technology, **51** 303
- [3.30] N. Basse, et al., Fusion Science And Technology **51**, 476, 2007
- [3.31] R. Bravenec, W. Nevins, RSI **77**, 015101, 2006.
- [3.32] D. Mikkelsen, M. Greenwald, J. Candy and R. Waltz, "Collisionality dependence of density peaking in H-mode plasmas in Alcator C-Mod", Bulletin of the American Physical Soc. 49th annual DPP meeting, Vol. **52**, No. 11, pg 212, 2007
- [3.33] Miskane F. and Garbet X., Phys. Plasmas 7, 4197, 2000.
- [3.34] Yankov V. V., Plasma Phys. Rep., **21** (1995) 719.
- [3.35] Baker D. R. and Rosenbluth M. N., Phys. Plasmas, **5** (1998) 2936
- [3.36] E. Marmor, J. Cecchi, S. Cohen, Rev. Sci. Instruments, **46**, 1149, 1975.
- [3.37] M. Greenwald, et al., PRL, **53**, 352, 1984.

- [3.38] S. Wolfe, M. Greenwald, R. Gandy, et al., Nucl. Fusion, **26**, 329, 1986.
- [3.39] E. Synakowski, PPCF, **40**, 581, 1998.
- [3.40] F. Jenko, et al., Phys. Plasmas. **7** 1904, 2000
- [3.41] M. Bitter, K. W. Hill, S. Scott, S. Paul, A. Ince-Cushman, M. Reinke, J. E. Rice, P. Beiersdorfer, M. F. Gu, S. G. Lee, Ch. Broennimann, and E. F. Eikenberry, "Passive Spectroscopy: Bolometers, Grating and X-ray Imaging Crystal Spectrometers", Proceedings of the International Workshop on Burning Plasma Diagnostics, Varenna, Italy, Sept., 2007
- [3.42] E.F. Jaeger et al., Phys. Rev. Lett., **90**, 195001, 2003.

4 Plasma Boundary

4.1 Highlights of Recent Research

Highlights of C-Mod's plasma boundary research are organized below under four topics: edge/SOL transport, operation with high-Z metal wall and boronization, hydrogenic retention, and divertor physics.

4.1.1 Edge Transport

4.1.1.1 Time-averaged Transport and Flows

Over the past five years, research on edge transport in Alcator C-Mod has continued to produce cutting-edge results in a number of areas. Some highlights include: (1) evidence that electromagnetic turbulence sets the observed pressure gradients near the last-closed flux surface, (2) identification of radial transport-driven edge plasma flows arising from ballooning-like transport asymmetries, which impact the toroidal rotation of the confined plasma and potentially explain the x-point dependence of the L-H power threshold, (3) unprecedented detailed information on turbulent structures in the scrape-off layer, using a unique set of gas-puff turbulence imaging systems, (4) an enlightening dimensionless scaling study of cross-field particle convection in the far scrape-off layers of DIII-D, C-Mod and JET.

Due in large part to C-Mod's prior contributions, it is now well established that the scrape-off layer (SOL) exhibits different transport physics in the regions 'near' and 'far' from the separatrix [1]. Moreover, recent experiments have uncovered evidence that pressure gradients near the separatrix are set by electromagnetic plasma turbulence both in L- and H-mode discharges [2,3]. Local pressure gradients, normalized by the poloidal magnetic field strength squared (i.e., α_{MHD}) are invariant in plasmas with the same normalized collisionality despite having vastly different currents and magnetic fields (Fig. 4.1.1). These data suggest that pressure gradients are clamped to a 'critical gradient' condition that is a function of local collisionality – a behavior that is broadly consistent with electromagnetic plasma turbulence simulations [4,5]. Pressure gradients in the H-mode pedestal are found to follow a similar scaling [6]. Thus, the near SOL forms the base of the H-mode pedestal and may play a key role in its formation and development. At higher collisionality (i.e. lower Λ , as defined in the figure), particle and heat transport across the separatrix increases dramatically despite a concomitant reduction in pressure gradients [7], rendering this 'phase-space' region inaccessible to experiment [2]. This behavior is consistent with a transport-defined tokamak density limit, as proposed by Rogers [5] and investigated recently in more

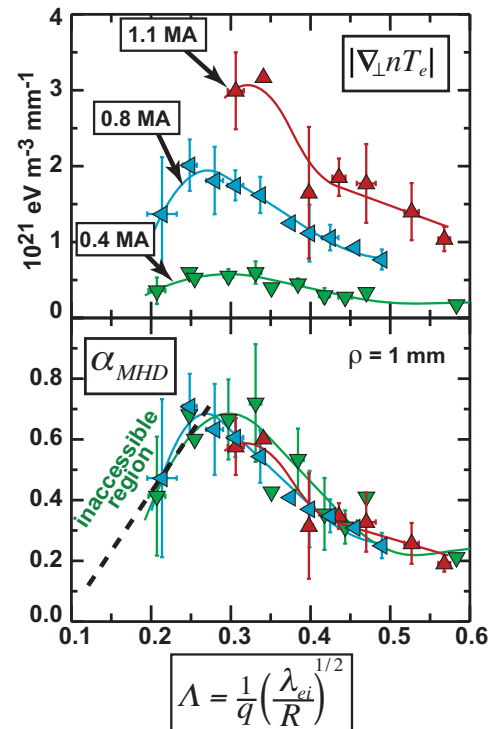


Fig. 4.1.1. Normalized pressure gradients, α_{MHD} , at a location 1 mm outside the separatrix versus inverse collisionality parameter, Λ .

theoretical detail by Guzdar [8].

Related experiments in C-Mod have revealed a rich interplay among anomalous cross-field transport, strong plasma flow along magnetic field lines in the SOL, magnetic topology and toroidal plasma rotation [9]. Near-sonic parallel plasma flows are observed in the high-field SOL, with their origins traced to a strong ballooning-like component of the cross-field transport on the low-field side. In magnetic topologies with $B \times \nabla B$ pointing toward the x-point (‘favorable $B \times \nabla B$ ’), such flows circulate the SOL in a helical pattern that projects toward the co-current direction (see Fig. 4.1.2). The confined plasma responds to this ‘flow boundary condition’ at the separatrix, acquiring a corresponding co- or counter-current increment to its intrinsic rotation, for $B \times \nabla B$ toward and away from the x-point, respectively. Moreover, the research suggests that this topology-dependent flow boundary condition may help explain the x-point dependence of the L-H power threshold observed in tokamaks [10]: in a set of otherwise

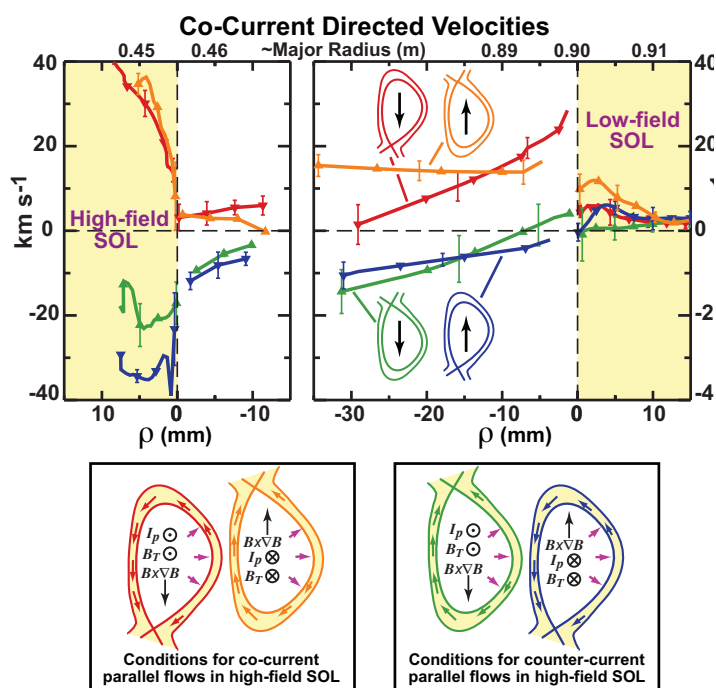


Fig. 4.1.2. Plasma flow profiles in ohmic L-mode plasmas from Langmuir-Mach probes (parallel flow velocities in the high- and low-field SOL regions) and CXRS diagnostics (toroidal velocities of B^{+5} on the low-field side and parallel velocities of D^+ on the high-field side, both inside the separatrix). Positive velocities indicate flow towards the co-current direction. The direction of transport-driven near-sonic parallel flows in the high-field SOL are seen to depend on x-point location; the confined plasma responds by rotating toroidally, at a velocity that is smaller than the toroidal projection of the parallel flows seen in the high-field SOL.

similar discharges, the L-H transition is seen to coincide with co-current plasma rotation achieving roughly the same value in both upper and lower-null topologies. However, with unfavorable $B \times \nabla B$, the flow boundary condition impedes co-current plasma rotation. Correspondingly, higher input power (which in itself tends to spin the plasma in the co-current direction through an increase in stored plasma energy [11]) is necessary to attain H-mode in this topology. Most recently, a similar connection has been observed among SOL flows, magnetic topology and pressure gradients in L-mode discharges [3]: Normalized pressure gradients near the separatrix (α_{MHD}) are systematically higher for favorable $B \times \nabla B$, i.e., when the resulting SOL flows ‘spin-up’ the confined plasma in the co-current direction. These data further support the notion that transport-driven edge flows influence plasma turbulence (presumably via flow shear) and affect the resultant ‘critical pressure gradients’ near the last-closed flux surface.

4.1.1.2 Research into the Underlying Edge/SOL Turbulence

The time-averaged characteristics of the perpendicular convective transport in the edge/SOL cannot at the present time be determined from a first-principles physics model. This is primarily because those characteristics are set by the properties of plasma turbulence. Research on C-Mod has made significant contributions to the study of the turbulence in this region. One of the goals of this research is to guide and verify first-principles models that have predictive capability. Some of the results of the last five years are reported here.

Experiments to image the turbulent structures and their dynamics have relied primarily upon “Gas-Puff-Imaging” (GPI) in D_α and He line emission [1]. This technique relies on the fact that the imagable emission fluctuations result from local fluctuations in density and temperature. The imaging showed that the turbulent structures were filamentary, aligned with the local field and with $k_{\parallel} \ll k_{pol}$. Measurements of the cross-correlation between the (Langmuir-probe-measured) floating potential and the (GPI-measured) D_α emission from toroidally-separated points within the same flux tube yielded correlation amplitudes of $\sim 30\%$ [Grulke PoP 2006]. Additionally, the density fluctuations in the cross-field plane of the correlation patterns were monopole features (blobs) associated with and located at the center of dipole patterns of the electric potential fluctuations [12]. The spatial orientation of the potential dipole perturbations is such that the resulting electric field causes a radially outward oriented $E \times B$ drift of the density-fluctuation pattern, consistent with basic models for radial blob propagation (e.g. [13]).

Using GPI with fast-framing cameras and 2D detector arrays has yielded additional detailed information about the structure and dynamics of the turbulent blobs/filaments. Time-delay cross-correlation analysis of movie images is used to produce 2D maps of the phase velocities of the dominant turbulent structures [14], and measurements of the wavenumber and frequency spectra have yielded other details of the spatial structure of the poloidal phase and group velocities [15]. As shown in Fig. 4.1.3, the poloidal phase velocities inside the separatrix and in the far SOL are in opposite directions, while in the near-SOL region features are observed to move in both directions. These new observations are presently being investigated.

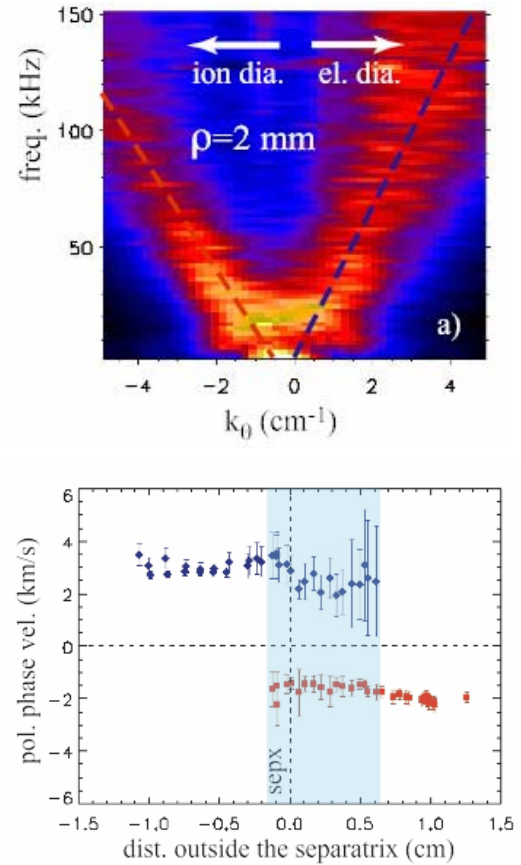


Fig. 4.1.3. (top) Time-averaged $(k_{\omega f})$ spectrum of the GPI emission from a view 2mm outside the separatrix. Two counter-propagating features are evident. (bottom) Time-averaged poloidal phase velocities of the turbulence, measured at the outboard midplane. The blue and points give the velocities of the features in the $(k_{\omega f})$ spectra that propagate in the electron and ion diamagnetic drift directions respectively. $V < 0$ is in the ion-diamagnetic drift direction.

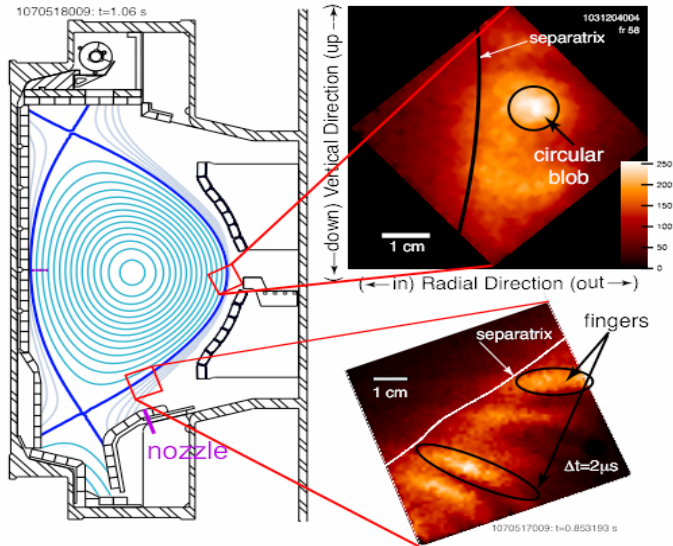


Fig. 4.1.4. 2D structure of the SOL turbulence at two poloidal locations. The filaments have circularly x-sections near the outboard miplane, but are elongated fingers in the high-shear region.

The poloidal variation of the SOL turbulence is also of great interest, especially because of its primary role in driving flows. We have shown that both the absolute and relative (density) fluctuation levels are much reduced at the inboard midplane compared with the outboard [9,16]. Recently we have studied the turbulence structure at a third poloidal location, i.e. in the high-shear region just outside the X-point of LSN plasmas. We find striking differences as compared to the outboard midplane region. While the filament cross-sections are approximately circular at the midplane (i.e. blobs), they are tilted, elongated fingers in the high-shear region. The viewing-geometry and two snapshot images illustrating

these different characteristics are shown in Fig. 4.1.4. Many of the observed structural aspects of the filaments in the high-shear region are approximately consistent with the shearing and flux expansion of circular flux tubes that are magnetically mapped from the midplane. The dynamical properties of the structures in the two regions indicate that they are related by electric potential perturbations extending along the local field. These observations are the first of their kind. The effects of shearing and flux expansion in the presence of the blobby, convective transport may have important consequences not only for the perpendicular, but also for the parallel transport.

One of the primary goals of studying turbulence in the C-Mod edge is to guide simulation models towards a predictive capability for the key time-averaged characteristics of the edge/SOL transport (Sect. 4.1.1.1) To date, experimental turbulence data from C-Mod has been compared

	Frequency spectrum	poloidal correlation length (cm)	radial correlation length (cm)	auto-correlation time (μ s)	$n_e^{\text{RMS}}/\langle n_e \rangle$ (%)
Experiment		1.3-2.1	0.9-1.6	12-20	20-30
GEM	similar to exp.	1.0	0.5-0.6	9	4-5

Table 4.1.1 Comparison of experimental turbulence characteristics with those from the simulation of the C-Mod SOL using the GEM code.

with simulations from a number of first-principles turbulence codes, e.g. NLET (3D non-linear fluid code) [16], ESEL (2D non-linear fluid code) [17], BOUT (3D non-linear fluid code with X-point), and GEM (3D non-linear gyrofluid code) [18]. An example of the comparison of C-Mod

experimental measurements in limiter plasmas with the GEM simulation is given in Table 4.1.1, where agreement is typically within about a factor of two.

In an effort to determine whether the convective nature of the C-Mod SOL was singular to C-Mod or more general to other tokamaks we organized collaborations with JET and DIII-D. L-mode discharges which were both dimensionlessly similar and dissimilar were obtained on all three tokamaks [19,20]. The profiles of n_e , T_e and ionization source were used to derive the radial ion flux as a function of radius in the SOL. This flux was interpreted as $n \cdot v_{\text{eff}}$. The convective velocity, v_{eff} , was strikingly independent of density on all three tokamaks (independent of v^*). The range in v_{eff} as a function of normalized radius is shown in Figure 4.1.5. Note that v_{eff} increases in radius in the far SOL reaching values of order 100m/s. These and further comparisons as a function of field imply that v_{eff} is independent of both β and ρ^* .

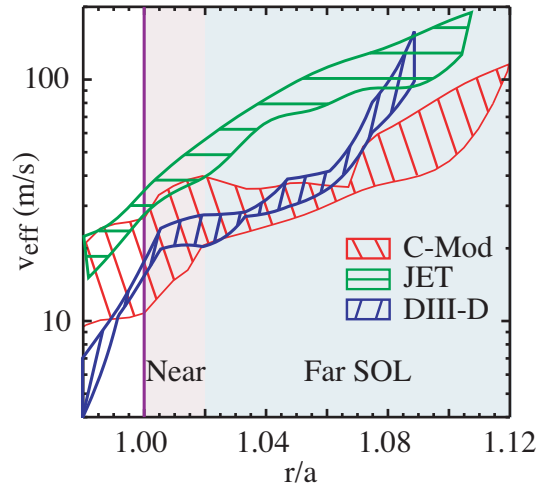


Fig. 4.1.5. Profiles of convection velocity vs normalized radius for C-Mod, JET and DIII-D.

As part of the same collaborative efforts, the radial ion flux reaching the main-plasma-chamber ‘wall’ was determined for both L- and H-mode plasmas in DIII-D [21,22]. The results indicate that time-averaged H-mode fluxes to the ‘wall’ tend to be lower than for L-mode by factors of 1-2. These results have been used to scale to ITER with the result predicting that wall flux densities in ITER will be similar to today’s experiments [23].

4.1.2 Boronization and High-Z Operation

While present-day tokamaks operate with boron-coated plasma facing components (PFCs) to achieve the best possible energy confinement such coatings will not make sense in ITER and reactors due to the long-pulses and high heat fluxes (erosion). C-Mod is particularly suited to study the absence of B coatings as the underlying PFCs are high-Z and so the compatibility with the core plasma is relevant to ITER and beyond. Boron coatings were removed prior to the 2005 run period [24,25] to provide a unique comparison of operation with or without boronized molybdenum PFCs. ICRF-heated H-modes were readily achieved without boron-coatings although the resultant enhancement in energy confinement was typically small ($H_{\text{ITER},89} \sim 1$). Molybdenum concentrations, n_{Mo}/n_e , rise rapidly up to 0.1% after the H-mode transition, cooling the plasma by line radiation, reducing confinement and/or causing a back H/L transition. After applying boron coatings, n_{Mo}/n_e was reduced by a factor of 10-20 with $H_{\text{ITER},89}$ approaching 2. Boronization also has a significant effect on the plasma startup phase lowering Z_{eff} , radiation, and lowering the runaway electron damage. The effects of each boronization are found to be limited in time, correlated to integrated ICRF input energy. Through the use of inter-discharge boronization and comparison of ICRF-heated and Ohmic H-modes [24-26] we demonstrated that the enhanced erosion of B, the Mo underneath, is due to acceleration of D and B ions in an ICRF-enhanced sheath potential. Experiments also showed that the erosion is localized, with

different locations linked to each antenna. This is consistent with previous measurements that found ICRF-enhanced sheath potentials, which appear only on flux tubes linked to the active antenna [27].

4.1.3 Fuel Retention

One of the advantages of high-Z metals for use in fusion reactors is believed to be their low retention of hydrogen (e.g. [28]). This laboratory-derived characteristic has not been verified in a tokamak. The retention and recovery of hydrogen (H) and deuterium (D) fuel in C-Mod has been studied [24,25,29]. C-Mod uniquely employs bulk high-Z molybdenum (Mo) as its plasma-facing armor material, with intermittent application of thin boron (B) films. The C-Mod wall materials are found to retain large fractions, ~20-40%, of the D₂ gas fuelled per shot, whether or not the Mo surfaces are bare or partially covered by B films. The retention appears to be linearly proportional to the ion flux to PFC surfaces, with ~1% D ions incident on the divertor surface being retained. There is no indication of the retention rate saturating over 15-20 s of plasma exposure. The retention is inconsistent with D in Mo retention from laboratory ion beam studies, which would predict rapid saturation of the fuel inventory in the wall after only a few seconds of exposure to C-Mod's plasma. The retention is also not consistent with co-deposition of the B since it occurs with cleaned Mo walls. Planned disruptions are exploited to recover H and D from the wall in C-Mod. The disruptions produce rapid heating of the wall surfaces, releasing the H/D from the wall for recovery by the pumps; a technique proposed for tritium recovery in ITER. It was shown that disruptions are effective for removing hydrogen absorbed into the wall during water exposure during vents. Overall control of the H/D wall inventory was demonstrated using frequent, planned disruptions, with the result that the C-Mod wall can be net depleted of fuel over a run day.

4.1.4 Divertor Physics

Much of C-Mod's research in period from 1995 to 2000 was focused on the physics of the divertor [30]. During that period important discoveries relating to power and particle-handling capabilities were made, e.g. divertor "detachment", different regimes of parallel transport, the influence of the geometry on detachment, and volume recombination. Recent important work has centered around C-Mod's capability to approach some of the conditions predicted for the ITER divertor. In particular, since it is believed that photon trapping will play an important role in determining the plasma conditions and pressure in divertors, research into the effects of radiation trapping of D₀ Lyman_α line radiation were benchmarked with data from the C-Mod divertor plasma [31]. This work was one of the US-assigned ITER tasks and as well as an ITPA task. In a related study the C-Mod divertor plasmas were modeled in the attempt to reproduce the

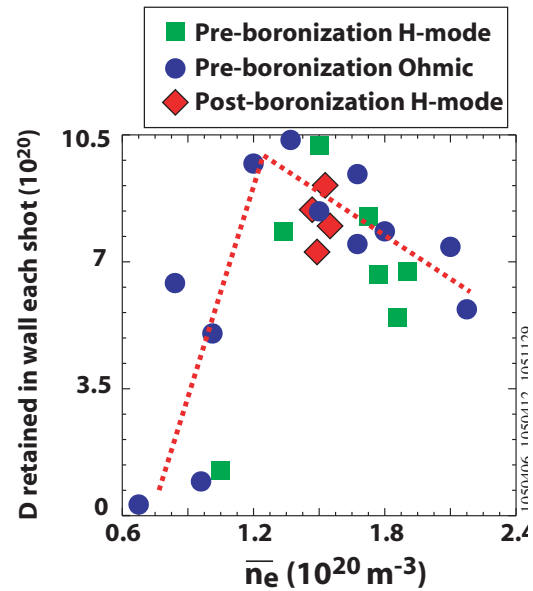


Fig. 4.1.3.1: Deuterium wall retention versus flattop line averaged density for varying levels of boron coverage & confinement mode. All discharges: $I_p=1$ MA, $B=5.4$ T.

measured neutral pressures over a range of densities. This proved to be surprisingly difficult, requiring inclusion of not only the effects of radiation trapping, but also neutral viscosity, elastic collisions between ions and neutral molecules, and modeling of the Private-Flux-Zone (PFZ – the region between the inner and outer divertor legs).

Other experimental work on C-Mod also showed the complexity of the PFZ. Under detached divertor conditions, significant plasma density was observed in the PFZ, inferred from the emission that resulted from volume recombination of the high density, cold plasma there [32]. The primary source of plasma for the PFZ was the ExB drift generated by the poloidal temperature gradient.

4.2 Proposed Research

4.2.1 Goals and Directions

The goal of the boundary physics program at C-Mod is to provide reliable physics-based descriptions of the coupled interactions between edge plasma, neutrals, and wall surfaces such that the overall performance of C-Mod and future reactors can be optimized: minimal core impurities (radiation, fuel dilution), maximal first-wall lifetime, minimal fuel retention, optimal divertor design for impurity/neutral compression and pumping. Progress can be measured according to the predictive capability that has been assembled; research goals are truly achieved when reactor-scalable, physics-based descriptions are identified and tested. As discussed in the previous sections, Alcator C-Mod has contributed substantially towards this goal over the past 5 years. However, further progress is clearly required in a number of science areas, particularly as Alcator C-Mod pushes forward with increased input power and discharge pulse length.

The following sections outline research plans in five key areas: *Edge plasma transport* (4.2.2) is aimed towards understanding the processes that determine the cross-field and along the field transport in the boundary region. This includes time-averaged profile and flux measurements as well as detailed spatial/temporal measurements of the underlying turbulence. *Plasma-surface interaction* (4.2.3) emphasizes the understanding of impurity source processes, in particular those generating molybdenum, and the screening of impurities from the core. *Divertor physics and fueling* (4.2.4) focuses on the processes that control the characteristics of the divertor including neutral (including He) transport, radiation transport, detachment physics, the role of divertor geometry and how the core plasma is fueled. *Plasma-facing materials* (4.2.6) focuses on the processes that control the hydrogenic fuel retention characteristics – specifically with high-Z materials, with the goal of developing an understanding of the level and control of the D/T reservoir in high-Z PFCs. We include a special section, *Demo-like divertor* (4.2.5), to describe plans in the boundary physics area that are specifically aimed at developing the high-Z divertor and boundary plasma conditions required for a reactor. This goal is coincident with support of reliable C-Mod operations needed for the advanced scenarios and burning plasma thrusts. Following the description of planned research in each of these areas, there is a table that summarizes in concise way the main *issues* to be addressed, the proposed *approach* for addressing them, the *diagnostics or facilities* to be used in addressing them, and the *modeling* that will be used in conjunction with the experimental effort. Closing out the description of our program are two sections; the first (4.2.7) details how the boundary research plans relate to the "priorities, gaps and opportunities" specified in the 2007 FESAC panel report; the second (4.2.7) prioritizes the areas in the boundary program and discusses their relation to an incremental budget.

From reading section 4.1 it is clear that the C-Mod program has made substantial contributions in a number of boundary physics areas. We will continue our strong emphasis on transport. In addition we will expand our efforts regarding understanding and controlling hydrogenic retention, the understanding of parallel transport from the upstream separatrix to the divertor, and the effect of the RF waves on the SOL and impurity generation.

In support of our expanded emphases we will be implementing several exciting new upgrades and capabilities:

- Demo-like divertor (4.2.5) with solid tungsten tiles, ambient temperature control, and minimal toroidal gaps, plus a new array of heat flux diagnostics (4.2.2.3)
- Implementation of several innovative diagnostics for analyzing plasma-facing surfaces both in-situ (4.2.3) and ex-situ (4.2.6).
- An expanded array of diagnostics for characterizing edge turbulence (4.2.2.2) and particle, momentum and heat transport (4.2.2.1, 4.2.2.3).
- New tools for optimizing boronization and wall conditioning (4.2.6) with toroidal magnetic field.

Plasma Boundary appendix (4.A) contains a timeline for upgrades and diagnostics related to power handling and the Demo-like divertor.

4.2.2 Edge Plasma Transport

As a result of the most recent C-Mod observations (section 4.1), a fundamental shift in our views of edge transport physics has occurred: transport in the near SOL in both L- and H-mode may be more appropriately described in terms of a critical gradient phenomena rather than a simple diffusive and/or convective transport paradigm, with electromagnetic turbulence setting the values of ‘critical pressure gradient’ there. These observations largely mimic the behavior of the H-mode pedestal and indicate that the near SOL may be viewed as an extension of the L- and H-mode pedestal onto the open field lines of the SOL. This behavior has important implications. First, it tells us that the power e-folding width of the near SOL may be inextricably tied to the width of the temperature pedestal – a key observation that impacts the scaling of SOL heat flux densities from present devices to ITER and power-producing reactors. Second, any first-principles physics model of the SOL must include both electromagnetic effects and also the detailed physics (which is not yet resolved) that self-consistently forms the steep ‘critical-gradient’ region near the last-closed flux surface – key elements that are not yet produced by first-principles numerical simulations. Finally, the transport physics in this region and its apparent sensitivity to plasma flows (Fig. 4.1.2) may hold the key towards understanding the local conditions required for an L-H transition.

Recognizing these developments, our transport research will concentrate on four principle thrusts during the next five years: (1) identify and understand the underlying transport physics of the near SOL region and its connections to the L and H-mode pedestals, (2) elucidate more fully the physics of the far SOL, e.g., the mechanisms that generate the observed intermittent ‘blobby’ transport and the key physical processes that will ultimately set the magnitude of main-chamber particle fluxes in future reactors, (3) explore transport physics in the divertor and x-point regions and how it connects to that in the ‘main chamber’ SOL, and (4) determine the physics and

scalings of the power e-folding width in the near SOL and how it maps to the heat flux ‘footprints’ at the divertor target.

In order to carry out these investigations, detailed, high resolution measurements of the time-averaged profiles (density, temperature, toroidal and poloidal flows, and cross-field transport fluxes) at a number of locations in the edge plasma are required. Equally important are high-resolution measurements of the turbulent eddy fields (spatial and spatial/temporal structure), also at multiple locations in the edge plasma. Finally, in order to study the physics that sets the heat fluxes to the divertor target, a fully instrumented divertor is required (Langmuir probes, calorimeter probes, surface temperature IR), combined with high-resolution divertor bolometry.

The planned complement of edge plasma transport diagnostics is shown in Figure 4.2.1, which builds upon C-Mod’s already extensive diagnostic set. Over the near term (2-3 years), we will fully exploit a number of recently installed diagnostics and tools, including: (1) upper divertor probe array and cryopump, (2) high-field edge, and low-field edge charge-exchange recombination spectroscopy (CXRS) views [33-35], which resolve toroidal and poloidal plasma flows, impurity and majority species ion temperatures, and impurity densities in the ‘pedestal’ region, (3) midplane, toroidally-viewing L_{α} array for SOL ionization profile measurements, (4) upgraded, high heat-flux handling scanning probes [36], including a ‘wall scanning probe’ on the high-field SOL for measuring SOL profiles and plasma flows both parallel and perpendicular to B , and (5) gas-puff turbulence imaging on both the outer midplane and near the lower x-point regions. In addition, we are planning new and/or improved diagnostics: (6) new divertor bolometry arrays and expanded L_{α} views (’09), (7) a Thomson scattering system for improved SOL profile measurements (SOLTS) (’11), (8) additional GPI turbulence imaging views (in the divertor and of one of the ICRF antennas) (’10), (9) expansion of the array of fiber-to-diode-based GPI views at the outer midplane to full 2-D (’10), and (10) a new diagnostic suite for the Demo-like Divertor, including embedded Langmuir probes, IR surface temperature and calorimeter sensors for detailed diagnosis of divertor plasma conditions including heat fluxes (’11) (see section 4.2.5).

Using this unique diagnostic set, we will explore edge transport phenomenology over a wide

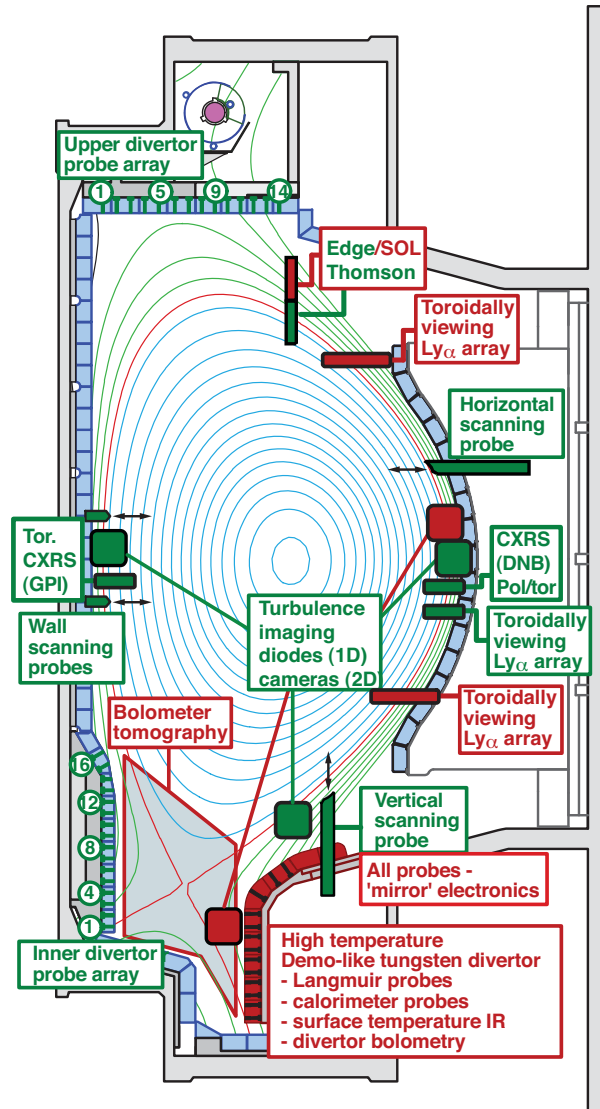


Fig. 4.2.1. Present (green) and expanded (red) edge plasma transport diagnostics set.

variety of plasma conditions (currents and fields, plasma species, magnetic topology, L/H mode, input power and radiation). This will allow us to formulate and test physics-based and semi-empirical hypotheses about underlying transport mechanisms. Our unique measurements will also be folded into comparisons with state-of-the-art turbulence and transport simulation codes (highlighted in following subsections). Such codes, if they are to be validated, must predict not only the observed time-averaged profiles/fluxes and their scalings with external engineering parameters (plasma currents, magnetic fields, plasma density) but also the observed turbulent eddy fields.

4.2.2.1 Time-averaged transport studies

Building on recent observations, we will use the expanded diagnostic set to further explore the ‘critical pressure gradient’ phenomenon near the last-closed flux surface, its connection to electromagnetic turbulence, and its sensitivity to the plasma flow patterns that naturally arise in the edge. In addition, we will explore how the pressure gradients of the near SOL ($\alpha_{MHD} \sim 1$) smoothly connect to the pressure gradients further up the H-mode pedestal ($\alpha_{MHD} \sim 8$). The edge Thomson system upgrade (SOLTS) will be very important in this regard, providing n_e , T_e profiles across the pedestal and separatrix to the limiter radius. Unlike the scanning Langmuir probes, which are typically limited to 3 scans per discharge, the Thomson diagnostic will continuously records profiles (~ 30 Hz) on every discharge and is unaffected by RF fields (a concern for Langmuir probe data). While certain ‘control parameters’, such as plasma collisionality, are seen to affect the observed ‘critical pressure gradient’ values in the edge, theory suggests that other ‘control parameters’ such as magnetic shear and/or plasma flow shear should also be observed. Perhaps the complex edge plasma flow patterns, which are not yet modeled by any transport code, are largely responsible for setting the breakpoint between the near and far SOL regions. (This feature is not yet reproduced by the turbulence codes.) Our unique set of diagnostics covering the region from the near SOL through the pedestal (scanning Langmuir-Mach probes, CXRS, gas-puff turbulence imaging and associated fast diode diagnostics) will be used to map out both the fluid and phase velocity profiles across the separatrix and into the SOL, with magnetic topology being a ‘control knob’ to systematically vary these flows (as well as varying *magnetic shear*). With the help of the new L_α diagnostics, cross-field particle fluxes will be tracked systematically, allowing us to map out flux gradient relationships over an expanded ‘phase-space’ of electromagnetic plasma fluid turbulence. We will continue to work using with our theory and modeling collaborators, including B. Rogers (Dartmouth), P. Guzdar (U. Md), M. Umansky, X.Q. Xu, R. Cohen, D. Ryutov (LLNL), B. Scott (IPP Garching), using the C-Mod data to challenge the models (see Table 4.2.1).

Another important topic is the conditions in the edge plasma at the onset of the L-H transition (i.e. gradients, rotation, flow shear,...) – what clues can we learn here about L-H transition dynamics? Data from ohmic L-H transitions (see Fig. 4.2.2) suggest a tantalizing connection: discharges just prior to the L-H transition are found to lie on a boundary very similar to that predicted by Guzdar [2,37]. Is this coincidence or evidence of a deeper connection? Is it the near SOL that initially triggers the transition? We hope to test the existence of this boundary in more detail in the upcoming campaigns, operating with an expanded range of plasma currents and probing edge conditions in more detail.

Finally, we aim to further elucidate the role of electromagnetic effects in the plasma turbulence by direct measurement. Using a novel scanning probe head with embedded coils, we will build upon our database of poloidal magnetic field fluctuations as a function of distance into the SOL. These will be compared with output from first-principles numerical computations (e.g., BOUT). In addition, with the help of a new ‘Mirror Langmuir Probe’ technique developed at MIT [38,39], there now exists the possibility of simultaneously measuring plasma density, electron temperature and plasma potential fluctuations, their k-spectra, and their correlations as a function of distance into the SOL using C-Mod’s standard 4-electrode scanning probes. If ballooning mode physics (resistive or ideal) does indeed play a prominent role in the near SOL, as suggested by the pressure gradient scaling with

α_{MHD} in Fig. 4.1.1, then the local phase delay between pressure and potential fluctuations should tend towards $\sim\pi/2$ in this zone, instead of ~ 0 for drift-wave turbulence [40]. In any case, we will test the viability of this diagnostic technique and develop it further, if necessary, to more generally interrogate plasma density, electron temperature and plasma potential fluctuations in the C-Mod SOL. This will provide valuable information on the dynamics of blob and ELM transport physics.

Strong parallel plasma flows are expected to exist near wall surfaces in the tokamak scrape-off layer, yet they are found to also exist in regions far from material surfaces. C-Mod experiments have shown these flows to be driven largely by ballooning-like cross-field transport asymmetries [9]. As indicated above, such flows may have important consequences for plasma discharges, in addition to transporting impurities in the boundary layer. They may influence the L-H power threshold (via changes in magnetic topology [10]) and/or change the flux-gradient relationships of local plasma transport in the near SOL [3]. With the recent improvements to our edge flow diagnostics (new scanning Langmuir-Mach probes, CXRS, gas-puff imaging) we will explore SOL flows, the physics of their origin and their influence on edge profiles/transport in further detail. An important goal is to determine how the strong flow of material towards the inner divertor leg returns into the confined plasma and forms a closed mass-flow loop – Is there a mechanism of cross field ion convection into the closed flux surfaces or the private flux zone? Or, does neutral fueling from the inner divertor leg dominate? The possible role of an inward fluctuation-induced particle flux will be investigated using the capabilities of the new inner-wall scanning probe system. Through dedicated experiments, we plan on quantifying the contribution that neutral recycling can possibly make to ‘close the flow loop’. This will involve a combination of particle flux measurements on the inner divertor surface and simple neutral transport modeling. Lastly, we will continue to compare our detailed flow measurements with those simulated by 2-D transport codes. In particular, flow measurements that span the separatrix on the high-field side provide a means to critically test the flow patterns produced by modelers, such as A. Pigarov (UCSD) using the UEDGE code [41]. We also will continue to work closely with

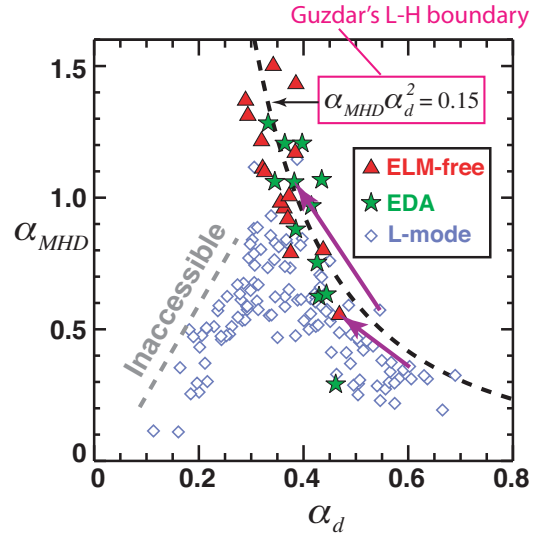


Figure 4.2.2: Normalized pressure gradient versus normalized (inverse) collisionality in the near SOL for a wide range of plasma conditions.

P. Catto (MIT) and A. Simakov (LANL) in analyzing the symmetry properties of the observed flows [42]. These analysis techniques can be used to extract the topology-dependent parts of the plasma flow field.

Table 4.2.1 - Active collaborations on transport in the near SOL, including flows		
Collaborators	Topics	Theory/Modeling
B. Rogers (Dartmouth), P. Guzdar (U. Md)	Electromagnetic turbulence, density limit, L-H transition	L-H transition theories, density limit theories
M. Umansky, X.Q. Xu, R. Cohen, D. Ryutov (LLNL)	Electromagnetic turbulence, role of x-point, blobby transport	BOUT, TEMPEST-future
B. Scott (IPP Garching)	Electromagnetic turbulence, drift-wave vs ballooning mode structures	DALFTI, GEM, GEMX-future
P. Catto (MIT), A. Simakov (LANL)	Edge plasma flows and toroidal rotation	Magnetic topology and flow symmetries
A. Pigarov, S. Krashininnikov (UCSD)	2-D modeling of SOL flows, critical gradients	UEDGE, blob formation theories

Transport processes in the far SOL are also important since they determine the conditions under which a ‘shoulder’ forms in the profile, increasing the level of plasma interaction with main-chamber wall surfaces (see 4.1.1). We hypothesize that the differences in SOL profiles between JET (weak shoulder) and C-Mod (strong shoulder) are due to differences in the opacity of the SOL to neutrals [19]. We have recently begun to explore lower density, reduced neutral opacity discharges on C-Mod, with the aim of unfolding such effects. These experiments will continue with the aid of the new C-Mod cryopump and with a new toroidal-viewing Lyman-alpha diode array to extract neutral profiles and ionization sources in the SOL. Drawing on these new tools and an expanded operational space we will: (1) Determine if the inferred weak dependence on dimensionless parameters holds over a much larger dataset; (2) Vary the neutral opacity over a much wider range, matching that of JET, and determine if the JET SOL profiles are achieved (without changes in transport); and (3) Compare the characteristics of the far SOL transport (v_{eff}) with that of local turbulence (e.g. phase velocities of striations/blobs). Augmenting the C-Mod work, we intend to continue inter-tokamak collaborations that include analysis of SOL data from DIII-D (H-mode), MAST and JET. This work is part of IEA/ITPA collaboration DSOL-5 and the ITPA high-priority research task, “Improve understanding of SOL plasma interaction with the main chamber.”

4.2.2.2 Turbulent transport studies

A second major component of C-Mod's edge transport research is the study the turbulent eddy fields that underlie the time-averaged transport and profiles. As discussed in Section 4.2.2, we have a large number of diagnostics with the capability of making detailed measurements of those eddy fields and their dynamics. The diagnostics are primarily imaging diagnostics that utilize GPI and probes. They make measurements at multiple locations, inboard, outboard near the midplane, outboard in the high-shear region, and at the divertor targets. The goals of these studies are 1) to characterize spatial structure of the eddies, their temporal dynamics, and the spatial variation of the eddy fields, 2) to use these measurements as stringent tests for first-principles models of turbulence in simulations of the C-Mod edge plasmas, and 3) to characterize changes in the turbulence during confinement regime transitions like the L-to-H-mode transition and to characterize the edge turbulence in the steady state phases of the different regimes. We now outline the research plans proposed in each of these areas.

The study of the spatial structure of the turbulence has been on-going for a number of years at C-Mod (see Section 4.1.1.2), with extensive measurements at the outboard and inboard midplane regions. Recent measurements, made in the high-shear region outboard of the typical Lower-Single-Null X-point, show clear differences when compared to those made near the midplane. We will continue to characterize the turbulence in the regions near the X-point with the goal of better characterizing the role of the high-shear region there in affecting turbulence *vis a vis* the rest of the SOL. While the turbulence in these regions is related via the parallel electric potential, we plan to elucidate the causes of both the structural and dynamical *differences* using 2D and 3D codes (like ESEL, GEM, and BOUT). Theoretical analysis [43,44] indicates that magnetic shearing and flux expansion near the X-point may have important consequences for parallel and perpendicular transport, both because of their effects on stability and because perpendicular perturbations are deformed into shapes for which the poloidal scale length approaches the ion gyro-radius. Some of these theoretical ideas will be tested, especially as they and turbulence in general relate to the crucial issues of parallel transport of heat and particles in the SOL and into the divertor (see Section 4.2.2.3). We plan an additional GPI view of the divertor plasma, i.e. in the region on the “other side” of the X-point and the high-shear regions. Turbulence-imaging measurements at multiple poloidal and toroidal locations (three existing and a fourth planned, see Fig. 4.2.1), as well as probe measurements at multiple poloidal and toroidal locations will provide excellent measurements of the spatial variations in the turbulent fields and tightly constrain the 2D and 3D simulations of them.

As is evident from the description above, comparisons of experiment with simulation are an important part of the

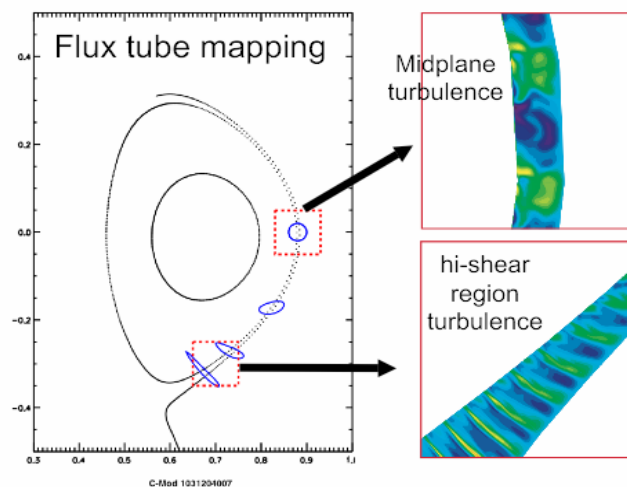


Fig. 4.2.3. BOUT simulation of C-Mod edge turbulence. X-sections of the turbulent density (δn_i) fields are shown on the right at the two locations imaged in the experiment. Compare with the exp. observations shown in Fig. 4.1.4.

research plan. Ultimately we desire (with the community) the ability to simulate, using a first-principles-physics model, the time-averaged profiles and perpendicular and parallel fluxes that we measure. With that capability the community can more confidently *predict* the power and particle profiles footprints in the divertor of future devices like ITER and Demo. At C-Mod we have working relationships with groups running the following turbulence codes (see sect. 4.1.1.2) - ESEL (2D non-linear fluid code) [45], BOUT (3D non-linear fluid code with X-point) [46], and GEM (3D non-linear gyrofluid code) [18]. Fig. 4.2.3 shows results from a simulation of the C-Mod SOL using the BOUT code, where predictions of the turbulent structures at two of the experiment's imaging locations can be compared with the experimental observations. In the simulation blobs are evident at the midplane, while 'fingers' are predicted in the high-shear region, qualitatively similar to the observation (shown in Fig. 4.1.4). We will continue to work with these groups to validate the codes with C-Mod's turbulence data. We will push to have the simulation start with the *flux* specified as a boundary condition and see if they can reproduce the measured radial profiles as well as the turbulence characteristics. In parallel we will seek to develop a robust experimental *measurement* of particles fluxes using the gas-puff-imaging-with-fast-cameras technique. Such a measurement would be very powerful in connecting the turbulent fields with the time-averaged profile measurements as well as with the simulation results. Some preliminary work on this subject has been done on RFX [47]. We will examine these techniques (with the group at RFX) and attempt to develop others that would yield the perpendicular particle flux.

The third major area of the proposed work on edge turbulence is concerns diagnosing differences in turbulence among different confinement regimes, the most notable of which are L- and H-mode. Previous C-Mod work on this [48] indicates that "microscopic" differences (e.g. in eddy size and frequency) are not obvious. Additionally, we have not yet found any precursor to the L-to-H-mode transition in the turbulence measurements. Yet, major time-averaged changes in the edge pedestal and in confinement are unmistakable. Thus we seek to examine the changes in turbulence at the microscopic level among the different confinement regimes. This will include detailed examination of turbulence changes at the L-H transition as well as a quantitative characterization of the turbulence in the steady state periods of the different regimes.

Finally, as part of the work on the structure and dynamics of the cross-field convective transport, we will be relating the turbulence measurements made using imaging with those made using probes. There is a need for this since it has not yet been shown that the results of the two diagnostics are fully consistent. For example, imaging diagnostics usually measure the radial propagation of a turbulent structure by tracking its enhanced emission signature over its lifetime within the field-of-view, while multi-tipped probes typically measure the floating potential at two or more points as an eddy/blob passes it and that is used to calculate the radial component of \mathbf{ExB} . In our search for scaling relations and trends in the edge turbulence we desire to combine and study results from many devices. For example, we are responsible for organizing the ITPA Research task "Inter-machine comparison of blob characteristics". Yet in this and other multi-machine studies, turbulence characteristics measured by both techniques (imaging and probes) are typically combined with the absence of understanding of possible systematic errors introduced by the technique. C-Mod has the most extensive complement of probes and turbulence-imaging diagnostics, and as such is well suited to study this issue.

4.2.2.3 Heat fluxes in the SOL and divertor

The prediction of plasma heat flux magnitude and profiles, and developing techniques to dissipate the plasma power, are critical areas of research with respect to projecting from current tokamaks and ITER towards future fusion reactors. This is easily seen by examining the requirements for the ARIES-AT fusion reactor [49]: $P_{\text{exh}} \sim 400$ MW of exhaust power, roughly three times larger than ITER, must be safely exhausted by conduction through the plasma-facing components (PFCs), but in a device that is actually smaller than ITER.

C-Mod will exploit its unique access to reactor power density levels among present devices as an instrument for determining if our understanding of parallel heat transport is correct, and whether heat dissipation techniques such as radiation and divertor detachment are compatible with clean high-performance core plasmas. Table 4.2.2 shows that with the proposed power upgrades to 8 MW (ICRH + LH heating), C-Mod achieves $P_{\text{exh}}/A_{\text{div}} \sim 10$ MW/m², commensurate with global power exhaust requirements on ARIES-AT.

It is important to note that C-Mod is not in fact held to the same steady-state technological limit for reactors ~ 10 MW/m² for actively cooled PFCs (limited by heat conduction, joining technology currently, etc.). Namely, unlike a reactor C-Mod can study the physics of heat exhaust while the divertor tiles are transiently heated (temperature diffusion time ~ 5 s), yet with an equilibrated upstream SOL “boundary condition” of ~ 4 - 5 s duration. The thermal limits of C-Mod molybdenum PFC tiles are ~ 44 MW/m² and 22 MW/m² for a 1 and 4 second discharge respectively (tungsten is $\sim 30\%$ higher than Mo). Thus C-Mod will have more “security” in exploring peak heat load conditions in excess of 10 MW/m² than will larger devices where the core equilibration time \sim current relaxation time \gg the tile equilibration time.

	C-Mod	JET	ITER	ARIES-AT
R (m)	0.67	2.96	6.2	5.2
B (T)	5.4 - 8	3.5	5.3	6
P_{exh} (MW)	6 (8)	25	150	400
P_{exh} / S (MW/m ²)	0.74 (0.99)	0.13	0.22	0.87
$P_{\text{exh}} / A_{\text{div}}$ (MW/m ²)	7.4 (9.9)	2.1	2	10.8
$T_{\text{sep}} \sim [P_{\text{exh}}/R]^{2/7}$ (eV)	150 (162)	155	184	250

Table 4.2.2 Power exhaust requirements for various tokamaks. Proposed C-Mod power upgrades for steady-state AT scenarios shown in parentheses. Definitions: Exhaust power, P_{exh} is the sum of alpha and external heating power, S is total plasma surface area, A_{div} is the area of divertor vertical target plates, T_{sep} is upstream separatrix temperature required for heat exhaust based on scaling from ITPA database $T_{\text{sep}} \sim (P_{\text{exh}}/R)^{0.28} q_{\text{cyl}}^{0.63}$.

While it is certain that C-Mod matches global reactor power exhaust based on $P_{\text{exh}} / A_{\text{div}}$, the issue of critical importance is the spatial distribution of the heat exhaust - in the SOL and at the various PFC surfaces - and whether the 10 MW/m^2 reactor limit is locally exceeded. The “boundary condition” for the exhaust to the divertor is the upstream separatrix T_e and separatrix electron temperature gradient scale length (λ_T), since these set the heat exhaust power flux density and width (assuming parallel electron heat conduction is the dominant heat transport mechanism). Recent analysis of a multi-machine SOL database of H-mode discharges [50,51] shows that $\lambda_T \sim R$ and does not depend on power exhausted into the SOL. This appears self-consistent with our observations that the near-SOL profiles reside at a critical gradient (4.2.2.1), presumably set by curvature-driven instability $\sim R$. The scaling also allows for simple calculation of upstream peak parallel heat flux (i.e. $q_{//,\text{sep}} \sim P_{\text{SOL}} / R^2$) which indicates that C-Mod is unique among present devices in being able to access the same $q_{//,\text{sep}} \sim 3 \text{ GW/m}^2$ as ARIES-AT (Fig. 4.2.4).

We believe these observations on $P_{\text{exh}}/A_{\text{div}}$ and $q_{//,\text{sep}}$, as well as more complex observations regarding SOL similarity which we do not present here, indicate that C-Mod provides an exceptional opportunity to study heat exhaust physics at reactor-relevant levels and thus motivates an enhanced research effort in this area. We will explore a range of discharges, from high density, high current ICRF-heated discharges to the lower density, lower current AT discharges. In particular we will document ARIES-AT levels of heat exhaust in AT scenarios (AT section), with $P_{\text{exh}} \sim 6\text{-}8 \text{ MW}$ and, if possible, demonstrate regimes where peak divertor heat flux is kept below 10 MW/m^2 as will be required for an actively cooled divertor (see section 4.2.5). This will be achieved at the same line-averaged density $\sim 2 \times 10^{20} \text{ m}^{-3}$ as ARIES-AT, and the role of upstream/core density in achieving acceptable q_{div} will be examined.

Research on C-Mod and elsewhere strongly motivates improved diagnostic capabilities that will be described in this section and 4.2.6. For example we note a previous multi-machine study of *downstream* divertor heat load profile widths [52], which indicates $\lambda_T \sim P_{\text{SOL}}$, but independent of R , i.e. the opposite observation as found upstream! While it is our opinion that the upstream diagnosis/scaling is more robust at this point, it clearly motivates improved capabilities for measuring divertor heat loads, i.e. how is the C-Mod divertor responding to upstream $q_{//} < 3 \text{ GW/m}^2$. Is there a reduction in peak power flux due to radiation or spreading across B (turbulence)? Analysis of the highest power C-Mod discharges (Fig. 4.2.4) achieved so far indicates that surface heat fluxes should be in the range $q \sim 8\text{-}16 \text{ MW/m}^2$, within the technology limits of the divertor, but also indicating that $\sim 75\%$ of $q_{//,\text{sep}}$ is

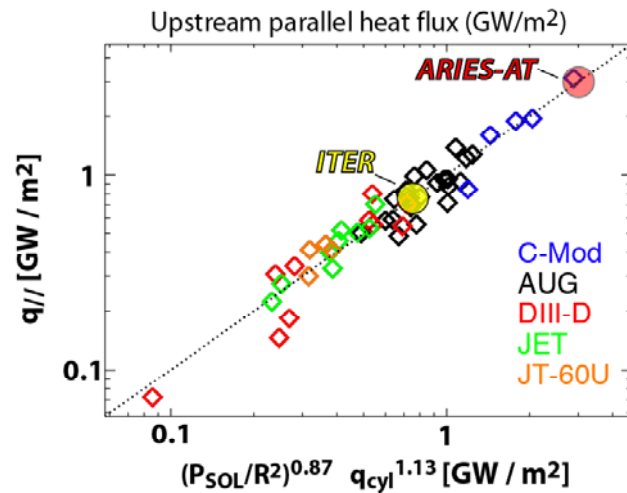


Figure 4.2.4: Regression analysis of parallel heat flux, $q_{//}$, at the upstream separatrix from a multi-machine database [50]. Scaling law results for ITER and ARIES-AT are overlaid assuming P_{SOL} is 70% of total exhaust power due to core radiation.

dissipated volumetrically before reaching the divertor target. However, because analysis is limited to Langmuir probes in the divertor target, there is no direct means to corroborate these values discussed above (heat fluxes, volumetric radiation, sheath transmission factor, etc.).

We propose to probe the scaling and underlying physics of the upstream $q_{||}$ profiles in more detail, attempting to experimentally determine what are the dominant contributions to $q_{||}$. A major advance will be to measure the possible contributions of ions to the heat exhaust. The analysis presented in Figs. 4.2.4 is typical of analysis of SOL heat exhaust in that the role of ions is ignored. However if $T_i/T_e \geq 2$ or there is substantial fluid flow (i.e. high Mach number) at the outer midplane, then the ions could make important contributions to the heat exhaust through conduction or convection respectively. The uncertain role of ions is essentially due to the fact that main ion species diagnosis of T_i and v_i profiles is required but not typically measured in tokamaks. Standard ion diagnosis in the SOL based on CXRS of trace impurity species is insufficient since the impurity ion temperature can be substantially different than the main ions. Therefore we are working to develop a new diagnostic to measure the main ion species T_i and v_i profiles in the pedestal and SOL for C-Mod, utilizing CXRS on the deuterium main ion species. We will develop analysis techniques that take into account that the deuteron charge-exchanges into a neutral species which is not tied to the field line it was born on. Both parallel (toroidal) and poloidal velocity measurements will be made in order to reconstruct the main ion flow vector profile near the separatrix (we note that this is highly complimentary to the C-Mod research effort on plasma flows). We will validate the technique by studying the role of ions in heat exhaust for He plasmas, for which standard CXRS is available on the He^{+2} . With upstream main ion profiles of T and velocity in hand (He or D CXRS), the contribution of ions to heat exhaust can be quantified, and its effect on “locating” the upstream separatrix will be included in the $q_{||,sep}$ analysis. To our knowledge this would be the first direct examination on the role of ions in heat exhaust. We will also improve the electron temperature profiles with the new SOL Thomson scattering system such that it covers the SOL and overlaps with the current edge Thomson measurement range as well as complementary T_e measurements with high spatial resolution from scanning probes.

We will document the divertor plasma and target response to upstream $q_{||}$. We want to address several questions here: Is there any anomalous cross-field energy transport that widens the $q_{||}$ profile? If so does turbulence play a role? How efficient is the divertor plasma in dissipating or spreading the power flow and how does that depend on divertor plasma conditions? Can we understand the sheath transmission factor at the targets? For this thrust, top priority will be given to accurate evaluation of peak and total power loads on the divertor since: a) estimated heat loads are close to the limit of 10 MW/m^2 for actively cooled PFCs, so they need to be accurately measured, b) accurate divertor heat flux measurements are required for quantifying global power balance in C-Mod, and c) for divertor protection on C-Mod during high power / long pulse discharges. Towards this goal we propose two initiatives: 1) installation of a new toroidally continuous divertor (section 4.2.5) and 2) installation of new power exhaust diagnostics in the lower divertor to complement the data now obtained from Langmuir probes. The first initiative is required to ensure toroidally uniform power deposition. This is important both for operationally avoiding leading edges (to improve the divertor power handling) and to provide global divertor power exhaust levels based on toroidally localized diagnostics. For heat load diagnostics we propose calorimeter probes and upgraded infrared (IR) thermography. An array of calorimeter probes [53], which are thermocouple-instrumented, thermally isolated bodies, inserted in the divertor plates, will provide unambiguous total heat flux measurements with $\sim 2 \text{ mm}$ spatial

resolution. The other complementary heat flux diagnostic will be upgraded IR imaging of the divertor. While interpretation of the IR is more difficult (especially given the low emissivities of W and Mo), imaging provides a means to assess spatial uniformity (e.g. presence of leading edges, local hot spots caused by RF interactions) as well as better (< 10 ms) time resolution than calorimeters. In addition, because embedded Langmuir probes in the divertor also provide profiles of particle flux and T_e , the ratio of q to ΓkT_e provides γ , the sheath energy transmission factor. Standard sheath theory predicts $\gamma \sim 7$, yet anomalous values of γ (low and high) have long been reported [54,55], and not understood. Routine measurement of γ will provide an invaluable database for this parameter of fundamental importance to power exhaust, and should provide new insights as to its controlling mechanisms by correlation to other global and local plasma parameters.

We cannot understand the transport of heat along and across the magnetic field without properly measuring the loss of power flow between the upstream SOL and the divertor surface. This is particularly challenging in an environment where neutrals can be a significant power loss channel. We propose that the divertor foil bolometry arrays be re-installed. These have the advantage of being easily calibrated and are accurate across the spectral range of divertor radiation (as well as for neutrals). AXUV photodiode arrays will be utilized in a complementary role, particularly for their time and spatial resolution as well as their insensitivity to neutral power losses. Both bolometer arrays, along with our standard complement of spectroscopic diagnostics, will greatly improve power accounting and diagnosis of the role of power losses in modifying the parallel power flow between upstream and the divertor surfaces.

The above experimental measurements from the upstream to the divertor plate will continue to be interpreted primarily through simple SOL power and particle accounting. This analysis (e.g. Onion-Skin modeling [56]) allows one to extract useful information about the roles of volumetric energy and momentum dissipation. It is also likely that results will confront the more complex 2-D SOL models, which have had difficulty predicting the details of heat and particle exhaust and other divertor characteristics (see Section 4.2.4), a confrontation which is all the more compelling given the exceptional access of C-Mod to reactor relevant plasma conditions.

Table 4.2.2 – Edge transport research thrusts			
Issue/topic/objective	Approach	Diagnostics/facilities	Modeling
Explore connections between ‘critical pressure gradients’ in near SOL, plasma flows/shear and magnetic shear	Map gradients and velocity profiles vs. edge ‘phase-space’ (α_{mhd}, Λ) and magnetic topology	Langmuir-Mach probes on high/low-field SOLs; GPI on high/low-field sides (mid-plane); Toroidally viewing Lyman-alpha arrays (’09); Scrape-off layer Thomson Scattering [SOLTS] (’11)	BOUT, GEM – influence of flow shear on SOL transport and near/far SOL profiles
Quantify Γ_{\perp} vs. ∇n in near SOL as validation test for turbulence codes	Use SOL particle balance model to infer Γ_{\perp} in near SOL as a function of α_{mhd}, Λ & topology		BOUT, GEM – attempt to match measured particles fluxes and SOL profiles
Test ‘phase-space’ boundaries as predictor of L-H threshold condition	Expand range of investigated I_p & B_T in Ohmic and ICRF heated discharges		Guzdar/Rogers L-H ‘phase-space’ boundary
Quantify \tilde{B}_p in near SOL as validation test for electromagnetic turbulence codes	Use scanning probe head with embedded coils to measure $\tilde{B}_p(\omega, k)$ for variety of edge conditions	Fast-scanning probe head with embedded coils	BOUT – compare measured $\tilde{B}_p(\omega, k)$ to code output
Look for direct evidence of ballooning-mode turbulence in near SOL	Record k-resolved phase delay between \tilde{P} and $\tilde{\Phi}$ in near SOL	Mirror Langmuir Probe electronics on fast-scanning probe	DALFTI simulations from B. Scott
Understand the mechanism(s) that closes the strong parallel mass-flow loop from low- to high-field SOLs	Investigate fluctuation-induced ‘inward pinch’ on high-field side	Scanning Langmuir probe in high-field SOL to record $\tilde{n}, \tilde{\Phi}$ -induced fluxes	KN1D – assess magnitude of inner div. neutral fuelling; UEDGE modeling (A. Pigarov)
	Assess potential role of neutral recycling on inner divertor	Γ_{div} via divertor probes; n & T_e profiles from high-field scanning probe	
Explore influence of SOL neutral opacity in affecting ‘shoulders’ in the far SOL	Measure profiles at low \bar{n}_e, I_p & B_T ; assess SOL shoulders; compare with DIII-D, JET, MAST	Upper divertor cryopump; toroidally viewing Lyman-alpha arrays (’09)	KN1D – match observed ionization profiles; assess role of neutral penetration/fueling

Table 4.2.2 – Edge transport research thrusts

Issue/topic/objective	Approach	Diagnostics/facilities	Modeling
Understand turbulence dynamics of particle transport in far SOL	Build statistical database of ‘blob’ characteristics and correlate with Γ_{\perp} ; Map spatiotemporal behavior to hi-shear regions and div. leg	GPI fast-camera views of hi-shear region, divertor, and ICRF antenna (’10); Langmuir-Mach probes on high/low-field SOLs;	‘Blob’ models of Myra & D’Ippolito (Lodestar), analytic predictions of Ryutov & Cohen (LLNL)
What is the interplay between the ‘microscopic’ SOL turbulence and the L-H transition?	Identify changes in edge turbulence across the L-H transition. Examine possible link between pedestal and SOL turbulence	Toroidally viewing Lyman-alpha arrays (’09); ‘mirror’ probe (’10); Upgraded fiber-to-diode GPI arrays (’10); SOLTS (’11)	BOUT (LLNL), GEM (Scott-IPP), 2D turbulence code of Myra & D’Ippolito, ESEL (Naulin, Garcia)
Gain predictive capability for Γ_{\perp} in the SOL	Provide detailed measurements of SOL turbulence characteristics to 1 st -principles fluid codes		
Explore scaling and underlying physics of upstream $q_{ }$ profiles	Measure upstream T_e/T_i profiles, divertor plasma conditions and heat fluxes on targets over wide parameter range; unfold electron & ion contributions to upstream $q_{ }$; measure sensitivity to shape and topology	SOLTS, main ion CXRS; Mach-probe flow measurements; Demo-like divertor (’11); div. target calorimeter probes (’11); upgraded IR thermography (’09); divertor bolometry (’09)	OEDGE-Onion-Skin modeling (Stangeby); EIRENE (Lisgo); ITPA SOL database
Test understanding of heat-flux mapping from midplane to divertor ‘footprint’ at reactor-level conditions			
Determine the role of ions in the parallel heat flow			
Continued development of dissipative-divertor scenarios at reactor-level heat fluxes	Explore strike-point sweeping, impurity-gas-puffing, divertor detachment at high power & long pulse		

4.2.3 Plasma-Surface Interactions

Understanding and controlling the various deleterious effects that arise from plasma-surface interactions (PSI) are critical for C-Mod and future fusion devices. Plasma-surface interactions are the root cause of impurities in the plasma, which can limit the core plasma performance, particularly in the case of Mo impurities [24]. In future long pulse devices, other effects of PSI (erosion, fuel retention, dust) will also pose serious operational limits. In this section we describe research in three areas, with a particular emphasis on developing several exciting and innovative PSI diagnostics. *Plasma-Facing Component (PFC) sputtering and the effect of ICRH-derived erosion* focuses on measuring the location, magnitude and cause of plasma + RF sputtering of both molybdenum and boron films. *Net Erosion and Near-surface transport* research seek to understand the fate of sputtered materials, and how the combination of ionization, redeposition and near-surface transport lead to net erosion of plasma-facing surfaces. *Dust studies* seek to understand the physical mechanisms controlling the transport of dust particles inside the vessel.

PFC Sputtering & the effect of ICRH-derived erosion - Understanding high-Z sputtering is a challenge because a number of plasma species, including impurities, can lead to Mo (or W) sputtering. Furthermore, the incident ion energies produced by the C-Mod edge plasmas (~10-100 eV), are typically very close to the sputter threshold, thus making sputtering extremely difficult to predict in tokamaks (see Figure 4.2.5). This picture of sputtering in C-Mod is further complicated by the effect of ICRH heating on sputtering through enhanced sheath voltages, i.e. sheath rectification [27]. C-Mod experiments have shown that sheaths are enhanced by the ICRF up to 100's of volts. Such sheaths leads to enhanced Mo erosion; indeed the main plasma (deuterium) can start to sputter Mo for energies > 100 eV (Figure 4.2.5). Therefore plasma core performance, plasma purity and heating, which is predominately ICRH, are all strongly coupled on C-Mod. The understanding, mitigation and reduction of the RF-sheath enhancement and ensuing Mo sputtering are critical goals of the C-Mod program over the next 5 years. We note that this is important both for C-Mod and for future fusion experiments that rely on ICRF heating (e.g. ITER, ARIES-AT). A related discussion, in the ICRF section (Chapter 5) of this proposal, emphasizes antenna changes and models of the processes that lead to the sheaths. Beside Mo sputtering, the erosion locations of the applied B films is also important, both with respect to maximizing the lifetime of B films and as a tool to understand the location and impact of Mo sources that arise after the B film is removed.

Due to the difficulty of predicting sputtering, particularly for Mo, our goal is to measure what precisely are the magnitudes and the poloidal/toroidal location of the Mo and B sputter sources.

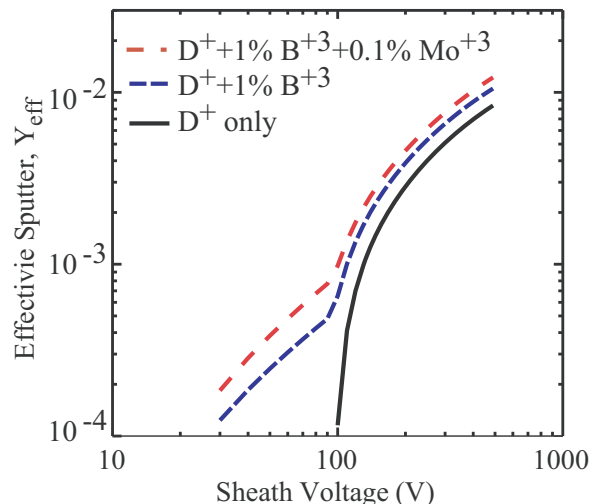


Figure 4.2.5: Molybdenum sputter yields and their dependence on incident species and sheath voltage.

This goal calls for an enhancement of our sputtering diagnostics. Currently, the locations of the sputter sources have been inferred two ways: 1) line of sight spectroscopic monitoring of neutral Mo and B lines; and 2) indirectly from the plasma response to boronization films applied at different locations. The former tells us the gross removal rate at the viewed location. The latter serves to inform us what regions of Mo erosion are most likely to affect the core plasma. While the spectroscopic views are fairly extensive at present, covering multiple poloidal locations and surfaces at one toroidal location, our plan is to significantly increase the number of surfaces monitored. In order for present spectroscopic measurements to be used to infer total impurity source rates (gross erosion) one must assume toroidal symmetry. However, because the RF antennas, their protection armor and the midplane protection limiters are toroidally discrete, localized spectroscopic measurements are inadequate.

We must measure the 3-D pattern of impurity sources in order to completely quantify and locate the Mo sources. To this end we will work towards line-filtered imaging of all the structures of interest. This will allow us to correlate and locate the Mo erosion sources, particularly that caused by RF-enhanced sheaths, with core Mo levels. A particular focus will be on monitoring the onset of Mo erosion after boronization, since this will provide valuable clues as to the most important location(s) for Mo sputtering. Mo atomic line emission will be difficult to image because the strongest atomic lines are in an unfavorable part of the visible spectrum for both camera sensitivity and interfering lines. Therefore *we are exploring the use of mixing Mo with “marker” elements, such as copper, that are more easily isolated with line filters.* The challenge here is to ensure that the marker material is indicative of Mo erosion. Preliminary tests have been carried out on candidate materials (e.g. Mo/Cu) in the PISCES facility, which we will analyze. *We will also exploit the newly installed Surface Science Station S³* (Fig. 4.2.7). The instrumented S³ probe head can be inserted into the SOL above the outer divertor. Because the sample can be retracted during operations, the S³ will allow us to test imaging analysis (e.g. of marker erosion) with surface analysis either in the S³ chamber or at the MIT accelerator facility (Section 4.2.6).

We will also develop specific tools to diagnose and advance our understanding of RF-enhanced sheaths. *Emissive probes will be installed on S³ in order to monitor sheath potential at various radial locations* (by scanning the probe head) and sheath-originating poloidal locations (by varying q_{95}) in the SOL. Emissive probes will also be installed at fixed locations around the chamber so that we have a direct measurement of sheaths on flux tubes connected to each antenna. *We are developing a second technique for inferring the sheath magnitude based on the line-shape of line emission from sputtered (and excited) atoms.* Shown in Fig. 4.2.6 are the varying spectral shapes for Mo as the incident D ion energy is increased, based on the Thompson distribution [57]. As the incident ion energy increases, the Mo I exhibits a stronger asymmetry in the line shape due to the ejection of higher energy atoms from the surface.

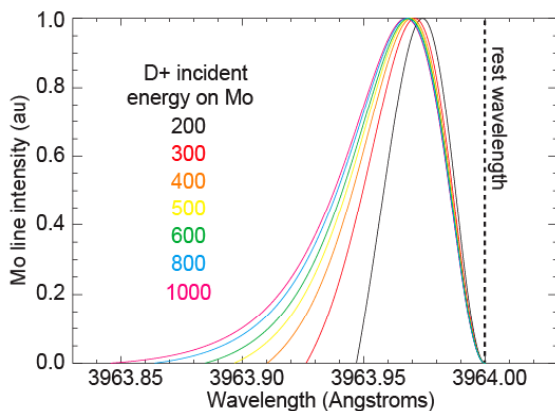


Figure 4.2.6: Predicted neutral Mo spectral shape as incident D ion energy is increase from 200 to 1000 V using the Thompson distribution with light ion corrections. The line shape becomes increasingly asymmetric as E_{D+} increases.

Net Erosion & Near-surface Transport - In order to understand and control impurity sources and core levels it is insufficient to measure only the gross sputter influxes of PFC materials. This is because the impurity must go through several intermediate steps, such as ionization, redeposition and near-surface / SOL transport, before entering the core plasma. These same processes also control the effectiveness of sputtering to lead to net erosion / deposition of the PFC surfaces, an issue that will be critical to the operational lifetime of steady-state fusion devices.

Several C-Mod results challenge conventional wisdom about what controls net erosion. The usual expectation is that when the mean free path for ionization of the sputtered impurity is less than the newly-formed ion's gyroradius it will be redeposited close to where it is eroded, thus leading to a net erosion much less (x100) than gross erosion. Such high redeposition efficiency is particularly expected for eroded Mo in the C-Mod SOL and divertor, where the sputtered atoms are slow, ionization MFPs are ~ mm, and the magnetic field is high. However, the inferred net erosion rates of B and Mo (B up to 20 nm/s, Mo ~ 0.2 nm/s) [24] imply lower prompt redeposition fractions. Furthermore, the extremely high net erosion of B illustrates that ICRH sheath rectification may pose a serious limitation for *all* plasma-facing materials, not just high-Z. Furthermore, the eroded Mo appears to very easily access the core plasma during ICRF H-modes, potentially indicating an RF-related perpendicular transport phenomenon such as convective cells. Thus we propose to install a GPI view of an antenna that will attempt to observe convective cells in front of the antenna.

The observations above strongly motivate an aggressive research program to substantially improve the diagnosis of net erosion of material surfaces. Several exciting new tools will be developed on C-Mod towards this goal.

The Surface Science Station (Fig. 4.2.7) will be able to expose material samples to well-diagnosed conditions in the SOL and, by a combination of spectroscopic monitoring (gross erosion) and surface analysis (net erosion /deposition), to assess the redeposition efficiency. The instrumented probe head also

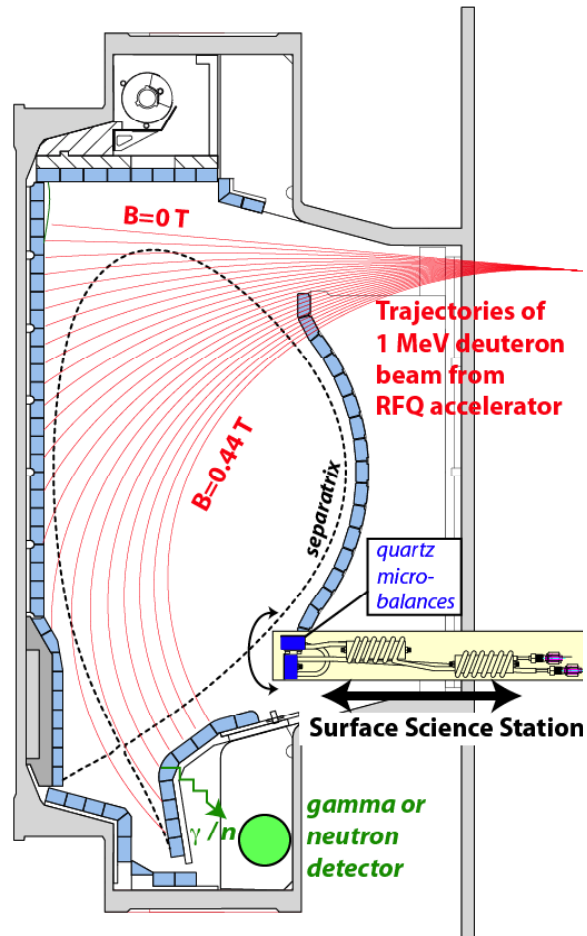


Fig. 4.2.7 In-situ surface diagnostics for plasma-facing components. In red, trajectories of a 0.95 MeV deuteron ion beam, produced by an RFQ accelerator, steered by a varying toroidal field. Resulting neutrons and gamma are measured to interpret surface properties. The instrumented Surface Science Station can be inserted and rotated to control exposure to SOL and conditioning plasmas. Shown is the head instrumented with quartz microbalances for erosion/deposition diagnosis.

allows for a wide variety of langmuir and emissive probes diagnostics, such as quartz microbalances.

An *accelerator-based in-situ surface diagnostic* will be tested at the proof-of-principle level on C-Mod (Fig. 4.2.7). The demonstration is a collaboration with the MIT Nuclear Science and Engineering department and is supported by a diagnostic development grant. The surface diagnosis is obtained by measuring the elastic and inelastic nuclear reaction products produced when a \sim MeV energy ion beam intercepts the surface. The large palette of so-called ion beam analysis (IBA) techniques can non-destructively resolve depth profiles of nearly every element in the surface (first \sim 10 microns of depth), which has made them the surface diagnostic of choice for ex-situ analysis. We will use a 0.9 MeV deuteron ion beam produced by a Radio-Frequency Quadrupole (RFQ) linear accelerator situated outside of the toroidal field coils, but connected to the tokamak vacuum, such that the mono-energetic D ion beam can enter the vessel in between plasma discharges. The RFQ is a compact (\sim 1 m length) source for the D ion beam and provides high time-averaged beam current \sim 0.1 mA.

A key innovation is exploiting the intrinsic toroidal magnetic field of the tokamak to steer the D ions (Fig. 4.2.7), via the Lorentz force, to the desired poloidal location at the material wall, thus

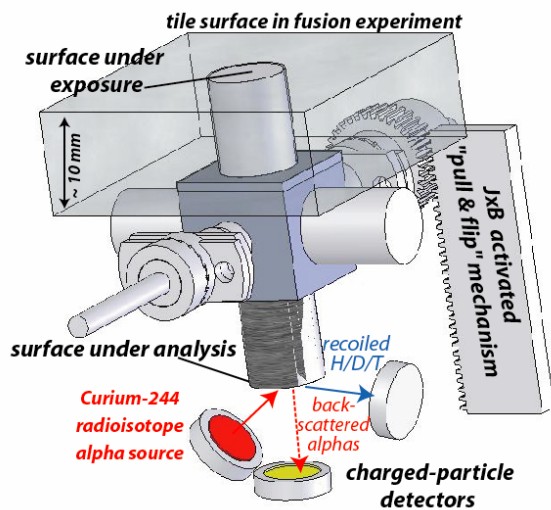


Fig. 4.2.8 A 3-D schematic of generic ARRIBA geometry with the mechanical mechanism, radioisotope source, and charged particle detectors behind a plasma facing surface.

providing high spatial resolution set by the beam spot size (\sim 1 cm), but with nearly complete poloidal coverage possible by varying the B field intensity. The necessary B fields are sufficiently small (\sim 0.4 T) such that continuous application of the field would be available. Deuterons feature large nuclear reaction cross sections with most elements expected in the wall surfaces, including the deuterium and tritium fuel, producing energetic gamma-rays or neutrons that can be measured by detectors in protected areas or external to the vessel. Knowledge of the beam fluence and energy, detector geometry and efficiency, and reaction kinematics allows one to extract the depth-resolved isotope/elemental concentrations where the beam intercepts the PFCs. Preliminary estimates show the technique allows for non-perturbing diagnosis of surface concentrations, film depth and deuterium/tritium fuel retention over a large poloidal portion of

the wall surfaces on a shot-to-shot basis.

Another PSI diagnostic development is *ARRIBA (Alpha Radioisotope Remote Ion Beam Analysis)*. ARRIBA features an in-situ ion beam analysis of surface where the high-energy ions are provided by an alpha-emitting radioactive source (Fig. 4.2.8). A novel mechanical movement design allows surfaces to be exposed and/or hidden in a controlled manner during shots, and also moved into a position behind the PFC surface where they can be analyzed. The technique thus provides for time-resolved, depth-resolved “ion beam analysis” of PFCs depth profiles and H/D detection. We will test a prototype version of ARRIBA using the Surface Science Station. A device like ARRIBA could be employed for continuous monitoring of film growth and fuel

retention on both plasma-receiving and hidden surfaces. Presently there is a strong need for the development of such measurements in burning plasma experiments like ITER.

Erosion/deposition models are useful to quantify and understand the experimental results. We have already developed a Monte Carlo model to describe the boron deposition on the quartz microbalances of S³ during boronization. This has been useful in helping describe the role of ion-neutral collisions and finite B⁺ gyro-radii in setting the pattern of boron deposition. This will be further expanded to extrapolate S³ measurements to not only B deposition on axisymmetric divertor surfaces, but also “3-D” structures such as protection limiters. Furthermore we propose a collaborative effort with Argonne National Laboratory (J. Brooks) to apply advanced erosion/deposition models (WBC, REDEP [58]) to C-Mod cases, in support of the all-metal PFC initiative of the US Plasma-Facing Component research community.

Dust Studies. In reactor-scale devices such as ITER, dust will be an important safety issue, since the potentially mobile dust particles will be radioactive due to tritium contamination and neutron activation. In order to understand the accumulation of dust in a tokamak, it is important to know not only what processes produce dust, but also how the dust is transported around the chamber. Theoretical and computational modelling of dust transport is in progress, such as DUSTT [59], but there is limited experimental data on dust transport in tokamaks. Proof-of-principle experiments during the previous campaign showed that frictional forces were the dominant force acting on the dust particles.

A diagnostic has been installed on Alcator C-Mod specifically to study the transport of dust in the scrape-off layer during normal plasma operation. It consists of a dust puffer system that injects boron particles (40-120 micrometers) into the outboard SOL near the divertor shelf. The dust is illuminated by intrinsic plasma light, blackbody emission from plasma heating and by a dedicated laser. The dust particles are imaged by two cameras, which can be filtered with narrow bandpass filters around the laser wavelength in order to reduce background plasma light. The two independent camera views provide stereoscopic imaging capability in order to unambiguously determine dust particle trajectories.

Table 4.2.3 – Plasma-surface interactions research thrusts

Issue/topic/objective	Approach	Diagnostics/facilities	Modeling
Understand physics and controlling mechanisms of sheath-rectification enhancement of erosion	Measure plasma potential on flux tubes near and far from antennas; characterize dependence on P _{RF} , plasma conditions and antenna design	Emissive probes at multiple locations ('10 - '12); Gridded energy analyzers ('12).	RF code modeling (Myra & D'Ippolito)
	Correspondence of sputtered Mo energies with enhanced sheaths	Imaging & Spectroscopic analysis of Mo I line ('10)	
	In-situ analysis of tile surface erosion, including limiters	ARRIBA ('10); RFQ ('10)	

Table 4.2.3 – Plasma-surface interactions research thrusts

Issue/topic/objective	Approach	Diagnostics/facilities	Modeling
Understand surface transport of sputtered impurities	Compare gross erosion (spectroscopy) with net erosion	Mo imaging ('10); RFQ ('10)	In-house Monte-Carlo modeling, REDEP (Brooks)
Understand dust transport	Inject dust into SOL and map trajectories	Dust injector & camera imaging ('09)	DUSTT (Pigarov)

4.2.4 Divertor Physics

The study of divertor physics was de-emphasized at C-Mod, and in the general community, around 2000 in favor of general SOL transport - a subject that was poorly understood. It was believed that a divertor “solution” – the radiative, partially detached divertor – had been found. However, since that time it has become apparent that divertor physics in more fluid-like ITER regimes has not been validated (by experiment) in the codes. Most code-experiment comparisons are single-machine, with the divertor and SOL in more kinetic, low opacity, regimes. The implication is that we have little confidence of proper predictions for divertor detachment (threshold and behavior, control of the detachment front location, the role of flows and $B \times \nabla B$ direction, effects on He pumping, etc.), as well as the treatment of power flow in the SOL (see section 4.2.2.3 on $q_{||}$). C-Mod plasmas are well-suited to address these concerns, since their SOL and divertor characteristics approach those of ITER.

Our intention is to continue our work to provide the unique information on recombination (the only quantitative measurement worldwide) and D_0 Lyman series absorption. We plan to implement new Ly_{α} chordal measurements through the divertor region, an advance over our previous single chord view of the x-point and inner divertor. Together with the existing visible views (providing Balmer series spectral measurements of the recombining region density and temperature), probe measurements, imaging of the recombination light and neutral pressures we will have the most detailed measurements of detached plasma characteristics. The comparison with modelling will continue to be a central part of this work through our collaborations with S. Lisgo of UKAEA Culham and Vladislav Kotov & Detlev Reiter of Juelich.

More recent changes in the C-Mod divertor geometry and capabilities open up other areas of divertor physics that need investigation. The new upper divertor has a flat-plate geometry together with a complete set of probe and neutral pressure diagnostics. Those characteristics provide a unique capability to compare, in one tokamak, the difference in operation between vertical-plate and the more open, flat-plate geometry. The latter is a simpler design and if it could be shown to have good enough properties relative to the vertical plate, it would significantly open up volume in reactor designs. More specifically we plan comparisons of the plasma profiles and detachment characteristics between the lower vertical-plate divertor and the upper, flat-plate. Modelling and physics arguments predict that the flat-plate divertor should have temperature profiles more peaked near the separatrix. Preliminary measurements in C-Mod show some inconsistencies with such a model. If the models are incorrect the implications for modelling and ITER are significant.

The new upper divertor measurements, together with the new upper divertor cryopump, will provide the opportunity to delineate the role of pumping in affecting divertor and SOL characteristics. Comparison of pumped and unpumped discharges in C-Mod has already shown

effects on the pedestal profile. Yet, when the pump is active the plasma profile across the divertor is almost identical to that without pumping, even though there is substantial particle removal rate by the pump (~150 torr-l/s). Correspondingly, the gas fueling rate must be increased to keep the discharge density constant. Obviously, this must affect plasma flows into the divertor – they must rise. An important question that we will investigate is whether divertor detachment can be influenced and controlled by such ‘pump and puff’ scenarios, elucidating the role that heat convection may have in divertor detachment physics.

A second major change in the C-Mod diagnostic complement is the complete coverage of the lower inner divertor with Langmuir probes. This has opened up the capability to properly study its characteristics with respect to detachment (occurring at lower densities than the outer divertor as commonly thought or, as recent C-Mod measurements indicate, at the same density as the outer divertor), the pressure profiles there in comparison to the outer divertor, and the role of flows and $B \times \nabla B$ direction in controlling divertor characteristics.

One major question that C-Mod started to address in the late 1990s was that of active control of divertor detachment. At the time it was shown that nitrogen gas was optimal for injection into the divertor to raise radiation, and lower temperatures to provide access to detachment [60]. The study of this important subject is now even more relevant as the C-Mod parallel power flows have risen and more attention is being paid to the divertor material – in the case of C-Mod solid tungsten and molybdenum tiles. Once the proper measurement of $q_{||}$ is made and understood it appears C-Mod can then directly address heat flux dissipation under ITER-like conditions (see section 4.2.2.3). This will be particularly relevant in the high-power advanced-tokamak scenarios.

Table 4.2.4 – Divertor physics research thrusts			
Issue/topic/objective	Approach	Diagnostics/facilities	Modeling
Understand the role of D_0 Lyman $_{\alpha}$ opacity in high density divertor plasma	Measure Ly_{α} , Ly_{β} , D_{α} emissions from divertor	D_0 Lyman $_{\alpha}$ arrays viewing divertor ('09), div. bolometry ('09)	Modeling using B2-Eirene by Lisgo, Kotov, and Reiter
Compare operation between ‘closed’ vertical target geometry with more-‘open’ flat target geometry	Change configuration between LSN (vertical target) and USN (flat target)	Embedded probe coverage of upper and lower targets, target calorimetry ('11), IR upgrade ('09)	
Understand differences in divertor legs as they relate to divertor detachment	Compare inner and outer divertor legs under detached divertor conditions with varying flow, puff & pump conditions		

4.2.5 Demo-like divertor

Current tokamaks have generally ignored the reactor-relevancy of the divertor and first-wall material and operating characteristics. Results from C-Mod, found during the current 5 year plan, indicate that we are far from being confident that the Demo requirements of tungsten tiles at high temperature (to anneal out neutron damage) can be compatible with low core W levels and low T retention in the PFCs. We see that gap in knowledge and understanding as a priority to address. More specific to C-Mod, our 5 year physics program calls for a combination of lower hybrid current drive ($\leq 3\text{MW}$), ICRF heating (6 MW), and steady-state density control with pulse length more than doubling to $\sim 4\text{ s}$ (see Table 4.A.1 in Appendix 4.A). Given that we already observe small melt areas of the divertor due to leading edge effects, the enhanced pulse lengths could lead to unacceptable divertor temperatures and damage (temperature rise is proportional to the square-root of pulselength) if efforts are not made to properly handle such deposited energies.

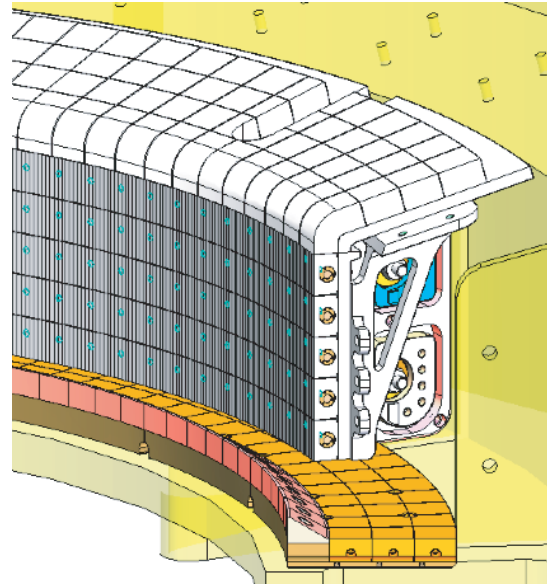


Fig.4.2.9: New lower outer divertor including tungsten lamella tiles in the high heat flux region (vertical section)

the square-root of pulselength) if efforts are not made to properly handle such deposited energies.

In the 2008-11 time frame, we will concentrate our efforts on developing and installing a new outer divertor optimized for addressing high power, long-pulse discharges with reactor-relevant materials and tile geometries. The divertor will also be optimized for both hydrogenic fuel retention studies as well as understanding the potential issues of operating W lamellae tiles under high heat fluxes at high temperature (Fig. 4.2.9). The first, and potentially most important, step will be the removal of leading edges in the high heat flux region. The current 5 large (8-10 cm) and 5 small (0.5 cm) toroidal gaps between the 10 divertor modules will be reduced to $\sim 1\text{ mm}$. This will be accomplished with 2 changes: 1) eliminate diagnostic openings in the high heat bearing vertical surface and 2) allow the outer divertor to expand in major radius with temperature increase while keeping its alignment from one module to the next. To estimate the average divertor temperature we assume that the outer divertor only loses heat through radiation between discharges (20 minutes) assuming an emissivity of 0.15 (mid-range for that given in the literature for Mo and W). The energy loss is then equated to the energy deposited during a discharge on the outer divertor, 1.5MW for 4 seconds, and a surface temperature of $\sim 600^\circ\text{C}$ is predicted. At that temperature ($\sim 600^\circ\text{C}$) the toroidal arclength of each module will be increased by 4 mm corresponding to an increase in major radius of 6.4 mm.

While the above calculation shows that in our highest energy deposition conditions the bulk outer divertor temperature will ratchet up to $\sim 600^\circ\text{C}$ over the course of a day we also want the capability to directly raise the divertor temperature for D retention and tungsten tile studies independent of the power loading. The heater/divertor design requirement is to reach as high as 600°C . It is well known that the diffusivity and surface recombination of hydrogenic species in Mo and W are exponentially increasing in temperature [61]. As discussed in section 4.2.6 higher tile temperatures allow us to access Demo-like regimes where the high D pressures in the near

surface which drive trap creation may be reduced by high diffusion into the bulk and recombination from the front surface. The new divertor temperature control capability will allow us to study this effect as a function of plasma flux/fluence and bulk/surface temperature.

The high temperatures of the outer divertor will also allow us to access W material properties above the ductile to brittle transition (DBTT) for tungsten (400 °C) and for molybdenum (~ room temperature). Thus the operation at a variety of temperatures will allow us to study the capability of the different materials to withstand thermal and mechanical shocks as their ductility varies.

Issue/topic/objective	Approach	Diagnostics/facilities
Develop divertor shape, tiles and configuration that supplies R&D information for ITER and beyond	Eliminate toroidal gaps in high-heat flux region	Demo-like divertor ('11); IR ('09) and calorimeter measurements ('11)
	Experience with manufacture & use of tungsten-lamella tiles	
	Operation at reactor-like temperatures (600 °C)	

4.2.6 Plasma-Facing Materials

Deuterium Fuel Retention - Based on concerns about tritium fuel retention in ITER (a safety issue) and relevance to eventual reactor operation, the tokamak and surface science community has been examining whether refractory metals, such as Mo and W, are truly significantly better than carbon plasma-facing components with respect to fuel retention. It is widely accepted that codeposition of fuel in carbon films is the primary reason for high fuel retention in carbon-clad tokamaks. In contrast, there is little tokamak experience concerning fuel retention with bulk high-Z refractory metals. As reported in section 4.1.3 C-Mod has already contributed to characterization of D retention in high-Z PFCs through experiments with Mo which, from the point of view of hydrogenic retention, is expected to be very similar to tungsten. *This research will continue to be a central focus of our program in the next 5 years.*

The current model of retention in C-Mod is that during intense plasma bombardment, as occurs in the divertor, recombination back into volatile molecular form at the material surface exposed to the plasma-interaction limits the loss of D from within the bulk material. This leads to D atom buildup near the surface and to high neutral pressures there, which in turn causing damage to the lattice and thus creating locations for D atoms to reside - so-called 'traps'. Such traps lead to long-term retention because the corresponding potential wells of the traps are much deeper than the thermal energy of the D atom; it cannot escape and diffuse to the surface without significant heating. In C-Mod, the retention of incident ion flux is typically in the range of 1-2% when averaged over all surfaces. The tokamak D retention rates (fraction of incident ion flux retained) inferred in C-Mod are at least an order of magnitude higher than those found in controlled laboratory experiments. A second difference to laboratory experiments is that the C-Mod retention shows a linear scaling with fluence whereas in laboratory experiments the scaling is in the range of the 0.5 to 0.7 power of the fluence. Our present judgment is that the above

differences between C-Mod and laboratory experiments could be due to several factors: 1) modification of the surface (impurities, roughness, damage) which could lead to changes in retention and/or recombination, 2) different structural makeup for the Mo and W, and 3) larger flux densities in C-Mod ($\leq 10^{24}/\text{s}/\text{m}^2$) in comparison to the ion beam experiments ($10^{19} - 10^{22}/\text{m}^2/\text{s}$). The creation of traps could be non-linear in flux density (and thus the D density within the surface).

The issue of surface effects will be addressed both with C-Mod experiments and through ex-situ laboratory experiments. Tiles exposed to C-Mod plasmas for a minimum of one campaign will be removed from C-Mod and used in retention experiments on linear devices with reasonably high flux densities - PISCES (UCSD) and PILOT-PSI (FOM). Retention for the C-Mod modified surfaces, and for polished surfaces, will be compared under plasma conditions similar to those in C-Mod. Finally, the retention as a function of depth in the tile will be measured with ion-beam analysis techniques and the D content integrated through the tile profile compared to that inferred from complete removal of the D retained through heating (Thermal Desorption Spectra or TDS). This work will be performed early in the 5 year period of this proposal.

We plan to monitor the surface composition and D retention in the surface directly using the new accelerator (RFQ) and ARRIBA diagnostics (see 4.2.3 for details). These diagnostics will come online for daily utilization 2-3 years into the 5 year research period and will allow direct in-situ interrogation of some fraction of the C-Mod tiles for D retention (with depth resolution) as well as the surface impurities. Then, as the surface conditions change, either through our intervention (e.g. boronization) or slowly over time through the migration of impurities around the vacuum vessel, we can correlate the differences in retention with the changes in surface condition.

The C-Mod divertor currently has one toroidal row of tungsten tiles in the high heat flux region. A first step in the comparison of W and Mo will be to remove tiles of both materials that have received similar particle fluences and study them using ion beam analysis ex-situ in the CLASS ion-beam facility (see below). As discussed above, when they become available, we will be able to monitor the differences directly as a function of time using the RFQ and ARRIBA diagnostics. Several years into the 5 year period we will first add additional W tile rows then later replace the outer divertor, the latter placing W tiles all through the high heat flux region of the outer divertor (see Section 4.2.5). In the case where the W tiles are only 2 adjacent rows we can then compare retention with the strike point on either the W vs Mo tiles there. When all the tiles are replaced with W we will compare retention between putting the strike point on the lower vs upper divertor (which is still planned to be Mo).

We need to better understand the D retention process with the goal of controlling it as well as extrapolating to ITER and reactor operation. We believe subjecting surfaces exposed to C-Mod plasmas to ITER-like conditions – primarily higher temperature and fluence – would be the best plan of study. This will be done with tiles removed from C-Mod and subsequently exposed to PISCES or PILOT-PSI plasmas, with retention measured as a function of fluence and temperature. In parallel we plan to vary the tile temperatures in C-Mod in the “Demo-like divertor” (Section 4.2.5). The outer divertor (‘11), where the W-lamellae tiles will be installed, will be heatable up to the range of 600 C, close to reactor-level temperatures. At higher temperatures, diffusivity and detrapping of D is much higher, which may allow for demonstration of D fuel recovery from the divertor. Also important, the surface recombination rate will increase by orders of magnitude, which could lead to a removal of the D trap formation by ion-irradiation described earlier and hence could dramatically reduce fuel retention.

We will explore the effect of strong divertor pumping on both fuel retention and H isotope recovery by exploiting the relatively new upper divertor cryopump. The cryopump provides the capability to make discharges with controlled density, but with substantially larger fuelling rates. In fact, the cryopump has already demonstrated a pump rate ~ 150 Torr-L/s at fixed plasma density with puffing, a fuelling rate ~ 10 times that required for ITER when normalized to plasma

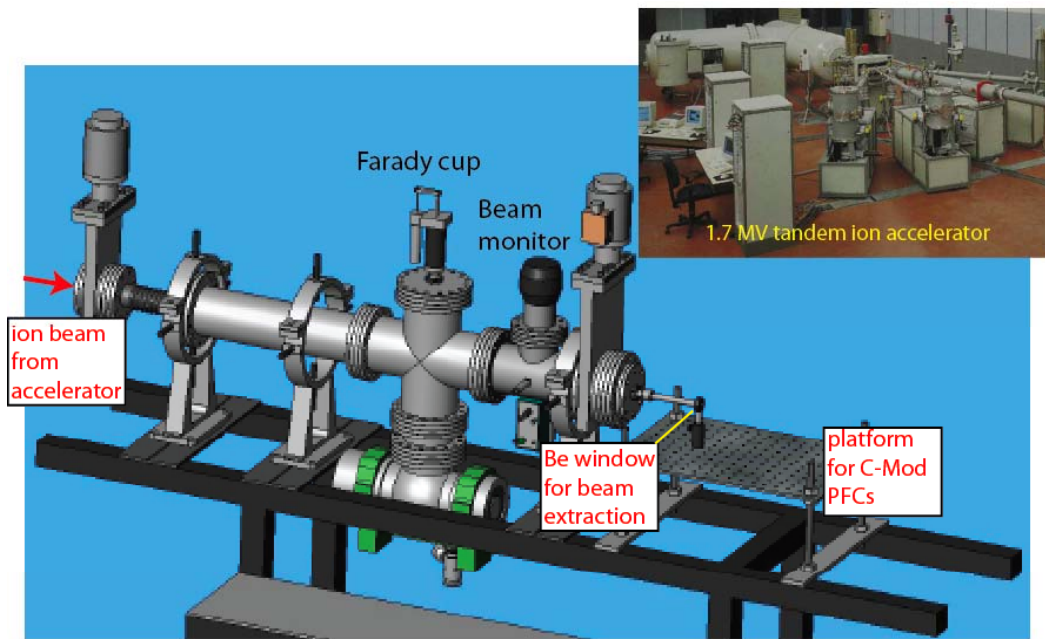


Fig.4.2.10 : External ion beam setup where C-Mod PFCs can undergo ion beam analysis in atmosphere. The insert shows the 1.7 MV tandem ion accelerator used in the CLASS facility at MIT.

size. This provides an interesting new tool to explore the physics of fuel retention in the C-Mod walls. For example, a key issue is enhancing H removal after vents to reach the levels of hydrogen fraction ($\sim 5\%$) required for efficient ICRF minority heating. The walls hold large amounts of water, which comes out at a sufficiently slow rate that weeks of regular discharges are required to reach this level. It is likely the H recovery can be enhanced by circulating D at a much faster rate through they system, since it appears from gas analysis that isotope exchange is the principal means to recover H. We will also explore the use of the cryopump to recover fuel previously retained in the wall, as was demonstrated on DIII-D [62].

Ex-situ surface analysis of plasma-facing components - The ability to analyze C-Mod PFC surfaces ex-situ will be greatly enhanced by the initiation of our new Cambridge Lab for Accelerator Studies of Surfaces (CLASS). The facility features a 1.7 MV tandem ion accelerator with dual sources (plasma and sputtering). This allows for an extremely wide variety of surface analysis techniques including Ruther Backscattering Spescctroscopy (for depth resolved film analysis), Elastic Recoil Detection (for surface H/D content) and Nuclear Reaction Analysis (for isotope sensitive depth profiling, and in particular, deuterium). CLASS is located in the building adjacent to C-Mod, making it extremely efficient to transport and analyze a large number of C-Mod PFC tile surfaces during vents. In addition, a dedicated “external” beam is being developed at CLASS in order to provide analysis of large PFC sections (Fig. 4.2.10). The external beam brings a proton beam through a thin window and a short distance of atmosphere, and onto the

surface. Beam induced gamma emissions are detected in order to measure quantities of interest, such as boron film thickness, in as little as a few seconds. Without the requirement for placing the PFCs under vacuum, it will be possible to rapidly produce 2-D “maps” of the surface quantities and fuel retention on PFC components while they are still mounted on support hardware and thus in the same orientation as in C-Mod. This will be very useful in assessing the poloidal and toroidal patterns of erosion and deposition, including considerations typically ignored such as the effects of leading edges.

Wall conditioning: boronizations & ECDC plasmas - Conditioning of the PFCs is a critical aspect for successful utilization of tokamaks. This is particularly true for C-Mod where, with the exception of the proposed actively heated divertor (4.2.5), the in-vessel temperature is limited to ~ 60-120 C. This low temperature makes preparation of the PFC surfaces for plasma operations more difficult, since it is too low for substantial cleaning of the surfaces through outgassing of the usual vacuum surface impurities (water, CO, hydrocarbons, etc.). Also, the influx of high-Z Mo from the walls and the accumulation in the core is well documented as an impediment to good plasma performance [24]. The two major conditioning techniques in use on C-Mod are ECDC (electron cyclotron discharge cleaning) and boronization film deposition. (We note that the two techniques are linked since boronization is accomplished with a high gas pressure ECDC plasma with 90% He – 10% diborane mixture.) The present system features ~ 2.3 kW of RF waves (2.45 GHz) launched into the vessel. A steady-state toroidal field (<0.1 T) is applied and varied to control the major radius of the EC resonance [63].

We propose to increase the available power, and possibly the frequency, of the ECDC system in order to substantially improve several aspects of PFC conditioning in C-Mod, which we now describe.

The higher power ECDC will allow for more aggressive discharge cleaning of the PFC surfaces between discharges and following vents. First of all, a simple argument is that more RF power will allow us to raise the surface temperature of tiles at regions of intense ECDC plasma ion flux, which is beneficial for H isotope removal and surface conditioning. We will also plan to improve recovery from disruptions using higher power ECDC. Following disruptions the combination of a varying current evolution, and the thick, conducting C-Mod vacuum vessel, often results in loss of position control and premature termination of the plasma, known as a “fizzle”. It often takes 2-3 fizzles after high current disruptions ($I_p > 1.2$ MA) before plasmas are recovered; this poses a serious loss of operational availability. Therefore solving fizzles with more aggressive wall conditioning to recover more constant surface conditions would be of great benefit to C-Mod. In addition such a demonstration will be of great interest to ITER which faces a nearly identical situation in recovering from disruptions: nearly all metal-walls, thick conducting vacuum vessel, and the requirement of PFC conditioning with magnetic field present.

The upgraded ECDC system should also provide better capabilities for boronization; namely higher deposition rates that are more localized to specific areas of the PFCs. Boronization is also being used as a tool for determining where the ICRF-derived erosion is strongest and affecting the plasma most (section 4.2.3). Lastly, it is being used in cases where core transport studies are the highest priority and the wall material is not of interest. Over the last year the Surface Science Station has revealed some important, and unexpected, aspects of boronization that indicate how to better optimize boron film deposition (Figure 4.2.11). It was observed that B film growth rate was strongly correlated only to local ion flux density, i.e. ionic deposition of B⁺ dominates over neutral B deposition. The magnitude of deposition (nm / min) directly increases

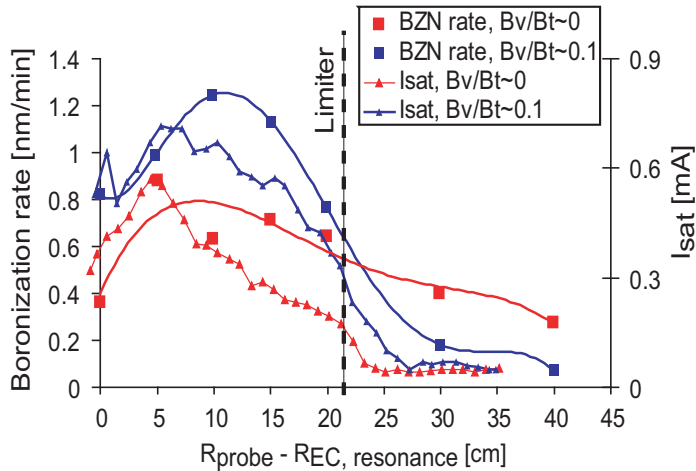


Figure 4.2.11: Surface Science Station diagnosis of boronization profiles vs. R . The measured B films deposition rate is found to be strongly correlated to the local ion flux density, I_{sat} . The addition of a vertical field (10% of toroidal field) increased ECDC plasma, and hence boronization rate.

the plasma density has become limited by ionization rather than total particle throughput. Increasing the RF power should increase the deposition rate.

One short-term solution for constant clean plasma conditions for core transport studies is to *use routine between-discharge boronization* occasionally during a run-day to keep the core Mo radiation low. Increasing the peak deposition rate by even a factor of two, to ~ 5 nm/minute, would have a significant impact on the ability to routinely apply substantial films (~ 25 - 50 nm) with between-shot boronizations without adversely impacting the tokamak operation. To obtain the higher density and B film growth rate needed for these higher boronization rates, we need more ionization through higher RF power, with vertical field applied. However, this may have limits with respect to improving localization of the films because the UH resonance location separates further from the EC resonance with increasing density, tending to broaden the plasma profile (Fig. 4.2.13). Therefore we will investigate the use of 2nd harmonic EC plasmas and/or higher frequency RF sources. If successful, this would reduce the radial footprint of the boronization film to < 10 cm, which would be greatly beneficial for avoiding film deposition in unwanted locations. Beyond the obvious benefits to operations, a more “precise” boronization tool will be helpful in better establishing those locations where Mo erosion adversely affects core performance. Finally, demonstrating effective ways of applying coating films with magnetic field present could be of great interest to ITER and other super-conducting devices.

with increasing flux density. The application of vertical field ($\sim 10\%$ of the toroidal field), by forcing the “draining” of plasma along B, caused the plasma radial width to decrease and typically peak the plasma density. Importantly, the peak plasma density ($\sim 2 \times 10^{16} \text{ m}^{-3}$), and hence peak B deposition rate, was not found at the electron cyclotron resonance, but rather ~ 10 cm outboard at the upper hybrid (UH) resonance [64]. Diagnosis showed that the plasma density and B film growth rate increased with increasing gas throughput, up to as much as 2.5 nm/minute B film growth rate, until a pressure ~ 10 mTorr was reached, beyond which the density and growth rates decreased. This indicates that

Table 4.2.6 – Plasma-facing materials research thrusts			
Issue/topic/objective	Approach	Diagnostics/facilities	Modeling
Understand why D retention in C-Mod is much greater than predicted by lab ion-beam experiments	Surface impurities - abrade mixed B/Mo layer before run period	Up-to-air access to C-Mod tiles in vessel	Utilize in-house model of D transport in Mo/B
	Lab studies of tiles exposed to C-Mod plasmas	CLASS ('09); PILOT-PSI ('09); DIONISOS ('10)	
	In-situ analysis of tile surface impurities and retention	RFQ ('10); ARRIBA ('10)	
Are there inherent differences between Mo and W for retention?	Operate with strike point on W tile rows vs. Mo tile rows	2 nd row of W tiles in lower divertor ('10)	In-house model, DIFFUSE, TMAP (Causey)
	Compared global retention and core impurities	Demo-like all-W heated divertor ('11)	
What are the roles of temperature, ion flux and/or fluence in affecting retention?	Vary the flux/fluence in C-Mod by varying operational parameters	Global retention; RFQ for local retention ('10)	
	C-Mod tiles studied in ex-situ lab	CLASS ('09), PILOT ('09)	
	Vary the ambient divertor temperature during operations	Demo-like divertor ('11)	
Optimize conditioning & boronization for C-Mod operations	Increase speed of boronization; Optimized boronization thickness in localized regions	Higher power ECDC ('10)	In-house Monte-Carlo boron deposition model
	Localize conditioning	Higher frequency RF for ECDC ('11)	

4.2.7 Relationship of boundary plans to FESAC 2007 "Priorities, Gaps and Opportunities" panel report

C-Mod's plasma boundary research program is aimed at solving a number of issues that must be confronted before building a full-scale reactor. As such, the program squarely addresses a number of "scientific and technical questions which must be answered before we are ready to proceed to Demo," as outlined in the recent FESAC report, with a heavy focus on theme B: "Taming the material surface". Below we outline which parts of our plan address the issues within the various themes: A "Creating predictable high-performance steady-state plasmas", B "Taming the plasma material interface", and C "Harnessing fusion power".

A.1 'Validated Theory and Predictive Modeling' - All of our studies in transport, divertor

physics, plasma-material interaction, and plasma-surface interaction have goals of both making direct connections to the underlying theory (e.g. $\alpha_{\text{MHD}}/\Lambda$, physical sputtering) and working with modelers to match the unique data that C-Mod can provide (e.g. turbulence characteristics, divertor Lyman series trapping, ...).

A.6 ‘Plasma Modification by Auxiliary Systems’: *Establish the physics and engineering science of auxiliary systems which can provide power, particles, current and rotation at the appropriate locations in the plasma at the appropriate intensity* - Our emphasis in Plasma-surface interactions (4.2.3) is aimed at understanding how the RF affects the plasma and how the plasma affects the RF with the goal of minimizing the deleterious effects commonly associated with RF (e.g. enhanced sheaths, non-thermal populations in the SOL).

B.8 ‘Plasma-Wall Interactions’: *Understand and control of all processes which couple the plasma and nearby materials* - Certainly the studies included in plasma-surface interactions (4.2.3) aimed at understanding and controlling the Mo sputtering are part of this mission. In addition, the general transport studies (4.2.2) and divertor physics (4.2.4) are aimed at predicting the plasma characteristics (particle and energy flux, energy distribution) at the material interface.

B.9 ‘Plasma Facing Components’: *Understand the materials and processes that can be used to design replaceable components which can survive the enormous heat, plasma and neutron fluxes without degrading the performance of the plasma or compromising the fuel cycle* - The Demo-like divertor (4.2.5) is directly aimed at divertor and tile design and development. Plasma facing materials (4.2.6) is aimed at developing the tools to better understand how those components fare in a plasma. Implicit in this issue is the question of fuel retention, which is clearly a central emphasis at C-Mod as described in 4.2.6 (Plasma-facing materials)

B.10 ‘RF Antennas, Launching Structures and Other Internal Components’: *Establish the necessary understanding of plasma interactions, neutron loading and materials to allow design of RF antennas and launchers, control coils, final optics and any other diagnostic equipment which can survive and function within the plasma vessel* - The study of Plasma-surface interactions (4.2.3) addresses important aspects of the plasma effects on internal components.

Lastly - the FESAC panel discussed the gap - *G-11. Understanding the elements of the complete fuel cycle particularly tritium breeding and retention in vessel components*. The addition of the Demo-like divertor (4.2.5) to our program directly addresses that gap.

4.2.8 Relative priorities of boundary program and relation to incremental budget

The planned boundary physics program encompasses research over a wide range of topics. The near-term research is enabled by our investments in the most-recently-installed diagnostics. As a result, the near-term emphasis is concentrated more on transport studies with an evolving emphasis on studies of plasma-facing materials and plasma-surface interactions. With respect to these latter issues, which have some urgency for input into the ITER design and research plan, we are looking forward to the installation of several important diagnostic tools including the new Demo-like divertor, the new SOL Thomson diagnostic and the RFQ PSI diagnostic. These will allow detailed measurements of fuel retention (RFQ), SOL power flow and divertor heat footprints (new divertor and SOL Thomson). Together with the new sheath-rectification diagnostics (emissive probes, spectroscopic and imaging diagnostics), we will begin to ramp up a program to investigate surface erosion/redeposition and the physics of RF-enhanced erosion of

surfaces.

Additional monies associated with the incremental budget would have a strong impact on our program. Our schedule calls for a significant R&D effort and capital expenditure, particularly for the new Demo-like divertor and the SOL Thomson systems, with the research time-line being set primarily by the design/fabrication/installation cycle of these elements. Incremental funding for such systems would minimize risk and ensure a timely development, with a higher chance that the results will be available for ITER decisions in a timely manner. At the same time, the research staff required to implement the planned diagnostics, maintain existing diagnostics and to execute the experimental program is also a limiting factor, with the ever-changing population of graduate students being an uncertain variable. In this regard, additional monies for staff and students would certainly enable a more aggressive and effective boundary research program in C-Mod, leading to both a better implementation/utilization of the planned diagnostics set and a better exploitation of C-Mod's unique research opportunities.

4.A Appendix for Plasma Boundary

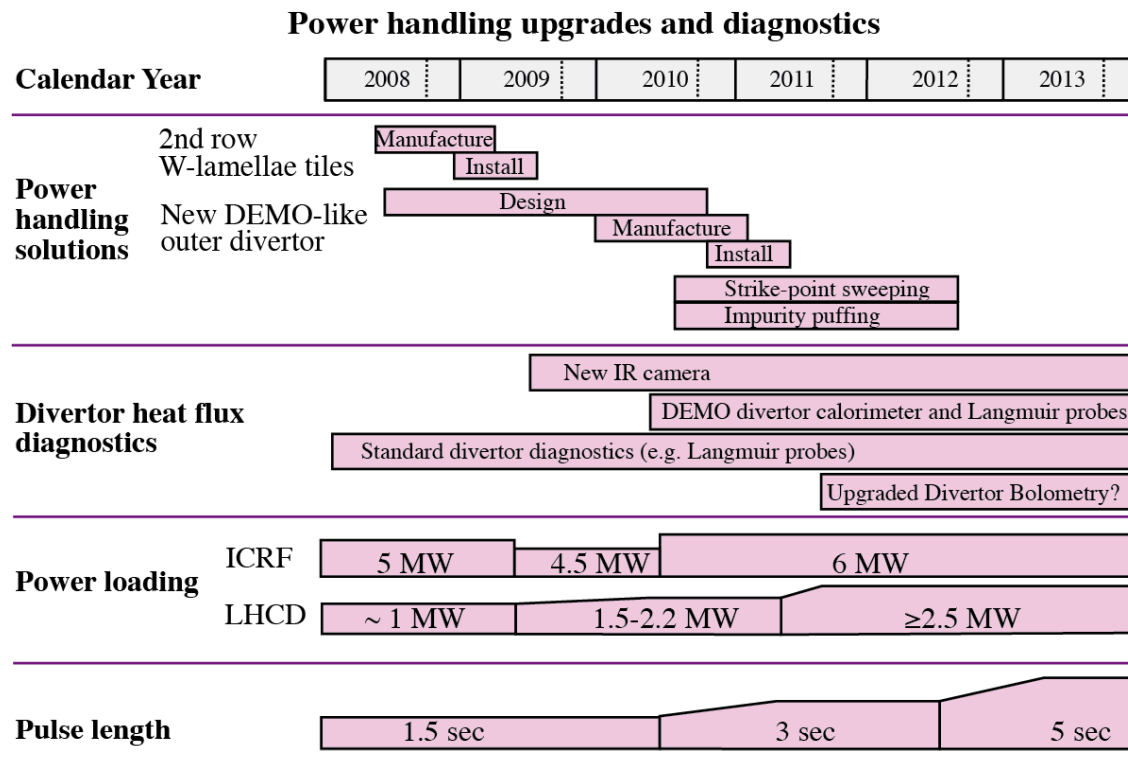


Table 4.A.1 Timeline for power handling upgrades and diagnostics.

Chapter 4 References

- [1] J. L. Terry, B. LaBombard, B. Lipschultz, M. J. Greenwald, J. E. Rice, and S. J. Zweben, *Fusion Science and Technology* **51**, 342 (2007).
- [2] B. LaBombard, J.W. Hughes, D. Mossessian, M. Greenwald, B. Lipschultz, and J.L. Terry, *Nuclear Fusion* **45**, 1658 (2005).
- [3] B. LaBombard, J. W. Hughes, N. Smick *et al.*, *Physics of Plasmas* **15**, 056106 (2008).
- [4] B. Scott, *Plasma Physics and Controlled Fusion* **39**, 1635 (1997).
- [5] B. N. Rogers, J. F. Drake, and A. Zeiler, *Physical Review Letters* **81**, 4396 (1998).
- [6] J. W. Hughes, B. LaBombard, J. Terry, A. Hubbard, and B. Lipschultz, *Nuclear Fusion* **47**, 1057 (2007).
- [7] B. LaBombard, M. Greenwald, R. Boivin *et al.*, "Density Limit and Cross-Field Edge Transport Scaling in Alcator C-Mod," in *Fusion Energy 2002* (Vienna: IAEA, Lyon, 2002), Vol. CD ROM file EX/D2-1 and http://www-pub.iaea.org/MTCD/publications/PDF/csp_019c/html/node120.htm.
- [8] P. N. Guzdar, R. G. Kleva, P. K. Kaw, R. Singh, B. LaBombard, and M. Greenwald, *Physics of Plasmas* **14**, 020701 (2007).
- [9] B. LaBombard, J. E. Rice, A. E. Hubbard *et al.*, *Nuclear Fusion* **44**, 1047 (2004).
- [10] B. LaBombard, J. E. Rice, A. E. Hubbard *et al.*, *Physics of Plasmas* **12**, 056111 (2005).
- [11] J.E. Rice, R.L. Boivin, P.T. Bonoli *et al.*, *Nuclear Fusion* **41**, 277 (2001).
- [12] O. Grulke, J L Terry, B LaBombard, and S. Zweben, *Physics of Plasmas* **13**, 012306 (2006).
- [13] S. I. Krasheninnikov, *Physics Letters A* **283**, 368 (2001).
- [14] J.L. Terry, S.J. Zweben, O. Grulke, M.J. Greenwald, and B. LaBombard, *Journal of Nuclear Materials* **337-339**, 322 (2005).
- [15] I. Cziegler, J.L. Terry, and B. LaBombard, *Bull. Amer. Phys. Soc.* **52**, 230 (2007).
- [16] J. L. Terry, S. J. Zweben, K. Hallatschek *et al.*, *Physics of Plasmas* **10**, 1739 (2003).
- [17] O. Grulke, *Bull. Am. Phys. Soc.* **49**, 59 (2004).
- [18] B. D. Scott, *Physics of Plasmas* **12**, 102307 (2005).
- [19] B. Lipschultz, D. Whyte, and B. LaBombard, *Plasma Physics and Controlled Fusion* **47**, 1559 (2005).
- [20] B. Lipschultz, P. Andrew, J. P. Coad *et al.*, "A Study of JET SOL Radial Transport Based on Particle Balance," in *Controlled Fusion and Plasma Physics* (European Physical Society, Geneva (2003), St. Petersburg, 2003), Vol. 27A, pp. 3.197.
- [21] D. G. Whyte, B. Lipschultz, P. C. Stangeby, J. Boedo, D.L. Rodakov, J. G. Watkins, and W. P. West, *Plasma Phys. & Cont. Fusion* **47**, 1579 (2005).
- [22] A. W. Leonard, J. A. Boedo, M. Groth, B. L. Lipschultz, G. D. Porter, D. L. Rudakov, and D. G. Whyte, *Journal of Nuclear Materials* **363-365**, 1066 (2007).
- [23] B. Lipschultz, X. Bonnin, G. Counsell *et al.*, *Nuclear Fusion*, 1189 (2007).
- [24] B. Lipschultz, Y. Lin, M. L. Reinke *et al.*, *Physics of Plasmas* **13**, 56117 (2006).
- [25] B Lipschultz, Y. Lin, E S Marmor *et al.*, *Journal of Nuclear Materials* **363-365C**, 1111 (2007).
- [26] S Wukitch, B Lipschultz, E S Marmor, Y. Lin, A. Parisot, M. L. Reinke, J. Rice, J L Terry, and C-Mod team, *Journal of Nuclear Materials* **363-365C**, 491 (2007).
- [27] B. Lipschultz, D. A. Pappas, B. LaBombard, J. E. Rice, D. Smith, and S. J. Wukitch, *Nuclear Fusion* **41**, 585 (2001).

- [28] R. Causey, K. Wilson, T. Venhaus, and W.R. Wampler, *Journal of Nuclear Materials* **266-269**, 467 (1999).
- [29] D. Whyte, B Lipschultz, J. Irby, R. Granetz, B LaBombard, J L Terry, and G.M. Wright, "Hydrogenic Fuel Recovery and Retention with Metallic Plasma-Facing Walls in the Alcator C-Mod Tokamak," in *21st IAEA Fusion Energy Conference* (Chengdu, China, 2006), pp. EX/P4-29.
- [30] B. Lipschultz, B. LaBombard, J. L. Terry, C. Boswell, and I. H. Hutchinson, *Fusion Science and Technology* **51**, 369 (2007).
- [31] S. Lisgo, P. Borner, C. Boswell *et al.*, *Journal of Nuclear Materials* **337-339**, 139 (2005).
- [32] C.J. Boswell, J.L. Terry, B. LaBombard, B. Lipschultz, and J.A. Goetz, *Journal of Nuclear Materials* **290-293**, 556 (2001).
- [33] R. McDermott, B Lipschultz, K. Marr, D. Whyte, and J W Hughes, *Bull. Amer. Phys. Soc.* **52**, 213 (2007).
- [34] A. Graf, M. May, P. Beiersdorfer, D. Whyte, B. LaBombard, N. Smick, and K. Marr, *Bull. Amer. Phys. Soc.* **52**, 214 (2007).
- [35] K. Marr, B Lipschultz, and R. McDermott, *Bull. Amer. Phys. Soc.*, NP8.00079 (2007).
- [36] N. Smick and B. LaBombard, *Bull. Amer. Phys. Soc.* **51**, 243 (2006).
- [37] P.N. Guzdar, R.G. Kleva, A. Das, and P.K. Kaw, *Physical Review Letters* **87**, 015001 (2001).
- [38] B. LaBombard and L. Lyons, *Rev. Sci. Instrum.* **78**, 073501 (2007).
- [39] L. Lyons, "Construction and operation of a Mirror Langmuir Probe Diagnostic for the Alcator C-Mod Tokamak," Masters Thesis, MIT, 2007.
- [40] B. D. Scott, *Physics of Plasmas* **12**, 062314 (2005).
- [41] A Yu Pigarov, S. Krasheninnikov, B LaBombard, and T. Rognlien, *Bull. Am. Phys. Soc.* **52**, 231 (2007).
- [42] Peter J. Catto and Andrei N. Simakov, *Physics of Plasmas* **13**, 052507 (2006).
- [43] D. Ryutov and R.H. Cohen, to be published in *Contrib. to Plasma Phys.* **48** (2008).
- [44] R. H. Cohen, B. LaBombard, D. D. Ryutov, J. L. Terry, M. V. Umansky, X. Q. Xu, and S. Zweben, *Nuclear Fusion* **47**, 612 (2007).
- [45] O.E. Garcia, V. Naulin, A.H. Nielsen, and J.J. Rasmussen, *Physical Review Letters* **92**, 165003 (2004).
- [46] X. Q. Xu, W. M. Nevins, R. H. Cohen, J. R. Myra, and P. B. Snyder, *New Journal of Physics* **4** (2002).
- [47] P. Scarin, of the RFX Team, private communication (2007).
- [48] J L Terry, N P Basse, I. Cziegler *et al.*, *Nuclear Fusion* **45**, 1321 (2005).
- [49] Farrokh Najmabadi, A. Abdou, L. Bromberg *et al.*, *Fusion Engineering and Design* **80**, 3 (2006).
- [50] A. Kallenbach, N. Asakura, A. Kirk, A. Korotkov, M.A. Mahdavi, D. Mossessian, and G.D. Porter, *Journal of Nuclear Materials* **337-339**, 381 (2005).
- [51] D. Whyte and B Lipschultz, "Scaling of upstream $q//$," in *ITPA divertor/SOL meeting* (Garching, Germany, 2007).
- [52] A. Loarte, S. Bosch, A. Chankin *et al.*, *Journal of Nuclear Materials* **266-269**, 587 (1999).
- [53] J. G. Watkins, C. J. Lasnier, D. G. Whyte, P. C. Stangeby, and M. A. Ulrickson, *Rev. Sci. Instrum.* **74**, 1574 (2003).
- [54] D. Buchenauer, J. W. Cuthbertson, J. A. Whaley, J. D. Miller, J. G. Watkins, R. Junge, W. P. West, and D. N. Hill, *Rev. Sci. Instrum.* **66**, 827 (1995).

- [55] S. Gangadhara, B LaBombard, B Lipschultz, and N. Pierce, *Bull. Am. Phys. Soc.* **41**, 1550 (1996).
- [56] P. C. Stangeby, J. G. Watkins, G. D. Porter, J. D. Elder, S. Lisgo, D. Reiter, W. P. West, and D. G. Whyte, *Journal of Nuclear Materials* **290-293**, 733 (2001).
- [57] M. W. Thompson, *Philosophical Magazine* **18**, 377 (1968).
- [58] J. N. Brooks and D. G. Whyte, *Nuclear Fusion*, 525 (1999).
- [59] A. Yu Pigarov, S. I. Krashennnikov, T. K. Soboleva, and T. D. Rognlien, *Physics of Plasmas* **12**, 122508 (2005).
- [60] J. A. Goetz, B. LaBombard, B. Lipschultz *et al.*, *Physics of Plasmas* **6**, 1899 (1999).
- [61] G. Wright, "The dynamic of hydrogen retention in irradiated molybdenum," Ph.D. Thesis, U. Wisconsin, 2007.
- [62] R. Maingi, G. L. Jackson, M. R. Wade, M. A. Mahdavi, P. K. Mioduszewski, G. Haas, M. J. Schaffer, J. T. Hogan, and C. C. Klepper, *Nuclear Fusion*, 245 (1996).
- [63] R. T. Nachtrieb, B. L. LaBombard, J. L. Terry, J. C. Reardon, W. L. Rowan, and W. R. Wampler, Elsevier. *Journal of Nuclear Materials* **266-269**, 896 (1999).
- [64] R. Ochoukov, B. Lipschultz, D. Whyte, N. Gierse, and S. Harrison, *Bull. Amer. Phys. Soc.* **52**, 216 (2007).

5 Wave Plasma Interactions

C-Mod exclusively uses RF for auxiliary heating (ion cyclotron range of frequency - ICRF) and current drive (lower hybrid range of frequency - LHCF) to heat and drive current for a wide range of plasma conditions. Both ICRF and LHCF are considered excellent candidates for future reactors and experiments, like ITER, for providing bulk heating[1] and current drive, respectively. For ICRF, the primary reason is that ICRF has been experimentally demonstrated to heat high performance plasmas on numerous experiments including deuterium-tritium discharges on TFTR[2] and JET[3], and has favorable scaling to burning plasmas. The LHCF has been demonstrated to provide efficient auxiliary current drive[4] and has been utilized in high confinement discharges with modified shear profiles[5]. We seek to develop an understanding of the underlying physics and technological issues associated with high power ICRF and LHCF operation. C-Mod is an excellent facility to investigate a number of unresolved physics and technological issues since the wave characteristics in C-Mod are similar to those expected in ITER. In ICRF, the single pass absorption in H minority heating in C-Mod can be more than 80%, similar to the expected single pass absorption in ITER. In the LHCF, the C-Mod system is optimized for off-axis current drive and operates at the ITER B-field and density resulting in similar wave accessibility and absorption physics as expected in ITER. Thus, the C-Mod experiments are well positioned to contribute to the evaluation of LHCF physics for ITER. Furthermore, C-Mod has several advanced diagnostics for RF wave fields and deposition that facilitate experimental verification of advanced simulation tools through collaboration with the SciDAC Center for Simulation of Wave Plasma Interactions (CSWPI).

5.1 ICRF

5.1.1 Research Highlights

5.1.1.1 Antenna coupling and Antenna/Plasma interactions

The application of ICRF for plasma heating and current drive is complicated by a number of physics and technological issues. We have investigated an array of topics in an effort to improve our understanding and operational capability. In C-Mod, we have operated two 2-strap (D and E antennas) and a 4-strap (J antenna) antenna at high power density ($>10 \text{ MW/m}^2$) and are expecting to install a new four strap antenna in FY09. The present antennas have the current world record for power density of any 4 strap antenna under all plasma conditions and we have the highest power density for a 2 strap antenna into H-mode.

The compatibility of high power ICRF with all metal plasma facing components (PFC) and high plasma performance is a critical issue for C-Mod and future devices, such as ITER. The key to high plasma performance on C-Mod has been determined to be the control of impurities,

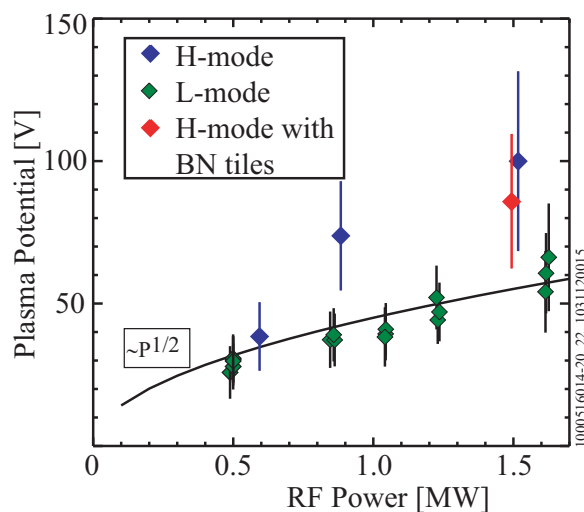


Figure 5.1.1: Plasma potential on magnetic flux tubes linked to the active antenna for H (blue) and L-mode (green) discharges with all metal PFCs and a representative H-mode with BN insulating tiles. The solid black line is proportional to the square root of the injected power.

particularly Mo, through boronization.[6] Experiments to identify the location of RF specific impurity sources showed that there are important molybdenum sources outside the divertor and away from the antenna and its limiters.[7] The mechanism is likely a result of enhanced sputtering due to RF sheaths resulting from rectified parallel electric, E_{\parallel} , fields generated by the RF.[8] In Figure 5.1.1, plasma potential measurements on field lines magnetically linked to the active antenna showed that the RF sheath is dependent on the plasma confinement mode, sheath voltage depended upon the square root of the RF power, and an RF sheath was still present with insulating limiter tiles. While the power dependence was expected, the dependence on confinement regime was unexpected and RF sheaths with an insulator is counter to previously published theoretical and experimental investigations.[9]

Antenna coupling has a significant impact on the antenna and matching network design, and ultimate voltage and power limits of an antenna. Therefore, understanding ICRF wave coupling physics and developing predictive tools, scalable to ITER and beyond, is critical for present and future ICRF utilization. Antenna coupling and the load presented by the antenna to the matching network depends primarily upon the edge density value and its profile.[10] The ICRF power, particularly at high power, modifies the edge plasma density and further complicates the coupling situation. In the ICRF regime, the wave is evanescent in the plasma edge, so-called evanescent layer, and begins propagating at the so-called cutoff density. In C-Mod, we have pursued both experimental parameter scans and numerical models to develop physical insight into the physics of ICRF antenna loading. A comparison of L and H-mode discharges, found that the H-mode loading variation is primarily determined by the H-mode pedestal height rather than the evanescent layer as observed in other experiments like DIII-D and Tore Supra.[11] Due sensitivity of sheath formation and electric characteristics to geometry, we have also collaborated with R. Maggiara of Politecnico de Torino on the experimental validation of an electromagnetic solver, TOPICA, that has a realistic ICRF antenna geometry coupled to a plasma full wave model, FELICE and TORIC. Initial comparison between experiment and simulation of the E antenna were encouraging.[12]

Plasma load variations are commonly encountered during L/H transitions and edge localized mode activity (ELM's). Recently, we have begun to study ELMs with fast digitizing of the reflection coefficient measurements. The relative perturbation of the reflection coefficient is dependent upon the ELM size and we can identify the so-called precursor, primary, and secondary ejections in the reflection coefficient time history. We also note that the time scale for the loading variation is faster than an L->H or H->L transition. We have investigated two strategies for maximizing delivered power to the plasma during load variations, both within a discharge and discharge to discharge. One was based on conjugate-T transmission line network. The system is passive and is based upon connecting two identical and independent antenna straps such that the reactive load variations essentially cancel at the input to the conjugate-T; thus the input impedance is resistive. We implemented such a network on the E antenna and found that the coupling between antenna elements was too strong resulting in destruction of load tolerance.[13] The loss of load tolerance was attributed to the strong coupling between the antenna straps.[14] Another approach is to deploy a real-time matching system to maximize the power transferred to the plasma by minimizing the VSWR. This system allows for improved experimental flexibility by allowing the antenna to be matched throughout a parameter scan, particularly density. We have implemented a fast ferrite, triple stub tuner (FFT) system into the E antenna matching network.[15] The origin of using ferrite tuning elements can be traced to work at DIII-D [16] and an initial implementation at ASDEX-U [17]. We have recently demonstrated the first successful implementation at high power (1.85 MW coupled) into H-mode and low VSWR maintenance over a wide range of

plasma conditions. Initial operation with ELMs shows that system matching was maintained throughout the discharge with low the reflection coefficient.

The voltage and power handling of an antenna can be limited by breakdown. In surveying antenna arc damage in C-Mod, DIII-D and ASDEX-U, the majority of the arc damage, and probable weak link, is located in the vacuum transmission line rather than the radiating element. We have a small test facility that can be operated with and without magnetic fields to investigate RF breakdown. Utilizing this test facility, we have identified that our operational antenna neutral pressure limits (voltage handling degrades to <10% of maximum) is a result of discharge formation. We also found that coaxial transmission line is more susceptible to multipactor than parallel plate transmission line with similar electrode spacing and a discharge will form at neutral pressures two orders of magnitude below the Paschen breakdown limit. In the presence of a B-field, the neutral pressure at which the discharge is initiated was further reduced for both coaxial and parallel plate transmission line geometry. We verified the test stand results with experiments on the C-Mod ICRF antennas where the antennas were operated into the tokamak backfilled with D₂ gas with and without a magnetic field found the discharge onset at nearly identical pressures as the observed neutral pressure limit.[18]

5.1.1.2 Propagation, Absorption and Mode Conversion Physics

C-Mod provides a unique opportunity to explore ICRF wave propagation, absorption, and mode conversion physics. These investigations are facilitated by a flexible ICRF system, access to sophisticated ICRF simulation codes (through CSWPI), and the availability of advanced diagnostics for RF wave measurements. Realizing high heating efficiencies in D(³He) discharges, where the single pass absorption is weak, is important for planned 2 MA, 8T operation in C-Mod and future experimental devices. We have observed that the heating efficiency is a sensitive function of the ³He fraction, more so than expected from theory and more sensitive than is observed for the H concentration in D(H). In L-mode, the heating effectiveness is similar to D(H) as determined by analysis of stored energy and H-mode thresholds.

We have extended the investigation of ICRF mode conversion and have made the first measurements of all three waves in the mode conversion region using Phase Contrast Imaging (PCI) diagnostic (DoE Diagnostic Initiative). Furthermore a synthetic PCI diagnostic has been implemented in TORIC in collaboration with the CSWPI.[19] The data

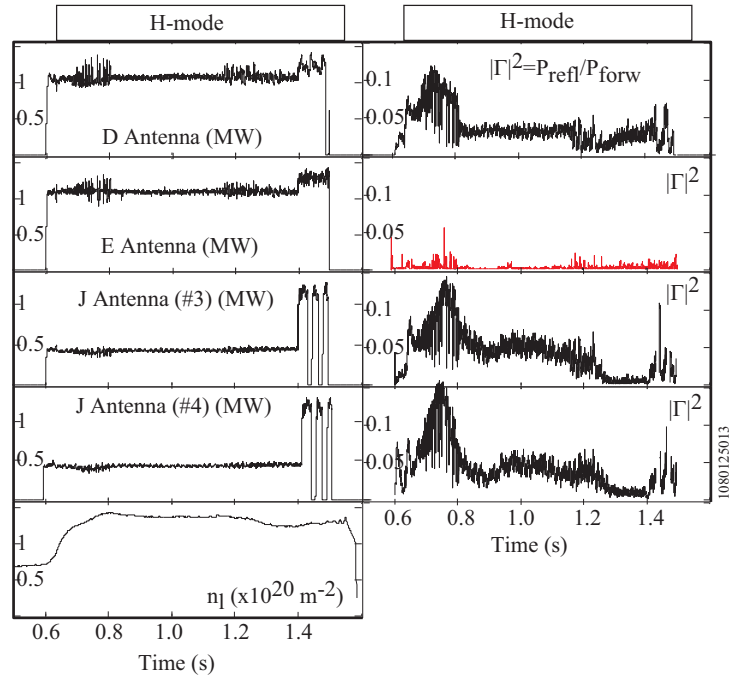


Figure 5.1.2: Comparison of the power reflection coefficient for a typical H-mode discharge highlighting the low power reflection coefficient maintained for the E antenna that utilizes the fast ferrite tuner system to maintain low reflections.

and simulation are in remarkable agreement suggesting that the physics model and numerical algorithm in TORIC models the mode conversion process very well.

We have investigated MCCD both experimentally and theoretically. We have found that MCCD is a good candidate for sawtooth pacing where the local current profile is modified to destabilize the sawteeth.[20] We have shown that the sawtooth period can be shortened or lengthened by changing the antenna phasing or deposition location. In Figure 5.1.3, the deposition location is just inside the $q=1$ surface and for counter (co-)current drive phasing the sawtooth period becomes longer (shorter) as

expected by modifying the local shear at the $q=1$ surface. Using a Fokker-Planck code (DKE [21]) to calculate the electron distribution function, we found that wave polarization and precise accounting of trapping reduced the expected driven current to ~ 50 kA for 3 MW power injected from previous estimate of 100 kA.[22] Previous work done on MCCD in TFTR [23] was simulated and found to be driven by mode conversion to ion cyclotron wave (ICW) instead of the reported ion Bernstein wave (IBW). These simulations have demonstrated that the fast wave mode converts to a combination of IBW and ICW and the balance between the two mode-converted waves is set approximately by the ratio β_p (plasma pressure to poloidal magnetic field pressure) where higher β_p results in mode conversion to IBW rather than ICW. For IBW current drive which dominates for near axis deposition, the driven current profile has a dipole structure; thus, MCCD in an advanced tokamak scenario on-axis is likely to be ineffective for on-axis current drive because the net current will be vanishingly small. However, MCCD experiments can provide important information regarding the inherent up-down asymmetry associated with the mode converted waves. Recent experiments sweeping the mode conversion location from inside to outside the $q=1$ surface with heating and current drive have shown that the heating phase may have net driven current. This would be consistent with the up-down asymmetry in the mode converted spectrum predicted by simulation.

5.1.2 Proposed Research

The goal of ICRF physics program is to provide first principle understanding of ICRF physics including antenna coupling and wave absorption such that it is a reliable heating and/or current drive actuator that can be utilized to optimize overall plasma performance, in C-Mod and future reactors, with minimum negative impact. Progress can be measured by both the identification of the principle plasma parameters through experimental scans and modeling and reactor-scalable, physics-based simulation capability has been achieved and validated. The research program can be organized along three major themes: antenna coupling and antenna/plasma interactions, wave propagation and absorption, and current drive and is summarized in Table 5.1.1. Although we would like to pursue all these topics aggressively, typically realities dictate some difficult prioritization. The highest priority is to

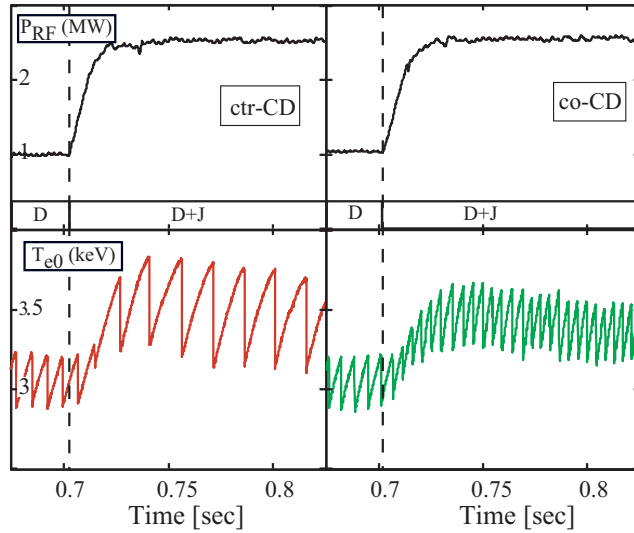


Figure 5.1.3: Modification of the sawtooth period utilizing MCCD with the deposition location peaked inside the $q=1$ surface.

Research Topic	Priority Justification
Antenna coupling and RF-Plasma Interaction	Progress aids the rest of the C-Mod program Is an important topic for ITER and future devices Leverages expertise in the boundary and RF groups
Wave Propagation, mode conversion and Absorption	Strong emphasis on simulation validation aids entire C-Mod program Leverages expertise in theory-modeling and experimental collaboration Lends itself well to student theses
ICRF Current/Flow Drive	LHCD is primary current drive tool. Benefits to the C-Mod program are less universal.

Table 5.1.1: ICRF Research topics and their justification of their priority given the realities of research resources.

develop an understanding the RF-plasma edge interactions in a tokamak with high Z first wall materials. This is because it is an important topic for ITER, future devices, and progress in this area aids the rest of the C-Mod physics program. Furthermore, C-Mod is well positioned for this research with an excellent boundary group that works closely with the RF group. Of nearly equal importance is investigating wave propagation and absorption physics which has a strong emphasis on validating simulation codes available through SciDAC CSWPI with advanced diagnostics. We have strong theory-experiment collaboration in this area and it also lends itself well to student theses. Furthermore the validation effort contributes to both future device like ITER and progress in validation of the codes benefits the rest of the C-Mod physics program. The lowest priority is for ICRF current/flow drive because the LH is the primary tool for driving current and the benefits to the C-Mod program are less universal. For example, the fast wave current drive is expected to be a useful tool for the advanced tokamak integrated scenarios but relatively unimportant for the H-mode integrated scenarios.

5.1.2.1 Antenna coupling and Antenna/Plasma interactions

An ideal ICRF system would have the generator isolated from the load and/or would be resilient to load variations and efficiently couple power to the plasma with minimum negative impact on the plasma. The coupling antenna structure, however, needs to be situated near the plasma edge and a number of issues associated with ICRF utilization arise from this feature: antenna coupling, dynamic loading variations due to ELMs and confinement mode transitions, voltage and power limitations, and impurity production. We prioritize our research effort according to a balance between enabling the overall physics program and issues expected in future experiments and reactors. For example, we have achieved high power density operation over a range of plasma parameter space, but many of the planned experiments discussed in the other sections are placing more stringent requirements on the ICRF antenna. Our approach is to place more emphasis on those issues that can yield the largest improvement without ignoring the smaller incremental steps that can yield 10% improvements. Table 5.1.2 summarizes the specific issues to be addressed in this section and the prospective diagnostics and codes instrumental to developing an understanding of these issues.

Particularly in a tokamak with metallic PFCs, impurity production associated with ICRF is critical to its utilization. Ample evidence from C-Mod and other devices indicates that the ICRF is enhancing the sheath potential. One of the primary questions regarding impurity production is the nature of the sheath formation. Are the sheaths formed as a result of

energetic electrons generated at the antenna or electron acceleration at the wall due to local interaction with the fast wave? We plan to characterize the RF sheaths under different confinement regimes, density, and antenna phase. This requires an upgrade to the present RF edge diagnostics. As mentioned in the edge physics section, we need to deploy an array of emissive probes on the limiters to improve coverage of field lines linked to the antenna. We also intend to implement retarding energy analyzers approximately in the same locations to measure the electron distribution and magnetic probes to monitor the wave field strength. The latter will be important for distinguishing the responsible mechanism. For example, if there is significant wave amplitude at the probe location, the sheath physics is local to that location. If however, the wave amplitude is low and a sheath is present this will indicate the mechanism likely at the antenna. The planned reflectometer will provide local density measurements and will provide an opportunity to monitor up-down asymmetries expected from convective cells. With the additional diagnostics and range of single pass absorption scenarios available, we can investigate so-called far field sheaths with the same antenna spectrum and assess its strength. Far field sheaths have been speculated to be the reason for low heating effectiveness of current drive phasing.[24] We will be able to monitor the plasma potential values and wave field strength for the same impressed spectrum with varying core absorption strengths. We would also like to identify the important impurity source locations. Therefore, we seek to develop marker materials to allow identification by spectroscopic imaging. This technique would allow rapid identification of source locations. In addition to identifying the location of the important molybdenum sources, we need to develop a technique to improve the boronization lifetime or reduce the impurity influx. We have successfully tested a set of vacuum sprayed boron coated tiles in-situ at relatively low heat flux locations. These tiles survived numerous disruptions without failure and one proposal would be to utilize these tiles on the RF and plasma limiters. The erosion location and average erosion rate could be deduced by placing a marker material under the boron. Another means is to reduce the parallel electric field excited by the antenna that should lead to a reduction in the sheath potential and the strength of the convective cells. Initially, we plan to utilize the TOPICA code to investigate the geometric effects on RF sheaths. However, we recognize that while the fields generated by the antenna are accurately calculated the self-consistent plasma response is still under development by the CSWPI project and others. As the new simulation capabilities develop, we will provide data for simulation validation. As discussed in the edge physics section, another outstanding question is why the RF source is apparently the most important source. One potential mechanism is that the convective cells driven by the RF-enhanced sheaths may be responsible for enhanced impurity penetration from a particular location. To investigate this we will perform experiments where the magnetic topology is changed to attempt to move the source location or change the direction of the convective cell. A related issue is the effect of RF heating on filament transport and we will begin by using the existing gas puff imaging diagnostic at low plasma current. Depending upon the results, we would like to expand this investigation to more standard 1 MA discharges.

We plan to continue our collaboration with the CSWPI and the Torino groups for validating the TOPICA code. In the near term, we will compare experimental measurements with the simulations and plan to simulate fast changes in loading to understand the antenna behavior during confinement changes associated with H-mode transitions and ELM's. With the addition of a new 4-strap antenna and associated edge reflectometer (in collaboration with Greg Hanson ORNL), we will have accurate edge density profiles and additional voltage and current measurements with high temporal resolution at the antenna. This will allow a significant improvement in the state of the art comparison between simulation and

Physics Issues	Approach	Diagnostics and Facilities	Modeling
Identification of RF impurity sources	Monitor marker tile materials Vary RF power and plasma current	<i>Marker tiles, spectroscopic imaging</i>	
Nature of RF sheaths	Measure plasma potential Vary RF power, phasing, single pass absorption, plasma current	<i>SOL reflectometers, emissive probes, RF magnetic probes, retarding energy analyzer</i>	<i>TOPICA/TORIC VORPAL</i>
Validation of RF wave coupling	Measure local density profiles Follow transient loads Measure antenna impedance with discharge	<i>SOL reflectometer, antenna current and voltage probes, and high frequency data acquisition</i>	<i>TOPICA/TORIC 3-D antenna model with current and voltage probes</i>
Voltage and power limits	Vary power and plasma conditions to find limits	<i>New 4 strap antenna, antenna video monitors, test stand</i>	

Table 5.1.2: Summary of physics issues, diagnostics and hardware, and codes where italics indicates new capability.

experiment: simulation incorporates realistic geometry and experiment has accurate density profiles and voltage and current measurements in the antenna itself. An emerging issue is the details of coupling between the antenna codes and the full wave codes. Presently, the antenna code solves Maxwell's equations up to some location, typically the protection tiles, assuming no plasma. The full wave codes used for wave propagation are valid inside the last closed flux surface, so there is a transition region in the scrape-off layer, where the loading is critically affected, and the modeling has significant simplifications. We will need an extensive set of measurements to understand the quality of the approximations made and their robustness over parameter space.

We also plan to continue to investigate the behavior of the FFT during plasma operation, particularly losses in the ferrites and nonlinear behavior with high circulating power. The latter is particularly important for situations where the antenna loading is low as in plasmas where the edge pedestals or evanescent layers are large. Another important area is operation in ELMing conditions and evaluation of the limits of the FFT as a function of ELM size and frequency is planned. During the next 5 years, we plan to install FFT's on all the transmitters to improve power transfer and increase experimental flexibility. To enable FFT operation, we plan to retain our comprehensive arc detection network in use with the prototype system. This system includes optical arc detectors in the FFT themselves, ratio of reflected to forward power, voltage limits, and current phase balance. The latter is located at the ground of the antenna and is sensitive to both amplitude and phase changes in the antenna strap current. This system is the primary protection against arcs developing at low voltage locations as has occurred on other devices.

We plan to continue utilizing our RF test stand to investigate RF breakdown physics. An outstanding question for the so-called neutral pressure limit is the initial fault. We plan to modify the setup to allow this fault scenario to be investigated and also plan to investigate the influence of magnetic field in parallel plate geometry at high power. This is motivated by the observation on C-Mod and a number of other devices where the ultimate voltage is set by locations where the RF electric field is parallel to the magnetic field.[25] We would like to quantify the voltage degradation between the cases of RF electric field perpendicular and parallel to the magnetic field.

The new 4-strap antenna will provide an opportunity to evaluate the effectiveness of a variety of ideas to improve antenna performance with respect to voltage/power handling and impurity production. The primary changes in the antenna compared to the J antenna are as follows: larger feedthrus, 30 Ω parallel plate vacuum transmission line (VTL), tungsten

Physics Issues	Approach	Diagnostics and Facilities	Modeling
D(³ He) minority heating effectiveness with low single pass absorption	Assemble database of H-mode discharges for comparison with D(H) heated H-modes	³ He monitor, stored energy, impurity radiation	TORIC AORSA
Investigate mode conversion regime	Locate mode conversion with PCI window Investigate mode conversion with other species mix	³ He monitor, high resolution ECE, <i>calibrated PCI</i>	TORIC Synthetic PCI
Characterize ICRF minority fundamental and 2 nd harmonic ion absorption	Scan RF power, plasma density. Measure ion distribution function	H concentration, <i>multichannel CNPA, CXRS-FI</i>	TORIC/CQL3D <i>TORIC/ORBIT-RF</i> Synthetic CNPA <i>Synthetic CXRS-FI</i>
Assess direct fast wave absorption	Obtain discharges with high temperature and electron beta Modulate RF power and monitor plasma response Scan plasma temperature and electron beta	<i>8 MW source</i> , high resolution ECE	TORIC

Table 5.1.3: Summary of wave propagation and absorption issues, important diagnostics, and codes where italics indicate new capability.

coated vacuum transmission line elements and antenna straps, and shielded radial feeders. We also plan to move the antenna strap closer to the plasma to improve the coupling and to have real time phase control. The larger feedthrus and 30 Ω transmission are intended to reduce the voltage in the VTL to avoid arcing and breakdown issues. The tungsten coating is to improve resistance to arcing because breakdown experiments done in the accelerator community have achieved higher electric fields with high melting temperature materials like molybdenum and tungsten compared to lower melting temperature materials like copper. An addition benefit is that tungsten is a potential material for antennas in future devices like DEMO where copper is unlikely to survive the expected heat load. Finally the shielded radial feeders are expected to decrease the unwanted fields excited by the antenna that lead to parallel electric fields which are rectified at the plasma sheath. A reduction in the RF sheath should reduce impurity production. Moving the current strap closer should improve coupling and allow higher power operation over larger range of plasma conditions. In addition to enabling current drive experiments, real time phase control will enable measuring the plasma impedance matrix within a single discharge.[probert] Measuring the impedance matrix will provide a more explicit validation experiment for TOPICA.

5.1.2.2 Propagation, Absorption and Mode Conversion Physics

C-Mod provides a unique opportunity to explore ICRF wave propagation, absorption, and mode conversion physics. These investigations are facilitated by a flexible ICRF system, access to sophisticated ICRF simulation codes (through CSWPI), and the availability of advanced diagnostics for RF wave measurements. A summary of the physics issues and their associated critical diagnostics, hardware, and codes is shown in Table 5.1.3.

We plan to expand the D(³He) H-mode discharge database to characterize the plasma performance and compare it with D(H) H-mode discharges. Operating the J antenna at 50 MHz (to couple to the ³He minority) and D and E antenna at 80 MHz (H minority), target discharges will have the same magnetic field, plasma current, temperature, and density. An outstanding question regarding D(³He) is the role of parasitic absorption, e.g. B minority resonance, loss mechanisms near the plasma edge. A similar parasitic minority resonance will be present in ITER from the planned use of beryllium coating on plasma facing

components (PFC's). In the near term, experiments are planned to move the parasitic ion edge resonances alternately into the plasma core or out of the plasma. Further experiments will also investigate the effect of additional heating power on heating efficiency with higher power density and consequently higher bulk plasma temperature, where we expect to increase the single pass absorption in D(³He). This work will also take advantage of new simulation capabilities where self-consistent ion distributions can be evolved within the simulation to investigate the impact of energetic ions on wave absorption.

A re-emerging area of interest is both fundamental and second harmonic heating where the former is the primary heating scenario in C-Mod and the latter is planned for ITER. For C-Mod, the ICRF is utilized to provide auxiliary heating in a majority of high performance discharges and validating the simulation codes used in discharge analysis is obviously important. For second harmonic, theoretical absorption calculations have indicated stronger damping than previously thought. Furthermore, recent developments in diagnostics and simulation capabilities have significantly improved the quality of the validation experiments and potentially could provide a fuller understanding of the fundamental minority and second harmonic ion absorption. At C-Mod, we have implemented a four-channel compact neutral particle analyzer (CNPA) based on operating small Si diode detectors in pulse-height analysis (PHA) mode and capable of measuring these energetic hydrogen minority ions through charge-exchange.[26] To interpret the CNPA data, a synthetic diagnostic was implemented in CQL3D [27] where the RF fields are calculated from TORIC and a comparison of this data is shown in Figure 5.1.4. We plan to build upon these initial results by adding new and upgrading current ion diagnostics: 8 (from 4) channel CNPA, fast ion loss scintillation probe (FIELD), and charge exchange recombination spectroscopy fast ion diagnostic (CXRS-FI) provide an opportunity to compare experimental results with those from advanced simulation capabilities being developed through CSWPI. The CNPA provides both spatial and distribution function data for confined energetic particles. The FIELD provides similar information for lost ions. The CXRS-FI will primarily provide spatial distribution of confined energetic ions.

Using the combination of diagnostics, we plan to investigate discharges with significant energetic ion populations, initially L-mode discharges, to validate the simulations. The primary complicating feature of H-modes is the higher density that increases the degree of difficulty associated with measurements of the energetic ion distribution. We will investigate a range of parameters to investigate the predictive capability of the simulation codes. We plan to investigate parameter scans of the plasma density, minority ion species and concentration, and antenna power and phasing and measure the effect on the fast ion distribution. For second harmonic absorption, initial experiments will investigate second harmonic H absorption and allow benchmarking of the simulations to experiment. Future experiments could examine the role of parasitic edge ion absorption, predicted by the codes which could have significant effects on impurity generation.

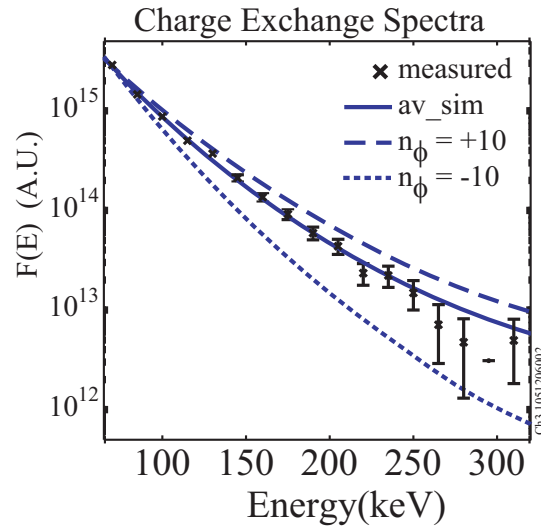


Figure 5.1.4: Measured charge exchange data from compact neutral particle analyzer for H minority heated discharge. Simulated data from TORIC-CQL3D compares favorably to the experimental measurement.

Current drive	Estimated driven current	Application
LHCD	>100 kA	Off axis current drive for AT
MCCD	<50 kA	Sawtooth stabilization physics Central seed current (back-up)
FWCD	<50 kA	Central seed current for AT
ICCD	<50 kA	Sawtooth pacing for H-mode

Table 5.1.4: Summary of RF current drive, estimated driven current, and their primary application.

We wish to revisit the mode conversion scenario for validation of the TORIC simulations with upgraded diagnostic capabilities. We have implemented a masking technique in the PCI system that relies on magnetic pitch angle dependence of the scattered signal to provide localization information along the measurement chord. This will allow us to explore the predicted up-down asymmetries associated with mode conversion and make detailed local measurements of the short wavelength modes. An optics upgrade will allow resolution of higher wavenumber (k) and when combined with the localization may allow observation of the rapid k up-shift associated with the mode converted waves. We have completed an improved calibration and spatial referencing upgrade that will allow a more accurate density fluctuation level and position to be determined. Furthermore, additional code to code benchmarking has identified an overestimation of the field strength in TORIC. Thus an outstanding issue from the previous analysis regarding amplitude discrepancies can potentially be resolved because of these diagnostic and code improvements. Taking advantage of this unique capability, studies will initially focus on D(3 He) and D(H) the primary species mixes used in C-Mod. An important aspect of these studies is comparing the measured wave spectrum with TORIC simulations. In collaboration with the RF Sci-DAC Initiative, we have local access to the MARSHALL and Beowulf cluster to perform fully resolved full-wave simulations routinely.

5.1.2.3 ICRF Current Drive

While not expected to be as efficient as LHCD, ICRF current drive, via mode conversion (MCCD) and ion cyclotron minority (ICCD) current drive, can be used to tailor the local current profile for controlling instabilities and Fast Wave current drive (FWCD) can provide the central seed current for fully non-inductive advanced tokamak scenarios. These current drive scenarios are listed in Table 5.1.4. In addition, these experiments will provide a good test of simulations and their associated current drive models and a summary is shown in Table 5.1.5.

An important application of MCCD for C-Mod is sawtooth pacing where the sawtooth period and amplitude are kept short to avoid monster sawteeth. The associated monster sawtooth crash has been observed to terminate high performance H mode discharges as shown in Figure 5.1.5, and also may prevent neoclassical tearing modes (NTM) by reducing or eliminating the seed island. A principle question yet to be addressed is sawtooth pacing in the presence of a substantial, stabilizing energetic ion population. We plan to investigate the MCCD power required to pace the sawtooth period in the presence of energetic ions generated by minority H absorption. We can scan the RF power, density, and plasma current to modify the energetic ion tail and measure the ion distribution with the CNPA and other

planned ion diagnostics. These experiments will be performed within the framework of the ITPA experiment MDC-5.

For the reference C-Mod advanced tokamak discharge, a central seed current of approximately 20 kA is required.[28] Fast wave absorption on electrons is a strong function of plasma β giving a centrally peaked absorption and current drive profile. Recent high performance discharges have been identified as good target discharges. In these discharges one set of antennas, D and E, can be utilized to raise the plasma temperature via standard minority heating scenario and utilize the J antenna at lower frequency (50 MHz) to heat via fast wave damping on electrons. In this scenario, the only parasitic ion absorption is minority boron and majority D. Initial experiments will focus on the deposition profile in a variety of conditions to determine the deposition profile and absorbed power fraction. Another issue will be impurity generation due to lower single pass absorption compared to hydrogen minority anticipated for these discharges. Tests of the driven current can also be performed and provide added data to experimentally benchmark the simulation codes and their respective current drive models.

A third current drive technique, ICCD, should be useful for local current profile tailoring, in particular sawtooth pacing. The physics of ICCD is complicated but essentially there are two regimes: classical and finite orbit. In the classical regime current is carried by passing particles and has peak efficiency near the critical energy. The finite orbit regime generates current as a result of finite width trapped particle orbits and requires highly energetic ion tails. C-Mod has access to both regimes and will allow benchmarking of simulation codes. For the classical regime, finite banana width simulations may not be necessary to calculate the driven current; however in the finite orbit regime, finite banana width will be required. Quantitative modeling of this scenario will require iterations between the full wave solver, TORIC or AORSA, and the Monte Carlo code ORBIT-RF available through CSWPI. Up to now, analysis has been qualitative.[] Since the two regimes have opposite dipole current profiles, one can demonstrate that both regimes exist simply by observing the change in sawtooth period.

5.1.2.4 Flow drive (MC)

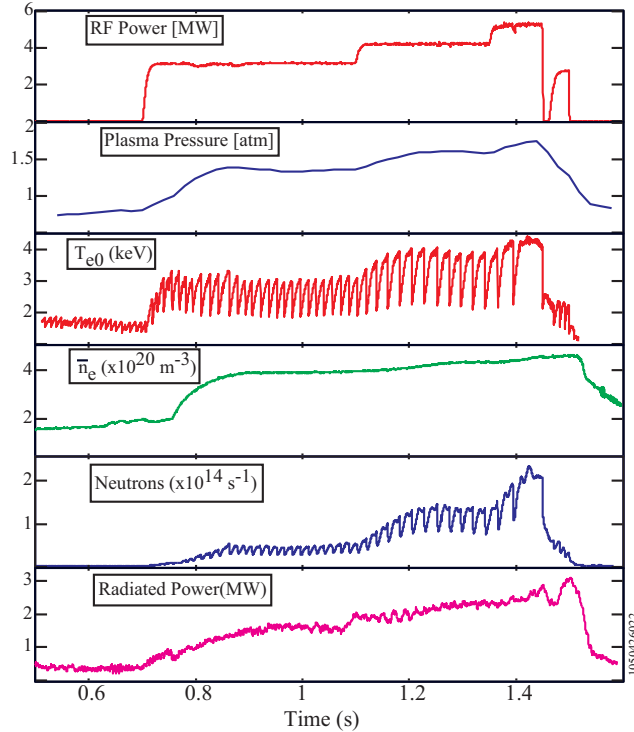


Figure 5.1.5: Example discharge where high performance phase is terminated by crash of monster sawtooth.

Physics Issues	Approach	Diagnostics and Facilities	Modeling
Assess MCCD power required to pace the sawteeth in the presence of energetic ions	Vary energetic minority energy by varying ICRF power of other antenna and density Modulate RF power and monitor plasma response with	³ He monitor, ECE, MSE, <i>polarimetry</i>	Porcelli model TORIC
Investigate FWCD	Obtain discharges with high temperature and electron beta Modulate RF power and monitor plasma response Scan plasma temperature and electron beta	high resolution ECE, MSE, <i>polarimetry</i>	TORIC
Assess ICCD	Scan RF power, plasma density. Measure ion distribution function Modulate RF power and monitor plasma response	H concentration, <i>multichannel CNPA, CXRS-FI</i> , MSE, <i>polarimetry</i>	TORIC/CQL3D <i>TORIC/ORBIT-RF</i> Synthetic CNPA <i>Synthetic CXRS-FI</i>
Assess MC flow drive	Obtain discharges with MC on low field side of magnetic axis Scan RF power, ³ He fraction	high resolution ECE, HIREX-sr	AORSA

Table 5.1.5: Summary of ICRF current and flow drive physics issues, approach, important diagnostics, and codes where italics indicate new capability.

Another research theme, relevant to triggering and controlling transport barriers, is RF driven flows. Theoretical calculations are difficult because one must calculate the plasma response in addition to the RF fields and resulting force. Experiments may provide insight into which of the many terms in these equations are important. For example flows can be driven by pondermotive forces or Reynolds stress. In the former case, damping on electrons may result in driven current but in the latter case damping on electrons will be small (electron to ion mass ratio is small) and ineffective. Depending on species mix, deposition location, and plasma current, the power can be channeled to ions or electrons. With upgraded diagnostics, the poloidal rotation, RF power deposition, and RF density fluctuation profiles can be simultaneously measured. These data will allow an assessment of the amount of poloidal flow, its profile, and its relation to RF wave propagation and absorption. Simulations have indicated that the scenarios most likely to drive significant sheared flow are those that have significant damping on ions near the cyclotron resonance where the forcing term switches sign as the resonance is crossed.[29] This suggests current drive experiments where the plasma conditions are tailored to maximize electron damping, while flow drive experiments will require different plasma conditions so that ion cyclotron damping will dominate. In C-Mod, this requires a mode conversion scenario where the fast wave mode converts primarily to an IBW on the low field side of the magnetic axis. Initially, experiments are planned utilizing the available antenna phasings and corresponding transmission network configurations. We plan to assess the poloidal flow characteristics for scenarios with predominantly ICW and IBW to test the code predictions. Depending on the flow drive success, RF driven flow shear can be investigated to determine RF power required to trigger or maintain internal transport barriers.

5.1.3 Relationship to FESAC and ITPA Activities

The ICRF research program supports the OFES long-term goal of “progress toward developing a predictive capability for key aspects of burning plasmas using advances in theory and simulation benchmarked against a comprehensive experimental database of

stability, transport, wave-particle interaction, and edge effects.” We have a heavy emphasis on validating RF and wave-particle physics and computational models thru comparison of experiments with access to wide range of RF absorption scenarios and diagnostics and advanced simulation codes.

In the 2007 "Priorities, Gaps and Opportunities" report, three themes were identified to help organize research plans in preparation for DEMO. The proposed ICRF research plan addresses both scientific and technical issues which must be addressed before proceeding to DEMO. Below we outline our plans that address issues within the various themes - A ‘Creating predictable high-performance steady-state plasmas’, B, ‘Taming the plasma material interface’; and C, ‘Harnessing fusion power’.

A.6 "Plasma Modification by Auxiliary Systems:" The primary goal of ICRF physics program is to provide first principle understanding of ICRF physics including antenna coupling and wave absorption such that it is a reliable heating and/or current drive actuator that can be utilized to optimize overall plasma performance with minimum negative impact on plasma. Listed below are a few highlighted issues to develop ICRF as an actuator for heating, current drive, and flow drive.

Issue	Approach	Diagnostics	Code
Nature of RF sheaths	Measure plasma potential Vary RF power, phasing, single pass absorption, plasma current	SOL reflectometers, emissive probes, RF magnetic probes, retarding energy analyzer	TOPICA/TORIC VORPAL
Validation of RF wave coupling	Measure local density profiles Follow transient loads Measure antenna impedance with discharge	SOL reflectometer, antenna current and voltage probes	TOPICA/TORIC
ICRF mode conversion	Locate mode conversion with PCI window Investigate mode conversion with other species mix	³ He monitor, high resolution ECE, calibrated PCI	TORIC Synthetic PCI
ICRF minority fundamental and 2 nd harmonic ion absorption	Scan RF power, plasma density. Measure ion distribution function	H concentration, multichannel CNPA, CXRS-FI	TORIC/CQL3D TORIC/ORBIT-RF
FWCD	Obtain discharges with high temperature and electron beta Modulate RF power and monitor plasma response Scan plasma temperature and electron beta	high resolution ECE, MSE, polarimetry	TORIC
MC flow drive	Obtain discharges with MC on low field side of magnetic axis Scan RF power, ³ He fraction	high resolution ECE, HIREX-sr	AORSA

B.8 ‘Plasma-Wall Interactions’: Since the role of RF sheaths can be important for sputtering and first wall erosion, understanding the interdependence of ICRF couplers and plasma-wall interactions is obviously important. We have an integrated program with the plasma boundary group which is summarized in the following table.

Physics Issues	Approach	Diagnostics and Facilities	Modeling
Identification of RF impurity sources	Monitor marker tile materials Vary RF power and plasma current	Marker tiles, spectroscopic imaging	
Nature of RF sheaths	Measure plasma potential Vary RF power, phasing, single pass absorption, plasma current	SOL reflectometers, emissive probes, RF magnetic probes, retarding energy analyzer	TOPICA/TORIC VORPAL

B.10 “RF Antennas, Launching Structures and Other Internal Components:" We investigate and develop solutions to technological and physics issues associated with the antenna/coupler and operations to enable successful RF operation. Listed below are a number of issues related to ICRF utilization.

Physics Issues	Approach	Diagnostics and Facilities	Modeling
Identification of RF impurity sources at antenna	Monitor marker tile materials Vary RF power and plasma current	Marker tiles, spectroscopic imaging	
Nature of RF sheaths near antenna	Impact of antenna geometry on sheath formation	SOL reflectometers, emissive probes, RF magnetic probes, retarding energy analyzer	TOPICA/TORIC VORPAL
Validation of RF wave coupling	Measure local density profiles Follow transient loads Measure antenna impedance with discharge	SOL reflectometer, antenna current and voltage probes	TOPICA/TORIC 3-D antenna model with current and voltage probes
Voltage and power limits	Vary power and plasma conditions to find limits Impact of refractory metals on antenna performance	New 4 strap antenna, antenna video monitors, test stand	

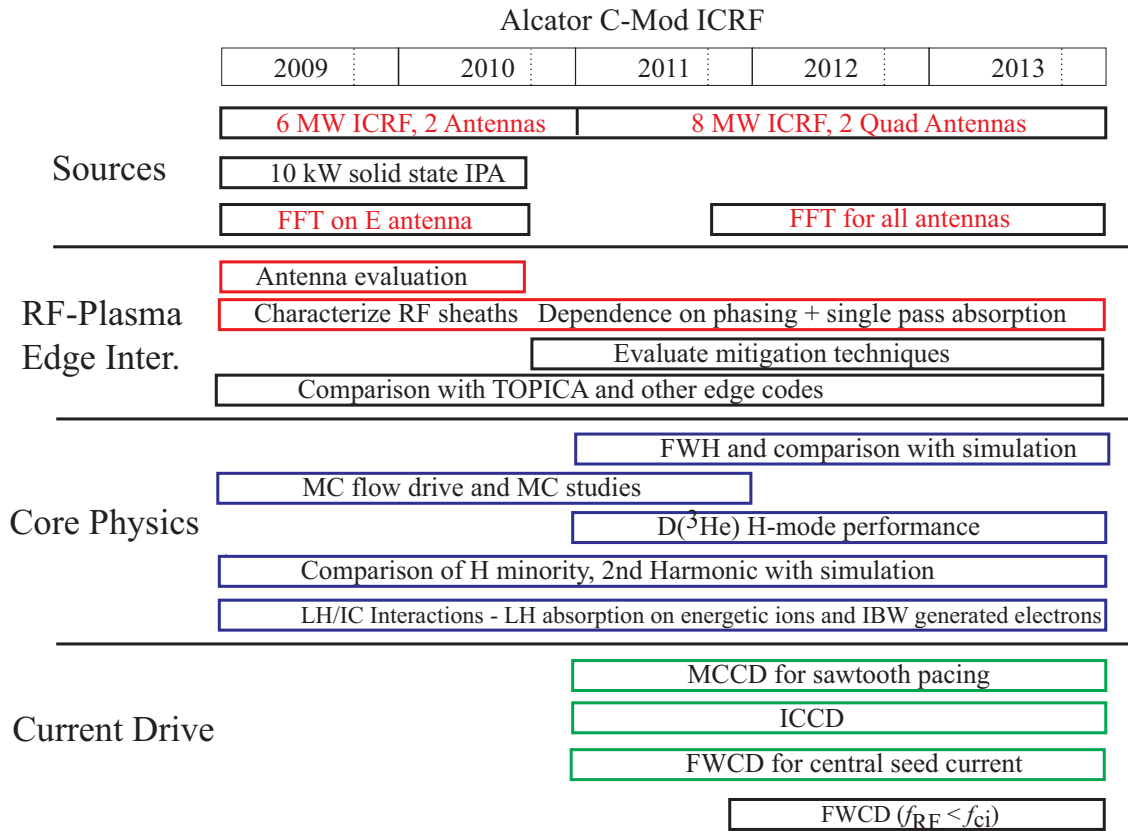
In the FESAC Priorities Panel 2005 waves and energetic particle recommendations, a fundamental issue identified is the interaction of electromagnetic waves with plasma. The proposed C-Mod research has three thrusts: optimize externally-launched wave spectra and power coupling limits; develop detailed understanding of wave propagation, absorption and plasma responses required for practical applications, and elucidate the interaction between waves, stability, and transport for potential development to control and optimize of fusion plasmas. Another area of interest is interaction of high energy particles with plasma and C-Mod can examine the interaction of energetic ions created via ICRF. C-Mod is well positioned to contribute on developing a fundamental understanding of energetic particle modes and these modes can be explored over a wide range of plasmas with access to sophisticated diagnostics and simulation codes.

Although no dedicated ITPA organization exists to address heating and current drive, C-Mod contributes in joint experiments utilizing the RF for localized tailoring of temperature, momentum, or current profiles. In the near term, we contribute to MDC-5, comparison of sawtooth control methods for NTM suppression

5.1.4 ICRF Research Objectives

Goal	Intermediate Objective	Date
Reliable antenna operation with minimum negative impact on antenna	Commission new 4 strap antenna	2009 and 2011
	Characterize RF sheaths with RF power, phasing, and single pass absorption	2010
	Evaluate sheath mitigation techniques	2012
Validate simulation against experiment	Measured antenna electrical characteristics comparison with TOPICA	2009
	Investigate mode conversion regime with PCI and compare with TORIC simulations	2010
	Characterize ICRF minority ion absorption with CNPA and CXRS-FI and compare with simulation	2011
	Investigate direct Fast wave absorption and compare with TORIC simulation	2011
	Examine ICRF 2 nd harmonic minority ion absorption with CNPA and CXRS-FI and compare with simulation	2012
Evaluate mode conversion flow drive	Investigate low field side mode conversion flow drive	2010
Develop ICRF current drive	Utilize MCCD for sawtooth pacing	2011
	Investigate FWCD for central seed current	2012
	Characterize ICCD for sawtooth pacing	2013

5.1.4 ICRF Research Schedule



- [1] ITER Physics Expert Group on Energetic Particles, Heating, and Current Drive, Nucl. Fus. 39, 2495 (1999).
 [2] J.R. Wilson et al., Phys. Rev. Lett. **75**, 842 (1995).
 [3] D.F.H. Start et al., Phys. Rev. Lett. **80**, 4681 (1998) and C. Gormezano et al., Phys. Rev. Lett. **80**, 5544 (1998).
 [4] C. Gormezano et al., Nuclear Fusion **47**, S285 (2007).
 [5] S. Ide et al., Nuclear Fusion **40**, 445 (2000) and X. Litaudon et al., Plasma Phys. Control. Fusion **44**, 1057 (2002).
 [6] B. Lipschultz et al., Phys. Plasmas **13** (2006) 056117.
 [7] S.J. Wukitch et al., J. Nuclear Materials **363**, 491 (2007).
 [8] J. Myra, 16th Topical Conference on RF Power in Plasmas, AIP Conference Proceedings **787** (2006) 3.
 [9] J.R. Myra et al., J. Nucl. Mater. **249**, 190 (1997); J. Sorensen et al., Nuclear Fusion **33**, 915 (1993); and J. Sorensen et al., Nuclear Fusion **36**, 173 (1996).
 [10] M.J. Mayberry et al., Nuclear Fusion **30**, 579 (1990).
 [11] A. Parisot et al., Plasma Phys. Control. Fusion **46**, 1781 (2004).
 [12] R. Maggiora et al., AIP Conf Proc **787**, 166 (2005).
 [13] A. Parisot, Master's thesis, Massachusetts Institute of Technology, 2005.
 [14] D. Swain et al., 23rd Symposium on Fusion Technology, P3T-B-460 (2004).
 [15] Y. Lin et al., Proc. of the 6th Technical Meeting on Control, Data acquisition and Remote Participation for Fusion Research, Fusion Eng. Design (accepted).
 [16] D. Remsen et al., 15th Symposium on Fusion Engineering, 1088 (1993).
 [17] F. Braun, 18th Symposium on Fusion Engineering, 395 (1999).
 [18] T. Graves et al., J. Vac. Sci. Technol. A **24**, 512 (2006).
 [19] E. Nelson-Melby, Ph.D. thesis, Massachusetts Institute of Technology, 2001; Y. Lin et al., Phys. Plasmas **11**, 2466 (2004); and S.J. Wukitch et al., Phys. Plasmas **12**, 056104 (2005).
 [20] A. Parisot, et al., Plasma Phys. Control. Fusion **49** (2007) 219-235.
 [21] J. Decker and Y. Peysson, Plasma Science Fusion Center Report, (2005) RR-05-3.
 [22] S.J. Wukitch et al., Phys. Plasmas **12**, 056104 (2005).

-
- [23] R. Majeski et al., Phys. Rev. Letters **76** (1996) 764.
- [24] J.E. Stevens, Plasma Physics and Controlled Fusion **32**, 189 1990.
- [25] H. Kimura et al, Nuclear Fusion **35**, 619 (1997).
- [26] V. Tang, Ph.D. thesis, Massachusetts Institute of Technology, 2007.
- [27] R.W Harvey and M.G. McCoy. The CQL3D Fokker-Planck Code. Technical Report Montreal Canada, IAEA TCM Advances in Simulation and Modeling of Thermonuclear Plasmas, 1992.
- [28] P.T. Bonoli et al., Nucl. Fusion (2000).
- [29] E. F. Jaeger *et al.*, Phys. Rev. Lett. **90**, 155001 (2003)

5.2 Lower Hybrid Range of Frequencies

The main motivation for Lower Hybrid Current Drive (LHCD) experiments on Alcator C-Mod is to use this form of current drive to augment the bootstrap current in producing and sustaining high performance, steady-state plasma regimes [1,2]. By this we mean plasmas with confinement exceeding the standard H-mode scaling and increased normalized beta β_N and β_{pol} , leading to substantial self-driven current. As outlined in Chapter 9, our target scenarios have full non-inductive current drive, with a majority of the current carried by bootstrap current and the remainder mainly driven by lower hybrid waves. Intermediate ‘hybrid’ scenarios are also of interest. Discharges will be maintained for durations substantially exceeding the resistive diffusion time, which in Alcator C-Mod is typically 100-300 ms, depending on T_e . For details, see Chapter 9 of this proposal, *Integrated Scenarios – Advanced Tokamak*.

An important secondary objective in carrying out the program of LHCD research is to inform the decision on implementing LHCD on ITER, which may be necessary if ITER is to achieve its steady-state goals. Key experimental contributions are concerned with coupling LH waves over substantial distances from the LH antenna to the plasma separatrix, and penetrating the H-Mode pedestal in order to effectively drive current in H-Mode regimes. An essential aspect of the LH program useful to ITER is the validation of advanced codes, such as the Fokker-Planck code CQL3D coupled with the ray-tracing code GENRAY and the full-wave code TORIC. In this regard, the comparison of measurements taken with an imaging hard X-Ray camera, a cyclotron emission spectrometer and the MSE system are invaluable in comparing with predictions of the synthetic diagnostics imbedded in the codes.

Fabrication of the Lower Hybrid launcher and transmitter was initiated as an MIE in FY 2000 and was completed on schedule in FY 2003. However, the repair of flaws found in the fabrication of the grill required its installation in Alcator C-Mod to be postponed until the beginning of 2005. Shortly after, it was found that the titanium used as the grill structural material reacted with hydrogen to form titanium hydride dust in quantities sufficient to force removal of the grill before meaningful LH experiments could be carried out. After fabricating a new grill from stainless steel, the LH launcher was again installed in Alcator C-Mod and LH experiments began in mid-2006. In effect, the LH experimental program was then delayed approximately two years relative to the schedule foreseen in the last 5-year Plan. Nevertheless, rapid progress has been made since these first experiments and the outlook for achieving the ambitious goals laid out for this program remains optimistic.

The LH program in Alcator C-Mod is planned to evolve in two phases. In the first phase, up to 3 MW of source power is to be coupled to a single LH launcher. Physics milestones for this phase included measurement and optimization of the coupling of the LH antenna to C-Mod plasmas, evaluation of the current drive efficiency, demonstration of current profile modification, and comparison of hard X-Ray profile measurements with predictions based on codes used in the simulations. All these milestones have been achieved and highlights of the results are described below.

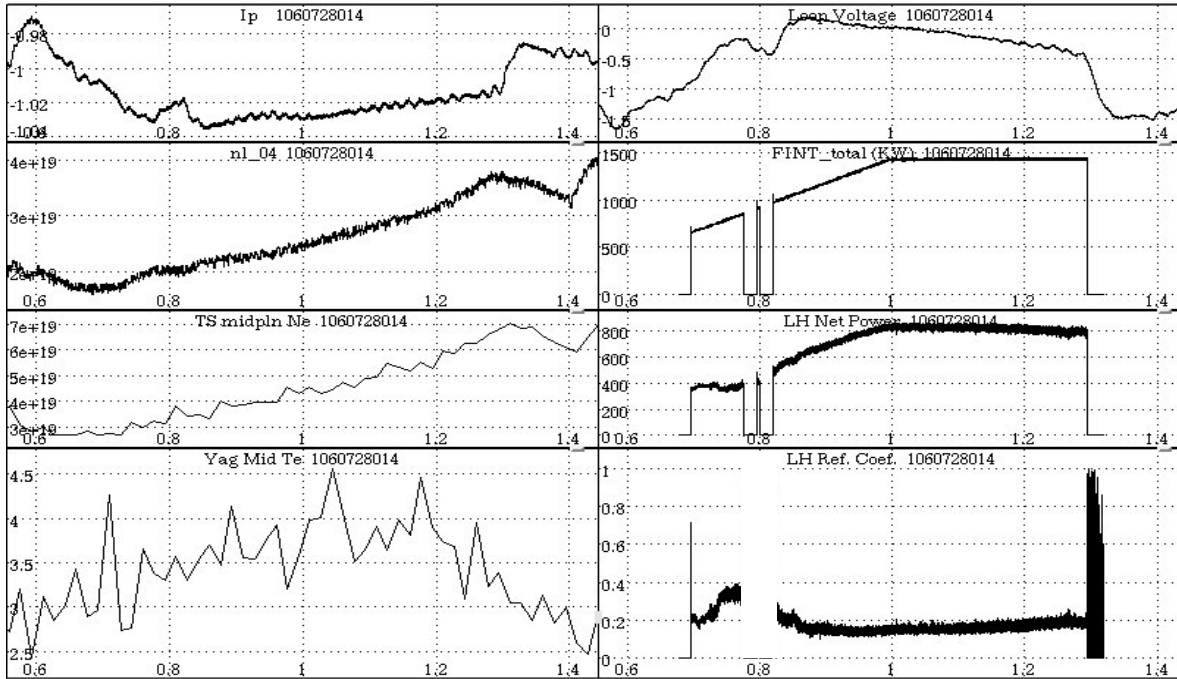


Figure 5.2.1 Example of discharge in which LHCD transiently reversed the loop voltage

In the second phase, the available source power is to be increased to 4 MW and applied to two independent launchers. The primary objective for this phase is to use LHCD as an actuator to modify the current profile and achieve the top level objective as outlined in the beginning of this Section. This second phase is scheduled to begin with installation of a second launcher in 2009. The experience gained in operating the first launcher, particularly in understanding the limits in its power handling capacity, are providing valuable input to the design of the second launcher.

5.2.1 Overview of recent LHCD results

RF power in the lower hybrid range of frequencies (4.6 GHz) is coupled to Alcator C-Mod plasmas by means of a grill composed of 88 waveguides arranged in 4 toroidal rows of 22 waveguides each [3]. The parallel index of refraction $n_{||} = k_{||}c / \omega$ of the launched waves is controlled by setting the phase progression of the electric field at the mouths of the waveguides facing the plasma; for example, with a 60° phase progression, the predominant component of the spectrum of launched waves is at $n_{||} = 1.6$, while at 90° , it is at $n_{||} = 2.3$. The phase progression, as well as the amplitude of the field at each waveguide mouth, is electronically controlled in real-time by an IQ modulator inserted between the output of a master oscillator and the input to each of 11 klystrons, which were originally purchased for Alcator C current drive experiments in the early-mid 1980's. Each klystron generates up to 250 kW of RF power at $f = 4.6$ GHz. Although the klystrons are capable of CW operation, the pulse length of the RF system is limited by the high-voltage power supply to ~ 5 s, which is also the maximum discharge length achievable in Alcator C-Mod at $B_T = 5.4$ T. The 5 s pulse length is substantially longer than the current redistribution time in Alcator C-Mod, which is typically 100 -300 ms.

When the LH power is applied to an inductively-formed discharge the loop voltage decreases in order to maintain the current at its feedback-controlled level. The most impressive example of this is illustrated in Fig. 5.2.1, which shows that the loop-voltage can be transiently reversed by 800 kW of LHCD power applied to a 1 MA discharge with central density of $\sim 5 \times 10^{19} \text{ m}^{-3}$. As the Ohmic power is replaced by RF power, the central temperature in this discharge increases to $\sim 4 \text{ KeV}$, indicating that the RF power is at least as efficient as the Ohmic power regarding its global heating effectiveness. By varying RF power density and current, we find that the fractional change in loop voltage is, over a wide range, roughly proportional to the parameter $P_{LH} / n_e I_p R_0$, as shown in Fig. 5.2.2. As is well known, in addition to the direct current drive by RF, there is a synergistic effect with the residual electric field due to the RF-produced non-thermal tail in the electron distribution function. When this is taken into account using a method due to Giruzzi [4] based on Fisch-Karney theory [5], the specific RF current drive efficiency is found to be $n_e I_{LH} R_0 / P_{LH} \approx 0.3 \text{ MA} / \text{m}^2 \text{ MW}$ [6]. This efficiency is consistent with the value derived from the simulations leading to the development of advanced steady-state regimes in Alcator C-Mod as outlined in the introduction to this Section.

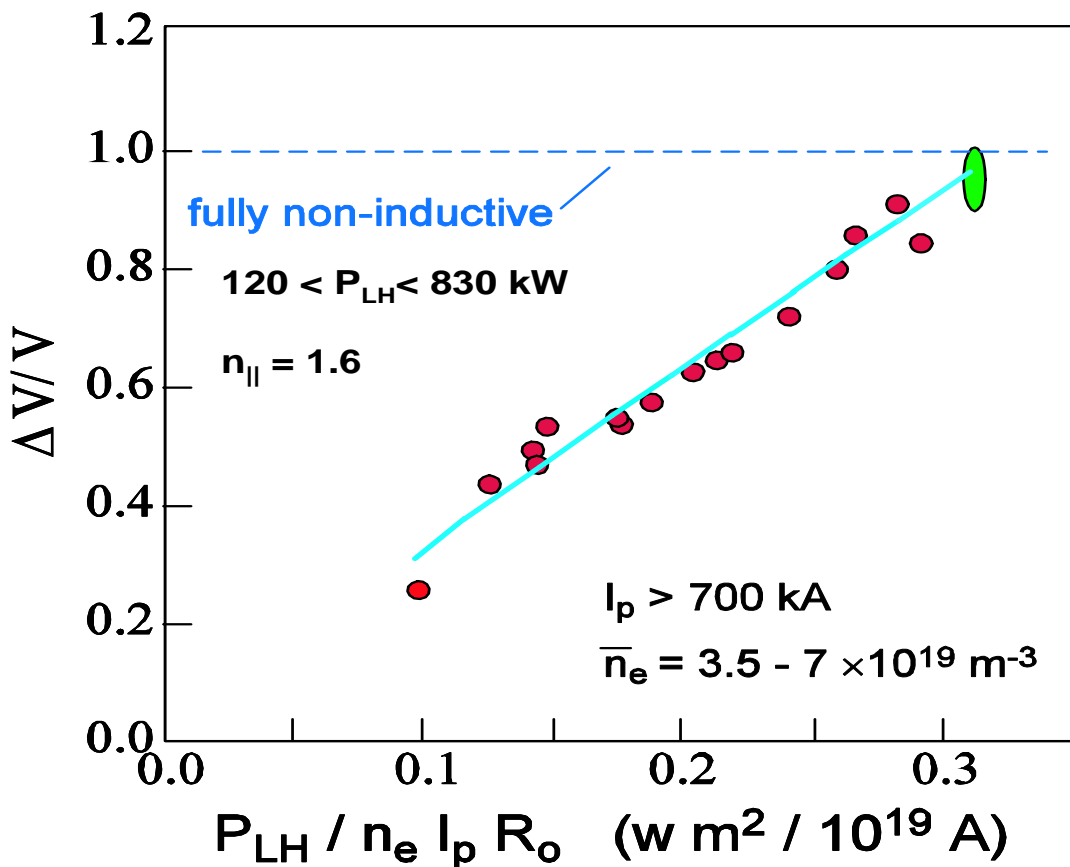


Figure 5.2.2 Fractional change in loop voltage vs. $P_{LH} / n_e I_p R_0$.

Production of advanced regimes requires not only an efficient external current drive, but also control of the current profile, which should be largely off-axis. The absorption of lower hybrid waves in current drive experiments takes place through Landau damping on the electron distribution function and is determined by a combination of the propagation of the lower hybrid rays in the plasma, including effects due to the toroidal upshift in $n_{||}$, as well as the radial temperature profile. Roughly, absorption occurs where $T_e(\text{keV}) \sim 30/n_{||}^2$; therefore the location of the driven current profile depends on both the temperature profile and the local value of $n_{||}$. The latter generally increases from its launched value as the LH rays propagate from the grill toward the plasma core. Evidence that the LH driven current in Alcator C-Mod is peaked off-axis stems from a number

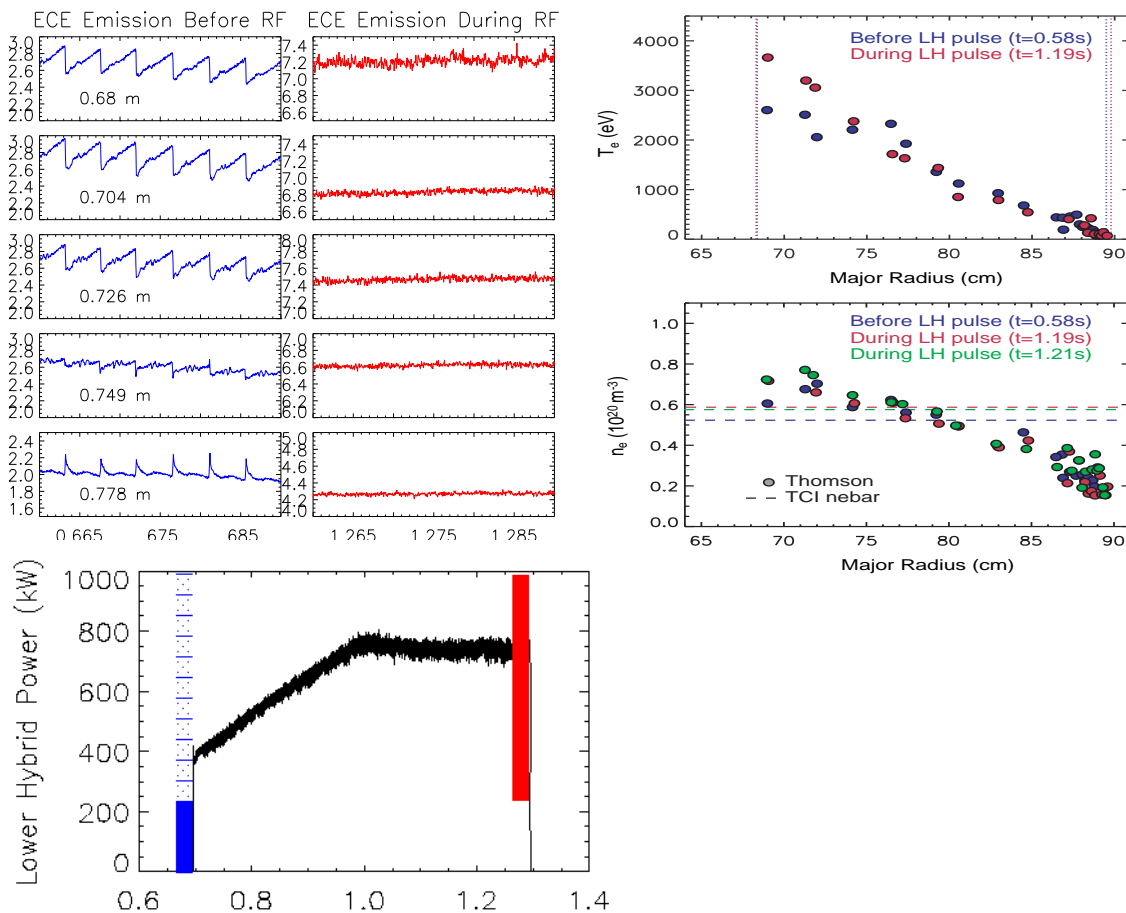


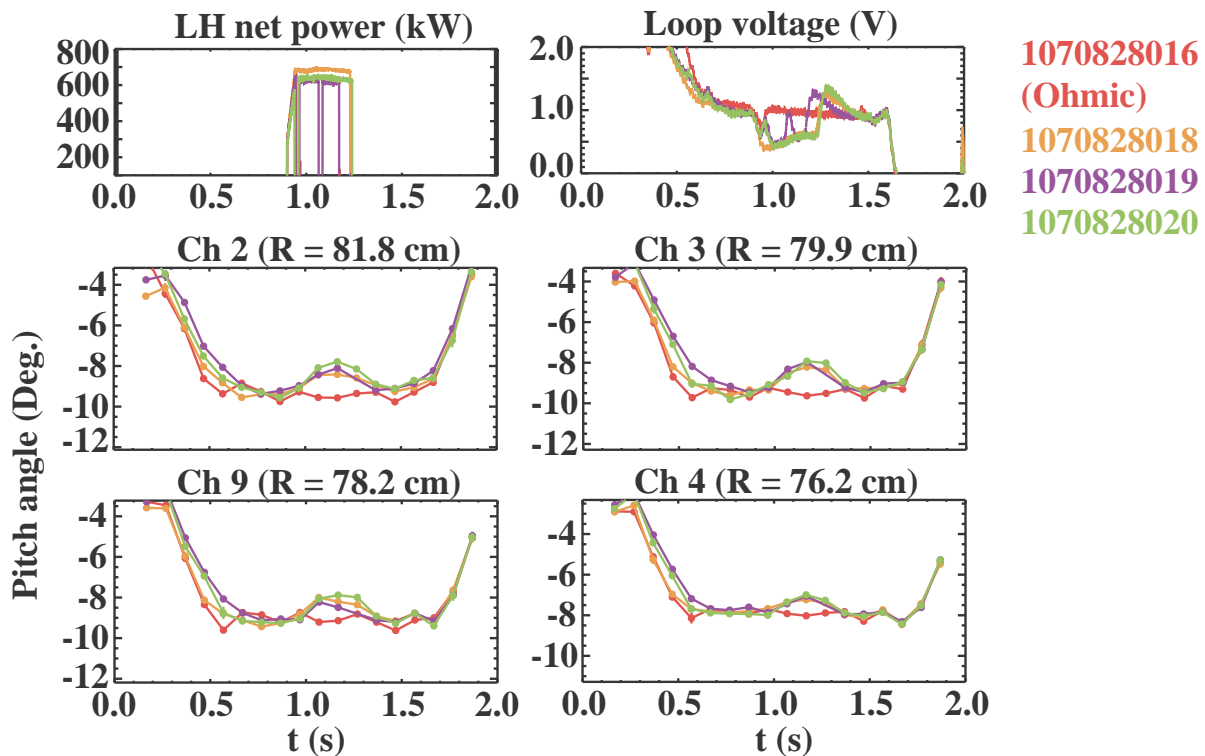
Figure 5.2.3 An example of stabilizing sawteeth by application of LHCD. With the sawteeth stabilized, the central temperature increased from 2.6 to 3.7 keV, while the density remains unchanged.

of independent observations, including indirect indications such as a decrease in the internal inductance deduced from EFIT and sawtooth stabilization, as well as more direct measurements

such as the spatial profiles of the hard X-Ray emission associated with the RF-driven tails in the electron distribution function, and preliminary MSE measurements of the current density profile.

Fig. 5.2.3 shows an example of a discharge in which 700 kW of LH power stabilized the sawtooth instability. With the sawteeth stabilized, the central electron temperature in this discharge rose from 2.6 keV to approximately 3.7 keV, while the plasma density remained unchanged. As a function of time after the RF is applied, the sawtooth inversion radius is observed to shrink and the sawteeth ultimately disappear. This can be explained by noting that with RF current drive (and fixed total current), the electric field is globally reduced leading to a reduction in the inductively driven component of the central current density j_0 . Since the LH driven current peaks off axis, j_0 is reduced thus raising the central q. When the central q reaches $q = 1$, the $m=1$ instability driving the sawtooth is quenched.

Figure 5.2.4. Time development of spatial profiles of Bremsstrahlung emission in the range 40 - 60 keV for three values of $n_{||}$. a) $n_{||} = 1.6$, b) $n_{||} = 2.3$ and c) $n_{||} = 3.2$. Inversion of these data shows that the peak emissivity progressively moves toward the plasma edge as $n_{||}$ increases



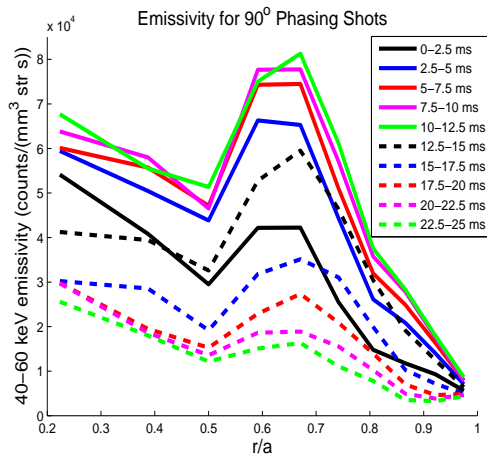
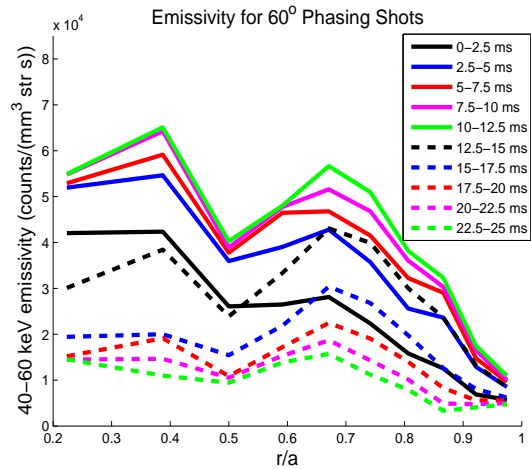
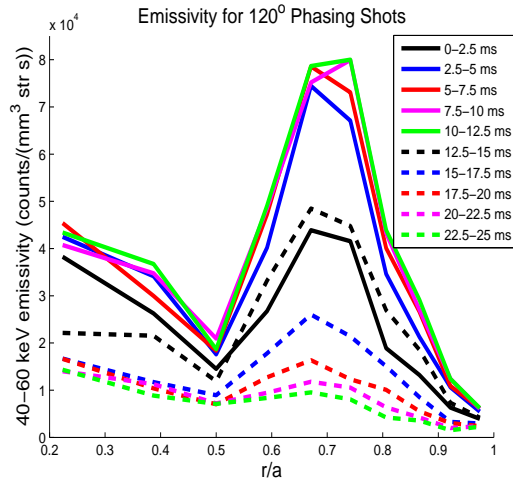


Figure 5.2.5. Time development of spatial profiles of Bremsstrahlung emission in the range 40 -60 keV for three values of $n_{||}$. a) $n_{||} = 1.6$, b) $n_{||} = 2.3$ and c) $n_{||} = 3.2$. Inversion of these data shows that the peak emissivity progressively moves toward the plasma edge as $n_{||}$ increases

Mod LHCD experiments, Bremsstrahlung profiles are routinely monitored by a 32 spatial channel X-Ray camera that spectrally resolves the photon emission over the range 20-200 keV in each channel. Since the absorption of LH waves depends on n_{\parallel} , varying the launched n_{\parallel} should affect the profile of bremsstrahlung emission. Results of an n_{\parallel} scan are shown in Fig. 5.2.4. In these data the LH power was square-wave modulated with a 25 ms period in order to minimize the effect of the LH on the target plasma and to make it possible to study the buildup and decay of the fast electrons. The spectral range of the collected photons was 40-60 keV. Increasing the launched n_{\parallel} shifts the radial peak of the photon emission, and presumably the region of LH wave

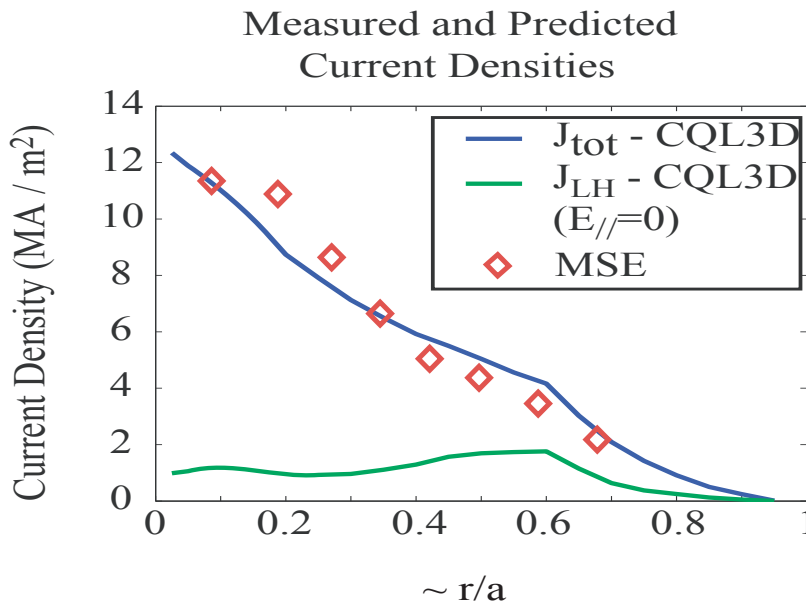


Figure 5.2.6 Inferred current density (diamonds) from MSE data in Figure 4 compared with total current from GENRAY/CQL3D simulation. Also shown is the LHCD current in the simulation, excluding the synergistic effect of the electric field

absorption, outward as one would expect. The relation between the emitted bremsstrahlung and the electron distribution function is complex, as is the relationship between the launched n_{\parallel} and its upshifted value where the LH power is absorbed. Quantitative interpretation of these data must therefore be carried out with the aid of CQL3D-GENRAY simulations as discussed in Chapter 10 in this proposal.

Successful implementation of MSE on Alcator C-Mod has made it possible to obtain the first direct measurement of the current profile with LHCD. Raw MSE data showing the pitch angle $\theta = \tan^{-1}(B_p / B_T)$ as a function of time in 3 LH discharges are shown in Fig. 5.2.5 where they

are compared with a reference inductive shot. The inferred current density for the LH shot 1070828020 is shown in Fig. 5.2.6, where it is also compared with the results of a CQL3D-GENRAY simulation (Chapter 10). Evidence for off-axis current drive is clearly seen from these figures; more detailed studies of the LH driven current profiles as functions of plasma and LH parameters using MSE are scheduled for the 2008 run campaign.

Comparison of the results of advanced simulations (including the imbedded synthetic diagnostics) with detailed diagnostic information described above suggests that the underlying physics of LHCD is fairly well understood and this lends confidence that LHCD will be a useful tool in developing advanced tokamak regimes in Alcator C-Mod. However, one issue that is not yet well in hand has to do with the compatibility of LHCD with H-Modes, an issue that is also of concern for ITER. For Alcator C-Mod, this issue concerns: i) maintaining sufficient density at the grill so that LH waves can be efficiently launched, which essentially requires $\omega_{p,grill} > \omega$; ii) propagating the LH waves through the H-mode pedestal (this should be easier on ITER since the density pedestal scale length will be longer than the wavelength, whereas in C-Mod they are of the same order); and iii) maintaining a sufficiently low H-Mode core density that the LHCD will have reasonable efficiency. An additional complication regarding item i) is that in Alcator C-Mod, the main heating method and therefore trigger for producing H-Modes is ICRH and the ICRH antennas affect the scrape-off layer in ways which can negatively affect the coupling of LH waves. We have found that this interference is limited to the D-port ICRF antenna which is magnetically connected to the LH grill located in the adjacent C-port. In the present port arrangement this leaves 3-4 MW of ICRH from the E- and J-port ICRH antennas still available for combined LH-ICRH H-Mode studies.

In general we have not found it difficult to maintain the density at the LH grill above the critical density required for coupling. To ensure that this will be the case, we have installed a gas puffing system in the gaps between the grill and its protective limiters, and this could be used to augment the density at the grill by RF ionization should it be necessary. However we have found that when the grill is recessed by ~ 5 mm from the protective limiters, coupling is poor even though strong local gas puffing allowed the critical density to be exceeded. These coupling studies are important for optimizing the power available for current drive, and are being continued in the present campaign.

The cryopump is a key tool in maintaining sufficiently low H-mode core density ($n_{core} \leq 2 \times 10^{20} \text{ m}^{-3}$) to ensure that the current drive efficiency ($\sim 1/n$) will be adequate to support advanced regimes, which generally require about 300 kA of driven current. Pumped discharges with upper X-point (grad B drift direction is down for ions) show promise as useful target discharges for this purpose (see Chapter 9.)

5.2.2 Research Plans

While the results of LHCD experiments are in large measure in accord with our understanding based on theory and simulation, a relatively disappointing aspect of the LH experience to date is the limited power (≤ 1.2 MW) that has been successfully coupled to C-Mod plasmas. There are two issues to be addressed here, namely i) relatively high losses in the transmission system ($\sim 50\%$), which limits the maximum available power to ~ 1.5 MW, and ii) breakdowns in the splitter and launcher system which often occur at a coupled power level of 700-800 kW. The positive aspect regarding item ii) is that with very few exceptions we have not experienced breakdown in the coupler containing the vacuum windows nor at the coupler-plasma interface. Nevertheless, success in using LHCD to develop nearly steady-state advanced modes will depend in mitigating these issues, as well as adding more RF capability. *Thus, the key elements in our proposal for the next 5 years are to increase the available klystron power to 4 MW and to develop a simpler launcher that has both lower loss and improved power handling capability.*

Regarding the increase in source power, we currently have 10 of the original klystrons working up to specification. Of the remaining 6, we are planning to refurbish 4 that are in need of repairs, including regunning. We are also getting quotations for at least 4 new tubes from the original manufacturer. In this regard, we are fortunate to be able to take advantage of a large klystron procurement contract (24 tubes) that has been made by the Chinese Institute for Plasma Physics with the same vendor, which we expect will bring the unit price down substantially for us. These klystrons are identical to the klystrons used as the source of power in our LH experiments, with the exception of the option of installation of a more robust collector. Assuming that at least 4 of our older tubes can be successfully brought back to the name-plate specification, this will bring our total to 18. Sixteen tubes would then provide a robust 4 MW of source power, and the remaining 2 tubes would be used as spares. We are also in discussions with the Chinese group to see if we might contribute to the EAST project through collaboration in exchange for additional klystrons.

The second element in our plan is development of a simplified coupler that would have lower loss and higher power handling capability. Fig. 5.2.7 shows an isometric of the new design. Key simplifying features are summarized in Table 5.2.1. The new coupler is far simpler and cheaper to fabricate, and we believe that it will have significantly higher power handling capability as well as reduced losses.

The schedule for installing the new coupler calls for it to be installed by the end of 2009, at which time we will also have both procured and repaired enough klystrons to bring the total number of working klystrons to 16 with possibly 2 spares. Sixteen klystrons will be split into two groups of 8 and used to power the two launchers. One group will power the present launcher, the other the new launcher. Assuming satisfactory performance from the new launcher concept, it will be reproduced and will replace the present launcher in 2011. With 2 MW source power for each launcher, we expect to couple 3 MW of LH power into C-Mod plasmas. Based on our measured current drive efficiency, this should be sufficient to drive ~ 300 kA as required in our advanced scenario simulations. The objectives for this aspect of the LHCD program are more fully described in Chapter 9.

The secondary goal of the C-Mod LHCD program is to develop the physics and practical aspects of LHCD for informing a decision on installing LHCD on ITER. The novel coupler that is being developed for the upgrade of the LH source power for Alcator C-Mod experiments may in fact have relevance to the design of a relatively simple and efficient LH launcher for ITER. Thanks to the encouragement of the ITER STAC, a proposal for a 20 MW LH system is being prepared for ITER. The reference frequency is 5 GHz, which is close to the 4.6 GHz used in Alcator C-Mod

Table 5.2.1. Comparison of new LH coupler design with present approach

Present Design	New Design
Three 3 dB power splitters	One 3 dB power splitter
Forward and rear waveguide assemblies formed from 25 plates with joint	One continuous waveguide feeding two adjacent columns, no joint
24 simultaneous window brazes required	Windows are brazed one at a time

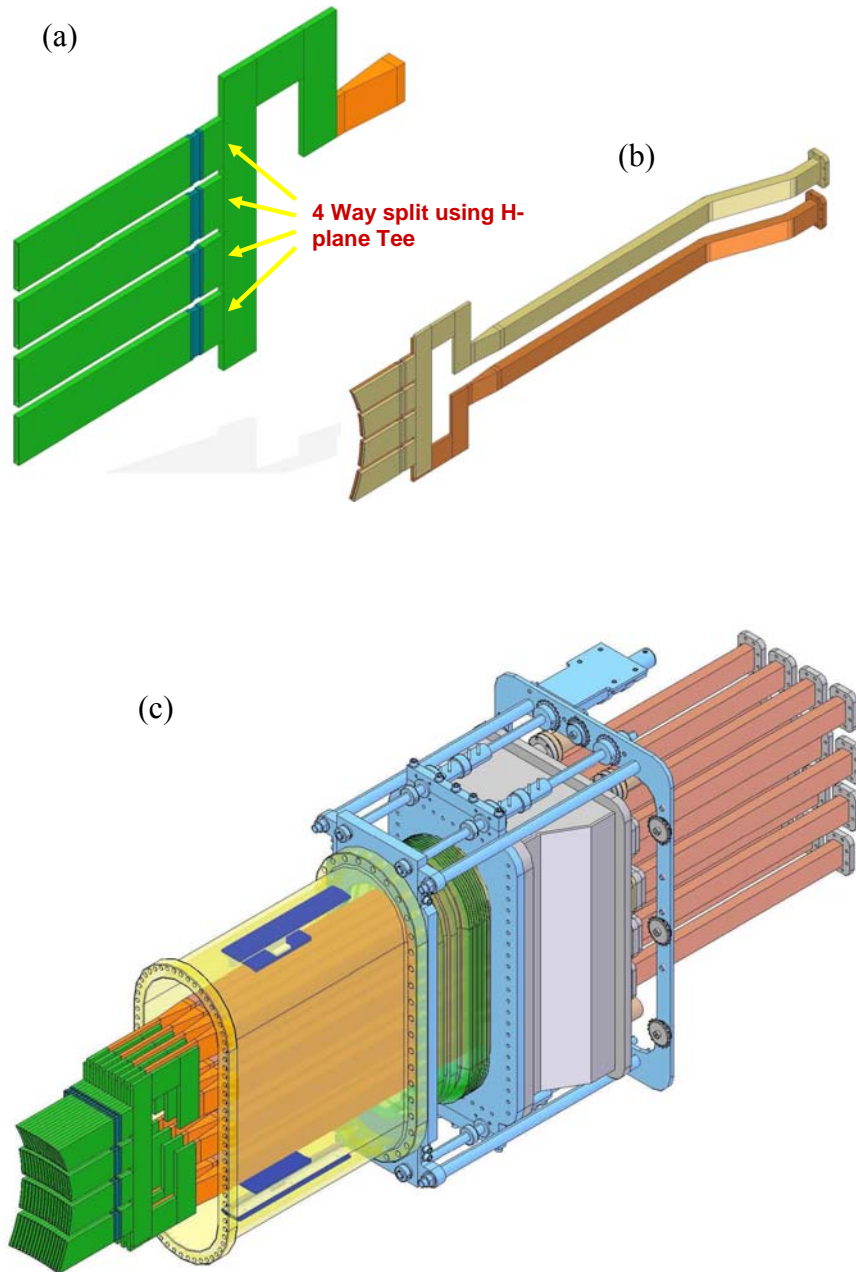


Figure 5.2.7 Isometric views of the new lower hybrid launcher concept. a) The power split in the vertical direction is by means of H-plane tees. b) The configuration for feeds to two adjacent columns. Standard WR187 waveguide is used to bring the power all the way to the 4-way splitter. c) The complete launcher assembly, showing that the feed to the coupler is via continuous waveguides

experiments. The effort to prepare the ITER proposal is being led by the European Party and members of the C-Mod LH team are actively involved. It is estimated that such an LHCD system could save about 30% of the V-Sec required for startup, which would be very significant both in facilitating low internal inductance startup as well as in extending ITER's pulse length. The LHCD program on Alcator C-Mod is highly relevant in providing both scientific and technological support for this LH system proposal

The essential task in developing the physics of LH current drive for ITER is to develop a comprehensive set of validated simulations that can be used to confidently predict the performance of a LHCD installation on ITER. This requires a detailed understanding and modeling of:

Plasma-grill interactions, including predictions of coupling efficiency and synergies (or anti-synergies) with the ICRH antennas, and power handling capability;

Long-distance coupling from grill to separatrix, including models that can be used to describe the plasma buildup in the scrape-off layer via localized gas puffing and interaction with the LHRF waves;

Propagation of LH waves in the scrape-off layer, through H-mode barriers, and toward the core plasma until they are absorbed ;

Interactions of the LH waves with the electron distribution function and validation of FP and QL models (including effects of trapping).

Regarding long-distance coupling, it should be noted that although the separatrix-grill spacing in C-Mod is limited to ~ 5 cm, the perpendicular wavelength is typically ~ 5 mm. Therefore measured in terms of λ_{perp} , long-distance coupling means about 10 wavelengths from the grill to the separatrix.

An additional issue of great interest and further study is whether there is a density limit for LHCD, beyond effects of reduced accessibility and/or the usual $1/n$ fall off in current drive efficiency. An example of a density dependent limiting process is the onset of parametric decay instabilities, which could cause the launched LH wave (or pump) to lose power as the result of decay into daughter waves or quasimodes. PDI decays into LH and IC waves have already been observed in our experiments, however it is not clear if significant power from the pump is being lost by this mechanism. We will continue to investigate power lost via PDI processes and determine whether this is indeed an efficiency-limiting mechanism at high density. Y. Takase from University of Tokyo is collaborating with us on this investigation.

Successful attacks on these issues will require the continuation of close coordination with the development of advanced simulations. This has been the case since the beginning of the LHCD program in Alcator C-Mod and has been invaluable to the rapid progress that has been made. (See also Chapter 10.) Especially useful in this regard are the simulated diagnostics imbedded in

the simulations, e.g., X-Ray profiles and spectra, non-thermal ECE spectra and MSE measurements of the pitch angle on the outer mid-plane, through which $j_{\phi}(r)$ can be reconstructed. Two new diagnostics which would assist in this effort and which are being considered are a vertically viewing ECE spectrometer, which could unambiguously resolve the spatial location of relativistically downshifted non-thermal ECE emission, and a reflectometer imbedded in LH grill to accurately characterize the density profile from the grill to the separatrix, and the effect of LHRF power on it. A similar reflectometer is being fabricated for ICRF coupling studies and our plan is to adapt it to be also used for LH coupling investigations on a time-shared basis. A third interesting possibility under investigation is to use the current multi-frequency reflectometer system now being used to study lower frequency fluctuations, e.g., QC modes, in a modified form to map out the spatial dependence of the 4.6 GHz LH wave fields. Many of the effects discussed and in the following table can only be adequately resolved by direct measurement of the LH wave fields. For this reason, we are also considering installation of a CO₂ laser scattering system, similar to that which was successfully deployed on Alcator C.

5.2.3 Tabular summary of research plans

Issue/theme/task	Approach	Tools
<p>Develop validated model to accurately describe LH wave propagation and absorption in diverted C-Mod plasmas, operating in both L- and H-mode</p>	<p>Measure 4.6 GHz wave fields in plasma and compare with ray-tracing and full wave code predictions.</p>	<p>Adapt presently existing multi-frequency reflectometer to detect 4.6 GHz density fluctuations</p> <p>Consider mounting CO₂ scattering experiment to directly detect 4.6 GHz density fluctuations</p> <p>Continue close collaboration with development of full-wave TORIC/CQL3D simulation for LH wave propagation.</p>
<p>Validate, to the extent possible, QL Fokker-Planck predictions regarding electron distribution function (and current drive) in presence of LH waves.</p>	<p>Compare predictions of X-Ray and cyclotron harmonic emissions from synthetic diagnostics embedded in CQL3D with measurement.</p>	<p>Existing 32 channel X-Ray spectrometer that resolves photon energies in range 20-200 keV</p> <p>Expanded MSE mid-plane pitch angle measurements to infer $j_{\phi}(r/a)$</p> <p>New tangentially viewing X-Ray spectrometer</p> <p>Existing horizontally viewing Michelson ECE spectrometer (100-1000 GHz).</p> <p>New vertically viewing wide band ECE spectrometer, 100 – 1000 GHz</p>
<p>Explore possible density limit to LHCD other than accessibility.</p>	<p>Measure 4.6 GHz wave fields in plasma; correlate with appearance and strength of parametric decay instabilities</p>	<p>Existing spectral analysis of reflected waves in grill at 4.6 GHz, downshifted by ion cyclotron harmonics</p> <p>Reflectometer and/or CO₂ scattering (as in first item) to detect wave fields at 4.6 GHz</p>

Issue/theme/task	Approach	Tools
Develop model to accurately predict coupling efficiency taking into account effect of LH power on grill density, density gradient	Measure reflection coefficient as function of grill density, gradient, RF power and effect of local gas puffing	<p>Several coupling codes, including Brambilla, TOPLHA and one under PSFC development</p> <p>Existing probes located in face of grill – vary flux surface shape to map gradient</p> <p>Existing gas puff in grill</p> <p>New reflectometer mounted in close proximity to grill</p>
Explore effectiveness of “long-distance” coupling, including propagation through H-mode pedestal	Investigate coupling efficiency, current drive efficiency as function of grill-separatrix distance (up to $\sim 5\text{cm}$, many λ_{perp} 's)	<p>Measurement of reflection coefficient grill</p> <p>MSE measurement of j_{ϕ}</p> <p>Measurement of wave fields beyond separatrix (see above)</p>

References

1. P. T. Bonoli, M. Porkolab, J. Ramos, et. al., PPCF 39,(1997)223
2. P.T. Bonoli, R.R.Parker, M. Porkolab, et.al., Nucl Fus 40,(2000)1251
3. P. Bonoli, R. Parker, et. al., Fusion Science and Technology 51(2007)401
4. G. Giruzzi, E. Barbato, S. Bernabei, et.al., Nuclear Fusion, 37 (1997) 673
5. N. J. Fisch, C. F. F. Karney, Phys. Rev. Lett.,54, 897(1985)
6. P. T. Bonoli, J. Ko, R. R. Parker, et.al., to be published in Physics of Plasmas

5.3 ICRF and LHRF Interactions

Our goal is to investigate issues related to compatibility between ICRF heating and LHCD and to enable tokamak performance optimization with the combination of ICRF and LHRF.

5.3.1 Coupling

Both ICRF and LHRF coupling are dependent upon the edge density profile with LHRF being much more sensitive due to the shorter wavelength. As seen in other tokamak experiments, for example JET and Tore Supra, the ICRF can modify the density profile significantly and result in difficult coupling conditions for LH. In C-Mod, we have successfully coupled LH power into both L and H-mode ICRF heated discharges. We have found that the LH coupler reflected power fraction and the fluctuation level significantly increases for discharges heated with the neighboring antenna. This effect was also dependent upon machine conditions particularly boronization. Future experiments will continue to examine the coupling dependence on plasma density, LH power, coupler distance to the plasma, and ICRF power. An additional reflectometer designed to measure the edge density profile (similar to the reflectometer in the new 4-strap ICRF antenna) will greatly improve the data quality and potentially our understanding. In addition, we plan to utilize TOPLHA to investigate and analyze the coupling under various conditions. Another potential issue we will monitor is the creation of edge energetic electrons by either the ICRF or LHRF and their impact on the plasma edge density profile. The planned addition of emissive probes and retarding energy analyzers on the plasma limiters will be important in monitoring their presence and impact on the edge profiles.

5.3.2 Core Interactions

The LH wave absorption can be modified by the presence of energetic ions and electrons. The choice of LH source frequency in ITER (≈ 5 GHz) is in part driven by the need to avoid parasitic absorption of the LH wave on fast fusion α -particles through ion Landau damping. In C-Mod we can approximate damping on alpha particles with ICRF generated minority ions. Using low density discharges, the minority tail energy can be ~ 300 keV and sufficient to interact with LH waves. Estimates show at $n_{||} \sim 1.5$ LH waves will absorb on ions if the ion energy is ~ 800 keV while $n_{||} \sim 3.5$ will interact with ~ 150 keV ions. Comparison of hard X-ray data alternatively with and without ICRF power can provide an experimental validation of the simulations.

Furthermore, a comparison fast ion data from CNPA and FIHD of discharges with low $n_{||}$ and high $n_{||}$ would provide an additional validation. A parameter scan of ICRF power and LH wave spectrum could provides an opportunity to test the simulation over a wide range of parameters. In addition, ICRF can also modify the electron distribution function through mode converted IBWs and create a population of energetic electrons that then readily interact LH waves. Since the mode converted IBWs can be localized off-axis, this may allow for deposition control of the LH waves.

6 Macroscopic Stability

The Alcator C-Mod macrostability research program addresses issues relevant to the overall C-Mod program goals, as well as within the context of international research thrusts. A large fraction of the MHD research on C-Mod involves close collaboration with other facilities, many through official ITPA-coordinated joint experiments. This leverages C-Mod's unique region of parameter space to better determine scaling laws relevant to ITER and future reactors. The C-Mod MHD program also has excellent connections with theory and modeling.

6.1 Highlights of Recent Research

6.1.1 Disruption Mitigation

Disruptions are one of the most urgent ITER physics issues. The development of practical disruption mitigation techniques is a critical item for any tokamak burning plasma experiment and reactor prototype. Disruption-related problems that are particularly severe for ITER and future reactor devices include thermal damage (ablation/melting) to divertor surfaces, $J \times B$ mechanical forces on conducting structures arising from halo currents, and runaway electron populations generated during the current quench by avalanche amplification. Injection of high-pressure jets of noble gas is proposed as a mitigation technique for ITER, and experimental tests of disruption mitigation with gas jets are a high-priority ITPA MHD task. A high-pressure gas jet system was installed on Alcator C-Mod, and very promising results have been obtained over the last few years [1,2]. Due to its ITER-like plasma pressure and energy density, as well as its very high current density and fast disruption timescale, C-Mod provides a very challenging test of this technique, both in terms of the gas jet penetration, and in the ability to radiatively dissipate at the required power levels. The C-Mod system was optimized to put the gas outlet nozzle very close to the plasma edge (2-3 cm) in an attempt to maximize the amount of noble gas delivered to the plasma. Experiments with pre-programmed firing of high-pressure gas jets into stable plasmas in Alcator C-Mod using high-Z gases (neon, argon, and krypton) have shown that halo

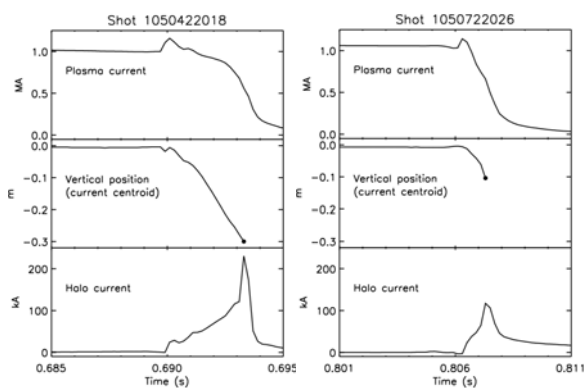


Figure 6-1 — Neon gas jet injection speeds up the current quench (right-hand case) compared to an unmitigated disruption (left-hand case). This allows less time for the plasma to move toward the divertor and results in less halo current.

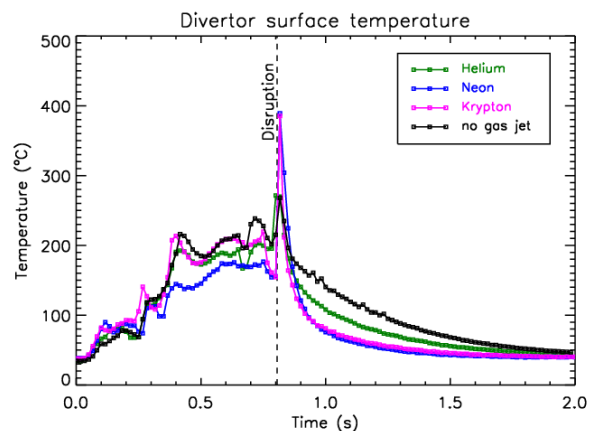


Figure 6-2 — High-Z gas jets quickly radiate away most of the energy, resulting in less heating of the divertor surfaces.

currents can be cut in half (Fig 6-1), and radiated energy fractions can be increased to over 80%, thereby reducing the thermal loads on divertor surfaces (Fig 6-2). The high-Z gases used in these experiments have relatively slow flow velocities (\sim sound speed), resulting in response times of 5-7 ms from the time the gas valve is fired. For real-time disruption mitigation, there are some situations (VDEs, for example) where it necessary to shorten this delay. Low-Z noble gases, such as helium, are faster, but have shown poor performance in terms of disruption mitigation on C-Mod. A possible solution is to mix a small percentage of high-Z gas with a lighter ‘carrier’ gas. Experiments on C-Mod using mixtures of argon and helium over a range of ratios have shown that an optimal mix of 15% argon with 85% helium minimizes the response time by several milliseconds, yet still mitigates halo current and thermal loads effectively. More recently, experiments involving real-time detection of VDEs and locked mode disruptions have been carried out using C-Mod’s digital plasma control system (DPCS). Real-time mitigation of VDEs in C-Mod is particularly difficult because of the short timescales involved, but these experiments have been nearly as successful as pre-programmed mitigation of stable plasmas.

These successful mitigation effects have been obtained despite the fact that the injected impurities do not penetrate far into the C-Mod plasma as neutral gas jets. Modeling of the gas jet effects using the 3D MHD code NIMROD reveals that rapid growth of tearing modes creates ergodic field regions over most of the plasma cross-section, which allows both rapid transport of impurity ions into the plasma core, as well as fast transport of thermal energy out to the radiating mantle [3]. Recently NIMROD has been modified to include impurity physics, such as ionization, transport, and radiation. Modeling of C-Mod helium and argon cases with this upgraded NIMRAD code clearly reproduces the specific differences seen for these two gases, such as the larger density increase for helium, as seen in the left graph of Fig. 6-3, and the gigawatt radiated power levels for argon (right graph).

6.1.2 Locked Modes and Error Fields

Alcator C-Mod has a set of eight external coils (above and below the midplane at each of four

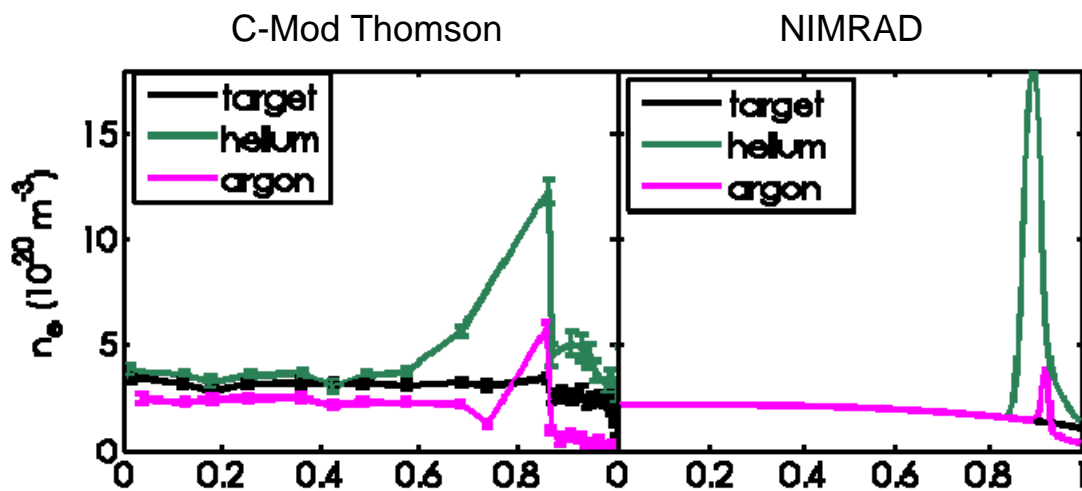


Figure 6-3 — Prior to the thermal quench, helium gas jet injection yields a larger increase in plasma electron density than argon injection (left). The radiated power as calculated by NIMRAD reaches the gigawatt level for argon gas jet injection (right). These are both consistent with experimental observations.

toroidal locations) that can be connected together in various configurations to produce non-axisymmetric perturbations with predominantly $n = \pm 1$ and/or $n = \pm 2$ structure. These ‘A-coils’ have been used to correct error fields on the machine in order to avoid locked modes. Two experiments studying B_T scaling and size scaling of the locking threshold have been completed as part of an ITPA series of joint experiments with JET [4]. The C-Mod results for toroidal fields higher than 4 tesla support the standard simple power law scaling of the error field locking threshold:

$$\frac{B_{pen}}{B_T} \propto n^{\alpha_n} B^{\alpha_B} q^{\alpha_q} R^{\alpha_R}$$

and yield a field scaling that goes like B^{-1} , as shown in Fig 6-4. For ITER’s size, this implies an error field threshold, $B/B \sim 10^{-4}$, which is well within the design capability of the ITER

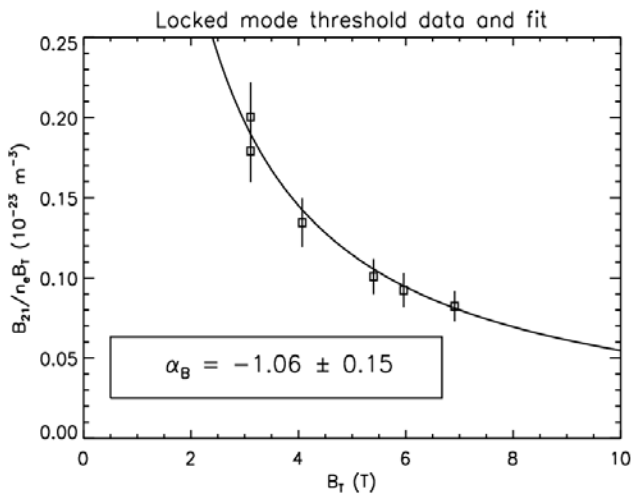


Figure 6-4 — An inverse scaling with B -field was found for the error field locking threshold under a particular set of controlled parameters on C-Mod.

correction coils. The identity experiments with JET also validate non-dimensional scaling over a factor of four in size, at least at medium and high toroidal fields. These ITPA experiments have now been declared officially closed. However, there is an additional, unmatched low-field point from C-Mod (at 4.1 T) which is inconsistent with a simple power law, but a corresponding low-field point from JET (at 0.6 T) is needed to verify its significance. JET is planning to acquire these data in the next year or two.

6.1.3 Alfvén eigenmodes

The stability of Alfvén eigenmodes (AEs) has been studied on C-Mod using a number of diagnostics including active MHD antennas, Phase Contrast Imaging (PCI), magnetic pick-up coils, a compact neutral particle analyzer (CNPA), and a hard x ray camera. Understanding the physics of AEs may be important for fusion burn control and controlling the loss of fast ions in ITER. Stable AEs are excited with the active MHD antennas to measure their stability properties. Magnetic pick-up coils and the PCI measure the AE fluctuations and their toroidal, poloidal, and radial structure. The CNPA and hard x ray camera are used to measure profiles of the fast ions and electrons, respectively. The Alfvén eigenmode data on C-Mod are compared with numerical results from the NOVA-K [5] code for mode structure and stability. TRANSP combined with TORIC is used to calculate the fast ion distribution for input into NOVA-K. Initial comparisons of the fast ion distribution have also been made with the AORSA/CQL3D [6] codes. A synthetic PCI diagnostic code was also written to compare NOVA calculated eigenmode structures with the line integrated PCI data. This combination of multiple diagnostics together with numerical analysis routines helps advance our understanding of Alfvén eigenmodes.

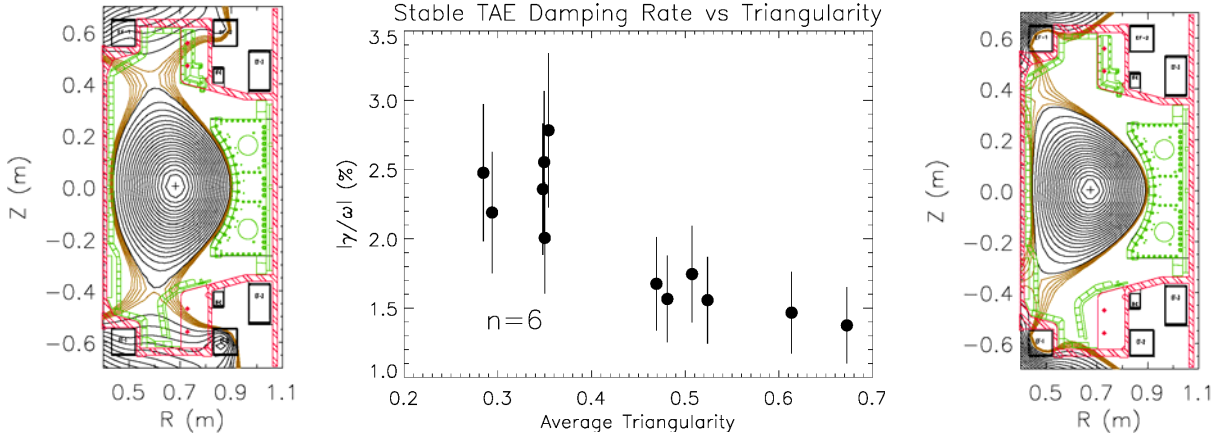


Figure 6-5 — Measured TAE damping rate vs average triangularity for $n=6$ modes together with the plasma poloidal cross-section equilibrium contours for the two extremes in triangularity.

The active MHD antennas generate an ITER-relevant intermediate- n toroidal mode spectrum ($|n|_{\text{fwhm}} \sim 16$) at the same toroidal field and density as in ITER to study the damping rate of stable Alfvén eigenmodes as a function of plasma parameters. Recent experiments have measured the damping rate of stable TAE resonances as a function of triangularity, ion ∇B drift direction, density, toroidal field, and ICRF power. The damping rate is seen to decrease for $n = 6$ modes with increasing triangularity (Fig 6-5), in contrast to the JET result for $n = 1$ [7] where increased triangularity increased the damping rate. These data suggest that the radial structure of moderate n modes is not dominated by edge shaping effects as it is for low n modes. Experiments to determine the effects of ICRF generated fast ions on the measured damping rate of stable modes showed an initial increase in TAE stability with increasing heating at low ICRF power, followed by decreasing stability above 1.5MW. Experiments are ongoing to better understand the change in the overall drive/damping rate in the presence of a fast ion tail.

The stability of AEs also depends on the confinement phase of the discharge; ICRF driven unstable AEs are usually found in the H-mode phase while in the preceding lower density L-mode phase the modes remain stable (Fig 6-6). Furthermore, the AEs found in H-mode rotate in the electron direction, which could imply an off-axis maximum in the fast ion distribution. Modeling with the NOVA-K code did indeed find core localized modes at the measured mode frequency when the Doppler shift due to plasma rotation is included and these modes rotate in the electron direction for an off-axis shifted fast ion profile [8]. However, radiative damping was found to stabilize the modes for the assumed profiles.

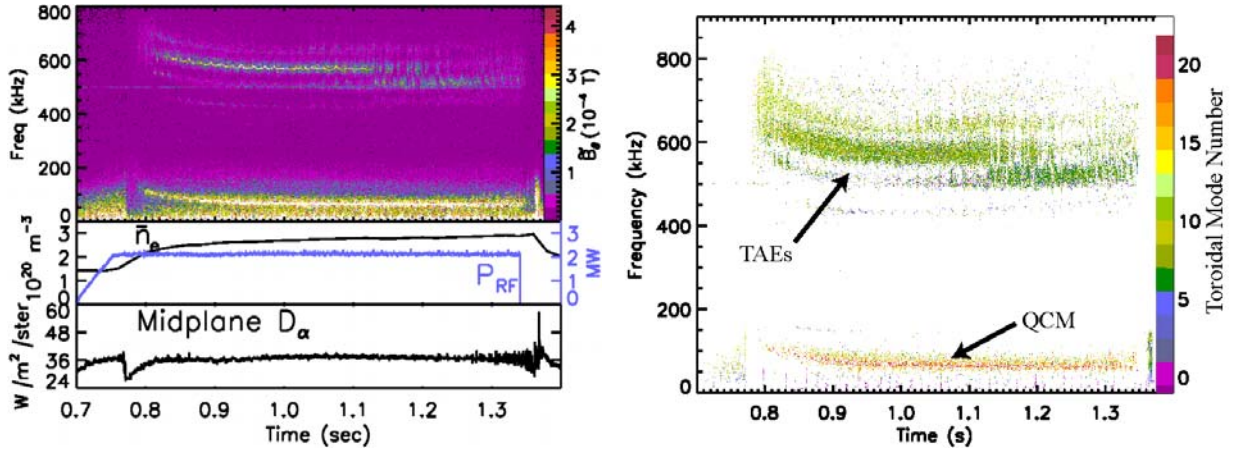


Figure 6-6 — a) Fourier spectrogram of a magnetic pick-up coil signal showing unstable TAEs during the H-mode phase of an ICRF heated discharge around 600 kHz. b) Toroidal mode number spectrum of the discharge in a) showing the TAEs have $6 \leq n \leq 11$ and that they rotate in the same direction as the quasi-coherent mode (QCM) in the electron diamagnetic drift direction.

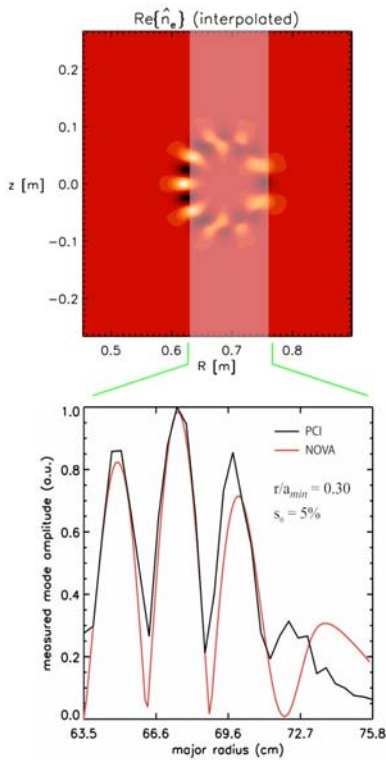


Figure 6-7 — Comparison of NOVA-calculated 2D mode structure of an Alfvén Cascade with the measured structure from PCI line-integrated along vertical chords, together with a synthetic PCI calculated signal from NOVA, showing good agreement.

Early heating in the current rise drives Alfvén cascades or reversed shear Alfvén eigenmodes (RSAEs) that are observed with both the magnetic pick-up coils and the PCI diagnostic. The cascades are excited at integer and half-integer values of q_{min} and exhibit a characteristic frequency ‘chirp’ up due to the mode’s sensitivity on $(q - q_{min})$, which is evolving throughout the I_p ramp up. The minimum in frequency of RSAEs on C-Mod has been found to scale as $\sqrt{T_e}$, as expected for geodesic acoustic modes according to theory [9]. Modeling the RSAE modes with the NOVA code together with a synthetic PCI diagnostic to calculate what the PCI signals should observe through their line integrated measurements shows good agreement with the observed structure of the modes and the calculated structure (Fig 6-7). So the radial structure and frequency time evolution of the modes can be combined to provide a measure of the evolution of the q -profile, particularly $q_{min}(t)$ as well as the structure of the eigenmodes. More recently, core localized RSAEs have also been observed with PCI in the current flattop leading up to sawtooth crashes and have been successfully modeled with NOVA [10].

Very early lower hybrid current drive (LHCD) during plasma initiation has also excited fast electron driven AEs that burst at integer and half-integer q values and allow a comparison between theory and experiment of

the fast electron distribution [11]. These modes give a very precise measure of the resonant q time evolution and together with theory allow a comparison of the fast electron energy predicted to drive these modes with measurements from the hard x-ray profile diagnostic.

6.2 Proposed 5-year MHD Research Program

6.2.1 Disruption Mitigation

High pressure gas jet experiments on Alcator C-Mod and other tokamaks have been very successful at mitigating two out of three of the important disruption effects, namely halo currents and thermal loads on divertor targets. Delivery times have been minimized on C-Mod by using optimal mixtures of high-Z noble gases with helium, and overall gas loads have been reduced enough to avoid operational delays due to post-gas jet recovery. These gas jet experiments will still continue for some time on C-Mod in conjunction with the development of real-time disruption detection algorithms for additional types of disruptions (locked mode, density limit, etcetera). In addition, the NIMROD/KPRAD (NIMRAD) modelling, which has been extremely useful in understanding the physics involved in gas jet mitigation, will continue to advance. However, there is still one disruption mitigation issue remaining that has not yet been resolved, namely the prevention and/or elimination of runaway electrons.

Disruption runaway electron studies

Disruptions on ITER may have the potential to generate several megamps of multi-MeV runaway electron (RE) beams during the current quench due to avalanching [12]. This problem is unique to ITER and future reactors because of their high plasma currents. In the absence of RE loss mechanisms, the avalanching process is exponentially dependent on I_p , so compared to today's ~ 1 MA machines, ITER's 15 MA will result in avalanche growth that is e^{15} , or 3×10^6 larger. So even though runaway electrons are not much of an issue on present machines, they could result in catastrophic damage to the ITER vacuum vessel if the RE energy dump is localized. This large difference between ITER and today's tokamaks makes it challenging to study the issue directly in current machines.

Avalanching growth of multi-MeV runaway electron population can be reduced and even eliminated by collisions with thermal electrons in the plasma, both free and bound. However, in the case of ITER, suppressing the avalanche process by means of collisional damping alone would require an enormous number of electrons. In the ITER Physics Basis [13], Rosenbluth derived a value of order 10^{22} electrons/m³ to suppress the avalanche process, under the assumption that there are no other loss mechanisms. This is two or more orders of magnitude greater than the requirements for mitigation of halo currents and thermal loads, based on extrapolation of results from current machines. Based on results from current experiments with regard to the low assimilation of gas atoms into the plasma, this would require the injection of roughly 1 kg of gas in ~ 10 ms. (The fastest current quench time in ITER is predicted to be 36 ms.) Furthermore, although it may be technically possible to realize this magnitude of injection in ITER, the consequences for the torus pumping system and tritium recovery plant are extremely severe, and post-gas injection recovery could take 12 hours or more due to cryopump regeneration.

Obviously one approach to exploring RE avalanche suppression in present machines would be to experiment with massive gas injection to study the feasibility of collisional damping. However, there are numerous hints that other RE loss mechanisms exist in current tokamaks, and studies on JT-60U have shown that B-field perturbations due to MHD modes are one such mechanism [14]. This suggests that huge gas loads may not be required, but a good understanding of RE physics is necessary in order to project this to ITER, because even a single large RE event could compromise the vacuum vessel.

Runaway electrons are not normally generated during disruptions in Alcator C-Mod. However, it may still be possible to study RE disruption physics because C-Mod has a lower hybrid current drive system which can routinely generate a population of fast electrons (~ 100 keV). Furthermore, the LH research program on C-Mod includes detailed study of the fast electron spatial profile, temporal evolutions, and energy spectrum using a sophisticated hard x-ray imaging diagnostic. In addition, one or more of the plasma video monitors observe(s) forward-cone synchrotron radiation from the fast electrons. Finally, C-Mod's A-coil set can provide a controllable source of non-axisymmetric B-fields which could possibly be used to study the effect of B-field perturbations on the confinement of runaway electrons. With LHCD to provide a seed of fast electrons, and hard x-ray and synchrotron diagnostics, and its A-coils, Alcator C-Mod has a unique capability to study RE confinement physics during disruptions IF it can be shown that the LH-generated fast electrons are indeed converted to runaways during the disruption. This needs to be demonstrated on C-Mod, but plausibility of this is greatly enhanced by recent observations from FTU [15] showing unambiguous effects of runaway electrons during disruption current quenches on shots where their LHCD was on (Fig. 6-8).

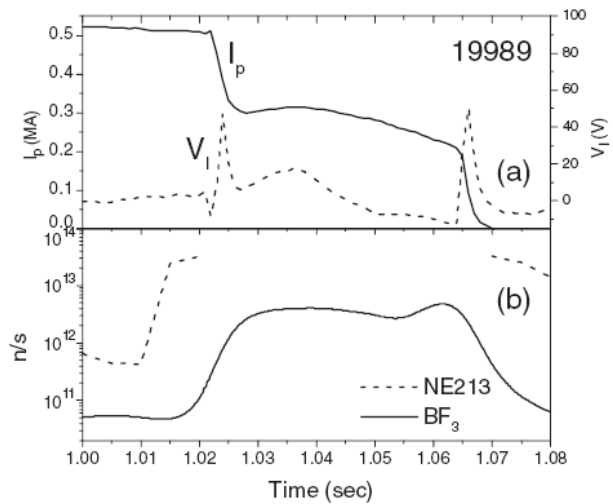


Figure 6-8 — Observation of 0.3 MA of runaway current during a disruption in FTU (plateau in current quench), along with photoneutrons detector with two instruments [15]

Based on this observation, we propose embarking on a research program to study the confinement and loss of runaways during disruptions in Alcator C-Mod using the tools that have been described. The first goal will be to demonstrate that runaways can indeed be generated during the current quench from the seed of fast electrons. Assuming that is successfully demonstrated, the hard x-ray and synchrotron diagnostics will be used to study the RE population and how it varies with applied B-field perturbations, and also with the spatial location of the seed electrons (by varying the LH phasing). In particular, applied non-resonant perturbations may be particularly attractive since they would not be expected to degrade confinement of the plasma prior to a disruption. The ultimate goal would be to find out if controlled, benign B-field perturbations could reliably suppress the formation and/or avalanching of runaway electrons during disruptions, and if so, to understand the physics well enough to extrapolate to ITER.

6.2.2 Effects of Non-axisymmetric Fields

Research on error field mode locking thresholds and scalings in Alcator C-Mod has been essentially completed. The A-coils are now routinely used with the plasma control system to reduce error fields, allowing for plasma operation at higher I_p and lower n_e . However, the non-axisymmetric perturbation fields produced by the A-coils can be used to study a number of other important phenomena.

Magnetic Braking of Rotation

Plasma toroidal rotation, particularly in a torque-free tokamak such as C-Mod, challenges our understanding of momentum transport in tokamaks. Moreover, plasma rotation provides effective, passive stabilization of high- β resistive wall modes and other MHD instabilities, and is therefore of practical interest to ITER. Understanding the physics of plasma rotation is necessary in order to predict the rotation behavior of ITER plasmas, and thus their MHD stability to certain modes. Neoclassical toroidal viscosity (NTV) theory [16] has been developed to provide this understanding. Elements of NTV theory have been tested on JET by applying $n = -2$ (i.e. non-resonant helicity) error fields to provide a control knob on rotation braking of the plasma (Fig. 6-

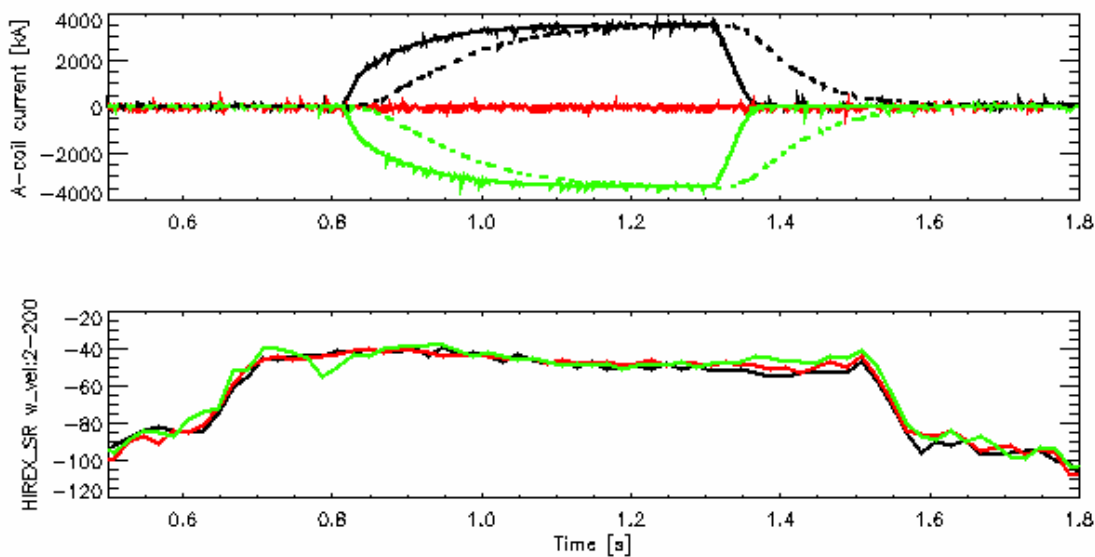


Figure 6-9 — Data from the initial experiment testing NTV theory on C-Mod. Top graph shows applied A-coil current and resulting $n = -2$ error field for a series of discharges. Lower graph shows measured core rotation. For this initial experiment a null result was obtained, in agreement with NTV theory.

9). The initial results from JET show that a transiently-applied non-resonant $n = 2$ field does indeed slow down the plasma rotation by an amount that is in agreement with NTV theory. Non-

resonant error fields have also been shown to have important effects on DIII-D. Experiments to test NTV theory on C-Mod, as part of a joint ITPA dimensionless identity experiment with JET, have just recently begun and will continue. The A-coils on C-Mod can produce an applied $n = -2$ error field structure very similar to that on JET, and plasmas with similar dimensionless parameters will be run. Rotation braking of the core and edge plasma can be measured spectroscopically through the Doppler shifts of x-ray (HIREX-Sr viewing argon) and visible (DNB-based CXRS viewing boron) line radiation as a function of time. The joint experiments are aimed at experimentally determining the toroidal viscosity in each machine, as well as the neoclassical velocity. These results from dimensionally different machines should provide a stringent test of NTV theory. A successful outcome would bolster our confidence in predicting rotational effects in ITER.

Resonant Magnetic Perturbation in the Edge

Experiments on DIII-D using applied $n = 3$ magnetic perturbations, which are resonant around the $q = 3$ surface in the pedestal region, have shown notable success at mitigating the effects of ELMs, and have even eliminated ELMs, without degrading overall confinement [17]. The resonant magnetic perturbations (RMP) are seen to modify the pedestal profiles, apparently by changing the transport in the edge, and thus the stability of the edge peeling/ballooning modes. Similar experiments on JET, using applied $n = 1$ edge-resonant fields, have also reduced the effects of ELMs [18]. Alcator C-Mod usually has type-I ELMs only in unusually high-triangularity H-modes, but the ability to modify and/or control edge pedestal profiles would be useful for studying transport in the pedestal region in all H-mode regimes. Using the present A-coil set, we are proposing to do similar $n = 1$ RMP experiments on C-Mod to study the effects on edge transport, and on ELMs in a machine without strong beam rotation. In addition, the RMP experiments on C-Mod could be designed so as to test the various theories for RMP suppression.

NTM Stability and Thresholds

In principle, resonant non-axisymmetric fields may affect the growth and stability of tearing modes on low-order rational surfaces, and thus the seed islands which are necessary to generate neoclassical tearing modes (NTMs). Therefore it may be possible to use the A-coils to study the non-linear NTM threshold physics, at least for the 2/1 mode. An upgrade to the A-coil set (see below) will allow the study of the 3/2 mode.

Proposed Upgrades to A-coil System

The present A-coils on Alcator C-Mod are mounted on the external surface of the igloo, which is about 3 meters from the plasma surface. For several of the proposed research items the magnitude of the non-axisymmetric field at the resonant surfaces is at the low end of the desired range. Ideally one would prefer to have the coils be much closer to the plasma, but the only available spaces in the C-Mod structure would be on the outboard surface of the vacuum vessel, or inside the vessel itself. Both options would place the coils in the high toroidal field region, and the resulting $J \times B$ forces are prohibitively high, so these options are not feasible. However, we plan an upgrade to add one or more additional power supplies, which will allow us to: (1) increase the current, and therefore field amplitude by a factor of two or more, and (2) allow for additional flexibility in generating different mode structures, particularly if the upgraded supplies are bipolar. In addition, with incremental funds it is also feasible to increase the number of A-coils to a set of 6 x 2, which would permit the generation of $n = \pm 3$ fields.

6.2.3 Axisymmetric Stability of ITER-like Equilibria

Advanced Controllers

ITER needs to be confident of axisymmetric control when operating close to machine limits. Both ITER and C-Mod could benefit from the development and testing of smart adaptive control algorithms beyond those that are in use on today's machines. This requires experimental investigation and verification on an ITER-like machine. C-Mod is a good facility in which to do this since we normally run ITER-like plasma shapes; we have a highly conducting vacuum vessel; and our equilibrium coils are relatively far from the plasma, similar to ITER. We intend to design and experimentally validate higher order controllers to improve controllability of high-elongation, high- ℓ_i plasmas. The Alcator control simulator tool (Alcasim) will be especially useful for investigating new control algorithms.

Noise Rejection

In order to reduce AC losses in its superconducting coils, the ITER control system has stringent limits on measurement noise and fluctuations in its feedback loop. C-Mod can address the issue of noise and how to suppress/reject it. We will analyze the sources of noise and pickups and estimate their effects on axisymmetric control (control precision, power supply and PF coil requirements, etcetera). We will also study noise suppression through the use of model-based filters.

Safe Scenarios

We also propose continuing our design work on 'safe scenarios' and other adaptive interpolation algorithms to be deployed in case of power supply saturation, including experimental validation of their effectiveness.

6.2.4 Neoclassical tearing modes (NTMs)

With the combination of high ICRF power and LH power, high $\beta_N \geq 1.7$ conditions should be achievable in C-Mod during the next few years, allowing access to regimes where neoclassical tearing modes are expected to go unstable. In addition, the cryopump allows controlled operation at low densities and therefore low collisionalities where NTMs are more likely to occur. This opens up research opportunities to study NTM physics at C-Mod conditions and parameters, including: (1) threshold β_N scalings, (2) critical seed island physics (by ramping β_N down), (3) rotation effects on the NTM threshold β_N , and (4) effects of non-axisymmetric fields on the NTM threshold (see previous section). Obviously a number of dimensionless identity experiments should be undertaken to test the validity of NTM theory. For example, such an experiment is already planned between C-Mod and DIII-D to determine if the threshold of $\beta_N \approx 1.7$ found on DIII-D will also be found on C-Mod at the corresponding dimensional parameters of $B_T = 5.3$ T, $a = 0.22$ m, and $n_e = 2.5 \times 10^{20} \text{ m}^{-3}$.

LHCD Stabilization of NTMs

A potential application of lower hybrid current drive (LHCD) on both C-Mod and ITER is for direct NTM stabilization. This has been accomplished with electron cyclotron current drive (ECCD) on DIII-D[19] and other tokamaks, but LHCD has the distinct advantage that its current

drive efficiency is notably higher than ECCD. The stabilization physics is also quite different; ECCD stabilization works mainly by driving current in a narrow profile centered on the island in order to replace the missing bootstrap current. In contrast, LHCD stabilization works mainly through the Δ' term, i.e. by modifying the current profile in the vicinity of the resonant surface. We have successfully demonstrated the use of LHCD to both stabilize and destabilize *classical* tearing modes by launching different $n_{//}$ spectra, as shown in Fig 6-10. The same Δ' modification with LHCD should carry over directly to NTM stabilization.

ICRF Stabilization of NTMs

Previous work on a number of tokamaks [20], including C-Mod, has shown that ICRF can modify sawtooth periods and even eliminate sawteeth under certain circumstances. The sawtooth crash is one of the principal ways that seed islands are generated, leading to the destabilization of NTMs. Therefore reducing the sawtooth crash amplitude and/or eliminating sawteeth altogether could effectively result in the suppression of NTMs. The possible RF techniques for doing this (ICRF, FWCD, LHCD, MCCD, ICCD) are discussed in detail in chapter 5.

6.2.5 TAEs and fast particle instabilities

To improve our understanding of Alfvén eigenmodes, upgrades to existing and new fast particle diagnostics are proposed together with enhancements to the numerical codes used to interpret the data. Diagnostic upgrades include possibly installing a second pair of active MHD antennas, enhancing the time resolution of the high spatial resolution ECE diagnostic, enhancing the CNPA to a multiple channel system to provide confined fast ion profiles, and perhaps installing a second PCI system to measure toroidal mode numbers of core localized modes. New fast particle

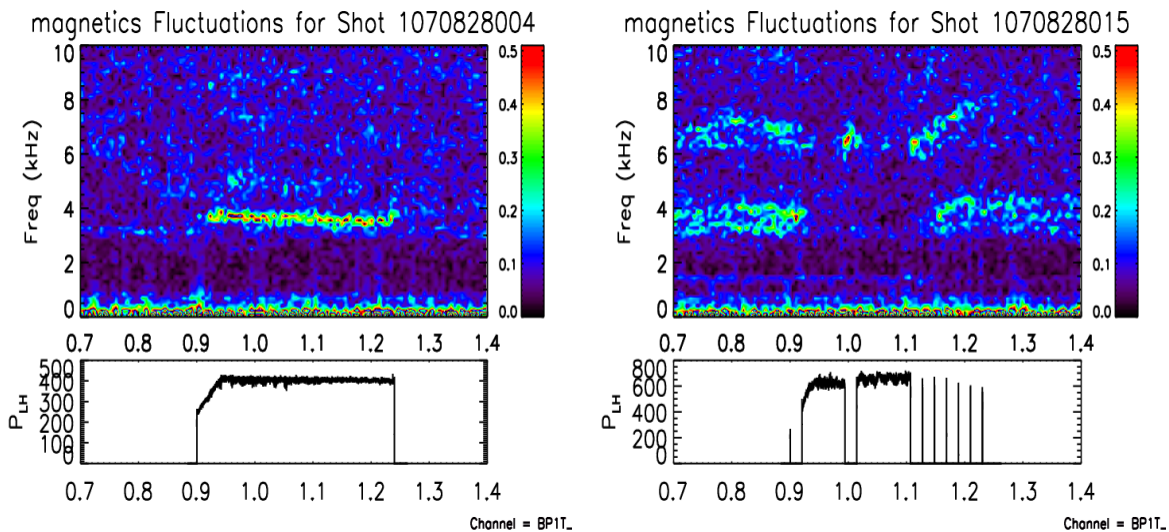


Figure 6-10 Examples of destabilization (left) and stabilization (right) of classical tearing modes using LHCD. The tearing modes show up in the B spectrograms (upper graphic on each side). The LH power is shown in the lower trace. The left case has $n_{//} = 2.3$, the right is $n_{//} = 1.6$.

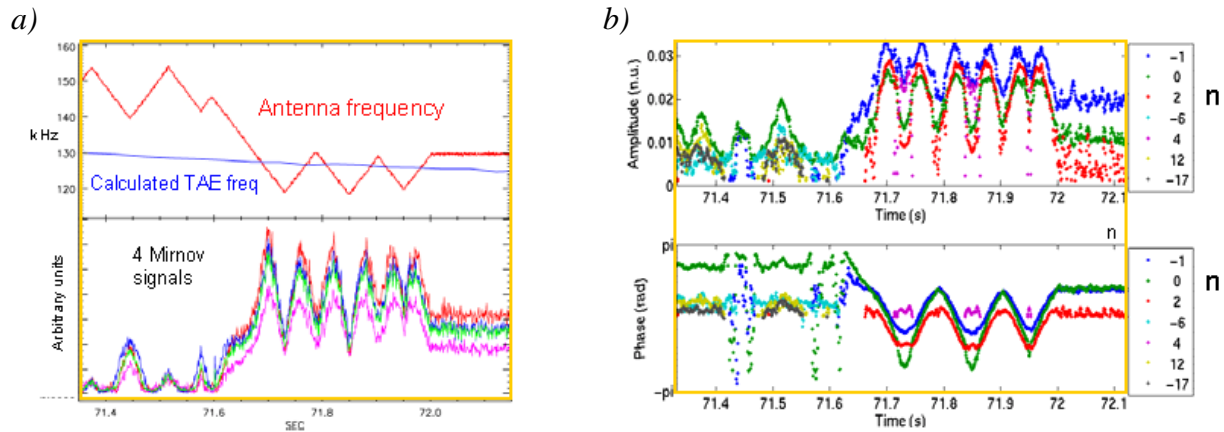


Figure 6-11 — a) Magnetic pick-up coil synchronously detected signals from four coils together with the sweeping TAE antenna frequency and calculated center of the TAE gap frequency vs time from $71.5 < t < 72.1$ s for JET shot 69586. b) SparSpec calculated amplitude and phase of the dominant toroidal modes. (Courtesy A. Klein)

diagnostics include a fast ion loss diagnostic (FIL) scintillator probe to measure the energy and pitch angle distribution of fast ions lost by MHD activity with high time resolution and a fast ion D_α (FIDA) diagnostic to measure confined fast ions with the diagnostic neutral beam (DNB). Enhancements to numerical codes used to interpret Alfvén eigenmode data include further improvements in the NOVA-K code for ICRF fast ion distributions in collaboration with PPPL, improvements to the AORSA/CQL3D codes to include finite orbit width effects, improvements to the TORIC code within TRANSP for ICRF distributions, use of the SparSpec [21] code to improve MHD mode analysis, and synthetic ECE and CNPA diagnostic codes to improve the comparisons between the codes and the measured data.

The study of the dependence of the damping rate of stable Alfvén eigenmodes on plasma parameters will continue with either one or two pair of active MHD antennas. With incremental funds, a second set of active MHD antennas will be installed on the opposite side of the tokamak toroidally, as has been done on JET, to be able to selectively excite even or odd n numbers and improve the signal-to-noise ratio of the excited stable modes. With only one toroidal location for exciting stable AEs, the excited mode spectrum is very broad with no selectivity. While it is not possible to selectively excite a given intermediate n number without having a large number of antennas all the way around toroidally, having two sets of antennas on opposite sides of the tokamak would allow selectively exciting even or odd n numbers, depending on the relative polarity of the two sets of antennas. An additional antenna pair would also provide twice as much flux, which would double the signal-to-noise ratio for measuring stable modes. Closed-loop frequency control should also be implemented for the active excitation of AEs, which would confine the excitation frequency to a narrow band around any observed resonance, as is done on JET. Real-time tracking of an AE decreases the band of the frequency excursions, increasing the time resolution of stable AE resonances. Further experiments are planned to study the effects of fast ions on the measured damping rate of stable AEs with either off-axis ICRF or choosing the active MHD frequency to correspond to more core localized modes near $q=1$. JET now has their intermediate n TAE antennas operational and high priority joint ITPA experiments comparing the scaling of TAE damping rates across plasma conditions between these devices are planned for the

coming years. MAST and JT-60U have also installed moderate n TAE antennas and are also taking part in these joint ITPA experiments. By comparing C-Mod damping rates taken at the toroidal field and density of ITER with results from the large size and high temperature plasmas of JET and JT-60U and results from the low aspect ratio MAST device, we hope to successfully extrapolate the results to ITER.

The collaboration between MIT and JET in the study of Alfvén eigenmodes has helped develop a new analysis code called SparSpec [21] for determining toroidal mode numbers. This code is based on algorithms originally developed by the astrophysics community for determining the smallest number of modes that could describe the orbit of a celestial object sampled at various times throughout a calendar year. Unequally spaced pick-up coils toroidally provide data that can be interpreted in the same way allowing the smallest number of modes to be determined that best describes magnetic fluctuations in a tokamak. This is particularly important for actively excited stable intermediate n modes since a broad spectrum of modes is excited, which can result in multiple n modes at approximately the same frequency. Ordinary Fourier analysis methods can only determine a single mode number at a given frequency. Figure 11 shows an example of SparSpec calculated mode numbers for modes excited with the JET intermediate n TAE antennas [22]. The SparSpec code has been successfully implemented on JET and will soon be used to analyze C-Mod magnetics data to determine the toroidal mode numbers of both stable and unstable modes.

Present comparisons between Alfvén eigenmode measurements and the NOVA-K code calculations have shown discrepancies in the mode stability for the measured direction of mode rotation. Anisotropy in the fast ion distribution function could be responsible for some of these discrepancies. So, a more accurate model of the ICRF distribution function needs to be included in NOVA-K calculations. Both the presently used TRANSP/TORIC calculations of the fast ion distribution and more sophisticated AORSA/CQL3D calculations need to be improved and used in NOVA-K. Enhancements to the AORSA/CQL3D codes including orbit width effects together with improvements in fast ion diagnostics such as the planned multi-channel CNPA to provide confined fast ion profiles will allow more detailed comparisons with experiments.

Another high-priority ITPA research topic is to determine if TAEs cause loss of the fast NBI or ICRF ions that couple the auxiliary heating power to the thermal plasma. Most other machines are concentrating on NBI, but an experiment is being planned on C-Mod to look for any reduction in ICRF heating efficiency due to driven TAEs. The active MHD antenna system, however, does not have sufficient power, so instead plans call for using the relatively strong beat wave produced by the interaction of the D and E ICRF transmitters. These are normally run at 80.0 and 80.5 MHz, resulting in a beat wave at 500 kHz which is clearly seen on the Mirnov pickup coils. With some effort, the frequency difference can be adjusted to 400 kHz, which is within the normal range of stable TAE modes in C-Mod. By varying the density, the TAE resonance can be excited at will with the strong beat wave, and possible reductions of heating efficiency in phase with the TAE excitations will be investigated.

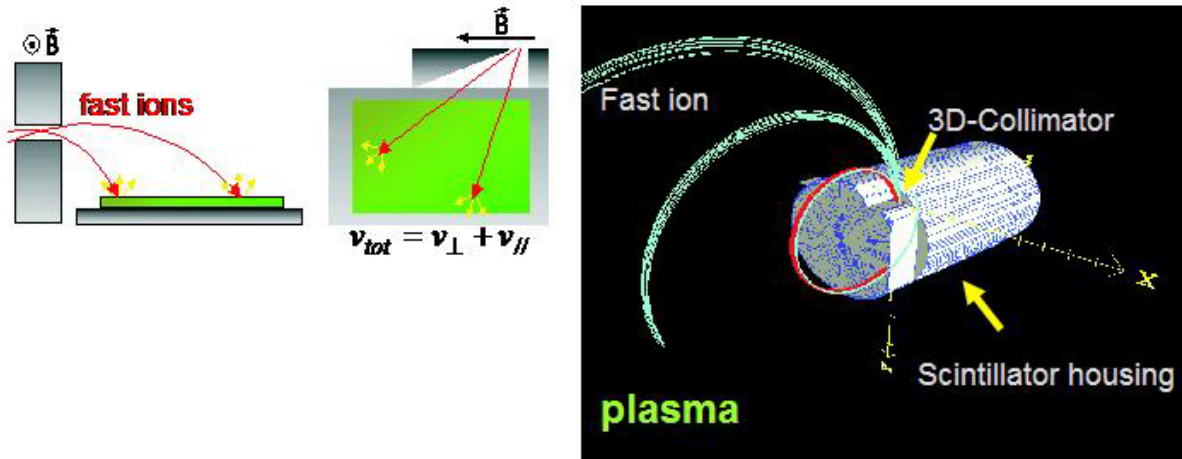


Figure 6-12 — Schematic diagram of the fast ion loss diagnostic scintillator probe on ASDEX Upgrade showing how fast ions lost from the plasma enter the slit and are mapped in 2D onto the scintillator plate dispersed in both gyroradius and pitch angle. (Courtesy M. Garcia-Muñoz)

A new fast ion loss diagnostic (FILD) scintillator probe that is presently being designed will measure lost ICRF generated fast ions to provide a more accurate measure of the effects of AEs and other MHD activity on the transport of fast ions. Figure 12 shows a schematic of a similar diagnostic that is used on ASDEX-Upgrade [23]. With a slit close to the plasma edge, fast ions gyrating along field lines strike a scintillator plate at a position that is dispersed according to the gyroradius and pitch angle of the fast ion. By splitting the image of the scintillator plate between a CCD camera and an array of fibers leading to photomultiplier tubes, both the 2D spatial and energy information can be obtained at standard CCD image rates as well as very fast (2 MHz) time histories of the fast ion loss rate. This allows the fast ion loss rate to be measured in phase with the TAE oscillations, quantifying the fast ion transport due to these modes.

With high power LHCD, the study of Alfvén cascades will be expanded by extending the reversed shear phase of the discharge and by providing a tool for modifying the current density profile. The addition of the motional Stark effect (MSE) diagnostic with the DNB, as well as the new polarimetry diagnostic, will provide additional measures of the q profile to compare with that found by comparison of the time evolution of the Alfvén cascade frequency with the theory of Alfvén cascades. It may also be possible to measure the ion-to-electron temperature ratio from the low-frequency rollover feature of the Alfvén cascade modes. Because of difficulties in determining the mode numbers of core localized Alfvén cascades from pick-up coils at the wall, a second PCI diagnostic may be added to the port adjacent to the existing PCI diagnostic to be able to measure the toroidal mode number by comparing chords between the two toroidal locations.

New high radial and time resolution ECE measurements implemented through our collaboration with the University of Texas at Austin should also be able to measure the local radial structure of the AEs. Additional pick-up coil limiters that have been installed at four toroidal locations around the machine also improve the toroidal mode number resolution for both the AEs and other MHD activity. A synthetic ECE diagnostic may also be developed for the NOVA-K code to

compare the calculated AE radial structure with the new measurements to better benchmark the code and improve consistency with calculated q profiles.

6.2.6. Summary of MHD research for ITER/ITPA

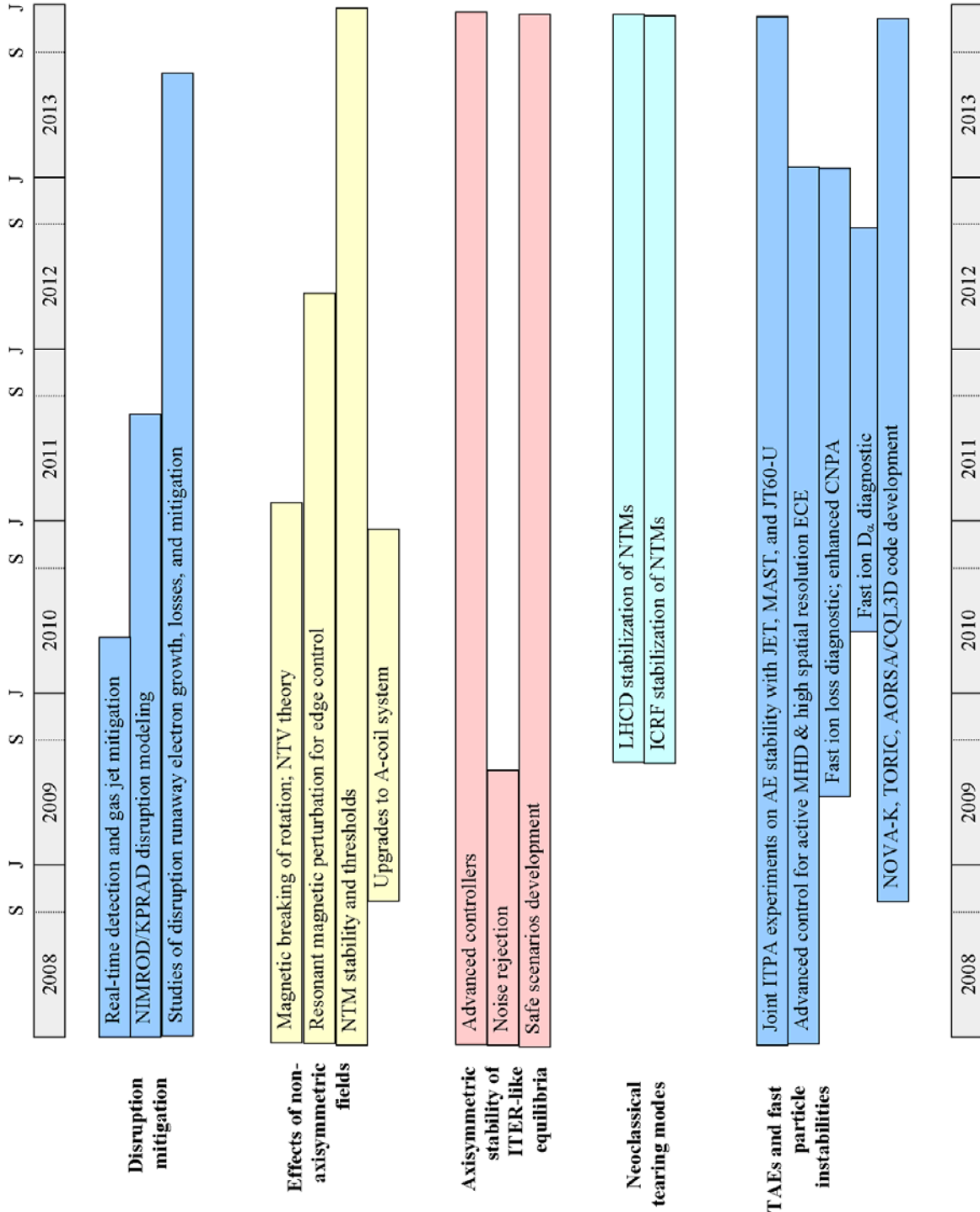
Description	JOINT Experiments	Notes on C-Mod Contributions
Disruption mitigation by massive gas jets	MDC-1 (DSOL-11)	Optimise gas mixture; injection quantity, real-time detection and triggering
Disruption runaway physics and mitigation	Under discussion	LHCD-driven seed; hard x-ray and synchrotron diagnostics
Vertical stability of ITER-like equilibria	MDC-13	Advanced controllers; noise characterization and rejection
Error field effects on NTMs	MDC-3	
Sawtooth control for NTM suppression	MDC-5	ICRF; LHCD
Current drive prevention/stabilisation of NTMs	MDC-8	LHCD modification of Δ'
TAE intermediate- n damping rates	MDC-10	Compare with JET
Fast ion losses and redistribution from TAEs	MDC-11	New fast ion loss detector
Rotation effects on NTMs	MDC-14	
Non-resonant magnetic braking	MDC-12	Compare with JET
Resonant magnetic perturbation effects on ELMs and pedestal	PEP-19	C-Mod will do $n = 1$

6.2.7. MHD Research Objectives

Research Goal	Intermediate Objectives	Approach/Key new diagnostics
Disruption mitigation, including runaway electrons	Finalize optimization of gas mixture, pressure, and injected quantity	Characterize P_{rad} fraction, I_{halo} , divertor ΔT , and response time vs gas jet parameters
	Continue development of real-time disruption prediction and mitigation activation for additional types of disruptions	DPCS programming; offline validation
	Continue collaboration with modelers on NIMROD/KPRAD simulations of gas jet disruption mitigation	
	Study physics of runaway electron physics during disruptions (loss mechanisms) and mitigation using unique C-Mod tools (LHCD, hard x-ray and synchrotron diagnostics, error-field coils)	Use LHCD to provide fast electron seed; Use A-coils to provide B-field perturbations. Specific diagnostics: hard x-ray PHA array, synchrotron imaging.
Study effects of non-axisymmetric fields	Magnetic braking of rotation; tests of neoclassical toroidal velocity (NTV) theory	Use A-coils in $n=2$ configuration. Specific upgrade: additional A-coil power supplies
	Explore resonant magnetic perturbations for affecting/controlling edge pedestals and ELMs	Use A-coils in $n=1$ configuration. Specific upgrade: additional A-coil power supplies.
	Explore effects on NTM seed islands	Use A-coils in 2/1 and 3/2 configurations. Specific upgrade: additional A-coil power supplies.
	Upgrade A-coil power supplies and coilset	
Characterize and improve axisymmetric stability of ITER-like equilibria	Develop advanced controllers for stability at higher elongation	Specific tools: Alcasim simulator
	Characterize effects of noise on feedback and develop noise rejection/suppression algorithms	'Noise' includes disturbances due to ELMs, L-H transitions, sawteeth, etc
	Develop 'safe scenarios' and adaptive algorithms in case of power supply saturation/failure	DPCS programming
Neoclassical tearing modes (NTMs)	LHCD stabilization of NTMs by modification of Δ'	Adjust plasma parameters and LH phasing to drive current at the $q=3/2$ and $q=2$ surfaces
	ICRF stabilization of NTMs by eliminating sawtooth seed islands	MCCD, FWCD
TAEs and fast particle instabilities	Characterize dependence of intermediate- n TAE damping rate on plasma parameters	Active MHD antennas; frequency sweeps
	Benchmarking codes (NOVA-K, AORSA/CQL3D) against experiment	
	Study TAE-induced fast ion loss (ICRF-generated ions)	Use beat frequency of D and E antennas to drive TAEs; look for ion losses. New diagnostics: fast ion loss, CNPA array

	Combine measurements and modeling of reversed shear AEs (Alfven cascades) to provide information on q-profile modification by LHCD	Temporal evolution vs mode number
	Combine measurements and modeling of reversed shear AEs (Alfven cascades) to provide information on q-profile modification by LHCD	Temporal evolution vs mode number
	Diagnostic upgrades (two more antennas; CNPA array, fast ion loss diagnostic, fast ion D_α diagnostic, 2 nd PCI)	

6.2.8. MHD Research Schedule



6.2.9 References

- [1] R.S. Granetz, D.G. Whyte, V.A. Izzo, *et al*, Nucl. Fusion **46** (2006) 1001-8.
- [2] R.S. Granetz, E.M. Hollmann, D.G. Whyte, V.A. Izzo, *et al*, Nucl. Fusion **47** (2007) 1086-91.
- [3] V.A. Izzo, Nucl. Fusion **46** (2006) 541-7.
- [4] S.M. Wolfe, I.H. Hutchinson, R.S. Granetz, *et al*, Phys. Plasmas **12** (2005) 56110-1-10.
- [5] C. Z. Cheng, (1992) *Phys. Reports* **211**, 1.
- [6] E. F. Jaeger, *et al.*, (2006) *Journal of Physics: Conference Series* **46**, 82.
- [7] D. Testa and A. Fasoli, (2001) *Nucl. Fus.* **41**, 809.
- [8] J. A. Snipes, *et al.*, (2007) *Proc. 10th IAEA TCM on Energetic Particles, Kloster Seeon*, P9.
- [9] B.N. Breizman, M.S. Pekker and S.E. Sharapov. (2005) *Phys. Plasmas* **12**, 1.
- [10] E.M. Edlund, M. Porkolab, L. Lin, *et al.*, to be published.
- [11] J. A. Snipes, R. R. Parker, A. Schmidt, G. Wallace, and P. E. Phillips, submitted to *Phys. Rev. Lett.*
- [12] M.N. Rosenbluth and S.V. Putvinski, Nucl. Fusion **37** (1997) 1355.
- [13] F. Perkins, *et al*, *Plasma Physics and Controlled Nuclear Fusion Research*, 1995, p 477-88 vol.2
- [14] R.Yoshino and S.Tokuda, Nucl. Fusion **40** (2000) 1293-1309.
- [15] J.R. Martin-Solis, *et al*, Phys. Rev. Lett. **97** (2006) 165002-1-4.
- [16] C. Shaing and J. D. Callen, Phys. Fluids **26** (1983) 1526.
- [17] T.E. Evans, *et al*, Nucl. Fusion **45** (2005) 595-607.
- [18] Y. Liang, *et al*, Phys. Rev. Lett. **98** (2007) 265004-1-5.
- [19] R. Prater, *et al*, Nucl. Fusion **43** (2003) 1555-69.
- [20] O. Sauter, *et al*, Phys. Rev. Lett. **88** (2002) 105001-1-4.
- [21] S. Bourguignon, H. Carfantan, T. Bohm, (2007) *Astronomy and Astrophysics* **462**, 379.
- [22] A. Klein, *et al.*, (2007) *Proc. 10th IAEA TCM on Energetic Particles, Kloster Seeon*, P4.
- [23] M. Garcia-Muñoz, (2006) *Max-Planck-Institut für Plasmaphysik*, IPP-Report II/12.

7 Pedestal Physics

On Alcator C-Mod, as in the broader tokamak community, research on the H-mode edge has been driven by the desire to understand the detailed physics processes which give rise to edge transport barriers (ETBs), and how these various mechanisms combine to determine the boundary values of density and temperature for the core plasma (*i.e.* the edge *pedestal*). ITER and other future devices present new challenges in this area, as they will require substantial pedestal pressure in order to obtain high energy confinement, yet the edge-localized modes (ELMs) that often characterize high performance discharges must be suppressed or constrained to small amplitude, in order to prolong the lifetime of divertor targets. In addition there are open questions surrounding the mechanisms governing the transition from L-mode to H-mode plasmas, and the capability of existing power threshold scalings to predict the required input power needed for ITER to obtain H-mode. Pedestal physics issues permeate a number of the other topical science subjects covered in this proposal, and are an integral component of the H-mode Baseline and Advanced Scenarios integration efforts (see chapters 8, 9). The C-Mod program is actively engaged in resolving these crucial questions with an aggressive experimental pedestal program. To achieve progress toward these goals, we commit resources to improving diagnostics in the scrape-off layer and pedestal regions; we plan dedicated experiments to study pedestal transport, edge relaxation mechanisms and L-H thresholds; and we engage theoretical colleagues in collaborations intended to enhance the interpretation of experimental results. Our progress on these fronts in the previous five years, and our plans for moving forward, are discussed below.

7.1. Highlights of recent research

7.1.1. H-mode edge transport and pedestal structure

We have taken advantage of edge diagnostics with millimeter-scale radial resolution in order to characterize the structure of H-mode pedestals, as well as their scalings with discharge parameters. In furtherance of scaling studies, we have taken advantage of ICRF tuning capabilities and alternate minority ion heating schemes in order to heat effectively over the available range of magnetic field in C-Mod, and this effort significantly increased the range of engineering parameters in which H-modes are obtained and characterized. Figure 7.1 demonstrates this expansion over an extensive range of toroidal field ($2.7 < B_T [T] < 8.0$) and plasma current ($0.4 < I_p [MA] < 1.7$). H-modes were

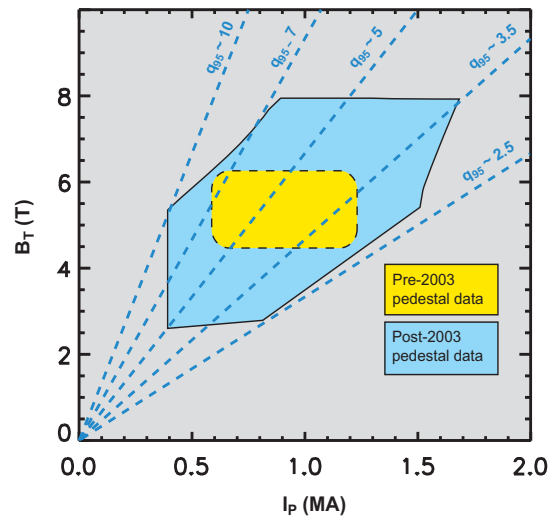


Figure 7.1: H-mode pedestal data set expansion in field-current operational space, 2003—2008.

obtained across this operational space with varying density and ICRF input power [1]. As a consequence, substantial variation in potentially significant local edge parameters was also obtained, so that quantities such as pedestal height and gradient could be mapped in a “phase-space” determined by either global or local parameters. Thus we achieve a twofold goal: first, determining operational recipes for obtaining desired pedestal parameters, and second, providing an extensive data set for testing theories that predict pedestal width and height. As discussed later in this chapter, both variation in plasma shaping and active pumping have also been used to extend our H-mode data set.

For several years the workhorse diagnostic for pedestal profile studies has been the edge Thomson scattering (ETS) diagnostic [2]; recently we have added CXRS diagnostics which have begun to provide spatially resolved measurements of temperature and velocities (poloidal and toroidal) of B^{+5} [3], quantities which should be well-coupled to the majority ion quantities: T_i , v_{i0} , $v_{i\phi}$. Agreement between CXRS and ETS generally is quite good, as demonstrated in Figure 7.2. We have to date found no significant discrepancy between pedestal profiles of T_i and T_e , for edge collisionality ν^*_{ped} in the range of approximately 0.5—5. Such agreement supports prior transport and stability analyses that assumed ion-electron equilibration within the pedestal.

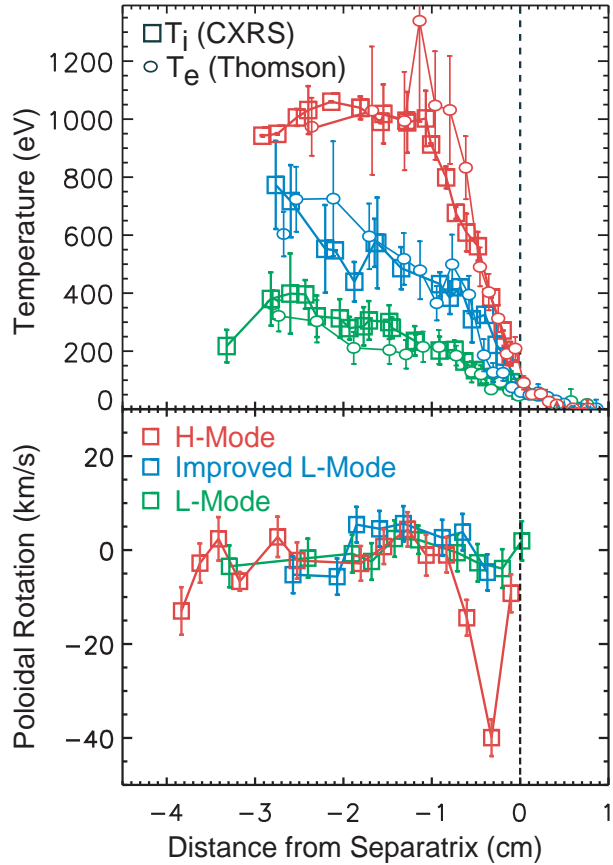


Figure 7.2: Examples of edge profiles from edge Thomson scattering (circles) and CXRS (squares) for three distinct confinement regimes.

Well-resolved measurements of T_i , v_{i0} and $v_{i\phi}$ from CXRS have begun to allow direct inference of the radial electric field E_r via the radial force balance equation. Figure 7.3 shows initial results from analysis of these data, demonstrating low E_r shear in L-mode, followed by the development of substantial E_r shear in H-mode, in qualitative agreement with results obtained on other tokamaks (*e.g.* [4]). In the ETB the well in E_r can reach depths of up to -250kV/m, a substantial fraction of which is accounted for by a strongly sheared poloidal velocity, such as that demonstrated in the H-mode of Figure 7.2. By reducing the temporal resolution from the more typical 15 ms to 5ms and less, the evolution of CXRS parameters can be tracked during both transient and steady H-modes for comparison with confinement properties. Experiments are planned in 2008 to obtain

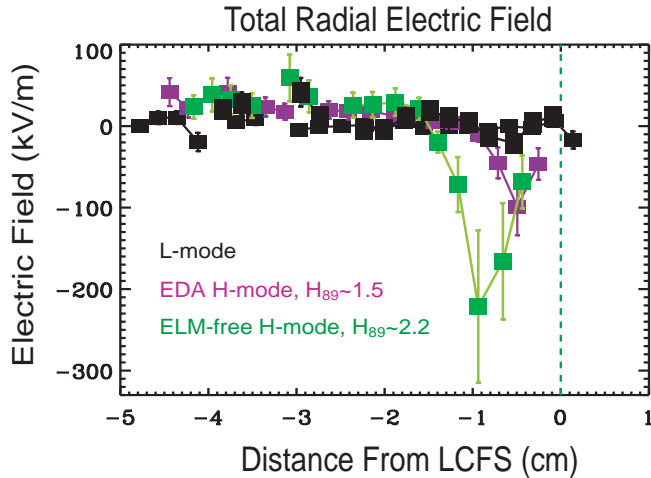


Figure 7.3: Radial electric field inferred from midplane CXRS measurements, in three distinct confinement regimes

additional CXRS data over a broad range of H-mode regimes and relate the electric field shear to pedestal quality and global confinement.

Pedestal width Δ remains one of the crucial uncertainties for the ITER H-mode scenario, despite the substantial leverage the quantity has on performance. For this reason, there is a substantial effort on all major tokamaks to identify the important physical mechanisms setting Δ . For

typical C-Mod equilibria, pedestal width is approximately 3—4% in normalized flux space, and exhibits little systematic variation with engineering parameters. We do observe wider pedestals on C-Mod both by running unusually low plasma currents ($I_p < 600 \text{ kA}$) [5] and by substantially modifying equilibrium shape (*e.g.*, by increasing triangularity) [6,7]. A possible reason for this is modification of the edge magnetic shear layer, as suggested by some modeling [8]. Ongoing experiments in 2008 will address this question in more detail. In the data set obtained over the wide range in B_T and I_p mentioned earlier, pedestal width does not scale explicitly with either the toroidal or the poloidal ion gyroradius. Nor does it scale inversely with the absolute plasma density, as would be predicted by simple models based on the penetration length of fueling neutrals [9]. In fact, kinetic modeling of edge neutrals in C-Mod H-modes indicates a strong self-screening of the pedestal to neutral fueling, the effect of which diminishes only as the overall pedestal density is reduced well below the typical operating point of $n_{e,\text{ped}} \sim 1.5\text{—}3.0 \times 10^{20} \text{ m}^{-3}$ [5]. These studies suggest that C-Mod is much less susceptible to details of edge neutral sources than larger, lower-field tokamaks, which for similar Greenwald fraction and safety factor, must run at considerably lower absolute density ($n \sim B_T/R_0$).

This question of the impact of neutral sources on the pedestal has been investigated via inter-machine pedestal matching experiments between C-Mod and other tokamaks. The general method involves adjusting engineering parameters (*e.g.* B_T , I_p , n_e) on two or more tokamaks in order to match dimensionless parameters (*e.g.* β , v^* , ρ^*) at the top of the pedestal. The subsequent comparison of the full pedestal profiles constitutes a check on whether the plasma satisfies scale invariance. Our first such experiment [10] was conducted on C-Mod and DIII-D, and it was successful at obtaining both matched pedestal profiles and non-dimensionally similar core confinement, as well as similar edge fluctuations. Because the ratio of dimensional density on two matched discharges scales with the ratio of minor radii according to $n_1/n_2 = (a_1/a_2)^{-2}$ (a factor of >5 when going from DIII-D to C-Mod), a pedestal width determined by neutral penetration length ($\propto 1/n$) should scale as a^2 . However, in the comparison of C-Mod and DIII-D, the

pedestal widths in flux coordinates matched; *i.e.*, $\Delta \sim a$. This result is highly suggestive of a weak contribution from neutral sources in setting pedestal structure. This work was followed by dimensionless similarity comparisons conducted between C-Mod and the JET tokamak [11,12], which have a size ratio of approximately 4. In this ITPA joint experiment (PEP-7), discussed further in Chapter 8, over an order of magnitude difference in edge density was required in order to obtain a dimensionless match at the pedestal top. In contrast to the DIII-D match, the JET and C-Mod non-dimensional pedestal profiles did not overlay exactly. T_e pedestals nearly matched, while the density pedestal on JET was shown to be wider in flux space, suggesting that the role of neutral sources on the pedestal can vary significantly with operating density, as determined to leading order by B_T/R_0 .

High edge densities in C-Mod result in a SOL and pedestal that are typically opaque to neutrals, a feature that limits to a large degree the edge fueling of H-modes. Instead, the density pedestal—and consequently the core particle inventory—on C-Mod are determined to first order by the plasma current, with the available neutral source playing a lesser role. Experimental characterization of particle transport was accomplished using high-resolution profiles of electron density and temperature, as well as emissivity of Balmer alpha light, allowing calculation of ionization rate profiles and effective particle diffusivity. Strong diffusivity wells were measured in the pedestal region, the depth of which increased strongly with I_p , highlighting the dominant role of plasma transport in regulating the H-mode density. Efforts to modify H-mode density through aggressive gas puffing and, more recently, enhanced neutral pumping, have revealed a remarkable stiffness in the density profiles, as seen in Figure 7.4. Increasing or reducing the neutral source available to fuel the pedestal seems to have the largest effect on the SOL density, with most of the pedestal modification coming in the temperature profile.

Throughout all efforts to modify the edge pedestal by adjusting sinks and sources of particles, as well as efforts to adjust heat flux, relatively stiff pressure profiles have been the usual observation. The emerging picture from these studies is that the H-mode pedestal structure is regulated by transport such that a “critical gradient” is maintained. This transport paradigm contrasts strongly with simple diffusive transport, and is more akin to models for core transport which assume operation near marginal stability. On C-

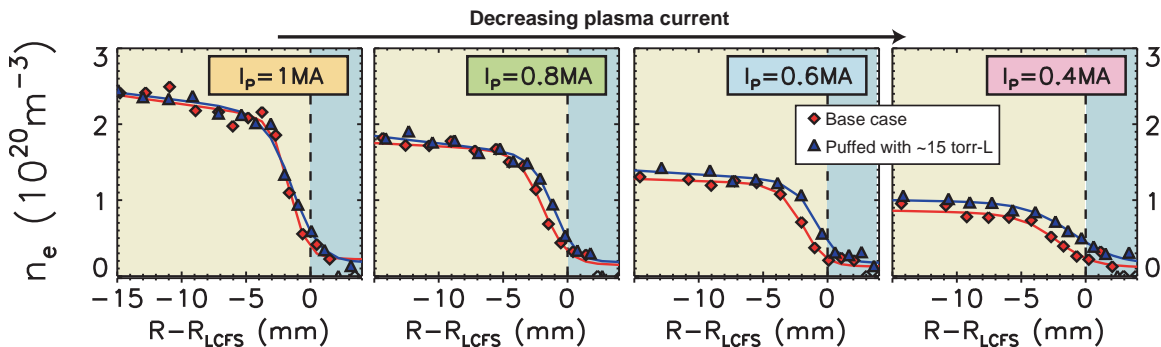


Figure 7.4: Density pedestals in steady EDA H-modes fueled by wall recycling only (red) and with supplemental gas puffing (blue). Clamped density gradients and resilience to core fueling, especially at the higher currents, are observed.

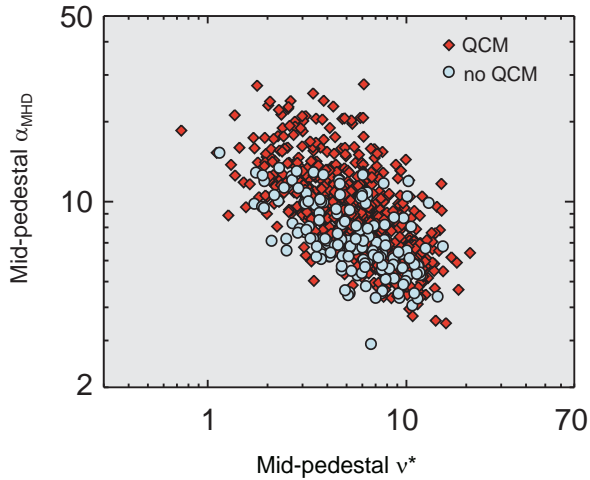


Figure 7.5: Non-dimensional H-mode pedestal pressure gradient ($\text{grad-p}/I_p^2$) as a function of collisionality over a wide range of I_p , B_T and density

Mod this trend is manifested in an H-mode edge density proportional to I_p , and an edge pressure that scales as I_p^2 . Over a wide range of dimensional engineering parameters, the H-mode edge is well characterized in terms of appropriately normalized pressure gradient (e.g., α_{MHD}) and collisionality v^* [13]. Figure 7.5 demonstrates the trend toward higher α_{MHD} (or the gradient in poloidal beta) in the pedestal as H-modes are made less collisional. Clustering in such a dimensionless phase space was also observed in the SOL of Ohmic plasmas [14], as discussed in Chapter 4.

Improved H-mode particle control has become a major priority on C-Mod, due to the desirability of low density H-mode targets for LHCD and advanced scenario targets, not to mention low collisionality plasmas for core and edge transport studies. Using a mixture of cryopumping (neutral source reduction) and magnetic balance control (pedestal plasma transport) to optimize the density pedestal, we are developing suitable H-mode targets and determining the limits of low density operation.

7.1.2. Edge stability, fluctuations

The typical relaxation mechanism for C-Mod's H-mode pedestal is the Quasi-Coherent Mode (QCM) [15], the phenomenon that underlies the Enhanced- D_α (EDA) H-mode. Much research defining the operational space for the EDA H-mode and characterizing the QCM has been done in the last five years. The QCM is a fluctuation of density, potential, and magnetic field [16], with a frequency spectrum peaked typically between 90 and 200 kHz. It is found to be aligned with the local field, i.e. $\mathbf{k} \cdot \mathbf{B} = 0$, with typical poloidal wavenumber values at the outboard midplane around $k_\theta \sim 1 \text{ cm}^{-1}$. The mode propagates in the electron diamagnetic drift direction with a phase velocity of a few km/s. The evidence that the QCM is responsible for the enhanced transport associated with the continuous relaxation of the density pedestal in EDA H-mode is: 1) the magnitude of the oscillation is observed to increase the time-averaged effective-particle-diffusion-coefficient ($D_{\text{eff}} \equiv -\Gamma_{\text{perp}}^{\text{meas}} / \nabla n_e^{\text{meas}}$), and 2) the absence of the fluctuation in "ELM-free" H-modes, in which both density and impurities accumulate. When the QCM is present it exists in the outboard (low-field) region and is *not* observed at the inboard midplane, consistent with a ballooning-like drive. The peak amplitude of the QCM in the outboard region is found in the edge pedestal region, just inside the separatrix, with a radial width ≥ 5 mm [17], leading to a non-zero amplitude outside the separatrix and qualitatively consistent with its transport enhancement. Fluctuations similar in character to the QCM have been reproduced on other tokamaks while attempting matched discharges [10, 18]. In one

ITPA joint experiment (PEP-12), discharges on C-Mod and the JFT-2M tokamak were run with matched shapes in order to compare and contrast EDA H-mode with the JFT-2M high-recycling-steady (HRS) regime. Despite a significant difference in aspect ratio and interesting differences in edge fluctuations, the two devices found that a similar recipe of increased edge q and v^* favored the appearance of EDA and HRS [18]. This experiment is discussed further in the following chapter.

Research on C-Mod has shown that the operational space boundaries for plasmas with the QCM (and thus EDA H-mode) can be defined by a multidimensional plasma parameter space of pedestal density and temperature, edge q , and plasma shape, with the mode favoring highly-shaped, high q , moderate temperature, high-density plasmas [6,19]. The edge profiles in the EDA regime are typically stable to ideal peeling/ballooning modes [20]. This, together with the fact that these H-modes typically have high $n_{e,PED}$ and lower $T_{e,PED}$ (thus high-collisionality), supports theoretical models showing a resistive character for the QC mode. It has also been demonstrated that MHD activity associated with the mode does not limit the growth of edge pedestal [19]. Thus, applying more heating power (>3.5 MW) to these high-collisionality H-mode plasmas leads to formation of higher edge pressure gradients and transition to a regime with high-frequency (“grassy”) ELMs.

As is evident from the preceding paragraphs, on Alcator C-Mod, ELMs are *not* the typical relaxation mechanism for the H-mode edge-pedestal, despite its often being close to the ballooning pressure-limit. However, small ELM regimes can be accessed with relative ease, with Type II (“grassy”) ELMs [19] and larger Type III ELMs [21] occasionally observed under appropriate conditions. Small ELM regimes are the subject of an extensive and ongoing ITPA joint experiment (PEP-16) between C-Mod, NSTX and MAST devices. There is also an operational space in C-Mod for which discrete,

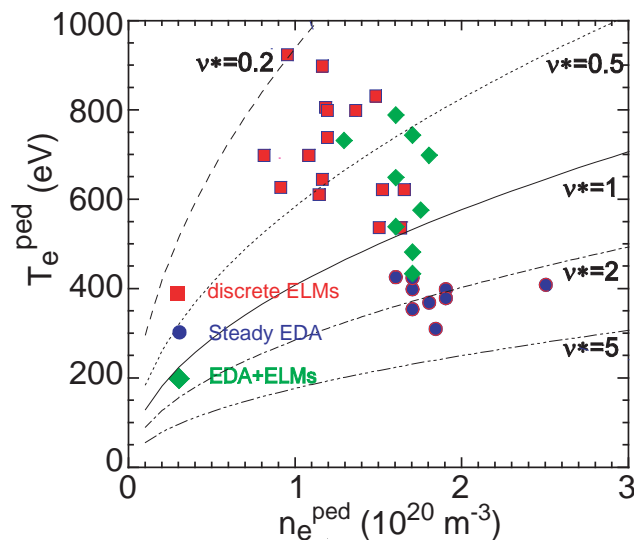


Fig. 7.6: Pedestal n_e, T_e space for highly-shaped C-Mod H-mode plasmas. The dependence of the relaxation mechanism upon collisionality (v^*) is apparent. q_{95} is 3.5 for these plasmas..

relatively large, Type I ELMs *are* the relaxation mechanism for the pedestal. This operational space is one of large triangularity for the lower half of the plasma ($\delta_{lower} > 0.75$), small upper triangularity ($\delta_{upper} \sim 0.15$), and a relatively low normalized collisionality in the pedestal ($0.2 < v^* = v_{ei}/v_{bounce} < 1$) [18]. The operational space for the pedestal and the relaxation mechanism for these atypically shaped plasmas are shown in Figure 7.6.

In studying the characteristics of the discrete ELMs [22], we find that the energy lost per ELM from the H-mode pedestal is typically ~10-20% of the total pedestal

energy. The ELMs exhibit relatively long-lived precursor oscillations of intermediate ($n \sim 10$) toroidal mode number. At the ELM “crash” a high frequency (~ 0.5 MHz), short-lived magnetic oscillation is initiated, and multiple plasma filament structures are expelled into the Scrape-Off-Layer. The initial ELM filaments, so-called “primaries”, are large perturbations to the SOL. For example, the filament perturbation increases the local D_α emission by factors ranging from 1.5 (just outside the LCFS) to ~ 100 . In the outboard midplane region the primary filaments have radial extents of 0.5-1 cm and typical radial propagation velocities of 1-2 km/s. The poloidal extent of the filaments is greater than the 4.5 cm diagnostic field-of-view. The initial filaments are followed by multiple, less perturbing “secondary” filaments. A perturbation at the *inboard* midplane is also generated at the ELM event, although it appears to be a response to the outboard perturbation and not a filament. We have analyzed stability of the pedestal profiles to peeling/ballooning modes in these ELMing plasmas using the MHD code ELITE (in collaboration with scientists at DIII-D). Similar to the earlier results, in which the profiles were shown to be marginally unstable in the range of pressure gradients where the grassy ELMs are observed [20], the profiles for which the large discrete ELMs occur are also marginally unstable. Both results are consistent with a model of the ELMs as non-linear manifestations of intermediate n , peeling/ballooning modes. The profiles of the plasmas exhibiting large discrete ELMs were also examined using the 3D resistive-MHD code, M3D, where it was seen that they were unstable, consistent with the ideal MHD analysis [23].

7.1.3. L-H transition dynamics and threshold studies

Understanding the trigger mechanisms and dynamics of the L-H transition have been a research priority on Alcator C-Mod, and the last five years have given rise to exciting new insights. Considerable progress was made in the study of SOL flows, contributing to a new understanding of the long-observed topology-dependence of the L-H power threshold [24]. As discussed in Chapter 4, near-sonic flows are observed in the high-field side SOL of single null plasmas, directed toward the inner divertor. As suggested by the diagrams in Figure 7.7, these flows are driven by strong radial flux at the low-field side, and may provide an edge boundary condition that works to “spin

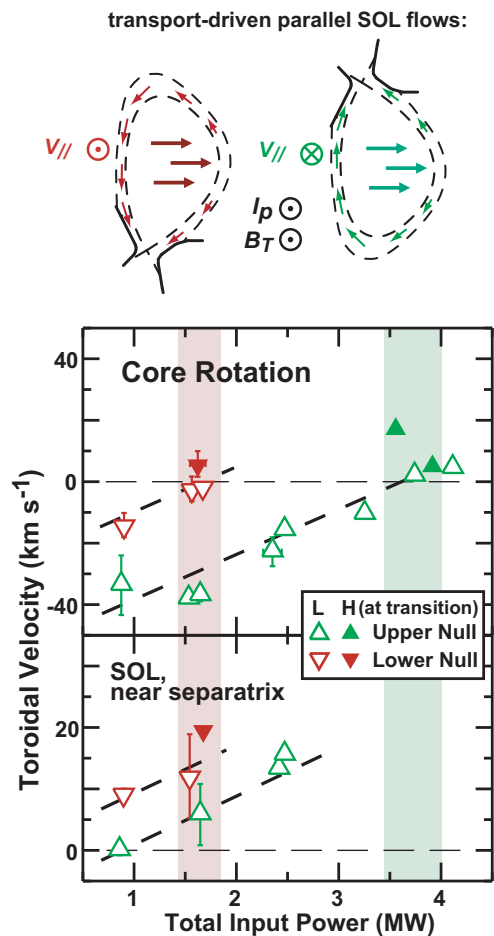


Figure 7.7: Transport-driven flows in the SOL and their correlation with core toroidal rotation

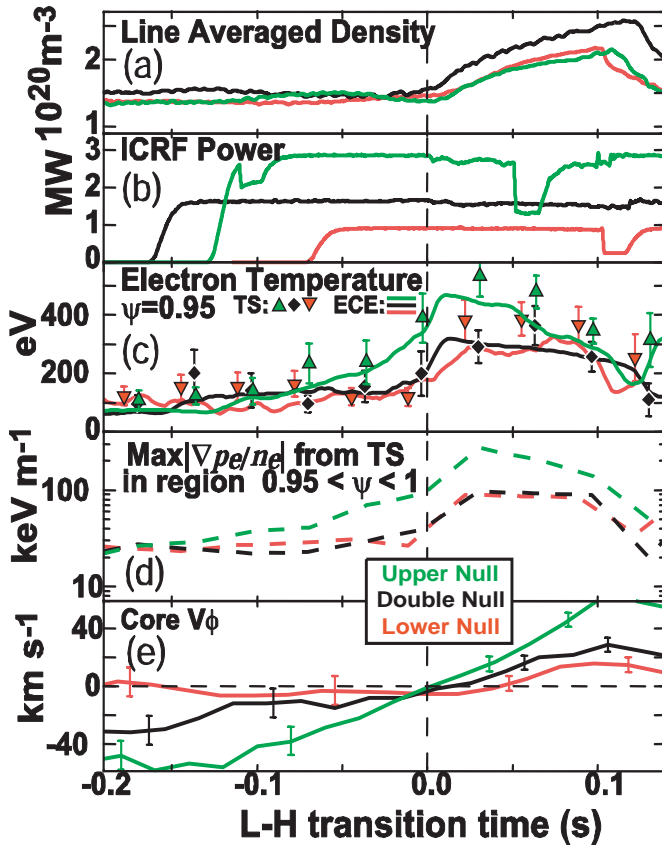


Figure 7.8: Time histories of three discharges exhibiting L-H transitions, near power threshold in USN, DN and LSN. Note that the core central rotation (e) is near a fixed value at the transition in each case.

up” the core plasma. HFS flows are directed co-current when ion grad-B is directed toward the active x-point, and counter-current when the opposite is true, and this reversal of flow at the inboard side appears to have an impact on the core rotation in the center of the discharge, as well as on the parallel flow velocities in the LFS SOL (see Figure 7.7). These quantities consistently undergo a co-current increase as the stored energy in the L-mode phase rises [25,26], with the L-H transition shown to occur at roughly the same value of plasma rotation, as measured either from the Ar^{+17} core toroidal rotation or the parallel flow velocity 2mm outside the separatrix. Figure 7.8 illustrates the differences in the pre-H-mode v_ϕ and its evolution preceding the L-H transition for three discharges with normal B_T orientation: lower single null (low P_{LH}), upper single null (high P_{LH}) and double null (intermediate in threshold

power). Given the presumed importance of edge flow shear in triggering L-H transitions, the results suggest that transport-driven SOL flows play a role in lowering or raising the L-H power threshold, by either promoting or impeding the L-H trigger.

Recent experiments have examined H-mode performance and characteristics of the L-H transition in discharges with unfavorable ion ∇B drift [1]. Interestingly, these discharges show a slow phase of edge evolution prior to the usual abrupt jump that marks the classic transition. In the pre-phase, which can last for several energy confinement times, temperature and temperature gradient rise continuously with constant applied ICRF heating, while magnetic fluctuations become gradually suppressed in the 50—100kHz range. A gradual drop in effective thermal diffusivity is inferred. As can be observed in Figure 7.8, the slow evolution in edge temperature is concurrent with a gradual spin-up of the toroidal velocity toward values normally observed at L-H transition. During the pre-phase, energy confinement can be surprisingly good, with H_{89} as high as 1.6, and temperature pedestals with $\nabla T_e \sim 200\text{keV/m}$, a figure that competes with our best H-mode pedestal gradients. An example of such an improved L-mode T_e pedestal can be seen in

Figure 7.2. The confinement enhancement associated with this operational regime evokes the “Improved L-mode” of ASDEX Upgrade [27].

At moderate to high density, the H-mode threshold increases with both density and toroidal field. At lower densities, many tokamaks have observed a sharp increase in the input power required to achieve H-mode. The minimum density below which the H-mode threshold power increases sharply is $n_{\text{th,min}} \sim 2\text{--}3 \times 10^{19} \text{ m}^{-3}$ on ASDEX-Upgrade, DIII-D, JET, and JT-60U but on C-Mod, this minimum occurs between $8\text{--}10 \times 10^{19} \text{ m}^{-3}$. Since ITER intends to operate with an L-mode target density of $5 \times 10^{19} \text{ m}^{-3}$, it is important to know where this low density limit will be for ITER. If this limit increases sharply with toroidal field, then ITER could have a similar low density limit as C-Mod, which would mean ITER would require two to three times the power predicted by the threshold scaling to achieve H-mode. Since the ICRF heating scheme on C-Mod is sensitive to large changes in the toroidal field, the initial C-Mod experiments instead checked the plasma current dependence of $n_{\text{th,min}}$ to see if it scales with the Greenwald density limit, $n_G = I_p/(\pi a^2)$. These initial experiments, which contribute to a high-priority ITPA joint experiment (CDB-11), indicated that $n_{\text{th,min}}$ does not scale with the Greenwald limit.

Characterizing the fast dynamics spanning the L-H transition helps to shed light on the rapidly evolving transport processes during this period, and may yield an understanding of the physics setting the fully-evolved pedestal structure. Although H-mode density rises to steady values on time scales of tens of milliseconds following an L-H transition, temperatures demonstrate much faster behavior. Fast ECE diagnostics [28] were utilized to study the evolution of edge T_e across L-H transitions with unprecedented temporal resolution. We observed that thermal barrier formation occurs in two distinct phases: first, an abrupt rise in temperature across the entire edge lasting approximately $500\mu\text{s}$; and second, a slower response lasting tens of milliseconds, which is consistent with the transition bringing on an abrupt drop in thermal diffusivity from approximately $0.5\text{m}^2/\text{s}$ to less than $0.1\text{m}^2/\text{s}$. [29,30] The input ICRF power flux had no observable effect on the duration of the fast T_e “jump”, although at power levels just above the L-H threshold, the jump was often followed by a slight downturn. This phenomenon appears to be related to L-H-L “dithering” cycles observed when power is marginal for triggering H-mode. Attempts to model the transition dynamics numerically used a spatially nonlocal fluctuation-flow model based on work by Diamond *et al.* [31]. Several experimental features, including the dithering oscillations but not the two-phase evolution, were reproduced.

7.2. Goals and directions for pedestal research

Although ETB research has yielded useful insights into the transport mechanisms underlying the pedestal structure, the field remains rich with further research opportunities. The fundamental goal of pedestal research is to project pedestals to larger tokamaks—ITER in the short term and power reactors in the far term. The general strategy for contributing to this forward projection is to leverage unique features and parameter space of C-Mod against results from other machines. To help accomplish this,

we will pursue an improved physics-based understanding of the pedestal profile characteristics, in particular the width of the ETB region and the gradients established within this narrow radial region. The interrelation of pedestal structure and edge relaxation mechanisms will receive further study, in both ELMy and ELM-suppressed regimes. We will also continue our investigation of the trigger mechanisms for H-mode in different configurations, and examine the role played by SOL plasma in determining H-mode power threshold. Experimental research will leverage an extensive and continuously improving set of edge diagnostics in which a great deal of investment has been made in the previous five years. Figure 7.9 highlights a number of the high spatial resolution ($<3\text{mm}$) diagnostics utilized (or planned) on C-Mod. Concentrated efforts will be made across many operational regimes to use measured profiles of plasma density and temperature, ion flow velocities (poloidal and toroidal), neutral density and radiated power to accomplish the experimental goals laid out in the following subsections. Tools for controlling pedestal transport and stability will also be investigated, and connections with theory will be made using available computational tools for pedestal simulation.

7.2.1 L-H threshold and transition studies

We will continue our efforts to identify the critical parameters responsible for triggering transitions from L- to H-mode and develop a physical understanding of their impact on ETB formation. Edge CXRS measurements of impurity temperature and poloidal and toroidal velocities will be crucial to these experimental efforts, as these measurements allow the inference of E_r profile in the vicinity of the separatrix. We will investigate the characteristic values of E_r shear associated with L-H transitions, as well as the concomitant pressure and velocity profiles. Comparisons of threshold conditions with ion

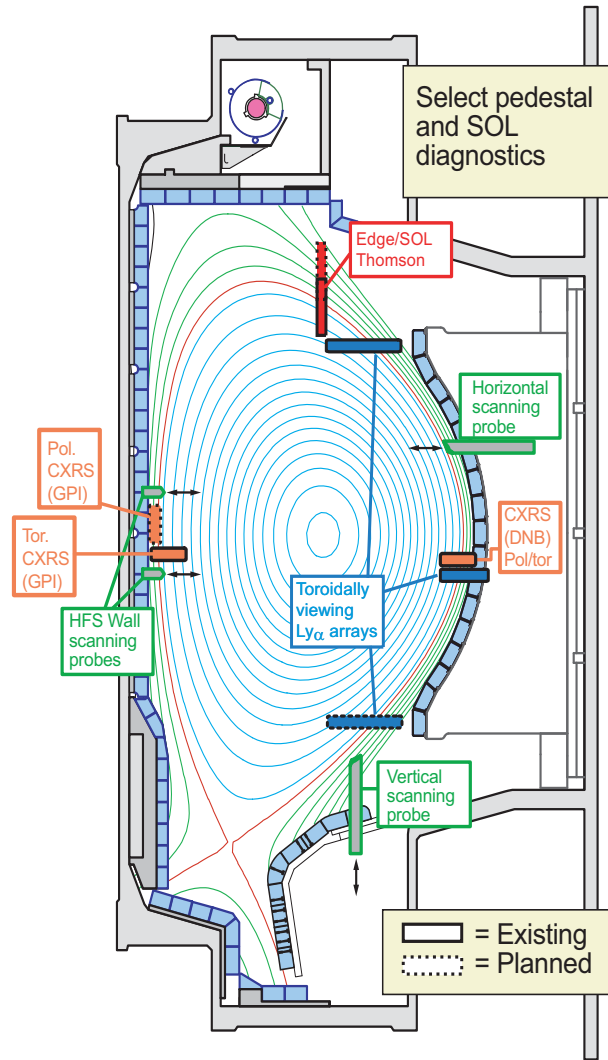


Figure 7.9: Existing and planned edge diagnostics pertinent to pedestal and L-H transition studies

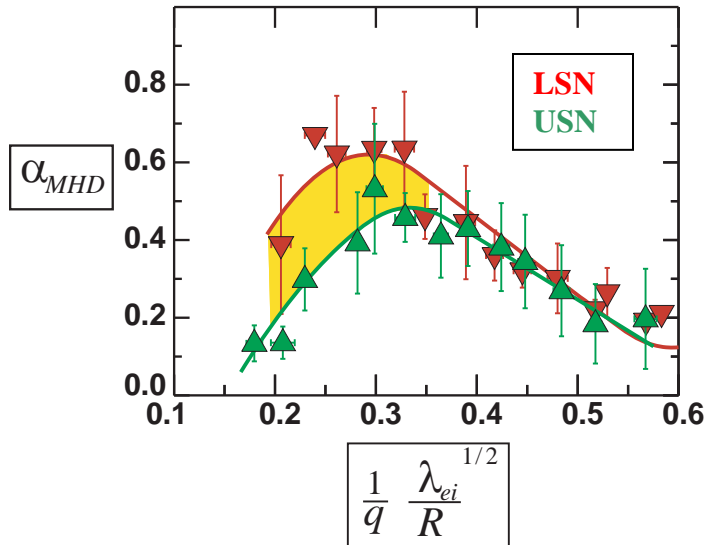


Figure 7.10: SOL “phase-space” in terms of non-dimensional pressure gradient and collisionality for LSN (red) and USN (green) Ohmic discharges. Discharges have the normal field direction

pressure gradients [32,33], as discussed in Chapter 4. These studies will take advantage of the set of poloidally distributed scanning Mach probes highlighted in Figure 7.9. By way of illustration, Figure 7.10 demonstrates the dependence of normalized pressure gradient α_{MHD} on collisionality in the near SOL of Ohmic discharges, for ion ∇B drift directed away from and toward the X-point. Significant differences in the obtained pressure gradient are observed at higher collisionalities, and simultaneous measurements indicate correlation of higher α_{MHD} with a more co-current flow velocity. To further study the relationships between flows, edge profiles and L-H transition thresholds, Ohmic transitions to H-mode will be assayed using scanning probes. A goal of these experiments will be to identify the locus or loci within the Ohmic SOL phase space (*e.g.* within the plot in Figure 7.10) corresponding to conditions favorable to the L-H transition. These results will be compared with the theoretical predictions of Guzdar [34].

Additionally, we will continue our research into the improved L-mode, described in Section 7.1.3, which achieves a substantial temperature pedestal and good energy confinement, with favorably low particle and impurity confinement. We will investigate the mechanisms that give rise to the drastically different levels of particle and energy transport, and work to actively control the suppression of the classical L-H transition and achieve steady state improved L-mode performance.

A number of outstanding questions connected to L-H threshold physics will be examined in the coming years. Recent observations showing a reduction in L-H power threshold in the presence of strong pumping will be revisited. The low density limit for H-mode formation described in Section 7.1.3 will be explored further to determine how factors

∇B drift directed toward (favorable) and away from (unfavorable) the active X-point will assist us in these investigations. Operation in unfavorable magnetic configurations (*e.g.* reversed field LSN or normal field USN) will be pursued further in order to study the slow L-H transitions described above and more carefully delineate the key local threshold parameters.

We will examine the possible connections between changes in L-H thresholds with ion ∇B drift direction and the variation observed in both SOL flows (*co- versus counter-current*) and Ohmic

like wall conditioning and neutral particle control affect results. Through ITPA-sanctioned collaboration with other tokamaks (CDB-11), the scaling of the low density limit will be examined with B_T and other parameters. Local minima in the L-H power threshold have been observed in MAST and ASDEX-Upgrade when running in close proximity to double null [35] (ITPA joint experiment PEP-6). We will determine if a similar reduction is evident on C-Mod. Throughout all of these studies, new diagnostic capabilities will be exploited to document edge profiles and rotation velocities. How these quantities evolve, and the resultant electric field shear changes, will be studied in detail in the near term by reducing integration time windows of the edge CXRS diagnostics to the millisecond level.

7.2.2 Transport within the pedestal region and ETB structure

For some time, pedestal models used to project toward ITER and other next-step devices generally have postulated profiles limited by stability to Type I ELMs, while less consideration has been given to what sets profiles in ELM-free H-modes, or between ELMs. In contrast to most other tokamaks, though, ELMs do not usually limit the pedestal on C-Mod, and our pedestal scalings have therefore been determined by other transport-based limits on profile gradients. This kind of result takes on potentially greater importance in light of the recent impetus to reduce the ELM size on ITER, or to find feasible ELM-free regimes with good energy confinement. Understanding the nature of the continuous transport processes that result in “stiff” pedestal profiles on C-Mod (and perhaps on other tokamaks) may be applied ultimately to model realistically edge profiles on next-step devices. We will continue to study the details of ETB gradients, now with the inclusion of ion temperature data from CXRS, and test whether the observed critical gradient phenomenology continues at lower values of edge v^* . Experiments aiming to systematically vary particle and heat fluxes through the ETB will be used to test the critical gradient hypothesis more carefully. In addition, the relationships between edge gradients and other local parameters (such as collisionality) will be tested further under alternate configurations (*e.g.* reversed field direction, extreme triangularity) and in Type I ELM regimes.

Neutral fueling of the edge pedestal will remain a focus area, particularly given the anticipated use of the cryopump as a density control tool. When operating within its normal range of density, C-Mod exhibits a higher neutral opacity in the SOL and pedestal than larger, lower-density tokamaks, effectively approaching that of ITER. This feature of C-Mod (and ITER) results in inefficient fueling from the edge, and, according to 1D modeling [5], a density pedestal which is only weakly influenced by neutral source. Over the next two years, we will pursue 2D modeling of the ionization source in the C-Mod edge, in order to establish firmly the range of density over which the pedestal is insensitive to details of the poloidal ionization distribution. Experiments will also be designed to produce H-modes at the ITER value of B_T , q_{95} , and determine the limits of edge fueling due to neutral opacity. Improved experimental measurements of neutral emissivity at multiple poloidal locations, highlighted in Figure 7.9, will be exploited as inputs into this interpretive modeling. This research will also benefit from more routine collection of upstream SOL T_e , n_e profiles, which will be provided by an upgrade to the

Thomson scattering diagnostics suite. Contributions will be made to an ITPA multi-machine profile database for the purposes of modeling the sources in several tokamaks.

The width of the pedestal region remains a considerable uncertainty when projecting to ITER and beyond. We will continue to explore pedestal width physics across H-mode regimes and work to understand the terms setting the spatial extent of pedestal transport suppression. In the process of pushing toward less collisional H-modes, it will be possible to assess whether neutral sources become important at lower density. Inspired by results that show pedestal widening at both extreme shaping, as in Figure

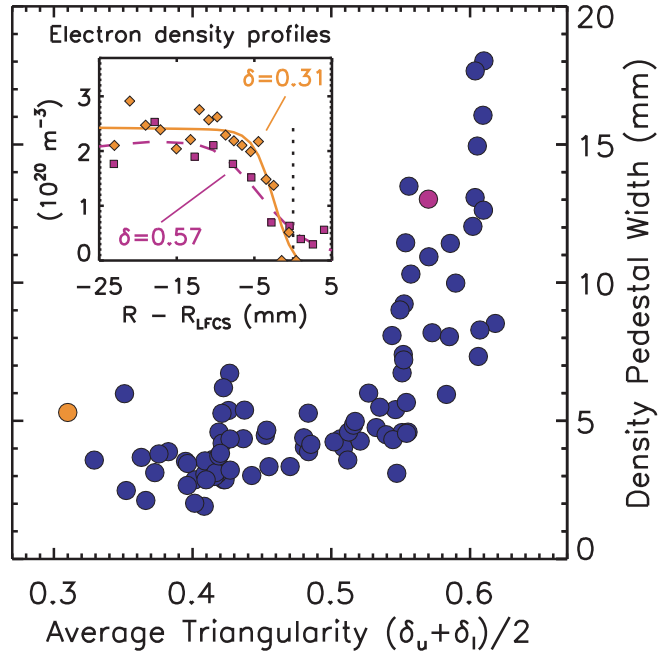


Figure 7.11: Measured density pedestal width in intra-discharge scans of triangularity. Sample profiles show differences in width and gradient at the extremes of δ

7.11, as well as at high edge q , [5,7] experiments are being planned to test the influence of edge magnetic shear on the ETB width. This will be studied with broad scans in triangularity, elongation and plasma current, as well as with scans of magnetic balance spanning the double null configuration. This H-mode work is complemented by Ohmic experiments in which we examine the connection between the layer of high magnetic shear associated with the X-points and the region of sharp gradient scale lengths observed in the near SOL of L-mode discharges.

Momentum transport through the pedestal region is another important topic that will receive enhanced emphasis in the coming five years. As discussed in Chapter 3, C-Mod is well suited for studies of intrinsic plasma rotation, due to the absence of externally applied torques. Evidence points to edge plasma flows as a significant source of angular momentum, which propagates into the core plasma. Understanding the momentum transport across the separatrix in both L-mode and H-mode will be a high priority.

7.2.3 Pedestal Relaxation Mechanisms

The primary goal for C-Mod's research on pedestal relaxation is to understand from first-principles the operational space for the various relaxation mechanisms. As is evident from Figure 7.6, different regimes can overlap somewhat, trending (for this shape) in a relatively continuous way as a function of the dimensionless collisionality, ν^* . Because of this, we hypothesize that the relaxation mechanisms are related by a similar physics

basis. It is presently generally believed that Type I ELMs are the non-linear manifestation of unstable peeling/ballooning modes [36]. We seek a similar level of understanding for the QC mode and other so-called “small-ELM” regimes, mainly because the occurrence of Type I ELMs in burning plasma experiments are predicted to limit the lifetime of materials as a result of their large transient heat and particle loads on the divertor plates. Small ELM regimes are being developed and explored in detail as a part of ongoing ITPA joint experiments (PEP-16) among C-Mod, NSTX and MAST. We will continue experimental study of the QC mode itself, employing the wide array of diagnostics that detect it. These include Phase Contrast Imaging, Gas-Puff-Imaging, reflectometry, probes, and magnetic pick-up loops. Using new edge ion diagnostics we will investigate the possibility that the QCM is related to the Kelvin-Helmholtz instability. We will attempt to relate the QCM to similar continuous relaxation mechanisms observed on other devices and also under theoretical investigation, *e.g.* the Edge Harmonic Oscillation (EHO) on DIII-D and AUG. Further exploration of the operational space boundaries for the various relaxation mechanisms will occur as we utilize C-Mod cryopumping and shaping capabilities. In those plasmas exhibiting Type I ELMs (presently those with large δ_{lower}), we plan experimental studies of the boundaries in operational space, more detailed examination of the ELM energy losses, and more detailed examination of the structure and dynamics of the ejected ELM filaments. Analysis of all of the stability boundary results will be helped greatly by the acquisition of a suite of data handling codes [37], developed at DIII-D, that assemble and fit profile measurements of kinetic quantities, and then reconstruct plasma equilibria using those and magnetic data (so-called “kinetic EFITs”). In collaboration with the DIII-D group, we plan to acquire this capability. In the next three years, experimental diagnosis of the QCM and ELMs will be aided by upgrades to fast edge imaging diagnostics and Doppler reflectometry.

7.2.4 Pedestal optimization and control

Not only can the H-mode pedestal serve as a boundary condition establishing core confinement, but it has been seen that global confinement can influence the pedestal structure, providing positive feedback under certain conditions [38]. As we push toward H-modes with higher performance and advanced scenario discharges, the impact of enhanced core confinement on the pedestal will be examined. Density and impurity control will be of paramount importance in these regimes of operation, and we will devote considerable time to defining the limits of density control via pumping and equilibrium shaping. Recent results in near double null configurations showed great promise for reducing density pedestals while still maintaining steady H-modes that were either EDA or with small ELMs. Figure 7.12 shows two H-mode discharges which are close to balanced double null, though with controlled scans of the separation of the primary and secondary separatrixes (SSEP). Millimeter order perturbations to SSEP are seen to regulate the density pedestal in a repeatable fashion, opening up windows of reduced collisionality and increased confinement. These equilibria also are excellent targets for particle control via the upper chamber cryopump. The pumped discharge shows an additional reduction in plasma density and an increase in $T_{e,\text{ped}}$, which in turn improves global confinement. Further work will be performed to optimize these discharges for reduced collisionality and study the associated pedestal scalings in these

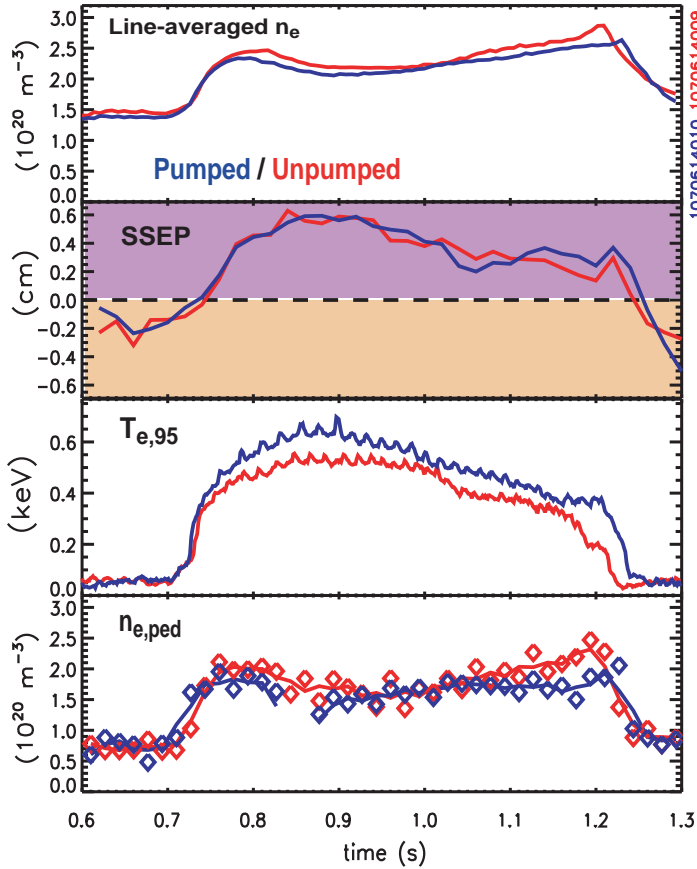


Figure 7.12: 800kA EDA H-modes in near double null configuration. The natural density of the unpumped (red) case is regulated by fine changes in magnetic balance. A discharge with cryopumping (blue) shows additional density reduction. In either case, $T_{e,ped}$ increases as $n_{e,ped}$ falls.

The flexibility of these experiments will be increased upon the implementation of power supply upgrades. In the longer term, as low collisionality H-mode targets are developed for LHCD, the potential exists for driving current close to the edge, thus externally modifying the edge magnetic shear. Since peeling/ballooning mode theory yields a fairly well-defined instability boundary in pedestal-current-density/pedestal-pressure space, we propose to test whether application of Lower Hybrid current drive as near to the pedestal as possible can influence the frequency of the ELMs. This work will extend our efforts to characterize the role of magnetic shear on pedestal width, as well. Additionally, we propose to investigate the external stimulation of continuous edge modes such as the QCM.

7.2.5 Exploiting theory and computational tools

A substantial development effort has been undertaken in the computational community to develop powerful tools for edge transport and stability calculations in the ETB region.

configurations. Further reduction in v^* is expected to help connect C-Mod pedestal results with those of larger, low-field machines, improving confidence in projections to ITER.

In addition to mapping out the operational space for edge relaxation mechanisms and understanding the “natural” scalings of pedestal width, we will explore the use of available tools to actively modify these pedestal phenomena. Utilizing those plasmas with Type I ELMs, we plan to test two methods for mitigating the ELMs. Encouraged by promising experiments on JET [39], where external coils were used for this purpose, we have begun to design ELM mitigation experiments using C-Mod’s external A-coil set. In the course of these experiments, the impact on pedestal structure of magnetic perturbations will be assessed.

One of the more successful codes, ELITE, has been utilized for comparisons with data from a number of devices, including C-Mod, to calculate the eigenfunctions and growth rates of ideal MHD modes within the context of the peeling-ballooning model for ELMs. As mentioned in Section 7.1.2, the resistive MHD code M3D is also being used to analyze edge stability. We will continue using these tools for ELM studies and also to study the QCM in the context of the kink/ballooning model. We will also take advantage of the burgeoning array of edge transport codes in development. The XGC0 code is a neoclassical edge transport code, developed mainly to model pedestal structure and edge flows with a self-consistent radial electric field. The usefulness of XGC0 should be enhanced considerably within the next five years by the completion of the XGC1 turbulence code, which will calculate the contribution of electromagnetic turbulence to transport in 3D geometry, complete with X-point. These codes will make possible more realistic calculations of flux-gradient relationships in the pedestal, and will produce predictions for pedestal structure and scalings which can be validated using C-Mod data.

Recently, increased focus has been placed on the integrated use of simulation codes, for the purposes of simulating complex time-dependent edge phenomena. Classic examples of these phenomena, which may be driven by multiple physical processes coupled in highly non-linear ways, include the L-H transition and the complete ELM cycle. While the goal of simulating these processes will not be realized for some time, progress in code development and integration is anticipated over the next five years, spearheaded by the SciDAC initiative known as the Center for Plasma Edge Simulation (CPES). We will work closely with the CPES to validate codes against C-Mod pedestal data and use the integrated workflow they develop to begin modeling time-evolving edge processes like H-mode evolution.

7.2.6 Research contributions to ITPA, ITER and FESAC priorities

7.2.6.1

Alcator C-Mod supports a number of high priority research tasks within the framework of the International Tokamak Physics Activity. Participation in joint experiments among multiple devices is strong in many topical areas. Table 7.1 lists several important ITPA collaborative experiments which bear on the topic of pedestal physics.

Table 7.1: Planned contributions to ITPA joint experiments

Description	ITPA designation	Notes on C-Mod contributions
Pedestal Structure and ELM stability in double null	PEP-6	H-modes in near DN and SN configurations will be compared in terms of profile structure and ELM stability. We will examine whether a local minimum in L-H threshold power exists at exactly DN.
Pedestal width analysis by dimensionless edge identity experiments	PEP-7	Discharges were designed to match non-dimensionally complementary JET discharges, with preliminary results described in Section 7.1.1. Analysis continues, and additional devices may add similarly matched discharges.
Comparison of small ELM regimes	PEP-13	q and v^* scans with high input power to map out boundaries of small ELM regimes
Small ELM regime comparison on C-Mod, NSTX and MAST	PEP-16	Experiments have accessed high power H-modes in double and single null configurations, achieving ELMy regimes for further study
Low density limit for L-H transitions	CDB-11	Providing data at high field, and evaluating impact of wall conditions, character of edge fueling

7.2.6.2

Both through ITPA experiments and through our locally motivated program, we plan to make contributions to a number of ITER priority tasks in this area:

- Improve predictive capability of pedestal structure
 - Cross machine comparisons to isolate physics setting pedestal width
 - Utilize profile database for integrated modeling of pedestal structure and transport comparison to experiment
 - Establish pedestal profile database for hybrid and advanced regimes

- Assess impact of ELM control techniques on pedestal structure
- Improve predictive and design capability for small ELM and quiescent H-mode regimes and ELM control techniques
 - Define magnetic field structure and magnitude required for ELM control, accounting for plasma response and field penetration
 - Assess applicability of low collisionality small ELM regimes
 - Test nonlinear MHD and turbulence models of ELM evolution
- Re-examine L-H power threshold at low density

7.2.6.3

The October 2007 report to the Fusion Energy Sciences Advisory Committee (FESAC) , “Priorities, Gaps and Opportunities: Towards A Long-Range Strategic Plan For Magnetic Fusion Energy”, indicated a number of scientific and technical issues, organized thematically, which must be resolved prior to the construction of a demonstration power reactor. Pedestal research on C-Mod will contribute to issues gathered under the theme of “Creating predictable high-performance steady-state plasmas,” and motivated as such:

The state of knowledge must be sufficient for the construction, with high confidence, of a device that permits the creation of sustained plasmas which meet simultaneously, all the conditions required for practical production of fusion energy.

Integration of high-performance, steady-state, burning plasmas (A2): Similarly to ITER, a reactor must exhibit high energy confinement while maintaining a low impurity content, and must achieve this without large, damaging ELMs. C-Mod pedestal research, in coordination with the H-Mode baseline scenario thrust, is increasingly focused on high-performance regimes with ELMs either benign or suppressed altogether. Both naturally occurring small- or no-ELM regimes and operation with externally determined relaxation of the pedestal will be explored. A research focus will be to compare with the results of other devices and determine the capability of extrapolating to ITER and Demo.

Validated Theory and Predictive Modeling (A3): Extensive pedestal and SOL measurements exist on C-Mod, and are continually being expanded, as discussed earlier. A major goal over the next five years is to assist in the validation/de-validation of developing edge/pedestal codes. Specific predictions of models which can be tested include flux-gradient relationships, ELM stability, edge flows and the coupling of momentum across the pedestal, and L-H transition triggers.

7.2.7 Summary of Research Objectives

The following table summarizes high-level objectives within each of the research themes covered in this section, along with new diagnostic or facilities upgrades (see Chapter 11 for details) that will enable our experimental studies, or computational tools that will be used in conjunction with experiment, where appropriate.

Thematic Research Goal	Intermediate Objectives	Enabling Tools
Characterize pedestal structure (and its impact on core confinement) in a manner scalable to future devices, through a physics-based understanding of edge plasma and neutral transport	Examine flux-gradient relationships in the ETB in various configurations and operational regimes	SOL TS, CXRS, Ly _α arrays (Upgrades in 2009—10)
	Study impact of neutral fueling on pedestal at reduced density/collisionality	
	Determine impact of edge magnetic shear on pedestal width	Pedestal database enhancements
	Characterize momentum transport through the ETB	
Understand the physical processes determining the operational space of edge relaxation mechanisms in H-mode	Refine map of edge operational space of ELMs and other transport-regulating modes in experiment	Fast H _α diode array upgrade (2009); Doppler reflectometry (2011)
	Extend the use of MHD stability codes in the identification of edge relaxation mechanisms	
	Compare characteristics of QCM with theoretical predictions	ELITE, M3D, BOUT, GA toolkit
Identify critical local parameters needed to trigger L-H transition ; understand how they relate to global threshold conditions	Diagnose profiles of edge flows, pressure profiles with improved temporal resolution	SOL TS, CXRS, Ly _α arrays (Upgrades in 2009—10)
	Investigate the evolution of radial electric field shear across the L-H transition, and in slow transitions; explore improved L-mode as a useful operating regime	
	Map L-H transition trigger conditions onto non-dimensional phase space; compare with theory	
	Identify scaling of low-density limit for H-mode access	
Develop methods for controlling pedestal structure and edge relaxation mechanisms that are compatible with high confinement	Regulate pedestals and confinement via shaping, topology	Correction coil upgrades (2013); Lower hybrid power/launcher upgrades (2009—10)
	Explore use of externally applied fields to relax pedestals, regulate ELMs	
	Utilize LHCD for pedestal/ELM modification	
	Investigate RF drive for continuous edge relaxation modes	
Validate edge simulation tools currently in development using experimental data	Compare pedestal structure and scalings with edge transport code predictions	XGC0, XGC1, ELITE, M3D; Kepler workflow as developed by CPES
	Validate simulation of dynamic events such as ELM cycle	

7.2.8 Pedestal Research Schedule

The timeline in Figure 7.13 provides an approximate guide to the timing for the aforementioned research within the pedestal physics topic. Because much of the physics work in this area is a continuously evolving process of discovery, experimental planning naturally must remain adaptive to developments that are currently unknown. That said, many physics topics are certain to hold programmatic interest over the next five years. It is mainly the focus among topics that is expected to shift over time, and the chart estimates the timing of those shifts. Some subtopics will naturally grow in priority upon the advent of enabling machine capabilities or availability of computational tools. Others are expected to maintain a high profile throughout the next period of the program.

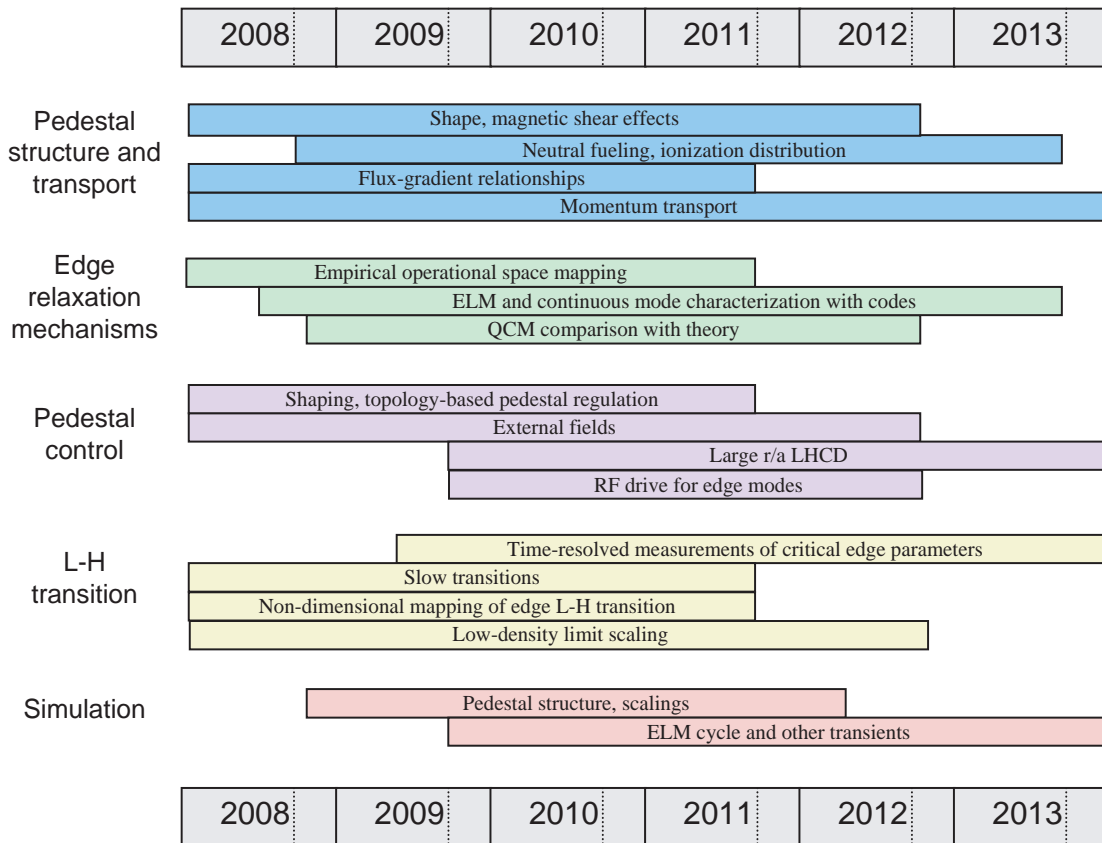


Figure 7.13: Approximate schedule for pedestal research

7.3. References

- 1 A.E. Hubbard *et al.*, Phys. Plasmas **14**, 056109 (2007).
- 2 J.W. Hughes *et al.*, Rev. Sci. Instr. (2001).
- 3 R. McDermott *et al.*, Bull. Am. Phys. Soc. **52**(16), 213 (2007); K. Marr *et al.*, *ibid.*
- 4 K. Burrell *et al.*, Plasma Phys. Control. Fusion **38**, 1313 (1996).
- 5 J.W. Hughes *et al.*, Phys. Plasmas **13**, 056103 (2006).
- 6 J.W. Hughes *et al.*, Phys. Plasmas **9**, 3019 (2002).
- 7 J.W. Hughes *et al.*, Fusion Sci. Technol. **51**, 317 (2007).
- 8 M. Sugihara *et al.*, Nucl. Fusion **40**, 1743 (2000).
- 9 M.A. Mahdavi *et al.*, Phys. Plasmas **10**, 3984 (2003).
- 10 D.A. Mossessian *et al.*, Phys. Plasmas **10**, 689 (2003).
- 11 G. Madisson *et al.*, 30th EPS Conference on Contr. Fusion and Plasma Phys., St. Petersburg, 7-11 July 2003 ECA Vol. 27A, P-1.109.
- 12 G. Maddison *et al.*, Bull. Am. Phys. Soc. **52**(16), 229 (2007).
- 13 J.W. Hughes *et al.*, Nucl. Fusion **47**, 1057 (2007).
- 14 B. LaBombard *et al.*, Nucl. Fusion **47**, 1658 (2005).
- 15 M. Greenwald *et al.*, Phys. Plasmas **6**, 1943 (1999).
- 16 A. Mazurenko *et al.*, Phys. Rev. Lett. **89**, 225004 (2002).
- 17 J.L. Terry *et al.*, Nucl. Fusion **45**, 1321 (2005).
- 18 A.E. Hubbard *et al.*, Plasma Phys. Control. Fusion **48**, A121 (2006).
- 19 D.A. Mossessian *et al.*, Phys. Plasmas **10**, 1720 (2003).
- 20 D.A. Mossessian *et al.*, Plasma Phys. Control. Fusion **44**, 423 (2002).
- 21 J.A. Snipes *et al.*, Plasma Phys. Control. Fusion **38**, 1127 (1996).
- 22 J.L. Terry *et al.*, J. of Nucl. Mat. **363-365**, 994 (2007).
- 23 J.L. Terry *et al.*, Bull. Am. Phys. Soc. **51**(7), 98 (2006).
- 24 B. LaBombard *et al.*, Phys. Plasmas, **12**, 056111 (2005).
- 25 B. LaBombard *et al.*, Nucl. Fusion **44**, 1047 (2004).
- 26 J.E. Rice *et al.*, Nucl. Fusion **45**, 251 (2005).
- 27 F. Ryter *et al.*, Plasma Phys. Control. Fusion **40**, 725 (1998).
- 28 R. Chatterjee *et al.*, Fusion Eng. Des., **53**, 113 (2001).
- 29 A.E. Hubbard *et al.*, Plasma Phys. Control. Fusion, **46**, A95 (2004).
- 30 A.E. Hubbard *et al.*, Phys. Plasmas **8**, 2033 (2001).
- 31 P.H. Diamond *et al.*, Phys. Plasmas, **2**, 3685 (1995).
- 32 B. LaBombard *et al.*, J. Nucl. Mat. (2007).
- 33 B. LaBombard *et al.*, submitted to Phys. Plasmas.
- 34 P.N. Guzdar *et al.*, Phys. Rev. Lett. **87**, 015001 (2001).
- 35 H. Meyer *et al.*, Nucl. Fusion **46**, 64 (2006).
- 36 P.B. Snyder *et al.* Phys. Plasmas **12**, 56115 (2005).
- 37 T. Osborne, http://web.gat.com/~osborne/python_d3d.html.
- 38 C.F. Maggi *et al.*, Nucl. Fusion **47**, 535 (2007).
- 39 Y. Liang *et al.*, Phys. Rev. Lett. **98**, 265004 (2007).

8 H-mode Integrated Scenarios – ITER Baseline

This research activity includes experiments and modeling aimed at supporting and optimizing the baseline ITER operating scenario, generally cutting across multiple science topics and often involving interaction and compatibility issues between different plasma processes or regions. It *integrates* work described in the preceding topical science sections, and corresponding Scientific Campaigns as defined by the 2005 FESAC panel on Scientific Challenges, Opportunities and Priorities for the US Fusion Energy Sciences Program. The overall theme of the program is to support development of the ITER H-mode (baseline) Scenario, by demonstrating operating regimes with relevant plasma parameters and control tools. The goal is to establish the physics basis required to extrapolate from present-day experiments to ITER.

This effort is complementary to the “Integrated Scenarios – Advanced Regimes” task described in the next chapter. Given the imminent construction of ITER, C-Mod is focusing its integration work to an even greater degree than previously on the target scenarios which are to be demonstrated and explored on ITER. The *Conventional H-Mode “Baseline” Scenario* (ITER Scenario 2) is relied on to provide the target $Q=10$ fusion performance. The operating point features an edge transport barrier but no core barrier and has positive shear, without external current drive; non-inductive fraction of $\sim 25\%$ comes primarily from bootstrap current. Target parameters are $q_{95}=3$, $\beta_N=1.8$ and

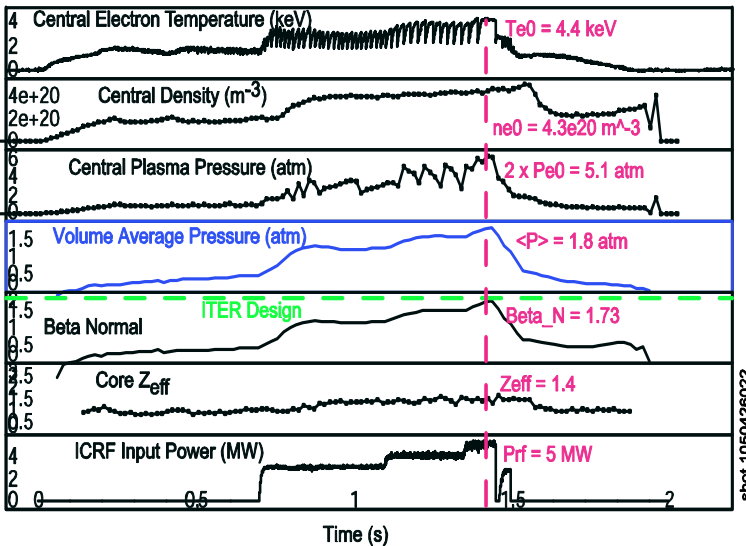


Figure 8.1: High performance C-Mod H-mode plasma with world record plasma pressure $\langle P \rangle = 1.8$ atm, at values of toroidal field, 5.4 T, and normalized beta, $\beta_N=1.73$, very close to those on ITER.

density $\sim 10^{20} \text{ m}^{-3}$, all similar to current C-Mod values.

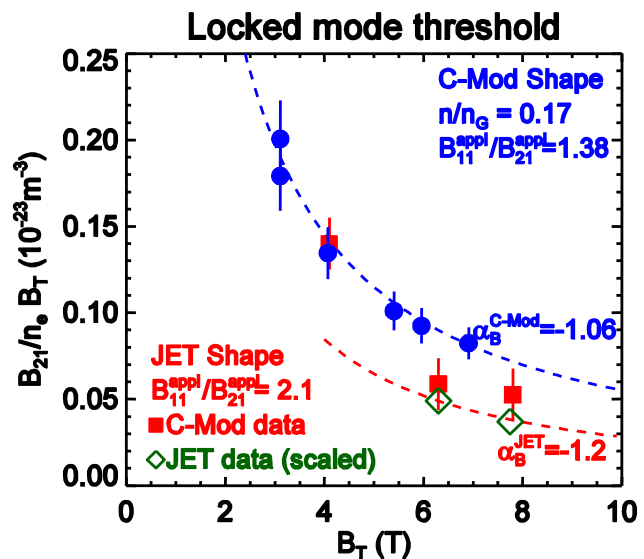
It should be recognized that, in ITER experiments as on C-Mod, ranges of parameters will be explored in each scenario. However, reaching these ambitious targets serves as a useful goal to focus attention on the challenging combination of conditions which must be simultaneously met on burning plasmas. This research therefore contributes most strongly to the second overarching theme of the US fusion sciences program, “*Create a Star on Earth*” (i.e. burning plasmas), as expressed by the 2005 FESAC panel.

8.1 Recent Research Highlights

Integrated H-mode scenario studies in C-Mod have resulted in improved plasma performance, enabling operation in regimes highly relevant to ITER. Increases in stored energy, 250 kJ, and volume averaged pressure, $\langle P \rangle = 1.8$ atm, were achieved with 5 MW of ICRF, shown in Figure 8.1. This is not only a C-Mod but a world record for $\langle P \rangle$ and , significantly, was achieved at the values of toroidal field, 5.4 T and normalized beta, $\beta_N=1.73$, very close to those planned on ITER. Good cleanliness was maintained, with $Z_{\text{eff}}=1.4$, below the ITER target. Results in this scenario are therefore encouraging for ITER and provide a relevant regime for many detailed topical physics studies, such as pedestal and ELM research, SOL and divertor studies, disruption mitigation, core MHD modes and RF-plasma coupling studies.

Experimental work in the Integrated Scenarios on C-Mod includes support for ITPA/IEA Joint Experiments, in conjunction with U.S. and international collaborators at NSTX, DIII-D, JET, MAST, and ASDEX-UG. These experiments exploit the high leverage provided by the unique C-Mod parameters for non-dimensional scaling studies.

The ITPA/IEA Joint experiment MDC-6, Low beta Error Field Experiments, begun in 2004, was completed in 2006 with experiments on C-Mod at 7.8 tesla. These experiments, led by T. C. Hender (UKAEA), were aimed at improving the prediction for the error field threshold for onset of locked modes in the low density ITER ohmic target plasma, and thereby validate the specification of the ITER error-field correction coils. JET and C-Mod were operated with matching shapes and non-dimensional plasma parameters at the ITER safety factor $q_{95}=3.2$, and with matching poloidal mode spectra for the imposed non-axisymmetric perturbing field. Following the standard plasma physics scalings, non-dimensional identity is imposed by maintaining the quantities $(aB^{5/4}, na^2)$, along with all naturally dimensionless quantities such as shape, safety factor, Z_{eff} , etc., constant; for ohmically-heated plasmas this combination should insure that the remaining scalar quantity $(\text{Ta}^{1/2})$ will also be constant., providing only plasma physics processes above the Debye scale are important. Previous results¹ had established the non-dimensional identity in the normalized perturbation threshold (B_{21}/B_T) between C-Mod (at 6.3 T) and JET (at 0.98 T), as well as a linear dependence of the threshold on plasma density. For extrapolation in major radius to ITER, it was necessary to establish the scaling of the threshold with field. Experiments at higher field on JET had indicated a power law scaling with toroidal field with an exponent $\alpha_B = -1.2$. However, experiments in 2005 on C-Mod at a lower field, 4.1 T, indicated a much



stronger scaling like $\alpha_B \approx -2.4$, which would have led to a rather pessimistic prediction for the ITER threshold. No corresponding dimensionlessly matched data was available from JET, and the C-Mod data employing the JET shape and perturbed mode spectrum was inconsistent with other C-Mod results² which found $\alpha_B = -1.1$, similar to JET and DIII-D. In 2006 additional experiments were undertaken on C-Mod, at a higher field of 7.8 T, which corresponded to an existing JET dataset at 1.3 T. The results were found to agree within error bars with the JET data, consistent over this range with a power law exponent $\alpha_B = -1.1$. Based on this scaling, the extrapolation to the ITER scale, using the non-dimensionally constrained expression $\alpha_R = 2\alpha_n + 1.25\alpha_B$, corresponds to $(B_{21}/B_T) = (0.9 \pm 0.5) \times 10^{-4}$ at the nominal ITER target density of $2 \times 10^{19} \text{ m}^{-3}$. The deviation from a simple power law form at lower C-Mod field remains unexplained, but may be related to observations of similarly strong field scaling reported by COMPASS-C and COMPASS-D.

C-Mod also carried out experiments in support of ITPA/IEA Joint Experiment PEP-7, “Pedestal width analysis by dimensionless edge identity experiments on JET, ASDEX-Upgrade, and C-Mod”. The goal of these experiments is to investigate the physics governing the width of the edge transport barrier in H-mode, which together with MHD stability determines the height of the pedestal and, because of the stiff profile associated with core transport, the overall confinement and reactivity of the ITER plasma. C-Mod obtained data³ for these investigations at a field of 7.8 T, with $q_{95} = 5.2, 4.2, \text{ and } 3.2$. These experiments were carried out using the D(He³) ICRF heating scenario at $f \approx 80$ MHz. The corresponding target field for JET (size ~ 4 times that of C-Mod) is 1.4 T. The JET experiments were completed in 2007, and results of the comparison reported by Maddison reported at the 2007 APS-DPP meeting⁴, and a publication is in preparation. The normalized pedestal profiles were found to be similar, but not identical; in particular, the density width is proportionally larger in JET, consistent with an intermediate condition in which both plasma transport and edge sources influence pedestal formation. Additional studies at higher β_{ped} and lower v^* are proposed.

A major emphasis of H-mode Integrated Scenarios research is characterization and optimization of pedestal relaxation phenomena. It is generally recognized that Type I ELMs, large intermittent MHD events which limit the pedestal pressure and provide particle exhaust, will be detrimental to survival of plasma facing components in ITER or a reactor. However, ELM-free H-modes suffer from impurity accumulation and uncontrolled density rise, due to the intrinsically high particle confinement. More benign edge relaxation mechanisms, including small ELMs and continuous fluctuations such as the quasi-coherent modes observed in the C-Mod EDA regime, have been observed in different devices. Studies of these phenomena involve elements of Transport, Boundary Science, MHD, and Wave-Particle interactions, and clearly satisfy the interdisciplinary criterion for “integrated” research.

Alcator C-Mod has participated in two ITPA Joint Experiments addressing these more benign relaxation regimes. A comparison was carried out for similar ranges of non-dimensional pedestal parameters between the Alcator C-Mod and JFT-2M tokamaks⁵. Shapes were matched apart from aspect ratio, which is higher on JFT-2M. The high recycling steady H-mode on JFT-2M and enhanced D-alpha (EDA) regime on C-Mod, both of which feature very small or no ELMs, were found to have similar access

conditions in $q95 - \nu^*$ space, occurring for pedestal collisionality $\nu_{ped}^* > 1$. Differences in edge fluctuations were found, with lower frequencies but higher mode numbers on C-Mod. In both tokamaks an attractive regime with small ELMs on top of an enhanced $D\alpha$ baseline was obtained at moderate ν^* and higher pressure. The JFT-2M shape, which is characterized by large δ_L , small δ_U , and relatively low elongation, $\kappa \sim 1.5$, favored the appearance of type I ELMs on C-Mod at lower ν^* and also resulted in the appearance of a lower frequency component of the quasicohherent mode during EDA.

Another set of experiments is being carried out in conjunction with the Spherical Torus facilities MAST and NSTX, to establish a dimensionless pedestal comparison between small ELM regimes in these devices and in conventional tokamak aspect ratio plasmas in C-Mod. These experiments, designated ITPA/IEA Joint Experiment PEP-16, complement the successful Joint Experiment on pedestal relaxation phenomena between C-Mod and JFT-2M, which operates at higher aspect ratio. Motivation for PEP-16 includes the identification of similarities and differences between the type-V ELM regime observed on NSTX and the EDA regime on C-Mod and HRS-mode on JFT-2M, as well as to the “small ELM” regime which develops at higher power on C-Mod. In addition to the comparison of edge relaxation mechanisms, these experiments, to be carried out with matched non-dimensional parameters *with the exception of aspect ratio* are also expected to contribute to the understanding of the scaling of the pedestal width.

C-Mod achieved the specified target pedestal temperature in the designated common lower single null (LSN) shape, and observed a brief period of small ELMs, although higher power is required to access the specified pedestal β . Partial results were also obtained in the experiments on MAST and NSTX. These initial experiments have resulted in some modification of the experimental design, including some modification to the target shape, to facilitate a three-way match in the non-dimensional parameters. The ITPA Joint Experiment is continuing, with additional results anticipated in 2008.

The C-Mod program is also addressing issues raised during the ITER Design Review. An example is an experiment concerning the scaling of the L-H threshold power at low density (Issue cards LH-2 and AUX-11). As noted on C-Mod several years ago, and subsequently on other facilities as well, the power required to access H-mode increases rapidly below some critical density, deviating from the general trend toward lower power as the target density is reduced. The ITER H-mode scenario is predicated on accessing H-mode at relatively low density, around $2 \times 10^{19} \text{ m}^{-3}$. However, the scaling of the low density bound is uncertain, and if the minimum in the power versus density relation is in fact near $5 \times 10^{19} \text{ m}^{-3}$ then the planned heating power in ITER could be insufficient to achieve H-mode operation. This issue is of critical near-term importance, since it impacts the specification of the ITER heating systems. Experiments on C-Mod in 2007 investigated the question of whether the low density limit scales with plasma current, *e.g.* as n/n_G . Such a scaling would be favorable for ITER, which proposes to access H-mode at a value of n/n_G above that which corresponds to the low density limit in C-Mod, at the same toroidal field. However, these experiments appear to rule out a scaling of the low density bound with current or Greenwald parameter, leaving the relevant scaling still to be determined.

As described in the MHD section, C-Mod also provided significant input to Issues raised at the ITER Design Review related to vertical stability and control⁶. These issues will continue to be addressed in dedicated C-Mod experiments modeling ITER startup, as well as development and validation of control options for ITER H-mode scenarios.

8.2 Research Plans

Over the next five years, a major emphasis of the C-Mod H-mode Integrated Scenarios research program will be to address important issues related to ITER construction and operation. Issues include:

- Compatibility of core and boundary, extending beyond the last closed flux surface to open field lines
- Interaction with plasma-facing materials, including heat-flux and particle control
- Control of the operating point, and also of the startup and approach sequence and shut-down phase

The program builds on previous results, as well as exploiting newly developed C-Mod capabilities, including the cryopump for particle control as well as enhanced diagnostics.

The C-Mod research program in this area is embedded in a world-wide effort in support of ITER. Continued participation in ITPA Joint Experiments and High Priority Tasks will leverage C-Mod's unique parameters and provide valuable input toward the development of improved physics understanding and predictive capability for ITER. Coordination and collaboration activities are being pursued among the major U.S. facilities, as well as within the world program. The scope of these activities ranges from closely coordinated Joint Experiments to complementary or related experiments on multiple facilities, and includes shared development and exploitation of tools and methods.

Modeling and analysis codes are key to Integrated Scenarios research, and development, benchmarking, and validation of these tools is both a goal and a requirement for this effort. In simulations supporting this research, a code such as TSC, which contains a model of the tokamak actuator systems and geometry, is used to advance the tokamak discharge subject to transport estimates from transport estimates of varying degrees of sophistication, ranging from empirical transport coefficients to physics-based models embodied in codes such as TGLF or GLF23. Transp runs are used to compute source terms due to ICRF (using TORIC-FPP module) and LHCD (presently employing the LSC code module, to be augmented by more advanced modules incorporating CQL3D-GENRAY). The resulting source terms are then employed to time advance the TSC simulation. Such simulation procedures are employed both for experimental design and for post-experiment interpretation and model validation.

Design of individual experimental discharges studied in the Integrated Scenarios program benefits from the use of the Alcasim code⁷, a MATLAB-Simulink application (developed by an MIT Nuclear Science and Engineering Department graduate student) which incorporates details of the C-Mod magnetics diagnostics, power supply characteristics, and digital plasma control system (DPCS). The time evolution of plasma parameters are taken from experimental data from actual or simulated discharges, and can be modified by the user through a graphical interface. This code is coupled directly to the C-Mod

Plasma Control System Operator interface, so that discharge programming can be evaluated off-line (software-in-the-loop), or even between plasma shots during an experimental run. This tool is also useful for developing and debugging new plasma control algorithms prior to on-line testing in C-Mod experiments.

In addition, sophisticated simulation models in standalone codes such as NIMROD, ELITE, and M3D in the MHD area, AORSA, TORIC, CQL3D, GENRAY in RF, XGC, GS2, and GYRO for Transport, are used for analysis of experimental results in these areas, and to provide guidance for experiments. Going forward, the Integrated Scenarios program will both benefit from and inform the development of the integration of such modules planned for the IPS (Integrated Plasma Simulator) being developed through the SWIM Prototype Fusion Simulation Project, as described in Chapter 10.

8.2.1 ITER H-mode Operational Scenarios

A major focus of the H-mode Integrated Scenarios research program over the next five years will be aimed at development, demonstration, and validation of operational scenarios for ITER operation. The C-Mod physics regime, machine capabilities and control tools are highly relevant to these tasks. Near-term experiments will address ITER rampup and shut-down scenarios, with particular attention to the need to maintain low internal inductance, $0.7 < l_i < 1.0$, in order to maintain vertical stability, and also to minimize heat loads to limiters and plasma-facing components during these phases of the discharge. As noted above, the ITER reference startup has been modified⁸ to include a faster ramp rate and early diversion in order to satisfy stability requirements. Simulations of this ramp-up require experimental validation, and experiments are being conducted at several facilities.

In addition to operation at the ITER field of 5.3 T, the C-Mod experiments feature high ohmic power and ITER-relevant auxiliary heating (ICRF, LH), metallic walls and conducting structures, and similar PF coilset and control issues. The goal of these experiments is to provide input for benchmarking the ITER simulations, particularly the transport assumptions, as well as evolution of impurities, heat loads, and electron density.

The experiment should demonstrate sufficient conditions, including detailed evolution of plasma shaping and density, possible use of auxiliary heating or current drive during the ramp-up, and requirement on control tools, to satisfy the criteria for the ITER startup, while identifying potential limitations due to MHD activity, runaway electron generation, heat loads or impurity generation, etc. ITER ramp-down scenarios will also be studied, with the aim of demonstrating safe routine shutdowns from nominal H-mode conditions ($\beta \sim 1.8$, $q_{95} \sim 3.2$, etc.) while maintaining divertor operation, control over the evolution of I_p , and of the plasma density. These near-term experimental investigations will inform design choices for the ITER coil and power supply system and first wall components, and help refine the reference operational scenarios.

In the longer term, C-Mod experiments will address aspects of the approach to and control of the nominal operating point. As noted previously, the layout of the C-Mod

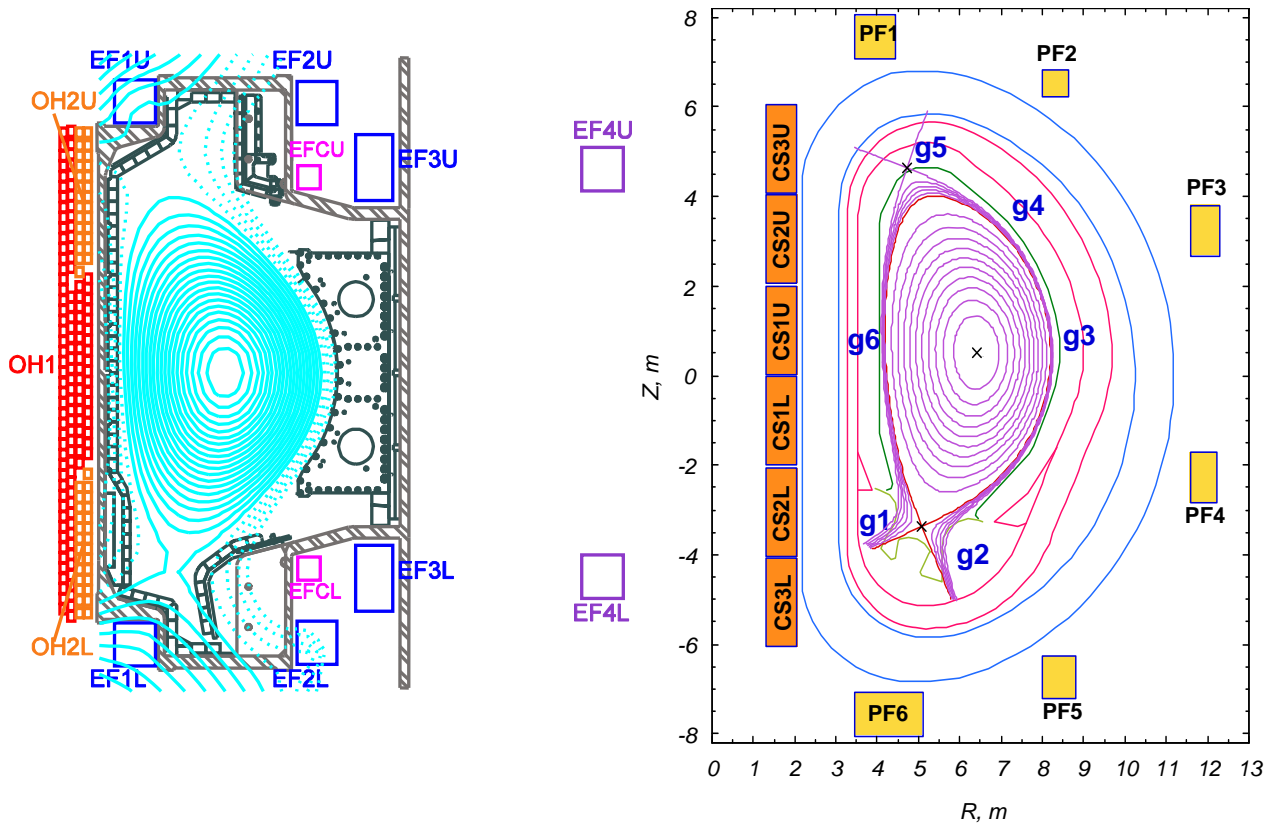


Fig. 8.2.1 C-Mod (left) and ITER (right) poloidal field coil sets have similar arrangement and functionality. Shape control depends on combinations of coils to maintain a small number of gaps, with minimal null space.

poloidal field coilset is rather similar to that of ITER. The central solenoid is used not only for inductive drive but is composed of separate coils which play an important role in plasma shaping. The PF ring coils are distributed around the poloidal cross-section, utilizing essentially all the available space not required for port access. There is no strict one-to-one correspondence between individual PF coils and the plasma shape parameters of interest, resulting in shape (and current) control algorithms that are inherently MIMO

(Multiple Input, Multiple Output) in character. C-Mod is therefore an appropriate test-bed for development and testing of control approaches and algorithms in a realistic tokamak environment, including the effects of noise, parasitic currents in conducting structures, effects of power supply nonlinearities, transient events, *etc.* These experiments also serve to benchmark the simulation codes used to design and validate control approaches for the ITER system.

Other H-mode experiments with direct relevance to ITER burning plasmas include burn control simulations. The digital plasma control system gives the capability to vary input RF power as a function of plasma temperature or neutron production, mimicking the alpha heating in a burning plasma. This will allow us to study the evolution and stationary states of a self-heated plasma, and to develop and test burn control techniques. These experiments will also provide a good test of the ability of control algorithms to deal with stable as well as potentially unstable operating points. The goal would be to demonstrate the ability to maintain constant “fusion power” in the presence of perturbations such as ELMs, sawteeth, MHD instabilities, density excursions, *etc.*

In addition to maintaining a potentially unstable operating point, burn simulation experiments would also address the issue of access to the operating point and burn termination. Of particular interest is to simulate the entry to the H-mode phase including (simulated) alpha-heating, in view of the small margin of the ITER auxiliary heating system with respect to the H-mode threshold. The safe termination of the burn and subsequent ramp-down and plasma termination is also an important topic for these simulation studies.

8.2.2 High performance Demonstration Discharges

Demonstration of high performance discharges with the ITER baseline non-dimensional parameters (excluding ρ^*) is in itself a challenging task which serves to increase confidence and provide benchmarking for models and codes used to develop and refine operational scenarios for ITER. Moreover, these demo discharges provide a platform for other ITER-relevant physics studies, and a reference comparison for more advanced scenarios. Issues to be addressed include optimization of pedestal characteristics for best core reactivity, while maintaining satisfactory divertor parameters and particle and energy exhaust. This work will apply and *integrate* the results from research in the Pedestal Physics, Core Transport, MHD, and Boundary Science programs.

Building on the successful high-power H-modes already demonstrated, with ITER field and β_N , H-mode high-performance scenario experiments will be extended toward conditions which are closer to those on ITER in other respects, especially collisionality and normalized current (I/aB). We have previously demonstrated ITER-shaped ohmic discharges with $\kappa > 1.8$ and $q \leq 3.2$ at the nominal ITER field of 5.3 T. This discharge shape is well-matched to the cryopump configuration. We propose to operate in this configuration at high ICRF power ($P > 5\text{MW}$) using D(H) minority heating with $f \approx 80\text{MHz}$, which provides high single pass absorption, comparable to the ITER ICRF heating scenario. This should provide an expanded parameter space for databases and extrapolation to ITER, as well as demonstrating operation at the ITER field, q_{95} , β , and

absolute pressure. Using the cryopump to reduce density below that set by natural evolution from the L-mode target, the resulting increase in T_e should cause a substantial reduction of v^* . These experiments will provide integrated tests of confinement, heating and power handling in a highly ITER-relevant regime. In addition to enhanced D_α , pedestal and confinement studies will focus more on the regime of small ELMs, which is attained at high power and pressure; this seems most promising for ITER. To this end, we will increase plasma current and explore the limits of q_{95} for which this regime can be attained; our highest pressure H-modes to date were at $q_{95} = 3.9$, while the ITER reference scenario is at $q_{95} \sim 3.2$.

Because ρ^* is not matched in these “demonstration discharges”, no single measure of collisionality is adequate to characterize all the relevant physical processes. It is therefore not possible in general for a single set of parameters to serve as the basis for extrapolation to ITER. Typically different phenomena will be best addressed at different absolute parameters in a given device, and a range of “collisionalities” is required for ITER H-mode validation experiments. Some transport effects may be well-characterized by the usual neoclassical $v_*^{neo} = (\epsilon^{-3/2} v_{ii} q R / v_{thi})$. Others, along with NTM physics and other MHD processes, will depend on v/ω_* , which, for fixed q and geometry, is larger than v_*^{neo} by a factor of ρ^* . Electron-ion equilibration depends on $v^{e/i} \tau_E$, which in turn depends on the ρ^* scaling of the transport. For gyro-Bohm scaling, $(v^{e/i} \tau_E) \sim v_*^{neo} (\rho^*)^2$, *i.e.* two powers of ρ^* . Figure 8.2.2 shows example parameters of C-Mod discharges which match the ITER H-mode operating point in β_N , q , shape, and each of these three measures of collisionality, as well as having the same field and therefore the same absolute pressure.

As shown, under the given transport assumption ($H_{89}=2$), between 5 and 6 MW of heating power should be sufficient to access the ITER β value over the range of required density; this power is consistent with C-Mod’s installed ICRF power. Typical density in high power H-mode discharges in C-Mod are in the range of 3 to $5 \times 10^{20} \text{m}^{-3}$, corresponding to the upper two collisionality matching points. High power H-mode operation in C-Mod at $q_{95} \sim 3$ and a density of $2 \times 10^{20} \text{m}^{-3}$, as required in order to match the projected ITER neoclassical v_* , is a challenge, both in terms of accessing the low-density condition and for maintaining a quasi-steady discharge at low Z_{eff} and P_{rad} . Furthermore, these low density conditions provide the most severe challenge to the divertor and plasma-facing components.

In addition to operation at the ITER field of 5.3 T, some high performance H-mode experiments will be carried out at 8 T, using the D(He³) heating scenario at $f \sim 80$ MHz. These experiments, while at higher than the ITER field, extend ρ^* scalings, and facilitate important ITPA intermachine experiments with larger, lower field tokamaks including JET, DIII-D and Asdex Upgrade

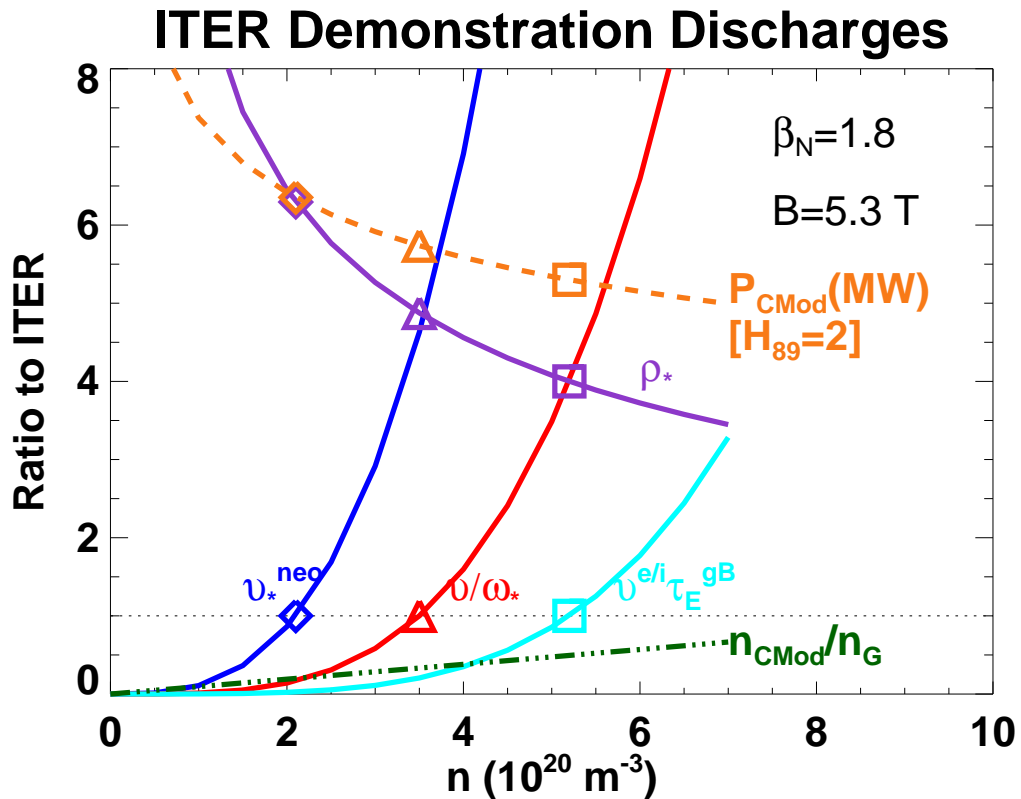


Fig. 8.2.2 Parameters of ITER H-mode demonstration discharges in C-Mod which match ITER in terms of three dimensionless measures of collisionality. Vertical axis corresponds to the ratio of the C-Mod parameters to the ITER nominal values for ρ_* (purple) and each collisionality parameter. Also shown are the power (MW) required for C-Mod (yellow) and the Greenwald density parameter of the C-Mod discharge.

Research into neoclassical tearing modes will be another topic of increasing importance. High performance H-modes are already close to predicted limits. With modest increases in β_N and decreases in v/ω_* , C-Mod will be positioned to provide important tests of NTM thresholds and RF stabilization techniques. Investigation of the use of LHCD for NTM stabilization by means of Δ' modification, initially being carried out by the MHD Physics topical area, will, if successful, be developed as a component of an integrated scenario for application to the ITER H-mode baseline case. Accessibility constraints will likely require these experiments to be carried out at densities close to those of ITER, around $1 \times 10^{20} \text{ m}^{-3}$.

It is perhaps worth noting that the issues and challenges that must be met for C-Mod to access this regime are similar to those faced by ITER. In both cases, the divertor and plasma facing components must deal with heat fluxes near the limits of the materials, and the impurity control must be compatible with maintaining low Z_{eff} and low radiated power from the core. The issue of hydrogenic retention in plasma facing components must be met in each case, in ITER because of tritium issues and in C-Mod because the

ICRF proton minority heating depends on a low hydrogen fraction in the plasma. C-Mod activities in response to this challenge are reported in the Boundary Physics chapter. In C-Mod, ICRF minority heating is employed as the primary auxiliary heating source to access and sustain the high performance plasma regimes of interest. For ITER ICRF is also employed as part of the complement of bulk auxiliary heating required to access the burning plasma regime. The devices face similar challenges in terms of RF power density at the antennas, compatibility of wave accessibility with the H-mode edge pedestal and ELM perturbations. These loading issues are being addressed at C-Mod through design of the ICRF antennas, and by utilization of a combination of active and passive load matching components, as described in the ICRF chapter. C-Mod operation has also identified an issue concerning interaction of the ICRF waves with high-Z metallic plasma facing components, as well as erosion of low-Z films used for wall conditioning. These issues, and measures undertaken and planned to resolve them, are described in sections 4.2.3 and 4.2.6.

8.2.3 Pedestal and ELM Control

For the H-mode baseline scenario, as for all scenarios with an H-mode edge transport barrier, control of the pedestal parameters and edge relaxation phenomena is crucial, both for setting the boundary conditions for the (stiff) core transport and for particle and impurity control. A particular challenge for C-Mod in this respect is in accessing regimes with sufficiently low collisionality. We propose to utilize the cryopump to extend our exploration of pedestal structure and edge relaxation mechanisms to lower collisionality regimes. The H-mode pedestal height is critical for determining the core profiles and confinement in ITER. Recent work, described in the Pedestal Physics section, extended C-Mod H-modes to lower v^* under specific circumstances, including high field (~ 8 T), unfavorable grad-B drift direction, and strong shaping. These regimes were characterized by higher pedestal T_e and lower pedestal density than our typical H-modes. Some of these cases also exhibited very steep pressure gradients. We will be continuing and extending our studies of these regimes, making use of the cryopump for additional particle control.

Experiments on C-Mod in the last few years have identified a regime of low-density H-modes with large ELMs. These plasmas were characterized by strong shaping, in particular by large values of lower triangularity. These experiments, described in the Boundary Physics section of this document, provided an opportunity to contribute to studies of ELM structure, dynamics and energetics. Using the cryopump, we will extend these studies to investigate ELM stability as a function of shape and collisionality. In particular, we should be able to pursue these studies in the ITER shape. Specific topics of interest include the further investigation, with improved diagnostics, of the high frequency magnetic oscillations observed at filament ejection, and the non-thermal electron generation associated with the ELM crash.

ELM mitigation has been identified as a major issue for ITER⁹, and consideration is being given to design changes which would incorporate additional non-axisymmetric coils for the purpose of reducing ELM effects by application of edge-resonant magnetic perturbations (RMP). We propose to follow up on a recently reported result from JET¹⁰ by evaluating ELM mitigation using $n=1$ perturbations produced by our non-axisymmetric coils (A-coils). Calculations indicate that the existing C-Mod A-coils are

capable of producing similar ergodization in the pedestal region to that required in the JET experiments, $\sigma_{\text{ch}} > 1$ outside the $\sim 90\%$ flux surface. Initial experiments carried out in 2008 using the strongly shaped equilibria which have provided the most reliable access to Type I Elms in C-Mod did not result in ELM suppression in the range of $3.3 < q_{95} < 3.9$. Future experiments in more ITER-like equilibria and employing alternative non-axisymmetric perturbations are proposed. The addition of a second power supply would also allow us to carry out experiments with $n=2$ RMP fields, which potentially have the advantage of not simultaneously exciting $2/1$ locked modes. In either case, an important aspect of the evaluation will include assessment of the magnetic braking of plasma rotation due to the (resonant and non-resonant) non-axisymmetric applied fields. The C-Mod case is particularly relevant to ITER in this respect, since there are no external torques due to the heating sources and the observed intrinsic rotation is the result of internal transport-driven processes. In view of the expense and technical complexity of incorporating internal coils into ITER or a reactor-scale device, the potential for ELM suppression of low- n perturbations achievable with external coil systems, as exemplified by the C-Mod A-coils or JET EFCC coils, is worthy of investigation.

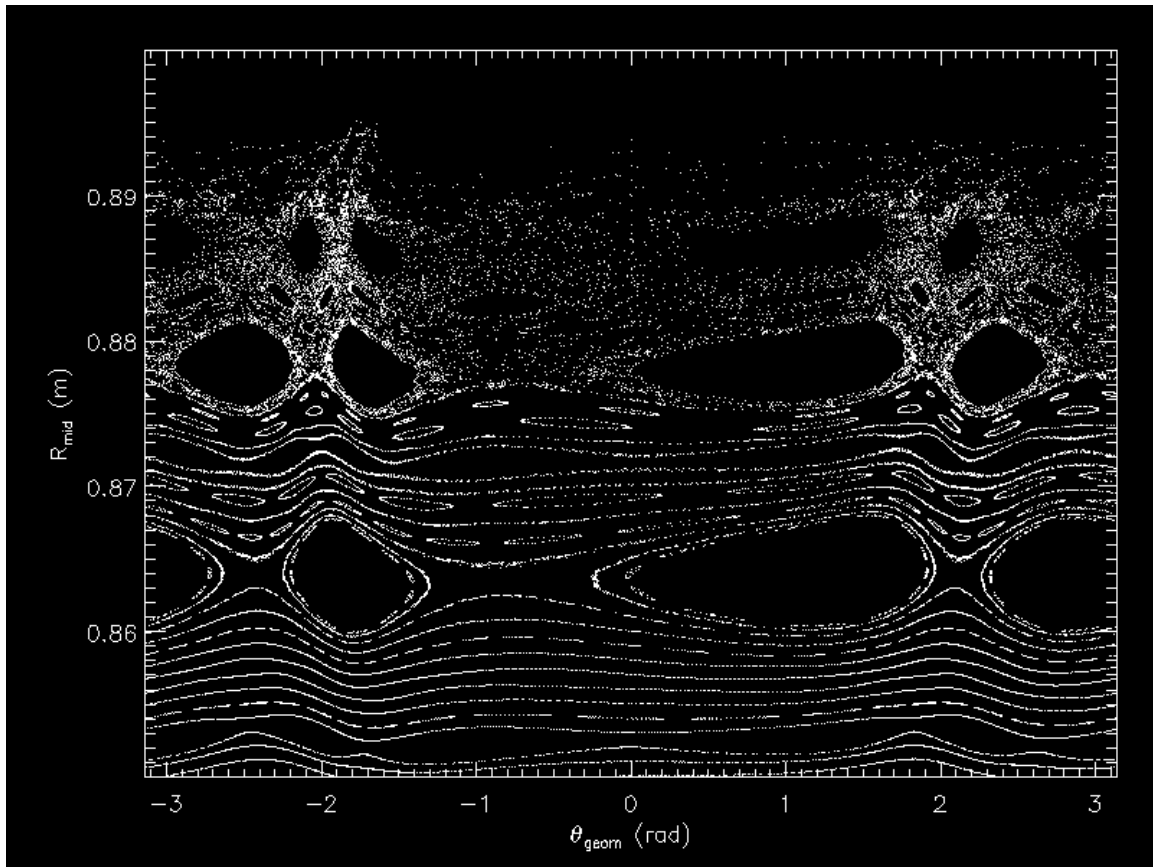


Fig. 8.2.3 Poincaré plot showing field ergodization in the outer region of C-Mod plasma using A-coils to produce a predominately $n=1$ perturbation. Intact island chains are produced inside $q=4$, while at larger radii the Chirikov (island overlap) parameter is above one, satisfying the conditions for ELM mitigation.

8.2.4 Power and Particle Exhaust – Plasma-Wall interaction

Research on testing PFC materials and coatings, and their impact on H-mode performance, will continue. C-Mod experiments feature divertor heat fluxes of ~ 0.5 GW/m², approaching that of ITER. Research will extend to include testing of new tungsten tile designs over a greater portion of the PFCs. As described in the Boundary Physics section, a complete toroidal band of tungsten lamellae tiles is presently installed in the outer divertor. The duration and input power of long-pulse experiments will be progressively extended, enabling even more demanding tests of all PFCs. Interaction with, and effects on, the core plasma will again be a key part of the experiments. The outer divertor modules are scheduled to be replaced in 2011 with a new structure featuring tungsten plasma facing components based on the presently installed lamella design. The new structure will be fully axisymmetric, with no leading edges, further increasing the power handling capabilities. In addition this divertor structure will be capable of DEMO-relevant operation at elevated temperature, up to 600C, providing improved hydrogenic retention properties.

We will continue to explore the prospects for radiative divertor H-mode scenarios on C-Mod at higher power than was available in past investigations. Moderately high radiated fractions are envisaged in most ITER experiments to reduce divertor heat loads. The issue and challenge here is to maintain high pedestal pressure and global confinement in conjunction with this edge and divertor radiation. Recent experiments have demonstrated the ability of the cryopump to pump injected radiating gases, allowing for additional control of the radiation fraction. Making use of this capability, along with the improvements in the plasma control system made possible by DPCS, we propose to revisit and extend our previous detached divertor control experiments¹¹ to ITER-like conditions. Puffing of impurity gases which radiate primarily in the divertor and SOL regions will be employed to increase the divertor radiation fraction and decrease the heat flux conducted to the divertor plates. Feedback on the puff rate together with pumping should enable us to maintain a constant ratio of edge radiation to total power. Upgrades to the divertor bolometry and thermography will facilitate these studies, as will the improved symmetry provided by the new divertor structure once it is installed.

Research to understand the physics of radiation trapping in the high n_0L C-Mod divertor will continue. C-Mod is the closest to ITER in this regard, and modeling predicts this will have important effects on detachment.

8.2.5 Control Algorithm Development and Validation

Another aspect of Integrated Scenarios research which will be receiving increasing attention at C-Mod and other facilities as ITER moves into the construction phase is the development and demonstration of robust machine protection algorithms and techniques. While development of these methods at C-Mod will be carried out initially under the auspices of the Operations and Control System tasks, incorporation of such techniques into routine operation at relevant parameters will be required. Robust fault sensing algorithms capable of identifying off-normal or unplanned conditions near operating

boundaries must be developed, validated, and demonstrated. The range of off-normal conditions which must be identified include failure of control system sensors, proximity to actuator limits, such as power supply voltage or current saturation, actuator failure, unanticipated variation from expected plasma behavior, and loss of plasma stability tending toward disruption. For each such condition reliable detection algorithms must be identified, with satisfactory look-ahead to enable appropriate remedial action and extremely low susceptibility to “false positives”.

One example of such machine protection actions is disruption mitigation using massive gas jet injection to ameliorate the effects of VDE's, as described in the MHD section. Experiments on C-Mod and elsewhere¹² are demonstrating the efficacy of the technique, and optimizing the amount and mixture of injected gas. A trigger algorithm based on detecting an incipient VDE by observing the amplitude of the error in the vertical position has been tested successfully¹³. Adequate time for actuation of the gas jet was demonstrated with a trigger threshold that should not lead to termination of controllable discharges, based on a database survey. However, implementation of the mitigation system using this algorithm has not been attempted on a routine basis, since on C-Mod the deleterious effects of unmitigated VDE's have not been considered sufficiently serious to warrant this step. In order to develop the database of experience required to qualify this technique for application on ITER, we propose to incorporate this algorithm into standard operation on C-Mod. Routine use of disruption mitigation will provide valuable operational experience leading to further optimization of the technique, as well as offering the potential for improved disruption recovery on C-Mod.

Another aspect of machine protection algorithms currently under development is a transition to an alternate, “safe” equilibrium trajectory, followed by graceful discharge termination, in response to power supply saturation. Such solutions have been proposed, and tested in simulations^{14,15}, but routine application of such nonlinear control methods in actual experiments is lacking. C-Mod is a suitable test-bed for such a scheme, since current saturation is frequently encountered in operation, particularly near the end of flat-top or in the ramp-down phase of discharges. The MIMO linear control scheme employed at C-Mod (7 shape parameters, plus plasma current; 9 independent power supplies) allows for only a rather small null space, rendering alternate solutions to the saturation problem without abandoning the original target equilibrium problematic. Similar considerations may be expected for the ITER shape control. Important issues for the design of such an adaptive response include the identification of appropriate alternative “safe” fallback equilibria, and the development of a smooth interpolation procedure between the original targets and the fallback. The stability of the intermediate equilibria during the transition is not guaranteed, and must be evaluated. Finally, the determination of the criteria used to instigate such an adaptive sequence leading to a graceful termination must be based on a trade-off between performance and safety margins: an early transition strategy based on proximity to the limit would avoid any non-linearity in response due to actuator saturation, but gives up some of the design range; delaying the response until the limit is actually reached risks disruption. In the case of ITER, which has very small margin in terms of coil currents in the nominal scenario, these trade-offs are especially critical.

While disruption mitigation is a necessary component of the ITER strategy, disruption avoidance is clearly a more desirable goal. Of necessity, the ITER scenarios require operation close to stability boundaries. Real-time estimation of the proximity of the operating point to instability, coupled with effective avoidance measures, would have significant benefits for robust operation. The ITER baseline H-mode scenario operates at modest $\beta_N \sim 1.8$, so the disruptive limit of primary concern is probably the $n=0$ vertical instability. Two approaches to estimation of the stability boundary seem feasible: evaluation of the operating point equilibrium elongation, I_i , *etc.*, for comparison to pre-computed closed loop stability margins; and direct observation of the plasma response to the control system drive. The latter method could be a relatively straightforward extension of the observer employed in the VDE mitigation system, while the former would require a more sophisticated real-time equilibrium calculation but could have the advantage of longer look-ahead capability, allowing more response time for modifying the discharge trajectory. An obvious adaptive response to detection of reduced stability margin would be to reduce the elongation, although such an approach must be applied in such a way as to reduce q_{95} below 3, so the current may need to be reduced as well.

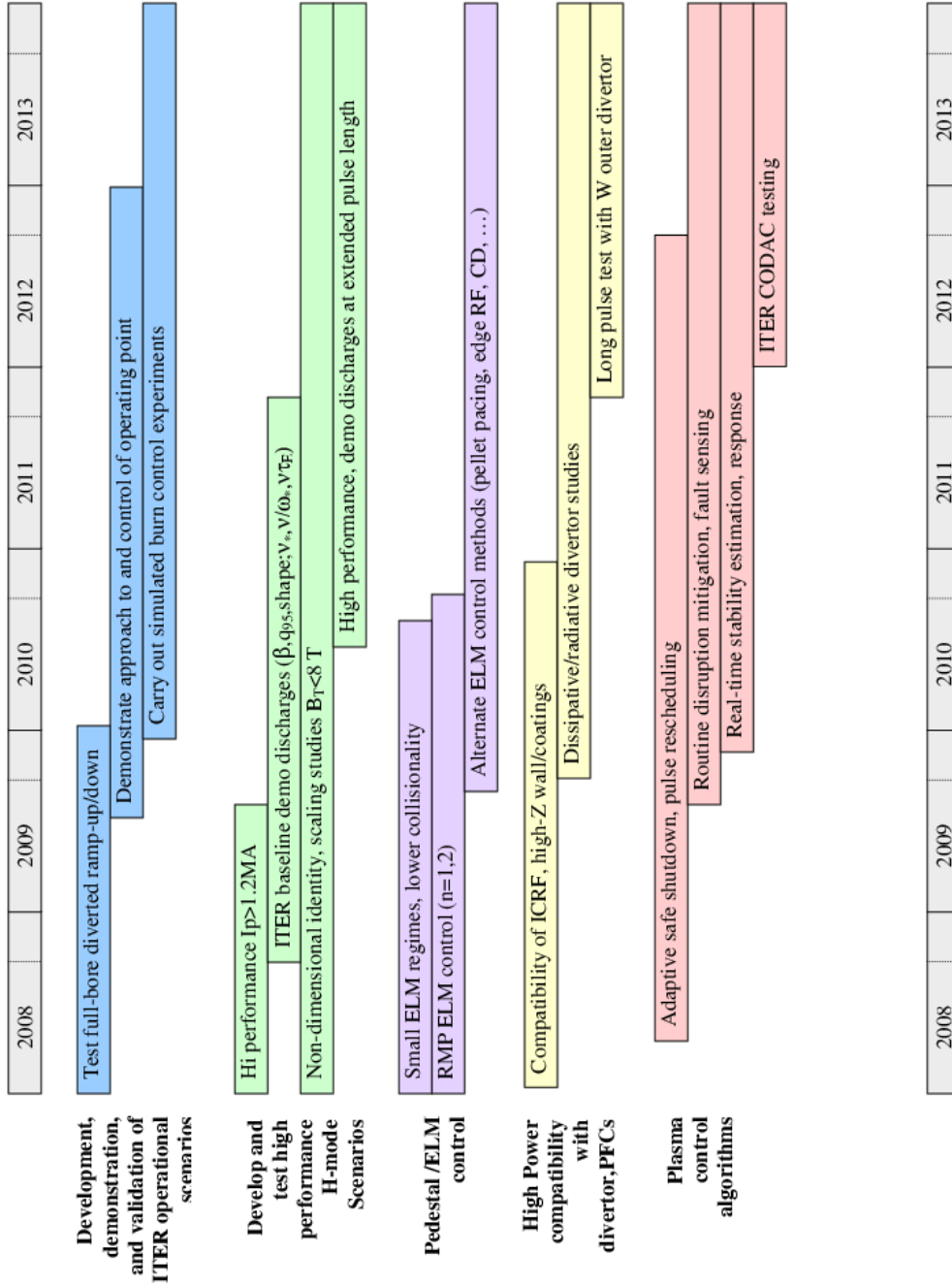
8.2.7 Goals and Objectives and Schedule

Table 8.2.1 Research Goals

Research Goal	Intermediate Objectives	Enabling Tools
Development, demonstration, and validation of ITER operational scenarios	Test ITER diverted full bore current ramp-up scenario	
	Test ITER ramp-down scenario	
	Demonstrate approach to and control of nominal H-mode operating point (shape, β , I_i , n_e , ...)	DPCS upgrades (software, sensors, actuators) PF Upgrades (EF2, EFC)
	Carry out simulated burn control experiments	DPCS enhancements ICRF antenna, FFT upgrades.
	Test LHCD control of NTM	LH Upgrade (2009-10)
Optimize pedestal relaxation mechanism with respect to core confinement, particle control, heat exhaust	Characterize shape, pedestal parameters resulting in small ELM regimes	
	Test low n/m RMP ELM control using A-coils	A-coil power supply upgrade
	Test ELM pacing using pellets, edge heating, CD	
Demonstrate high power operation with acceptable divertor heat loads, steady-state density	Determine and implement requirements for compatibility of ICRF and high-Z metal walls and/or low-Z coatings	Improved PFC's, limiter upgrades SPRED spectrometer
	Develop techniques for controlling dissipative/radiative divertor while maintaining acceptable pedestal parameters	Divertor bolometry Divertor piezo valves Outer Divertor upgrade IR camera upgrade
	Evaluate W divertor for long pulse operation	Outer divertor upgrade IR Camera upgrade
Develop and test high performance H-mode scenarios	Operate at ITER-scaled physics parameters q_{95} , β , and (v^* or v/ω_* or $v_{ei}\tau_E$), shaping and geometry	ICRF Upgrades PF Power Supply Upgrades
	Evaluate influence of pedestal parameters, relaxation mechanisms on core performance	

	Evaluate evolution of core radiation, impurities for extended pulse lengths	
Test ITER-relevant plasma control algorithms	Develop and test control algorithms which mimic the ITER configuration, dynamics	DPCS software, host enhancements EF2/EFC Power supply upgrade
	Develop robust fault sensing and mitigation techniques for off-normal events, including real-time adaptive control methods for safe shutdown	
	Develop real-time stability boundary estimation and response	
	Trial implementation of elements of the ITER CODAC	

H-mode Research Schedule



8.3 Contributions to ITPA/ITER and FESAC Priorities

Experimental work carried out under Integrated Scenarios – H-mode thrust includes support for ITPA/IEA Joint Experiments. Currently open experiments and those completed during the previous five year period are summarized in the following table. In some cases the C-Mod experiments are conducted jointly between the Integrated Scenarios and one or more of the Topical Science Groups, so there will be some overlap between this table and similar ones found in other chapters.

Summary of Integrated Scenario (H-mode) Work for ITER/ITPA

Description	JOINT Experiments	Notes on C-Mod Contributions
Confinement scaling, v^* scans at fixed n/n_G	CDB-4	Initial experiments performed, higher β operation required
ρ^* scaling along ITER relevant path at both low and high β	CDB-8	Will require further development of low density H-modes at high current.
L-H threshold power at low density	(CDB-? Proposed, under discussion)	Initial C-Mod experiment completed
Scaling of spontaneous rotation with no external momentum input	TP-6.1	Exploit improved profile measurements
Pedestal width analysis by dimensionless edge identity experiments on JET, ASDEX Upgrade, Alcator C-Mod and DIII-D	PEP-7	Experiments completed 2007; Publication in prep.
Comparison between C-Mod EDA and JFT-2M HRS regimes	PEP-12	Experiments completed 2005
C-MOD/NSTX/MAST Small ELM regime comparison	PEP-16	In progress
Role of Lyman absorption in the divertor	DSOL-5	See also Boundary physics
Low beta error field experiments	MDC-6	Completed 2006
Non-resonant magnetic braking	MDC-12	Initial C-Mod experiment 2007 Higher T_i case pending
Simulation and validation of ITER startup to achieve advanced scenarios	SSO-5	Addressing both AT and H-mode baseline scenarios; see also Integrated Scenarios-AT

The H-mode Integrated Scenarios program is also committed to providing timely response to ITER issues presented independent of the ITPA structure.

The 2005 FESAC panel on “Scientific Challenges, Opportunities and Priorities for the U.S. Fusion Program” did not identify a “campaign” corresponding to Integrated Scenarios research. Rather, this program, and also the AT Integrated Scenarios program,

integrates the results of the various campaigns on Macroscopic Plasma Physics, Multi-scale Transport Physics, Plasma Boundary Interfaces, Wave and Energetic Particles, and Fusion Engineering Science, with the aim of developing a consistent simultaneous solution to the problems facing production of a burning plasma in ITER. The research contributes most strongly to the second overarching theme identified in the FESAC report: “create a star on earth”, that is, “to produce, study and control a burning plasma – plasma whose high temperature is sustained by the heat produced by fusion reactions”. The program also includes elements which contribute to the third overarching theme, to “develop the science and technology to realize fusion energy”.

In developing and testing scenarios in support of H-mode operation of ITER, and in providing data against which to benchmark simulation codes, the research contributes to the first of the long term goals of the U. S. Fusion Energy Sciences program:

Predictive Capability for Burning Plasma: Progress toward developing a predictive capability for key aspects of burning plasmas using advances in theory and simulation benchmarked against a comprehensive experimental database of stability, transport, wave-particle interaction, and edge effects.

Furthermore, in developing improved operational techniques and integrated solutions this research is also well aligned with the second of the long term goals:

Configuration Optimization: Progress toward demonstrating enhanced fundamental understanding of magnetic confinement and improved basis for future burning plasma experiments through research on magnetic confinement configuration optimization.

While the principal focus of the H-mode Baseline Integrated Scenarios research thrust is on ITER operation, the research also contributes either directly or indirectly, by supporting a potential next step U. S. facility, to addressing some of the gaps identified in the FESAC report “Priorities, Gaps and Opportunities: Towards a Long-Range Strategic Plan for Magnetic Fusion Energy”. In particular, the work addresses issues relevant to Theme A “Creating predictable high-performance steady-state plasmas”, and Theme B “Taming the Plasma Material Interface”. Theme C “Harnessing fusion power” is mainly concerned with the technology of the fusion power cycle, and is outside the scope of the C-Mod program.

Sub-theme A.2 of the FESAC document is concerned with “Integration of high-performance steady-state burning plasmas”. To the extent that the C-Mod H-mode Integrated Scenarios research contributes to the achievements of these conditions in ITER, this research is indirectly supportive of this issue. In the absence of actual burn, the integrated scenarios including burn simulation experiments may be considered to provide some direct contribution in this topic.

A.3 Validated Predictive Modeling: A key aspect of the proposed research is to provide suitable benchmarking and validation for computational models of plasma performance employed for ITER, and by extension, applicable to the DEMO step as well.

A.4 Control: Development and demonstration of suitable control algorithms is a key theme of the proposed H-mode Integrated Scenarios research program. This contributes directly the issue described in the FESAC report: *Investigate and establish schemes for*

maintaining high-performance burning plasmas at a desired multi-variate operating point with a specified accuracy for long periods without disruption or other major excursions.

A.5 Off-normal Plasma Events: Sensing and avoiding or mitigating such off-normal events is identified as an important aspect of the control algorithm development theme of the proposed C-Mod research program in this area.

A.6 Plasma Modification by Auxiliary Systems: Under the corresponding topical areas, C-Mod research is aimed at developing the physics and engineering science of ICRF and LHCD systems for plasma heating and current drive. The Integrated Scenarios research provides the context for demonstrating the application of both the science and technology under relevant conditions and validating their consistency with the requirements of a high performance sustained plasma.

The second major theme, “Taming the plasma material interface”, deals with issues which are explicitly addressed in the C-Mod program (with the exception of nuclear issues). These are

B.8 Plasma-Wall Interactions: *Understand and control of all processes which couple the plasma and nearby materials.*

B.9 Plasma Facing Components: *Understand the materials and processes that can be used to design replaceable components which can survive the enormous heat, plasma, and neutron fluxes without degrading the performance of the plasma or compromising the fuel cycle.*

B.10 RF Antennas, Launching Structures and Other Internal Components: *Establish the necessary understanding of plasma interactions, neutron loading and materials to allow the design of RF antennas and launchers, control coils, final optics and any other diagnostic equipment which can survive and function within the plasma vessel.*

8.4 References

- ¹ S. M. Wolfe, et al., *Physics of Plasmas* **12**, 056110 (2005)
- ² R. S. Granetz, et al., *Bull Am Phys Soc* **50**, 316 (2005)
- ³ A. E. Hubbard, et al., “H-mode pedestal and threshold studies over an expanded operating space on Alcator C-Mod.”, *Physics of Plasmas* **14**, 056109 (2007)
- ⁴ G. Maddison, “Dimensionless pedestal identity plasmas on Alcator C-Mod and JET”, *Bull. Am. Phys. Soc* **52** (2007).
- ⁵ A. E. Hubbard, *et al.*, “Comparisons of small ELM H-Mode regimes on the Alcator C-Mod and JFT-2M tokamaks”, *Plasma Phys. Control. Fusion* **48** (2006) A121–A129
- ⁶ M. Ferrara, I. H. Hutchinson, S. M. Wolfe, “Inductance, stability and noise in C-Mod vertical control relevant to ITER”, draft report, Sept 5, 2007.
- ⁷ M. Ferrara, I.H. Hutchinson, S.M. Wolfe, J.A. Stillerman, and T.W. Fredian, “Alcasim Axisymmetric Simulation Code for Alcator C-Mod”, *Proceedings of the 45th IEEE Conf. On Decision and Control*, San Diego, CA (Dec. 2006)
- ⁸ Y. Gribov, *et al.*, “Revision of plasma startup in ITER Scenario 2”, SSO ITPA Topical Group Meeting, Garching, (1-12 Dec 2007).
- ⁹ A. Loarte, *J. Nucl. Mater.* **313-316**, 962 (2003).
- ¹⁰ Y. Liang, *et al.*, “Active Control of Type-I Edge-Localized Modes with n=1 Perturbation Fields in the JET Tokamak”, *Phys. Rev. Lett.* **98**, 265004 (2007).
- ¹¹ J. Goetz, *et al.*, “High confinement dissipative divertor operation on Alcator C-Mod”, *Physics of Plasmas* **6**, 1899 (1999).
- ¹² R. S. Granetz, *et al.*, “Gas Jet Disruption Mitigation Studies on Alcator C-Mod and DIII-D”, *proc. 21st Int’l Atomic Energy Agency Fusion Energy Conference*, Chengdu, China 16-21 Oct. 2006, paper IAEA-CN-149/EX/4-3. (<http://www-naweb.iaea.org/napc/physics/FEC/FEC2006/html/node222.htm#44609>)
- ¹³ R. S. Granetz, *et al.*, “Real-time VDE mitigation with gas jets, and mixed gas jets on Alcator C-Mod”, *Bull. Am. Phys. Soc.* **51** (2006).
- ¹⁴ G. Ambrosino, M. Ariola, A. Pironti, A. Portone, M. Walker, “A control scheme to deal with coil current saturation in a tokamak” *IEEE Transactions on Control Systems Technology* **9**, 831 (2001)
- ¹⁵ M. L. Walker, D. A. Humphreys, E. Schuster, “Some Nonlinear Controls for Nonlinear Processes in the DIII-D Tokamak”, *Proceedings of the 42nd IEEE Conference on Decision and Control*, Maui, HI, (Dec 2003).

9 Integrated Scenarios: Advanced Regimes

9.1 Highlights of recent research

The five-year period ending in 2008 has seen the beginning of a significant experimental effort towards developing integrated scenarios for advanced regimes on C-Mod, with an emphasis on relevance to ITER and beyond. This effort has been based on prior, and continuing, integrated modeling of attractive scenarios. By ‘advanced regimes’, we mean regimes with a greater degree of control of plasma profiles, leading to improved confinement and/or increased non-inductive current fraction with respect to the standard H-mode regimes covered in the previous chapter. These range from so-called ‘hybrid’ scenarios, with $q(0)$ near one, to fully non-inductive scenarios with reversed shear and higher bootstrap fraction. Exploration of each of these scenarios is planned on ITER, whose needs provide a focus for our research.

In this early phase of advanced scenarios research, the emphasis has been on building up and exploiting control tools, and on developing suitable target scenarios. Significant progress has been made in multiple areas, most notably in far off-axis current profile control with the new Lower Hybrid Current Drive system, and in reducing density in L and H-mode plasmas. Regimes of improved core confinement have been greatly extended in parameter space, and long pulse operation demonstrated at higher input power. Accompanying and guiding the experimental program has been development and use of integrated scenario models and improvements in ICRF and LHRF modeling. A few highlights from each of these areas are summarized below.

9.1.1 Current Profile Control

Control of the current profile $j(r)$ is crucial for the development of all advanced scenarios. The primary tool for this on C-Mod, complementing those in use on other US facilities, is lower hybrid current drive. Details of the successfully implemented LHCD system and its results are given in Chapter 5 (Wave Plasma Interactions). Particularly encouraging for Advanced Scenarios research is the good agreement between observed LHCD, as evidenced by loop voltage drops, hard x-ray profiles, and most recently Motional Stark Effect measurements of $j(r)$, and the predictions of LH models [1]. Deposition and current drive are strongly off-axis (typically $r/a \sim 0.6-0.8$), as desired and predicted. Control of the deposition radius by varying the launcher phasing, and thus the launched N_{\parallel} spectrum, has been demonstrated, as illustrated in Figure 9.1. While initial experiments were done at moderate powers, up to 1 MW, and for a limited range of plasma parameters, these results give increased confidence in extrapolation to modeled scenarios at higher powers and a wider range of parameters.

In 2007, LHCD was successfully combined with ICRF heating, in both L-mode and H-mode plasmas. This is critical for integrated scenarios, which require hot, high confinement plasmas. In contrast to some results elsewhere [2], in a well conditioned machine there is no major difficulty in coupling both waves simultaneously, with the

exception of the ICRF antenna immediately adjacent to the LH launcher. Further optimization using localized gas injection is being carried out in 2008. The

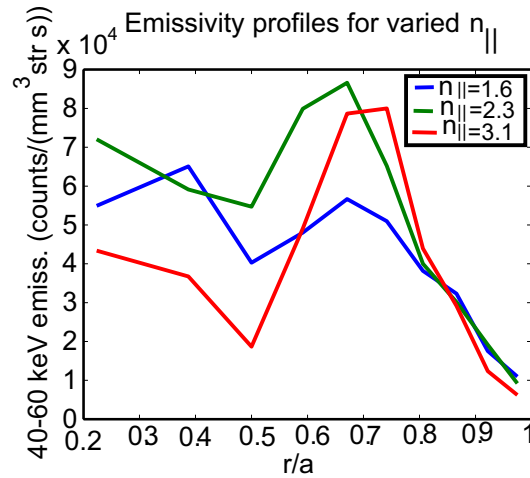


Figure 9.1: Variation of Hard X-Ray emissivity profiles at 40-60 keV as the peak N_{\parallel} launched from the LH antenna is varied, an indicator of the LH deposition location. As expected, the highest N_{\parallel} (red curve) corresponds to the most off-axis emissivity, peaked at $r/a \sim 0.7$.

addition of ICRH into L-modes increased the electron temperature from 2 to 4 keV, further localizing the deposition of LH waves. As expected, the deposition radius increases, as evidenced by broader profiles of hard x-ray emission. Some of these experiments used so-called ‘improved L-modes’ [3] with $B \times \nabla B$ drift away from the active divertor, to maintain low densities even with significant ICRF heating, while achieving edge thermal barriers and moderately improved energy confinement ($H_{ITER89-P}$ up to 1.6) [4].

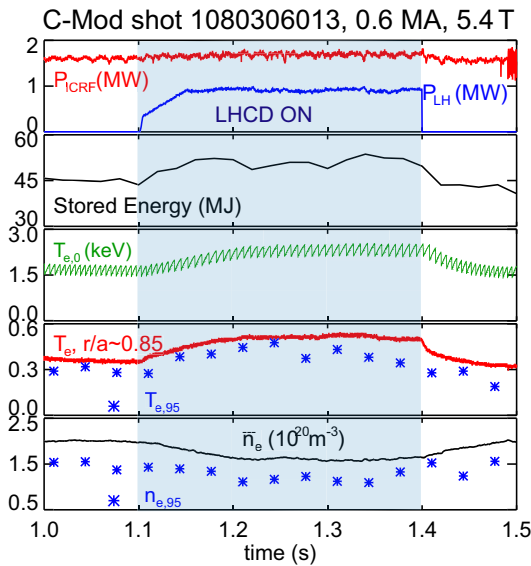


Figure 9.2: Evolution of core and edge parameters for a discharge in which LHCD at $N_{\parallel}=2.3$ was injected into a 600 kA H-mode.

Coupling of LH waves into H-modes, important for steady-state scenarios on ITER as well as on C-Mod, has also been demonstrated. The available power (~ 500 kW) during initial H-mode experiments in 2007 was too low to drive significant current at these higher densities. Very recently, experiments using increased LH power, up to 1 MW, and reduced H-mode densities resulted in clear and positive effects on the edge and core plasma, illustrated in Figure 9.2. Clear signatures when LH was injected included drops in loop voltage of typically 30% and increases of hard x-ray and other non-thermal emission. An unexpected benefit was a clear

and reproducible modification of edge pedestals and particle transport, as evidenced by further reduction in pedestal and core density, and radiated power, and a 50% increase in pedestal temperature. Core temperatures, stored energy and global confinement all modestly increased. This mechanism, which is not yet understood, may offer a new means of edge barrier control. Because of the strong T_e increase, separating LH heating and current drive effects on loop voltage is difficult. Initial modeling indicates that heating dominates, but that some localized off-axis current is driven.

Experiments have begun to exploit LHCD and ICRF, both alone and together, as tools to modify current profile evolution. A recent example is shown in Figure 9.3, in which heating and current drive are applied during slow current ramps. Even a modest amount of LHCD (0.4 MW) leads to a significant delay in the onset of sawteeth by up to 175 ms. This is clearly a current drive rather than heating effect; much higher powers (2.4 MW) of ICRH alone had only a moderate effect, with a 30-50 ms delay. Combining ICRH and LHCD gave an even larger delay of 250-375 ms, with an estimated LH driven current of 100 kA in this case. The weak effect of heating alone, in contrast to other experiments, is expected due to the short τ_{CR} on C-Mod (typically 0.1-1 s, depending on T_e and Z_{eff} , and ~ 0.2 s in these experiments). However, tailoring the early phase of the discharge may be useful to transiently obtain desired $j(r)$ profiles and modify transport. Time dependent simulations with the Tokamak Simulation Code TSC were used in planning this and other experiments, and afterwards to model several discharges in detail. Much more work remains to be done in exploiting our new $j(r)$ control tools for advanced scenarios, as discussed in section 9.2.

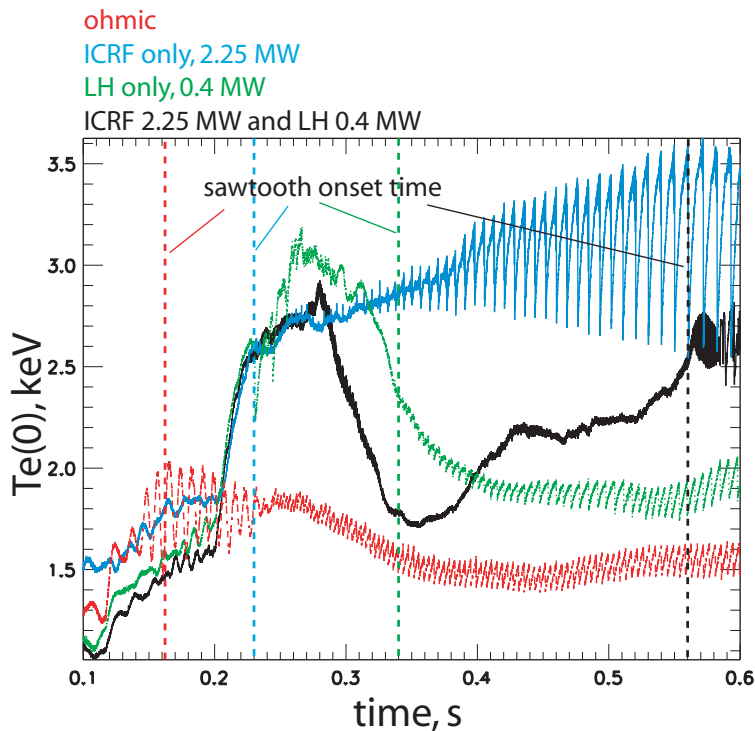


Figure 9.3: Comparison of sawtooth onset times in a series of 600 kA similar discharges with slow I_p ramps, with application of ICRH, LHCD or both. Compared to the ohmic reference (red), ICRH alone gives a modest delay, while the combination of heating and CD (black) gives the largest effect on q_0 . Note ECE signals may include a non-thermal contribution during LH.

Progress was also made in the development and understanding of ICRF Mode Conversion Current Drive (see Chapter 5 (Wave Plasma Interactions)). Clear modification of sawtooth periods, in agreement with expectations, was shown when phase and location of current drive were varied near the $q=1$ surface (Figure 9.4) [5]. However, experiments and recent modeling indicate that MCCD may not drive large current on-axis. Central current drive using fast waves is possible when electron temperatures are high, as is expected, and may be more promising for use in non-inductive scenarios. Experiments are planned during 2008 using ICRF at 50 MHz in combination with minority heating at 80 MHz to raise $T_e(0)$. Bootstrap current drive is also crucial, and depends largely on tailoring of heating and core transport, as discussed in section 9.1.3.

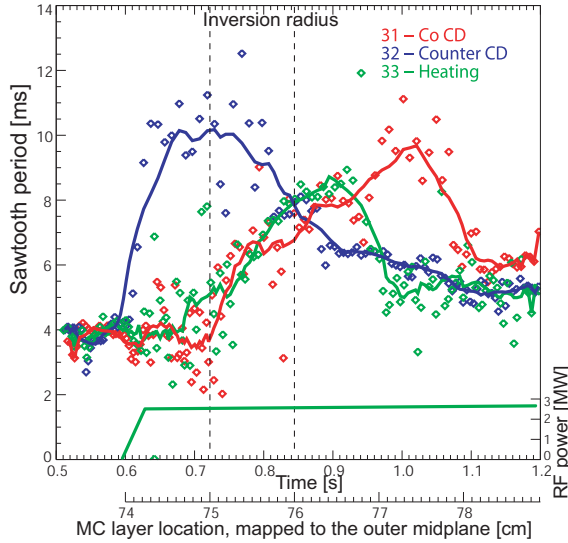


Figure 9.4: Modification of the sawtooth period effected by Mode Conversion Current Drive. The period varies substantially as the MC deposition layer is scanned across the $q=1$ surface. The effect reverses with co vs counter injection, clearly indicating local current drive [5].

9.1.2 Density Control

Electron densities on C-Mod, due to its compact size and high current, tend to be much higher than on most other tokamaks. Typical steady ‘Enhanced D-Alpha’ H-modes with I_p 0.8-1.2 MA have line averaged densities in the range $3-5 \times 10^{20} \text{ m}^{-3}$ and H-mode pedestal densities of $2-4 \times 10^{20} \text{ m}^{-3}$. Such densities are too high for good LH wave accessibility or current drive efficiency – recall that for fixed ‘efficiency’ η_{LH} , driven current is inversely proportional to density, while increasing $N_{||}$ for accessibility decreases η_{LH} . Ongoing studies of pedestal scalings have shown that in the absence of puffing or pumping, n_{ped} is primarily sensitive to plasma current I_p , with a weaker dependence on target n_e [6-8]. A minimum target density is typically needed to produce steady, as opposed to ELM-free, H-modes. By reducing I_p to 600 kA and optimizing L-mode density, we succeeded in developing steady H-modes with significantly lower density, $n_{e,ped} = 1.4 \times 10^{20} \text{ m}^{-3}$. Using only 3.5 MW ICRH, measured central electron temperatures reached 5 keV, as shown in Fig. 9.5 (a,b). High temperatures are important for good off-axis absorption of lower hybrid waves, as well as contributing to high pressures and bootstrap currents. These discharges proved also to have excellent confinement, with $H_{ITER89-P}$ up to 2.1, as well as reduced collisionality. Modeling of these discharges with various simulation codes, including ACCOME, TSC-LSC and CQL3D, shows good LH accessibility and off-axis current drive. Current predicted using CQL3D is shown in Figure 9.5(c).

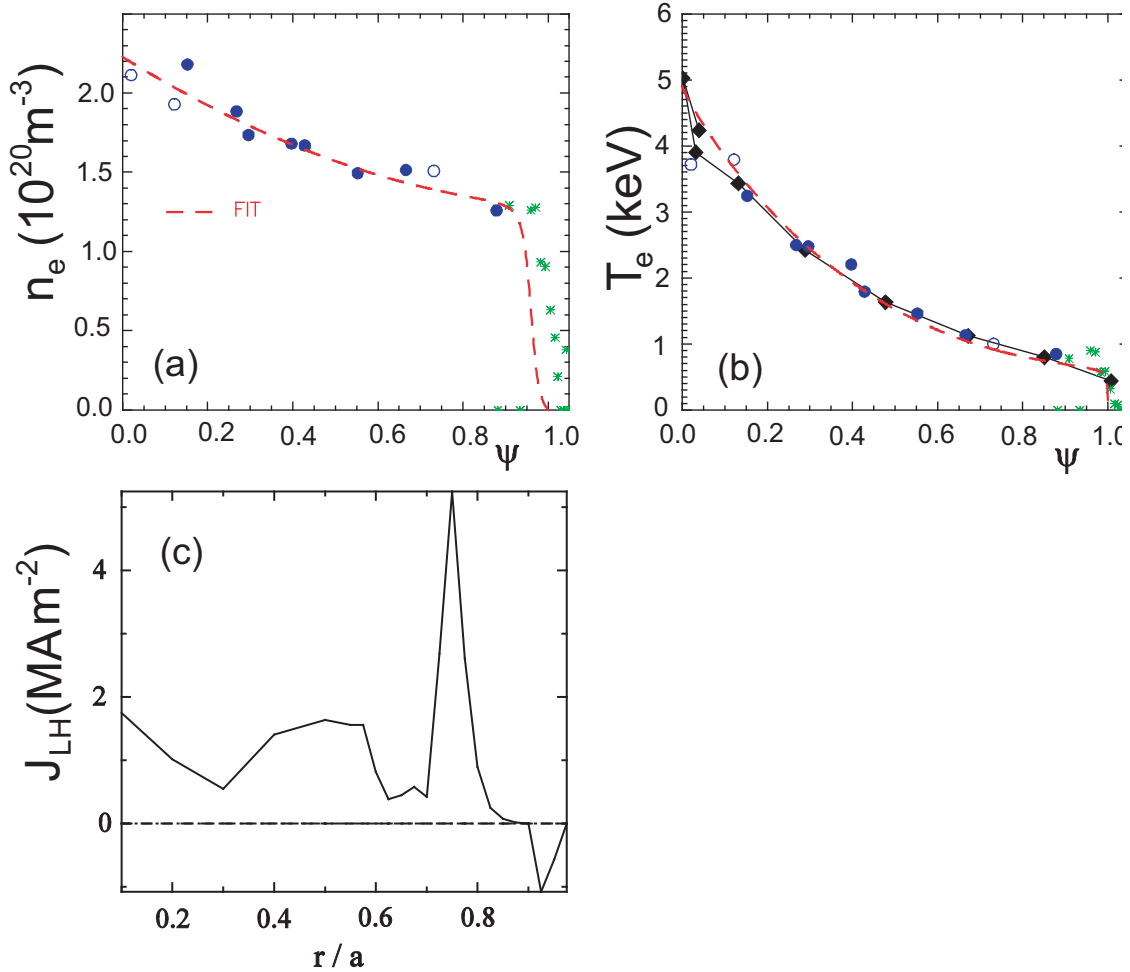


Figure 9.5: Experimental electron density (a) and temperature (b) profiles for a low density H-mode discharge developed as a potential LHCD target, with $I_p=600$ kA, $B_T=5.4$ T and $P_{RF}=3.5$ MW. The driven current which would result from applying 2.0 MW of LHCD, with launched $N_{/0}$ of 2.33, to this discharge was computed using CQL3D, showing good accessibility and peaking at $r/a \sim 0.75$ (c) [9].

The commissioning of a cryopump in the upper vacuum vessel of C-Mod in 2007 provided an important new density control tool. As described in Chapter 11 (Facilities), this novel slot design performed according to specifications, with a pumping speed of nearly 10,000 l/s for a range of shapes, and has been used routinely in a range of experiments. As expected, plasma density control is highly sensitive to magnetic balance, with strongest pumping for upper null or near double-null plasmas. Control is also affected by magnetic field direction, due to the in-out asymmetry of divertor recycling.

Density control is most straightforward in L-mode plasmas, where line averaged densities have been maintained at preprogrammed densities down to $7 \times 10^{19} \text{ m}^{-3}$. Local neutral pressures at the ICRF antennas are reduced, improving ICRF performance, and density excursions due, for example, to outgassing of ICRF or LHCD antennas or to diagnostic gas puffing, are minimized.

The situation for H-mode plasmas is more complicated since, as mentioned above and described in detail in Chapter 7 (Pedestal Physics), pedestal density is strongly influenced by particle transport. Although separatrix densities are decreased, the initial rise of pedestal density at the L-H transition is generally too rapid to be controlled by the cryopump. However, there is a gradual reduction during some sustained H-modes. Pedestal temperatures tend to rise, suggesting a positive influence on energy transport. Maintaining steady H-mode at reduced density and collisionality continues to be a challenge. Some promising cases in which n_{ped} is reduced by the cryopump have been achieved at moderate current, 600 kA, which is of interest for advanced scenarios, with reversed field and current, or with dynamically varied magnetic balance. Exploring and optimizing the operational parameters (field, current, topology) for density control in H-mode, and the newly observed ‘pumpout’ effect of LHCD, will be a priority in 2008.

9.1.3 Extension of Improved Core Confinement Regimes

Our long-term targets for advanced scenarios on C-Mod, and those for DEMO, have high bootstrap current fractions. Given the relatively high field of C-Mod, this is a significant challenge. Increasing core confinement over the standard H-mode regime is extremely helpful in this regard, and may be needed to achieve sufficiently high β_{pol} . Important open questions have been raised by ITPA groups as to whether internal transport barriers can be achieved in ITER and reactor relevant conditions with strongly thermally coupled electrons and ions, and without external rotation drive. C-Mod naturally operates in these conditions.

Experiments on C-Mod prior to 2003 had shown strong peaking of density profiles, and reduction of both particle and energy transport to near neoclassical levels, when ICRF heating was deposited off-axis, at or outside about $r/a=0.5$. This ITB regime differs from those seen elsewhere in that it occurs in plasmas with normal, monotonic shear and modest rotation and Shafranov shift; ExB shear does not appear to be dominant in the formation phase. An attractive feature, made possible by the variable frequency of ICRF heating on C-Mod, is that addition of modest levels of on-axis heating after barrier formation raises the particle transport level, stabilizing core densities and radiation at a desired value. The possibility to actively *control* transport levels is extremely advantageous for scenario optimization. In general, potential concerns of regimes with internal transport barriers (ITBs) have been uncontrolled accumulation of impurities, leading to radiative collapse, or steepening of pressure gradients, leading to MHD instabilities. Optimized transport coefficients, which could be controlled using feedback loops, would alleviate these issues.

Significant progress has been made in the past few years on understanding the mechanism for the changes in transport, exploiting improved diagnostics and using non-linear gyrokinetic modeling. These results are described in Chapter 3 (Transport). There have also been major extensions of the parameters over which transport barriers occur, which are encouraging from the perspective of advanced scenarios. By increasing the

levels of off-axis heating to 3 MW, it was possible to couple up to 1.8 MW inside the barrier, resulting in dramatic increases of, and peaking in, the central temperature as well as density; central pressures of up to 0.4 MPa were achieved (Figure 9.6) [10]

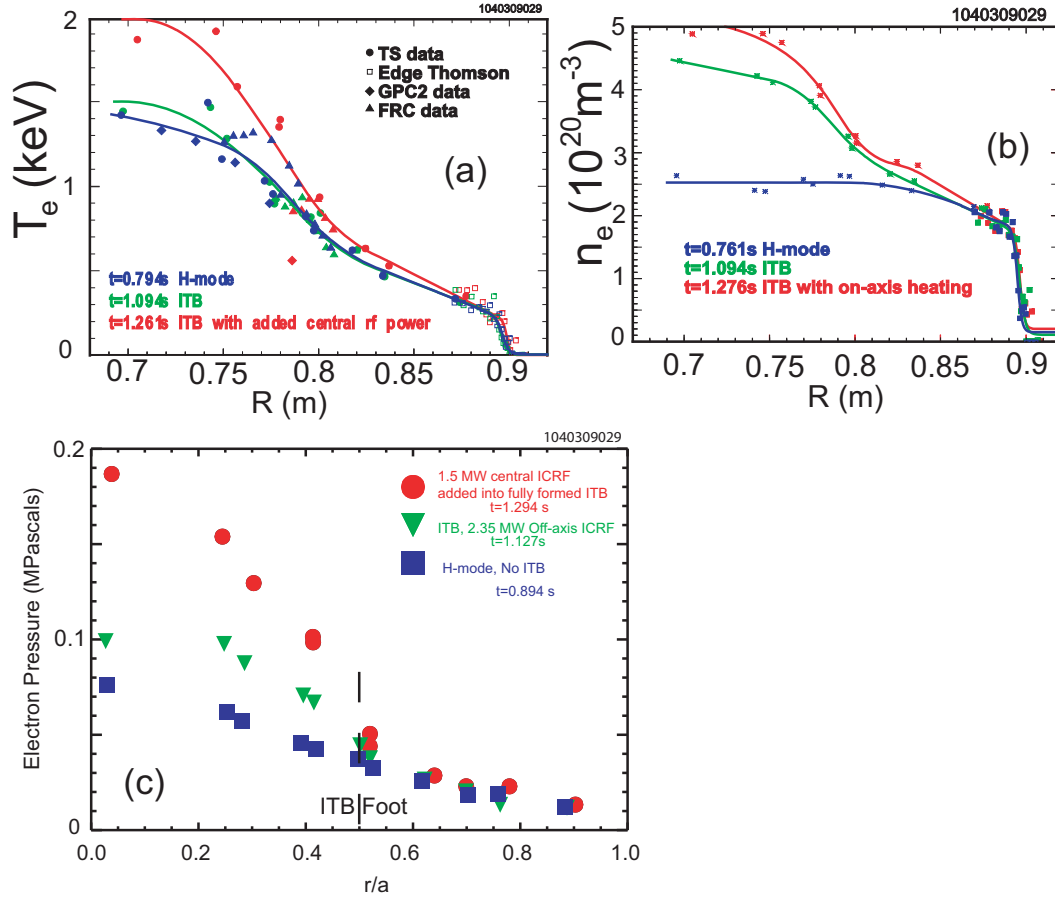


Figure 9.6: Electron temperature (a) density (b) and pressure (c) profiles during a high power double-barrier C-Mod discharge. H-mode profiles are shown in blue. Application of 2.3 MW off-axis ICRH only causes peaking in n_e (green points). Adding 1.5 MW of central ICRF (red) leads also to peaked T_e profiles and extremely high central pressures, as well as controlling the impurity and density increase.

The density in this example, with $B_T=4.5$ T and $I_p=0.76$ MA, is too high for effective LH accessibility and current drive. However, other experiments have extended the range in which ITBs are produced to $B_T=2.8$ -6.4 T, $I_p=0.4$ -1.2 MA and q_{95} as low as 2.7, using different ICRF frequencies and heating scenarios. This has proven that the barrier formation with off-axis heating is robust and clarified the scaling of barrier width, which depends on q_{95} rather than directly on field [10]. Very wide barriers, extending to near the edge transport barrier, are produced at low q_{95} .

As for standard H-modes, lower densities are achievable with ITBs at reduced I_p . Figure 9.7 shows profiles from a recent example with $I_p=0.45$ MA. TSC modeling shows that with addition of on-axis heating, up to 30% bootstrap current should be achievable even without LHCD. Furthermore, the density is low enough for LHCD in the off-axis region

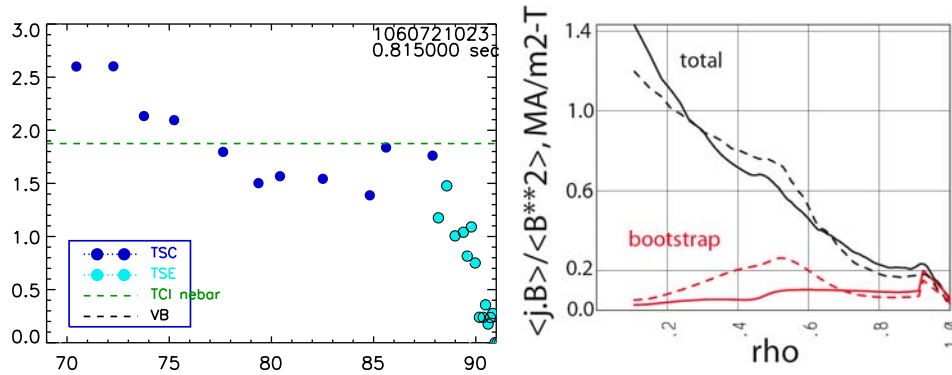


Figure 9.7 (a) Density profile from a 450 kA discharge with internal transport barrier. (b) Current profiles modeled using TSC code, based on the same discharge. Solid lines are computed using actual H-mode profiles, dashed are predictions assuming an ITB with some central heating.

outside the ITB. As discussed further in Section 9.2, future experiments will focus on core transport reduction in discharges with shear modified or reversed by LHCD.

9.1.4 Long Pulse Demonstration with ICRF Heating

Another goal of advanced scenario operation is to extend pulse lengths for several seconds, enabling fully equilibrated electrons and ions. The TF and other magnets are capable of running five second pulses (at 5 T), which will require partially non-inductive current drive, while τ_{CR} is naturally short ($\sim 0.1-1$ s) due to the compact size of C-Mod. As discussed in Chapter 4 (Plasma Boundary), handling the extremely high parallel and perpendicular heat fluxes at full heating and current drive power on C-Mod, which exceed those on ITER and are prototypical of DEMO, is a challenge.

Experiments performed in 2005 succeeded in making significant advances on this front, increasing pulse lengths in L and H-mode RF-heated plasmas to 3.2 s flat top and nearly 4 seconds total pulse length, and input energy to 6.3 MJ, all C-Mod records (Figure 9.8). New fast cameras were used to monitor ‘hot spots’ in the divertor, and the heat load was spread through strike-point sweeping, increasing confidence of use of these techniques for our advanced scenarios with LHCD. No significant difficulties in power handling of either the molybdenum tiles, or of prototype tungsten tiles which are being tested to aid possible designs for ITER, were encountered in these experiments. Subsequent improvements to ICRF power supplies, and the addition of LHCD, will allow higher input powers and longer pulses in future experiments.

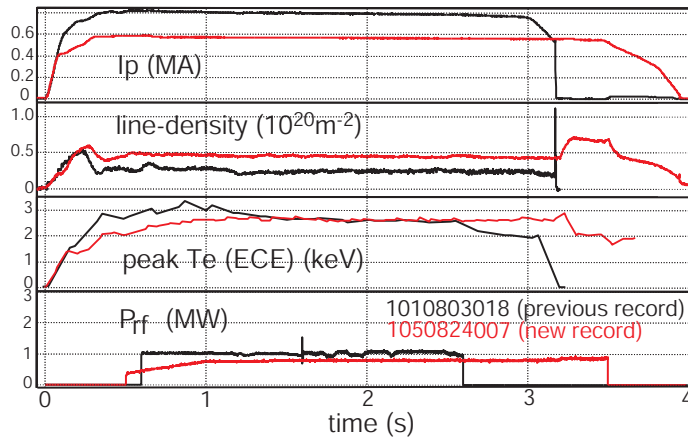


Figure 9.8: Long pulse experiments in 2005 (red) significantly extended the durations of the current flat top (top trace) and RF power (bottom trace) compared to prior limits in 2001 (black)

9.1.5 Integrated Scenario Modeling

Through a C-Mod – PPPL collaboration, significant progress has been made in the area of time dependent modeling of integrated scenarios. We have used the time dependent TSC code to simulate experimental discharges in C-Mod with fast current ramp-up and intense ICRF heating in improved core confinement regimes [see subsection 9.1.3]. These simulations employed thermal diffusivities from a micro-instability-based L-mode model due to Coppi-Tang [11]. The diffusivity is manipulated to give a temperature profile as close as possible to the experimental temperature profile. To model higher confinement scenarios, the overall confinement is increased by making the multiplier in front of χ smaller everywhere, so the pedestal temperature is also increased. A self-consistent ICRF model that computes the power partition between ions and electrons is not used in these simulations. Instead, the power transfer from the minority hydrogen tail to background electrons and ions is estimated based on previous TRANSP simulations using FPPRF/TORIC [9]. We have also used TSC with the lower hybrid (LH) current drive code LSC [12] to simulate the LH current profile control experiments in C-Mod described above. We plan to continue using the LSC code for near term modeling activities in 2008-9 and then move to the more sophisticated CQL3D-GENRAY code [13] in the period from 2010-2013. Further plans are given in section 9.2.7.

9.2 Proposed Research 2009-2013

During the next five years, the Integrated Scenarios research will shift from an emphasis on tool development and modeling of target scenarios to a focused effort on demonstrating, and documenting the performance of, a range of ‘advanced’ regimes. The central questions guiding this research are:

- Over what range of densities and confinement regimes can lower hybrid current drive be used to control $j(r)$?
- Which advanced regimes are feasible in the burning plasma relevant conditions of strongly coupled electrons and ions and no external particle or momentum input?
- What are the confinement and stability properties of these regimes?

Given the strong similarity of the tools and key parameters on C-Mod to those proposed on ITER, our aim is to inform the selection of auxiliary systems, and guide the development of advanced scenarios, for ITER operation.

9.2.1 Current Profile Control

The successful experiments with the first phase of the LHCD system on C-Mod have both confirmed our expectations of current drive efficiency and off-axis deposition, and underscored the need for significant increases in coupled power for use in advanced scenarios. While full non-inductive current drive was achieved with about 1 MW of LH power, this was only possible in L-mode plasmas with $n_e(0) \sim 0.5-1 \times 10^{20} \text{ m}^{-3}$. Driven current in higher density plasmas was much lower, and clear shear reversal has not yet been demonstrated. Accordingly, a very high priority in the C-Mod hardware upgrades is a progressive increase in LHCD power. This will begin in FY09 with the installation of a second LH launcher, redesigned to reduce losses and increase power handling in order to couple a greater fraction of the installed source power. After gaining experience with this, it is planned to replace the first launcher with one of this design in FY11. Additional klystrons will be added to fully utilize two launchers. With 4 MW source power in place by FY09, launched power of 1.5 to 2 MW is expected; the replacement of the first launcher with a second of the new design should provide 2.5 to 3 MW total capability into plasma.

With this higher power, modeling and simple extrapolation predict much increased current drive levels. We will be able to benchmark simulations of majority LH current drive over a wider range of plasma density. An example scenario modeled using TSC, with a profile typical of a moderate density L-Mode on C-Mod, and $\bar{n}_e \sim 10^{20} \text{ m}^{-3}$, similar to ITER H-modes, is shown in Fig 9.9. This assumes $P_{LH}=3 \text{ MW}$ and gives 66% LH driven current. Increased electron temperature from 3.5 MW ICRH ($T_{e0} = 6 \text{ keV}$ in this case) gives strong predicted single-pass LH absorption, peaked at $r/a \sim 0.8$. Other models give somewhat different profiles, and comparison with experiments will help validate and improve each of them. Experiments with a range of magnetic field, in particular reduced values (to $\sim 4 \text{ T}$), will assess the limits for which good accessibility and efficiency can be achieved, given $N_{||}$ variation in the plasma. These will inform plans for later integrated scenarios.

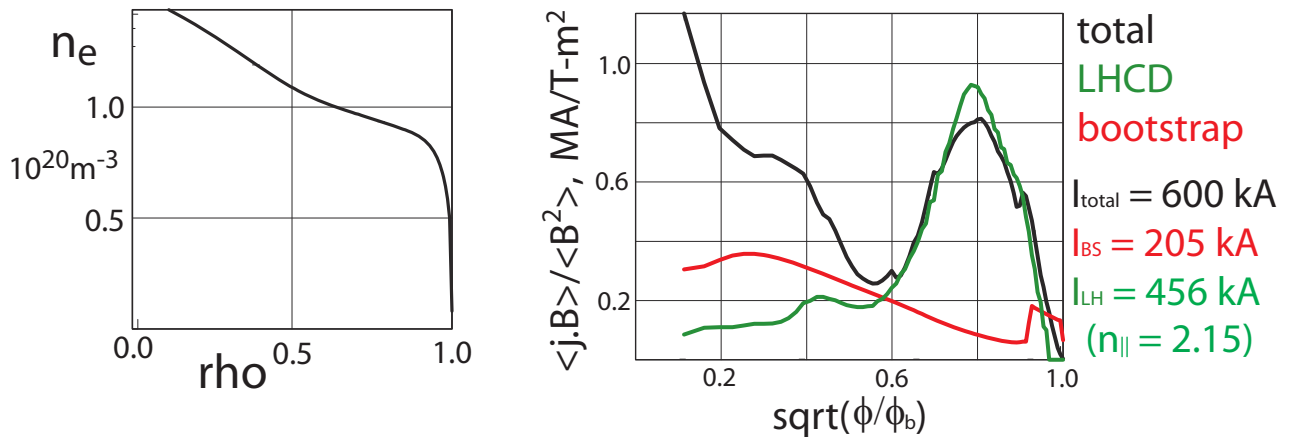


Figure 9.9: TSC simulation of a non-inductive scenario with relatively low density (a), leading to 66% LH current drive but relatively low bootstrap fraction (b).

Experiments to study lower hybrid current drive into H-mode plasmas are crucial both for potential application to ITER, and for advanced scenarios on C-Mod with high confinement and bootstrap current. There is relatively little information available from other experiments in this density and frequency range, and concerns have been raised about propagation through the steep density gradients in an H-mode pedestal. C-Mod provides a stringent test in this regard due to its very narrow barrier widths, typically a few mm. While good coupling (low reflection coefficients) has already been demonstrated, and the initial LHCD experiments reported in Section 9.1.1 are encouraging, the increased powers available in 2009 may be necessary for substantial current profile modification and to give a definitive measurement of LHCD efficiency and localization. Minimizing the H-mode density through a combination of cryopumping and variation of plasma parameters (I_p , L-mode density) and magnetic configuration (topology, shaping), as well as the apparent particle transport effect of the LH itself, will also be important. Comparison with new full wave LH models [14] will be particularly interesting for these H-mode cases.

While LHCD will be our primary current profile control tool, a modest amount of on-axis current drive will also be highly advantageous. In partially inductive scenarios, the strongly peaked T_e resulting from central ICRF tends to peak $j(r)$, making shear reversal challenging. Modeling shows that with full non-inductive current drive, $q(0)$ tends to rise, affecting LH damping and possibly the stability of the equilibrium. The addition of even modest amounts (~ 10 - 20 kW) of FWCD on-axis would limit $q(0)$ to below 2.5. Mode Conversion Current Drive on-axis could also possibly fill this role, and experiments to study further both of these CD techniques are described in Chapter 5 (Wave Plasma Interactions). Simultaneous minority and fast wave absorption should be feasible, but needs to be studied further both in models such as TORIC and in experiments.

For all of this program on current profile control, reliable, sensitive and routine measurements of $j(r)$ are of course essential. Accordingly, additions and upgrades to current profile diagnostics are a top priority for C-Mod facility improvements, described in more detail in Chapter 11. While MSE has measured LHCD, offsets due to stresses on lenses, and other issues, complicate analysis. Changes to in-vessel optics are planned in 2008 and 2009 to alleviate these issues. Other planned improvements include a more optimal view and increases to radial resolution. As a complement to the MSE diagnostic, in particular for central $j(r)$ measurements in higher density regimes for which beam penetration can be poor, a new multi-chord FIR polarimeter is also being developed, and is planned to be implemented in FY09.

9.2.2 Hybrid Scenario

This scenario, so-named because it is in a sense intermediate between the H-Mode and steady state scenarios, has weak core shear and $q_{\min} \sim 1$. This has been shown to provide modest core and global confinement improvement [15,16] and be sensitively dependent on current profile [17] though the mechanisms for the sawtooth avoidance and transport reduction are as yet unclear. The promising results on a number of tokamaks around the world have led ITER to include this scenario in its operational and scientific plans. The proposed ITER scenario has $\beta_N=2.8$ and 50% non-inductive fraction, projecting to $Q=10$ performance at reduced current ($q_{95}=4$) with respect to the baseline H-mode scenario, and allows increased pulse lengths and neutron fluence [18].

However, a number of uncertainties and open issues for extrapolation to the ITER regime have been identified by the ITER team and ITPA groups and can be addressed by C-Mod experiments. Most hybrid experiments to date have been in scenarios with $T_i > T_e$, and dominant NB heating, leading to strong external rotation drive. Indications are that reducing T_i/T_e , or rotation, tend to reduce the confinement enhancement over H-Mode [19, 20]. Establishing and documenting the performance of an attractive ‘hybrid’ scenario on C-Mod, which has no momentum drive and has strongly coupled electrons and ions, would be important. The ‘recipe’ for establishing the flat shear characteristic of this scenario elsewhere has been to heat during the current ramp. MHD activity related to NTMs appears to help maintain the flat $q(r)$ in the flat-top; it is not clear how this mechanism will extrapolate to the different parameters of ITER. As noted above, early heating alone tends not to significantly affect $j(r)$ on C-Mod. Shear modification by LHCD is thus needed on C-Mod. Use of LHCD would help establish whether this external technique can establish and maintain the ‘hybrid’ scenario and, if so, how the performance of the regime compares.

Given that relatively modest modification of the shear profile is needed to access the hybrid scenario, we plan to explore this regime early in the C-Mod five-year program. Initial experiments will begin in 2008, though the higher LHCD powers available in 2009 may prove necessary. Reduced density H-modes with EDA or small ELMs will be suitable LH target plasmas for these studies. We expect to start at $q_{95} \sim 5$, for which scenario modeling shows that shear modification will be significant, and progressively

decrease q_{95} towards the ITER target of 4. ICRF power scans will be used to vary β , found elsewhere to be important for improved confinement. Experiments will be carried out in coordination with ASDEX Upgrade and other tokamaks, as part of ITPA joint experiments. Documentation of pedestal parameters in the hybrid scenario will be an important part of these studies, since there is evidence elsewhere that both core and

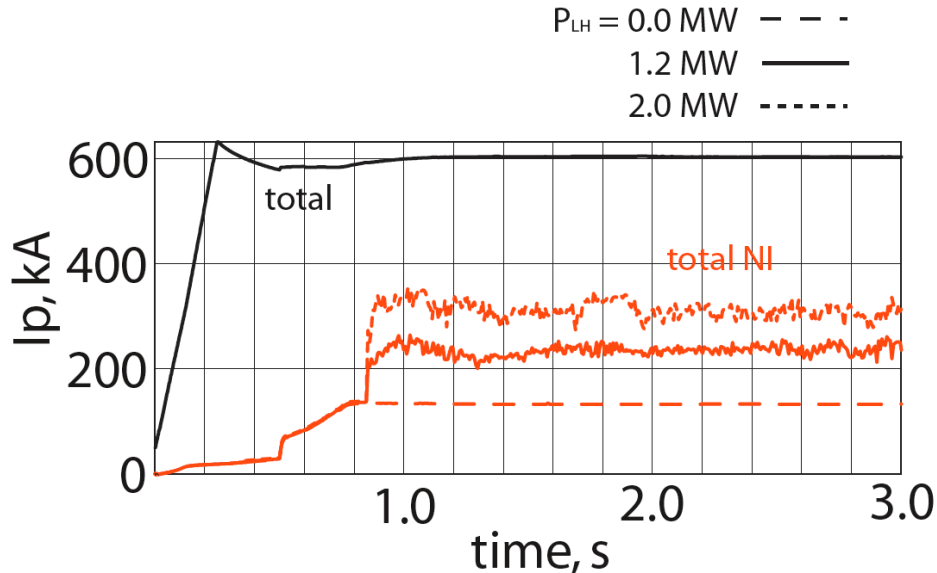


Figure 9.10. TSC modeling of predicted non-inductive current drive based on an experimental 600 kA H-mode, with varying LHCD power levels. In the simulation, ICRH is turned on at 0.5 s and LH power is turned on at 0.85 s. With 2.0 MW LHCD, the non-inductive (NI) current fraction reaches 50%.

edge transport can contribute to improved confinement [21]. Modeling is being used to prepare for these experiments, and will help assess the LHCD, bootstrap and any anomalous contributions to shear modification. For example, Fig 9.10 shows a time-dependent TSC simulation of a discharge based on an actual 600 kA, 5.4 T C-Mod H-mode. The predicted non-inductive current fraction is about 30% with 1.2 MW LHCD, rising to the ITER target of 50% with 2 MW LHCD. Central q rises above one even at the lower power. However, further reduction in shear is desirable. Further experiments under consideration include variation of magnetic field, to increase beta and modify the ICRH profile, and assessment of the effects of sawtooth modification via MCCD on the magnetic shear profile.

9.2.3 Non-inductive Scenarios

Scenarios in which most or all of the current is non-inductively driven are the chief focus and top priority of the five-year advanced scenario program on C-Mod. Such advanced regimes were the primary motivation for the installation of the LHCD systems [22, 23],

are planned for ITER, and are the basis for attractive tokamak reactor designs such as ARIES-RS and ARIES-AT [24, 25]. As for the H-mode and hybrid scenarios, C-Mod parameters will be prototypical of ITER and DEMO in several respects. Non-inductive scenarios will be challenging and will require the full complement of planned ICRF and LH upgrades, as well as the divertor upgrades to handle this power for longer pulses. For these reasons, emphasis on such experiments will increase later in the proposal period.

Target parameters for C-Mod scenarios are guided by plans for ITER and by ARIES-RS studies. The ITER “steady-state” scenario relies on strong off-axis current drive to produce weak or reversed shear profiles with $q_{\min} \sim 2$ and $q_{95} \sim 5$. Projected confinement improvements ($H_H \sim 1.2$) lead to $\beta_N = 3.0$, close to the ideal stability limit, and allow 100% non-inductive current drive and long pulse (~ 3000 s) operation at a reduced fusion gain, $Q = 5$. Successful demonstration of this regime on ITER would be an important step towards an attractive tokamak DEMO. Lower hybrid current drive is under serious consideration for producing this scenario, as it has the highest off-axis CD efficiency. TRANSP-TSC simulations of the main projected scenario (‘Reference Scenario 4’), using LHCD in addition to EC, NBI and ICRF heating and current drive, indicate approximately 50% bootstrap current and 50% external current drive [18, 26].

C-Mod similarly plans, during the period of this proposal, to stay within the no-wall MHD limit of $\beta_N \sim 3.0$. A target ITER demonstration scenario has the following parameters:

- > 90% non-inductive current drive.
- 50% bootstrap fraction.
- 40-50% RF current drive (LHCD plus possible FWCD and/or MCCD).
- $q_{95} \sim 5$
- pulse length > 2-3 τ_{CR} (3-4 secs)

A more ambitious target, relevant to ARIES and other proposed next-step devices, and consistent with more optimistic ITER transport projections, would be 70% bootstrap fraction. As discussed below, reaching this target depends on the degree of confinement improvement which is achievable, and on resolving performance issues with metal walls and very high ICRF power densities. It is recognized that increased self-driven current, while desirable for a reactor in many respects, carries with it increased difficulty of control and risk of off-normal events. Study of scenarios with progressively increased f_{BS} over the course of this research period will enable a comparison of their respective benefits and difficulties.

As noted above, near full non-inductive current drive was quite readily achieved during the first experimental campaign with the LHCD alone, using L-mode targets. Given the high field and density of C-Mod, however, achieving high bootstrap fractions, while simultaneously maintaining high LH driven current, is expected to be a greater challenge – there are many tradeoffs between optimal parameters for LH and bootstrap drive. Typical bootstrap fractions of present high current, high performance H-modes are much lower. Since bootstrap current scales with β_{pol} , raising f_{BS} should be easiest at reduced current. Recent experiments and scenario modeling for C-Mod have used $I_p = 600$ kA.

This has the added advantage that H-mode densities tend to be lower and more easily controlled. A range of q_{95} and β_N will be explored, comparing performance at different toroidal fields.

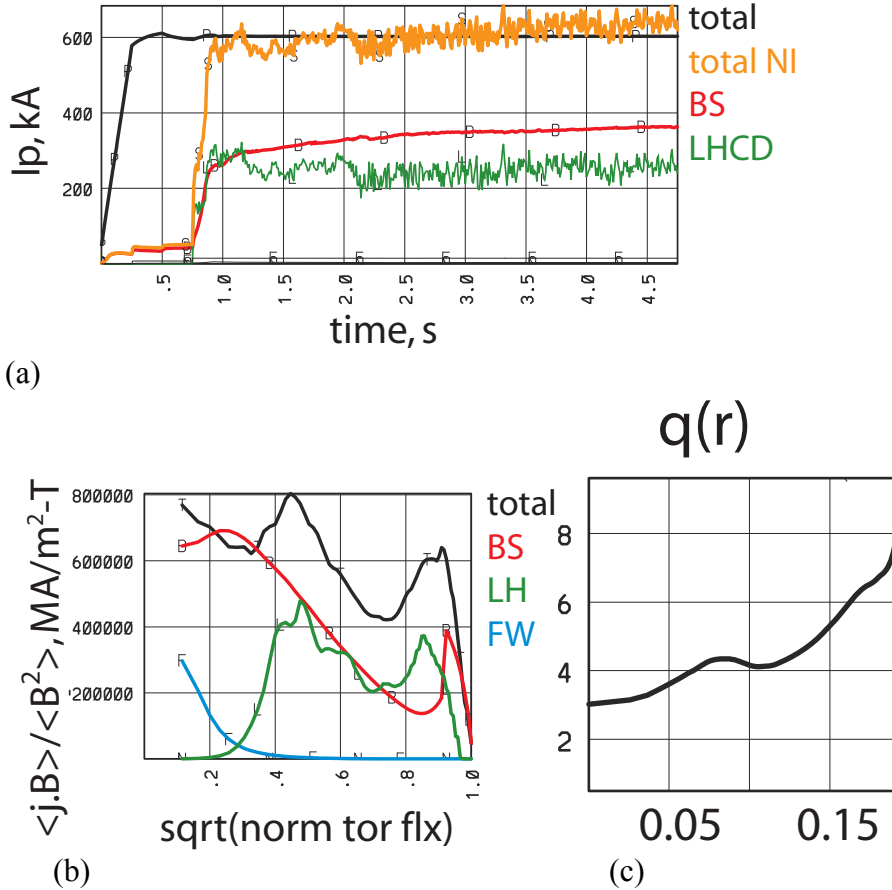


Figure 9.11: Time (a) and radial (b) profiles from TSC simulation of a non-inductive scenario with majority bootstrap fraction, using density profiles similar to those in recent H-mode discharges and applying 2.5 MW of LHCD and 4 MW ICRF.

As an example of the scenarios being considered, Figure 9.11 shows a recently modeled scenario with $I_p=600$ kA, $B_T=5.4$ T and $q_{cyl}=5.5$. A density profile similar to that of H-modes obtained in 2007 with the cryopump has been assumed. Temperature profiles and stored energy are derived assuming input power of 4 MW ICRF and 2.5 MW LHCD, with a confinement enhancement factor of $H_{ITER98y} = 1.44$. It should be noted that C-Mod generally finds a density scaling of τ_E rather weaker than the ITER98y scaling, so that $H_{ITER98y} > 1.2$ is fairly typical for lower density H-modes such as these, even without shear modification. LH waves are launched at $N_{//0} = 2.35$ and $\Delta N_{//} = 0.2$. The simulation predicts full non-inductive current drive, with time evolution as shown in Fig 9.11(a). 60% of the current is bootstrap-driven with β_{pol} approaching 2, and most of the remainder driven by LHCD. A small amount (15 kA) of on axis FWCD is included in

the simulation to limit $q(0)$ and help the equilibrium converge. This scenario is thus quite attractive though not yet fully optimized. In particular the j_{LH} profile in this case, shown in Figure 9.11 (b), is broader than in some other modeled and experimental scenarios, leading to $q(r)$ (c) which is substantially broadened but only locally reversed. Variation of plasma and LH parameters, including exploitation of the capability to launch different $N_{//}$ from the two LH launchers, and comparisons with more complete LH models such as that in CQL3D, are being used to optimize the far off-axis current drive.

The advanced scenarios research program will of course not focus on producing a single demonstration discharge but will explore a range of scenarios, allowing us to assess their properties and relative attractions. Lower density, higher temperature target plasmas typical of the ‘improved L-mode’, with intermediate confinement $H_{ITER98y} \sim 0.8$, should allow higher LH current drive fractions up to 75%. Alternatively, comparable LH current could be driven for lower coupled power, useful in the campaigns before the full LH complement is available. However, the bootstrap fraction would be reduced to $\sim 25\%$ due to the lower confinement.

These 5.4 T scenarios have relatively high q and thus low $\beta_N \sim 1.6$, avoiding MHD limits. We will also assess, in models and experiments, scenarios with lower B_T (4 or 4.5 T), and thus lower q_{cyl} (4.1-4.6). Lower ICRF frequency will be used to maintain near-central heating. Half of our current power is currently tunable from 50-80 MHz, with the remainder fixed at 80 MHz. The planned upgrade of all transmitters (in FY12/13, with incremental funds) to enable tuning will be advantageous for this scenario. Due to the weak scaling of confinement with field, stored energy and bootstrap current will to first order be unchanged. However, β_{tor} and β_N will be correspondingly higher. This would enable assessment of MHD instability limits, for example their dependence on shaping and kinetic profiles, as was done numerically in early modeling studies [23].

It is recognized, however, that there are tradeoffs with LH current drive, in that wave accessibility is worse at lower B. Higher launched $N_{//}$ will be needed, giving lower current drive efficiency. The feasibility and priority of reduced B scenarios will be reassessed following the LHCD experiments over a range of B_T and n_e planned in FY08-09, as well as further integrated simulations. If successful in increasing β to the no-wall limit, which is predicted to occur at $\beta_N \sim 3$, we will, in collaboration with other institutions, begin assessing and designing active or passive systems to stabilize modes and allow further increases. However, fabrication and installation of such systems would, under expected budgets, have to be deferred to a later research period.

9.2.4 Control of Core Transport

In planning the above scenarios, we have conservatively assumed only a modest enhancement over present H-mode confinement, and profile shapes similar to those in current H-modes. Reductions in core transport would of course be highly beneficial in increasing bootstrap current as well as plasma pressure. We will continue to explore and expand regimes with internal transport barriers. Once we become able to substantially modify shear profiles in H-mode plasmas, the focus of these experiments, in close

coordination with the Transport topical group, will shift to investigating the effect of $j(r)$ on barrier formation and confinement. Based on many results elsewhere, eg. [27], it is expected that particle and energy barriers will form more readily in regions with flat or reversed shear, even with central rather than off-axis heating. Strong core n_e and T_e gradients would increase local bootstrap current, further broadening $j(r)$ and tending to reduce central current and shear. If successful, such double-barrier scenarios have the potential to increase bootstrap fractions in non-inductive discharges to 70% or possibly higher. This, given our rather similar conditions of field and density, would be of great interest to DEMO studies.

A new and exciting area of research, made possible by the localized deposition and variable frequency of our ICRF heating, would be to explore the effects of heating profile on barriers formed via shear reversal. In particular, we will assess whether it is possible, as in present barriers formed by off-axis heating, to *control* the degree of particle and energy transport by adjusting the heating profile. If this can be done reliably, controlling impurity accumulation and keeping pressure gradients below MHD limits, it would make core barrier regimes extremely attractive.

9.2.5 Core-edge Integration in Advanced Scenarios

An important aspect of the “integration” of scenarios in advanced regimes is understanding and optimizing the interactions of edge/SOL, pedestal and core plasmas. C-Mod, with its record heat fluxes and strong research programs in Boundary and Pedestal physics, is very well placed to address these challenging issues. Core-edge integration is thus a top priority.

There are several aspects to this interaction, which will be able to be studied at different periods in this proposal. As mentioned in Section 9.1.2, transport in the pedestal strongly influences the density profiles in H-mode plasmas. While external control (puffing, pumping) can influence profiles under some conditions, edge physics is already a key consideration in planning integrated experimental scenarios. C-Mod has an extensive dataset of pedestal parameters in inductive H-mode regimes. Once advanced regimes are established, an important new area of research, to be carried out in conjunction with ITPA joint experiments, will be to assess the similarities and differences of pedestals in these regimes. Close coordination with the Pedestal topical group will continue. Other experiments [28] suggest that increasing β_{pol} leads to higher pedestals, though given the strong edge-core correlations, causality is difficult to establish.

A more challenging task is to study and optimize the effects of high power non-inductive plasmas on the SOL, divertor and other plasma facing components. As discussed in Chapter 4 (Plasma Boundary), because plasma densities need to be lower for advanced scenarios in order to have efficient LHCD, power handling is even more difficult than in baseline high performance H-modes. Depending on assumptions of in-out power asymmetries, average heat loads on the divertor plates, P_{exh} / A_{div} , a useful figure-of-merit (or difficulty) for power handling, are 7-10 MW/m². These exceed those expected on ITER and are in the range expected on ARIES-AT. This is near the technological

limit for steady state power handling of actively cooled PFCs. For expected SOL densities, peak upstream parallel heat flux, for low radiation fractions, could reach $q_{//,sep} \sim 1000 \text{ MW/m}^2$. Because the C-Mod divertor is inertially cooled, these high fluxes should be tolerable for short pulses, but local increased Mo temperature may, in some cases, prove to limit the duration for which non-inductive scenarios can be sustained. Recall that, for plasmas with a large non-inductive fraction, the magnets, heating and other C-Mod engineering systems are capable of five-second pulses; a flat top target of four seconds would allow sustainment and equilibration of advanced regimes for multiple current relaxation times. This concern has motivated the proposed redesign of the outer divertor, including use of all tungsten in the highest heat-flux regions, and addition of diagnostics to document thermal excursions and protect against possible damage. Also crucial for high pressure and bootstrap fraction discharges, which require both high ICRF power and excellent confinement, is an understanding and amelioration of impurities produced by RF sheaths, through antenna optimization and/or improved wall conditioning techniques (see discussion in Chapters 4 and 5).

A new area of study, which is both critical for possible extrapolation of advanced regimes to DEMO [24, 25], and perhaps necessary to achieve the longest pulse lengths on C-Mod, is that of integrating with radiative divertors. For both hybrid and non-inductive regimes, controlled puffing of gasses which radiate primarily in the plasma edge will be used to increase the radiation fraction and thus decrease the heat flux conducted to the divertor. This has previously been done with success in H-mode plasmas, though with some reduction in global confinement depending on the gas used [29, 30]. It will certainly be more challenging in these lower density, higher power, regimes. The key issue is what effect edge radiation will have on the improved confinement of advanced regimes, and to what extent high bootstrap fraction plasmas can be maintained simultaneously with high edge/SOL radiation fractions. Optimizing plasma density to allow both sufficiently high SOL collisionality and good LHCD efficiency is another crucial challenge – a solution is not assured *a priori*. C-Mod results in this area will be useful in planning ITER scenarios and could particularly influence machine designs for next step devices.

9.2.6 Real Time Control

Real time plasma control in support of Advanced Integrated Scenario research at C-Mod will entail development of improved plasma control capabilities and require enhancements to digital plasma control system (DPCS) capabilities. The key issues in plasma control for advanced scenarios involve profile control, including control of temperature and density as well as current density or $q(\psi)$ profiles. Furthermore, as the advanced scenarios program approaches the goal of fully non-inductive current sustainment, with high bootstrap fraction, control of the plasma shape while maintaining the loop voltage at zero (no inductive drive) will be required. Finally, since some scenarios target plasmas with β_N approaching the no-wall limit, methods for real-time estimation of the stability boundary, and operational techniques for disruption avoidance, will become important.

In the near-term, plasma control efforts associated with the AT program are concentrated on developing suitable target plasmas such as slow current ramp scenarios with early diversion, for application of ICRF heating and lower hybrid current drive to control the $q(\psi)$ profile. For these initial experiments, the application of these actuators to modify the conductivity profile and source non-inductive current is open-loop. The results of these experiments will also provide data which can be used to develop controller algorithms for eventual feedback control of optimized current profiles. Development of control algorithms for maintaining zero loop voltage is also being pursued, in support of non-inductive current sustainment experiments.

Beginning in 2009, we plan to incorporate additional sensor signals appropriate to real-time determination of plasma kinetic and magnetic field profiles as inputs to the DPCS. We will also begin developing observer algorithms for profile quantities of interest, both from the standpoint of feedback control and for stability estimation. Real-time equilibrium reconstruction will also be implemented in DPCS. These developments will require extension from the present single-cpu system to a multiple-cpu architecture, with control loops operating on multiple time scales.

Additional actuators will also need to be brought under real-time control in order to achieve closed loop operation of AT discharges. Interfacing of the ICRF transmitters to the DPCS system, enabling feedback control of the primary heating power to maintain the desired operating point, is proposed to be implemented first. One planned application is to use some of our ICRH power to simulate the core heating which would be created by alpha particles in a burning plasma and could make control of non-inductive plasma regimes much more challenging. In the longer term, an interface to the lower hybrid system, allowing feedback of both power and phase in order to control the driven current profile, will be implemented.

To enable steady-state application of the radiative divertor edge regimes discussed in the previous subsection, real-time control of gas input to maintain a desired level of radiation will be needed. Integration with advanced scenarios will build on the development planned for H-mode scenarios, including implementation of appropriate radiation diagnostics.

In addition to incorporation of suitable sensors, observer algorithms, and actuators, development of robust model-based control algorithms will be required for stable realization of the AT scenarios. The control of current profiles will be particularly challenging for fully non-inductive “steady-state” discharges, especially as the fraction of bootstrap current is increased. The intimate interaction of the kinetic and magnetic profiles in these discharges, close to MHD stability limits, may require real-time estimation of proximity to the stability boundaries. Approaches to this problem could include evaluation based on a library of stability code outputs, compared to real-time equilibrium reconstructions; or on the use of active MHD spectroscopic evaluation of stability by determination of the damping rate of stable modes, as demonstrated (in open loop) for the resistive wall mode [31].

9.2.7 Integrated Scenario Modeling

During the period from 2009-2013 we plan to carry out progressively more realistic simulations of improved core confinement discharges, LH current profile control experiments, and advanced tokamak operating modes using TSC. In the near term we shall perform simulations of discharges with current ramp up and ICRF heating only using a combined TSC – TRANSP approach, which has been successfully applied to time dependent ITER simulations. Here the TSC code is used to advance the discharge for a short time, the TRANSP code is then used to compute self-consistent ICRF heating source terms using FPPRF/TORIC, and finally the TSC equilibrium is advanced in time using these new heating source terms. The same calculation can be done including a LH current drive source as computed by LSC, which can be called from either TSC or TRANSP. These types of calculations will be invaluable in terms of identifying the combinations of ICRF heating power, LH current drive power, and current ramp rate that maximize the bootstrap current fraction and shear reversal radius.

We also anticipate that the gyro-Landau fluid transport module TGLF will be available in 2009 for use in TSC, making it possible to perform predictive simulations of C-Mod discharges. As discussed in Chapter 10 in the Theory and Simulation Highlights, we have shown through a detailed benchmarking exercise [32] that predictions of LH current obtained from an adjoint evaluation of the current drive efficiency in combination with a 1D ($v_{||}$) power deposition calculation systematically underestimate the driven LH current by about 20-30%, relative to 2D (v_{\perp} , $v_{||}$) Fokker Planck – ray tracing treatments such as CQL3D - GENRAY. In order to correct this deficiency we plan to take advantage of a new simulation architecture (the Integrated Plasma Simulator or “IPS”) being developed through the SWIM Fusion Simulation Project, expected to be available for this application in ~ 2010. Through this architecture, the AORSA and TORIC ICRF solvers, the CQL3D-GENRAY code, and the TSC code can all communicate through an interface called the Plasma State. Thus, more realistic time dependent simulations will become possible using TSC, since it will communicate with the most advanced simulation codes for ICRF heating and LH current drive.

This state-of-the-art suite of integrated simulation codes will be applied to the full range of advanced experimental scenarios outlined above, ranging from hybrid scenarios with flat shear, to high bootstrap fraction H-mode and ITB non-inductive scenarios for which the ability to predict core transport in regions with modified shear will be particularly useful. As is currently the case, modeling will be used both in planning experiments and as an aid to their interpretation and improvement. Model-experiment comparisons will be used to benchmark codes being used to simulate ITER scenarios, thus serving either to increase confidence in such simulations or to improve them where needed.

9.2.8 Summary of Research Objectives and Proposed Schedule

The research topics outlined above will of course be investigated largely in parallel, and are interrelated. However, we expect the emphases to evolve as new tools, both experimental and modeling, become available and regimes are explored. As an approximate guide to the proposed program, Figure 9.12 summarizes the principle sub-topics and anticipated timeline. It should be noted that the timing of the various scenarios reflects primarily the schedule of needed upgrades, in particular of LHCD, rather than their relative priority. While most of the needed upgrades are included in the guidance budget, fully exploiting them and making optimal progress on all of the proposed topics would require some increased experimental time associated with the incremental budget request.

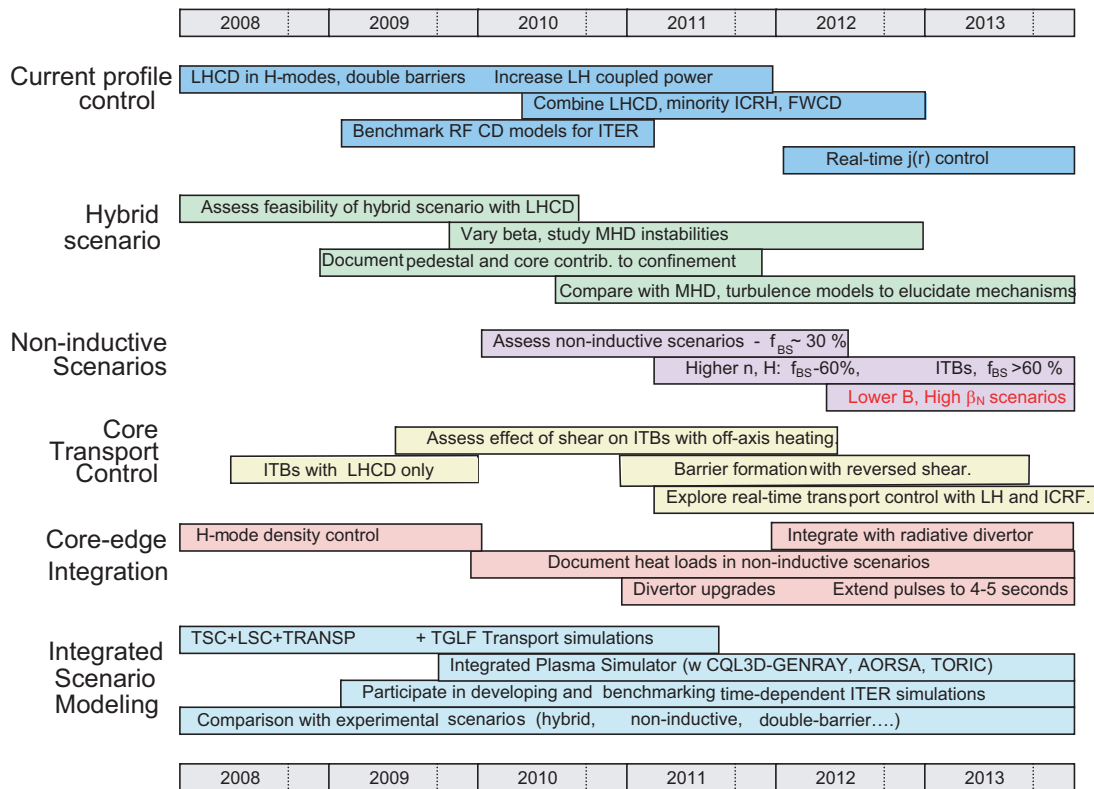


Figure 9.12. Proposed schedule for Advanced Scenarios research program. Items shown in red italics are contingent upon facilities upgrades which require incremental budget increases, and would have to be deferred under the baseline budgets. Fully exploring all of the subtopics would also require some increase in experimental time over guidance budgets.

A set of major experimental research goals and accompanying intermediate objectives which we aim to accomplish progressively during the proposal period is outlined in Table 9.1. Some of the major facility and simulation tools needed for each goal are also listed; these considerations have informed the above schedule. An accompanying program of integrated scenario modeling will be used to guide and interpret all of the experiments

specified here. These related goals and objectives for may be found in Chapter 10 (Theory and Simulation).

Table 9.1. Research goals and intermediate objectives for the Advanced Scenarios research program. Objectives shown in italics are again contingent upon facilities upgrades which require incremental budget increases, and may not be achievable under guidance budgets.

Research Goal	Intermediate Objectives	Enabling tools
Demonstrate current profile control by LHCD and FWCD in a range of confinement scenarios	Assess LH accessibility and efficiency in H-modes.	Cryopump, Phase I LHCD, MSE upgrades (2008-10), Polarimetry (2009)
	Combine LHCD with high power ICRF and FWCD, and compare with predictions of CQL3D and TORIC.	
	Develop diagnostic and control capability to test real-time control of current profiles.	Real-time $j(r)$, DCPS upgrades for LH control (~2011)
Assess feasibility and properties of “hybrid scenario” established and maintained by external LHCD with coupled electrons and ions, and no momentum input, for extrapolation to ITER.	Demonstrate core shear reduction in H-Mode plasmas using LHCD.	LHCD second antenna (2009), MSE.
	Assess changes in local and global confinement, including relative roles of pedestal and core.	
	Contribute to intermachine comparisons and model benchmarking, and to predictions and scenario development for ITER hybrid scenario.	TSC/TRANSP (2009), Plasma State (2010), TORIC LH (2010)
	Study MHD stability and β scaling in “hybrid” scenarios.	<i>Upgraded FMIT 50-80 MHz for highest β (incremental)</i>
Demonstrate and assess properties of non-inductive scenarios with varying contributions of external and bootstrap current, for multiple τ_{CR} .	Study non-inductive scenarios with majority LHCD.	LHCD Phase II complete; 2 improved launchers, 16+ klystrons (2011)
	Extend studies to higher confinement regimes with majority bootstrap current.	
	Explore feasibility of double-barrier regimes with improved core confinement and $f_{BS} \sim 70\%$.	
	Contribute to intermachine comparisons and model benchmarking, and to predictions and scenario development for ITER steady state scenario.	TSC/TRANSP (2009), Integrated Plasma Simulator (2010), CQL3D-TORIC LH (2010)
	Extend duration of non-inductive regimes to > 3 secs.	DEMO-relevant divertor (2011)
	<i>Study reduced B_T regimes with increased β_N and assess and optimize ideal MHD limits. If limits are observed, prepare for stabilization methods to increase β_N.</i>	<i>Upgraded FMIT 50-80 MHz (incremental).</i>
Demonstrate and understand control of core transport using RF tools in with coupled electrons and ions, and no momentum input.	Study rotation and barrier formation in L-mode plasmas with LHCD.	HIREX-Sr, CXRS, LHCD phase I
	Study effect of shear modification by LHCD on core barriers formed with off-axis ICRF.	LHCD 2 nd antenna (2009), MSE, polarimetry (2009)
	Assess core transport reduction in centrally heated H-mode plasmas with shear reduction by LHCD.	LHCD Phase II (2010-11)

	Explore techniques for <i>controlling</i> particle and energy transport by varying ICRF and/or LHCD actuators.	
	If successful, demonstrate real-time control of core transport, temperature and/or density using RF actuators.	DCPS upgrades for kinetic inputs (2009)
Document and optimize edge barrier, SOL and divertor properties in long-pulse advanced scenarios.	Evaluate and optimize the use of active pumping for low density edge barriers compatible with LHCD.	Cryopump, shape control.
	Document pedestal and ELM properties in advanced scenarios, and contribute to international studies.	See above for hybrid, steady state scenarios.
	Assess SOL and divertor heat fluxes in high power non-inductive scenarios.	Divertor IR upgrade (2010), calorimeter (2011)
	Implement control techniques and Plasma Facing Component upgrades needed to enable extension of non-inductive regimes for several seconds.	DEMO-relevant divertor (2011), DCPS upgrade to feed back on divertor bolometer (2012)

9.2.9 Contributions to ITPA and ITER Needs

C-Mod experiments are uniquely ITER-relevant in many respects, including:

- an all-metal wall,
- high heat loading,
- equilibrated ions and electrons,
- no external momentum or internal particle sources,
- an opaque divertor and
- high magnetic field.

Furthermore, C-Mod is the only experiment in the world that can test LHCD in these conditions. Our results will thus contribute strongly to a recent ITER Science and Technology Advisory Committee recommendation to prepare a plan for early implementation of LHCD, with the potential to resolve many of the open physics issues.

As noted above, the target parameters of our advanced scenarios, both hybrid and steady state non-inductive, have been chosen to closely match those projected for ITER. Research aimed towards demonstrating these integrated scenarios thus contributes strongly to a range of ITER needs, as identified by the 2007-2008 list of *ITPA High Priority Research Tasks* recently compiled by the ITPA Coordinating Committee. A summary of the most important contributions expected in the time frame of this proposal is given below, by Topical group. The strongest connections of this research are with the Steady State Operations and Transport Physics ITPA groups. We note that in the anticipated reorganization of ITPA, these efforts may shift to a new, broader, “Integrated Operational Scenarios” topical group. There is overlap with some of the issues identified in the Topical Science areas - the key challenge is to *simultaneously* address the many physics and technology issues which will be encountered on ITER. Many of these issues will be addressed partly through participation in ITPA joint experiments. Current ones

are listed in Table 9.3, and we anticipate further experiments will be planned and executed throughout the five year period.

Table 9.2: Principal anticipated contributions of C-Mod research in Advanced Scenarios thrust to high priority ITER research needs identified by ITPA.

<p>Steady State Operation</p>	<ul style="list-style-type: none"> • Joint experiments: Focus on qualifying candidates for ITER scenarios. <i>Hybrid experiments beginning in 2008, steady state later.</i> • Continue the focussed modeling-benchmark activity on ITER Hybrid and steady state scenarios, using standard/common input data. <i>MIT researchers are heavily engaged in this work, and C-Mod data will particularly enable LHCD benchmarking.</i> • Feedback control: Develop database of control tools. Continue development of profile control methods. <i>Particular contributions in current profile control with LHCD.</i> • Pedestal studies: Continue documentation and complete the analysis of pedestal in advanced scenarios. <i>C-Mod will contribute for both hybrid and steady state scenarios.</i> • The breakdown and current rise of ITER, in particular requirements for advanced scenarios. Joint experiments and code simulations. Recommendations for ITER simulations. <i>Experiments and modeling underway in 2008.</i>
<p>Transport Physics</p>	<ul style="list-style-type: none"> • Utilize upgraded machine capabilities to obtain and test understanding of improved core transport regimes with reactor relevant conditions, specifically electron heating, Te-Ti and low momentum input, and provide extrapolation methodology. <i>C-Mod uniquely features all of these conditions, and will study both hybrid and steady state scenarios.</i> • Develop and demonstrate turbulence stabilization mechanisms compatible with reactor conditions, e.g. shear-stabilization, shear flow generation, q-profile. Compare these mechanisms to theory. <i>C-Mod will study core transport reduction in both normal and reversed shear.</i> • Study and characterize rotation sources, transport mechanisms and effects on confinement and barrier formation. <i>Strong emphasis on momentum-free rotation.</i>
<p>Confinement Database and Modelling</p>	<ul style="list-style-type: none"> • Resolve the differences in β scaling in H-mode confinement. <i>Planned C-Mod experiments will vary β, in a unique parameter range which will test scalings.</i> • Develop a reference set of ITER scenarios for standard H-mode, steady-state, and hybrid operation and submit cases from various transport code simulations to the Profile DB. <i>This thrust will contribute steady-state and hybrid datasets, in ITER-relevant conditions to benchmark simulations.</i> • Develop common technologies for integrated modeling, e.g. frameworks, code interfaces, data structures.
<p>Pedestal & Edge Physics</p>	<ol style="list-style-type: none"> 1. Improve predictive capability of pedestal structure 1-3: Establish pedestal profile database for hybrid and advanced regimes <i>C-Mod will extend its pedestal contributions to these regimes.</i> 2. Improve predictive and design capability for small ELM and quiescent Hmode regimes and ELM control techniques. <i>Most C-Mod H-modes are in small ELM and quiescent regimes, which should integrate well with advanced scenarios.</i> 2-6: Assess applicability of low collisionality small ELM regimes. <i>Advanced scenarios will extend C-Mod pedestals to lower v^*, seek to maintain small or no ELM regimes and assess their compatibility with these core regimes.</i>
<p>MHD</p>	<ul style="list-style-type: none"> • Study NTMs in Hybrid Scenarios, the effect of plasma rotation, validate ECCD control models against data (including modulation) and specify diagnostics for

	NTM detection. <i>Hybrid scenarios may access these modes, in momentum-free conditions.</i> <ul style="list-style-type: none"> • For RWMs understand mode damping particularly at low rotation. <i>High β_N steady state scenarios may access these modes, again in momentum-free conditions.</i>
--	---

Table 9.3: Planned contributions of C-Mod research in Advanced Scenarios thrust to current ITPA joint experiments. Additional contributions are expected in future years.

Description	JOINT Experiments	Notes on C-Mod Contributions
Document performance boundaries for steady state target q-profile	SSO-1	<i>Expected later in five-year period.</i>
Qualifying hybrid scenario at ITER-relevant parameters	SSO 2.1/TP-2	<i>Experiments planned starting 2008, using LHCD.</i>
MHD in hybrid scenarios and effects on q-profile	SSO-2.2/CDB-8	<i>Planned 2009-10</i>
ρ^* dependence of confinement and stability in hybrid scenarios	SSO-2.3	<i>Planned 2009-10</i>
Modulation of actuators to qualify real-time profile control methods for hybrid and steady state scenarios	SSO-3	<i>Focus on LHCD</i>
Documentation of the edge pedestal in advanced scenarios	SSO-PEP-1/ PEP-20	<i>First hybrid scenarios, later steady state.</i>
Simulation and validation of ITER startup to achieve advanced scenarios	SSO-5	<i>In progress 2008.</i>
Determine transport dependence on T_i/T_e ratio in hybrid and steady-state scenario plasmas	TP-2	<i>Will contribute key data with $T_i=T_e$, in strongly coupled regime.</i>
Transport dependence of high performance operation on low external momentum input	TP-4	<i>C-Mod scenarios have NO external momentum input.</i>

9.2.10 Relationship to US Fusion Program Priorities

While C-Mod research on integrated advanced scenarios is targeted particularly towards ITER needs, it should be noted that it also makes strong general contributions to fusion science. Many issues at the forefront of fusion research are those involving interaction of multiple topical areas or ‘campaigns’. This is highlighted by the *Recommended areas of US ‘opportunity for enhanced progress’* in the 2005 FESAC report, which identified 12 top priorities for fusion program resources. Of these, the Integrated Scenarios thrusts contribute most directly to

Integrated understanding of plasma self-organization and external control, enabling high-pressure sustained plasmas,
 which in fact summarizes well the overall goal of the C-Mod scenarios research.

Other FESAC priority areas in which the integration research makes strong and unique contributions are:

- *Extend understanding and capability to control and manipulate plasmas with external waves.*

- *Resolve the key plasma-material interactions, which govern material selection and tritium retention for high-power fusion experiments.*

While the latter is often seen as a boundary physics area, in practice needs are driven, and limits challenged, by the demanding parameters of advanced scenarios.

In terms of the principal long-term performance measures for FY 2015 established for the FES program, Integrated Advanced Scenarios research contributes primarily to Goal 2: *Configuration Optimization: Progress toward demonstrating enhanced fundamental understanding of magnetic confinement and improved basis for future burning plasma experiments through research on magnetic confinement configuration optimization*

Success, worldwide, in demonstrating and understanding advanced scenarios and resolving issues for their extrapolation to burning plasma and reactor regimes is fundamental to optimizing the tokamak configuration.

The research also contributes strongly to the first FES goal:

Predictive Capability for Burning Plasma: Progress toward developing a predictive capability for key aspects of burning plasmas using advances in theory and simulation benchmarked against a comprehensive experimental database of stability, transport, wave-particle interaction, and edge effects.

Developing and testing integrated models of all of this physics is a key component of our research, and will provide the most stringent test of our predictive capability.

Looking further ahead at fusion research needs, a 2007 FESAC panel on “Priorities, Gaps and Opportunities: Towards a Long-Range Strategic Plan for Magnetic Fusion Energy” released a report on anticipated research needs in parallel with, and beyond, ITER. Advanced Scenarios research contributes in a number of areas, perhaps most directly to Issue 2: “*Integration of high-performance, steady-state, burning plasmas*”. While C-Mod is of course not a burning plasma experiment, it operates in the high field, high absolute pressure regime that will be required for such a demonstration, and uses many of the same RF tools proposed for DEMO. Research will also contribute strongly to Issue 3: *Validated theory and predictive modeling* and Issue 4: *Control*.

The high heat fluxes of C-Mod in fact exceed those on ITER and approach those of ARIES designs. Our research in the core-edge integration area aims to contribute strongly to the development of next-step US facilities which are being considered in the strategic plan to fill other ‘gaps’, such as a steady state high heat flux device along the lines of the suggested “Initiative 4” to resolve Plasma Facing Component and other edge and materials issues (gaps G-9, G-10).

9.3 References

[1] P. T. Bonoli et al, “*Lower hybrid current drive experiments on Alcator C-Mod: Comparison with Theory and Simulation*”, APS Invited talk 2007, paper submitted for publication in Physics of Plasmas.

- [2] L. Colas, A. Ekedahl, M. Goniche *et al*, Plasma Physics and Controlled Fusion **49**, B35 (2007).
- [3] F. Ryter, W. Suttrop *et al*, Plasma Phys. Control. Fusion **40**, 725-729 (1998).
- [4] A. E. Hubbard, J. W. Hughes, *et al*, Physics of Plasmas **14** (5) 056109 (2007).
- [5] A. Parisot, S.J. Wukitch, P. Bonoli, *et al*, Plasma Phys. Controlled Fusion **49**, 219-235 (2007).
- [6] J.W. Hughes, D.A. Mossessian, A.E. Hubbard, B. LaBombard and E.S. Marmor, Physics of Plasmas **9** (7), 3019 (2002).
- [7] J.W. Hughes, B. LaBombard, D.A. Mossessian, A.E. Hubbard, J. Terry, T. Biewer and the Alcator C-Mod team, Physics of Plasmas **13**, 056103 (2006).
- [8] J. W. Hughes, B. Labombard, J. Terry, A. Hubbard and B Lipschultz, Nuclear Fusion **47**, 1057-1063 (2007).
- [9] P. T. Bonoli, R. Parker, S. J. Wukitch *et al*, Fusion Science and Technology **51**, 401 (2007).
- [10] C. L. Fiore, D.R. Ernst, J. E. Rice *et al*, Fusion Science and Technology **51**, 303 (2007).
- [11] W. M. Tang, Nucl. Fusion **26**, 1605 (1986).
- [12] D. W. Ignat, Nucl. Fusion **34**, 837 (1994).
- [13] R. W. Harvey and M. G. McCoy, “*The CQL3D Fokker Planck Code*”, Proceedings of the IAEA Technical Committee Meeting on Simulation and Modeling of Thermonuclear Plasmas, Montreal, Canada (1992), (USDOC NTIS Document No. DE93002962).
- [14] J. C. Wright, E. J. Valeo, C. K. Phillips, P.T. Bonoli, and M. Brambilla, Communications in Computer Physics, **3** (2008).
- [15] T.C. Luce *et al.*, Nucl. Fusion **45** (2005) S86.
- [16] C. Gormezano, A.C.C. Sips, T.C. Luce *et al*, Nuclear Fusion **47** (6) S285-S337 (2007).
- [17] J. Stober, A.C.C. Sips *et al*, Nuclear Fusion **47** (8) 728-737 (2007).
- [18] C.E. Kessel, G. Giruzzi, A.C.C. Sips *et al*, Nuclear Fusion **47** (2007) 1274-1284.
- [19] A.C.C. Sips *et al*, Nuclear Fusion **47** 1485 (2007).
- [20] M. R. Wade for the DIII-D team, Nuclear Fusion **47** S543 (2007).
- [21] C.F. Maggi *et al*, Nuclear Fusion **47** 535 (2007).
- [22] P.T. Bonoli, M. Porkolab, J.J. Ramos, W. Nevins and C. Kessel, Plasma Phys. Control. Fusion **39** 223-236 (1997).
- [23] P.T. Bonoli, R.R. Parker, M. Porkolab *et al*, Nuclear Fusion **40**(6) 1251 (2000).
- [24] F. Najmabadi and the ARIES team, Fusion Engineering and Design **41** 365-370 (1998).
- [25] F. Najmabadi and the ARIES team, Fusion Engineering and Design **80** 3-23 (2006).
- [26] W.A. Houlberg, C. Gormezano *et al*, Nuclear Fusion **45**(11) 1309 (2005).
- [27] E. J. Synakowski, Plasma Phys. Control. Fusion **40** (5), 581-596 (1998).
- [28] Y. Kamada *et al*, Plasma Phys. Control. Fusion **42** (5A) A247-A253 (2000).
- [29] Goetz 1999] J. Goetz *et al*, Physics of Plasmas **6** 1899 (1999).
- [30] A. E. Hubbard, B. Lipschultz *et al*, *Pedestals and Confinement in Alcator C-Mod H-modes*, Proceedings of 26th EPS Conf. on Control. Fusion and Plasma Physics (Maastricht, 1999) (European Phys. Soc.), Vol. 23J, p. 13-16. (1999).

- [31] H. Reimerdes, *et al.*, “Active MHD Spectroscopy on the Resistive Wall Mode in DIII-D and JET”, 31st EPS Conference on Plasma Phys. London, ECA Vol. **28G**, P-2.184 (2004).
- [32] P. T. Bonoli, R. W. Harvey, C. E. Kessel *et al.*, 21st IAEA Fusion Energy Conference, (Chengdu, China, October 16 21, 2006) Paper IT/P1-2.

10 Theory and Simulation

10.1 Introduction

Alcator C-Mod benefits from an extensive program of theory and modeling support in many areas including core transport physics, MHD phenomena (energetic particles and MHD stability), wave – plasma interactions, integrated scenario modeling, pedestal and edge studies, and plasma boundary. This support has several components: (1) Formal collaborations with Princeton Plasma Physics Laboratory (PPPL), University of Texas at Austin, and with the IPP – Garching, (2) Individual initiatives between C-Mod personnel and theorists within MIT (PSFC Theory Group) and outside MIT, (3) Collaborations with the SciDAC Center for Simulation of Wave – Plasma Interactions (CSWPI), the SciDAC Center for the Study of Plasma Microturbulence, and two Fusion Simulation Projects – the Center for Simulation of Waves in MHD (SWIM) and the Center for Plasma and Edge Studies. Research activities in this area emphasize a common theme that consists of providing for basic advances in theory and simulation capability, validation of physics models in the different areas by comparisons between experimental measurement and synthetic diagnostic codes, and using the validated simulation capability to plan and interpret experiments. Through our participation in the various ITPA Topical Groups (see section 10.4.3) we have also been active in applying this predictive capability to critical issues in the upcoming ITER device.

10.2 Highlights from 2003 – 2007

10.2.1 ITB Formation and Control, Direct Observation of TEM Turbulence

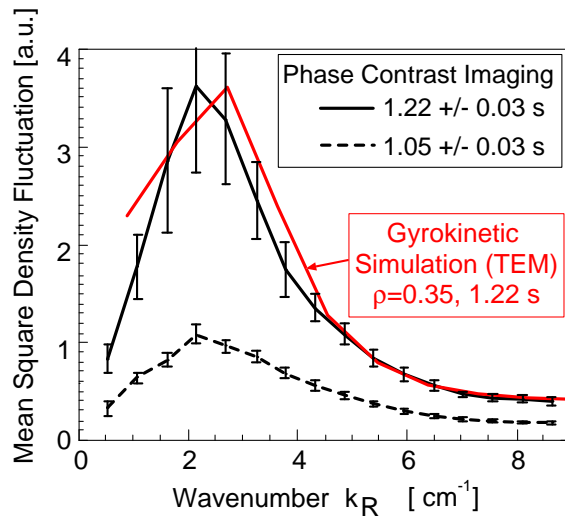


Figure 10-1: Comparison of mean square density fluctuations from PCI in the frequency range 20 - 80 kHz, with a GS2 nonlinear simulation, using the new synthetic PCI diagnostic. Two times shown for PCI, before on-axis heating (1.05 s), and during on-axis heating (1.22 s). During on-axis heating, TEMs dominate the spectrum.

Mechanisms for the formation and control of the Alcator C-Mod internal transport barrier [10.1, 10.2], by off-axis and on-axis ion cyclotron resonance heating (ICRH) respectively, were elucidated in a series of detailed gyrokinetic turbulence simulation studies. Trapped electron mode turbulence was predicted to play a strong role in limiting the density gradient [10.3, 10.4], providing a strong temperature dependence that allows control with on-axis ICRH. This work led to the first realistic nonlinear gyrokinetic simulations of TEM turbulence, and the discovery of a nonlinear upshift in the TEM critical density gradient, due to zonal flows [10.3, 10.5]. We developed a synthetic phase contrast imaging

diagnostic for the GS2 gyrokinetic code [10.5, 10.6] which made possible the first direct comparison of simulated and measured turbulent wavelength spectra [10.5, 10.6] for a tokamak plasma. Application of this diagnostic to ITB cases, in which linear stability analysis shows that TEMs should dominate the spectrum, allowed direct observation of TEM turbulence [10.5, 10.6]. As shown in Fig. 10-1, the nonlinear gyrokinetic simulations closely reproduce the shape of the wavelength spectrum measured by PCI. This direct observation was further confirmed by an upgraded PCI diagnostic. Utilizing a phase plate mask, the enhanced fluctuations during on-axis ICRH were confirmed to propagate in the electron diamagnetic direction. The TEM work was presented in invited talks at the American Physical Society Division of Plasma Physics Annual Meeting 2003, the Sherwood International Fusion Theory Conference 2004, 2004 IAEA Fusion Energy Conference [10.4], 2006 IAEA Fusion Energy Conference [10.5], 2006 EU-US Transport Task Force Workshop [10.7], and 2007 International Sherwood Fusion Theory Conference, as well as numerous contributed talks and posters. A recent PhD thesis focused on triggering mechanisms for the ITB, and featured extensive linear and nonlinear gyrokinetic simulations [10.8, 10.9].

10.2.2 Tool Development for Gyrokinetic Turbulence Simulations of Experiments

We have developed a web interface linking gyrokinetic simulation codes to experimental data. The interface incorporates GS2_PREP [10.10], which was widely used for several years, and provides sophisticated data preparation capabilities. The web site includes run management and a custom written java-based plotter for data visualization. The web site will be further developed and should be made available for use in 2008. To better utilize density and temperature profile data on C-Mod, we developed a sophisticated profile fitting tool, fiTS, with a graphical interface. This tool can automatically fit density and temperature profiles, making use of all available data, for all available times in a discharge. The resulting smooth profiles can then be used in TRANSP, and subsequently in gyrokinetic turbulence and other types of simulations.

10.2.3 Detection of Mode Converted ICRF Waves, Simulation Predictions, and Model Validation

Experimental measurements of mode converted ICRF waves have been made with a Phase Contrast Imaging Diagnostic (PCI) in the Alcator C-Mod tokamak [10.11]. These measurements initially presented puzzling results because the short wavelength mode was detected on the low field side of the mode conversion layer and at a much longer wavelength ($\approx 7 \text{ cm}^{-1}$) than what would be expected for ion Bernstein wave (IBW) excitation [10.11]. However, the PCI measurements were actually carried out in a three ion species plasma with parameters $B_0 = 5.8 \text{ T}$, 33% H, 23% ^3He , 21% D, $T_e \approx T_i \approx 1.5 \text{ keV}$; where it was recognized that the detected mode would not be the expected IBW, but rather a longer wavelength electromagnetic ion cyclotron wave (ICW) [10.12] that is coupled to the fast wave through the presence of a poloidal magnetic field component. The correct dispersion relation for this case [10.11] indicated that indeed a short wavelength mode (the ICW) is excited to the low field side of the usual IBW mode conversion layer. Massively parallel computer simulations of this ICW mode conversion

scenario in C-Mod were performed using the TORIC [10.13, 10.14] and AORSA [10.15, 10.16] field solvers and an example of one such simulation using TORIC is shown in Fig. 10-2. The longer wavelength ICW are apparent in the simulation above and below the tokamak midplane and can be seen propagating back to the low field side of the mode conversion layer at $-2 \leq X(\text{cm}) \leq 0$, where $X=R-R_{\text{axis}}$. Evidence of the shorter wavelength IBW can also be seen at the midplane. In Fig. 10-2, the fast wave is incoming from the low field side at $X \approx 20$ cm. The simulated mode converted wave fields from TORIC have also been used successfully used in a synthetic diagnostic code to predict the detected PCI signal [10.11, 10.17], lending further confidence in the capability of the full-wave solvers to accurately predict the detailed mode converted wave field structure. Referring to Fig. 10-3 it can be seen that the shapes of the measured and predicted PCI signals are in good agreement. The simulated PCI spectra in Fig. 10-3 include all of the toroidal modes coupled by the ICRF antenna in the experiment.

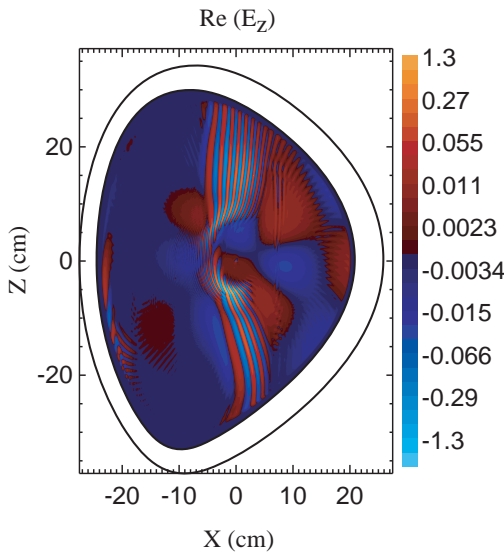


Figure 10-2: TORIC simulation of the ICW mode conversion scenario for Alcator C-Mod using a numerical grid of 240 (N_r - radial) \times 255 (N_m - poloidal) modes [10.14].

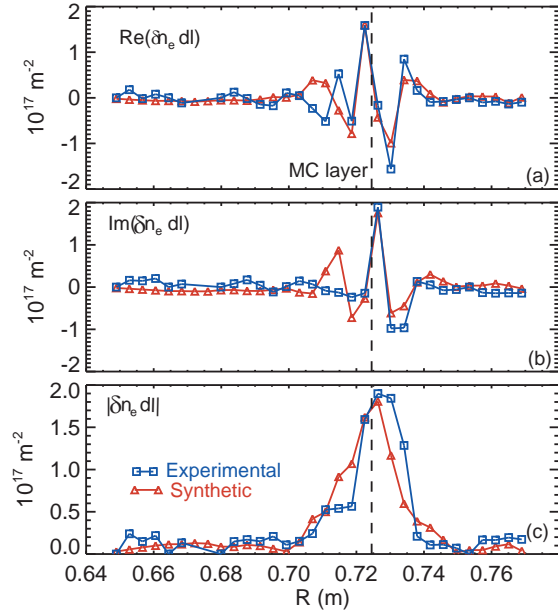


Figure 10-3: Comparison of measured PCI signal with synthetic diagnostic code prediction for ICW mode conversion in Alcator C-Mod [10.17].

These comparisons between predicted and simulated wave fields not only help to validate the physics contained in the simulation models, but allow us to use these numerical tools to provide guidance for mode conversion current drive and flow drive experiments on Alcator C-Mod and to assess the viability of these techniques in ITER. It is important to point out that the massively parallel simulations described in this subsection and the

following two subsections were performed in collaboration with the SciDAC Center for Simulation of Wave – Plasma Interactions.

10.2.4 Quasilinear Evolution of Nonthermal Ion Distributions

Radio-frequency heating in the ICRF regime is the sole means of auxiliary heating on Alcator C-Mod and the primary heating schemes are minority hydrogen (H) or minority (^3He), both in deuterium majority plasmas. Furthermore, second harmonic tritium cyclotron damping in deuterium is planned for bulk plasma heating in the burning plasma Scenario 2 in the ITER device. It is therefore critical to establish a predictive capability for ion cyclotron resonance heating (ICRH) experiments on C-Mod as well in future devices. A self-consistent simulation of ICRF heating requires a description of two different aspects of the wave-plasma interaction: (a) wave propagation and absorption in the plasma and (b) the quasilinear response of the plasma to the wave heating. The long time scale response of the plasma distribution function f_0 can be obtained from a bounce-averaged, zero-orbit width Fokker-Planck equation. This is a nonlinear problem in which the energetic ions generated by the waves can significantly alter the wave propagation and absorption in the plasma. Through the RF SciDAC Center (CSWPI), the AORSA global-wave solver [10.15] has been combined [10.18] with the CQL3D bounce-averaged Fokker-Planck code [10.18] and the SIGMAD module for evaluation of the plasma response for arbitrary particle distributions [10.20] to simulate the quasilinear evolution of nonthermal ion distributions in ICRF heating. A re-formulation of the quasilinear operator [10.18] enables calculation of the velocity space diffusion coefficients directly from the global wave fields in differential form. To obtain self-

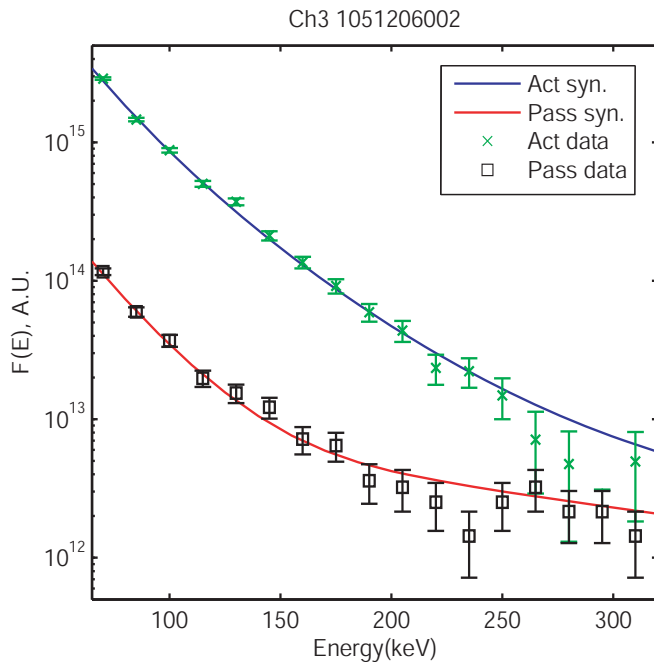


Figure 10-4: Comparison between measured and simulated active and passive charge exchange spectra for the minority heating in Alcator C-Mod [10.21].

consistency, AORSA and CQL3D are iteratively coupled (using the Python scripting language) in a stand-alone system in which both codes communicate and interact automatically on the same computing platform (the Cray XT3/XT4 Jaguar at ORNL).

We have used the 3D $(r, v_{\perp}, v_{\parallel})$ nonthermal minority ion distribution function computed by AORSA-CQL3D in a synthetic diagnostic for passive and active neutral particle analysis [10.21]. This compact neutral particle analyzer (CNPA) diagnostic is used on C-

Mod to measure the energy distribution of the minority hydrogen tail. A comparison of the predicted and measured neutral particle diagnostic signals is shown in Fig. 10-4. The spectra are normalized to the first CNPA data point for clarity and the error bars are based on counting statistics only. The agreement between the measured and simulated spectra is remarkably good [10.21]. It is thought that the failure of the simulated spectra to reproduce the positively sloping region in the passive data may be due to the omission of finite ion drift orbit effects in the AORSA-CQL3D simulation.

10.2.5 Simulations of Lower Hybrid Current Drive in Alcator C-Mod

Lower hybrid current drive (LHCD) experiments have been carried out on the Alcator C-Mod tokamak using a radio-frequency (RF) system at 4.6 GHz. Up to 900 kW of LH power has been coupled and driven LH currents have been inferred from magnetic measurements by extrapolating to zero loop voltage, yielding an efficiency of $n(10^{20} \text{ m}^{-3})I_{\text{LH}}(\text{A})R(\text{m})/P_{\text{LH}}(\text{W}) \approx 0.25$. We have simulated [10.22] the LH current drive in these discharges using the combined ray tracing / 3D $(r, v_{\perp}, v_{\parallel})$ Fokker Planck code GENRAY – CQL3D [10.19] and found similar current drive efficiencies. The simulated profiles of current density from CQL3D, including both ohmic plus LH drive have been found to be in good agreement with the measured current density from a Motional Stark Effect (MSE) diagnostic. Measurements of nonthermal x-ray emission confirm the presence of a significant fast electron population and the 3D $(r, v_{\perp}, v_{\parallel})$ electron distribution function from CQL3D has been used in a synthetic diagnostic code to simulate the measured hard x-ray data. Two examples of these types of simulations and comparisons with experiment are shown in Figs. 10-5(a) and 10-5(b).

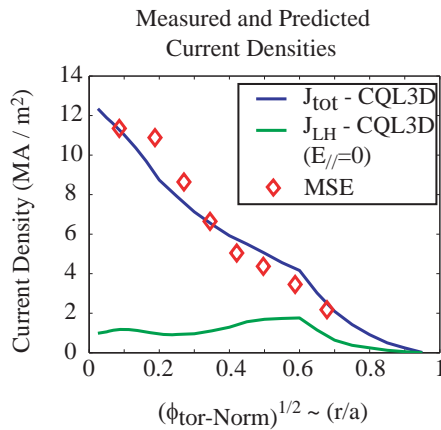


Figure 10-5(a): Comparison of the measured current density profile from the MSE diagnostic (red diamonds) with the simulated current density (ohmic plus LH) from CQL3D (blue line) for discharge 1070828018 at 1.16 sec. Also shown for reference is the LH current density profile from a CQL3D simulation corresponding to a zero DC electric field.

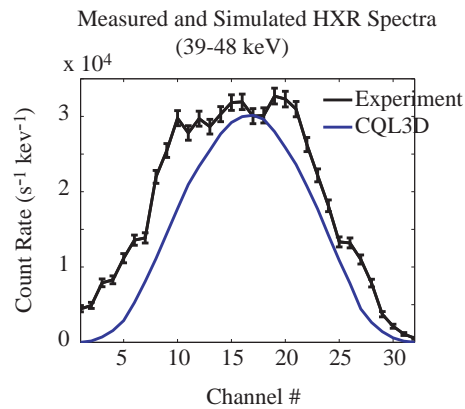


Figure 10-5(b): Comparison of the measured and simulated hard x-ray spectra for discharge 1070828018 at 1.16 sec. The experimentally measured spectrum at 44 keV (the 39-48 keV energy bin) corresponds to the solid black line and the simulated spectrum corresponds to the solid blue line and includes radial diffusion.

The current density and hard x-ray profiles for this C-Mod discharge were simulated using GENRAY - CQL3D and the synthetic diagnostic for hard x-ray emission. The relevant parameters for this simulation were $B_0 = 5.4$ T, $I_p = 0.81$ MA, and $n_e(0) = 1.05 \times 10^{20} \text{ m}^{-3}$, $T_e(0) = 2.61$ keV, $Z_{\text{eff}} = 3.0$, and $P_{\text{LH}} = 685$ kW. The relative waveguide phase used in these experiments was 75° , which corresponds to a characteristic n_{\parallel} for the forward lobe of 1.95. The CQL3D simulation employed a velocity dependent radial diffusion coefficient with $\chi_{\text{fast}}(0) = 0.04 \text{ m}^2/\text{s}$, where $\chi_{\text{fast}}(0)$ was chosen so that the integrated current in the simulation (ohmic plus LH) matched the experiment. The measured and simulated current density profiles (ohmic plus LH) are shown in Fig. 10-5(a). The agreement between measurement and simulation is quite good with both profiles showing a “shoulder” or flattening in the current density at $r/a \approx 0.6$, providing evidence of off-axis LH current generation at that location. The discrepancy in current density at $r/a \approx 0.2$ is thought to be a consequence of the presence of sawteeth in the experiment, an effect that is not included in the model. As a reference point we have also included the LH current density from CQ3D in the zero loop voltage limit [green curve on Fig. 10-5(a)], which corresponds to about 210 kA of integrated LH current. The full simulation [blue curve in Fig. 10-5(a)] was obtained using the measured loop voltage (0.6 V) so that the LH current in the simulation also included the synergy from the DC electric field, which has been estimated to be about 300 kA. Finally, a comparison of the measured and simulated raw hard x-ray spectra is shown in Fig. 10-5(b). The agreement between the predicted and measured profiles is remarkably good in that the peak values of both agree without any renormalization of the simulated data. On the other hand, the simulated spectra are narrower than the measured spectra along chords 1-7 and 25-32 which correspond to sight lines passing through the lower and upper regions of the plasma respectively. These comparisons between simulation and experiment are considered to be crucial in order to establish confidence in our ability to accurately predict the velocity-space and spatial structure of LHRF-generated electron distributions in ITER, where LHCD is under consideration for off-axis current profile control in advanced tokamak operating modes (Scenario 4) as well as for volt-second savings and pulse extension in the H-Mode Scenario 2.

10.2.6 Macroscopic MHD – Alfvén Eigenmodes and Cascades

The stability of Alfvén eigenmodes (AEs) has been studied on C-Mod using a number of diagnostics including active MHD antennas, Phase Contrast Imaging (PCI), magnetic pick-up coils, a compact neutral particle analyzer (CNPA), and a hard x ray camera. The Alfvén eigenmode data on C-Mod have been compared with numerical results from the NOVA-K code [10.23] for mode structure and stability. TRANSP [10.24] combined with TORIC [10.13] is used to calculate the fast ion distribution for input into NOVA-K and initial comparisons of the fast ion distribution have also been made with the AORSA/CQL3D [10.18] codes. A synthetic PCI diagnostic code was also written to compare NOVA calculated eigenmode structures with the line integrated PCI data. This combination of multiple diagnostics together with advanced simulation capability helps advance our understanding of Alfvén eigenmodes. Furthermore, understanding the physics of AEs may be important for fusion burn control and controlling the loss of fast ions in ITER.

The development of Reversed Shear Alfvén Eigenmode (RSAE) theory has expanded to include the effects of Alfvén wave coupling to geodesic-acoustic modes at low frequencies. This had the important effect of raising the minimum frequency, from essentially zero to approximately 150 kHz in Alcator C-Mod. A theoretical model of this effect [10.25] shows that the minimum frequency, in the absence of significant rotation or perturbing fast-ion effects, should scale as $T_e^{1/2}$. This scaling has been confirmed through PCI measurements of RSAEs during the current-ramp phase in C-Mod, and is presented in Fig. 10-6. Numerical investigations with the NOVA code show good agreement with the experiments and show the importance of the temperature gradient terms also reported in reference [10.25].

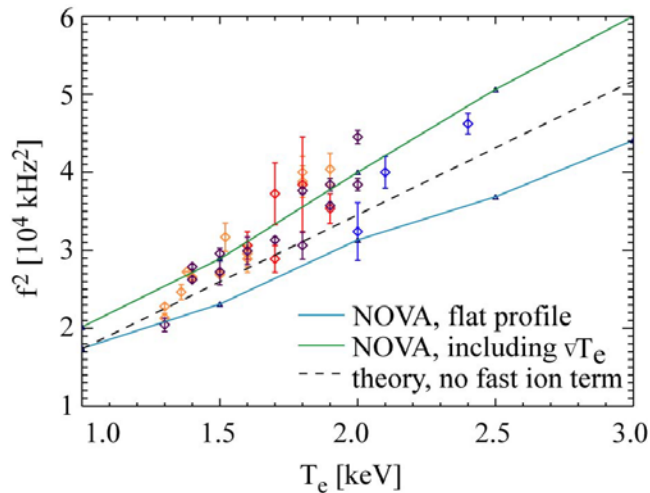


Figure 10-6: Compilation of minimum frequency measurements of RSAEs from PCI data. The trend shows a strong correlation between f_{\min}^2 and T_e . Comparison of NOVA data and a theoretical form also show generally good agreement when realistic temperature gradients are included.

The analytical techniques using PCI have been expanded to include a “synthetic diagnostic” code that has proven useful in making comparisons between measurement of line integrated density perturbations from PCI and eigenmodes calculated by NOVA [10.26]. These techniques have been applied to ascertain the radial position of q_{\min} (the minimum of the q -profile in a reversed shear plasma). The ability to localize q_{\min} is an additional constraint useful in understanding the plasma equilibrium and represents a further use of RSAEs for “MHD spectroscopy”.

10.2.7 Macroscopic MHD - Gas – Jet Mitigation Studies on Alcator C-Mod

We have used the massively parallel NIMROD code to simulate gas-jet mitigation experiments on Alcator C-Mod [10.27]. The NIMROD physics kernel solves the nonlinear, 3D, time-dependent two-fluid equations with neo-classical effects in toroidal geometry of arbitrary poloidal cross section. Shown in Fig. 10-7 is a NIMROD simulation of a gas-jet mitigation in C-Mod that demonstrates how the equilibrium edge is rapidly cooled. A 2/1 mode appears first (left panel) and stochastic fields form at the edge, eventually destroying all field lines outside the $q=1$ surface. The second and third panels (moving left to right) show how a 1/1 mode levels the core temperature by swapping the cold island with the hot magnetic axis. Electron temperature profiles

simulated during this thermal quench are found to resemble the profiles measured with Thomson scattering.

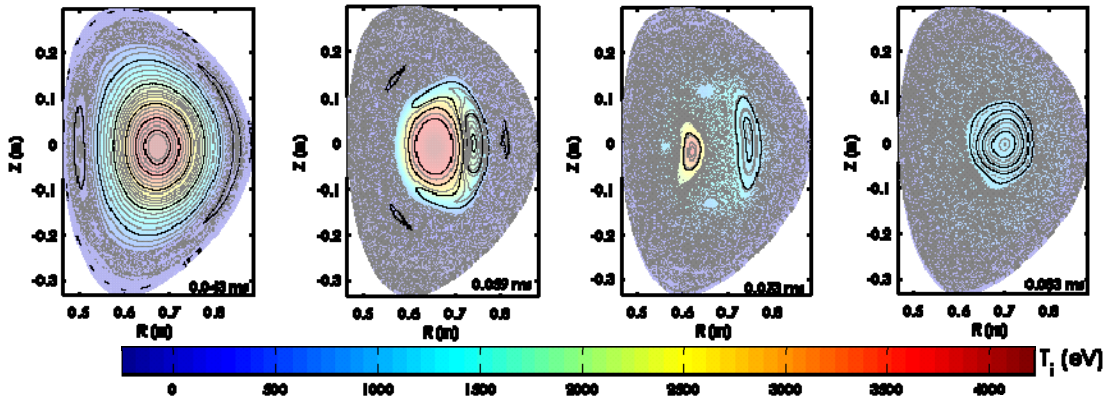


Figure 10-7: NIMROD simulation of gas jet mitigation experiment on Alcator C-Mod.

Finally, the NIMROD code has been combined with a code for impurity transport (KPRAD) and simulations have been performed that successfully capture density profile differences observed between Helium and Argon jet penetration experiments on C-Mod.

10.2.8 Integrated Scenario Modeling

During the period from 2003-2007 an important advance was made in the establishment of a time dependent predictive capability for integrated scenario modeling in Alcator C-Mod. Through a C-Mod – PPPL collaboration, the time dependent TSC code was used to simulate experimental discharges in C-Mod with fast current ramp-up and intense ICRF heating in improved core confinement regimes. The MHD equilibrium in these simulations is advanced using the free boundary solver in TSC that takes into account the actual poloidal field (PF) coil set in C-Mod. The simulations employed thermal diffusivities from a micro-instability-based L-mode transport model [10.28]. The diffusivity is manipulated to give the temperature profile (as close as possible) to the experimental temperature profile. The overall confinement is increased by making the multiplier in front of χ smaller everywhere, so the pedestal temperature is also increased. A self-consistent ICRF model that computes the power partition between ions and electrons is not used in these simulations. Instead, the power transfer from the minority hydrogen tail to background electrons and ions is estimated based on previous TRANSP simulations using FPPRF/TORIC [10.29]. We have also used TSC with the lower hybrid (LH) current drive code LSC [10.30] to simulate LH current profile control experiments in C-Mod. We plan to continue using the LSC code for near term modeling activities in 2008 and then move to the more sophisticated CQL3D-GENRAY code [10.19] in the period from 2008-2013. The development and validation of integrated models for transport, heating, and plasma control (current and pressure) is crucial in order to plan and optimize experiments in future device such as ITER.

10.2.9 New PSFC Parallel Computer Cluster

A new computer cluster has been installed at the MIT Plasma Science and Fusion Center. The facility is expected to greatly facilitate interaction between theory and the C-Mod tokamak experiment, to aid scientific discovery within the PSFC theory program, and to help train students. Nonlinear gyrokinetic simulations of plasma turbulence can now be done in-house. Full-wave lower hybrid field simulations with TORIC, which required six days on the older 48 processor PSFC Theory Cluster, can now be done in 4.6 hours. A well resolved, two species GS2 nonlinear simulation of electrostatic trapped electron mode turbulence, which was previously impossible in-house, completes in less than 8 hours on the new cluster. A radial profile of the maximum linear growth rate, for a C-Mod case, can be computed in about 10 minutes. The new cluster is ideal for frequent production runs that require hundreds, rather than thousands, of processors.

The new cluster consists of 256 AMD Opteron processor cores in 64 nodes, each connected by Infinipath and gigabit networks, with 4 gigabytes memory and 250 gigabytes disk per node, a head node, a spare node, 2.5 terabytes RAID storage, and remote console management. The high speed, very low latency Infinipath network not only more than doubles real world performance, but also allows an upgrade to 512 processor cores through a drop-in replacement with quad-core processors, while doubling the memory. The cluster is supported in roughly equal amounts by the PSFC DoE Theory Grant, Alcator C-Mod DoE Grant, and PSFC New Initiatives funding, and MIT provided a new air conditioning system.

10.3 Work Expected to be Completed in 2008 and Proposed Work for 2008-2013

10.3.1 Gyrokinetic Turbulence Simulations of Experiment

In 2008, we plan to continue gyrokinetic simulations of TEM turbulence, emphasizing recent ITB cases with improved PCI measurements with spatial localization. Additional comparisons with GYRO will be pursued in addition to GS2. This should allow us to conclusively identify ITG turbulence, which is generally not localized to a narrow region of the plasma cross-section, as TEM turbulence is in ITB cases. The dramatically improved HIREX and charge exchange measurements of ion temperature and toroidal rotation profiles will be extremely useful in these studies. We expect to release the web interface between gyrokinetic codes and experiments in 2008, with support from the SciDAC Center for the Study of Plasma Microturbulence.

Over the next five year period, we plan to carry out scaling studies comparing simulated and measured wavelength spectra for core fluctuations. These studies would involve dedicated experiments and simulations, aimed at not only validation, but elucidating the mechanisms underlying well-known trends, such as favorable current scaling, unfavorable power scaling, and aspect ratio scaling. We have proposed experiments to verify the ballooning structure of turbulence. With the new HIREX and charge exchange measurements of toroidal rotation, we can much more directly address possible mechanisms for spontaneous toroidal rotation. With some code enhancements, GYRO and GS2 can be used to simulate momentum transport and to investigate core momentum pinches. Recent HIREX data has revealed a toroidal momentum inflow in the outer half

of the plasma cross-section. The improved measurements also allow us to investigate impurity transport. The C-Mod ITB provides an excellent demonstration of impurity accumulation in the presence of peaked density profiles. The accumulation is very sensitive to on-axis heating, which is consistent with the role of TEM turbulence [10.3]. However, neoclassical inflows are known to play a role. A detailed investigation would help us better understand the role of fluctuations in the neoclassical parallel momentum balance, which would also shed light on possible anomalous poloidal rotation. Lower hybrid heating and current drive should have a very strong effect on ITB's in C-Mod through the electron temperature, the loop voltage, and the magnetic shear. Our previous gyrokinetic simulations have found negligible anomalous particle pinches at C-Mod collisionalities, leaving only the neoclassical pinch to peak the density profile to form the ITB. Therefore, if ITBs form in steady state LH heated discharges with zero loop voltage, evidence will exist for an anomalous particle pinch, at much higher collisionalities than expected. At ITB densities, the LH current drive efficiency is much lower, and access is more challenging, though still possible with the aid of the cryopump to reduce H-Mode densities. We also plan to support ongoing ohmic density scans, which access low collisionality regimes in which the electron channel dominates. These studies, combined with detailed simulations, could reveal fundamental physics underlying electron transport.

10.3.2 Pedestal and Edge Studies

Recent impurity (Boron) density, temperature and flow profile measurements by McDermott, Marr and co-workers [10.31, 10.32] have resulted in a reliable radial electric field profile in the pedestal of C-Mod in H-mode. The pedestal of C-Mod is collisional, its associated large negative radial electric field profile highly localized, and neutral beam injection absent, so these results may provide a clean and striking test of whether recent Pfirsch-Schlüter predictions for the radial electric field [10.33, 10.34] can shed any light on pedestal behavior and radial electric field profiles. These theoretical expressions retain crucial geometric features not contained in the original large aspect ratio, circular flux surface expression of Classen [10.35] which were not totally satisfactory but nonetheless gave collisional results large enough to possibly be relevant at the very edge of DIII-D [10.36].

A more challenging test is to compare the Pfirsch-Schlüter prediction for the shape of the radial electric field profile by adjusting the boundary condition on the toroidal flow so it matches at one point (i.e., the separatrix or top of the pedestal). This adjustment is necessary since there is no way to know how much momentum is transiently exchanged with the magnetic field coils and neutrals before the plasma reaches a near steady state. To make this comparison the background plasma density profile and an ion temperature profile are needed. Since the ion temperature profile is not available in C-Mod, the Boron and/or electron temperature (from Thomson scattering) profiles will be employed. Measurements in Helium plasmas are also expected in the near future making both the plasma density and ion temperature available. Using the plasma density and temperature profiles along with the magnetic field geometry and the boundary condition on the flow, the Pfirsch-Schlüter expressions for the radial electric field will be determined by demanding that the radial flux of toroidal angular momentum vanish. Comparisons to the

measured profiles will then be possible to try to determine the relative importance of anomalous and neoclassical effects on the radial electric field profile in an H-mode pedestal.

Comparisons of experimental and theoretical predictions for banana regime plasmas deeper into the core are still not possible since suitable theoretical expressions for the radial electric field are not available. Recent work [10.37] corrected the pioneering work of Ref. [10.38] but both treatments are incomplete since they ignore the poloidal variation of the electrostatic potential [10.39]. Consequently, a reliable banana regime expression for the radial electric field is yet to be determined.

The Boron flow measurements also provide a means of rather generally determining the poloidal variation of the density [10.32] and a means of examining the effects of magnetic topology on flows inside the separatrix. Previous work and work being completed examines the impact of magnetic topology on flows in the scrape-off layer [10.40, 10.41, 10.42]. If the Boron flows inside the separatrix are assumed to be neoclassical then it may be possible to determine some information about the background radial ion temperature profile as well. It is clear from these C-Mod experimental results that the poloidal flow of the impurity Boron is in the correct direction and about the right magnitude to agree with the Pfirsch-Schlüter expression for the impurity poloidal flow [10.43, 10.44, 10.45].

As already discussed in Chapter 7, a substantial development effort has been undertaken in the computational community to develop powerful tools for edge transport and stability calculations in the ETB region. One of the more successful codes, ELITE [10.46], has been utilized for comparisons with data from a number of devices, including C-Mod, to calculate the eigenfunctions and growth rates of ideal MHD modes within the context of the peeling-ballooning model for ELMs. As mentioned in Section 7.1.2, the resistive MHD code M3D [10.47] is also being used to analyze edge stability. We will continue using these tools for ELM studies, and will also take advantage of the burgeoning array of edge transport codes in development. The XGC0 code [10.48] is a neoclassical edge transport code, developed mainly to model pedestal structure and edge flows with a self-consistent radial electric field. The usefulness of XGC0 should be enhanced considerably within the next five years by the completion of the XGC1 turbulence code, which will calculate the contribution of electromagnetic turbulence to transport in 3D geometry, complete with X-point. These codes will make possible more realistic calculations of flux-gradient relationships in the pedestal, and will produce predictions for pedestal structure and scalings which can be validated using C-Mod data.

Recently, increased focus has been placed on the integrated use of simulation codes, for the purposes of simulating complex time-dependent edge phenomena. Classic examples of these phenomena, which may be driven by multiple physical processes coupled in highly nonlinear ways, include the L-H transition and the complete ELM cycle. While the goal of simulating these processes will not be realized for some time, progress in code development and integration is anticipated over the next five years, spearheaded by the SciDAC initiative known as the Center for Plasma Edge Simulation (CPES). We will

work closely with the CPES to validate codes against C-Mod pedestal data and use the integrated workflow they develop to begin modeling time-evolving edge processes like H-mode evolution.

10.3.3 ICRF Mode Conversion and Flow Drive Studies

The localized nature of IBW and ICW wave absorption makes these waves attractive for current profile and pressure profile control. We plan to carry out both theoretical and numerical work in this area as follows. Theoretical studies on the mode conversion of fast Alfvén waves to ion Bernstein waves and ion cyclotron waves will continue in 2008. Our aim is to determine the conditions which optimize conversion to one or the other wave in C-Mod. The change in the parallel wave number predicted in a ray tracing treatment and a comparison with the full wave codes will be pursued. From full wave electromagnetic field solvers it is evident that two dimensional effects are important in determining the coupling to IBW and ICW. A one-dimensional (in space) model is clearly not adequate to describe the mode conversion process. Extensions to two dimensions which include toroidal effects will be pursued. We also plan future work on the synergistic effects of ICW and IBW with lower hybrid waves. Previous work has shown that IBWs can assist in increasing the lower hybrid current drive efficiency. The role of ICW in the synergistic process needs to be determined. Since two dimensional spatial effects are important in the conversion to IBWs and ICWs, one needs to include toroidal effects into the quasilinear diffusion operator that describes the interaction of electrons with the waves. This is presently being pursued theoretically and will be part of the ongoing research program. The quasilinear diffusion operator will include both spatial and momentum space diffusion coefficients. The formulation will be valid for waves in the ion cyclotron, lower hybrid, and electron cyclotron range of frequencies. Thus, it will be useful not just for ICRF and LHRF experiments on Alcator C-Mod, but also for studies on other machines where ECRF is used.

In the near term (2008-2010) we plan to carry out a detailed inter-code study, comparing the electric field structures computed by the AORSA and TORIC field solvers in both the ICRF mode conversion and minority heating regimes. It should be noted that in order to achieve agreement between the simulated and measured PCI signals plotted in Fig. 10-3, it was necessary to rescale the simulated signal by about a factor of 10^{-2} . Preliminary comparisons of the predicted electric fields from TORIC and AORSA indicate the TORIC electric field is larger than the AORSA field by a factor of 6-10, consistent with the need to rescale the computed PCI signal downward. Furthermore, the AORSA field was found to be in agreement with theoretical estimates. The research plan to proceed forward is therefore to first investigate and correct the source of the electric field normalization error in TORIC. Then the inter-code electric field comparisons will be re-done for the minority and mode conversion cases, in order to establish that TORIC is in reasonable agreement with AORSA. Finally we will re-do the comparisons between the simulated and measured PCI spectra shown in Fig. 10-3, as well as expanding the comparisons to other mode conversion cases.

Implementation of the synthetic PCI diagnostic code for mode converted ICRF wave detection affords an excellent opportunity to begin formulating a set of metrics for this synthetic diagnostic calculation. Certain ICRF experiments have been performed in Alcator C-Mod that may provide a test bed for establishing such metrics. In these experiments the concentration of ^3He in a deuterium majority plasma was scanned from (5-30) % [10.29]. The absorption of mode converted ICRF waves on electrons was measured as a function of ^3He concentration and a clear transition was seen as the absorption physics changed from minority ^3He absorption to mode conversion electron heating. These experiments can be carried out again, now using the PCI diagnostic to document this transition. The diagnostic measurements can then be simulated using the wave fields from TORIC or AORSA in the synthetic PCI diagnostic. The synthetic diagnostic should be capable, as a zero order check, of reproducing the transition from minority heating to mode conversion electron heating as evidenced by a turn-on in the PCI signal as the ^3He concentration is increased.

During FY2008-2013 we also plan to use massively parallel simulations to understand and guide sawtooth modification experiments on Alcator C-Mod using mode conversion current drive (MCCD). Now that the capability exists to routinely compute the electron deposition of mode converted IBW and ICW using the parallel TORIC code, this code has been combined with an adjoint evaluation of the current drive efficiency in a calculation that includes the effect of large parallel wavenumber variation on the current drive efficiency [10.29]. We also plan to carry out numerical studies of the power partition between electrons and ions for ICW mode conversion schemes in Alcator C-Mod. The goal here will be to optimize absorption of the ICW by ion cyclotron damping in the three ion species mode conversion scenario in Alcator C-Mod [10.11, 10.14, 10.16], in order to identify viable ICRF flow drive scenarios. This work will be carried out in conjunction with the theoretical studies discussed above. This work should also benefit greatly from the new x-ray imaging spectrometer that has been installed on C-Mod, that will provide an unprecedented measurement of rotation profiles in a torque free plasma.

10.3.4 Linear and Nonlinear ICRF Antenna Coupling Studies

Understanding the linear and nonlinear processes that affect ICRF antenna coupling will be crucial in order to insure success of the ICRF experimental program on C-Mod. This knowledge base will also contribute to developing a predictive capability for ICRF antenna design and operation that will be critical for ITER. Theory and simulation work in this area will proceed on C-Mod as follows. In order to develop a predictive capability for the linear antenna response, the 3D antenna simulation code TOPICA [10.49] and the full-wave solver TORIC are currently being modified for integration. During 2009-2013 we plan to complete this integrated package in collaboration with the RF SciDAC Center. This self-consistent linear calculation will ensure that the poloidal and toroidal spectrum of RF modes at the core boundary are consistent with the RF current distribution in the detailed 3D, CAD-based antenna model used by TOPICA. In addition to providing more quantitatively correct core responses, areas of high thermal loading and high electric fields can be identified and eliminated or reduced with suitable antenna design modifications. Presently, the TORIC code uses a simple current distribution at the wall

to model the antenna and model important 3D antenna features. This can be improved upon by providing an interface to couple with a dedicated antenna code such as TOPICA. TOPICA is able to handle the actual 3D geometry of ICRF antennas with curved, solid straps, a general-shape housing, Faraday screen, etc. and is presently coupled to a 1D plasma loading model, the FELICE code [10.50].

We have modified the 2D TORIC code in order to replace the 1D FELICE model. Schematically, full wave and antenna codes are coupled through boundary conditions at a 2D plane that separates the plasma from the antenna. For each code, responses are calculated for a complete set of sources at the interface. Equating these sources then provides a self-consistent solution for the integrated system. To implement this technique, TORIC was modified to calculate these boundary responses. Figure 10-8 shows initial results from a TORIC calculation of the admittance $Y_{m,m} = B_m/E_m$ for a single toroidal mode, in this case $n_\varphi = 10$. The four component matrices break down the result in terms of plasma wave polarizations relative to the equilibrium magnetic field. The 1D

result would be analogous to retaining just the diagonal terms in each sub-matrix, that is, values where $m = m'$. As can be seen, the 2D case is still diagonally dominant, but there is significant structure in the response beyond just the driven mode. These results will be

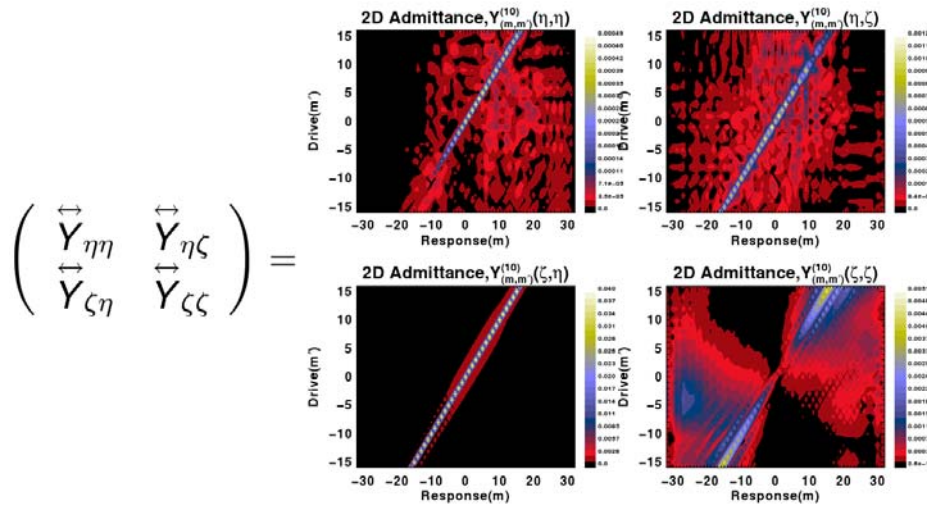


Figure 10-8: The admittance matrix from a TORIC simulation, $Y_{m,m}=B_m/E_m$, for $n_\varphi = 10$ above, is composed of four sub-matrices representing the self- and cross- admittances for the two polarizations, ζ (parallel) and η (perpendicular) to the equilibrium magnetic field. In this example 31 poloidal modes are driven and 63 poloidal modes are measured.

used to self-consistently couple the full-wave code TORIC and the antenna code TOPICA through impedance matching boundary conditions. (The impedance, Z , is just the inverse of the admittance, i.e. $Z = Y^{-1}$), thus providing the complete linear response of the ICRF antenna – plasma system.

Formation of nonlinear RF sheaths has been recognized as a major physics issue for ICRF antenna operation in Alcator C-Mod as well as in future devices such as ITER [10.51]. Past work on RF sheath effects used methods based on the vacuum RF field approximation to evaluate the sheath potential given the RF fields. This method gave useful information on near field sheaths, but was hard to quantify for other kinds of sheaths. Recent work in the RF SciDAC Center [10.52] has now taken the first steps towards a quantitative theory of RF sheath formation that allows a self-consistent calculation of the linear RF fields in plasma and the detailed spatial distribution of the nonlinear sheath potential. In particular, techniques have been developed for calculating the sheath potential from a suitable boundary condition (BC) in the RF wave solver. For weak RF sheaths, a modified form of the conducting wall BC that analytically takes into account the misalignment between the magnetic flux surface and the conducting boundary (antenna, limiter, or wall) yields a self-consistent result for the sheath properties without nonlinear iteration. For stronger RF sheaths or large misalignment, a general sheath BC was derived [10.52] to replace the conducting wall BC in full-wave propagation and antenna codes. In this case, the tangential component of the RF E field at the entrance to the sheath is non-zero due to a sheath capacitance term. A nonlinear root finder determines the RF fields, the sheath potential, and the sheath width self-consistently at each spatial point on the boundary (thus giving an accurate spatial distribution of the sheath effects). Sheath power dissipation can also be included in the BC. During 2008 we plan to complete implementation [10.53] of this sheath metal wall BC in the TORIC ICRF solver. This work will be carried out in close collaboration with the RF SciDAC Center.

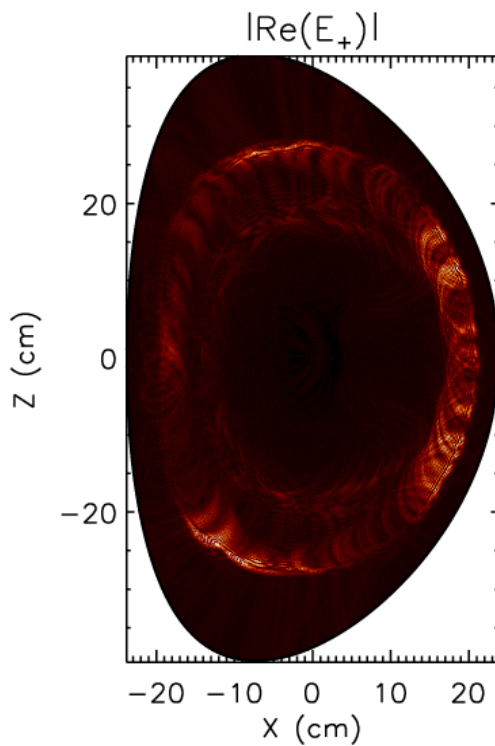


Figure 10-9: Full-wave LH field simulation for Alcator C-Mod using a fast wave launch with direct conversion to the slow LH wave [10.57].

10.3.5 Self-Consistent LHCD Simulations

Analyses of LHCD experiments carried out thus far on Alcator C-Mod (see subsection 10.2.5) have employed self-consistent calculations from combined ray tracing Fokker Planck models (GENRAY – CQL3D). However, these types of wave propagation treatments neglect important full-wave effects such as focusing and diffraction that are known to be important [10.54]. During FY2009-2013 we shall carry out integrated, self-consistent simulations of LH current drive by combining an antenna model, a full-wave solver, and a Fokker-Planck solver. For the antenna, we will use an analytical model, developed by Brambilla [10.55] which agrees well with experiments. A parallel version of the TORIC code, specialized to the LH range of frequencies (TORIC LH) [10.56] will be employed. Our initial full-wave simulations of LH waves used a version of TORIC that coupled only to a fast wave, which then had to mode-convert to the desired LH slow wave [10.57]. An example of this type of field simulation is shown in Fig. 10-9 using a spectral resolution of 1000 (Radial) \times 1023 (Poloidal) modes. The parallel field solve in Fig. 10-9 can be performed in about 1 hour of wall clock time on the CRAY XT3/4 at ORNL using 4096 processor cores.

This code has now been modified to provide a direct slow-wave launch and is now being parallelized and tested on the Cray XT3/4 Jaguar computer at ORNL and on our new local computing cluster Loki [10.56]. The parallel LH TORIC solver will then be coupled to the zero orbit width Fokker Planck solver CQL3D to enable self-consistent LHCD analysis. Through the RF SciDAC collaboration, the parallel TORIC solver has already been modified to compute the plasma response due to nonthermal electrons (and ions). These model advances will provide the capability required to calculate the driven LH current using the complete toroidal antenna spectrum with self-consistent RF fields and electron non-Maxwellian distribution functions. The self-consistent 3D electron distribution function from the TORIC LH-CQL3D simulation will be used in synthetic diagnostic codes for hard x-ray and nonthermal electron cyclotron emission (ECE) and the results will be compared with the corresponding diagnostic measurements. In order to understand differences in the treatment of wave propagation from full-wave and ray tracing treatments we plan to compare the synthetic diagnostic predictions obtained from the TORIC LH (full-wave) – CQL3D calculation with the predictions from the GENRAY (ray tracing)-CQL3D simulations. Specifically, ray tracing treatments neglect the effects of focusing and diffractive broadening of the wave spectrum that is accounted for in full-wave calculations. This can lead to differences in the spatial and velocity space distribution of fast electrons and LH current density that can be measured with the hard x-ray and Motional Stark Effect (MSE) diagnostics.

10.3.6 ICRF Minority Heating

An accurate computation of the 3D ion distribution generated during minority ICRF heating in C-Mod is critical to several other areas of research on C-Mod including MHD studies of Alfvén cascades and Alfvén eigenmodes, sawtooth modification experiments using minority ICRF, analysis of internal transport barrier (ITB) plasmas induced and heated by ICRH, and analysis of ICRF heated plasmas with significant toroidal rotation.

The coupling between the AORSA full-wave solver and CQL3D described in subsection 10.2.4 will also be carried out for the ICRF TORIC solver and CQL3D. The plasma response in TORIC has been modified (as noted above) to be valid for nonthermal ion (and electron) particle distributions, so that self-consistent minority heating studies can also be carried out by iterating TORIC and CQL3D until a converged distribution function and quasilinear diffusion coefficient are achieved. The 3D ion distribution functions from this combined model will also be used in a synthetic diagnostic code for the Compact Neutral Particle Analyzer and compared with experimental measurements, as was done with the 3D ion distribution from the combined AORSA-CQL3D simulation. This type of inter-code comparison will provide a useful assessment of where the finite ion Larmor radius expansion used for the plasma response in TORIC is valid, by comparing with a solver (AORSA) where no such approximation was made in deriving the conductivity operator. It is also possible to start to establish metric standards for the synthetic CNPA diagnostic by performing minority hydrogen (H) heating experiments in C-Mod where the (H) fraction is scanned from a few percent up to 10-20%. In this case the measured CNPA signal should decrease as the minority tail energy decreases at higher (H) concentration ($\geq 10\%$). The CNPA signal simulated with the synthetic diagnostic code should also reproduce this trend.

In order to assess the role of finite ion drift-orbit effects in ICRF minority heating we plan to collaborate with researchers in the RF SciDAC Center who are working on combining the AORSA and TORIC full-wave solvers with a Monte Carlo orbit code ORBIT RF. This type of model has already shown promise in understanding the interaction between high harmonic fast waves and fast neutral beam ions in the DIII-D tokamak [10.58] and should elucidate the importance of finite ion drift-orbit diffusion in minority ion heating and sawtooth stabilization schemes in C-Mod. An obvious step in assessing the role of finite ion orbit effects will be to employ the statistical fast ion distribution functions from the full-wave – ORBIT RF calculations in a the synthetic diagnostic code for the CNPA, and compare with the diagnostic code predictions from a full-wave – AORSA simulation.

10.3.7 MHD Studies of Reverse Shear Alfvén Eigenmodes

Alfvén eigenmodes studies on Alcator C-Mod emphasizing PCI has changed focus from the current-ramp to the flattop portion of the discharges where RSAEs are frequently observed during the sawteeth. This is a unique and important finding, as it challenges theories of the reconnection and the subsequent relaxation. The plasmas in which these modes are observed are at the extreme edge of the operational space, being generally found at low density and high ICRH power. These observations have been used to determine that q_{\min} following the sawtooth crash drops to about 0.95 or greater. These findings are supported by simulations from NOVA which has shown that $q=1$ RSAEs should be present and unstable given an ICRH generated fast-ion population. These modes show the feature of being excited to different amplitudes in shots of similar nature, as defined by the scopes. These observations, in addition to the fact that these modes have yet to be reported in the numerous Alfvén eigenmode studies on other machines where neutral beam heating is commonplace, suggest that the details of the fast-ion distribution are critical. During the period from 2009-2013 we plan to use the combined

AORSA/TORIC and CQL3D models (see subsection 10.3.6) to accurately describe the 3D(v_{\perp} , v_{\parallel} , r) fast ion distribution function generated in these experiments in C-Mod. Important features of these particle distributions will then be included in the NOVA simulations.

Present comparisons between Alfvén eigenmode data and the NOVA-K code have found discrepancies in the mode stability for the measured direction of mode rotation. Anisotropy in the fast ion distribution function could be responsible for some of these discrepancies. So, a more accurate model of the ICRF distribution function needs to be included in NOVA-K calculations for this reason also. Both the presently used TRANSP/TORIC calculations of the fast ion distribution and more sophisticated AORSA/CQL3D calculations need to be improved and used in NOVA-K. Enhancements to the AORSA/CQL3D codes including orbit width effects together with improvements in fast ion diagnostics such as a proposed multi-channel CNPA to provide confined fast ion profiles will then allow more detailed comparisons with experiments.

The collaboration between MIT and JET in the study of Alfvén eigenmodes has helped develop a new analysis code called SparSpec [10.59] for determining toroidal mode numbers. This code was originally developed by the astrophysics community for determining the least number of modes that could describe the orbit of a celestial object sampled at various times throughout a calendar year. Unequally spaced pick-up coils toroidally provide data that can be interpreted in the same way allowing the smallest number of modes to be determined that best describes magnetic fluctuations in a tokamak. This is particularly important for actively excited stable intermediate n modes since a broad spectrum of modes is excited, which can result in multiple n modes at approximately the same frequency. Ordinary Fourier analysis methods can only determine a single mode number at a given frequency. The SparSpec code has been successfully implemented on JET and will soon be used to analyze C-Mod magnetics data to determine the toroidal mode numbers of both stable and unstable modes.

10.3.8 Theory and Modeling Support - Plasma Boundary

Comparisons of experiment with simulation are an important part of the research plan in the plasma boundary area. The ultimate goal in this area is to simulate, using a first-principles - physics model, the time-averaged profiles and perpendicular and parallel fluxes that are measured in C-Mod. Validation of this type of physics model will be an important step in developing the capability to confidently predict the power and particle profiles footprints in the divertor of future devices like ITER and DEMO. At C - Mod we have working relationships with groups running the following turbulence codes - ESEL (2D non-linear fluid code - developed at Riso Nat Lab.) [10.60], BOUT (3D non-linear fluid code with X-point developed at LLNL) [10.61], and GEM (3D non-linear gyrofluid code developed at IPP-Garching) [10.62]. We will continue to work with these groups to validate the codes with C-Mod's turbulence data. There is a specific interest in starting these simulations with the flux specified as a boundary condition and observing if they can reproduce the measured radial profiles as well as the turbulence characteristics. Additionally, we will work with our theory and modeling collaborators, including: B. Rogers (Dartmouth) and P. Guzdar (U. Md).

10.3.9 Integrated Scenario Modeling Studies

During the period from 2009-2013 we plan to carry out more realistic simulations of improved core confinement discharges, LH current profile control experiments, and advanced tokamak operating modes using TSC. Simulations at present lack realistic ICRF heating sources, more advanced calculations of the LHRF-generated current, and a first principle-based transport calculation. In the near term we shall perform simulations with a more realistic ICRF heating source, using a combined TSC – TRANSP approach, which has been successfully applied to time dependent ITER simulations. Here the TSC code is used to advance the discharge for a short time, the TRANSP code is then used to compute the ICRF heating source terms using FPPRF/TORIC, and finally the TSC equilibrium is advanced in time using these new heating sources. This allows the use of the more realistic model in TRANSP for ICRF heating. The same calculation can be done including a LH current drive source as computed by LSC, which can also be called from TRANSP. A second area where an important model advance will be implemented in the time dependent scenario studies is in the LH current drive calculation. Recently, we have shown through a detailed benchmarking exercise [10.63] that predictions of LH current obtained from an adjoint evaluation of the current drive efficiency in combination with a 1D ($v_{||}$) power deposition calculation systematically underestimate the driven LH current by about 20-30%, relative to 2D (v_{\perp} , $v_{||}$) Fokker Planck – ray tracing treatments such as CQL3D - GENRAY. The GENRAY-CQL3D module should be implemented within TRANSP by 2010, making it possible to compute more realistic LH current drive with the TSC-TRANSP approach. We also anticipate that the gyro-Landau fluid transport module TGLF will be available in 2009 for use in TSC, making it possible to perform predictive transport simulations of C-Mod discharges. These types of calculations will be invaluable in terms of identifying the mixture of ICRF heating power, LH current drive power, and current ramp rate that maximizes the bootstrap current fraction and shear reversal radius in both standard and improved confinement regimes in C-Mod.

Finally, we plan to take advantage of a new simulation framework (the Integrated Plasma Simulator or “IPS”) being developed through the SWIM Fusion Simulation Project. Through this architecture, the CQL3D-GENRAY codes can communicate with TSC through an interface called the “Plasma State”. It is also important to note that the AORSA and TORIC ICRF solvers also are part of the IPS, so that self-consistent minority ICRF heating calculations can also be interfaced to TSC through the IPS. Here, the full-wave solvers employ the most recent fast ion distribution function in their dielectric response and in turn re-evaluate the quasilinear operator for use in the Fokker Planck solver. Thus, more realistic time dependent simulations can be carried using this framework since TSC can communicate with the most advanced simulation codes for ICRF heating and LH current drive. The codes and architecture comprising the Integrated Plasma Simulator have been implemented on parallel computing clusters at PPPL and Oak Ridge and in 2008 we plan to investigate the viability of implementing the IPS on the new Loki computing cluster at the MIT PSFC.

10.4.1 Simulation Codes, Applications, and Contributors

Simulation Code	Application	Contributors
GS2	Non-linear gyrokinetic stability (Flux tube)	D. Ernst (MIT) W. Dorland (U. of Md.)
GYRO	Non-linear gyrokinetic stability	D. Ernst (MIT) J. Candy (GA)
ELITE	MHD Stability for intermediate to high n ballooning modes	P. Snyder (GA)
M3D	Nonlinear 3D MHD Stability	W. Park (PPPL) L. Sugiyama (MIT)
XGC0 / XGC1	5D edge gyrokinetic code	C. S. Chang (NYU)
TORIC	2D FLR ICRF field solver	J. C. Wright & P. T. Bonoli (MIT) M. Brambilla & R. Bilato (IPP)
AORSA	3D All-orders ICRF field solver	E. F. Jaeger (ORNL)
CQL3D	3D bounce averaged Fokker Planck solver (ICRF, LHRF, ECRF)	R. W. Harvey (CompX)
TOPICA	3D electromagnetic antenna code	R. Maggiora (Torino)
FELICE	1D FLR ICRF solver	M. Brambilla (IPP)
TORIC LH	2D LHRF field solver	M. Brambilla (IPP) J. C. Wright (MIT)
NOVA-K	Kinetic MHD stability with energetic particles	N. Gorelenkov (PPPL)
SparSpec	Alfven Eigenmode stability at high n-number	JET
TRANSP	Transport analysis code	D. McCune (PPPL)
FPPRF	Bounce averaged ion Fokker Planck analysis with coupling to full-wave solvers	D. McCune (PPPL)
TSC	Tokamak Simulation Code with free boundary MHD solver and transport.	C. Kessel (PPPL)
LSC	Lower Hybrid Current Drive Code with ray tracing plus adjoint solution of Fokker Planck equation.	C. Kessel (PPPL)

Simulation Code	Application	Contributors
TGLF	Trapped Gyro-Landau Fluid (linear stability)	R. Waltz (GA) J. Kinsey (GA)
ESEL	2D nonlinear fluid -stability	O. E. Garcia (Riso Nat'l Lab)
BOUT	3D non-linear fluid -stability with X-point	X. Xu (LLNL)
GEM	3D non-linear gyrofluid	B. Scott (IPP)
IPS	Integrated Plasma Simulator - Framework for combining simulation codes.	D. Batchelor (ORNL)

10.4.2 Research Goals and Objectives

The following table summarizes high-level objectives within each of the research themes covered in this section, along with the simulation capability or diagnostic that will enable our theoretical and experimental studies.

Thematic Research Goal	Intermediate Objectives	Enabling tools
Understand ITB formation and control in C-Mod plasmas.	<ul style="list-style-type: none"> - Finish gyrokinetic simulations of ITB plasmas using GYRO and GS2 to distinguish ITG vs. TEM turbulent roles. - Simulate momentum transport and pinches with GS2 and GYRO and compare with HIREX data. - Assess role of magnetic shear modification due to LHCD in ITB formation. 	<ul style="list-style-type: none"> - Synthetic diagnostic codes in GS2 and GYRO. - Modifications to GYRO and GS2 to compute momentum transport and pinches. - HIREX measurements of rotation.
Develop a predictive theoretical capability for the radial electric field in the C-Mod pedestal.	<ul style="list-style-type: none"> - Compare Pfirsch-Schlüter predictions for E_r in the pedestal with E_r inferred from experiment. - Compare neoclassical flow predictions with measurements. 	<ul style="list-style-type: none"> - Measurements of impurity density, temperature, and flows in SOL.
Develop a predictive simulation capability for pedestal phenomena in C-Mod.	<ul style="list-style-type: none"> - Continue MHD stability studies of ELM's in C-Mod using the ELITE and M3D codes. - Validate XGC0 and XGC1 code predictions for pedestal structure and scalings against C-Mod data. - Simulate L-H transitions and ELM cycles in C-Mod using integrated codes developed through SciDAC Projects, as models become available. 	<ul style="list-style-type: none"> - Implement tools to process accurate kinetic EFIT profiles (from experiment) for use in ELITE and M3D. - Implementation of XGC0 and XGC1 by the CPES SciDAC Center.
Understanding linear ICRF antenna coupling in C-Mod	<ul style="list-style-type: none"> - Simulate dependence of antenna loading in C-Mod as a function of edge density and density profiles (L- vs. H-mode). - Apply coupled antenna model to new 4-strap antenna to identify antenna "hot spots". 	<ul style="list-style-type: none"> - Coupled TORIC-TOPICA codes. - Antenna loading measurements. - SOL density profile measurements.
Understanding role of nonlinear far field sheaths in C-Mod ICRF heating schemes.	<ul style="list-style-type: none"> - Simulate strong single pass damping regimes – D(H) - Simulate weak single pass damping regimes – D(³He) 	<ul style="list-style-type: none"> - Implementation of metal wall BC in TORIC solver. - Post-processing diagnostic in TORIC for RF sheath dissipation.

10.4.2 Research Goals and Objectives

Thematic Research Goal	Intermediate Objectives	Enabling Tools
Develop predictive capability for ICRF Flow drive and Mode Conversion Current Drive in C-Mod plasmas.	<ul style="list-style-type: none"> - Inter-code comparison of AORSA & TORIC mode converted wave fields and comparisons with theory. - Validate predictions for ICW/IBW electric fields from AORSA and TORIC against PCI measurements in C-Mod using a synthetic diagnostic code. - Validate predictions for RF flow drive by IBW/ICW using predicted electric fields from AORSA and TORIC in a synthetic diagnostic code against HIREX rotation data. - 	<ul style="list-style-type: none"> - Synthetic diagnostic code for PCI and PCI measurements. - Poloidal rotation measurements from HIREX diagnostic.
Develop predictive capability for LH current drive (LHCD) experiments on C-Mod that can be extrapolated to ITER.	<ul style="list-style-type: none"> - Assess full-wave effects on LH wave propagation in C-Mod using TORIC LH. - Validate synthetic diagnostic codes for hard x-ray, soft x-ray emissivity, and LHRF current density using measurements on C-Mod and predicted distributions from CQL3D-GENRAY and CQL3D-TORIC LH. 	<ul style="list-style-type: none"> - TORIC LH simulations on Loki cluster. - Coupling of full-wave TORIC LH and CQL3D. - Synthetic diagnostic codes for hard x-ray and soft x-ray emission. - Hard x-ray and ECE measurements of nonthermal electrons. - MSE measurements of toroidal current density.
Develop a predictive capability for 3D fast ion distributions generated by minority ICRH in C-Mod.	<ul style="list-style-type: none"> - Validate the 3D fast ion minority distributions predicted by TORIC-CQL3D and AORSA-CQL3D against C-Mod data using a synthetic diagnostic code for CNPA. - Assess role of finite ion drift orbit effects in C-Mod by comparing CNPA synthetic diagnostic code predictions using Monte Carlo orbit code distributions with zero-orbit width Fokker Planck distributions. 	<ul style="list-style-type: none"> - Coupling of TORIC to CQL3D. - Coupling of AORSA & TORIC to ORBIT RF. - Synthetic diagnostic code for CNPA. - Measurements of fast ion tails in C-Mod using CNPA diagnostic.
Elucidate the role of ICRF-generated fast ion distributions in Alfvén eigenmode (AE) and Alfvén Cascade excitation.	<ul style="list-style-type: none"> - Compare NOVA-K predictions for mode stability using realistic fast ion distribution representation. - Use SparSpec code to predict and analyze toroidal mode number spectrum of stable and 	<ul style="list-style-type: none"> - Accurate parameterization of 3D fast ion distributions from AORSA/CQL3D and TORIC/CQL3D in NOVA-K. -

	unstable AE's.	- Implementation of SparSpec code on C-Mod Linux cluster.
--	----------------	---

10.4.2 Research Goals and Objectives

Thematic Research Goal	Intermediate Objectives	Enabling Tools
Develop a predictive capability for heat fluxes at the plasma boundary of C-Mod.	- Validate the ESEL, BOUT, and GEM nonlinear fluid codes against edge turbulence data from the C-Mod.	- Implement simulation codes with the flux specified boundary conditions in C-Mod.
Develop the integrated simulation capability for modeling C-Mod discharges with LH current profile control and ICRH	- Carry out simulations of C-Mod discharges with ICRH and / or LHCD using a combined TSC-TRANSP approach. - Carry out simulations of C-Mod discharges using the Integrated Plasma Simulator (IPS) to include self-consistent ICRH (CQL3D-AORSA/TORIC) and LHCD (CQL3D-GENRAY) sources.	- Implementation of GENRAY-CQL3D in TRANSP. - Implementation of coupled AORSA/TORIC with CQL3D for ICRH and coupled GENRAY-CQL3D for LHCD in the IPS. - Implementation of the IPS framework on Loki.

10.4.3 Relationship of Theory and Simulation to ITER / ITPA Topical Areas

Theory and simulation work on Alcator C-Mod supports a number of high priority research tasks within the framework of the International Tokamak Physics Activity. The table below summarizes these connections.

ITER / ITPA Topical Area	Contributing Activity in Theory and Simulation
Scrape Off Layer and Divertor	<ul style="list-style-type: none"> - Improve understanding of plasma transport to targets and walls through validation of simulation codes (ESEL, BOUT, and GEM).
MHD	<ul style="list-style-type: none"> - Application of NIMROD + KPRAD simulation model to simulate gas jet injection mitigation experiments on C-Mod helps to develop reliable disruption prediction methods. - Application of NOVA-K with realistic fast ion distributions and SparSpec codes to AE and Alfvén cascade experiments in C-Mod contributes to the understanding of intermediate-n AE's and energetic particle modes.
Steady State Operation	<ul style="list-style-type: none"> - Comparison of synthetic diagnostic codes for CNPA, PCI, hard x-rays, and ECE contribute to ICRF and LHRF code benchmarking activities. - TSC simulations of ramp-up, hybrid, and steady state scenarios in C-Mod with ICRH and LHCD contribute to the focused modeling-benchmark activities for ITER hybrid and steady state scenarios.
Transport Physics	<ul style="list-style-type: none"> - ICRF flow drive and LHCD simulations for C-Mod contribute to the development of turbulence stabilization mechanisms compatible with reactor conditions. - GS2 and GYRO simulations of ITB's with ICRH and LHCD in C-Mod contribute to the understanding of improved core transport physics in reactor relevant plasmas with $T_e \approx T_i$ and low momentum input.

10.4.3 Relationship of Theory and Simulation to ITER / ITPA Topical Areas

ITER / ITPA Topical Area	Contributing Activity in Theory and Simulation
Confinement Database and Modeling	<ul style="list-style-type: none"> - Simulation of C-Mod integrated scenarios using the Integrated Plasma Simulator (IPS) and Plasma State frameworks contribute to the development of common technologies for integrated modeling.
Pedestal and Edge Physics	<ul style="list-style-type: none"> - Simulating edge turbulence data in C-Mod using the ESEL, BOUT, and GEM non-linear fluid codes will contribute to the testing of non-linear MHD and turbulence models of ELM evolution and will improve the capability for small ELM regimes. - Using the XGC0 and XGC1 codes to simulate the pedestal structure and scalings measured in C-Mod will contribute to improving the predictive capability of pedestal structure. -

10.4.4 Theory and Simulation Support for Long Term Goals of OFES

The Theory and Simulation research program on Alcator C-Mod supports the OFES long term goal stated as “Progress toward developing a predictive capability for key aspects of burning plasmas using advances in theory and simulation benchmarked against a comprehensive experimental database of stability, transport, wave – particle interactions, and edge effects.” Theory and Simulation research on Alcator C-Mod also contributes toward filling the following gap areas identified in the FESAC Planning Panel Report:

G-1: Sufficient understanding of all areas of the underlying plasma physics to predict the performance and optimize the design and operation of future devices.

G-2: Demonstration of integrated, steady-state, high-performance (advanced) burning plasmas, including first wall and divertor interactions.

G-7: Integrated understanding of RF launching structures and wave coupling for scenarios suitable for Demo and compatible with the nuclear and plasma environment.

References

- [10.1] C. L. Fiore, D. R. Ernst, J. E. Rice *et al*, Fusion Science and Technology, **51** (3), April 2007, p 303-16.
- [10.2] G. Greenwald, N. Basse, P. Bonoli *et al*, **51** (3), April 2007, p 266-87.
- [10.3] D. R. Ernst, P. T. Bonoli, P. J. Catto *et al*, Phys. Plasmas **11**(5) (2004) 2637.
- [10.4] D. R. Ernst, N. Basse, P. T. Bonoli *et al*, Proc. 20th Int'l. Atomic Energy Agency Fusion Energy Conference, Vilamoura, Portugal, 1-6 November 2004, oral paper IAEA-CN-116/TH/4-1.
- [10.5] D. R. Ernst, N. Basse, W. Dorland *et al*, in Proc. 21st Int'l. Atomic Energy Agency Fusion Energy Conference, Chengdu, China, 16-21 October 2006, oral paper IAEA-CN-149/TH/1-3. (http://www-pub.iaea.org/MTCD/Meetings/FEC2006/th_1-3.pdf)
- [10.6] D. R. Ernst, N. P. Basse, W. Dorland *et al*, submitted to Physical Review Letters Nov. 16, 2007.
- [10.7] D. R. Ernst, 11th EU-US International Transport Task Force Workshop, Marseille, France, September 4-7, 2006.
- [10.8] K. Zhurovich, PhD Thesis, MIT Dept. of Nuclear Science and Engineering, 2007.
- [10.9] Zhurovich, C.L. Fiore, D.R. Ernst *et al*, Nucl. Fusion **47** (9) (September 2007) 1220-1231.
- [10.10] D. R. Ernst *et al*, Phys. Plasmas **7**(2) 615 (2000).
- [10.11] E. Nelson-Melby, M. Porkolab, P. T. Bonoli *et al*, Physical Review Letters **90**, 155004 (2003).
- [10.12] F. W. Perkins, Nuclear Fusion **17**, 1197 (1977).
- [10.13] M. Brambilla, Plasma Phys Controlled Fusion **41** 1 (1999).
- [10.14] J. C. Wright *et al*, Physics of Plasmas **11**, 2473 (2004).
- [10.15] E. F. Jaeger, L. A. Berry, E. D'Azevedo *et al*, Physics of Plasmas **9**, 1873 (2002).
- [10.16] E. F. Jaeger, L. A. Berry, J. R. Myra *et al*, Phys. Rev. Lett. **90** 195001-1 (2003).
- [10.17] Y. Lin, A. Parisot, S. Wukitch *et al*, Plasma Physics and Controlled Fusion **47**, 1207 (2005).
- [10.18] E. F. Jaeger, R. W. Harvey, L. A. Berry *et al*, Nuclear Fusion **46**, S397 (2006).

- [10.19] R. W. Harvey and M. G. McCoy, “The CQL3D Fokker Planck Code”, Proceedings of the IAEA Technical Committee Meeting on Simulation and Modeling of Thermonuclear Plasmas, Montreal, Canada (1992), (USDOC NTIS Document No. DE93002962).
- [10.20] R. J. Dumont, C. K. Phillips, and D. N. Smithe, *Physics of Plasmas* **12**, 042508 (2005).
- [10.21] V. Tang, R. Parker, P. T. Bonoli *et al*, *Plasma Physics and Controlled Fusion* **49**, 873 (2007).
- [10.22] P. T. Bonoli, J. Ko, R. Parker *et al*, accepted for publication in *Phys. Plasmas* (2008).
- [10.23] C. Z. Cheng, (1992) *Phys. Reports* **211**, 1 (1992).
- [10.24] R. Hawryluk, in *Physics of Plasmas Close to Thermonuclear Conditions*, Eds. B. Coppi, G.G. Leotta, D. Pfirsch, R. Pozzoli, and E. Sindoni (CEC, Brussels, 1980), Document EUR FU BRU/XII/476/80 p. 19.
- [10.25] B.N. Breizman, M.S. Pekker and S.E. Sharapov, *Phys. Plasmas* **12**, 1 (2005).
- [10.26] E.M. Edlund, M. Porkolab, L. Lin *et al*, to be published (2008).
- [10.27] R. Granetz, D. G. Whyte, V. A. Izzo *et al*, *Nuclear Fusion* **46**, 1001 (2006).
- [10.28] W. M. Tang, *Nucl. Fusion* **26**, 1605 (1986).
- [10.29] P. T. Bonoli, R. Parker, S. J. Wukitch *et al*, *Fusion Science and Technology* **51**, 401 (2007).
- [10.30] D. W. Ignat, *Nucl. Fusion* **34**, 837 (1994).
- [10.31] R. M. McDermott, B. Lipschultz, K. Marr, D. Whyte and J. W. Hughes, *Bull. Am. Phys. Soc.* **52**, 213 (2007).
- [10.32] K. Marr, B. Lipschultz, and R. Mc Dermott, *Bull. Am. Phys. Soc.* **52**, 213 (2007).
- [10.33] P. J. Catto and A. N. Simakov, *Phys. Plasmas* **12**, 012501 (2005).
- [10.34] S. K. Wong and V. S. Chan, *Phys. Plasmas* **14**, 122501 (2007).
- [10.35] H. A. Classen and H. Gerhauser [*Czech. J. Phys.* **49** (Suppl. S3), 69 (1999)].

- [10.36] J. S. deGrassie, K. H. Burrell, L. R. Baylor, W. Houlberg and J. Lohr, *Phys. Plasmas* **11**, 4323 (2004).
- [10.37] S. K. Wong and V. S. Chan, *Phys. Plasmas* **12**, 092513 (2005).
- [10.38] M. N. Rosenbluth, P. H. Rutherford, J. B. Taylor, E. A. Frieman and L. M. Kovrizhnykh *Plasma Phys. Controlled Nucl. Fusion Res.* **1**, 495 (1971).
- [10.39] S. K. Wong and V. S. Chan, *Phys. Plasmas* **14**, 122501 (2007).
- [10.40] P. J. Catto and A. N. Simakov, *Phys. Plasmas* **13**, 052507 (2006).
- [10.41] P. J. Catto and A. N. Simakov, *Phys. Plasmas* **14**, 029901 (2007);
- [10.42] A. Simakov, P. Catto and B. LaBombard, submitted to *Phys. Plasmas* (2008).
- [10.43] Y. B. Kim, P. H. Diamond and R. J. Groebner, *Phys. Fluids* **B3**, 2050 (1991).
- [10.44] P. Helander, *Phys. Plasmas* **8**, 4700 (2001).
- [10.45] A. N. Simakov and P. J. Catto, *Phys. Plasmas* **13**, 052507 (2006).
- [10.46] P.B. Snyder *et al*, *Phys. Plasmas* **9**, 2037 (2002).
- [10.47] W. Park, E. V. Belova, G. Y. Fu *et al*, *Phys. Plasmas*, **6**, 1796 (1999)
- [10.48] C. S. Chang and S. Ku, *Phys. Plasmas* **11** (2004) 2649
- [10.49] V. Lancellotti, D. Milanesio, R. Maggiora, G. Vecchi, and V. Korytsya *Nucl. Fusion* **46** S476 (2006).
- [10.50] M. Brambilla, *Nucl. Fusion* **28** 549–563.
- [10.51] S. J. Wukitch, *Bull. Am. Phys. Soc.* **52**, 142 (2007).
- [10.52] D. A. D’Ippolito and J. R. Myra, *Phys. Plasmas* **13** 102508 (2006).
- [10.53] D. Richman and J. Wright, *Bull. Am. Phys. Soc.* **52**, 156 (2007).
- [10.54] G. Pereverzev, *Nucl. Fusion* **32**, 1091 (1991).
- [10.55] M. Brambilla, *Nucl. Fusion* **16** 47 (1976).
- [10.56] J. C. Wright, E. J. Valeo, C. K. Phillips and P. T. Bonoli, to be published in *Communications in Computer Physics* (2008).
- [10.57] J. C. Wright *et al*, *Nucl. Fusion* **45** 1411 (2005).

- [10.58] M. Choi, V. S. Chan, R. I. Pinsky, *et al*, Nucl. Fusion **46** 409 (2006).
- [10.59] S. Bourguignon, H. Carfantan, T. Bohm, Astronomy and Astrophysics **462**, 379 (2007).
- [10.60] O. E. Garcia, V. Naulin, A. H. Nielsen, and J. Juul Rasmussen *et al*, Phys. Rev. Lett. **92**, 6 (2004).
- [10.61] X. Q. Xu, R. H. Cohen, T. D. Rognlien, and J. R. Myra J.R., Phys. Plasmas **7** 1951 (2000).
- [10.62] B. Scott, Plasma Phys. Control. Fusion **45**, A385–A398 (2003).
- [10.63] P. T. Bonoli, R. W. Harvey, C. E. Kessel *et al*, 21st IAEA Fusion Energy Conference, (Chengdu, China, October 16 21, 2006) Paper IT/P1-2.

Chapter 11

Facilities

We will continue over the next five years to provide the tools needed to carry out C-Mod physics goals. These include many improvements to the ICRF systems to both maintain source power and to automate tuning. Source power for the Lower Hybrid System will be increased, and two new more efficient launchers will be installed. The outer divertor will be upgraded to accommodate the higher heat loads and to test ITER relevant tungsten lamella tiles. We will continue to improve diagnostic systems, data acquisition hardware and software, magnet power supplies and plasma control. We show current major machine parameters for the Alcator C-Mod facility in Table 11.1.

TABLE 11.1

Major Facility Parameters for Alcator C-Mod

Major Radius (m)	0.68
Minor Radius (m)	0.21
Maximum Elongation	1.85
Maximum Triangularity	0.85
Maximum Toroidal Field (T)	8.11 (9 T design)
Maximum Plasma Current (MA)	2.02 (3 MA design)
Plasma Volume (m ³)	1
Maximum Discharge Length (s)	<5
Maximum Stored Plasma Energy (kJ)	250
Vessel Volume (m ³)	4
TMP Pumping Speed N ₂ (l/s)	2000
Effective Pumping Speed N ₂ (l/s)	500
Ohmic Heating Power (MW)	2.7
ICRF Source Power (MW)	8
Lower Hybrid Source Power (MW)	3
Peak Utility Power (MW)	24
Peak Extracted Power Alternator/Flywheel (MVA)	400 design
Total Stored Energy Alternator/Flywheel (GJ)	2

11.1 Highlights of Recent Research

Several major engineering systems came on line over the past five years including the lower hybrid system, upper divertor cryopump, and major improvements to our ICRF systems. We also continued to improve control and data acquisition systems.

11.1.1 Tokamak Systems and Diagnostics

A major accomplishment during the last proposal period was operation of the Lower Hybrid system with up to 1200 kW of coupled power and substantial amounts of plasma current drive [1,2]. An unexpected challenge during this process was the development of stainless steel couplers to replace the original titanium ones that degraded dramatically in the C-Mod plasma environment. New techniques had to be developed to braze the alumina vacuum windows to the coupler waveguides. We show an in-vessel picture of the couplers and lower hybrid protection limiters in Fig. 11.1. A very large effort was also required to bring on line a remarkable array of control and protection instrumentation [3-9]. These systems allow for very flexible phase and amplitude control of the klystrons, and thus the launched spectrum, with rapid changes possible during a plasma discharge [10]. We have also made important progress in the design of new lower hybrid launchers Fig.11.2. A novel 4-way splitter design will be used to greatly simplify the fabrication of the new launcher. In Fig. 11.3 we show a simulation of the splitter indicating proper power splitting and relative phase at the four output ports. Sixteen splitters will be used in each launcher. They will be fed by standard WR-187 waveguide and will require a much simplified feed system compared to our current launcher.

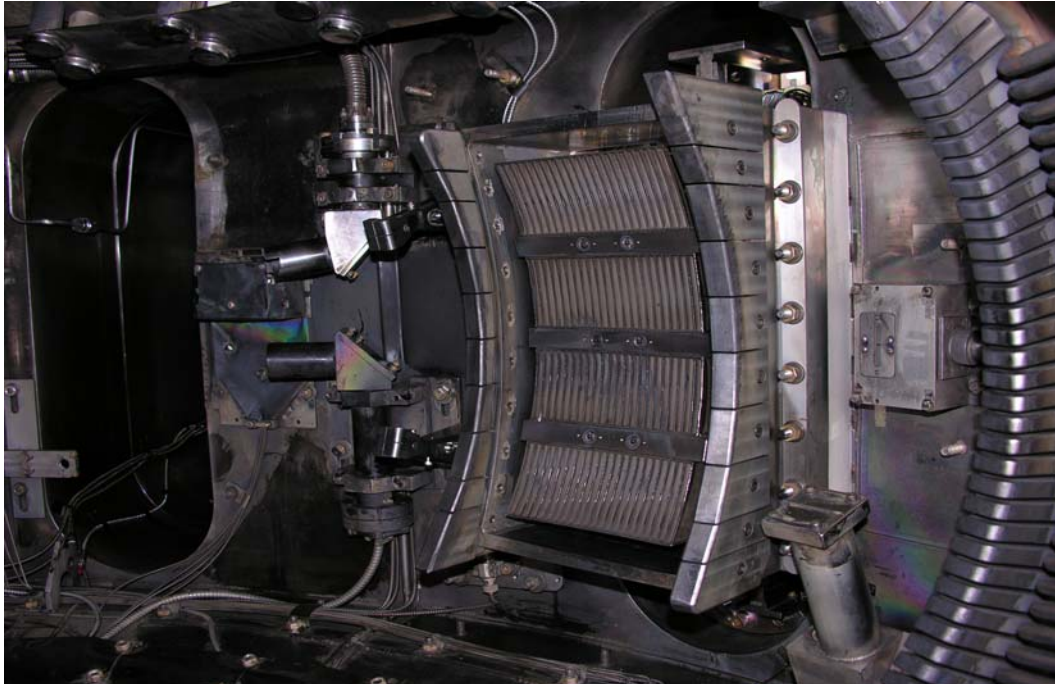


Figure 11.1 Lower Hybrid couplers and molybdenum protection limiters

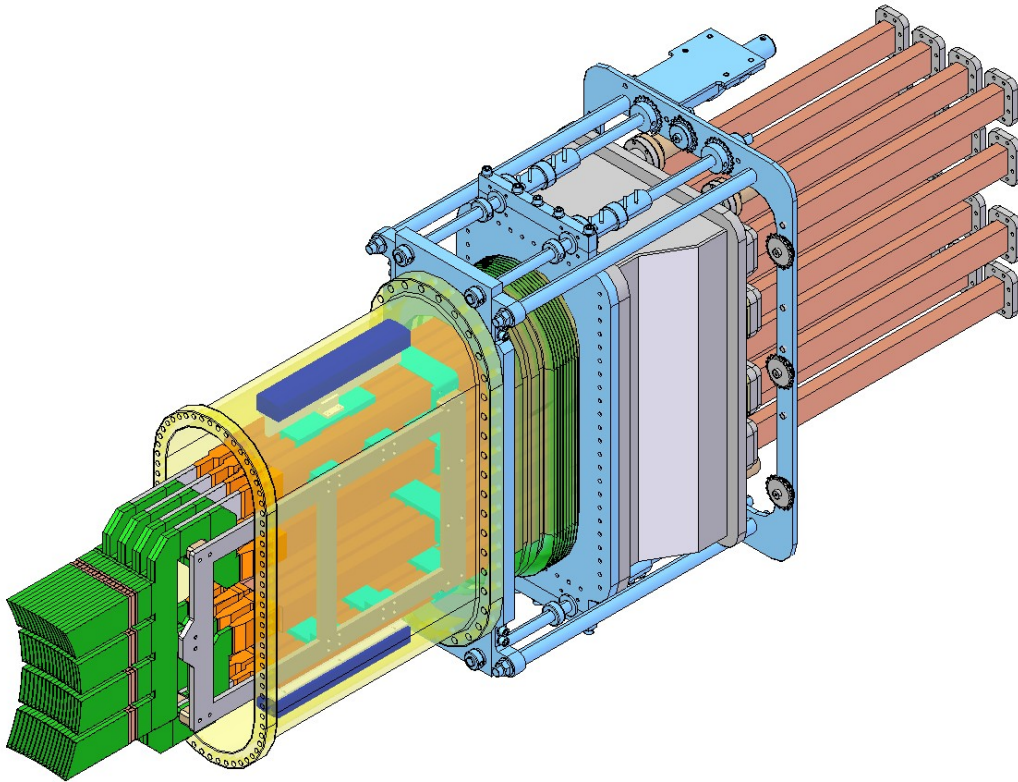


Figure 11.2 Design of the new launcher is shown. Couplers are fed by new 4-way splitters (both shown in green). Standard waveguides feed the splitters providing a very low loss transmission system.

Another major accomplishment has been the design, fabrication, and installation of the upper divertor cryopump which became operational during the FY2007 run campaign [11]. The design is unique among the world's tokamaks, employing an array of gas-pumping slots that penetrate the upper divertor target. This geometry enables the use of a single toroidal loop of liquid helium, operating in an efficient 'pool boiling' regime. A system pumping speed of 9,600 l/sec for D_2 gas has been achieved, matching that of the full-scale prototype system used to refine the design before installation. Neutral pressures in the upper divertor during upper-single-null plasmas (USN) are found to meet or exceed pressures in the lower chamber during lower-single-null (LSN) – evidence that the slot geometry and baffling structures are performing as intended. Very high steady-state pumping throughputs (exceeding ~ 140 torr-l/s) have been demonstrated in USN. Reliable and efficient operation of the pump has been established, synchronized with the standard C-Mod shot cycle and consuming only 60 to 90 liters of liquid helium during a full day of

operation. A picture of the upper divertor hardware and pumping slots is shown in Fig.11.4. This system has already proved to be very reliable and is being used during most C-Mod run days. In Fig.11.5 we show the cryopump during installation. The liquid nitrogen cooling shield is clearly seen.

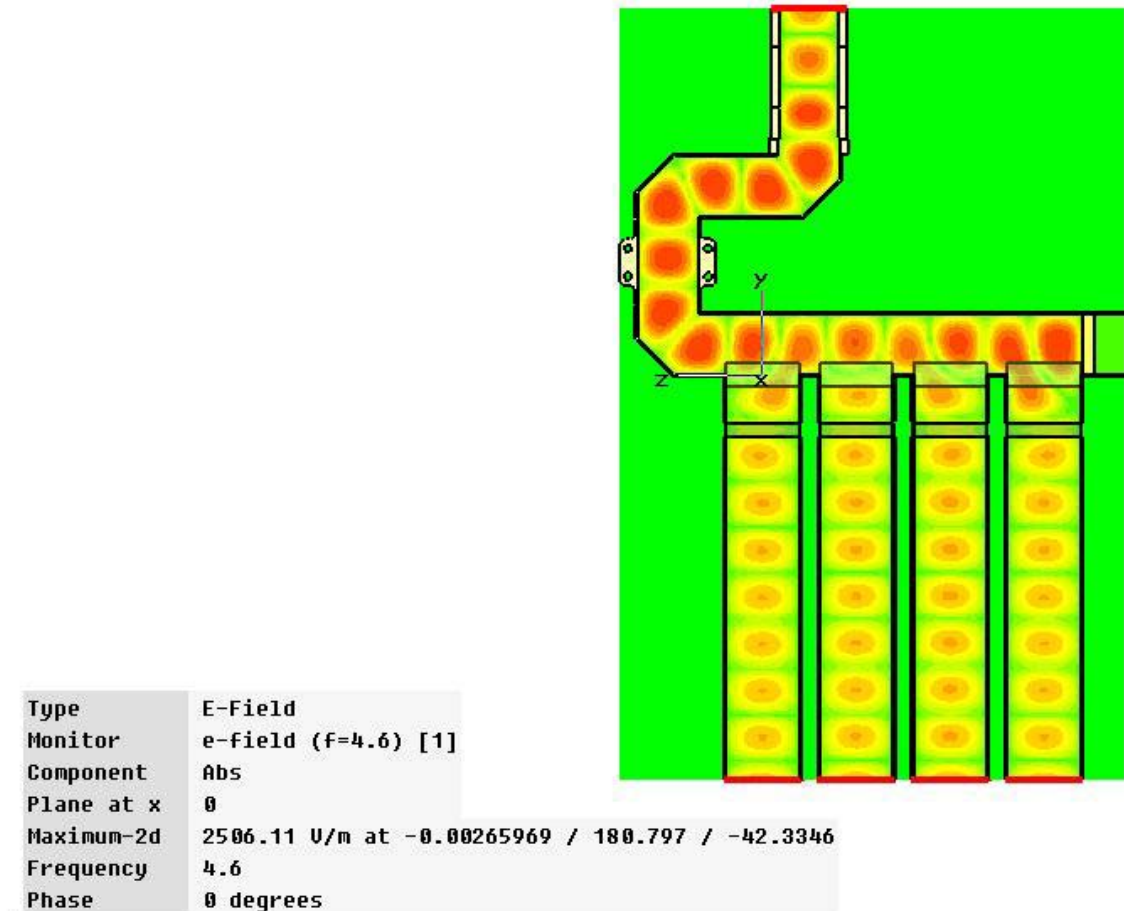


Figure 11.3 The electric field of the propagating waves in the 4-way splitter is shown. Power is fed into the splitter at the top of the figure through a transformer which matches the WR-187 waveguide to the splitter. Both amplitude and phase balance are very good in this design.

We have continued to develop ITER relevant upgrades to our first wall. A set of tungsten brush tiles were installed and tested on C-Mod in FY2005. We have more recently installed a toroidal belt of 120 tungsten lamella tiles Fig. 11.6 They have performed well during two run campaigns, and will very likely be the design basis for the new outer divertor upgrade planned for FY2011.

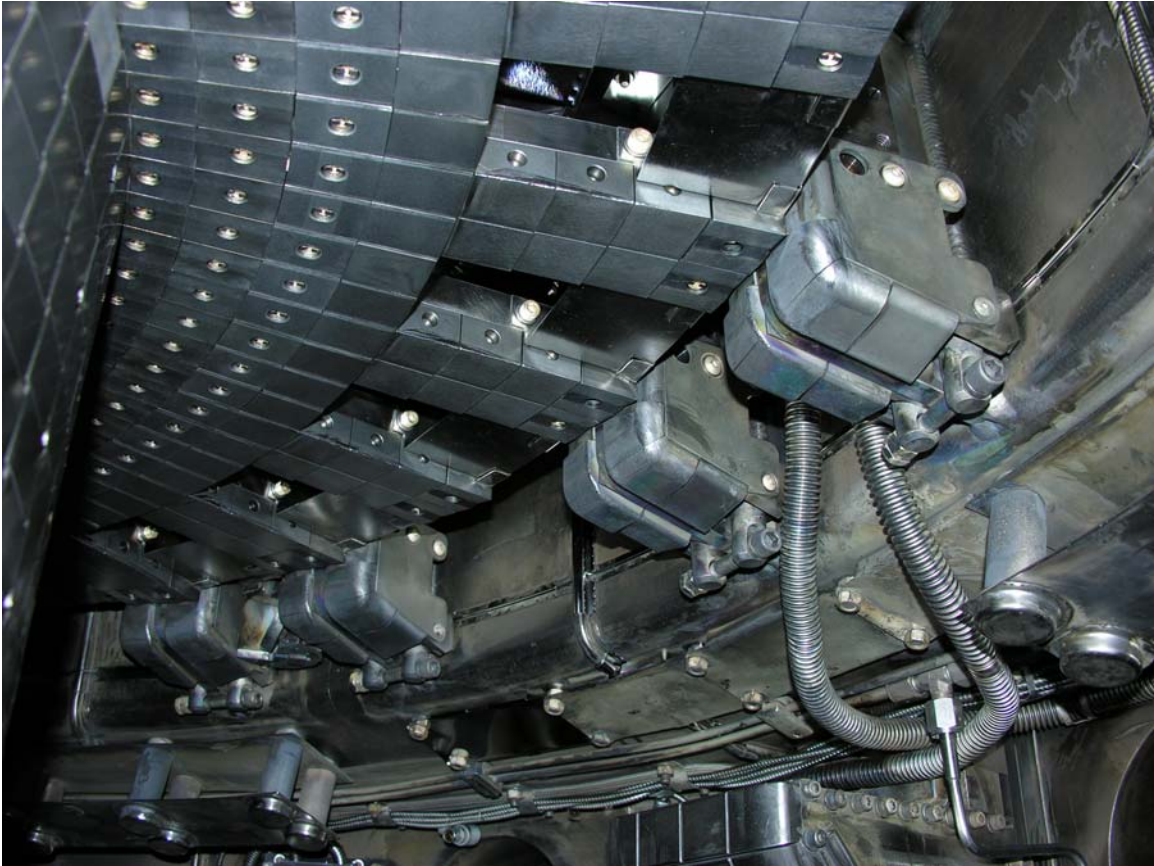


Figure 11.4 View of upper chamber showing protection tiles and pumping slots. Upper strike point can be moved near the slots to control pumping. The cryopump is inboard of the slots above the protection tiles. Baffles at the outboard end of the slots help control gas flow.

Many upgrades and improvements have been made to the ICRF systems. The rf control and protection system for all transmitters has been upgraded. Improvements have also been made to the switch gear and crowbar systems. Several improvements have been made to the J-Port 4-strap antenna and transmission line components to increase its power handling capability.

We have also worked to bring the fast ferrite tuner (FFT) prototype into operation. This system, feeding the E-Port antenna, has proved to be of great help in maintaining coupled power to the plasma. It has maintained a good match to plasmas that have resulted in faults on the other antennas, and has required less attention from the ICRF operators. We have worked to reduce the rf voltages seen by the FFTs, using pre-matching techniques, in an effort to increase the power handling capability of these devices. We plan to install FFTs on all antennas by FY2012.

We have continued to improve machine related instrumentation. Scanners needed to monitor TF temperatures and joints resistances, and to monitor vessel temperatures have been upgraded. The PC to PLC interface software has been upgraded and important new capability including the ability to log data very rapidly to MDSplus has been added.



Figure 11.5. A view of the upper cryopump during installation. The liquid nitrogen shield is shown along with some of the liquid nitrogen feeds. Bellows in the feed-lines allow the cryopump to be assembled from three sections that can be passed through ports separately.

Important machine operating parameters are now available online. MDSplus scopes allow trend information to be displayed remotely.

Major inspections of the 225 MVA alternator and flywheel were successfully completed in FY2003. Several minor inspections have taken place over the grant period to ensure safe operation of these vital systems.

In an effort to improve the diagnostic capabilities for measuring profiles of plasma rotation and ion temperature on Alcator C-Mod, an imaging x-ray spectrometer has been designed and installed in collaboration with PPPL. This instrument uses spherically bent quartz crystal and a set of 2D x-ray detectors to image the entire plasma cross section with a spectral resolving power of approximately 10,000 and a vertical chordal resolution of about 1 cm. Line emission from highly ionized states of argon and molybdenum are measured at frame rates up to 200Hz. Using spectral tomographic techniques the line integrated spectra can be inverted to determine impurity density, velocity and temperature profiles.

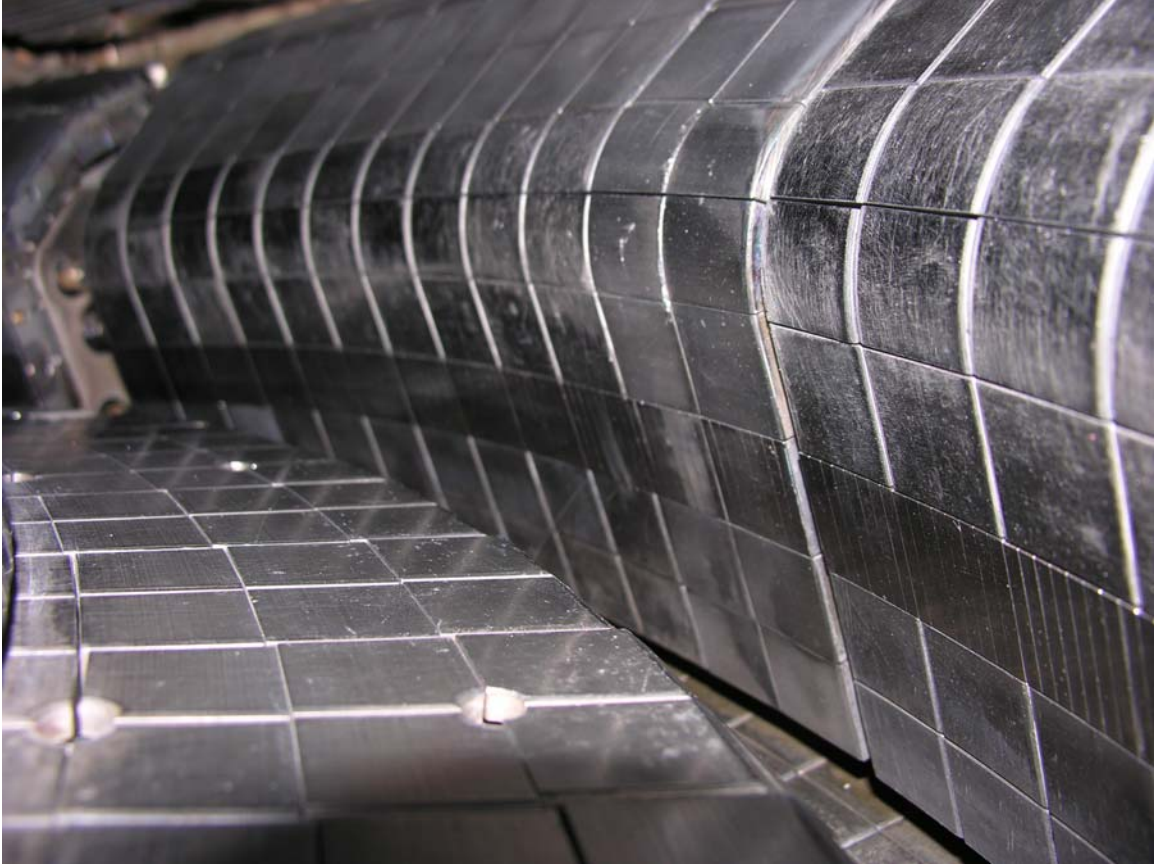


Figure 11.6. Tungsten belt of lamella tiles. These tiles have successfully endured two run campaigns and are expected to provide the design guidance for our outer divertor upgrade.

Another new diagnostic, the Surface Science Station (S^3) has been installed to provide detailed information about deposition on the vacuum vessel wall from boronization and other plasma processes. Understanding the deposition process is critical to developing better boronization techniques. The main diagnostic tools on S^3 include two quartz micro balances (QMBs), one viewing radially and the other viewing poloidally/ toroidal, and a Langmuir probe for n_e and T_e measurements. This diagnostic is capable of linear translation along the major radius for $R > 0.58$ m.

We have begun fabrication of an FIR polarimeter diagnostic for C-Mod. A dual FIR laser system, FIR detectors, waveplates and polarizers have been procured. In addition, a set of retro-reflectors has been installed on the inner wall, and a shuttering system has been developed to protect them during boronization. We have very successfully run a CO_2 interferometer using these retro-reflectors and shown that very good density measurements can be made, and that vibration levels from the inner wall are not too severe for operation of a polarimeter system. Faraday rotation techniques have also been investigated on C-Mod in a effort to pick the best technique for the FIR system.

The edge Charge Exchange Spectroscopy (CXS) system includes both toroidal and poloidal DNB viewing periscopes on the low field side as well as a high-field side

toroidal periscope, which uses an inner wall gas puff to localize its measurement. The system enables concurrent measurements of poloidal and toroidal velocity as well as the temperature and density of impurity ions in the edge pedestal region ($0.8 < r/a < 1.08$) with 3 mm radial resolution. The periscopes are coupled via fiber optics to high throughput Kaiser spectrometers and Photonmax CCD cameras capable of taking data on millisecond time scales, although an integration time of 5ms is typically employed due to signal level limitations. This system has demonstrated the existence of an impurity ion temperature and density pedestal, large poloidal velocity shear, and a steep negative radial electric field well just inside the LCFS during H-mode operation. In future campaigns, this diagnostic will be used to examine the structure and parametric dependence of the edge radial electric field, to probe low and high field side velocity and density asymmetries, and to provide a key measurement to connect core and SOL flow measurements for momentum transport studies.

A gas injection system has been installed to improve the coupling of the LH launcher by locally increasing electron density in front of the antenna. Similar gas injection systems on other Lower Hybrid systems (JET, ASDEX) have been shown to improve wave coupling, particularly in the presence of high power ICRF. Two pre-existing capillaries were rerouted inside the C-Mod vacuum vessel in the fall of 2007. These capillaries are used to inject D₂ gas into the area between the LH launcher and the LH limiters. The capillaries are mounted at fixed locations in the upper right and lower left corners of the limiter box (viewing out radially).

Alcator C-Mod now has an outboard hard x-ray diagnostic designed to detect Bremsstrahlung radiation from LH-driven nonthermal electrons. Thirty-two chords span the poloidal cross-section of the plasma, giving a spatial resolution of ~1 cm. Each chord terminates at a CZT solid-state detector, whose output is fed into a pre-amplifier and then into a pulse shaper card. The pulse train is sent to a digitizer and then stored in raw format for each shot, allowing for flexible time and energy binning during post-processing with a maximum time resolution of ~1 microsecond. The entire camera is encased in a lead shield, with a pinhole at the front of the camera. Inner aluminum shielding attenuates lead k-shell radiation. This system has provided important information about the lower hybrid driven electron distribution.

MSE has successfully measured off-axis current drive due to LHCD for the first time in Alcator C-Mod. We observed LH-driven changes in the local pitch angle of up to 15%, and the inferred current density profile is in qualitative agreement with CQL3D simulations. The cause of a long-standing MSE reproducibility problem has been identified: temperature variations in the in-vessel MSE optics cause mechanical stress and associated stress-induced birefringence that yields spurious changes in the polarization angle. Design changes are under investigation to eliminate this problem, including replacing the in-vessel lenses with spherical mirrors. In addition, a long-standing anomaly in MSE calibrations based on a beam firing into a gas-filled torus has been resolved. Experimental observations, supported by theoretical calculations, indicate that polarized light emitted from beam neutrals that ionize, gyrate about magnetic field lines, and then re-neutralize at a random gyro angle contaminates the measurement. The deleterious effect on the calibration was significantly reduced by pivoting the diagnostic neutral beam toroidally by 7°.

We have also made improvements or added new capability to the bolometry, gas puff imaging, magnetics, core and edge Thomson Scattering, fast scanning probes and probe arrays, neutral particle, neutron, plasma video and ultra high speed cameras, active MHD [12], neutral pressure, halo/Rogowski, PCI, and interferometry diagnostic systems. The Long Pulse Diagnostic Neutral Beam has developed into a reliable diagnostic system [13].

11.1.2 Data Acquisition and Computing

The C-Mod data acquisition and computing systems have evolved to meet the challenge of rapidly growing demands. Currently almost 8,000 channels of diagnostic data are acquired and made available for analysis and display between discharges, with over 2 GB of data added to the archive for every shot. The hardware system is based on a highly distributed network of servers and workstations which has allowed incremental upgrades to match the rise in demand and to take advantage of new technology developments. MDSplus, the data acquisition and management software system developed for C-Mod, has proven to be an extremely powerful and flexible tool (see <http://www.mdsplus.org/>). Its success has led to its adoption by teams from many other experiments.

A new all-digital plasma control system (DPCS) has been developed and deployed on C-Mod [14]. On its first day of operation in 2005, DPCS successfully replaced the original hybrid control system. The system, based on off the shelf CPCI components, has evolved to include nonlinear signal processing, and real time computing. The flexible structure of the PCS software allows the user to incorporate custom procedures at various stages of the real-time computation loop. Many have been implemented and successfully tested, and are routinely active during C-Mod runs. They include fizzle detection, input offset subtraction, active MHD antenna control, disruption mitigation, lock-mode detection and Kalman filtering. Work is on-going for the implementation of non-linear adaptive interpolation algorithms to respond to off-normal events and avoid potential disruptions. Some of these procedures significantly benefited from off-line benchmarking with Alcasim simulations [15, 16, 17]. Alcasim is a large Matlab-Simulink application including models of the tokamak and plasma, the magnetic diagnostics, the control system and the poloidal power supplies. Plasma parameters are read from reconstructed equilibria, and the database-driven approach greatly reduces the simulation time without sacrificing the accuracy. Alcasim has been used to perform axisymmetric non-linear simulations of plasma discharges: examples of applications include the analysis of the stability of C-Mod plasmas and the benchmark of advanced algorithms such as a real-time vertical position observer based on a Kalman filter and an adaptive non-linear algorithm which will anticipate and avoid the saturation of poloidal field power supply control currents.

New PC to PLC interface software, RSVIEW, has been implemented for all engineering systems. This software provides much better trending capability with update rates as high as several samples per second. These data are now stored using the new MDSplus continuous data stream capability. Magnet and vessel temperatures, vacuum conditions,

RGA spectra, and instrumentation current and voltages can now be recorded at fast time scales relative to a shot cycle time, viewed using MDS Scopes, and then processed using IDL.

The computer systems and associated infrastructure continue to be improved to handle increasing data loads. The transition from OpenVMS based servers and workstations to predominantly Linux-based systems has been completed [18]. Currently, the control room is outfitted with 46 high powered Linux workstations used by scientists and engineers for control, data analysis and visualization applications. In addition, there are 7 shared server systems for providing data acquisition, data archiving, web server, database and backup functions. All C-Mod data acquired since the first days of operation in 1991 are accessible online. To provide this capability approximately 16TB of RAID disk storage has been installed.

A new web based electronic logbook has been developed [19]. The new logbook is accessible using any web browser and enables the user to view and make new entries. There are currently over 160,000 text entries in the logbook, most manually entered by users during experimental runs. The logbook information is stored in a database structure, making it fully searchable using SQL software tools. This tool provides an invaluable resource for finding data and documenting experimental conditions. The logbook interface provides automatic updating and displays the current operational state of the machine. Summary information about each C-Mod run is available via the web including logbook entries, mini-proposals key personnel, shot information and plots of key measurements.

The use of technology to improve off site collaboration is becoming more and more important [20]. Two new video conference facilities have been constructed and are regularly used. All C-Mod group meeting and many technical meetings are attended remotely by remote collaborators. The C-Mod group participated in the development of the fusion GRID [21,22], which is being used to manage remote code invocation for TRANSP.

There have also been significant changes in the data acquisition technology used on the C-Mod experiment. The majority of the data is now acquired using CPCI boards instead of CAMAC modules. These boards provide low cost, high speed data acquisition enabling us to keep up with the expanding data acquisition requirements. These boards, or the servers associated with them, have high-speed Ethernet connections, allowing rapid transmission of acquired data to the storage archives.

Throughout the life of the project, there has been an ongoing effort to upgrade the local area network (LAN) to carry the higher traffic loads from an increasingly faster array of computers. Currently the LAN is based on switched 1 GB technology with a Gbps backbone. Connectivity to the outside world is via a T3 (45 Mbps) line provided through ESnet.

A set of three large project screens have been installed in the front of the C-Mod control room to replace the hardwired engineering displays which had been used since the experiment's commissioning. The new technology allows displays to be more easily customized for ongoing operations.

11.1.3 MDSplus

MDSplus software maintenance, bug fixes and ongoing support for off-site installations continues to be a major activity for the MDSplus development group. New support for data acquisition hardware was added, with emphasis on CPCI devices which is increasingly prevalent. Support for new IEEE-1394 camera models has been added. Site specific work has been done for experimental groups at Columbia University, PPPL, University of Wisconsin, LDX (MIT/Columbia University), DIII-D, UCLA, and University of Washington.

The major software development activity in recent years continues to be the support and enhancement of the MDSplus Data System which now runs on a wide variety of computing platforms. MDSplus is by far the most widely used data system in the international fusion program. It is used in its entirety for the data acquisition and analysis systems for TCV (EPFL - Switzerland), RFX (IGI - Padua), NSTX (PPPL), Heliac (ANU - Australia), MST (U. Wisconsin), HIT, TIP, TCS and ZAP (U. Washington), PISCES (UCSD), CHS (NIFS - Japan), LDX (MIT), HBT-IP and CTX (Columbia U.) and of course C-Mod. It is used to store processed data for DIII-D, for the collaborative data archives assembled by the ITPA, and for the inputs and outputs of several widely used codes, including EFIT, TRANSP and GS2. JET and ASDEX-Upgrade are using MDSplus as a remote interface to existing data stores, and KSTAR has adopted it as a data acquisition engine for data stored in other formats. The result is a de-facto standard which greatly facilitates data sharing and collaborations across institutions. At the same time, the breadth and variety of uses for MDSplus has increased the burden of supporting and documenting the system. A web site, <http://www.mdsplus.org> has been built to support the widespread user base and documentation is currently undergoing a major upgrade. The web site has been converted completely to a WIKI based system which makes it much easier to manage and update. MDSplus users worldwide are encouraged to participate in keeping the MDSplus online documentation accurate and up to date. Installation kits for all the supported platforms have been built and can be accessed this web site. MDSplus installation kits are upgraded frequently and made available on the MDSplus web site for a number of computing platforms. To date there have been over 5000 downloads of MDSplus installation kits

The MDSplus system has also been enhanced with the addition of some capabilities for handling the storage of continuous data streams [23]. Prior to these enhancements, MDSplus was suitable for storing only pulse based data but now it is possible to append data from continuous data sources. For example, much of the trending data such as the monitoring of the vacuum and cooling systems of the C-MOD experiment are now recorded using MDSplus. These enhancements will make it possible to use MDSplus on experiments with long pulse or continuous operation where it is impractical to wait for

the pulse to complete before acquiring and analyzing the data. This feature is currently in use at the C-Mod experiment at MIT for storing continuous trend data and for storing data from high speed cameras.

The MDSplus developers are actively participating in design discussions for the ITER CODAC system to ensure that the system used on ITER includes many of the valuable capabilities provided by MDSplus.

11.2 Proposed Research

We show in Table 11.2 below an availability plan for the next five years consistent with the research goals expressed in previous chapters of this proposal. We show both a baseline plan and what could be done with incremental funding (shown in red). Our major goals include providing as much rf power as possible while also providing the needed diagnostics and machine hardware to move the physics program forward.

TABLE 11.2
Availability Dates for New Systems and Inspections

	2008	2009	2010	2011	2012	2013
ICRF						
IPA to 10 kW	X					
New 4-strap Antennas		X	X			
Lower Z _p at 80 MHz (all FMITS)		X				
Variable Freq #1 and #2 FMITS					X	
FMIT Upgrades to 120 MHz						X
FFT all Transmitters					X	
Switchgear/Crowbar Upgrades						X
High Voltage Power Supply Upgrade						X
FPA procurements	X			X	X	
Lower Hybrid						
4th LH cart		X				
2nd and 3rd LH Launcher (3rd replaces 1st)		X		X		
LH HVPS Upgrade		X				
LH Water System Upgrade		X				
klystron rebuilds	X	X	X	X		X
new klystrons	X				X	
TPS Upgrade			X			
Boundary						
Outer Divertor Upgrade				X		
Improved PFCs	X	X	X			
Limiter Upgrades		X				
Operations						
alternator/flywheel inspection	X			X		
cryo upgrade		X				
machine inspection		X				
Helium recovery system			X			
ECDC/Boronization Upgrades	X					

DAQ Upgrades		X	X	X	X	X
Data Archives		X	X	X	X	X
Network Infrastructure (10 Gbps)		X	X	X	X	X
Workstations and Personal Computers		X	X	X	X	X
Online data storage		X	X	X	X	X
PSFC computing upgrade					X	
Digital Plasma Control System			X	X	X	X
Vacuum Equipment		X	X	X	X	X
EF2 upgrade						X
EFC upgrade				X		
Correction Coil Upgrade (MHD)						X
Diagnostics						
DNB Power System and Cntrl Upgrade			X			
MSE Upgrade (in vessel)		X				
MSE Upgrade (external optics/electronics)			X			
Californium/Cal Source		X				
Thomson Scattering Upgrades			X			
polarimetry (L_n, ~b)		X				
divertor probe arrays and upgrades	X	X	X			
Flux Loop Upgrade	X	X				
fast ion loss diag						X
runaway electron diag						X
reflectometry upgrade		X				
Doppler reflectometry				X		
HECE view					X	
Multichannel CNPA		X				
antenna reflectometry upgrade			X			
CO2 scattering			X			
SPRED Spectrometer		X				
In-Situ Accelerator (wall films)			X			
IR Camera Upgrade			X			
Upper Divertor TC Upgrade			X			
Fast Diode Array Upgrade		X				
Two New GPI Views		X				
High Harmonic ECE				X		
Reflectometry fluc at 4.6 GHz	X					
Inner Edge GPI/CXRS	X					
Outer Edge GPI/CXRS		X				
CXRS Measurement of Fast Ions			X			
Operation (weeks)	15	10	14/25	14/25	14/25	14/25
	2008	2009	2010	2011	2012	2013

11.2.1 Tokamak Assembly and Power Systems

A primary engineering task during FY2008 and FY2009 will be the inspection of the tokamak. C-Mod has operated very reliably since the last inspection in FY2002, with over 13,000 machine cycles at $B_t > 5$ T. C-Mod will be completely disassembled and all components of the machine will be carefully checked. The TF sliding joint felt-metal will be a major focus of the inspection, and we will be prepared to replace felt-metal contacts as required. OH coax joints will also be carefully inspected and reconditioned if required. The vessel heater system, machine instrumentation, cooling manifolds, bus connections, and cryostat will be refurbished and improvements made as indicated by the inspection results. During FY2008 we will also perform routine inspections of the alternator and flywheel. High Pots and tomographic ultrasonic testing of critical components will be done, as well as inspections of all the bearings. Refurbishment of instrumentation will continue.

As available power levels from the rf systems increase and pulse lengths are extended, impurity generation from the current outer divertor will become more of an issue. Changes were made to the inner divertor in FY2002 to upgrade it to accommodate these higher heat flux and fluence levels. Changes to the outer divertor are now planned that will allow it to function more robustly during high performance, longer pulse, operation of C-Mod. The new design will consist of a continuous toroidal belt without open spaces at vertical ports, in contrast to the current outer divertor design. The design of the plasma facing surface will be a simple cylinder that will be much easier to fabricate and install than the current outer divertor Fig. 11.7. We plan to use a tungsten lamella plate design, similar to the row of tungsten plate tiles currently installed in the high heat-flux region of the outer divertor. The new divertor will be designed to be bakeable, and operate reliably at an average temperature of 600 C, which should be beneficial for the removal of hydrogenic species. The new outer divertor will become available in FY2011.

Upgrades to the liquid nitrogen cooling system will simplify the control of the nitrogen flow and also improve the speed at which the magnets can be cooled. Improvements to the liquid nitrogen cooling system will also be considered during the machine inspection.

Given incremental funding, we will upgrade our EFC and EF2 power supplies in FY2010 and FY2013. The EF2 supply will be designed for faster response and will go from a 2 quadrant to a 4 quadrant supply. The EFC supply response time and current range will be improved. These upgrades will allow greater shape control, improved stability, and higher plasma current capability.

11.2.2 RF Systems

We will make upgrades to the lower hybrid system in FY2008 and FY2009 to increase the lower hybrid power coupled to the plasma and add the ability to generate compound spectra from the launchers. The number of klystrons will be increased from 12 to 16 with the addition of a 4th klystron cart. Available source power will then increase from 3 to 4 MW. We will also add a 2nd lower hybrid launcher in FY2009. The new launcher

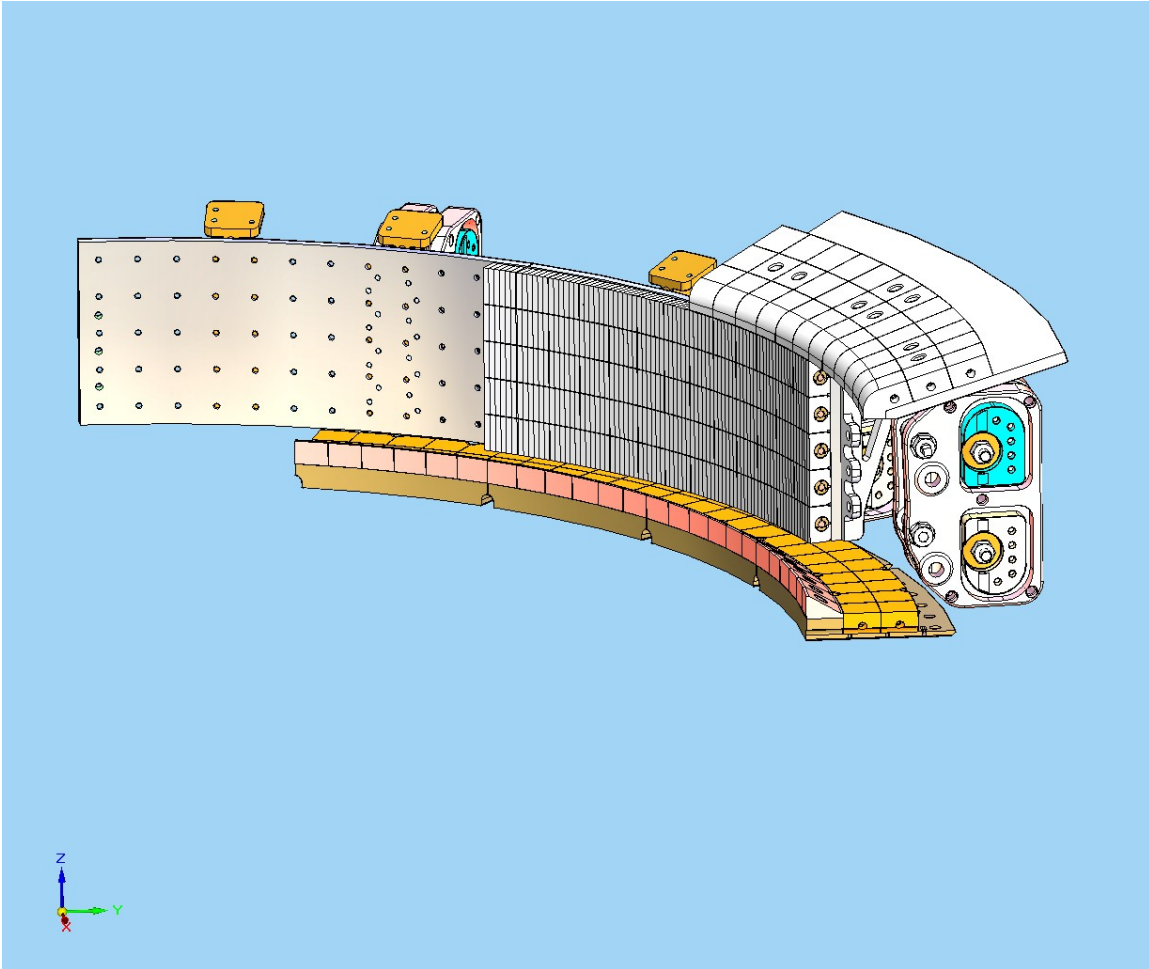


Figure 11.7. A conceptual design of the lower divertor upgrade is shown. W-lamella tiles forming cylindrical belts will be used in the high heat flux regions. Existing vessel gussets are shown providing support for divertor components.

will make use of the new 4-way splitter design recently developed and tested, significantly simplifying design and fabrication. We will both refurbish old klystrons and buy new ones so that 16 klystrons, and an acceptable number of spares, will be available for operation. We will continue to upgrade protection and control systems for both the klystrons and the launchers (complete by FY2010). These new systems will integrate high speed digitizers and field programmable gate arrays with rf and optical detector signals to protect the klystrons, launchers, and couplers. Upgrades will be made to both the klystron water cooling system and the high voltage power supply to support the additional klystrons and long pulse operation by FY2009. A second new launcher will replace the first launcher in FY2011 allowing another increase in coupled lower hybrid power.

We will also continue to improve and upgrade our ICRF systems. New 4-strap antennas will be installed in FY2009 and FY2010 that have been designed to reduce rf sheath

rectification effects while freeing up port space for diagnostics Fig. 11.8. FFT systems will be added to all rf antennas by FY2012. Changes to the FPA output cavities will lower the impedance and provide better coupling to the transmission lines in FY2009. Tube based IPA components will be replaced with solid state ones, for enhanced reliability (FY2008). New switch-gear and solid-state crowbar units will be added to significantly reduce the complexity of our protection systems and increase their availability (FY2013). Upgrades to the high voltage power supplies will be made in FY2012 and FY2013 to provide more robust voltage regulation and improved reliability. This upgrade will allow full ICRF power to be maintained over a broader range of plasma conditions.

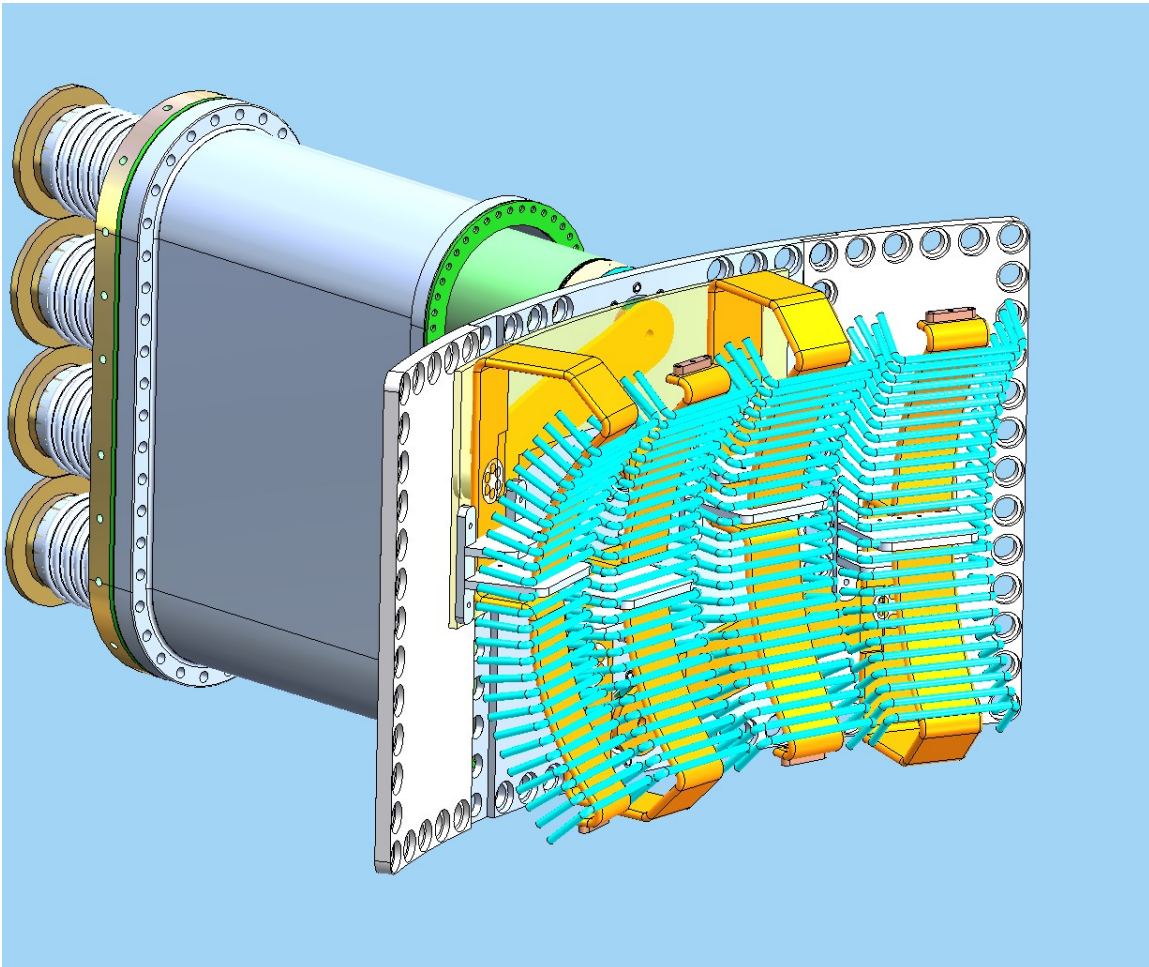


Figure 11.8. New 4-strap antenna showing current straps, Faraday screen, vacuum feeds, striplines, and supporting back plate. Box enclosure is not shown.

The deposition of boron on first wall surfaces is required for high performance operation of C-Mod. We have traditionally boronized using approximately 2 kW of microwave power at 2.45 GHz, with an applied toroidal field to provide a cylindrical electron cyclotron resonant surface. New measurements with the S³ diagnostic have indicated that

more fundamental power at a higher frequency would improve the efficiency of this process and the precision by which the coatings are applied. We plan to upgrade our boronization system in both available power and to a higher frequency to take advantage of this new information. We are also investigating the use of molybdenum tiles with thick boron coatings in areas most affected by rf induced boron erosion (FY2009). A small number of such tiles have been installed in C-Mod for two run campaigns without noticeable degradation.

11.2.3 New Diagnostics and Diagnostic Upgrades

DNB Power System and Control Upgrade – An upgrade of the long pulse DNB system is proposed that would provide direct feedback on beam current to achieve constant output beam current using arc current as the actuator. Replacement of the proprietary Russian control sequencer and java control software with one of our own design will simplify operation and modification and allow use of readily available equipment. Upgrade of the existing DNB power to utilize an ultracapacitor storage system will provide a much more efficient power grid interface and facilitate faster turn-on of each modulation pulse to allow better use of short modulation cycles. Replacement of the analog-based control system with digital controls will allow more flexible control of the beam parameters. The addition of beamline apertures, one of which is water cooled, will improve the spatial resolution of the beam related diagnostics.

MSE Upgrades – Modifications will be made to the in-vessel collection optics in 2008 and 2009 to reduce the effects of thermally induced stress birefringence in the MSE lenses. This change may involve replacing the lenses with aspheric mirrors. We will also move the view to the midplane. We will improve the spatial resolution of the MSE system by a factor of two in FY2010 with the addition of new fibers, image dissectors, detectors, and data acquisition.

Californium Calibration Source – Californium is an intense emitter of neutrons and is used to calibrate C-Mod neutron diagnostics. Its half life of less than three years mandates its periodic replacement which is planned for FY2009.

Thomson Scattering Upgrades – The next significant upgrade to the Thomson scattering diagnostic set will be a dedicated instrument measuring electron temperature and density profiles in the scrape-off layer. The new diagnostic will be designed to complement the existing edge TS, which is optimized to cover the H-mode pedestal, and will effectively reduce the lower bounds on measurable n_e , T_e and extend radial coverage into the SOL. The design goal will be to have several spatial measurements with 2–3mm radial resolution. Whereas currently SOL profiles are obtained with scanning Langmuir probes, which limits data collection mostly to low-power and Ohmic discharges, SOL TS routinely will provide upstream profiles for use in studies of SOL particle and heat transport, across a broad spectrum of operational regimes. Diagnostic design will proceed in FY2008–09, followed by procurement and deployment in FY2010.

Polarimetry – A multi-chord poloidally viewing, ITER relevant, FIR polarimeter will be available in FY2009 on C-Mod. This system will operate at 117.73 μm , a wavelength with acceptable refraction and sufficient Faraday rotation to provide high quality data. This system will supplement the MSE system, particularly during high density operation.

Flux Loop Upgrade – During the machine inspection period redundancy will be increased on critical flux loop measurements. Non-functioning loops will be replaced.

Fast Ion Loss Diag – This new diagnostic will provide high time resolution (1 MHz) measurements of the energy spectrum of the fast ions that leave the plasma due to Alfvén eigenmodes or other large amplitude MHD activity such as NTMs. The envisioned energy range is from 50 keV to 400 keV. This diagnostic will use the toroidal field to image the ions onto a scintillator. It will become available in FY2013.

Runaway Electron Diagnostic Integration – The hard x-ray camera (HRX), visible video cameras viewing synchrotron radiation, and IR and visible cameras looking at outer limiters, will be integrated into a system capable of monitoring runaway electrons by FY2013.

Reflectometry Upgrade – In collaboration with PPPL we will continue upgrades to the reflectometry system to improve correlation measurements and extend the density range of the diagnostic.

Doppler Reflectometry – A reflectometry system will be installed in FY2011 optimized to study the propagation and k-spectra of density fluctuations in C-Mod.

High Harmonic ECE – The instrument will be capable of providing ECE data from approximately 150 to 1000 GHz. A scannable, vertically viewing chord measurement of the harmonic content of the radiation is expected to be a good measure of the energy of the non-thermals and in fact may provide a more direct indication of the distribution function of the non-thermals than our imaging X-Ray system. Simulations and theoretical development of this diagnostic are underway.

Reflectometry Measurements of Fluctuations at 4.6 GHz – A reflectometry channel will be added with sufficient bandwidth to allow direct observation of density fluctuations caused by lower hybrid waves.

New GPI/CXRS Systems – New outer and inner plasma edge CXRS views will be added at gas puff imaging locations to better measure poloidal flow velocities.

CXRS Diagnostic for Fast-ions – The fast-ion population in the plasma can be detected, and its density and energy distribution measured, via charge exchange of the fast-ions with an injected beam of neutral hydrogen. The newly formed fast neutral is then observed as Doppler-shifted H_{α} emission which stands out as a wing in the ambient background spectrum of D_{α} . The newly formed fast neutral retains the velocity vector of the fast ion. The rate of production of fast neutrals from fast ions is a well-understood process. Thus, the spectral measurements of the fast neutrals provide detailed information on the kinetics and the density of the fast ion population. The emission is detected in the visible spectral region using standard optical techniques. Light is collected from the plasma along individual chords, which intersect with the neutral beam. Thus, the measurement is localized to the beam intersection region. The light from each chord is spectrally analyzed in a high-throughput, imaging spectrometer. This instrumentation is much like that already in use for charge exchange spectroscopy on C-Mod. We expect this diagnostic to become available in FY2010.

Horizontal ECE View – The ECE radiometer that UT-FRC provides for C-Mod yields 32 channels of high temporal and spatial resolution data on each shot. At 5.4 T, the most common field for C-Mod experiments, the channels cover the plasma from the magnetic axis to the low-field-side separatrix. At lower fields, the measurement range shifts away from the magnetic axis but still provides coverage through the H-mode pedestal region. At higher fields, the pedestal data are lost. We plan to increase the magnetic field range of the measurements by extending the low end of the frequency range of the diagnostic. A second planned upgrade is to move the ECE optics to the horizontal midplane. Since the FRCECE is incident at a 15° angle, there is a mixing of poloidal and radial resolution. The inherent radial resolution of the FRCECE is approximate 7mm but due to the off-axis angle, the poloidal resolution results in a few centimeters actual radial resolution. An on-axis midplane horizontal view would recover the 7mm radial resolution.

Multichannel CNPA – The combination of the DNB, ICRF, and cryopump for controlled low density operation and long pulse AT scenarios provide the necessary conditions to measure the confined fast ion distribution with the Compact Neutral Particle Analyzer. The currently operating 3-channel system will be upgraded to measure a 5 chord profile across the plasma cross-section, and provide measurements of the ICRF generated fast ion tail energies out to at least 300 keV.

Antenna Reflectometry – The density profile in front of the ICRF antennas is currently not measured to the accuracy required to be useful in modeling rf coupling to the plasma. A new reflectometer diagnostic, being fabricated in collaboration with ORNL, will provide detailed electron density profiles in front of the new 4-strap antenna. The invessel waveguide is being incorporated directly into the antenna design.

CO₂ Scattering – A scattering system similar to that successfully employed on Alcator C [24, 25] will be used to study lower hybrid waves and the parametric decay instability on C-Mod. This system would be a vertically viewing small angle system capable of

resolving fluctuations in the range of 30 cm^{-1} and up. Laser power in the 100 W range and a detector array with 10 to 20 channels would be required.

SPRED Spectrometer – A new vacuum ultraviolet spectrometer will be installed on C-Mod to complement the McPherson spectrometer given incremental funds. It will have a wide spectral range (5-20 nm and 1-5 nm) with gratings interchangeable between shots. It will be able to monitor bright resonance lines of low-z impurities. It will also be able to monitor multiple impurity lines simultaneously, and will have resolving power (100-700) sufficient for measuring intensity of lines for impurity density analysis.

In-Situ Accelerator – An accelerator mounted in a horizontal port will be used to illuminate the C-Mod vacuum wall from the inner wall down into the divertor region. A combination of electrostatic steering and adjustments of the C-Mod toroidal field will allow sweeping of this beam over this extensive range. Detectors mounted in-vessel will monitor the neutron and gamma ray production and be able to determine details of surface composition. This system will allow the first ever in-situ measurements of wall conditions to be made.

Divertor TC Upgrade – These thermocouples will be a key diagnostic in our study of parallel power flow to the divertor targets (Section Boundary X.2.2). Thermally isolated in small plugs in the divertor targets, they will have good spatial and temporal resolution.

IR Camera Upgrade – This camera will be used to measure surface temperatures with high spatial and temporal resolution. It will view toroidal sections of the outer divertor, the divertor slot, and the inner wall. Some of the thermocouples described above will be within its field-of-view and will serve to calibrate the measured emissivity with the near-surface tile temperature. The camera will be used for the study of parallel power flow to the divertor targets (Section Boundary X.2.2), disruption mitigation studies, and divertor materials studies.

Fast Diode Array Upgrade – The present system images a local gas puff (Gas-Puff-Imaging) with two radial rows of views crossed by one poloidal column of views at the outboard midplane. The system has 1 MHz time resolution, fast enough to follow most turbulence time-scales of interest. We plan to upgrade the system to full 2D imaging with a ~ 10 (radial) $\times 10$ (poloidal) array. This will augment the fast camera imaging at the same location (presently limited to ~ 250 kHz time resolution) with a system with 1 MHz time resolution.

Two New Gas-Puff-Imaging (GPI) Views – These new views will supplement the present set of three views at different poloidal locations (inboard and outboard midplane and high-shear region outboard of the lower X-point). We plan one view for the imaging

turbulence in the divertor (Section Boundary X.2.2 and PPPL/C-Mod collaboration Section) and the second for imaging near an ICRF antenna in our investigations of possible convective cells set up by the ICRF fields (ICRF Section).

Impurity Injector – A new laser blow-off system will be installed for studies of impurity transport beginning in FY2009. Using a multi-pulse, 10 Hz, YAG laser, the system will be capable of injecting a variety of non-intrinsic, non-recycling impurities. During each shot, a fast piezo-driven mirror will allow multiple injections, and remote control of the input optics will allow the amount of impurity in one injection to be varied from shot to shot. Measurements of the injected impurities will be made with existing and upgraded x-ray and UV diagnostics.

Divertor Probes – We will add probe arrays to the new outer divertor and also expand and upgrade probe electronics and data acquisition hardware during FY2008, FY2009, and FY2010.

11.2.4 Data Acquisition and Computing

While a large part of MDSplus software development and support for off-site users is funded as a separate line item in the C-Mod cooperative agreement, many of the new developments are targeted at, and motivated by local needs. The ongoing MDSplus development projects include long pulse extensions and extended node attributes both of which are being used locally. Much of the regular maintenance and development is done in response to needs and problems that are identified by the C-Mod community. C-Mod is usually the first consumer of new MDSplus features.

The C-Mod computing infrastructure will continue to be updated. The local area network (LAN), currently switched Gbit Ethernet, will be upgraded to 10G Ethernet in the near future. We plan to connect the data servers directly to this backbone at full speed. Upgrades to workstation connections will depend on needs and costs. Improvements in network architecture are planned, which should improve overall robustness by segmenting the LAN into separate routing domains. External connections, provided by ESnet, will be upgraded by using a high-speed fiber network procured by MIT to connect into the new ESnet/Internet2 infrastructure. In the near future, the link speed will be increased to 1 Gbps with further upgrades as needed. Disk arrays will be added to accommodate the growing C-Mod data archive. There are currently 10 TB of data archived, with several TB of new data currently coming in every year at a rate which is doubling every 2.1 years Fig. 11.9. Servers will be replaced and added as needed. We will migrate existing between shot analysis jobs from user workstations to dedicated computers. User workstations will be replaced as they become obsolete in order to keep up with the increasing requirements for data analysis and visualization. Generally one quarter to one third of the systems need to be upgraded or replaced each year. Strategies

for off-line storage (tape) which can keep up with the increasing data loads will be reviewed. New procurements are anticipated in this area.

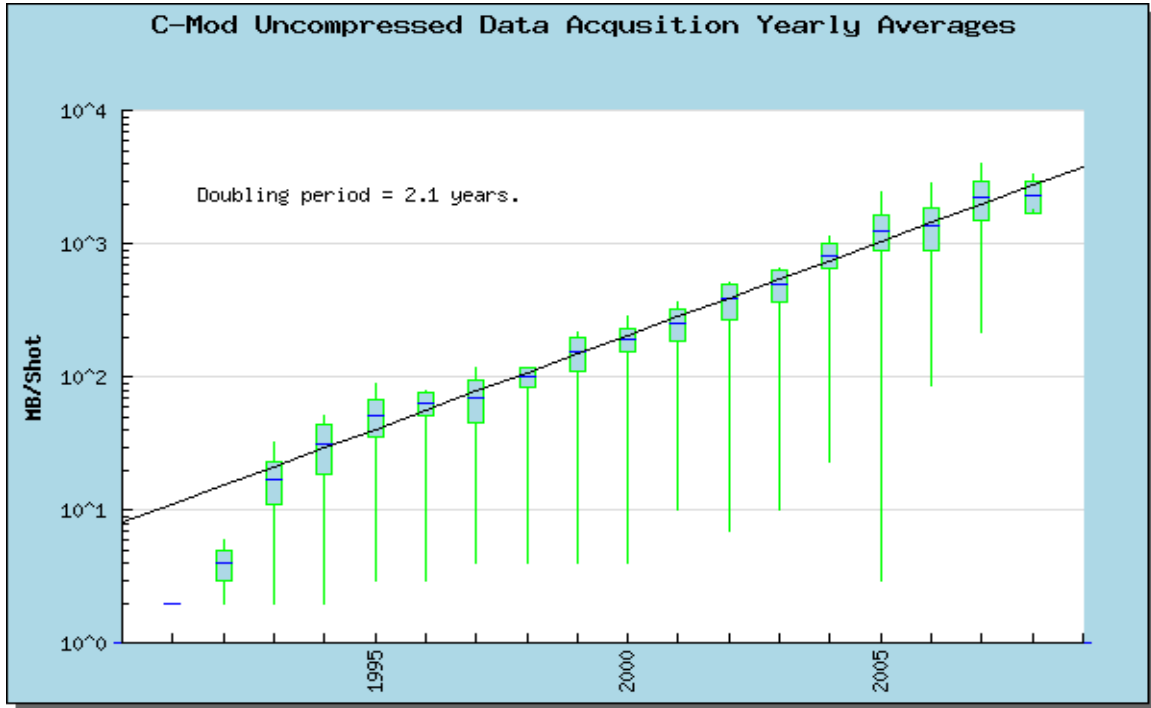


Figure 9. Total data acquired per shot is plotted for each year of C-Mod operation. The average increase is about 40% per year, leading, so far, to a 100 fold increase over the active life of the experiment.

The data acquisition system is being migrated from older CAMAC based hardware to modern CPCI and other platforms. This trend will continue, with most new diagnostics using the newer hardware platforms. The stable of hardware types will continue to expand, and spares will be acquired for the module types in use. Expansions to the current CAMAC based timing system (1 MHz) will be done using CPCI replacement hardware (10 MHz).

We will continue to migrate PC to PLC control software to RSVIEW. This task has been completed for the current engineering systems, and we will continue with upgrades to the diagnostic systems.

As we continue to develop new and more complex uses of the DPCS, computationally intensive routines might exceed the tight time constraints of the fast vertical control loop (100us/cycle). Therefore multi-processing capabilities and multiple time-base control schemes are required. A major upgrade of the DPCS hardware and software will involve the implementation of these advanced solutions.

Collaboration, in particular with off site personnel, is becoming a more and more important aspect of our operation. Most meetings are conducted with off site participants and a percentage of runs are led by session leaders from off-site. As the available tools evolve, they will be tested and applied as appropriate. Improved tools for screen sharing and informal remote communications are actively being sought. There are plans to leverage some of the capabilities of the new MIT SIP based phone system. Separate funding is being sought to investigate rich presence, social networking and geographic metaphors to enhance ad-hoc collaborations. A WIKI will be created for C-Mod users to document common data system tasks. As graduate students and visitors cycle through the PSFC they need a place to reference and document the institutional knowledge about MDSplus, and the MDSplus installation at C-Mod. This WIKI can become a first place for new users to look for site specific 'How-Tos'.

The PSFC currently has three Beowulf compute clusters. One owned exclusively by Alcator and the other two run by the theory division and shared by several groups. Over the next five years the Alcator owned cluster will be retired and the new, shared 256 core cluster will be upgraded. This will provide significant computing resources to run modeling codes locally at the PSFC.

11.2.5 MDSplus

Support for remote MDSplus sites will be increasing as the number of sites and the number of users increases. An ongoing effort to improve online documentation and to train local support staff at each of the major sites where the code is used will be made. The plan is to continue to hold a MDSplus users meetings on a biennial basis. The next meeting is scheduled in conjunction with the IAEA technical meeting in France in 2009. MDSplus software maintenance will continue to be a principal activity

We anticipate adding enhancements to the long pulse extensions as we gain more experience with their use. Some of the visualization tools will be enhanced to better handle continuous data streams.

Maintenance and enhancement of MDSplus will continue to be a major software development activity over the next five years. We anticipate that the long pulse capabilities of MDSplus will continue to be refined and enhanced as the fusion community gains more experience in the use of these features. Many of the MDSplus visualization tools will be enhanced to improve the handling of streaming data and very long records. Along with the long pulse enhancements, there are plans to reengineer the internal expression evaluation capabilities of MDSplus using a common scripting language such as Python. The expression evaluation capabilities in MDSplus are one of its most powerful features and porting this to a scripting language would make that facility easier to maintain and develop. Compared to TDI, it would also provide users with a more familiar scripting language and one with better error reporting, debugging tools and documentation.

Support for additional data acquisition devices – particularly CPCI will be provided as useful modules are identified.

11.3 References

- [1] S. Bernabei, J.C Hosea, C.C. Kung, G.D. Lesser, J. Rushinski, J.R. Wilson, R.R. Parker, M. Porkolab, “Design of a compact lower hybrid coupler for Alcator C-Mod”, *Fusion Science and Technology* 43, pp. 145-152, 2003.
- [2] G.D. Loesser, J. Rushinski, S. Bernabei, J.C. Hosea, J.R. Wilson, “Design and engineering of the Alcator C-Mod lower hybrid current drive system”, 19th IEEE/NPSS Symposium on Fusion Engineering”, Atlantic City, NJ, Proceedings, pp. 20-22, 2002.
- [3] M. Grimes, D. Gwinn, R. Parker, D. Terry, J. Alex, “The Alcator C-Mod lower hybrid current drive experiment transmitter and power system”, 19th IEEE/NPSS Symposium on Fusion Engineering (SOFE), Atlantic City, NJ, 16-19, 2002.
- [4] D. Terry, et.al. “Lower hybrid low power microwave active control system design, installation and testing on Alcator C-Mod”, 20th IEEE/NPSS Symposium on Fusion Engineering , San Diego, CA, Proceedings, pp 524-527, 2003.
- [5] P. Koert, G. Wallace, R. Parker, D. R. Terry and S. J. Wukitch, “New microstrip Directional Coupler Design for Side of Waveguide in Lower Hybrid Current Drive System on Alcator C-Mod”, 21st IEEE/NPSS Symposium on Fusion Engineering, Knoxville, TN, Proceedings, 2005.
- [6] D. R. Terry, R. Parker, J. Liptac, A. Kanojia, D. Johnson, P. Koert, G. Wallace, D. Beals, R. Vieira, N. Basse, S. Wukitch, W. Burke, W. Beck, M. Grimes, D. Gwinn, S. Bernabei, N. Greenough, J.R. Wilson, “Commissioning of the Lower Hybrid Current Drive System on Alcator C-Mod”, 21st IEEE/NPSS Symposium on Fusion Engineering, Knoxville, TN, Proceedings, 2005.
- [7] W. Burke, D. R. Terry, H. Kennedy, J. Stillerman, P. Milne, J. McLean, “The coupler protection system upgrade for lower hybrid current drive on Alcator C-Mod”, 22nd IEEE/NPSS Symposium on Fusion Engineering, Albuquerque, NM, Proceedings, 2007.
- [8] P. Koert, P. MacGibbon, W. Beck, J. Doody, D. Gwinn, “High power water load for lower hybrid current drive at 4.6 GHz on Alcator C-Mod, 22nd IEEE/NPSS Symposium on Fusion Engineering, Albuquerque, NM, Proceedings, 2007.
- [9] D.R. Terry, W. Burke, A. Kanojia, P. MacGibbon, D. Johnson, R.R. Parker, R.F. Vieira, G. Wallace, W. Beck, P. Koert, J. Irby, J.R. Wilson, N. Greenough, D. Gwinn, “Lower Hybrid Current Drive on Alcator C-Mod: System Design, Implementation,

Protection, Calibration and Performance”, 22nd IEEE/NPSS Symposium on Fusion Engineering, Albuquerque, NM, Proceedings, 2007.

[10] G. Wallace, et al., “Lower hybrid coupling experiments on Alcator CMod”, 17th Topical Conference on Radio Frequency Power in Plasmas, Clearwater, FLA, in press.

[11] P. Titus, J. Zaks, R. Vieira, D. Gwinn, B. Labombard, “C-MOD CRYOPUMP DESIGN AND ANALYSIS”, 21st IEEE/NPSS Symposium on Fusion Engineering, Knoxville, TN, Proceedings, 2005.

[12] W. Burke, W. Cochran, J. Sears, J. Snipes, S. Wolfe, X. Zhong, “Real Time Control of the Active MHD Diagnostic on Alcator C Mod”, 21st IEEE/NPSS Symposium on Fusion Engineering, Knoxville, TN, Proceedings, 2005.

[13] D. F. Beals, R. Granetz, W. Cochran, W. Byford, W. L. Rowan, A. A. Ivanov, P. P. Deichuli, V. V. Kolmogorov, and G. Shulzhenko, “Installation and Operation of New Long Pulse DNB on Alcator C-Mod”, 21st IEEE/NPSS Symposium on Fusion Engineering, Knoxville, TN, Proceedings, 2005.

[14] J.A. Stillerman, M. Ferrara, T.W. Fredian and S.M. Wolfe, “*Digital real-time plasma control system for Alcator C-Mod*”, Fusion Engineering and Design, Volume 81, 1905-1910, 2006.

[15] Alcasim simulation code for Alcator C-Mod, M. Ferrara, I.H. Hutchinson, S.M. Wolfe, J.A. Stillerman, T.W. Fredian. Mathematical Modeling and Control of Plasmas in Magnetic Fusion, San Diego CA, May 2006.

[16] Alcasim Axisymmetric Simulation Code for Noise and Stability Analysis on Alcator C-Mod, M. Ferrara, I.H. Hutchinson, S.M. Wolfe, J.A. Stillerman, T.W. Fredian. Annual Meeting of the APS Division of Plasma Physics, Philadelphia PA, November 2006.

[17] Alcasim Axisymmetric Simulation Code for Alcator C-Mod, M. Ferrara, I.H. Hutchinson, S.M. Wolfe, J.A. Stillerman, T.W. Fredian. Proceedings of the 45th IEEE Conf. on Decision and Control, San Diego CA, December 2006.

[18] T. Fredian, M. Greenwald, J. Stillerman, “Migration of Alcator C-Mod Computer Infrastructure to Linux”, Fusion Eng. And Design 71, 89, 2004.

[19] T. Fredian, J., J. Stillerman, “*Web based electronic logbook and experiment run database viewer for Alcator C-Mod*”, Fusion Eng. And Design, 81, 1963, 2006.

[20] J. Stillerman, D. Baron, T. Fredian, M. Greenwald and H. Schulzrinne, “Communications Fabric for Scientific Collaboration” to be published in Fusion Engineering and Design, Available online.

[21] D. P. Schissel, J. R. Burruss, A. Finkelstein, S. M. Flanagan, I. T. Foster, T. W. Fredian, M. J. Greenwald, C. R. Johnson, K. Keahey, S. A. Klasky, K. Li, D. C. McCune, M. Papka, Q. Peng, L. Randerson, A. Sanderson, J. Stillerman, R. Stevens, M. R. Thompson and G. Wallace, Building the US National Fusion Grid: results from the National Fusion Collaboratory Project, Fusion Engineering and Design Volume 71, Pages 245-250., 2004

[22] J. Burruss, T. Fredian, M. Thompson, "Security on the US Fusion Grid", Fusion Engineering and Design 81, 1949, 2006.

[23] T. Fredian, J. Stillerman and G. Manduchi, "MDSplus Extensions For Long Pulse Experiments", to be published in Fusion Engineering and Design, available online.

[24] "Study of Driven Lower Hybrid Waves in the Alcator Tokamak Using CO₂ Laser Scattering." C. M. Surko, R.E. Slusher, J. J. Schuss, R. R. Parker, I. H. Hutchinson, D. Overskei and L. S. Scaturro, *Phys. Rev. Lett.* **43**, 1016 (1979).

[25] "Spectrum and Propagation of Lower Hybrid Waves in the Alcator C Tokamak." R. L. Watterson, Y. Takase, P. T. Bonoli, M. Porkolab, R. E. Slusher, and C. M. Surko, *Phys. Fluids (Rapid Communications)* **28**, 2622 (1985).

12 Collaborations

The C-Mod program is carried out with broad collaborative participation. While this proposal is formally for the portion of the work funded through MIT, the plans assume collaborative efforts that continue at approximately constant level (for the guidance program), with incremental increases that are in tandem with those at MIT for the total proposed budget. Major collaborations are ongoing with the Princeton Plasma Physics Laboratory (section 12.1) and the University of Texas at Austin (12.2), along with a smaller effort at the Los Alamos National Laboratory focused on infra-red imaging. Many smaller groups of collaborators at Universities and Laboratories, both domestic and international, are integral participants in the research (see table 12-1). MDSplus, whose development efforts are led at MIT, is now in use by a large number of major fusion facilities around the world. Support for these installations, and further development of the software, are ongoing, and our plans are detailed in section 12.3.

Table 12-1 Institutions with C-Mod collaborations

Domestic	International
Princeton Plasma Physics Lab	ASIPP/EAST Hefei
U. Texas FRC	Budker Institute Novosibirsk
U. Alaska	C.E.A. Cadarache
UC-Davis	C.R.P.P. Lausanne
UC-Los Angeles	Culham Lab
UC-San Diego	ENEA/Frascati
CompX	FOM Nieuwegein, Netherlands
Dartmouth U.	IGI Padua
General Atomics	IPP Garching
LLNL	IPP Greifswald
Lodestar	ITER Organization Cadarache
LANL	JET/EFDA
U. Maryland	JT60-U, JFT2-M/JAEA
MIT-PSFC Theory	KFA Jülich
ORNL	KFKI-RMKI Budapest
SNLA	LHD/NIFS
U. Texas IFS	Politecnico di Torino
U. Wisconsin	U. Toronto

12.1 Collaborations: PPPL

PPPL has maintained a broad and active collaboration with Alcator C-Mod for over a decade, focusing on several areas of expertise. The level of effort has been approximately at the level of \$2 million annually (Table 12.1), with a larger budget during FY03 to support design and fabrication of the first Lower Hybrid system.

	2003	2004	2005	2006	2007	2008	2009	2010
Funding (\$M)	3.1	2.1	2.1	2.2	2.0	2.1	2.1	2.1
FTE	11.6	5.7	4.3	4.4	4.9	4.6	4.6	4.6

Table 12.1. Historical level of effort for the PPPL / C-Mod collaboration. Funding numbers are budgeted, inflation-corrected (2008 dollars). Full-time-equivalents (FTE) include research and engineering activities.

Major programmatic activities have included:

- Heating and current drive hardware: design and fabrication of the first Lower Hybrid launcher and coupling hardware and J-port ICRF antenna.
- Diagnostic development: Motional Stark Effect (MSE) for $q(r)$; high-speed Gas Puff Imaging (GPI) of edge turbulence; curved x-ray crystal spectrometer for $T_i(r)$, $V_\phi(r)$; and a swept-frequency reflectometer for fluctuation correlation lengths.
- Physics research: Lower Hybrid current drive; ICRF heating and current drive; advanced plasma scenario development; edge turbulence; comparison of transport behavior with numerical turbulence codes.
- Support: TRANSP support for transport analysis; and engineering support for LHCD, ICRF systems and diagnostics.

Research proposed for the 2009-13 period continues most of these activities with an increased emphasis toward physics research that utilizes the new heating, current drive, and diagnostic capabilities that were installed in the 2003-8 campaign.

12.1.1 Highlights of Recent Research

12.1.1.2 Lower Hybrid Current Drive and Ion-Cyclotron Heating

PPPL has been an integral participant in the LHCD program on C-Mod since its inception. Princeton personnel have been involved with the design, construction, installation, calibration and operation of the system. Princeton proposes to continue this collaborative work throughout the FY 2009-2012 period. As discussed in Chapter 5, initial experiments with the system have demonstrated that it behaves qualitatively as expected from previous experience and theory.

12.1.1.3 Development of Advanced Plasma Scenarios

The advanced tokamak concept consists of high β_N , 100% non-inductive current, strong plasma shaping, and good energy confinement, all self-consistent with ideal MHD stability and plasma transport.

In the 2007 run campaign a successful series of experiments were completed to examine slower plasma current ramps, simultaneous injection of ICRF and LH power in the current ramp, demonstration of the LHCD effects on the current profile, and operation at lower plasma currents. These were aimed at preparing for direct control of the safety factor profile in the plasma current ramp and flattop using heating from ICRF and heating and current drive from the LH, and target 100% non-inductive plasmas when the LH power is increased. The plasmas were all at $I_p = 600$ kA, and generally remained in L-mode.

Simulations with the Tokamak Simulation Code were performed prior to the experiment to aid in selecting discharge conditions, in particular to examine the effects of the plasma current ramp, timing of the ICRF and LH injection, and onset of the H-mode. These simulations indicated that the earliest injection of power and the H-mode produced strong distortions to the q-profile. Additional simulations were then performed after the experiments to model several discharges in detail. Overall, the observed discharge behavior could be reproduced fairly well, although there were variations in the sawtooth onset time, which served as our measure of the current profile in these experiments. It was determined that utilizing accurate electron temperature profiles in the simulations was important for matching the q-profile evolution, as expected due to the similar time-scales for energy confinement and current diffusion in C-Mod. Discharges with only 0.4 MW of LH delayed the sawtooth onset by up to 175 ms, relative to Ohmic discharges. The simulation of these discharges indicated that 200 kA of LH current may have been driven during the current ramp when the background DC electric field is significant, and then drops to about 65 kA in the flattop. When ICRF heating is combined with LHCD, the sawtooth onset time was delayed by 250-375 ms. Due the higher electron temperature from the ICRF heating, the LHCD is estimated to be about 100 kA, for 0.4 MW of LH power.

For the upcoming 2008 run campaign, the emphasis will be on a plasma current of 450 kA, which is more likely to approach high non-inductive current fraction, establishing H-modes on a regular basis, increased LH power, higher ICRF power, longer discharge pulse lengths, and routine incorporation of the motional Stark effect (MSE) diagnostic for the current profile. The current profile and discharge evolution effects demonstrated in

the 2007 campaign with a plasma current of 600 kA are expected to be amplified in the lower plasma current discharges. In addition, the lower plasma current is likely to reach higher non-inductive current fraction, lower loop voltages, and strong q-profile distortions from the LHCD. Previous experiments have shown that 450 kA discharges can be produced routinely, with good confinement and robust H-modes.

12.1.1.4 Motional Stark Effect diagnostic

In support of the LHCD and Advanced Scenarios programs on Alcator C-mod, PPPL has designed, fabricated and installed a motional Stark effect (MSE) diagnostic to measure the profile of magnetic field pitch angle (q-profile) in Alcator C-Mod [1, 2]. The diagnostic views light emitted by a diagnostic neutral beam (DNB) that injects in the horizontal midplane. Originally the DNB injected directly perpendicular to the torus, but for reasons discussed below it has been re-oriented to pivot at a toroidal angle of 7° . MSE measures the pitch angle along ten spatial channels that span the region $R = R_o$ to R_o+a .

MSE diagnostic systems on other tokamaks typically have no in-vessel optics other than a single vacuum window at the outer torus wall. The compact nature of the C-Mod torus precludes wide-angle tangential views and so a complex polarization-preserving optical relay system was implemented as illustrated in Figure 12.1.3.1. In other respects the C-Mod MSE design resembles that on TFTR, DIII-D, and NSTX.

The MSE diagnostic operated throughout the entire 2003-08 program period, however its performance has been limited by a number of technical problems, some of which are now understood to be a consequence of the unique in-vessel optics design and the DNB injection geometry.

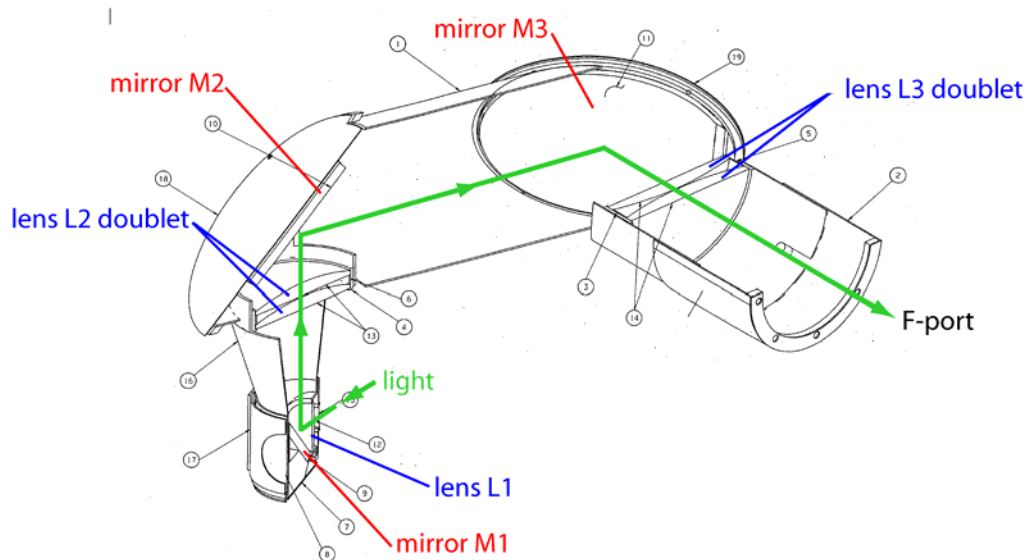


Figure 12.1.3.1. Schematic of in-vessel MSE optical components.

Disruption-induced vibrations originally caused significant damage to several in-vessel optical components. This problem has been eliminated through re-design of the optical support mechanisms to eliminate all contact between glass and metal surfaces.

The photon count rate was increased ten-fold by replacing aged photomultiplier tubes with high quantum-efficiency avalanche photodiodes. This improvement has reduced the statistical uncertainty in pitch angle measurements to acceptable values ($<0.2^\circ$) in low-density plasmas typical of the conditions prevalent during LHCD experiments.

Two technical problems dominated MSE research studies during the 2003-08 program: lack of reproducibility and anomalous behavior in beam-into-gas calibrations. As discussed below, the causes of these problems have been identified. This understanding is the basis for a re-design of the MSE in-vessel optical system which should resolve the problems prior to the 2009 run campaign.

Reproducibility:

The C-Mod MSE diagnostic experiences spurious variations of order $\sim 5^\circ$ in the measured pitch angle at the plasma edge, well in excess of the desired $\sim 0.2^\circ$ accuracy. As illustrated in Figure 12.1.3.2, similar variations have been observed over the course of a single day during beam-into-gas calibration experiments.

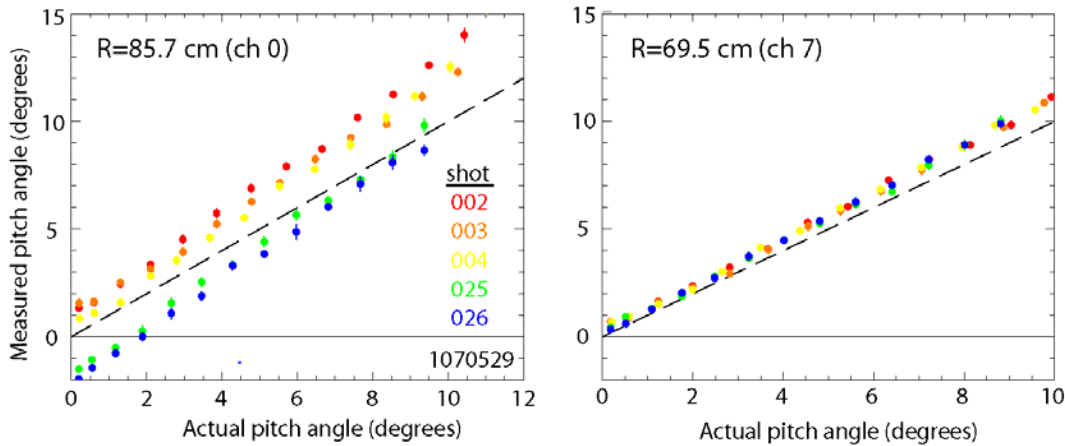


Figure 12.1.3.2. Reproducibility of pitch angles measured by MSE during beam-into-gas calibration experiments. MSE channels viewing the plasma edge show variations of several degrees over the course of a run day.

Measurements taken at the end of FY07 showed that the reproducibility problem is caused by thermal stress-induced birefringence in the “L-2” lens doublet (Figure 12.1.3.1). The in-vessel MSE optics experience temperature variations of order 100 Celsius over the course of a run day due to the combined effects of plasma heating, ECDC, TF cooling and vacuum vessel heating. The mechanical stress associated with these temperature variations

induces birefringence in the lenses, which rotates the polarization direction of light passing through the lenses.

The effect of thermal stress-induced birefringence on the measured pitch angles has been demonstrated by illuminating MSE with a constant, polarized light source while the optics canister was heated locally near the L2 lens doublet with a heating tape. Spurious pitch angle changes of order 10° were observed as the L2 region was heated 80 Celsius over the course of 20 minutes.

Anomalous behavior of beam-into-gas calibrations

The MSE diagnostic is first calibrated by illuminating it with a linearly polarized light source that is rotated through 360° at atmospheric pressure in absence of magnetic fields. This is supplemented by ‘beam-into-gas’ calibrations to account for possible Faraday rotation in the in-vessel lenses and stress-induced birefringence at the vacuum window. The beam-into-gas calibration measures the magnetic field pitch angle with MSE as the DNB is injected into a torus filled with low-pressure gas as known magnetic fields are applied by the toroidal and vertical field coils. Based on the optical properties of the MSE optical components, we expected the corrections in pitch angle from Faraday rotation and birefringence at the vacuum window to be less than 1° .

The actual behavior is rather different: with the DNB in its original orientation (perpendicular to the torus), the measured pitch angle differed from the actual pitch angle by as much as $\pm 10^\circ$. The mechanism for this anomalous behavior is now understood: if the DNB is oriented perpendicular to the torus, the beam ions have zero parallel velocity and their residence time in the MSE viewing sightline is limited only by the very slow grad-B drift. Consequently, most beam ions re-neutralize via charge exchange on the torus gas before leaving the MSE viewing footprint and then emit an $H\alpha$ photon *while moving at a random gyro angle*. The polarization direction of the light emitted by the beam neutrals is defined by the Lorentz electric field ($\mathbf{E} = \mathbf{V} \times \mathbf{B}$), thus the secondary neutrals generate light at a different polarization direction than the desired, primary beam neutrals.

To reduce the residence time of the beam ions in the MSE viewing sightline, prior to the 2007 run campaign the DNB was re-oriented by imposing a 7° pivot in the toroidal direction. As illustrated in 12.1.3.3, this change substantially reduced the anomalous behavior of the beam-into-gas calibration by decreasing the population of secondary beam neutrals and hence their contribution to the total $H\alpha$ emission [3, 4]. There remains a smaller anomaly of up to a few degrees in the edge channel, because the time scale for beam ions to charge exchange is still not large compared to the time to drift out of the MSE sightline. Numerical calculations indicate that the error introduced

by the secondary beam neutral emission should vary linearly with the torus pressure, and this is borne out by measurements.

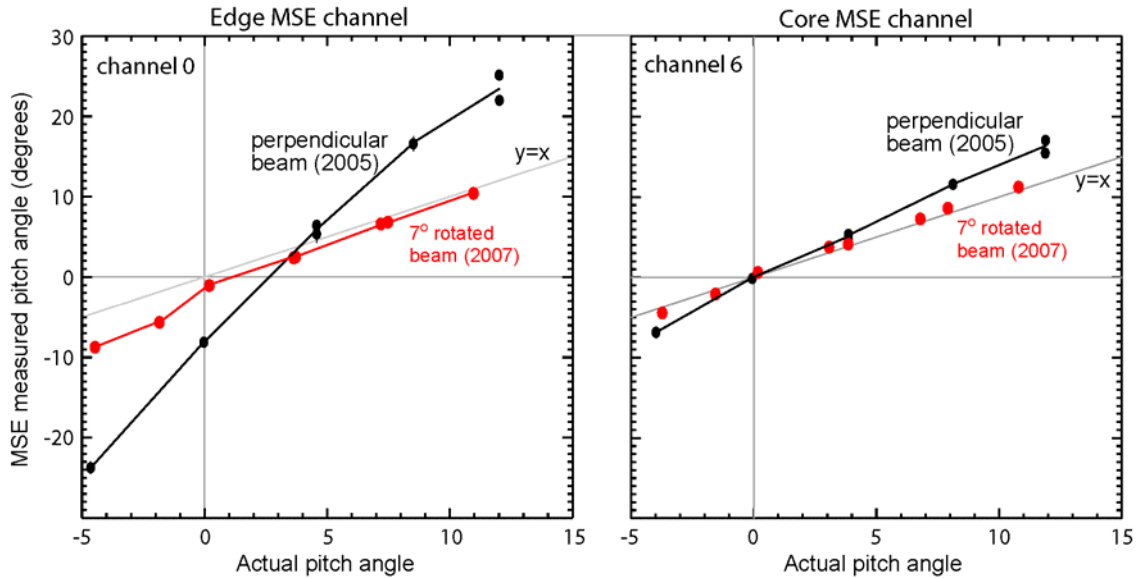


Figure 12.1.3.3. Comparison of the MSE beam-into-calibration before and after pivoting the DNB by 7° in the toroidal direction.

Both measurements and calculations indicate that the spurious pitch angle changes induced by secondary beam neutral emission is a function of the actual angle of the magnetic field line. This work suggests that the errors can be reduced significantly by performing the MSE beam-into-gas calibration at selected values of pitch angle. At other pitch angles, the calibration may be carried out at low torus pressure (at the cost of increased statistical uncertainty) or as a function of torus pressure to allow the results to be extrapolated to the zero-pressure limit.

First measurements of changes in current density by LHCD

The shot-to-shot offsets induced by stress-induced birefringence preclude direct use of the measured pitch angles to constrain the magnetic equilibrium as reconstructed by EFIT. Instead, we construct an in-situ calibration by comparing the pitch angles inferred from EFIT during the Ohmic phases of the plasma to those measured by MSE [4]. This procedure has provided the first measurements in Alcator C-Mod of changes in the current density profile by Lower Hybrid Current Drive [5] as described in Section 5.

12.1.1.5 Polarimeter Development

The MIT PSFC is leading an effort to design and fabricate a 20 channel polarimeter to measure the electron density and current profiles. This work is discussed in the Alcator C-Mod 5-year plan. Through FY2007-9, PPPL is supporting this effort at the level of about 0.25 FTE through design assistance primarily in the area of component and vendor selection.

Procurement for a prototypical one-channel system is underway. Fabrication and testing is expected to be completed early in FY08, allowing a proof-of-principle measurement to be carried out before the start of the C-Mod machine inspection in late Spring 2008.

12.1.1.6 Edge Turbulence / Boundary Physics

The goal of this research is to help solve the generic tokamak problem of overheating and erosion of divertor plates. The fundamental cause of this problem is the relatively small scrape-off layer (SOL) width of heat and particles, which causes the plasma to hit the divertor in a narrow zone only ~ 1 cm wide. The width of this zone is determined by the fairly well understood parallel connection length, and by the not-well-understood cross-field turbulent transport in the SOL. Therefore a potential solution to this divertor problem is to understand the turbulent transport in the SOL and to learn how to control it.

Although much is already known about edge turbulence from basic theory [6] and from direct measurements [7], we are just beginning to obtain a quantitative understanding of the relationship between the two. Significant progress in this direction has been made at C-Mod during the past five years, and during the next five years we want to extend this success to perform detailed quantitative tests of specific edge turbulence models. We also plan to test specific methods to control the edge turbulence on C-Mod to ameliorate the divertor heat and erosion problem.

The most recent results from this period provided the first 2D images of edge turbulence taken near the X-point region of a tokamak, as illustrated in Fig. 12.1.5.1(a). These images show a highly elongated structure in the near-radial direction, which is similar to the structure expected from the flux tube mapping model developed by Ryutov and Cohen [8]. However, the predictions from this model are (so far) not quite aligned with the experimental results, as shown in Fig. 12.1.5.1(b). A more detailed comparison between experiments and modeling is planned for the C-Mod 2008 run, including simultaneous imaging at the midplane and X-point regions.

Another interesting experimental result from this period concerns the cross-correlation between the SOL turbulence as measured by the gas puff imaging diagnostic (GPI) and by a movable Langmuir probe [9]. A significant cross-correlation coefficient was found between these two diagnostics over a rather large distance of ~ 3 m. along a B field line,

and the potential structure of a ‘blob’ was mapped out using this correlation method. This potential structure was found to be qualitatively similar to the poloidal dipole structure expected from simple analytic blob theory. However, the radial propagation speed of the blobs was approximately constant vs. radius, and so not consistent with these simple blob models.

During this period several different comparisons were made between C-Mod edge turbulence measurements and computational simulations of edge turbulence. The most recent results involved a direct comparison between the GEM code of Scott [6] and the turbulence measured near the outer midplane SOL of C-Mod for an inner-wall limited, near-circular discharge optimized for this comparison. The resulting frequency spectrum comparison as shown in Fig. 12.1.5.2 is fairly encouraging, as is the agreement within a factor-of-two of the poloidal correlation lengths; however, the relative fluctuation level in the simulation was about x5 lower than that in the experiment. Additional turbulence measurements were made during the 2007 run which included scans of the B field and density in this configuration, and the simulation results for these scans are in progress.

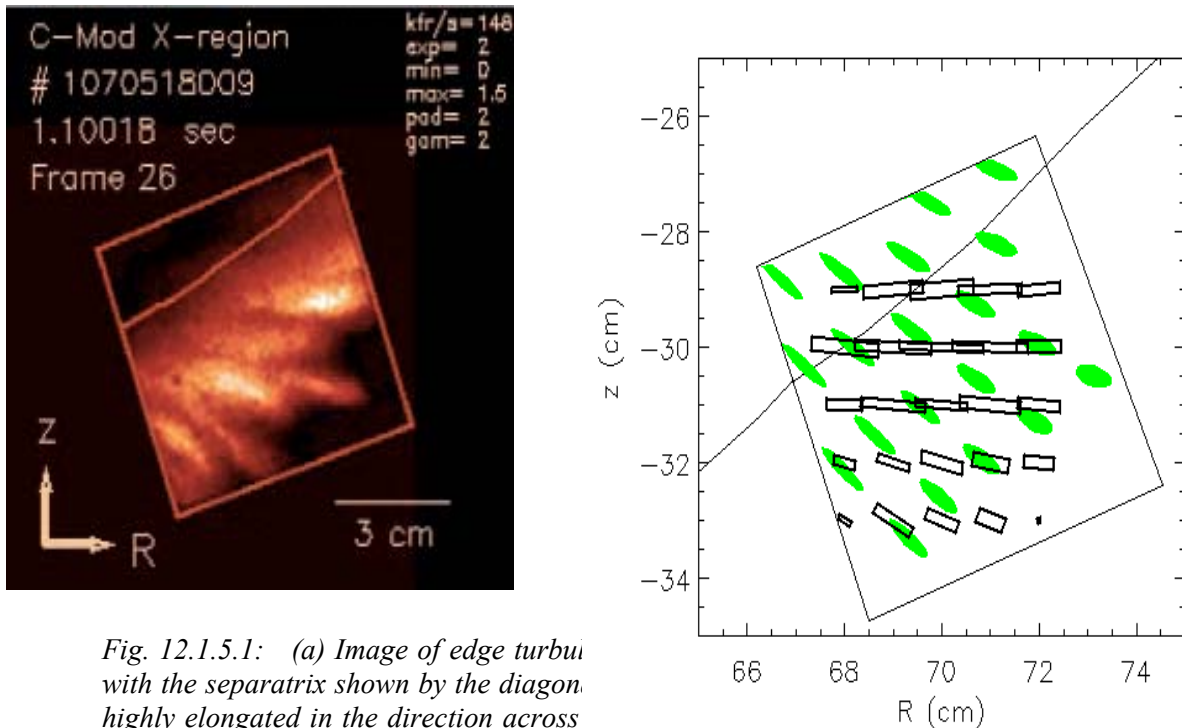


Fig. 12.1.5.1: (a) Image of edge turbul with the separatrix shown by the diagonal. highly elongated in the direction across of the shape of the observed turbulent structures (black rectangles) with a model based on magnetic flux tube mapping of circular structures from the outer midplane (green ellipses).

A comparison between edge turbulence simulations using the LLNL BOUT code and C-Mod edge turbulence measurements is shown in Fig. 12.1.5.3 [8]. The radial and poloidal correlation and the relative fluctuation levels from the code were found to agree with the experimental data to within a factor-of-two for this lower single null divertor case. However, the autocorrelation times derived from the code were about x5 shorter than those derived from the measurements. The BOUT code results were at least

qualitatively consistent with the radial blob propagation speed and also with the 2D images near the X-point shown in Fig. 12.1.5.1. An earlier comparison of the k-spectrum and fluctuation level between the NLET edge simulation code of Hallatschek and the C-Mod SOL turbulence measurements was described in [10].

In summary, during the past five years we have used new diagnostics and experiments on Alcator C-Mod to test the theory and simulation of edge turbulence. We have so far found an encouraging, but partial, agreement between experiment, theory and simulation. This naturally leads to the following proposals to extend this research and to explore its potential to solve of the divertor heat load and erosion problems of tokamaks.

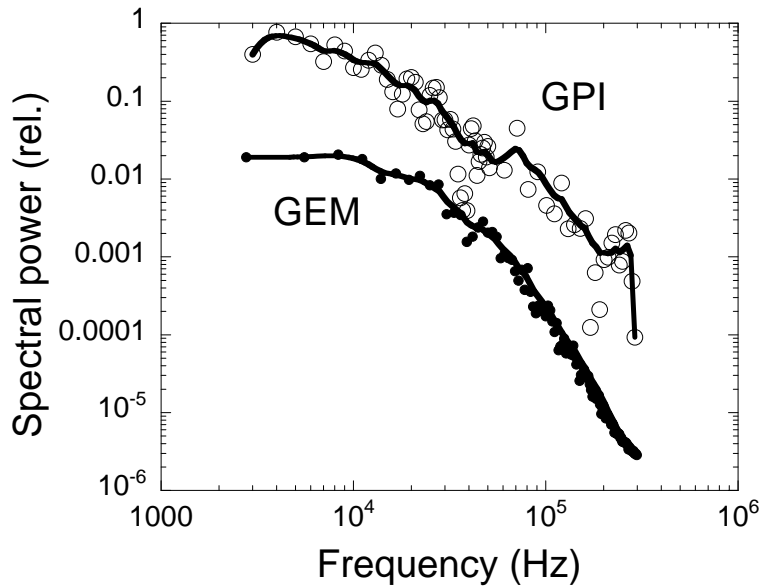


Fig.12.1.5.2: Comparison between C-Mod GPI data and the GEM code of Bruce Scott [7] for the frequency spectrum of SOL turbulence near the outer midplane.

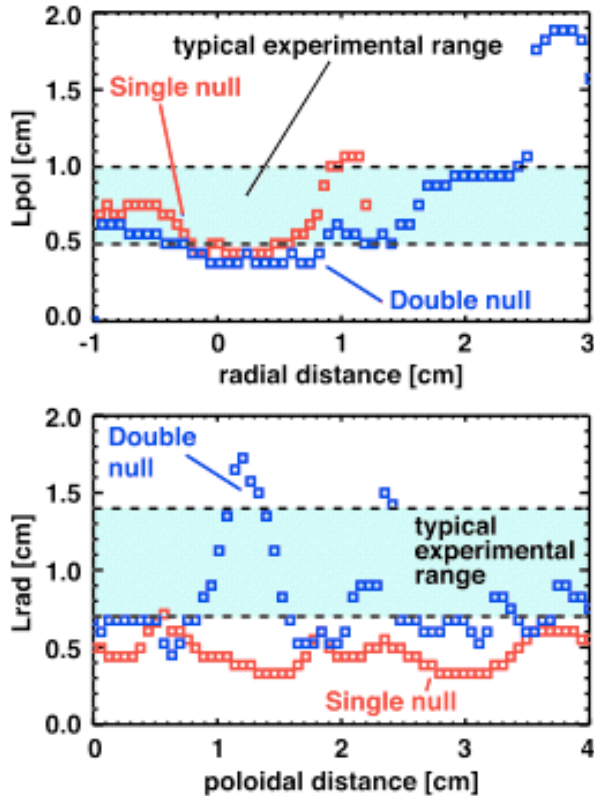


Fig. 12.1.5.3 Comparison between C-Mod GPI data and the BOUT code for the radial and poloidal correlation lengths of SOL turbulence near the outboard midplane [8].

12.1.1.7 Development of x-ray crystal spectrometer

For many years, profiles of impurity ion temperature and rotation speed have been measured on Alcator C-Mod with a set of five discrete x-ray crystal spectrometers that provide spatial and temporal resolution of ~ 3 cm and < 50 ms respectively [11]. Several factors have recently stimulated interest in developing an ion profile diagnostic with improved spatial and temporal resolution: the installation of a second harmonic electron cyclotron Te diagnostic with high resolution (32 chords, 1 MHz) [12]; the discovery of internal transport barriers with small gradient scale lengths [13], and the discovery of significant ion toroidal rotation velocities even in the absence of zero beam torque [14].

During the 2003-8 program, PPPL and the PSFC jointly developed a novel x-ray spectrometer which utilizes a spherically-bent crystal and a 2D position-sensitive detector to provide spectra from highly charged ions from multiple sightlines through the plasma. A proof-of-principle spectrometer was demonstrated on Alcator in 2003 using a multi-wire proportional counter [15], but the 400 kHz global count rate capability of this detector limited the time resolution to > 100 ms. The recent commercial development of higher-performance detector modules (Pilatus II [16]) with a count rate of 1 MHz *per*

pixel removes this limitation and makes possible x-ray measurements of ion temperature and rotation speed with significantly better spatial and temporal resolution.

The new diagnostic commissioned in April 2007 [17] utilizes two quartz crystals to resolve the x-ray W lines from helium- and hydrogen-like Argon. A single PILATUS detector views hydrogen-like emission from the plasma core, and a set of three detectors views the full vertical extent of the plasma ($\Delta z = 70$ cm). Chordal profiles of impurity density, temperature, and rotation speed are measured over the region $r/a = 0 - 0.8$ with ~ 1 cm spatial resolution (~ 50 chords) and ~ 10 ms time resolution. Statistical uncertainty in the ion temperature is $< 1\%$ for densities of typical Alcator C-Mod plasmas ($n_e > 10^{20} \text{ m}^{-3}$).

Recent work has focused on improvement of inversion techniques to infer local values of temperature and rotation speed from the chord-integrated measurements.

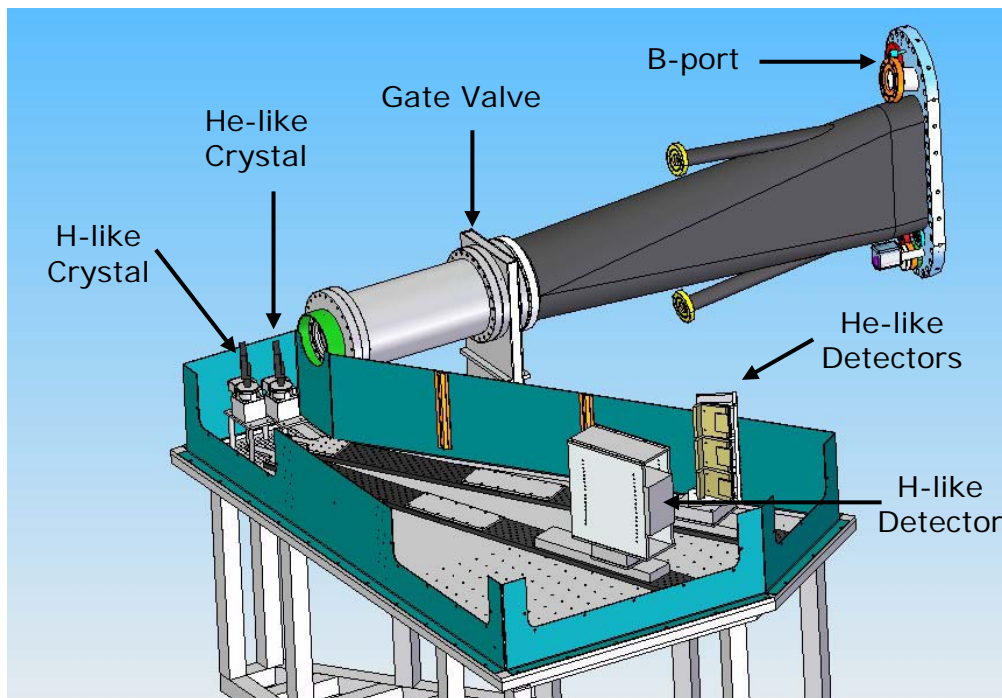


Figure 12.1.6.1. Configuration of the Alcator C-Mod curved x-ray crystal spectrometer.

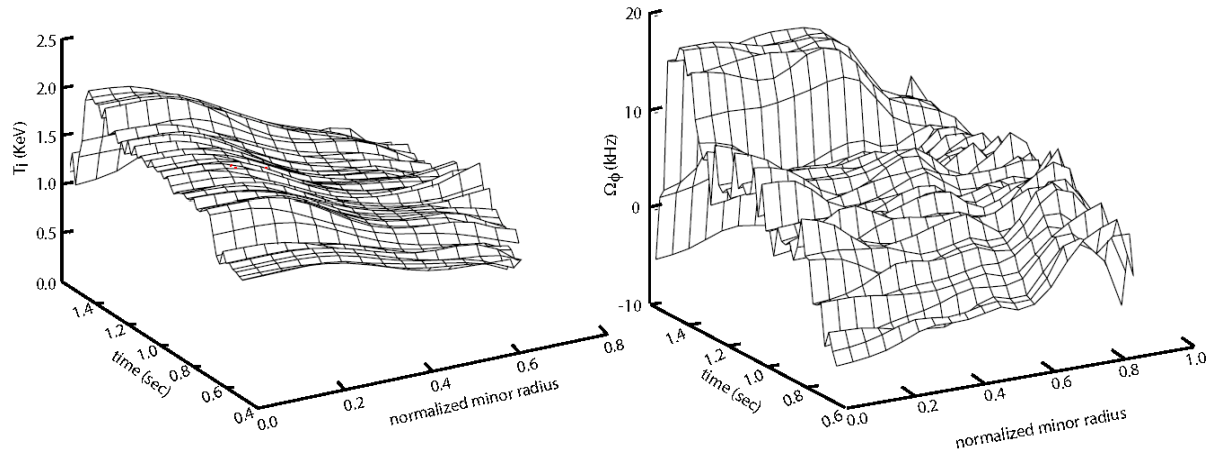


Figure 12.1.6.2. Profiles of local impurity ion temperature and rotation speed inferred from inversion of chordal profiles measured by the curved x-ray crystal spectrometer (shot 1070830013).

12.1.1.7 Swept-frequency reflectometer

Hardware

A 130-140 GHz swept-frequency reflectometer diagnostic to measure electron density fluctuations has been designed and fabricated by PPPL for use on Alcator C-Mod [23,24]. The frequency range corresponds to plasma densities in the range $1.5 - 2.4 \cdot 10^{20} \text{ m}^{-3}$, which is relevant to several regimes of interest for C-Mod transport studies:

- the plasma edge of H-Mode discharges;
- the ‘foot’ of the density profile in plasmas with an internal transport barrier (ITB); and
- in the core of L-Mode discharges.

The diagnostic system is designed to measure both the amplitude and radial correlation length of electron density fluctuations which are key parameters for testing numerical models of plasma turbulence. The system was installed prior to the start of the FY07 C-Mod run campaign, unfortunately one of its principle components (140 GHz Gunn diode) failed shortly thereafter. A new 140 GHz Gunn diode has subsequently integrated into the system and successfully tested at PPPL. Two other technical problems were encountered during FY07 and early FY08: failure of a 130 GHz mixer and weak signal-to-noise ratios, the latter due to excessive losses in the waveguide system that transport microwave power from the source to the launching/receiving antennas and back to the receiver.

A refurbished reflectometer with new mixers and low-loss waveguides will be installed in early FY08. We expect to obtain first measurements of density fluctuation correlation length with the system during the C-Mod 2008 run campaign.

Modeling

Heterodyne reflectometer systems can separate phase and amplitude fluctuations that are measured at the detector. In the ‘phase screen’ model for reflectometry, phase fluctuations originate in a thin slab near the reflection layer. Away from the cut-off layer, amplitude fluctuations emerge from interference between rays scattered from different places at the cut off layer. Both amplitude and phase carry information regarding the density fluctuations near the cut-off.

The conventional method to obtain both phase and amplitude information from a reflectometer system is to employ an I/Q detector which gives both the sine and cosine part of the reflected signal; the phase and amplitude information can be obtained when the DC offsets that are added by the I/Q detector to the signals are removed. A software package for the analysis of heterodyne reflectometer signals that was originally developed for the PPPL reflectometer at JT-60U [25] has been ported to the C-Mod workstations. In this package, the DC offset removal from the reflectometer signals has been implemented and with the corrected signals power spectra of phase, amplitude and the complex signals can be made. It can also be used to obtain cross correlations between different reflectometer channels. PPPL will continue to support and develop this software package and use it as an important tool to analyze the C-Mod reflectometer data.

To compare reflectometer-measured density fluctuation levels and correlation lengths against turbulence simulations, one must take into account the non-linear response of the reflectometer system to density fluctuations [26, 27]. In the last eight years a 2D reflectometer simulation code [28] has been developed at PPPL to extract density turbulence properties from the measured reflectometer signals. This code has been applied successfully in the interpretation of reflectometer data from different devices: JT-60U [29], LAPD [30], DIIID [31] and for a design study of a DIIID reflectometer imaging system [32] and the ITER reflectometer system [33].

12.1.1.8 Transport experiments

Global nonlinear GYRO simulations of turbulent transport in C-Mod low-density H-mode plasmas with peaked density profiles suggest a new mechanism for understanding this phenomenon [34]. Preliminary measurements of the ion temperature profile made in 2007 with the new imaging x-ray spectrometer reveal that the ion temperature is not well coupled to the electron temperature in these lower density plasmas, and that the ion temperature gradient scale length is significantly longer than L_{Te} for $r/a \sim 0.5$. Such reductions weaken the ITG drive relative to standard high-density H-modes in C-Mod, and the simulations show that modes with $k_{\theta}\rho_s > 0.6$ produce an inward particle flux that cancels an outward flux at lower $k_{\theta}\rho_s$ and results in a null net flux at about the density

gradient seen in the experiments. Artificially raising the collisionality does not change the null flux result, but using an ion temperature profile that is close to the electron temperature leads to an outward particle flux.

The empirically deduced collisionality dependence of H-mode density peaking in C-Mod plasmas may arise through the collisionality dependence of ion-electron temperature equilibration that enables the relaxation of the ion temperature profile in lower collisionality plasmas. This process may also operate in RF heated AUG and JET plasmas, but it probably is not occurring in NBI heated AUG and JET plasmas because the strong central ion heating would not permit relaxation of the ion temperature profile. In ITER and other reactor scale plasmas, the temperatures will be well equilibrated so there could be no relaxation of the ion temperature profile and this mechanism could not produce a pinch. It is therefore imperative to establish more firmly whether the relaxation of the ion temperature profile is real and to understand how this leads to a particle pinch.

Quantitative studies comparing measured and predicted temperature gradients were carried out with the aim of investigating whether the nonlinear upshift [35] of the critical gradient threshold for ITG turbulence was operative in highly collisional C-Mod plasmas. In the standard picture, nonlinearly driven zonal flows limit turbulent eddy size, so that just above the *linear* critical gradient, transport increases only slowly with increased drive. If this picture is correct, experimental measurements should correspond to higher gradients, where zonal flows themselves go nonlinearly unstable and transport increases rapidly above an ‘effective’ critical gradient (producing the ‘Dimits shift’ [35]). Our simulations extended the original model by including a nonadiabatic electron response and collisions, which enter the problem in two competing ways. First, by reducing the kinetic electron response, high collisionality can weaken the drive. Second, by damping zonal flows, which are predicted to be the main nonlinear damping mechanism for the turbulence, collisions could lead to higher transport. For the C-Mod parameters studied, simulations showed that the first effect dominated, leaving the Dimits shift intact and explaining past results where measured temperature gradients in C-Mod were found to be significantly higher than those predicted by widely used models [36].

PPPL proposed and led an experiment that separated the H-mode formation transients from ITB formation and demonstrated that off-axis heating broadens the temperature profile. The high radial resolution of the FRC-ECE system provides local measurements of the electron temperature gradient, and we clearly demonstrated that L_{Te} at the location of the ITB foot is reduced when ICRF heating is moved from the magnetic axis to $r/a \sim 0.5$. This scenario will enable future experimental determination of the threshold condition by producing controlled small changes in L_{Te} .

12.1.1.9 TRANSP development and support

Technical support

The C-Mod tokamak was the first facility to run TRANSP at PPPL as a remote service, and the first to transport TRANSP input and output data through MDS+ servers. Now, these practices are common throughout the fusion community. The earliest C-Mod TRANSP runs were done using a VMS-based TRANSP production engine in the 1990s. Through separate funding (SciDAC Fusion Collaboratory), a unix-based service, the TRANSP Fusion Grid, was introduced in FY-2003. In that year, over a period of a few months, C-Mod transitioned from the legacy VMS-based service to the Unix-based service. In FY-2006, the SciDAC Collaboratory funding ended, but the Fusion Grid TRANSP was continued with experimental project and collaboration funding, as it had become the basis of all TRANSP run production. Labor for maintenance and support of this production service is covered by combined funding from NSTX at PPPL and the PPPL collaborations with C-Mod, DIII-D, and JET.

TRANSP users can find information on access to the TRANSP service and its input and output at the website <http://w3.pppl.gov/TRANSP>. Users can monitor the progress of their runs at this site. Crashed runs are analyzed by PPPL TRANSP experts, and repaired or referred back to the user for data corrections as appropriate. The labor to support this is also funded jointly by experimental projects and collaborations at PPPL.

Table 12.1.9.1 summarizes C-Mod TRANSP utilization since 2003 (data on VMS service runs in 2003 was not available to be counted):

Fiscal year	Number of TRANSP suns	CPU hours
2003	21	120
2004	315	574
2005	164	340
2006	459	3256
2007	207	1138
total	886	5740

Table 12.1.9.1. Utilization of TRANSP by Alcator C-Mod.

Code development

During the previous five-year program (2003-2008), total labor funding for TRANSP support from C-Mod remained constant at the level of approximately 0.25 FTE. Approximately half of this effort is dedicated to production support and half to code development.

Development of TRANSP ICRF modeling capabilities has been largely but not exclusively motivated by the C-Mod experimental program. There has also been

interest from those using TRANSP for JET and ITER studies, although the ITER work has generally been voluntary (i.e. unfunded).

As a result of collaboration with C-Mod and IPP/Garching, TORIC was introduced as an ICRF modeling tool in TRANSP starting in 1999. In the early 2000s there was some effort (never completed) to create an “NTCC module” that would encompass ICRF wave codes with a Fokker Planck model for plasma response. Nevertheless, this effort contributed to the modernization of TORIC. Between FY-2003 and FY-2005, the PPPL TRANSP team contributed to TORIC portability by removing the software’s dependency on licensed software (the NAG math library). This effort involved importing freeware FFT software and various www.netlib.org freeware math library replacements interpolation and special functions. TORIC was also re-organized as a dynamically allocated FORTRAN-90 code with improved programming practices. In terms of physics capabilities, the new TORIC was enhanced with the ability to treat up-down asymmetric numerical MHD equilibrium geometry in the target plasma.

In FY-2006, the re-organized TORIC was made available (by John Wright at MIT) in a CVS server, and well-designed procedures were developed for receiving TORIC code version updates from the physics authors (John Wright and Paul Bonoli at MIT and original author Marco Brambilla, and Roberto Bilato at IPP/Garching) for installation in TRANSP. A rigorous file-based data capture method was devised that allowed sufficient data from select TRANSP time slices to be captured to allow precise reproduction of ICRF wave code results in a standalone version of TORIC with additional diagnostic output and visualization capabilities provided (useful for debugging and verification of results).

In FY-2007 and FY-2008, the TORIC source was moved to an SVN repository at IPP/Garching. PPPL tested the MPI-parallel version of TORIC and did some preliminary design work on a “stateless server” that would allow time dependent TRANSP runs to access MPI-parallel TORIC through its file interface. JET scientists (Irina Voitsekhovitch and Jim Conboy) were shown the TRANSP/TORIC interface and code update procedure, and were so put in a position to collaborate with us on future software development efforts.

In all these years, a 1980s era legacy zero banana width bounce averaged Fokker-Planck (FP) model FPPMOD has been used within TRANSP to estimate the plasma response to the ICRF wave field—minority species RF absorption and transfer of power to the thermal plasma. The fusion community has developed a better-validated, better-supported FP code (CQL3D) and the long term plan has been to replace FPPMOD with CQL3D in TRANSP. Sufficient manpower to carry out this important upgrade has not been available.

In the FY-2005 to FY-2007 time frame, TRANSP’s Lower Hybrid RF code (LSC) was also exercised for C-Mod simulations. This modeling, however, had several limitations and moreover the LSC code is “dead” in the sense that its authors have

retired and there are no longer any active LSC experts in fusion research. Consequently, there is a need to upgrade Lower Hybrid modeling tools in TRANSP.

12.2 Proposed Research

12.1.2.1 Lower Hybrid Current Drive and Ion-Cyclotron Heating

During the 2009-2013 period, LHCD operations will be extended to full performance parameters with the addition of a second launcher and associated klystrons. Experiments will concentrate on detailed comparisons between measurements and theory. This will require improvements and/or additions to the diagnostic set, as well as improvements in the modeling packages. These packages are also actively worked in parallel by a collaborative team including PPPL and MIT researchers under the SCIDAC initiative.

Princeton proposes to assist the design of the new launcher by applying commercial 3D EM analysis codes to the waveguide power splitting design as a check on MIT's design and to evaluate the consequences of arbitrary plasma conditions (reflections). In addition, PPPL will participate in the fabrication of the second launcher in 2011.

Comparisons with theory require detailed coupling, propagation and wave adsorption codes. Traditionally, due to the short wavelengths of the lower hybrid waves, ray tracing codes have been used to follow the wave propagation. Recently, through the SCIDAC initiative, the full wave code TORIC, originally written for ICRF frequencies, has been extended to higher frequency. Calculations with this interim version of the code have already indicated differences with the predictions of ray-tracing that are more in line with the experiments. It is believed that wave diffraction, which is not handled in the ray-tracing code, is responsible for the differences in predicted absorption. Future efforts within the SCIDAC effort will add non-Maxwellian distribution functions and a self-consistent Fokker-Planck calculation of the electron distribution function in the presence of the RF wave and the DC electric field to yield a state of the art prediction of the current drive magnitude and distribution. PPPL scientists will then apply the code to C-Mod data.

12.1.2.2 Development of Advanced Plasma Scenarios

For the 5 Year period spanning 2009-2013 the primary focus is to produce advanced tokamak discharges on C-Mod utilizing the increased ICRF and LH powers, the cryopump, and current profile measurements from MSE and Faraday rotation. These discharges will approach 100% non-inductive current, demonstrate current profile control, and be optimized by utilizing density control, slower plasma current ramps, and internal transport barriers (both ICRF induced and LHCD-reverse shear induced). In addition, efforts will be made to raise the operating β_N value by lowering the toroidal field, access high H-mode pedestal temperatures and global confinement to enhance the bootstrap current fraction, and establish on-axis CD from the ICRF to provide a seed current for $q(0)$ control when the plasma current becomes completely non-inductive. In

addition to the more aggressive advanced tokamak scenarios, hybrid discharges, which have approximately 50% non-inductive current fraction, will be pursued. The primary focus will be on the unique environment of C-Mod, with no external momentum input, all RF heating, and LH off-axis current drive. This should provide a critical test of the improved performance observed for neutral beam driven hybrid discharges from other tokamaks, and establish guidance on projecting and operating hybrids in ITER.

The efforts to expand and improve simulations for the C-Mod advanced scenarios development will continue, emphasizing time-dependent evolution, ICRF and LH source modeling and benchmarking, and integration of reliable plasma transport models. TSC/LSC free-boundary evolution code will remain the main driver for time-dependent simulations, with greater integration of TRANSP source models over time. The cross-checking and integration of GENRAY/CQL3D and TORIC-LH into time-dependent simulations which typically use the Lower Hybrid Simulation Code (LSC) will become a standard for discharge modeling. This provides a good model for the use of integrated simulation modules which is being developed through the Fusion Simulation Project and ultimately for use in ITER for discharge design and interpretation.

12.1.2.3 Motional Stark Effect Diagnostic

The major objective for the Motional Stark Effect (MSE) diagnostic during the 2009-13 program is to resolve technical issues that currently limit its performance and thereby to realize its potential to provide routine, accurate q-profile measurements.

Data analysis

At present, we compute a q-profile from the pitch-angle profile measured by MSE using a technique based on an analytic equilibrium developed by Giannella et al. [xx]. During the early part of the five-year program, we will implement the standard analysis technique of using the measured pitch angles as a fitting constraint in numerical (EFIT) magnetic equilibrium reconstructions [yy].

Eliminate effects of stress-induced birefringence

As discussed in Section 12.1.3, the MSE diagnostic currently suffers from poor reproducibility in its pitch-angle measurements, with variations of several degrees over the course of a run day being typical. Extensive testing has revealed that thermal stress-induced birefringence in the in-vessel optics, and in the “L2” lens doublet in particular, is the underlying cause of this anomalous behavior.

Several approaches to either reduce/eliminate the stress-induced birefringence or to compensate for it through additional calibration activities will be evaluated during early FY08 with a goal of selecting the most promising technique by March. Design, fabrication and calibration of new MSE hardware will commence immediately and will continue through the C-Mod machine ‘inspection’ starting ~May 2008. A refurbished MSE diagnostic that is immune to stress-induced

birefringence will be available when C-Mod resumes plasma operation in the spring of 2009. The approaches under consideration are:

- Eliminate one or more of the five in-vessel lenses. Replace one or more of the three flat in-vessel mirrors with curved mirrors to provide the focusing that is currently performed by the lenses.
- Create new MSE viewing system that can view the DNB at a favorable geometry without need for in-vessel optics. This approach mimics the MSE configuration on other tokamaks, but may be difficult due to port access limitations and interference from diagnostic and RF antenna hardware.
- Install a heating or cooling system to maintain the MSE in-vessel optics at constant temperature. This approach eliminates the stress-induced birefringence by eliminating the temperature gradients that generate the stress.
- More frequent re-calibrations of MSE. Recent changes to the support mechanism for in-vessel lenses decouple them from dimensional changes to the MSE optics canister. This improvement should increase the time constant for changes in stress-induced birefringence to many minutes. Simple 'beam-into-gas' calibrations of MSE performed either on alternate shots or in a post-shot phase may therefore provide acceptable accuracy. This approach will be evaluated during the FY2008 run campaign.

Effect of secondary emission from beam neutrals during beam-into-gas calibrations

As discussed above, large anomalies in the pitch angles measured by MSE during routine beam-into-gas calibration exercises are now understood to be a consequence of 'secondary' emission from beam neutrals. These anomalies have been reduced significantly in magnitude, but not eliminated, by pivoting the DNB thereby reducing the residence time of the beam ions in the MSE viewing sightline.

Both theoretically and empirically, the confounding effects of secondary beam emission on the MSE calibration has been shown to be linear function of the neutral density. The neutral density in plasmas is orders of magnitude lower than that during beam-into-gas calibration shots, therefore we expect that secondary beam emission is a negligible source of error during MSE measurements of pitch angle in plasmas. Consequently, we believe that secondary beam emission is *not* the cause of the observed poor reproducibility of pitch angle measurements in plasmas.

Going forward, MSE will rely more strongly on 'in-vessel' calibrations in which the diagnostic measures the pitch angle of light from a polarized light source that is

slowly rotated through 360° while the torus is at atmospheric pressure with no applied magnetic fields.

To check for Faraday rotation (which is expected to be small) and other potential technical problems, beam-into-gas calibrations will be performed while the torus pressure is ramped, so that the deleterious effects of secondary beam neutrals can be eliminated by extrapolating the measurements back to zero torus pressure.

In addition, we will calibrate MSE *in plasmas* by ramping the plasma size in time, thereby sweeping the plasma edge past successive MSE spatial channels. The pitch angle measured by MSE is then compared to the value computed from equilibrium construction (EFIT), which is highly accurate at the edge. The feasibility of this technique was demonstrated in 2007 for the outer five MSE channels. For inner channels, we will cross-calibrate against the pitch angle inferred from the location of the $q=1$ surface implied by the sawtooth inversion radius.

Spatial resolution

The spatial resolution of individual MSE channels is defined by two parameters: the image size of the MSE viewing footprint ($\Delta R \sim 1$ cm), and the width of the diagnostic beam ($\Delta R = W_{\text{beam}} \cos \theta$ where θ is the sightline-DNB angle). Spatial resolution is acceptable at the plasma edge, where the beam is nearly perpendicular to the MSE viewing sightlines, but at the plasma core the current beam width $W_{\text{beam}} \sim 10\text{-}12$ cm yields $\Delta R \sim 6$ cm corresponding to $\Delta r/a = 0.27$.

At the start of FY2008 a water-cooled variable aperture ($W_{\text{beam}}=4\text{-}12$ cm) was installed in the DNB calorimeter to reduce the beam width and thereby improve spatial resolution. By itself, this aperture will not significantly reduce the beam footprint in the plasma due to divergence of the individual beamlets. The PSFC plans to design and install a second, conductively/radiatively cooled aperture further down the DNB beamline closer to the plasma during 2008-09. The two-aperture system should improve the spatial resolution of individual MSE channels by a factor ~ 2 with acceptable reduction in signal strength. PPPL will assist the design of the second aperture by providing calculations of the estimated heat load, including the effect of beamlet divergence.

Pending an assessment of the overall MSE system performance following upgrades to eliminate effects of stress-induced birefringence, in \sim FY10-11 PPPL will evaluate the merit of doubling the number of spatial channels (10 \rightarrow 20).

12.1.2.4 Development of polarimeter

Installation of the 20-channel PSFC-developed polarimeter is expected in 2009. PPPL will continue to provide design and physics consultation services as needed during the commissioning and operational phase of the diagnostic.

12.1.2.5 Edge Turbulence / Boundary Physics

Understanding edge turbulence and transport

This research will continue to develop diagnostics and perform experiments on C-Mod to test theories and simulations of edge turbulence. This work will be closely coordinated with Jim Terry and Brian LaBombard of C-Mod, along with theorists and modelers of edge turbulence, with other experimental groups studying edge turbulence e.g. on NSTX and DIII-D, and it will also be applied to ITER and other future machines wherever possible. These comparisons will include both the turbulence properties and transport effects in various conditions including Ohmic plasmas (which are still not understood), L-H transitions, density limit phenomena, and the effects of ICRH and lower hybrid waves.

Specific goals for the C-Mod for 2009-2013 include the following:

1. Extend the present gas puff imaging diagnostic to include two new views, as illustrated in Fig. 12.2.5.1. One new view will include the outer upper divertor leg and outer upper strike point, in order to see the turbulence which as it nears and contacts the divertor plate, and to look for predicted divertor-region instabilities [8]. The other new view would be focused on the side of an ICRF antenna, possibly with zoom capability.
2. Extend the detector technology and data analysis techniques to better extract the 2D space vs. time flow fields of the edge turbulence, e.g. GAM and zonal flows. This would require a moderate increase in the camera framing rate to ~ 1 MHz, which might become available in the near future. Alternatively, the GPI fast diode arrays of Jim Terry can be extended from two linear 12 channel arrays to a full 10x10 2D array. Existing analysis techniques [39] can then be adapted and extended for use with the C-Mod data.
3. Continue and extend the comparisons of C-Mod edge turbulence with the simulations by Bruce Scott of Garching. The first step is to compare the existing experimental results on the scaling with gyroradius and collisionality with his GEM gyrofluid simulations [6]. This will be followed by comparisons with his edge gyrokinetic code GEM-X, presently under development. These comparisons will focus on the outer midplane region.
4. Continue and extend the comparisons of C-Mod edge turbulence with the BOUT code of LLNL. These comparisons will focus on the poloidal dependence of the turbulence, and will use both the existing X-region view and the new upper divertor and strike point view. The previous BOUT results on the physics of the L-H transition and the density limit can also be checked with dedicated experiments.
5. As soon as they become available, we will begin to compare the C-Mod results

with the comprehensive edge simulation codes being developed by the CPES and LLNL groups (i.e. XGC-1 and Tempest). These codes should be able to use global inputs such as particle and heat fluxes, rather than the measured edge profile inputs used in the GEM and BOUT codes. Thus these codes, once validated, could be used to *predict* edge and SOL properties of C-Mod and also ITER and other future devices.

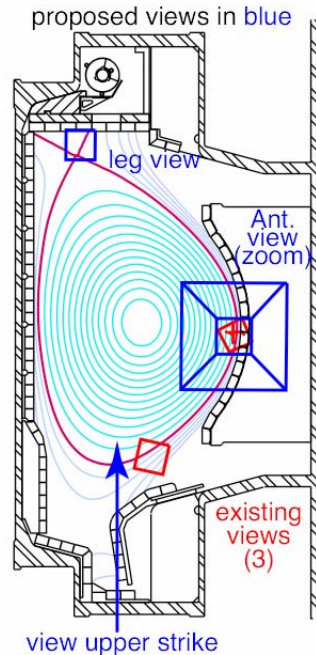


Fig.12.2.5.1: Existing (red) and proposed (blue) gas puff imaging diagnostic views on C-Mod. The new views would provide 2D imaging of the upper divertor outer leg and divertor plates strike points, and a variable-zoom view of the SOL in the shadow of an ICRH antenna.

6. Compare the experimental results and simulation results with analytic theories wherever possible, since these theories can provide of level of understanding not easily obtained from simulations alone. Examples of such analytic theories [e.g. 8,40] include those on radial propagation and birth of SOL blobs, the blob-induced density limit, possible resistive X-point modes or sheath-driven instabilities, and zonal flow-induced shear stabilization of edge turbulence.

Active control divertor plate heat load / erosion

The ultimate result of the work described above would be the ability to predict the edge and SOL properties of future tokamak devices such as ITER. This would allow the design of an optimized tokamak edge, at least within the constraints set by the required

core plasma and device geometry. However, given what is known about ITER [41] and any future DEMO, there will probably still be an excessive heat load and erosion on the divertor plates. Thus it is important to investigate potential methods to actively control the SOL in current devices like C-Mod, in particular, to learn how to widen the SOL width as much as possible. Attempts to test such schemes would also be interesting checks of our understanding of the basic physics.

Specific goals include the following:

1. Investigate the direct effects of ICRH waves on edge turbulence and transport, e.g. due to convective cell generation by RF-driven sheath potentials in the SOL [42]. This will require experiments to discriminate against the indirect effects of ICRH heating on the edge plasma profiles. Initial measurements can be made using the existing GPI and Langmuir probe diagnostics, but definitive measurements will need the new GPI view in the vicinity of the ICRH antenna (Fig. 4).
2. Investigate the direct effects of lower hybrid waves (LHW) on edge turbulence and transport, e.g. due to radial electric fields driven in the SOL by fast electron loss, as seen in Tore-Supra and HT-7 [43]. Other possible effects of LHW are scattering of the turbulence by (time-averaged) wave fields, parametric instabilities, pondermotive forces, edge current drive or edge heating. These effects may well depend on the parallel spectrum of the launched waves, which is highly controllable in the C-Mod LHW antennas.
3. Investigate the effects of edge fueling and geometry on edge turbulence and transport, e.g. due to the effects of parallel flow generation by deuterium puffing, cooling due to edge radiation or detachment, changes in the magnetic topology, and variation of the gaps between the separatrix and the limiters. Each of these effects could plausibly change the driving or damping of edge turbulence, but careful experiments will be needed to isolate the essential physics, since each of these can also indirectly modify the edge plasma profiles.
4. All the research listed above could be done without any major changes to the hardware of C-Mod, and all these techniques could be directly applicable to the existing ITER design. However, if these ‘knobs’ are not sufficient to control the SOL width, we will propose significant hardware changes to test specific new ideas. Possible ideas include asymmetric divertor plate biasing for convective cell generation, divertor plate tilting for increased edge turbulence drive, or an ergodic magnetic divertor. Some other ideas and previous experiments on active SOL control are discussed in Ref. [7].

12.1.2.6 X-ray crystal spectrometer (XCS)

We expect the curved x-ray crystal spectrometer (installed April 2007) will be a mature

diagnostic by the start of the 2009-13 five year program, providing routine chord-integrated profiles of impurity ion temperature, toroidal rotation speed. Similarly, we expect that algorithms to unfold the local values of temperature and rotation speed from the chord-integrated measurements which are currently being developed (FY07, FY08) will also be mature and that their accuracy will have been validated by the start of the five year plan. PPPL will support transport experiments on C-Mod with data analysis from XCS throughout the duration of the five year program.

In addition, we propose to explore the possibility of inferring characteristics of the electron velocity distribution function by comparing intensity ratios of particular emission lines. It has been shown previously [44] that the calculated intensity ratio of suitably chosen x-ray lines is a sensitive function of electron temperature and that the measured ratio agrees with the electron temperature measured by Thomson scattering [435]. The electron temperature measured by XCS also agrees quite well with measurements by Thomson scattering and ECE on Alcator C-Mod.

We propose to investigate the possibility of exploiting the high XCS count rates observed on central channels (>10 MHz / chord) to measure electron temperature fluctuations. This would involve the use of (a) fast detectors with slits that are configured primarily to measure line ratios only; (b) larger crystals with 3x higher throughput; and (c) different crystals (SI or Ge versus quartz) with 2-5x higher reflectivity. Calculations to assess the feasible temporal and amplitude resolution will be carried out in 2008-09 under a separate contract. Assuming these calculations indicate that acceptable performance is possible ($F > 50$ kHz, $\Delta T_e/T_e \sim 1\%$), fabrication and installation would follow in 2009-10.

12.1.2.7 Additional diagnostics for LHCD studies

At present, the energy spectrum of non-thermal electrons driven by Lower Hybrid waves is measured with a 32 chord, radially-viewing pinhole hard x-ray camera developed by the PSFC. The radial profile measurements provided by this diagnostic have been compared to detailed modeling and indicate a slightly broader x-ray profile than expected from CQL3D calculations.

The x-ray emission from suprathermal electrons becomes highly anisotropic and intense in the forward cone when the effective tail temperature exceeds ~ 100 keV and so measuring the anisotropy yields information about the electron distribution function [44, 45].

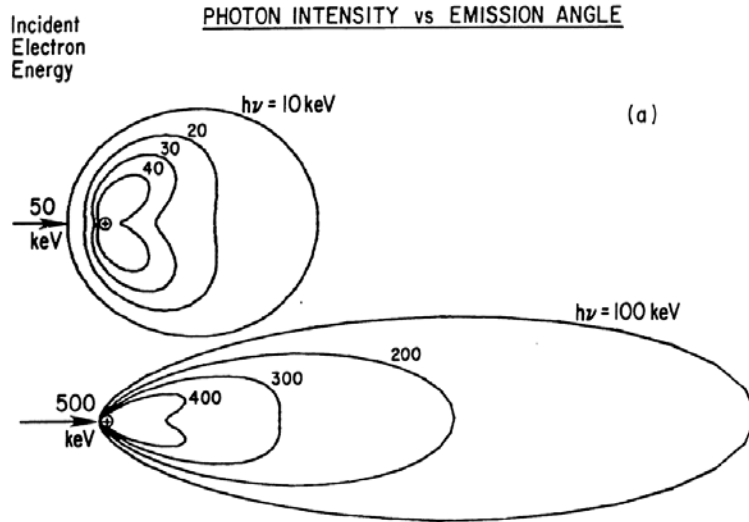


Figure 12.2.7.1. Angular distribution of x-ray emission from suprathreshold electrons.

Most of the equipment needed for a single-channel hard x-ray diagnostic (detectors, amplifiers, HV bias supplies) is currently available at PPPL. We propose to assemble and install a single-channel, tangentially-viewing energy-resolving x-ray diagnostic on Alcator C-Mod during the early part of the five-year program. The radiation “temperature” measured in this fashion is more sensitive to the peak absorbed power density than the existing perpendicular viewing diagnostic. The major engineering consideration is port access and space available for shielding.

Other diagnostics that PPPL will participate in include the possibility of installing a scanning probe to the new lower hybrid launcher to measure the edge density profile immediately in front of the wave coupler.

12.1.2.8 Swept-frequency Reflectometer

A number of the critical microwave components in the swept-frequency reflectometer are 10-20 years old and are approaching end-of-life. To improve reliability, we propose to replace several microwave components including mixers and Gunn diodes during the 2008-2009 C-Mod machine inspection.

PPPL will continue to provide technical support for the reflectometer diagnostic during the 2009-13 period as well as data analysis and modeling. This will include support of the PPPL 2D reflectometer simulation code to extract density turbulence properties from the measured reflectometer signals. The measured fluctuation amplitudes and correlation lengths will be a key input to detailed tests of theoretical models of plasma turbulence discussed under the Transport section of this report.

12.1.2.9 Transport studies

PPPL participates actively in the design and analysis of experiments dedicated to improved understanding of local particle, momentum and heat transport in the core plasma. Particular areas of emphasis include time-dependent transport analysis using the TRANSP code and validation of codes that simulate turbulent transport.

Several new diagnostic capabilities will be available during the 2009-13 reporting period that facilitate new and improved experimental tests of microturbulence models. These include the curved x-ray crystal spectrometer and CXRS and for high-spatial-resolution impurity density, T_i and V_ϕ profiles; MSE and a polarimeter for $q(r)$ profiles, and the swept-frequency reflectometer for measurements of the correlation length of density fluctuations. In parallel, over the same period we expect to use new 'diagnostic simulation' codes to relate the results from gyrokinetic/gyrofluid microturbulence codes to fluctuation diagnostic measurements.

Plasma transport validation studies will apply first-principles gyrokinetic turbulence simulation codes to steady-state plasmas, and the computationally more affordable TGLF model will be used for both time dependent and steady state discharges. The gyrokinetic codes GYRO and GS2 are already employed in this work, and when the GEM and GTC codes are released for general use we will use those as well. For some tasks the TGYRO code will be most appropriate, and when that code has demonstrated that it can robustly make self-consistent predictions of plasma profiles we will use it. While code-to-code benchmarks are common for heat transport, we will need to carry out benchmarks for momentum and particle transport since these topics have received very little attention. Particle transport generally requires higher resolution and completeness to achieve sufficient accuracy for validation, so these benchmarks will be very important. The GS2 and GYRO codes already include all the physics that is presently expected to be important in most C-Mod plasmas and calculate heat, particle, and momentum transport, so we should be able to conduct these benchmarks in the initial phases of each topical study.

The capability to compare predictions of microturbulence theory against experiment in multiple transport channels simultaneously, and/or transport channels and fluctuation characteristics (amplitude, frequency spectrum, radial correlation length) simultaneously is particularly valuable. When only one observable is compared at a time, there is often sufficient 'wobble-room' within the uncertainties of the input parameters (such as temperature gradients) to the microturbulence codes to match the experimentally-observed radial fluxes of heat, particles, or momentum. This is particularly true when the plasma is close to marginal stability. By comparing multiple channels in the same plasma it becomes possible to reduce the range of predicted quantities: for example, after the ion temperature gradient has been adjusted to match ion heat transport, we can ask whether the toroidal momentum and particle fluxes are accurately predicted and whether the predicted density fluctuation amplitude and radial correlation length are correct. Some of these quantities may have sensitive dependences on other poorly determined quantities (e.g., magnetic shear) so a strategy of successive refinement of the input parameters may

require a number of experimental measurements to provide data both for refinement and for testing against measurements not used in the refinement process.

Validation of particle transport predictions will focus on the low-collisionality peaked density H-mode regime and on H-L back transitions (which also features a remarkable improvement in ion thermal transport). Initial simulations of the peaked density H-mode plasmas are described in the PPPL Collaboration Highlights and future validation work will focus on understanding the detailed mechanism that produces the pinch; several theoretical processes might play a role and all the relevant physics is included in the simulations. We also hope to propose experimental tests of this mechanism by varying the key parameters (tentatively these are the relative strengths of ITG and TEM drive), and by comparing density fluctuations with measurements by the reflectometers and PCI diagnostics. The H-L back transitions are dynamic and will be modeled with a predictive transport code; we expect that the observed changes in the density profile will affect the ion heat transport, and the response of the ion temperature profile will affect the ITG drive so comprehensive coupled simulations will be required.

Studies of intrinsic rotation and momentum transport are important in themselves for understanding how to predict rotation in ITER, which could affect ELMs, macroscopic stability, L-H transitions, and reductions in transport cause by ExB shear. C-Mod is particularly well suited to studies of intrinsic rotation because the rotation speed can be measured in all regimes, and without the complication of neutral beam torque (ITER will also not have large external torques). C-Mod studies will complement work in strongly driven plasmas and in lower collisionality plasmas in TCV, which can also measure toroidal rotation in all regimes without strong external torques.

With no internal torque sources, steady state intrinsic rotation profiles produce null fluxes of toroidal momentum. These can be most conveniently predicted with a time-dependent simulation (based on the TGLF model, for instance), and this result can be confirmed by using the TGLF prediction as input for a ‘first principles’ simulation by GYRO (which includes the ExB shear pinch and the Coriolis pinch). If the models succeed in predicting the direction and magnitude of the intrinsic rotation, including the density threshold for reversal of intrinsic rotation direction and reversal of direction in L vs H modes, we would use ‘numerical experiments’ with the models to identify the key parameters and propose further experiments.

Additional opportunities for testing the models are provided by the dynamic phase of transition between the low and high density states of intrinsic rotation, as well as by changing the plasma boundary between USN and LSN to change the boundary rotation direction; this can be done without perturbing the core density or temperatures and thereby offers a very clean test of momentum transport. These time dependent validation scenarios will only be possible with a transport model embedded in a semi-predictive code that is coupled to experimental measurements (the ‘first principles’ codes are too computationally expensive for this work).

Impurity particle transport experiments based on laser blow-off edge sources are planned, and the previously reported experimental finding of no impurity pinch in L-mode plasmas provides a strong qualitative test; this one is also very important for devices such as ITER that cannot tolerate impurity accumulation. Both of the experimentally-oriented ‘first principles’ turbulence simulation codes are capable of calculating impurity transport (this is not the case, however, for the more affordable TGLF transport model). Planned validation efforts include searching for significant pinches in the code results, comparing the experimental and predicted particle diffusivities for a variety of impurity elements and varying q profiles. Since the impurity injection is non-perturbing it is possible to do the simulations before the experiments, and thereby to optimize the experiments. Preliminary simulations with multiple impurities show that interactions between species is not common (the presence or absence of different impurities does not affect the results much), and that the commonly employed D, V ansatz for particle flux does represent the simulated impurity transport.

We also propose to document T_i and T_e profiles and their gradient scale lengths and compare with GYRO and other turbulence codes. We expect that in most C-Mod plasmas the experimentally achievable temperature gradient scale lengths will be larger than or equal to the effective critical gradient scale lengths set by ITG/TEM and/or ETG modes. In some cases it should also be possible to measure density fluctuation amplitudes and radial correlation lengths to enable a broader comparison with theory. Studies in a variety of plasma regimes will experimentally determine important parametric dependences and enable a broad test of theoretical expectations.

12.1.2.10 TRANSP code development

Looking forward to FY-2009 and beyond, known priorities for RF modeling code development in TRANSP are:

- Maintain up-to-date TORIC capability in TRANSP; in particular, update to a future version of TORIC which treats non-Maxwellian target fast ion populations.
- Replace FPPMOD with CQL3D for the plasma response.
- Upgrade/replace the Lower Hybrid code in TRANSP.
- Deploy a stateless server for MPI-parallel RF wavefield calculations, that can be shared amongst multiple TRANSP jobs in production queues at PPPL.

Significant progress in these areas will require an increased level of support by the PPPL/C-Mod collaboration even when combined with support from other projects with similar goals. To this end, we note that the JET TRANSP user community and management have identified ICRF modeling improvement as their top priority for near term TRANSP code development. The JET PPPL collaboration has recently increased its TRANSP support/development combined budget significantly (from 0.2 to 0.7 FTE total). In addition, there are related activities in the SWIM and RF SciDAC projects.

In the SWIM SciDAC, Doug McCune is developing a portable tool for representation of model plasma time slices—the Plasma State module. This module contains data for (tokamak) machine description, MHD equilibrium, profiles, and file references to more elaborate datasets containing e.g. fast particle distribution functions. In the SWIM SciDAC, the plan is to use the Plasma State to couple CQL3D and multiple RF wave codes (TORIC, AORSA) in an integrated model.

TRANSP can already read and write Plasma State objects—it does so to communicate with the TSC code in a client-server arrangement, that was developed as part of a predictive enhancement project for TRANSP (the PTRANSP project). So, it should be possible for TRANSP to leverage the SWIM software development.

The SWIM SciDAC software elements are not mature, and so, specification of schedule for deployment of specific capabilities based on these elements is not possible at this time.

12.1.2.11 ICRF engineering and technical support

PPPL will continue to provide engineering and technical support for the C-Mod ICRF systems on an as-called basis. The level of PPPL technical assistance requested by the C-Mod ICRF group has been small for several years (~0.1 FTE), and we expect trend to continue through the 2009-13 campaign.

12.1.3 Proposed Research (incremental budget)

Increased participation in C-Mod experiments (\$1400): The C-Mod research proposal under incremental funding includes an increase in the yearly experimental run time from 14 to 25 weeks, an increase of 78%, starting in 2010. This makes run time for additional experiments in which PPPL participates, and requires additional support for PPPL-maintained diagnostics. We propose to increase the level of physics support by about 1.0 FTE for the years 2010-2013 to allow increased effort mostly in the areas of LHCD, Advanced Scenarios, edge turbulence measurements, and transport analysis.

Fabrication of variable-frequency RF sources (\$1000k): PPPL proposes to fabricate two new 2 MW variable-frequency RF sources for use in the C-Mod ICRF system. Upon completion, the entire C-Mod ICRF system will have frequency control over the range 40-80 MHz, thereby providing flexible control over the ICRF heating profile for use in generating and controlling Advanced Tokamak plasmas and transport experiments. Fabrication is expected to commence in FY2011 with completion in FY1012.

These will provide considerably greater flexibility in the ICRF heating profile that is useful for improved generation and control of Advanced Plasma scenarios. Construction will begin in FY2010.

CQL3D integration into TRANSP (\$350k): We propose a two-year incremental effort, supported jointly by the PPPL/C-Mod collaboration and NSTX, to increase the rate of progress integrating the CQL3D/GENRAY code into TRANSP. CQL3D is an all-frequencies, multispecies (ions and/or electrons), 2D-in-velocity, 1D-generalized radius, relativistic, bounced-averaged Fokker-Planck code that models LHCD, ICRF, EBW, and HHFW heating and current drive. The funding would primarily support additional efforts by the TRANSP computer scientists for integration activities.

Support for improved edge microturbulence codes (\$150k): We propose to subcontract to Lodestar Research, Inc. to improve modeling of ‘blob’ formation and propagation. Specifically, we propose to use the SOLT code to study the effects of collisionality and divertor sheath physics on edge turbulence in Alcator C-Mod, including simulations of GPI data using atomic physics models (\$50k/year for 3 years).

GPI diagnostic for very small-scale turbulence (\$100k): We propose to extend the gas puff imaging (GPI) diagnostic to a wider range of space and time scales in C-Mod. This requires developing a more highly localized gas injector to improve the spatial resolution, and a higher framing rate camera to improve the time resolution (\$50k/year for two years).

12.1.4 Summary of work related to ITER/ITPA

Description	JOINT Experiments	Notes on PPPL Contribution to C-Mod research
Density profiles at low collisionality	CDB-9	Evaluate whether collisionality effect is caused by i-e equilibration.
Impurity transport in peaked density H-modes	Under discussion	Compare impurity transport & pinch with microturbulence codes
Scaling of spontaneous rotation with no momentum input	TP-6.1	Support $V\phi$ profile measurements; compare profiles & pinches with GYRO
Inter-machine comparison of blob characteristics	DSOL-15	Contribute to design of new GPI views; physics analysis; compare to edge turbulence codes.
Document performance boundaries for steady-state target q-profile	SSO-1	Measure q-profile with MSE; develop plasma scenarios (TSC)
Qualifying hybrid scenario at ITER-relevant parameters	SSO-2.1	Measure q-profile with MSE; control q-profile with LHCD; develop plasma scenarios.

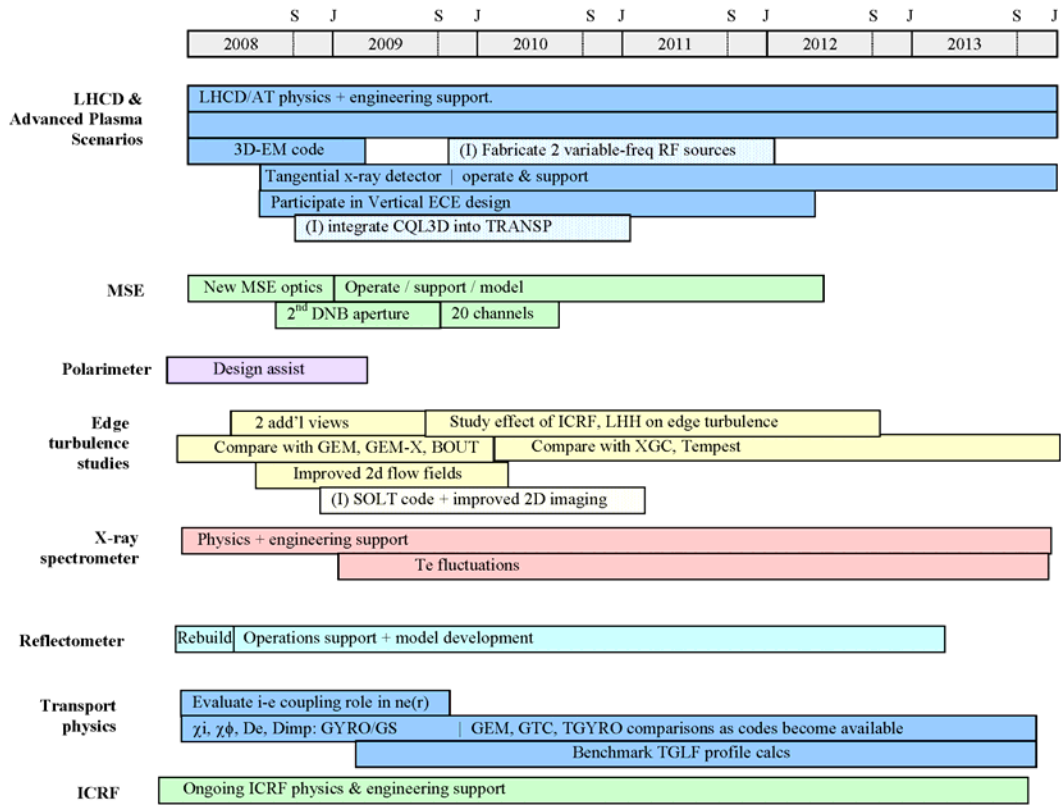
MHD in hybrid scenarios and effects on q-profile	SSO-2.2	Measure q-profile with MSE; control q-profile with LHCD; develop plasma scenarios.
Modulation of actuators to qualify real-time profile control methods	SSO-3	MSE, LHCD.
Simulation and validation of ITER startup to achieve advanced scenarios	SSO-5	Develop & model plasma scenarios (TSC, TRANSP, TGLF), MSE & LHCD.

12.1.5 PPPL Research Objectives within the Alcator C-Mod program

Research Goal	Objectives ('guidance' budget)
Routine, accurate q-profile measurements	Design/fabricate new MSE optics.
	Improve spatial resolution (DNB aperture; with PSFC).
	Design assistance for polarimeter
Measure T_i and V_ϕ profiles with x-ray spectrometer.	Continued diagnostic support & analysis.
	Test feasibility of Te fluctuation measurements.
LHCD	Provide continued physics & operations support as LH systems are extended to full performance.
	Apply emerging RF analysis codes developed by SCIDAC (e.g. TORIC) to model LHCD physics.
	Fabricate 1-channel tangential hard x-ray diagnostic.
	Assist design of new LHCD launcher (EM analysis code).
Edge turbulence	Fabricate & install two telescopes (upper strike point and ICRF antenna views)
	Extend detectors & analysis techniques for improved measurement of 2D flow fields
	Compare measured turbulence with GEM, GEM-X, BOUT, XGC-1, Tempest codes.
	Study effects of edge fueling and geometry on turbulence
	Study effect of ICRF and LH waves on edge turbulence.
Transport experiments	Evaluate role of i-e coupling in observed collisionality dependence of density peaking.
	Extend GYRO/GS2 comparisons of ion heat transport versus experiment to include momentum & particle transport, including pinches, in steady-state plasmas.
	Compare GEM, GTC, TGYRO code predictions to measured transport & turbulence when these codes are

	released publicly.
	Benchmark TGLF predictions of plasma profile evolution in steady-state and time-dependent plasmas.
Reflectometer	Continued operation, maintenance, physics analysis in support of turbulence/transport experiments.
	Replace aged components for improved reliability.
TRANSP	Continued technical support (debug crashed runs).
	Upgrade to version of TORIC that treats non-Maxwellian fast ions.
	Deploy a stateless server for MPI-parallel RF wavefield calculations.

Research Goal	Objectives (incremental budget)
LHCD, Advanced scenarios, turbulence, transport edge MSE,	Increased physics manpower allocation (1.0 FTE in 2010-13) to exploit & support increased C-Mod run time.
Heating profile control for Advanced scenarios plasma	Fabricate two 2 MW tunable RF sources (40-80 MHz).
LHCD understanding and modeling. physics and	Integrate CQL3D into TRANSP.
Improved edge turbulence understanding	Apply SOLT code to study the effects of collisionality and divertor sheath physics on edge turbulence.
	Localized gas puff and higher frame-rate GPI camera for better spatial/temporal resolution of edge turbulence.



References

- [1] N. Bretz, D. Simon, R. Parsells, “A motional stark effect instrument to measure $q(r)$ on the C-mod tokamak”, Rev. Sci. Instrum. **72** (1) 1012-1014 Part 2 Jan 2001.
- [2] N. P. Basse, A. Dominguez, E. M. Edlund, C. L. Fiore et al., “Diagnostic systems on Alcator C-Mod”, Fusion Science and Technology 51 (2007) 476-507.
- [3] S. Scott, J. Ko, I. Hutchinson, H. Yuh, “Effect of secondary beam neutrals on MSE: theory”, 49th Annual meeting, APS Division of Plasma Physics, November 12-16 2007, Orlando, FL, paper NP8.00087.
- [4] J. Ko, S. Scott W. Rowan, R. Granetz et al., “Effect of secondary beam neutrals on MSE: experiment”, 49th Annual meeting, APS Division of Plasma Physics, November 12-16 2007, Orlando, FL, paper NP8.00086.
- [5] P. T. Bonoli, J. Ko, R. Parker, A. Schmidt et al., “Lower hybrid current drive experiments on Alcator C-Mod: Comparison with Theory and Simulation”, invited paper APS 2007, to appear in Physics of Plasmas.
- [6] B.D. Scott, Plasma Phys. Cont. Fusion **49** (2007) S25
- [7] S.J. Zweben et al, Plasma Phys. Cont. Fusion **49** (2007) S1
- [8] R.H. Cohen et al. Nucl. Fusion **47** (2007) 612
- [9] O. Grulke O et al, Phys. Plasmas **13** (2006) 012306
- [10] J.L. Terry et al, Phys. Plasmas **10** (2003) 1739
- [11] J. E. Rice, E. S. Marmer, “Five-chord high-resolution x-ray spectrometer for Alcator C-Mod”, Rev. Sci. Instrum. **61** (1990) 2753.
- [12] R. Chatterjee, P. E. Phillips, J. Heard, C. Watts, R. Gandy, A. Hubbard, “High resolution ECE radiometer for electron temperature and profile measurements on Alcator C-Mod”, Fusion Engineering and Design 53 (2001) 113-121.
- [13] C. L. Fiore, J. E. Rice, P. T. Bonoli, R. L. Boivin et al., “Internal Transport barriers on Alcator C-Mod”, Phys. Plasmas **8** No. 5, May 2001 p. 2023-28.
- [14] J. E. Rice, W. D. Lee, E. S. Marmor, N. P. Basse, et al., “Toroidal rotation and momentum transport in Alcator C-Mod plasmas with no momentum input”, Phys. Plasmas **11** (5) 2427-2432 May 2004.
- [15] M. Bitter, K. W. Hill, B. Stratton, A. L. Roquemore, D. Mastrovito, S. G. Lee, J. G.

- Bak, M .K. Moon, U. W. Nam, G. Smith, J. E. Rice, P. Beiersdorfer, B. S. Fraenkel, “Spatially resolved spectra from a new x-ray imaging crystal spectrometer for measurements of ion and electron temperature profiles (invited)”, *Rev. Sci Instrum* **75** (10) 3660-3665 Part 2, Oct. 2004.
- [16] Ch. Broennimann et al., “The PILATUS 1M Detector,”, *J. Synchrotron Radiation* **13**, 120 (2006).
- [17] M. Bitter, K. W. Hill., S. Scott, S. Paul, A. Ince-Cushman M. Reinke, J. E. Rice, P. Beiersdorfer, M. F. Fu, S. G. Lee, Ch. Broennimann, and E. F. Eikenberry, “Passive Spectroscopy Bolometers, Grating- and X-Ray Imaging Crystal Spectrometers”, Varenna (invited)
- [18] M. Bitter, K. W. Hill, S. Scott, A. Ince-Cushman, M. Reinke, J. E. Rice, P. Beiersdorfer, M. F. Gu, S. G. Lee, Ch. Broennimann, and E. F. Eikenberry, “A novel x-ray imaging crystal spectrometer for Doppler measurements of ion temperature and plasma rotation velocity profiles”, IAEA International workshop “Challenges in Plasma Spectroscopy for Future Fusion Research Machines”, Jaipur, India 20-22 February 2008.
- [19] B. Stratton, M. Bitter, K. W. Hill, S. Scott, A. Ince-Cushman, M. Reinke, J. E. Rice, P. Beiersdorfer, M. F. Gu, S. G. Lee, Ch. Broennimann, E. F. Eikenberry, R. Barnsley, “Progress on Imaging x-ray crystal spectroscopy”, 13th Meeting of the ITPA Topical Group on Diagnostics, Chengdu, China Oct 29- Nov 2, 2007.
- [20] M. Bitter, K. W. Hill, S. D. Scott, A. Ince-Cushman, J. E. Rice, P. Beiersdorfer, M. –F. Gu, J. Dunn, S. G. Lee, C. Broennimann, E. F. Eikenberry, “ITER-relevant developments of X-ray imaging crystal spectrometers on NSTX and Alcator C-Mod”, talk given at the 1st Workshop on Diagnostic Developments for Burning Plasmas, February 6-8, 2007, General Atomics, San Diego.
- [21] M. Bitter, Ch. Brennimann, E. F. Eikenberry, K. W. Hill, A. Ince-Cushman, S. G. Lee, J .E. Rice, S. Scott, “Application of Pilatus II detector modules for high resolution X-ray imaging crystal spectrometers on the Alcator C-Mod tokamak’ poster presented at the 15th International Room Temperature Semiconductor Detector Workshop, October 29 – Nov. 4 2006, San Diego, California.
- [22] G. Bertschinger, M. Goto, O. Marchuk, M. Bitter and the TEXTOR-team, “Space resolved measurements of plasma parameters using x-ray spectroscopy of He-like argon”, 33rd EPS conference on Plasma Phys. Rome, 19-23 June 2006 ECA Vol. **30I**, P-2.153 (2006).
- [23] C. C. Kung, G. J. Kramer, G. D’ Amico, E. Fredd, S. Scott, J. R. Wilson, J. Hosea, A. Dominguez, “Grounding techniques for designing RF / Microwave diagnostic systems”, unpublished.

- [24] C. C. Kung, G. D' Amico, G. J. Kramer, E. Fredd, C. Brunkhorst, S. Scott, J. Hosea, "Grounding, DC supplies, and controlling signal issues for a tunable reflectometry system"
- [25] Shinohara et al., Rev. Sci. Instrum. **70** (1999) 4246.
- [26] R. Nazikian et al., Phys. of Plasmas. **8** (2001) 1840.
- [27] G.J. Kramer et al., Rev. Sci. Instrum. **74** (2003) 1421.
- [28] E. Valeo et al., Plasma Phys. Contr. Fusion **44** (2002) L1.
- [29] R. Nazikian et al., Phys. Rev. Lett. **94** (2005) 135002.
- [30] G.J. Kramer et al., Plasma Phys. Contr. Fusion **44** (2002) L11.
- [31] G. Wang et al., Nucl. Fusion **46** (2006) S708.
- [32] G.J. Kramer et al., Plasma Phys. Contr. Fusion **46** (2004) 695.
- [33] G.J. Kramer et al., Nucl. Fusion **46** (2006) S846.
- [34] D. Mikkelsen, M. Greenwald, J. Candy and R. Waltz, "Collisionality dependence of density peaking in H-mode plasmas in Alcator C-Mod", Bulletin of the American Physical Soc. 49th annual DPP meeting, Vol. **52**, No. 11, pg 212, 2007.
- [35] A. Dimits, et al., Phys. Plasmas **7**, 969, 2000
- [36] D. Mikkelsen et al., "Nonlinear simulations of Drift-wave turbulence in Alcator C – Mod", proceedings of 19th IAEA Conference on Fusion Energy, Lyon, 2002.
- [37] R. Giannella, et al., Rev. Sci Instrum. **75** (2004) 4247.
- [38] C.B. Forest, et al., Phys. Rev Lett. **73** (1994) 2444.
- [39] T. Munsat et al, Rev. Sci. Inst. **77** (2006) 103501; G. McKee et al, Rev. Sci. Inst. **77** (2006) 10F110
- [40] J.R. Myra et al, Phys. Plasmas **13** (2006) 112502, D. D'Ippolito et al, Phys. Plasmas **062503**; S. Krasheninnikov et al, Phys. Plasmas **14** (2007) 102503
- [41] B. Lipschultz et al, Nucl. Fusion **47** (2007) 1189
- [42] D. D'Ippolito et al, Phys. Plasmas **13** (2006) 102508
- [43] R. Zagorski et al, Plasma Phys. Cont. Fusion **49** (2007) S97 ; B.J. Ding et al,

Phys. Plasmas 11 (2004) 207

- [44] S. Von Goeler, J. Stevens, W. Stodiek, S. Bernabei, et al., “Course on diagnostics for fusion reactor conditions”, Vol. 1, Varenna, Italy (1982) 87.
- [45] S. Von Goeler, J. Stevens, S. Bernabei, M. Bitter et al., “Angular-distribution of the Bremsstrahlung emission during lower hybrid current drive on PLT”, Nuclear Fusion 25 (11) 1985, p. 1515-1528.

12.2 Collaboration: Fusion Research Center, The University of Texas at Austin

12.2.1 Overview and Summary

The Fusion Research Center (FRC) of the University of Texas at Austin proposes to operate, maintain, and upgrade diagnostics for Alcator C-Mod and to conduct experiments on the C-Mod tokamak to advance our understanding of plasma transport and turbulence. The diagnostics augment the existing capabilities of the C-Mod group and permit new experiments to quantify the relations between turbulence and transport. Specifically, the FRC will contribute an electron cyclotron emission (ECE) heterodyne radiometer, a charge exchange recombination spectroscopy (CXRS) diagnostic which can also be used for spectroscopy of passive emission from ambient species, and a beam emission spectroscopy diagnostic which can also be used to monitor the performance of the diagnostic neutral beam (DNB). The experiments of primary interest are precision measurements of electron temperature scale lengths for investigation of critical gradients and impurity transport and rotation to improve our empirical understanding of transport barriers. Major diagnostic upgrades will result in ECE measurements of electron temperature at lower toroidal magnetic fields as will be needed to support lower hybrid experiments and in CXRS measurements of fast ion distributions. Both of these upgrades will support lower hybrid experiments. The fast ion diagnostic will also support studies of fast ion transport by Alfvén eigenmodes as planned for the MHD program and deposition studies in the wave-particle interactions program.

During the previous phase of this collaboration, we operated and upgraded an electron cyclotron emission radiometer, a CXRS diagnostic which can also be used for ambient spectroscopy, and a BES diagnostic. We also conducted limited turbulence simulations. Besides measuring the electron temperature profile, the ECE diagnostic was applied to high precision measurements of gradient scale lengths. The CXRS diagnostic contributed ion temperature, impurity density and rotation measurements, and spectroscopy of ambient species. From these followed measurements of radial electric field, shear suppression, and impurity transport. The BES diagnostic was applied to improvements in the understanding of the radial extent and mode structure of the quasi-coherent mode. Throughout this period, we have improved the integration of the collaboration by actively participating in the experiments and by making available the data from these diagnostics.

12.2.2 Planned Research

Search for critical gradients in C-Mod L-mode discharges

Simulations based on critical gradient transport models can produce results consistent with observed transport. Some research on other devices has found no evidence of critical gradients.[12.2.1] On C-Mod, we plan to revisit these experiments with different experimental techniques. Critical gradients in L-mode discharges will be sought as a function of ICRF heating power in the core. The principal instrumentation will be a high resolution ECE diagnostic with the capability of detecting scale length changes with unparalleled accuracy. Incremental heat pulse diffusivity will follow from the scale lengths. The experiment is underway, but initial investigations fell victim to high

radiation loss which masked the thermal transport. More appropriate plasma conditions will be sought.

During previous campaigns, we measured temperature scale lengths (L_{Te}) using small changes in the magnetic field.[12.2.2] Small ramps, $\sim 1\%$, in the toroidal field move the ECE viewing volume along the profile a distance equal to the channel spacing. The change in signal during the ramp provides the gradient and the average signal provides the temperature. The ratio of these two quantities is L_{Te}

$$L_{Te} = T_e / \nabla T_e = \frac{\overline{ECE}(t)}{\frac{\Delta ECE(t)}{\Delta R}} \Bigg|_{\text{during ramp}}$$

which has very high accuracy since it is independent of the calibration of the detectors.

This is a quantity that we can recommend for use in simulation as being the very best available. This technique provides a direct measurement of the temperature scale length that is independent of the channel-to-channel calibration. The high spatial resolution is important since only very small changes ($< 1\%$) in the toroidal field are required to make these measurements. Small changes in the toroidal field are less likely to perturb the plasma.

Since we have already applied this method of scale length measurement in other experiments, it is expected to work well for the critical gradient studies. As an example of previous application, Figure 12.2.1 shows χ_e inferred from the measured temperature scale lengths. It is compared with an empirical formula (Taroni-Bohm) and with the TRANSP calculation of χ_e for similar discharges.

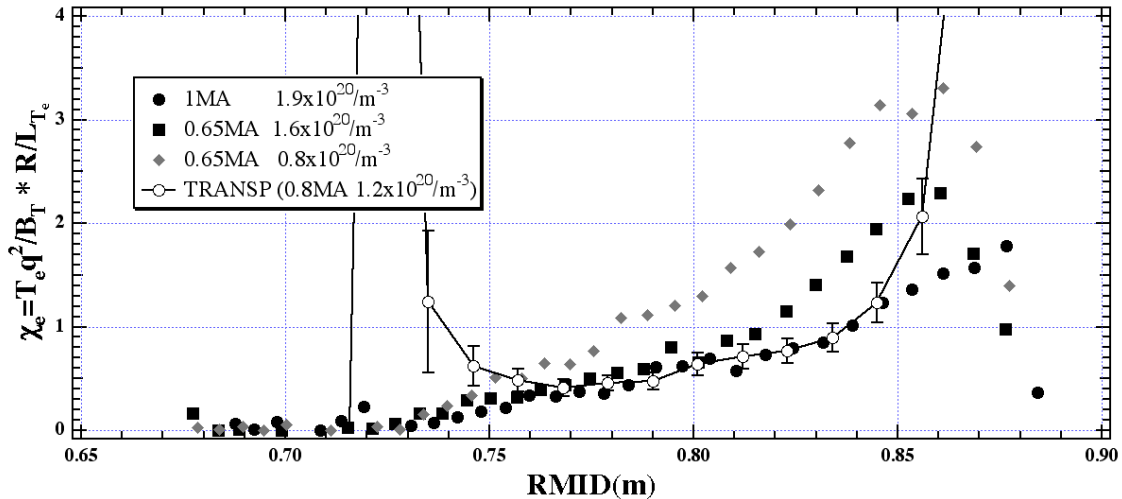


Figure 12.2.1 Detailed measurements of the local L_{Te} using the FRCECE system are used to calculate χ_e from the Taroni-Bohm empirical formula. This is compared to the calculation of χ_e from a TRANSP run for similar conditions.

Thermal Transport Barriers in ITB Discharges

We plan measurement of L_{Te} during ITB discharges. Sawtooth heat pulse experiments have suggested that there may possibly be a thermal barrier in the C-Mod ITB.[12.2.3]

While there is direct evidence for a particle barrier, strong direct evidence for a thermal barrier would add considerably to our understanding. The scale length measurement works best when the discharges have small or no sawteeth. ITB discharges with no sawteeth are common on C-Mod. These discharges are ideally suited to local measurement of L_{Te} using field ramps. Any change in the local L_{Te} would be very important in understanding any thermal transport barriers.

Transport of Light Impurities

Light impurity transport experiments will be pursued on C-Mod first to characterize light impurity behavior for various discharge regimes and then to contribute these new results to further investigations of impurity transport drives and to the differences between transport of light and heavy impurities. Some experiments have begun.[12.2.4] There is renewed interest in impurity transport which has resulted in new suggestions for turbulence driven impurity transport pinches.[12.2.5,6,7] Differences between the transport of light and heavy impurities have been observed on other devices [12.8]. With the ability to measure turbulence and to measure profiles of heavy and light impurities, this is an excellent research opportunity for C-Mod. In these experiments, UT-FRC would contribute light impurity transport.

B^{+5} density profiles can be measured on essentially every C-Mod discharge. This follows from the development of the CXRS diagnostic. An example for an ITB discharge is shown in Figure 12.2.2.

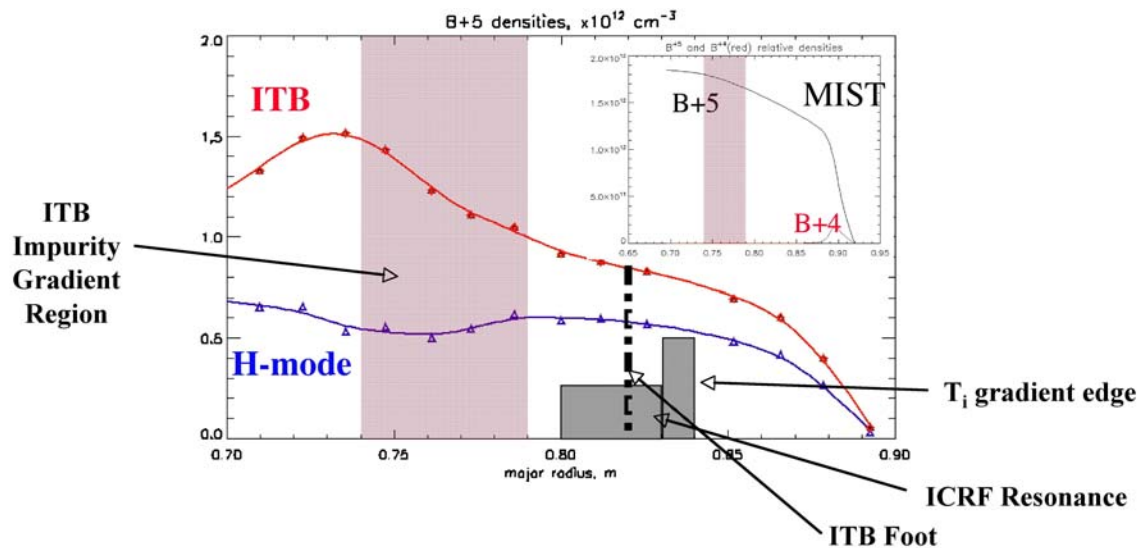


Figure 12.2.2. B^{+5} density profiles during an ITB. The impurity gradient is interior to the ICRF resonance region and the first indications of the particle and thermal transport enhancements.

Heavy impurity (argon) measurements have long been available on C-Mod.

An interesting feature of impurity transport is that heavy and light impurities behave differently in the more interesting confinement modes. Possibly this would be one of the many issues to consider in the choice of wall materials. In ITB discharges, light impurities display peaking but less so than heavy impurities. [12.2.8] Similarly, in low

collisionality experiments, light impurity profiles are not strongly peaked but heavy impurities show core accumulation. [12.2.9,10]

We will explore the physics of the transport and the difference between heavy and light impurities in particular. This can be correlated with radial electric field and expected shear suppression and with measurements of turbulence via phase contrast interferometry. In light of increased theoretical work in this area which was mentioned earlier, we expect that progress can be made.

The role of turbulence suppression in the formation of the ITB

Does shear suppression of turbulence play the strong role in ITB formation that it does in H-Mode formation? E_r is readily measured in the region of the ITB foot ($\rho \sim \rho_{ITB}$) using CXRS. Examples of our own work are in [12.2.11,12] $E \times B$ shearing rates follow from these.

$$\omega_{E \times B} = \frac{(RB_\theta)^2}{B} \left(\frac{\partial}{\partial \psi} \right) \frac{E_r}{RB_\theta}$$

Maximum linear growth rates determined using GS2 [12.2.13] can then be compared to the shearing rates. PCI measurements are also available for direct comparison to turbulence. Figure. 12.2.3 is an example from a recent presentation[12.2.12] of shearing rates.

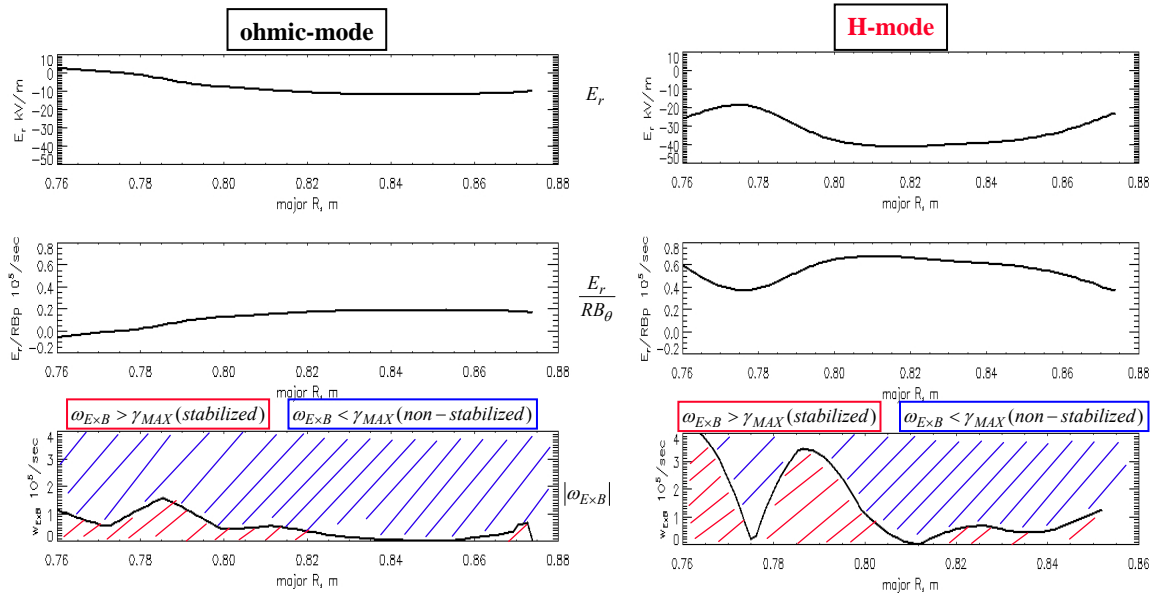


Figure 12.2.3. Calculated E_r and progression to the shearing rate. Comparison between ohmic and H-mode. Shot: 1070718018.

ELM Studies

Discrete and relatively large ELMs occur reproducibly in high triangularity, low v^* region of C-Mod operating space. We supported the C-Mod program investigating these

ELMs.[12.2.14] The FRCECE was able to see fast thermal transport in the ELMs along with a “filament” as seen in non-thermal emission in the edge plasma. The temperature changes detected by the FRCECE, along with a local measurement of density changes, can determine the energy transported in an ELMs. The filament and energy transport are linked to an onset of a magnetic perturbation that marks the “break-away” of a filament that propagates into the SOL as seen in the fast diode imaging array. It is speculated that magnetic reconnection can result in parallel electron acceleration generating the filament. Both the low and high field side pedestals are perturbed before the filament ejection. It is estimated that 10-25% of energy in the pedestal is transported by the ELM even though the pedestal is not destroyed.

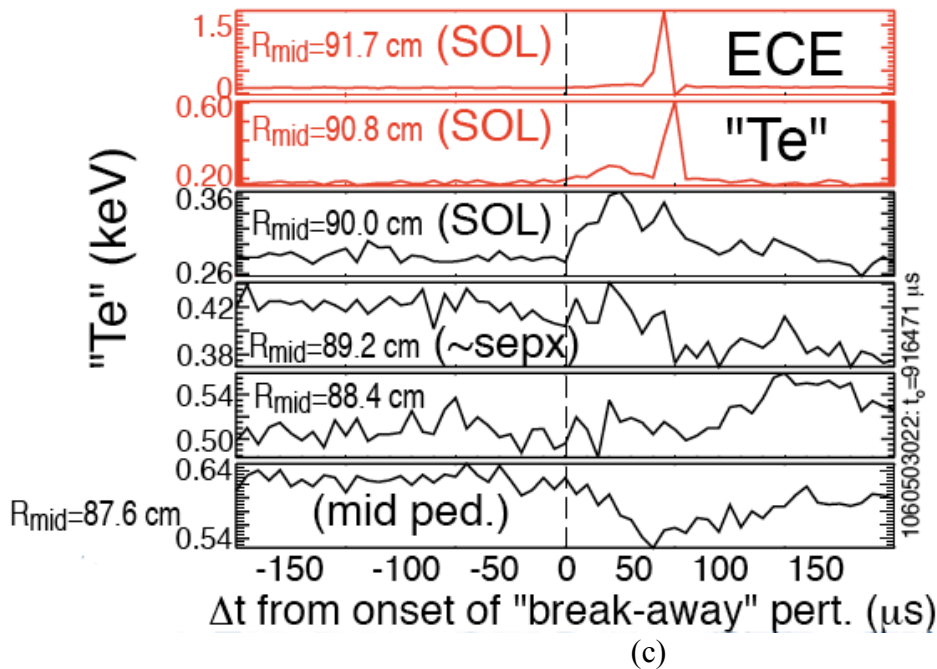
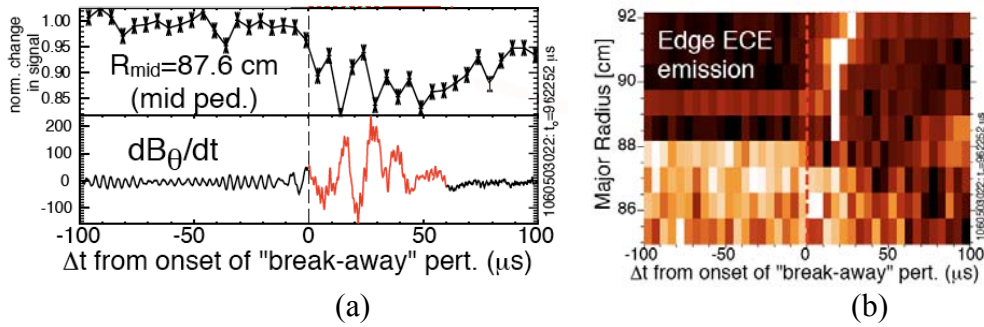


Figure 12.2.4 Onsets of perturbation and “break-away” perturbation are nearly coincident. The ECE emission shows a “filament” also ejected along with a temperature perturbation in the edge profile.

Experimental Plan

The FRCECE has been able to measure fast changes in the edge temperature profiles during ELMs. However, only line integrated density measurement has so far been possible on C-Mod. The BES system should be able to resolve local changes in the

density during these ELMs. With the addition of a local density measurement, BES, and the FRCECE temperature changes the energy transported in the ELM perturbation can be determined. The magnitude of the energy transported in the ELM and how it relates to the overall transport in the plasma is an important factor in operation of future machines such as ITER. This work will be in support of the C-Mod program on heat fluxes in the SOL and divertor.

Doctoral Thesis: Transport Studies on Alcator C-Mod Tokamak Using Charge Exchange Recombination Spectroscopy by Igor Bepamyatnov

This will include some of the work on poloidal rotation, E_r , impurity transport, and turbulence suppression during the formation of the ITB. From the diagnostics development section which is presented below, it will include calibration techniques and error analysis.

12.2.3 Diagnostics and Planned Development

High Resolution Electron Cyclotron Emission (ECE) Radiometer

Upgrades are planned for the FRCECE system to make it available for low-field LH experiments and to take full advantage of the systems innate high bandwidth. A summary of the present system will provide needed context. The upgrades will then be described in that context.

The FRCECE system is unique due to its high frequency (234-306 GHz), large number of channels (32), high spatial resolution (~ 0.6 cm x 2 cm) and wide video bandwidth (1 MHz), which facilitates measurements of complete temperature profiles (on the low field side with a toroidal field of 5.4 T) and fluctuation amplitudes. The diagnostic has been installed on a radial port of the Alcator C-Mod tokamak. It consists of a set of in-vessel collection optics that focus the ECE emission onto a set of overmoded waveguides that then carry the emission to the radio frequency receivers.

Two heterodyne receivers are used to cover the 80 GHz bandwidth. The 234-270 GHz and 270-306 GHz band are down-converted to 4-40 GHz bands, using the local oscillator frequencies of 115 GHz and 133 GHz (a frequency doubled 66.5 GHz LO), which then feed two second harmonic mixers. The mixer blocks have a net RF to IF gain of 10 dB, and employ an anti-parallel diode pair configuration to enhance the second harmonic mixing efficiency and eliminate the fundamental mixing response. The mixers are fed by an integrated diagonal feed horn structure coupled to a fundamental WR-4 waveguide machined into the mixer block. The IF signal from these mixers are split into 32 channels, band-pass filtered and detected using square-law detectors. The output of the detector is amplified by a video amplifier with a 1 MHz response and digitized. The wideband video amplifiers were developed at the University of Texas to reduce the cost of the IF section.

The ECE radiometer that UT-FRC provides for C-Mod yields 32 channels of high temporal and spatial resolution data on each shot. At 5.4 T, the most common field for C-Mod experiments, the channels cover the plasma from the magnetic axis to the low-field-

side separatrix. At lower fields, the measurement range shifts away from the magnetic axis but still provides measurements through the pedestal. At higher fields, the pedestal data is lost. An extension of the frequency range either to higher or lower frequency would benefit C-Mod experiments. We plan to increase the range of the measurements by extending the low end of the frequency range of the diagnostic.

The data acquisition system will be upgraded from a PCI system to a CPCI system. The FRCECE PCI system is one of only a few remaining at C-Mod, thus, an upgrade would make the FRCECE compatible with most of the other diagnostics and reduce the need for the special programming which is now required. Also, we would increase the sampling frequency to 500kHz that would allow fluctuation measurements on all 32 channels for frequencies up to 250 kHz. This would cover many of the interesting fluctuations already observed in the limited number of high frequency channels now available.

The third upgrade is to move the ECE optics to the horizontal midplane. Though on a radial port, the ECE optics are slightly below the midplane. The spatial resolution is decreased by this off-axis location. Also, the diagnostic is more sensitive to non-thermal emission as might be expected during LHCD experiments.

Extend the measurement range of the ECE diagnostic to lower magnetic fields

The ECE diagnostic can cover lower magnetic fields by extending the ECE frequency range to lower frequencies, Figure 12.2.4. This choice is made with careful consideration for the difficulty of the addition and the contribution that it might make to C-mod program.

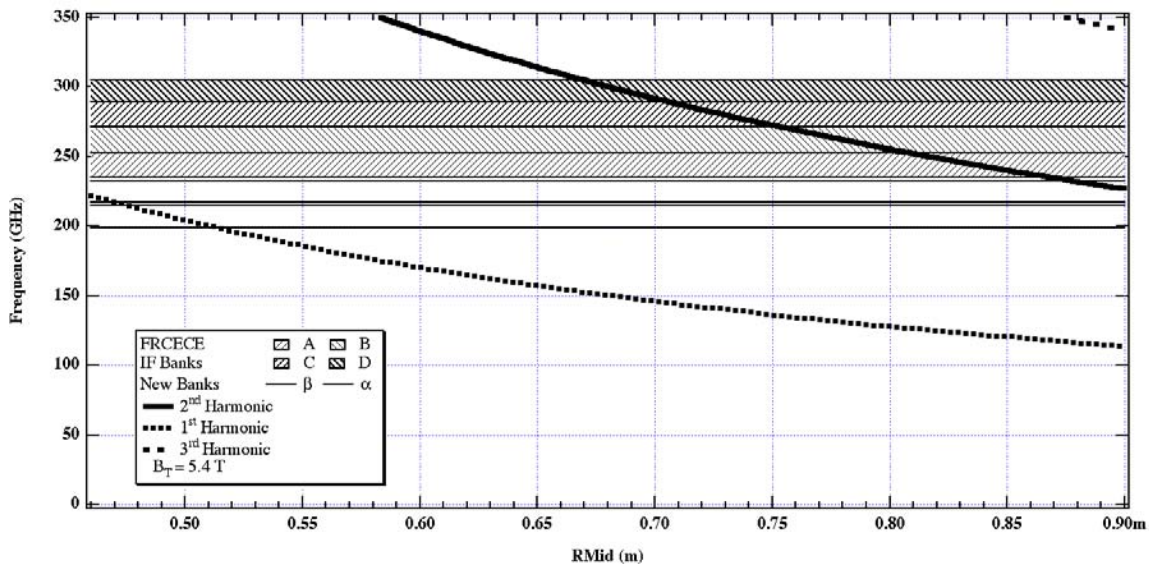


Figure 12.2.4 FRCECE channel locations for a 5.4 T plasma. Each of the four IF banks of channels (A, B, C, D) in the existing system has 8 channels covering the frequency bands shown by the hatched regions. The frequency bands covered by the two proposed banks are shown just below the existing bands as α and β . The large solid curve is the 2nd harmonic frequency as a function of radial position. Also shown are the fundamental and third harmonic frequencies.

In its present form without the proposed upgrade, the radiometer is optimized for observations at 5.4 T. When we ask whether this system would work for ITER, we find that without modification it would cover a frequency range adequate for measurement of

T_e in the proposed ITER plasma from the magnetic axis to within 10 cm of the low-field-side separatrix. Were we to increase the frequency of the C-Mod system in our proposed upgrade, the local oscillators and RF section would become a very difficult development project. It is unlikely that we would find the support for difficult undertaking when ITER will not require higher frequencies. Simply put, this may be the wrong environment for diagnostic development at higher frequency.

We lose some profile capability on C-Mod for experiments at higher field (at 6.3 T only the outer half of the minor radius is covered). The radiometer still covers the critical region outside the $q = 1$ surface including both the ITB zone and the pedestal. This is where the action is in C-Mod. The core can still be covered by existing grating polychromators so our decision to extend the diagnostic to lower frequency rather than higher frequency would not limit operations

Numerous experiments are conducted at lower fields including H-modes and ITB discharges which are intended to improve our understanding of barrier physics. At these fields for these experiments, the edge of the plasma is lost to measurement by the radiometer. It might at first seem that at lower fields, channels for the existing diagnostic would simply move to the high field side of the plasma where they would continue to sample T_e in the gradient region and possibly (for sufficiently low fields) in the plasma edge. Unfortunately, the channels that would sample on the high field side are subject to greater refraction, which reduces the quality of the T_e data. Although the refraction can be used to advantage to allow measurement of density fluctuations, the primary goal must remain the measurement of T_e and that requires providing additional channels at lower frequency. With the forgoing motivation, we now move on to a discussion of the proposed upgrade.

The only addition for this particular upgrade will be a new RF section covering 199 to 232 GHz, Figure 12.2.4. For the low fields, the new RF section will be coupled to the plasma radiation by the insertion of a quasi-optical switch into one of the over-moded waveguides. This new RF section will be connected to two of the existing IF sections. The high frequency RF section is switched out so we still have 32 channels with the upper 16 channels now covering the lower frequency range. This change over will be relatively simple with only a mirror insertion in the waveguide (the quasi-optical switch) and two RF cables from IF banks C and D reconnected to the new RF section. Note that the original configuration with the banks A, B, C, and D will be easily switched back and forth from the new configuration α , β , C, and D depending on the needs of the experiment.

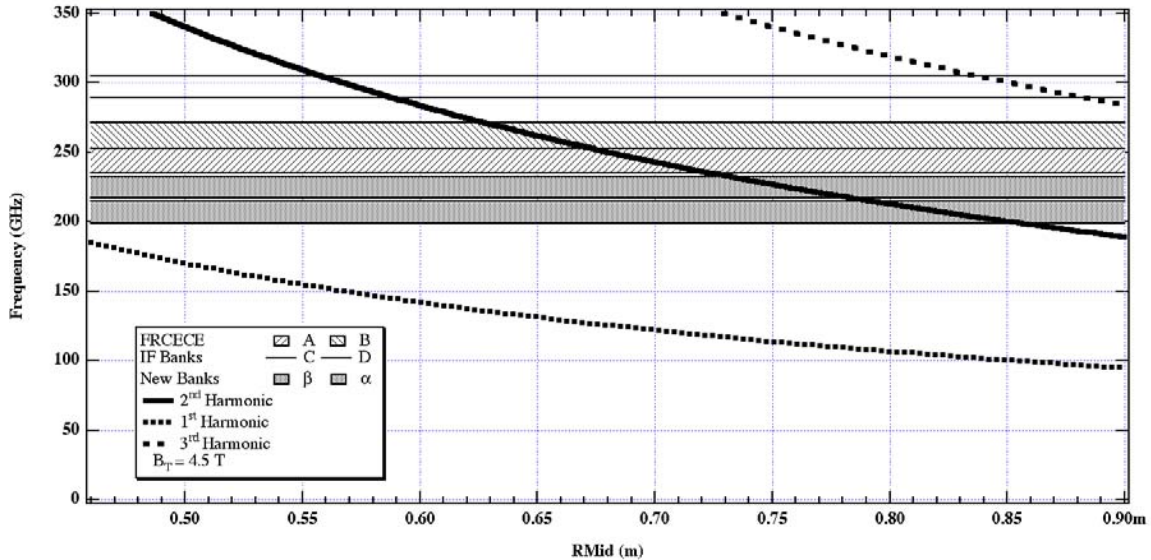


Figure 12.2.5 FRCECE channel locations for 4.5T toroidal field. The fundamental, 2nd and third harmonic are shown. Banks C and D have had their frequency range changed to the ones shown by the addition of a new RF section, banks α and β .

The main cost in this upgrade will be the development of a new RF section, consisting of a wide bandwidth mixer (44 GHz bandwidth) and a second local oscillator (44 GHz) mixer combination to downshift of the upper IF 22 GHz band. There is some difficulty in getting the wide bandwidth at these lower frequencies. The quasi-optical switch will be designed and constructed at the UT-FRC. Additional magnetic shielding will be employed in the redesigned RF box which is needed for the addition of the third RF section.

Data Acquisition Upgrade

The present PCI based data acquisition system for the FRCECE employs a dedicated computer stuffed with data acquisition cards. This older configuration of cards in a stand-alone computer require special attention when the data system is periodically updated. To better fit in with the standards at C-Mod, we plan to convert FRCECE data acquisition to a CPCI system. The newer system will allow higher sampling speeds, up to 500 kHz for a 32 channel low cost card, ACQ196CPCI. The present system has a bandwidth of 100 kHz for all 32 channels. This has limited the fluctuation measurements since there are observed fluctuations observed on other diagnostics at higher frequency, including QC modes and some broadband fluctuations around 200 kHz. The new system will allow all the channels to observe fluctuations up to 250 kHz.

After this upgrade, we will retain the ability to measure at frequencies up to 2 MHz for specific opportunities and only for a limited number of channels. The anti-aliasing filter amplifiers for the system will need modification to allow for the higher frequencies. These boards were designed and built at the FRC so upgrading will not be a significant additional cost. The addition of a CPCI system will also make upgrading of the very fast channels, up to 2 MHz, relatively easy for those occasions when high frequency is needed, for the search for induced TAE modes.

Move the FRCECE system to the horizontal midplane

The FRCECE utilizes an internal antenna system consisting of a poloidally-focusing elliptical mirror that couples to two smaller toroidally-focusing parabolic mirrors that then couple into the two over-moded waveguide transmission lines. The main antenna is in close proximity to the plasma and collects radiation at a 15° angle. This angle was required to work around the conflicts with the large number of other diagnostics installed at this port (F port). We are proposing to move the FRCECE to use the existing C-Mod ECE collection optics. There are a number of reasons for this change. Firstly, F-port is heavily used for other diagnostics and there are inevitable conflicts and risk of misalignment for the FRCECE mirrors and waveguide system. Also, the internal antenna is in close proximity to the plasma and has thus become coated during heavy boronization. This has resulted in significant changes in the FRCECE signal which can lead to uncertainties in the temperature measurements. Additional diagnostics are planned for F-port that would increase conflicts. These would all be alleviated by the proposed modification.

The C-Mod ECE collection system has similar spatial resolution to the FRCECE system: it is near diffraction limited. Due to the previous mentioned conflicts in F-port, the FRCECE system is at a 15° angle to the plasma centerline, and this results in a coupling between the poloidal and radial resolution. The FRCECE channel bandwidth (1.5GHz) would lead to a radial resolution of approximately 6 mm. However, the poloidal antenna pattern, as shown in Figure 12.2.5, due to the 15° angle increases the radial resolution across flux surfaces to a few centimeters. The C-Mod ECE collection system is on axis so better radial resolution would be obtainable.

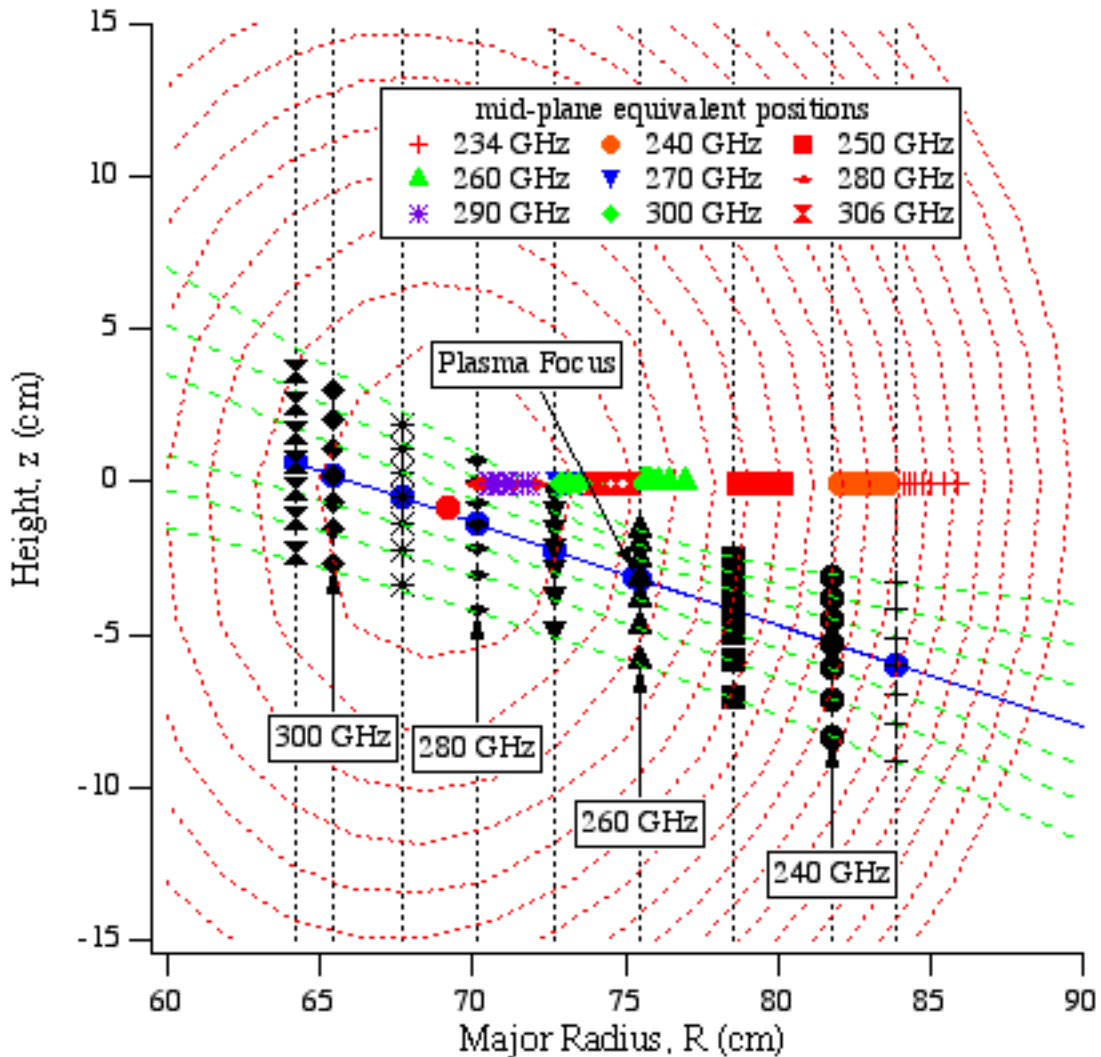


Figure 12.2.6. Improvement in radial resolution by placing the FRCECE optics on-axis. Rays that enter the FRCECE optics are shown in green and this defines the vertical extent of plasma observed by each FRCECE channel. The vertical extent observed by a particular channel maps to an extended radial range.

Refraction effects have been observed in the FRCECE data. In some high-density C-Mod plasmas, temperature profile measurements on the high field side are modified by refraction in the high-density regions. An on axis view would minimize these effects. Cut-off of the FRCECE signal is also observed at lower densities than are seen in the C-Mod ECE system due to refraction of the off-axis FRCECE in the high density core plasma.

Utilizing the C-Mod ECE optics would also allow the RF and IF section to be removed from the C-Mod cell which has restricted access during plasma operation. Removal then leads to two significant benefits. There have been significant problems resulting from RF system proximity to the high fields in C-Mod. This led to the failure of the local oscillators and the need to add magnetic shielding to specific components. Second, placement of the RF and IF section outside the cell would allow the quicker change over

for the switch between RF sections which was described above since cell access would not be required.

In order to accomplish this, a coupling between the C-Mod ECE system and the two FRCECE RF sections will need to be designed. This will involve the C-Mod and FRC group so the existing system will not be adversely affected. Details will need to be worked out in the time period before the proposed transfer is scheduled. .

CHARGE EXCHANGE RECOMBINATION SPECTROSCOPY

We operate, maintain and upgrade a charge exchange recombination spectroscopy diagnostic to measure ion temperature, T_i , poloidal rotation, v_θ , and toroidal rotation v_ϕ , of a boron impurity as well as to measure the distribution of the fully-stripped boron n_B v_I in the plasma. From these, the radial electric field

$$E_r = \frac{kT_\sigma}{e_\sigma} \left[\frac{1}{n_\sigma} \frac{\partial n_\sigma}{\partial r} + \frac{1}{T_\sigma} \frac{\partial T_\sigma}{\partial r} \right] - v_{\sigma\theta} B_z + v_{\sigma z} B_\theta$$

can be inferred. Two optical systems are used to acquire the data, a poloidal and a toroidal optical system. The poloidal optical system views are distributed along the beam trajectory, and in the plasma range $67.8 < R < 91.0$ cm (Figure 12.2.7, red chords). The second optical system (generally described as the toroidal system) is mainly toroidal but with a minor poloidal component over the width of the DNB. This system views the plasma (along the beam) over a narrower range $74.2 < R < 86.3$ cm (Fig 12.2.7, blue chords). The temporal resolution of the CXRS data acquisition system is $\Delta\tau > 12.5$ ms when all 45 views are simultaneously observed.

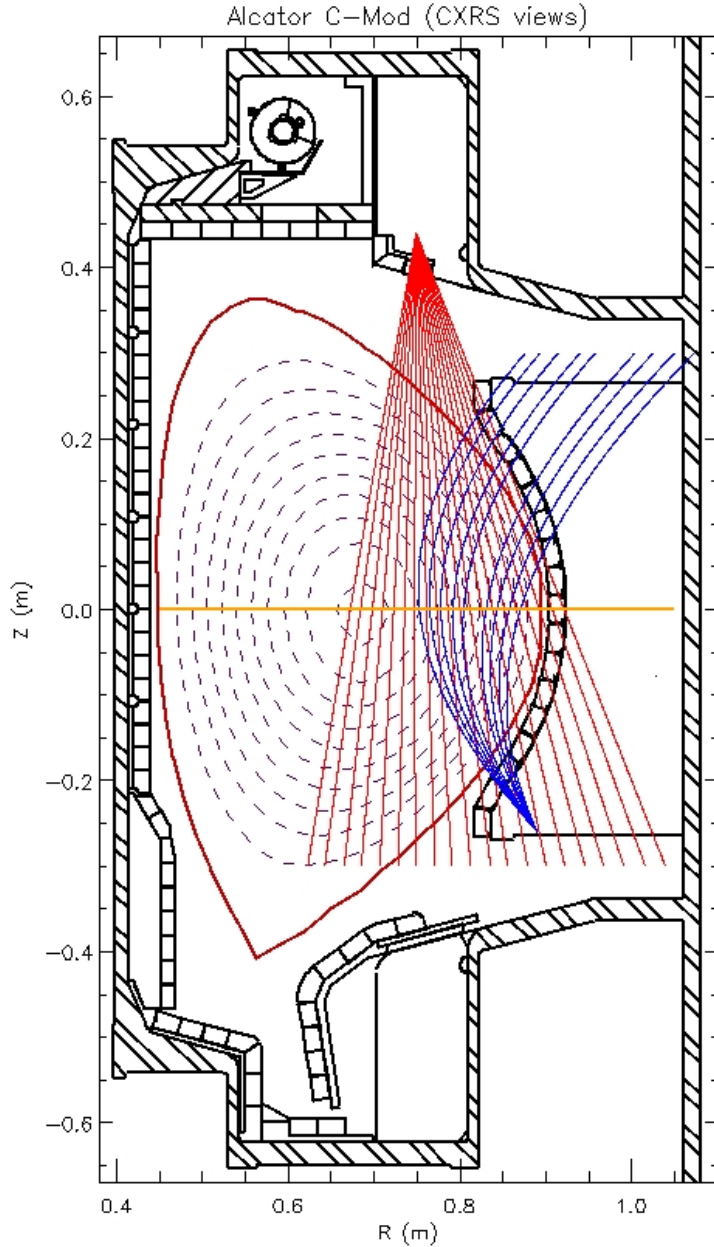


Figure 12.2.7. Two sets of view chords intersect with the neutral beam (yellow center-line) to collect emission from the B^{+4} ions that are formed in the interaction of B^{+5} ions with the neutral beam. The poloidal coverage (red) is $67.8 < R < 91.0$ cm, toroidal chords are traced (blue) starting from an out-of-paper-plane and ending in-plane. Toroidal coverage: $74.2 < R < 86.3$ cm

The region is rich in opportunity for physics studies of transport. One is the opportunity for improving understanding of transport barrier confinement. First, the region of measurement covers the foot of the C-Mod ITB, the region in which the transition to improved confinement occurs. Note that E_r is critical for interpretation of turbulence diagnostics. An example is the interpretation of turbulence phase velocity measurement from BES, reflectometry, or PCI by identifying $E \times B$ rotation. It can also support

interpretation of gyro-kinetic codes via measurements which will lead to accurate “quench rule” estimates and interpretation of turbulence codes and diagnostic analysis by characterization of shearing rate. The measurement of E_r is so critical to physical understanding that sometimes we lose sight of the independent importance of the individual measurements (poloidal rotation, toroidal rotation, impurity profiles and ion temperature) that contribute to E_r . Each provides critical information and rich opportunities for physics studies and all will be included here as well.

Proposed diagnostic upgrades

The diagnostic upgrades proposed for this period include replacement of the toroidal optics with a system that provides coverage similar to that of the poloidal system and increases the throughput of the system. At least one additional set of optics will be added that does not view the beam to allow alternative background subtraction schemes. Spectrometer modifications will be made to simplify calibration.

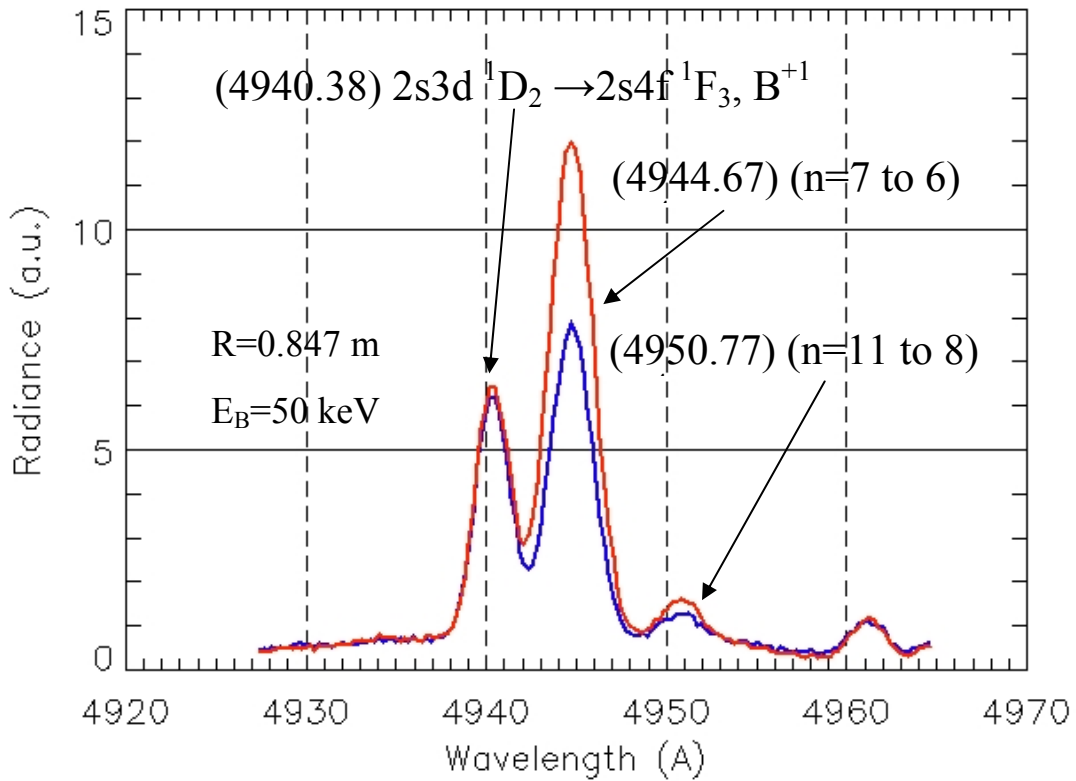
Toroidal Optical System

The range of view covered by the toroidal optical system is narrower than that of the poloidal system. This limits the range over which E_r can be inferred. Attempts to investigate toroidal momentum transport are also limited by this. The toroidal optical system that is presently installed can be improved through the use of improved shuttering techniques and improved fiber optics based on the lessons learned since its installation many years ago.

Background Subtraction

The spectrum viewed is a combination of ambient and charge exchange spectra (See Fig. 12.2.8 (a)). In the analysis of the spectra, it is necessary to remove the spatially averaged ambient emission from the more valuable spatially localized CXRS emission (blue component in Fig 12.2.8 (a)). There are several methods for background subtraction. The one in use at present is to modulate the beam (See Fig. 12.2.8 (b)). We propose to add two new ones. One of these is to use our detailed knowledge of the spatial and temporal temperature and density of the plasma to predict transients in the ambient background. As a second technique, we plan to install an additional set of optics which will view a portion of the plasma near to the DNB but offset from it so that the beam excitation is not evident.

(a)



(b)

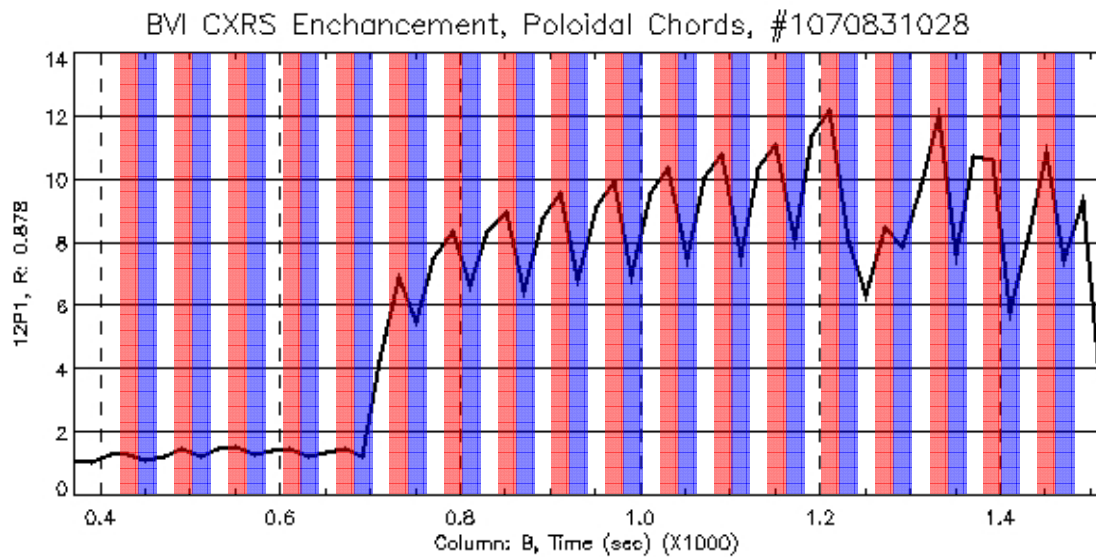


Figure 12.2.8. Beam modulation method. (a) Typical CXRS emission spectrum. Red spectrum is acquired during the DNB pulse. Blue spectrum is acquired during the following DNB OFF frame. (b) CXRS B+4 (n=7-→6) spectral line intensity time history. Red stripes are time intervals when beam is ON. Blue stripes are time intervals when beam is OFF.;

Spectrometer Improvements

The data from many plasma chords is introduced to the imaging spectrometer through many fiber optics. The location of the chords in the entrance plane of the spectrometer is arranged so that the spectrally resolved image at the exit plane matches the rectangular pixel matrix of the camera used as the detector. The location of the chords in the entrance plane was determined theoretically. The fibers will be relocated based on experiment. This will simplify some aspects of the data analysis.

BEAM EMISSION SPECTROSCOPY

The BES diagnostic is a filter spectrometer with eight discrete channels. These are distributed between $R=0.70$ m and $R=0.89$ m. The spatial resolution is approximately 5 mm, and the temporal resolution is 200 kHz.

The BES diagnostic will be used for measurements of narrow band fluctuations, and that role is well established. If possible, its role will be expanded to DNB attenuation and diameter. Measurements of the neutral beam density are required where boron absolute or relative densities are needed. For example, boron densities are needed for impurity transport measurements and for CXRS based E_r measurements. The diameter of the beam is measured at two locations. One of those is provided by BES. It is near the focus of the beam and is located in the plasma. When supplemented by a measurement near the output of the beam, accurate determination of the beam size throughout the plasma is assured. It may also be possible to configure the BES diagnostic to directly measure the beam attenuation. Beam attenuation is typically inferred from detailed measurements of plasma parameters and simulation using various cross sections. We would not need to depend on this simulation if we develop means for interpreting BES measurements.

CXRS DIAGNOSTIC FOR FAST IONS ON C-MOD

Introduction

Fast-ion populations in Alcator C-Mod plasma can be detected by their interaction with a diagnostic neutral beam.[12.2.15] This will contribute to two active research areas on C-Mod. One is the validation of the physics models for RF deposition physics via minority ions. (Wave Plasma Interactions) The other is the study of Alfvén eigenmodes (Global Stability) via their diffusive effect on fast ion populations.

Experimental Method

The fast-ion population in a plasma can be detected and its density and energy measured via charge exchange of the fast-ions with an injected beam of neutral hydrogen. The newly formed fast neutral is then observed as Doppler-shifted H_α emission which stands out against the wing of the broad ambient background spectrum of plasma D_α . The newly formed fast neutral retains the velocity vector of the fast ion. The rate of production of fast neutrals from fast ions is a well-understood process. Thus, the spectral measurements of the fast neutral provide detailed information on the kinetics and the density of the fast ion population.

The emission is detected in the visible spectral region using standard optical techniques. Light is collected from the plasma along individual chords, Fig. 12.2.9a, which intersect with the neutral beam. Thus, the measurement is localized to the beam intersection

region. The light from each chord is spectrally analyzed in a high-throughput, imaging spectrometer such as that in Fig. 12.2.9b. This instrumentation is much like that already in use for charge exchange spectroscopy on C-Mod. In fact, one step in the development path is to test the technique using some of the existing CXRS instrumentation.

Diagnostic Development Path

- Simulate the emission expected on C-Mod.
- After completing a simulation that indicates success for the measurements, the Wide-View CXRS diagnostic will be used for an inexpensive proof of principle. Only one optical component in the system will be changed. This is the grating in the spectrometer. Fast ions will be created using ICRF or Alfvén eigenmodes. The emission will be analyzed with emphasis on understanding the signal to noise and using it to estimate the limits of detectability for the fast ions.
- With success in the previous area, dedicated optics will be developed and fielded. This will include a spectrometer/imaging-detector system and optics for plasma views. The latter may be a completely new set of optics or one of the existing views after modification to add views for the fast ion diagnostic.

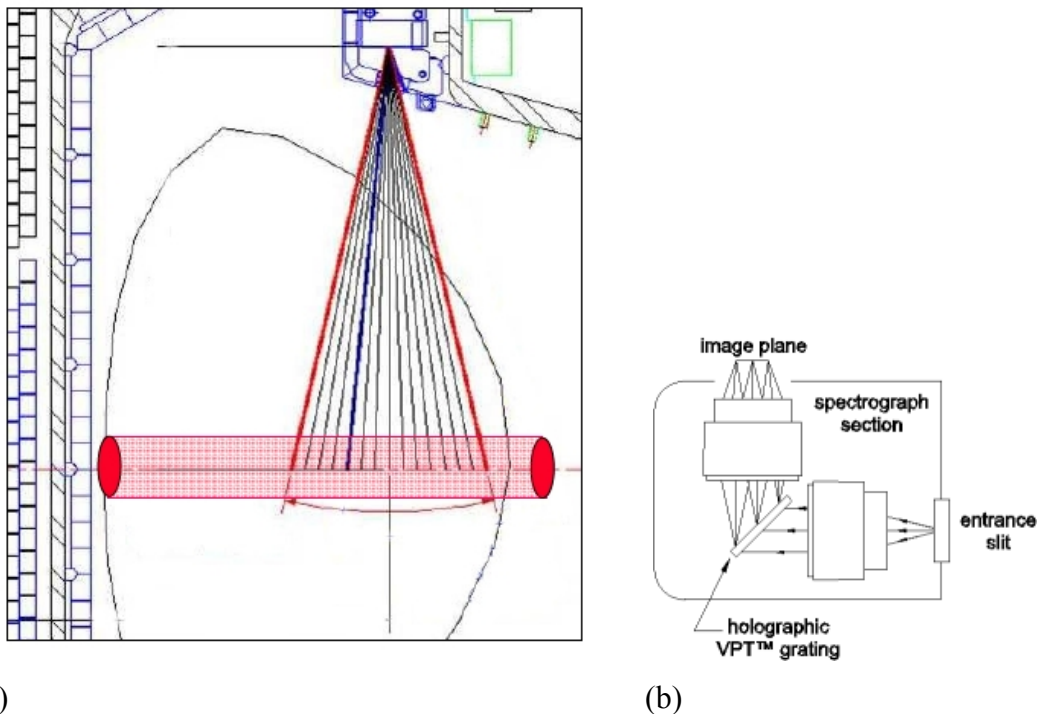


Figure 12.2.9. A typical set of view chords intersect with the neutral beam to collect emission from the fast neutrals that are formed in the interaction of fast ions with the neutral beam (panel a). The emission is transported to the spectrometer via fiber optics (not shown). A state-of-the-art high-throughput imaging spectrometer (panel b) provides spectral analysis of the emission which is detected and digitized with a fast, high-sensitivity camera (not shown).

12.2.4 Personnel

The Fusion Research Center of the University of Texas at Austin assigns 1.7 professional FTE's and 2 graduate students to the C-Mod program. The high-spatial-and-temporal-resolution FRCECE diagnostic, the Wide-View CXRS diagnostic, and the Beam Emission Spectroscopy systems are all the responsibility of the FRC. The FRC staff participate in conducting experiments on C-Mod, supporting the experiments of others, and in C-Mod operations.

12.2.5 References

[12.2.1] J.C. DeBoo, S. Cirant¹, T.C. Luce, A. Manini, C.C. Petty, F. Ryter, M.E. Austin, D.R. Baker, K.W. Gentle, C.M. Greenfield, J.E. Kinsey and G.M. Staebler, Nucl. Fusion 45, 494, 2005

[12.2.2] "Temperature Scale Lengths and ETG Models for C-Mod", P. Phillips, 16th US Transport Task Force Workshop and 9th Joint US-EU Workshop, Madison, Wisconsin, 2-5 April 2003

[12.2.3] S. J. Wukitch, et al. Phys. Plasmas 9, 2149 (2002).

[12.2.4] "Light impurity transport at an internal transport barrier in Alcator C-Mod," paper in preparation.

"Ohmic and RF Heated ITBs in Alcator C-Mod," William L. Rowan, Igor O. Bespamyatnov, C.L. Fiore, et al., Abstract:NP8.00072, 49th Annual Meeting of the Division of Plasma Physics, November 12–16 2007; Orlando, FL

[12.2.5] C. Angioni and A. G. Peeters, Phys. Rev. Lett 96, 095003, 2006.

[12.2.6] N. Dubuit, X. Garbet, et al., Phys. Plasmas 14, 042301, 2007.

[12.2.7] R Guirlet, et al., Plasma Phys. Control. Fusion 48, B63–B74, 2006

[12.2.8] R. Dux, et al., Nucl. Fus. 44, 260, 2004.

[12.2.9] H. Weisen, et al., Nucl. Fus. 45, L1, 2005

[12.2.10] M. E. Puiatti, et al., Phys. Plas. 13, 042501, 2006

[12.2.11] "Studies of H-mode Pedestal Width through Gyrokinetic Microstability Analysis of the Top of the Pedestal," R. V. Bravenec, W. L. Rowan, I. O. Bespamyatnov, R. J. Groebner, T. Osborne, J. Candy, G. M. Staebler, DIII-D team, M. Greenwald, Alcator C-Mod Team, W. Dorland, 2006 Transport Task Force Meeting , Apr 4, 2006 - Apr 7, 2006, Myrtle Beach, SC, USA

[12.2.12] "Impurity poloidal rotation and other CXRS measurements for $0.1 < \rho < 1.0$ in Alcator CMod plasmas," Igor O. Bespamyatnov, William L. Rowan, , et al., Abstract:NP8.00077, 49th Annual Meeting of the Division of Plasma Physics, November 12–16 2007; Orlando, FL

[12.2.13] M. Kotschenreuther, G. Rewoldt, and W. M. Tang,
Comput. Phys. Commun. **88**, 128 (1995).

[12.2.14] “Investigation of Edge Localized Modes in Alcator C-Mod”, J. L. Terry, et al,
GI1.00004, 48th Annual Meeting of the Division of Plasma Physics, October 30 -
November 3, 2006; Philadelphia, PA

[12.2.15] W W Heidbrink, et al, Plasma Phys. Control. Fusion 46 1855, 2004

12. 3 MDSplus

Recent Highlights

The major software development activity in recent years continues to be the support and enhancement of the MDSplus Data System which now runs on a wide variety of computing platforms. MDSplus is by far the most widely used data system in the international fusion program. It is used in its entirety for the data acquisition and analysis systems for TCV (EPFL - Switzerland), RFX (IGI - Padua), NSTX (PPPL), Helic (ANU - Australia), MST (U. Wisconsin), HIT, TIP, TCS and ZAP (U. Washington), PISCES (UCSD), CHS (NIFS - Japan), LDX (MIT), HBT-IP and CTX (Columbia U.) and of course C-Mod. It is used to store processed data for DIII-D, for the collaborative data archives assembled by the ITPA, and for the inputs and outputs of several widely used codes, including EFIT, TRANSP and GS2. JET and ASDEX-Upgrade are using MDSplus as a remote interface to existing data stores and KSTAR has adopted it as a data acquisition engine for data stored in other formats. The result is a defacto standard which greatly facilitates data sharing and collaborations across institutions. At the same time, the breadth and variety of uses for MDSplus has increased the burden of supporting and documenting the system. A web site, <http://www.mdsplus.org> has been built to support the widespread user base and documentation is currently undergoing a major upgrade. The web site has been converted completely to a WIKI based system which makes it much easier to manage and update. MDSplus users worldwide are encouraged to participate in keeping the MDSplus online documentation accurate and up to date. Installation kits for all the supported platforms have been built and can be accessed this web site.

MDSplus software maintenance, bug fixes and ongoing support for off-site installations continues to be a major activity for the MDSplus development group. New support for data acquisition hardware was added, with emphasis on CPCI devices which have become increasingly popular. Support for new IEEE-1394 camera models has been added. Site specific work has been done for experimental groups at Columbia University, PPPL, University of Wisconsin, LDX (MIT/Columbia University), DIII-D, UCLA, University of Washington. A list of active fusion sites is appended at the end of this document.

The MDSplus system has also been enhanced with capabilities for handling storage of continuous data streams. Prior to these enhancements, MDSplus was suitable for storing only pulse based data but now it is possible to append data from continuous data sources. For example, much of the trending data such as the monitoring of the vacuum and cooling systems of the C-MOD experiment are now recorded using MDSplus. These enhancements will make it possible to use MDSplus on experiments with long pulse or continuous operation where it is impractical to wait for the pulse to complete before acquiring and analyzing the data. This feature is currently in use at the C-Mod experiment at MIT for storing continuous trend data and for storing data from high speed cameras.

MDSplus installation kits are upgraded frequently and made available on the MDSplus web site for a number of computing platforms. To date there have been over 5000 downloads of MDSplus installation kits.

The MDSplus developers have been included in design discussions for the ITER CODAC system to ensure that the system used on ITER includes many of the valuable capabilities provided by MDSplus.

Plans

Support for remote MDSplus sites will be increasing as the number of sites and the number of users increases. An ongoing effort to improve online documentation and to train local support staff at each of the major sites where the code is used will be made. The hope is to continue to hold an MDSplus users meetings on a biennial basis. The next meeting is scheduled in conjunction with the IAEA technical meeting in France in 2009. MDSplus software maintenance will continue to be a principle activity

We anticipate adding enhancements to the long pulse extensions as we gain more experience with their use. Some of the visualization tools will be enhanced to better handle continuous data streams. The KSTAR and EAST tokamaks have expressed particular interest in these developments.

There has also been some exploratory work done investigating the use of high level programming languages such as Python for re-implementing the existing MDSplus expression evaluation capabilities and we expect some of this work to continue. The expression evaluation capability found in MDSplus is one of the most important features of the system but is also is the most difficult software to maintain or enhance. Porting this functionality to a language such as Python should improve its maintainability and make it far easier for MDSplus developers and users to add new capabilities to the system.

Support for additional data acquisition devices – particularly CPCI will be provided as useful modules are identified.

Partial List of MDSplus sites.

US:

- PSFC - MIT
- PPPL
- GA
- U. Wisconsin
- U. Texas
- UCLA
- Columbia

- U. Washington
- Auburn University
- Los Alamos
- University of Maryland
- University of Utah
- U.C. Irvine
- SAIC, San Diego
- UCSD
- LBL
- NASA, Huntsville
- Ad Astra Rocket, Houston, TX

International:

- IGI- Padua, Italy (RFX)
- EPFL – Lausanne, Switzerland (TCV)
- EFDA-JET – Culham, UK (JET)
- UKAEA – Culham, UK
- IPP-Garching, Germany
- CEA – Cadarache, France (TORE-SUPRA)
- Kurchatov Institute of Nuclear Fusion – Moscow, Russia
- IPP – Hefei, China (HT-7, EAST)
- Korean Basic Science Institute, Taejon, S. Korea (KSTAR)
- NIFS – Toki, Japan
- Australia National University, Canberra (HELIAC)
- ENEA - Frascati, Italy
- University of Quebec
- Institute for Plasma Research, Gandhinagar, India
- Ad Astra Rocket Company, Liberia, Costa Rica

13 Key Personnel and Publications

M.I.T. is a university, and so has a somewhat different organizational structure from, for example, an industrial corporation or a national laboratory. In addition to the familiar faculty tenure track, M.I.T. has a parallel career structure for research scientists and engineers which gives them an identifiable promotion path and appropriate security. There are three levels above the post-doctoral position: “Research Scientist/Engineer”, “Principal Scientist/Engineer”, and “Senior Scientist/Engineer”. A Senior Scientist is the research equivalent of a full professor, and comparable review procedures to those on the academic side are required for promotion to the Principal and Senior levels.

13.1 Resumes of Key Personnel

The resumes of selected personnel are given in this section to indicate the very high quality of research and engineering expertise represented in the Alcator group. An additional factor that cannot be adequately conveyed in this way, but that is of great importance, is the many years of experience as a group that Alcator has. A dynamic research group is ideally more than the sum of its individual members. Working together as a team for a period spanning twenty years has developed a mutual respect and understanding in all levels of the group that brings out the best in every member.

Dr. Earl S. Marmor
Senior Research Scientist, Department of Physics, and Alcator Project Head
Principal Investigator, Alcator Project

Education

B.Sc. (Hons., Physics), University of Manitoba (1972)

M.A. (Physics), Princeton University (1974)

Ph.D. (Physics), Princeton University (1977)

Professional Experience:

Dr. Marmor is a Senior Research Scientist in the Department of Physics and Head of the Alcator project at the MIT Plasma Science and Fusion Center. He has overall responsibility for the activities of the Alcator research program.

Dr. Marmor's main research interests are: high temperature plasma diagnostics, atomic physics of low, medium and high Z ions, and particle transport and plasma wall interactions in tokamak plasmas.

As a graduate student at Princeton University, Dr. Marmor helped to develop a technique to introduce an intense beam of low energy neutral atoms into the edge of a tokamak plasma discharge. This technique, known as laser impurity injection, has found subsequent application in fusion related experiments worldwide.

From 1979 through 1987, Dr. Marmor was co-principal investigator of the Plasma Wall Interactions Task of the Alcator Project. From 1984 to 1987, Dr. Marmor was Principal Investigator of the High Resolution X-Ray Spectroscopy Development Project at the Plasma Fusion Center. He worked closely with Dr. John Rice on this project, and, in addition to ion temperature profile measurements, they made the first clear observations of charge transfer, from intrinsic neutral hydrogen, to highly stripped impurity ions, in a tokamak plasma.

In 1986, Dr. Marmor proposed a novel diagnostic technique to measure the internal magnetic fields and current density profile in tokamaks. Proof of principle experiments were carried out on Alcator C. This work continued with a very successful collaboration at the TFTR facility in Princeton. In related experiments, it was discovered that lithium wall conditioning can profoundly influence the particle dynamics in carbon walled tokamaks, and all of TFTR's highest fusion power D-T operation was achieved with the help of intense lithium pellet wall coating. In ongoing experiments on Alcator C-Mod, the Li pellet imaging technique is being used to measure internal poloidal magnetic field profiles.

Dr. Marmor has served on a number of advisory panels, including the DIII-D PAC, the NCSX-PAC, the Fusion Energy Sciences Advisory Committee, the Next Step Options Advisory Committee, the US-ITER Project Technical Advisory Committee and the Executive Committee of the University Fusion Association. He currently serves on the Advisory Council of the US Burning Plasma Organization. Dr. Marmor is a fellow of the APS.

Publications:

Rice, J.E.; Ince-Cushman, A.; Degraessie, J.S.; Eriksson, L.-G.; Sakamoto, Y.; Scarabosio, A.; Bortolon, A.; Burrell, K.H.; Duval, B.P.; Fenzi-Bonizec, C.; Greenwald, M.J.; Groebner, R.J.; Hoang, G.T.; Koide, Y.; Marmar, E.S.; Pochelon, A.; Podpaly, Y., “Inter-machine comparison of intrinsic toroidal rotation in tokamaks”, *Nuclear Fusion* **47**(2007) p 1618.

Marmar, E.S., “The Alcator C-Mod program”, *Fusion Science and Technology* **51**(2007) p 261.

Lipschultz, B.; Lin, Y.; Reinke, M.L.; Hubbard, A.; Hutchinson, I.H.; Irby, J.; LaBombard, B.; Marmar, E.S.; Marr, K.; Terry, J.L.; Wolfe, S.M.; Whyte, D., “Operation of Alcator C-Mod with high-Z plasma facing components and implications”, *Physics of Plasmas* **13** (2006) p 056117.

Rice, J.E.; Hubbard, A.E.; Hughes, J.W.; Greenwald, M.J.; LaBombard, B.; Irby, J.H.; Lin, Y.; Marmar, E.S.; Mossessian, D.; Wolfe, S.M.; Wukitch, “The dependence of core rotation on magnetic configuration and the relation to the H-mode power threshold in Alcator C-Mod plasmas with no momentum input”, *Nuclear Fusion* **45**(2005), p 251.

Fiore, C.L.; Bonoli, P.T.; Ernst, D.R.; Greenwald, M.J.; Marmar, E.S.; Redi, M.H.; Rice, J.E.; Wukitch, S.J.; Zhurovich, K., “Internal transport barrier production and control in Alcator C-Mod”, *Plasma Physics and Controlled Fusion* **46**(2004) p B281.

Lin, Y.; Wukitch, S.; Bonoli, P.; Nelson-Melby, E.; Porkolab, M.; Wright, J.C.; Basse, N.; Hubbard, A.E.; Irby, J.; Lin, L.; Marmar, E.S.; Mazurenko, A.; Mossessian, D.; Parisot, A.; Rice, J.; Wolfe, S.; Phillips, C.K.; Schilling, G.; Wilson, J.R.; Phillips, P.; Lynn, A., “Investigation of ion cyclotron range of frequencies mode conversion at the ion-ion hybrid layer in Alcator C-Mod”, *Physics of Plasmas* **11**(2004) p 2466.

Hubbard, A.E.; Carreras, B.A.; Basse, N.P.; Del-Castillo-Negrete, D.; Hughes, J.W.; Lynn, A.; Marmar, E.S.; Mossessian, D.; Phillips, P.; Wukitch, S., “Local threshold conditions and fast transition dynamics of the L-H transition in Alcator C-Mod”, *Plasma Physics and Controlled Fusion* **46**(2004) p A95.

Lee, W.D.; Rice, J.E.; Marmar, E.S.; Greenwald, M.J.; Hutchinson, I.H.; Snipes, J.A., “Observation of anomalous momentum transport in Tokamak plasmas with no momentum input”, *Physical Review Letters* **91**(2003) p 205003/1.

Rice, J.E.; Bonoli, P.T.; Fiore, C.L.; Lee, W.D.; Marmar, E.S.; Wukitch, S.J.; Granetz, R.S.; Hubbard, A.E.; Hughes, J.W.; Irby, J.H.; Lin, Y.; Mossessian, D.; Wolfe, S.M.; Zhurovich, K.; Greenwald, M.J.; Hutchinson, I.H.; Porkolab, M.; Snipes, J.A., “Pressure profile modification of internal transport barrier plasmas in Alcator C-Mod”, *Nuclear Fusion* **43**(2003) p 781.

Sunn Pedersen, T.; Granetz, R.S.; Marmar, E.S.; Mossessian, D.; Hughes, J.W.; Hutchinson, I.H.; Terry, J.; Rice, J.E., “Measurements of large poloidal variations of impurity density in the Alcator C-Mod H-mode barrier region”, *Physics of Plasmas* **9**(2002) p 4188.

Prof. Miklos Porkolab
Professor of Physics; Director, MIT Plasma Science and Fusion Center
Co-Principal Investigator, Alcator Project

Education:

B.A.Sc. (Engineering Physics), University of British Columbia (1963)

Ph.D. (Applied Physics), Stanford University (1967)

Professional Experience:

Professor Miklos Porkolab is an internationally recognized physicist, well known for his work in both experimental and theoretical plasma physics. He is the MIT Plasma Science and Fusion Center Director and the Head of the PSFC Physics Research Division. He has received his Ph.D. in Applied Physics at Stanford University in 1967, and thereafter joined the Princeton Plasma Physics Laboratory where he rose to the position of Senior Research Physicist and Lecturer with the rank of Professor in the Astrophysical Sciences Department in 1975. While at Princeton University, Professor Porkolab carried out pioneering experimental and theoretical research in the area of nonlinear wave-wave and wave-particle interactions, parametric instabilities and RF plasma heating experiments on magnetically confined fusion plasma experiments. In 1976 Professor Porkolab spent one year at IPP, Garching, Germany, under the auspices of the Humboldt Foundation as a winner of the "US Senior Scientist Award." In 1977 Dr. Porkolab joined MIT as a professor in the Physics Department and since then he has led several pioneering experiments in radio frequency heating and non-inductive current drive on both the Versator II and the Alcator C tokamaks. For this work, Professor Porkolab shared the 1984 American Physical Society "Excellence in Plasma Research Award." From 1986 through the present time, Prof. Porkolab has participated actively on the Alcator C-Mod experimental program as RF Group Leader, and contributed to the DIII-D ICRF experimental program at General Atomics where he initiated the highly successful fast wave electron heating and current drive experiments. In 1993-1995 Professor Porkolab was actively involved in the design of TPX as the Heating and Current Drive Physics Task Leader. He also served on the TPX Council, and later on ISCUS, the ITER Scientific Council, US, and more recently served on the VLT Program Advisory Committee. From 1991 through 2001 Professor Porkolab was the Editor of Physics Letters A, Plasma Physics and Fluid Dynamics subsection. He also represented the US Plasma Physics community for six years on the International Union of Pure and Applied Physics (IUPAP) Commission-16 (Plasma Physics) (1991-1997). In 1992-1995 he served as a member of the National Research Council Sub-panel on Plasma Science. He is author or co-author of more than 200 publications, has served on numerous occasions on the APS executive committee, he is a Fellow of the American Physical Society, has served on various DOE committees, and has been past chairman of the Gordon Research Conferences (1978) and the International High Power RF Conference in Boston (1993). He has also taught advanced plasma physics courses at both MIT and Princeton and supervised the thesis work of more than a dozen doctoral students. He is past Vice-Chair of the University Fusion Association (1997) and Vice-Chair (1998) and Chair (1999), Plasma Physics Division, American Physical Society. From 2003 to 2006 he was the Chairman of the Board, Fusion Power Associates, a non-profit organization advocating the development of fusion power. Fellow of the American Association for the Advancement of Science (AAAS) since 2005. The Hungarian Nuclear Society awarded The Karoly Simony Memorial Plaque and Prize to Professor Miklos Porkolab at its annual meeting November 29 in Budapest. The award was given in recognition of "outstanding achievements and contributions to plasma physics and fusion research." Professor Porkolab's current research interests include advanced tokamak physics research on the Alcator C-Mod tokamak at MIT, including heating and profile control

with RF waves, study of transport and plasma turbulence and RF wave propagation using phase contrast imaging techniques on both C-Mod and DIII-D. More recently his interests have expanded to the experimental study of magnetic reconnection in plasmas on the MIT Versatile Toroidal Facility. These phenomena are important to both space plasma (earth's magnetotail and solar prominences) and laboratory fusion plasma experiments. Since 1995 he has been the Director of the Plasma Science and Fusion Center at MIT.

Publications:

M. Porkolab and R.P.H. Chang, "Nonlinear Wave Effects in Laboratory Plasmas: A Comparison Between Theory and Experiment," *Reviews of Modern Physics* **50** Issue 4, 745-795, (1978).

P.T. Bonoli, M. Porkolab, J.J. Ramos, W. Nevins, C. Kessel, "Negative Magnetic Shear Modes in Operation in the Alcator C-Mod Tokamak near the Bata Limit," *Plasma Physics and Controlled Fusion* **39** n 2, 223-236 (1997).

M. Porkolab, A Bécoulet , P T Bonoli C Gormezano , R Koch , R J Majeski , A Messiaen , J M Noterdaeme , C Petty, R Pinsker, D Start and R Wilson, "Recent Progress In ICRF," *Physics, Plasma Physics and Controlled Fusion* **40**, A35-A52, (1998) www.iop.org/EJ/abstract/0741-3335/40/8A/004.

Mazurenko, M. Porkolab, D. Mossessian, J.A. Snipes, X.Q. Xu, W.M. Nevins, "Experimental and Theoretical Study of Quasi Coherent Fluctuations in Enhanced D_{alpha} Plasmas in the Alcator C-Mod Tokamak," *Physical Review Letters* **89**, n 22, 225004 (2002).

E. Nelson-Melby, M. Porkolab, P.T. Bonoli, Y. Lin, A. Mazurenko and S.J. Wukitch, "Experimental Observations of Mode-Converted Ion Cyclotron Waves in a Tokamak Plasma by Phase Contrast Imaging," *Physical Review Letters* **90**, n 15, 155004-1 (2003).

M. Porkolab, J.C. Rost, N. Basse, J. Dorris, E. Edlund, Liang Lin, Y. Lin, S. Wukitch, "Phase Contrast Imaging of Waves and Instabilities in High Temperature Magnetized Fusion Plasmas", *IEEE Transactions on Plasma Science* **34**, n 2, 229-234 (2006).

R.I. Pinsker, M. Porkolab, W.W. Heidbrink, Y. Luo, C.C. Petty, R. Prater, M. Choi, D.A. Schaffner, F.W. Baity, E. Fredd, J.C. Hosea, R.W. Harvey, A.P. Smirnov, M. Murakami and M.A. Van Zeeland, "Absorption of fast waves at moderate to high ion cyclotron harmonics on DIII-D," *Nuclear Fusion* **46**, n 7, S416-S424 (2006).

L. Lin, E.M. Edlund, M. Porkolab, Y. Lin and S.J. Wukitch, "Vertical Localization of Phase Contrast Imaging Diagnostic in Alcator C-Mod", *Review of Scientific Instruments* **77**, n 10, 10E918-1-3 (2006).

J. Egedal, W. Fox, N. Katz, M. Porkolab, K. Reim and E. Zhang, Laboratory Observations of Spontaneous Magnetic Reconnection," *Physical Review Letters* **98**, n 1, 015003-1-4 (2007). <http://link.aps.org/abstract/PRL/v98/e015003>

P.T. Bonoli, R. Parker, S.J. Wukitch, Y. Lin, M. Porkolab, J.C. Wright, E. Edlund, T. Graves, L. Lin, J. Liptac, A. Parisot, A.E. Schmitt, V. Tang, W. Beck, R. Childs, M. Grimes, D. Gwinn, D. Johnson, J. Irby, A. Kanojia, P. Koert, S. Marazita, E. Marmor, D. Terry, R. Vieira, G. Wallace, J. Zaks, S. Bernabei, C. Brunkhorse, R. Ellis, E. Fredd, N. Greenough, J. Hosea, C.C. Kung, G.D. Loesser, J. Rushinski, G. Schilling, C.K. Phillips, J.R. Wilson, R.W. Harvey, C.L. Fiore, R. Granetz, M. Greenwald, A.E. Hubbard, I.H. Hutchinson, B. Labombard, B. Lipschultz, J. Rice, J.A. Snipes, J. Terry, S.M. Wolfe, and the Alcator C-Mod Team, "Wave-Particle Studies in the Ion Cyclotron and Lower Hybrid Range of Frequencies in Alcator C-Mod," *Fusion Science and Technology Journal* **51**, n 3, 401-36 (2007).

Prof. Ian H. Hutchinson
Professor and Head of Department of Nuclear Science and Engineering, MIT.
Coprincipal Investigator, Alcator Project

Education:

B.A. (Physics), Cambridge University (1972)

Ph.D. (Physics), Australian National University (1976)

Professional Experience:

Dr. Hutchinson is Head of the Nuclear Science and Engineering Department at MIT, which he has led since 2003.

He has been engaged in experimental plasma physics research since 1973. As a Commonwealth Scholar at the Australian National University, he gained extensive practical experience on one of the earliest tokamaks to operate outside the Soviet Union. He played a leading role in the research on Alcator A and C as Principal Research Scientist and co-leader of the MHD and operations section.

He worked on reversed field pinch experiments at the Culham Laboratory from 1980 to 1983 where he made landmark measurements of magnetic turbulence structure showing that it could explain the energy transport. He returned to M.I.T. in 1983 as a member of the Nuclear Engineering department faculty. He was responsible for coordination of the MHD aspects of the Alcator C-Mod proposal and design, and directed the entire Alcator project, from 1987 on.

His personal scientific contributions span many areas of plasma physics, including the first direct measurement of anomalous resistivity during MHD disruptions and of hollow current profiles during current rise, the first observations of polarized tokamak electron cyclotron radiation and development diagnostics of thermal and nonthermal electron distributions based on it, fundamental theory of Mach probes to measure plasma flow, observations of spontaneous tokamak plasma rotation.

In addition to approximately 150 journal articles on a variety of plasma phenomena, Dr. Hutchinson is the author of the standard monograph on measuring plasmas: *Principles of Plasma Diagnostics*, the second edition of which was published by Cambridge University Press in 2002. He has served on numerous national fusion review panels. He was a member of the editorial board of *Physics of Fluids B*, the *New Journal of Physics*, and was editor in chief of the journal *Plasma Physics and Controlled Fusion* from 2000-2004. His present personal research interests include plasma momentum transport, MHD instability suppression and measurement, real-time plasma control, plasma radiation, interactions of flowing plasmas with solid objects and dust particles, and tokamak boundary phenomena. In addition to his research, he teaches graduate courses at M.I.T. on plasma and fusion physics and is the author of the computer program TtH a TeX to HTML translator, widely used for web-publishing of mathematics. He is a fellow of the American Physical Society and of the Institute of Physics. He is the current Chairman of the Division of Plasma Physics of the American Physical Society.

Publications:

I.H. Hutchinson, R. Boivin, F. Bombarda, et al., (C-Mod Group), "First Results from Alcator C-Mod," *Physics of Plasmas* **1**, 1511 (1994).

I.H. Hutchinson, S.F. Horne, G. Tinios, et al., "Plasma Shape Control: A General Approach and its Application to Alcator C-Mod," *Fusion Technology* **30** 137 (1996).

J.E. Rice, M. Greenwald, I.H. Hutchinson, et al., "Observations of Central Toroidal Rotation in ICRF Heated Alcator C-Mod Plasmas," *Nuc. Fusion* **38**, No. 1, 75 (1998).

I.H. Hutchinson, J.E. Rice, R.S. Granetz, J.A. Snipes, "Self-Acceleration of a Tokamak Plasma during Ohmic H Mode," *Phys. Rev. Lett.*, **84** No. 15 (2000) 3330.

I.H. Hutchinson, R. Boivin, P.T. Bonoli, et al., "Overview of Recent Alcator C-Mod Results," *Nucl. Fusion* **41** No. 10 (2001) 1391.

I.H. Hutchinson, "Electromagnetic Wall Torques from Magnetically Confined Plasmas", *Plasma Phys. Control Fusion* **43** (2001) 145.

I.H. Hutchinson, "Excited-State Populations in Neutral Beam Emission," *Plasma Phys. Control. Fusion* **44** No. 1 (2002) 71.

W.D. Lee, J.E. Rice, E.S. Marmor, M.J. Greenwald, I.H. Hutchinson, et al., "Observation of Anomalous Momentum Transport in Tokamak Plasmas with No Momentum Input," *Phys. Rev. Lett.* **91** No. 20 (2003) 205003.

Wolfe SM, Hutchinson IH, Granetz RS, Rice J, Hubbard A, Lynn A, Phillips P, Hender TC, Howell DF, La Haye RJ, Scoville JT "Nonaxisymmetric field effects on Alcator C-Mod" *Phys. Plasmas* **12**, 056110 (2005).

T P Graves, S J Wukitch, B LaBombard, I H Hutchinson "Effect of multipactor discharge on Alcator C-Mod ion cyclotron range of frequency heating", *J. Vac. Sci. Techn. A* **24** 512-516 (2006).

Dr. Paul Bonoli
Senior Research Scientist

Education:

BS (Electrical Engineering) Cornell University (1976)
MS (Electrical Engineering) Cornell University (1978)
PhD (Electrical Engineering) Cornell university (1981)

Professional Experience:

Paul Bonoli is currently a Senior Research Scientist at the Plasma Science and Fusion Center at the Massachusetts Institute of Technology. He specializes in theoretical and computational plasma physics in the areas of radio frequency heating and current drive in toroidal confinement devices (tokamaks). He has developed detailed simulation models for radio frequency heating and current drive experiments, which include wave propagation, Fokker Planck, and transport calculations. These codes are used widely throughout the international fusion community.

He received the Ph.D. in electrical engineering from Cornell University in 1981, under Professor Edward Ott. He then joined the Physics Department at the Massachusetts Institute of Technology as a post-doctoral associate under Professors Bruno Coppi and Miklos Porkolab. In 1984 he became a research scientist at the Research Laboratory of Electronics at MIT. He then joined the research staff at the MIT Plasma Science and Fusion Center (PSFC) in 1986 and rose to the rank of principal research scientist in 1989. He became leader of the RF Interactions and Modeling Group at the PSFC in 1992. Dr. Bonoli is the co-author on over 45 papers in refereed journals.

Dr. Bonoli is currently the principal investigator for the SciDAC Center for Wave – Plasma Interactions (CSWPI) and for the NSTX High Harmonic Heating and Current Drive Project at MIT. He is also currently serving as the co US Team Leader of the ITPA Working Group on Steady State Operations. He was the co US Team Leader for the TPX Current Drive and Heating Physics Design Team. Previously, he conducted modeling studies of electron cyclotron heating (ECH) in the CIT/BPX Projects and was co-principal investigator of the ITER Lower Hybrid Current Drive Physics Program at MIT.

Dr. Bonoli is a fellow of the American Physical Society and has served twice as a member of the International Sherwood Controlled Fusion Theory Conference Executive Committee. He has also been a consultant at the Lawrence Livermore National Laboratory and at Hydro-Quebec.

Publications:

P.T. Bonoli, J. Ko, R. Parker *et al*, “Lower hybrid current drive experiments on Alcator C-Mod: Comparison with Theory and Simulation”, submitted to *Physics of Plasmas* (2008).

P. T. Bonoli, R. Parker, S. J. Wukitch *et al*, “Wave-particle studies in the ion cyclotron and lower hybrid ranges of frequencies in Alcator C-Mod”, *Fusion Science and Technology* **51**, 401-436 (2007).

P. T. Bonoli, D. B. Batchelor, L. A. Berry *et al*, “Evolution of nonthermal particle distributions in radio frequency heating of fusion plasmas”, *Journal of Physics* **78**, 012006 (2007).

V. Tang, P. T. Bonoli, R. R. Parker, J. C. Wright, R. S. Granetz, R. W. Harvey, E. F. Jaeger, J. Liptac, C. L. Fiore, M. Greenwald, J. H. Irby, Y. Lin and S. J. Wukitch, “Experimental and numerical characterization of ion-cyclotron heated protons on the Alcator C-Mod tokamak”, *Plasma Physics and Controlled Fusion* **49**, 873 (2007).

P. T. Bonoli, D. B. Batchelor, L. A. Berry, M. Choi, D. A. D’Ippolito, R. W. Harvey, E. F. Jaeger, J. R. Myra, C. K. Phillips, D. N. Smithe, V. Tang, E. Valeo, J. C. Wright, M. Brambilla,

- R. Bilato, V. Lancellotti, and R. Maggiora, "Evolution of nonthermal particle distributions in radio frequency heating of fusion plasmas", *Journal of Physics* **78**, 012006 (2007).
- E.F. Jaeger, L.A. Berry, S.D. Ahern, R.F. Barrett, D.B. Batchelor, M.D. Carter, E.F. D'Azevedo, R.D. Moore, R. W. Harvey, J.R. Myra, D.A. D'Ippolito, R.J. Dumont, C.K. Phillips, H. Okuda, D.N. Smithe, P.T. Bonoli, J.C. Wright, and M. Choi, "Self-consistent full-wave and Fokker Planck calculations for ion cyclotron heating in non-Maxwellian plasmas", *Physics of Plasmas* **13**, 056101 (2006).
- J.C. Wright, L.A. Berry, P.T. Bonoli, D.B. Batchelor, E.F. Jaeger, M.D. Carter, E. D'Azevedo, C.K. Phillips, H. Okuda, R.W. Harvey, D.N. Smithe, J.R. Myra, D.A. D'Ippolito, M. Brambilla and R.J. Dumont, "Nonthermal particle and full-wave diffraction effects on heating and current drive in the ICRF and LHRF regimes", *Nuclear Fusion* **45**, 1411 (2005).
- S.J. Wukitch, Y. Lin, A. Parisot, J.C. Wright, P.T. Bonoli *et al.*, "ICRF mode conversion physics in Alcator C-Mod: Experimental measurements and modeling", *Physics of Plasmas* **12**, 056104 (2005).
- J.C. Wright, P.T. Bonoli, M. Brambilla, F. Meo, E. D'Azevedo, D. B. Batchelor, E. F. Jaeger, L. A. Berry, C. K. Phillips and A. Pletzer, "Full Wave Simulations of Fast Wave Mode Conversion and Lower Hybrid Wave Propagation in Tokamaks", *Physics of Plasmas* **11**, 2473 (2004).
- J.C. Wright, P.T. Bonoli, E. D'Azevedo, and M. Brambilla, "Ultrahigh resolution simulations of mode converted ion cyclotron waves and lower hybrid waves", *Computer Physics Communications* **164**, 330 (2004).

Dr. Martin Greenwald
Senior Research Scientist

Education:

BS (Physics), Massachusetts Institute of Technology (1973)

BS (Chemistry), Massachusetts Institute of Technology (1973)

MA (Physics), University of California (1975)

PhD (Physics), University of California – Berkeley (1978)

Professional Experience:

Dr. Greenwald is the leader of the transport program on Alcator C-Mod, and heads the group responsible for data acquisition and computing. He is also head of the Office of Computer Services for the PSFC. He is a member of the Fusion Energy Sciences Advisory Committee (FESAC), recently chairing a panel charged by the Undersecretary of Energy to develop the technical underpinnings for a long-term strategic plan for the development of fusion energy.. Dr. Greenwald currently heads the program advisory committee for the CPES (Center for Plasma Edge Simulation) project. He is a past chairman of the Transport Task Force and has served on many program advisory committees, working groups, visiting committees and U.S. DOE review committees. He is an associate editor of the journal “Physics of Plasmas”, an APS Fellow and former APS/DPP Distinguished Lecturer in Plasma Physics.

Since joining the Plasma Fusion Center in 1978, Dr. Greenwald has conducted physics research on the Alcator A, C, and C-Mod tokamaks, including studies of energy and particle transport, pellet fueling, density limits, neutral particle measurements, and studies of energetic ion dynamics. He was part of the original design team for Alcator C-Mod. His recent work has focused on particle and impurity transport, on the role of critical gradients in determining plasma temperature profiles, on the EDA H-mode regime, and on the role of turbulent transport in determining the tokamak density limit. This latter work is aimed toward defining a "first principals" theory for the limit with the long term goal of obtaining reliable predictions and extrapolations to future machines. Dr. Greenwald recently served as part of a three person advisory group, reporting the leader of the ITER CODAC (Control, Data Acquisition and Communications) group, working in that capacity on the conceptual design for the ITER data systems. He was also a leader in the Fusion collaboratory project (2002-2006), a multi-institutional project to develop tools and methodology in support of collaborative research and remote participation on experimental facilities.

Publications:

Lister, J. B., Farthing, J. W., Greenwald, M., Yonekawa, I., “The ITER CODAC conceptual design”, *Fusion Engineering and Design* **82**, 1167, 2007.

LaBombard B, Smick N, Greenwald M, et al., “The operational phase-space of the edge plasma and its sensitivity to magnetic topology in Alcator C-Mod”, *J. Nuclear Materials*, **363**, 517, 2007.

M. Greenwald, C. Angioni, J.W. Hughes, J. Terry, H. Weisen, “Density Profile Peaking in Low Collisionality H-modes”, *Nucl. Fusion* **47**, L26, 2007.

M. Greenwald, N. Basse, P. Bonoli, R. Bravenec, E. Edlund, D. Ernst, C. Fiore, R. Granetz, A. Hubbard, J. Hughes, I. Hutchinson, J. Irby, B. LaBombard, L. Lin, Y. Lin, B. Lipschultz, E. Marmor, D. Mikkelsen, D. Mossessian, P. Phillips, M. Porkolab, J. Rice, W. Rowan, S. Scott, J. Snipes, J. Terry, S. Wolfe, S. Wukitch, K. Zhurovich, “Confinement and Transport Research in Alcator C-Mod”, *Fusion Science and Technology* **51**, p 266, 2007.

Terry, J. L., Cziegler, I., Hubbard, A., Snipes, J., Hughes, J.W., Greenwald, M., LaBombard, B., Lin, Y., Phillips, P., Wukitch, S., “The dynamics and structure of edge-localized-modes in Alcator C-Mod”, *J. Nuclear Material* **363**, 994, 2007.

Zhurovich, K., Fiore, C. L., Ernst, D. R., Bonoli, P. T., Greenwald, M., Hubbard, A. E., Hughes, J. W., Marmor, E. S., Mikkelsen, D. R., Phillips, P., Rice, J. E., “Microturbulent drift mode suppression as a trigger mechanism for internal transport barriers on Alcator C-Mod”, *Nucl. Fusion* **47**, 1220, 2007.

M. Greenwald, Andelin, D., Basse, N., Bernabei, S., Bonoli, P., Bose, B., Boswell, C., Bravenec, R., Carreras, B., Cziegler, I., Edlund, E., Ernst, D., Fasoli, C., Ferrara, M., Fiore, C., Granetz, R., Grulke, O., Hender, T., Hosea, J., Howell, D.H., Hubbard, A., Hughes, J., Hutchinson, I., Ince-Cushman, A., Irby, J., LaBombard, B., LaHaye, R., Lin, L., Lin, Y., Lipschultz, B., Liptac, J., Lisgo, S., Lynn, A., Marmor, E., Marr, K., Mikkelsen, D.R., McDermott, R., Mossessian, D., Parisot, A., Parker, R., Phillips, C., Phillips, P., Porkolab, M., Redi, M., Rice, J., Rowan, W., Sampsell, M., Schilling, G., Scott, S., Scoville, J.T., Smick, N., Snipes, J., Stangeby, P., Tang, V., Terry, J., Ulrickson, M., Wallace, G., Whyte, D., Wilson, J., Wright, J., Wolfe, S., Wukitch, S., Youngblood, B., Yuh, H., Zhurovich, K., Zweben, S., “Overview of Alcator C-Mod Program”, *Nuclear Fusion* **45**, S109, 2005.

M. Greenwald, D. Schissel, J. Burruss, T. Fredian, J. Stillerman, J. Lister, “Visions for data management and remote participation on ITER”, proceedings of the 10th International Conference on Accelerators and Large Physics Control Systems, Geneva, Switzerland, 2005.

LaBombard B, Hughes JW, Mossessian D, Greenwald M, Lipschultz B, Terry JL, “Evidence for electromagnetic fluid drift turbulence controlling the edge plasma state in the Alcator C-Mod tokamak”, *Nucl. Fusion* **45**, 1658-1675, 2005

M. Greenwald, “Beyond Benchmarking – How Experiments and Simulations Can Work Together in Plasma Physics”, *Computer Physics Communications* **164**, 1-8, 2004.

Dr. Robert S. Granetz
Principal Research Scientist

Education:

S.B. (Physics), Massachusetts Institute of Technology (1977)

S.M. (Nuclear Engineering), Massachusetts Institute of Technology (1977)

Sc.D. (Physics), Massachusetts Institute of Technology (1982)

Professional Experience:

Dr. Granetz is a principal research scientist on the Alcator C-Mod project, coordinator of the diagnostic neutral beam (DNB) collaboration, and MHD program leader, with primary responsibilities for performance of the DNB program, disruption studies, magnetics instrumentation, and x-ray imaging instrumentation. Currently he is also responsible for run planning and scheduling of C-Mod operations. Dr. Granetz's research has concentrated on the study of MHD instabilities and disruptions in tokamaks. He has also made important contributions to the understanding of current-rise instabilities, the sawtooth instability, and pellet injection. Dr. Granetz has also taught graduate student courses in plasma physics and fusion for the Department of Nuclear Engineering.

Shortly after joining the Alcator staff in 1982, Dr. Granetz began investigating the feasibility of applying tomographic reconstruction techniques to do x-ray imaging of tokamak plasmas. In 1985 Dr. Granetz was invited to be a visiting scientist at the JET project in Europe, and he concentrated on the analysis of data from the soft x-ray arrays. He has helped pioneer the use of x-ray tomographic imaging for studying the physics of MHD instabilities and plasma equilibria, particularly with respect to the fast sawtooth crash. Dr. Granetz returned from JET in 1987 to take on his present responsibilities for the Alcator C-Mod project. One of Dr. Granetz's principal areas of research on C-Mod has been the study of disruptions, particularly halo currents and disruption mitigation. He developed instrumentation which clearly showed the magnitude and toroidally-asymmetric nature of halo currents, and compiled a large database that formed the bulk of the ITER disruption design constraints. He has also experimented with a number of concepts for reducing disruption effects, including high-Z doped 'killer' pellet injection and neutral point operation. Most recently this disruption mitigation research has utilized high-pressure gas jets to successfully reduce halo currents and divertor thermal loads. Dr. Granetz is currently developing techniques to study the physics and mitigation of disruption-generated runaway electron populations.

Dr. Granetz has also been responsible for managing the procurement and installation of a diagnostic neutral beam, for coordinating DNB-related physics research on C-Mod with scientists from collaborating institutions, and for planning upgrades to the beam systems.

Publications:

R.S. Granetz, E.M. Hollmann, D.G. Whyte, V.A. Izzo, et al, "Gas Jet Disruption Mitigation Studies on Alcator C-Mod and DIII-D", *Nucl. Fusion* **47** (2007) 1086-91.

D.G. Whyte, R. Granetz, M. Bakhtiari, V. Izzo, T. Jernigan, J. Terry, M. Reinke, B. Lipschultz, "Disruption Mitigation on Alcator C-Mod Using High-pressure Gas Injection: Experiments and Modeling Toward ITER", *J. Nucl. Mat.* **363-365** (2007) 1160-1167.

R. Granetz, D.G. Whyte, V.A. Izzo, et al, "Gas Jet Disruption Mitigation Studies on Alcator C-Mod", *Nucl. Fusion* **46** (2006) 1001-8.

S.M. Wolfe, I.H. Hutchinson, R.S. Granetz, J. Rice, et al, "Nonaxisymmetric Field Effects on Alcator C-Mod", *Phys. Plasmas* **12** (2005) 056110.

J.A. Snipes, et al, "Energetic Particle Physics Studies on Alcator C-Mod", *Fusion Sci & Tech.* **51** (2007) 437-450.

J. Irby, D. Gwinn, W. Beck, B. LaBombard, R. Granetz, R. Vieira, "Alcator C-Mod Design, Engineering, and Disruption Research", *Fusion Sci. & Tech.* **51** (2007) 460-475.

D.F. Beals, R. Granetz, A.A. Ivanov, et al, "Installation and Operation of New Long Pulse DNB on Alcator C-Mod", *Proc. SOFE05* (2006) 4019009.

J.A. Snipes, D. Schmittiel, A. Fasoli, R.S. Granetz, R.R. Parker, "Initial Active MHD Spectroscopy Experiments Exciting Stable Alfvén Eigenmodes in Alcator C-Mod", *Plasma Phys. & Controlled Fusion* **46** (2004) 611-620.

J.A. Snipes, R.S. Granetz, et al, "Beta-limiting MHD Activity and Mode Locking in Alcator C-Mod", *Plasma Phys. & Controlled Fusion* **44** (2002) 381-393.

T. Sunn Pedersen, R.S. Granetz, et al, "Measurements of Large Poloidal Variations of Impurity Density in the Alcator C-Mod H-mode Barrier Region", *Phys. Plasmas* **9** (2002) 4188.

Dr. Amanda E. Hubbard
Principal Research Scientist

Education:

B.Sc. (Mathematics and Engineering), Queen's Univ. at Kingston, Ontario (1983)

Ph.D. (Plasma Physics), Imperial College of Science and Technology, University of London, U.K. (1987)

Professional Experience:

Dr. Hubbard has since 2001 been the leader of the Advanced Tokamak Task Force on Alcator C-Mod, coordinating research on control of plasma transport and current profile via LHCD and ICRF, aiming at the development of high performance integrated scenarios in 'advanced' regimes. She is also responsible for Electron Cyclotron Emission diagnostics and an active researcher in H-mode 'pedestal' and transition physics.

Dr. Hubbard was one of the first graduate students on the JET tokamak in the UK, where she pioneered the use of reflectometry as a density profile diagnostic. Following her graduation she remained at JET for a year and worked on particle transport and H-mode and ELM studies. From 1988 through 1991, Dr. Hubbard was a research scientist at the Centre Canadien de Fusion Magnetique, where she helped develop both electron cyclotron (ECE) diagnostics and a lower hybrid current drive (LHCD) system at the Tokamak de Varennes.

Since joining the Alcator C-Mod group in 1991, she has developed and exploited several

ECE diagnostics. A primary research interest has been the outer region in which a transport barrier (or pedestal) forms in the H-mode regime. A key contribution was the observation that the L-H transition occurs when a threshold in edge electron temperature or a closely related local variable is exceeded. These results helped stimulate comparison with theories and similar studies on other tokamaks. From 1998-2001, she coordinated pedestal studies on C-Mod. The discovery and characterization of the steady state, high confinement, "Enhanced D-alpha" (EDA) H-mode regime was a noteworthy result of the group effort. Dr. Hubbard has been a member of the ITPA Pedestal Physics expert group, and its predecessor ITER expert group, since its inception in 1997 and collaborates with groups on a number of US and international tokamaks. She has given several review talks on pedestal issues.

Dr. Hubbard has been involved in multiple fusion community activities, serving on the Federal Energy Sciences Advisory Committee panels on Burning Plasmas (2002), Fusion Development Path (2003) and Fusion Program Priorities (2005). She has also served on several APS and conference organizing committees, and is currently Chair of the Council of the U.S. Burning Plasma Organization.

Publications:

A.E. Hubbard *et al*, “H-mode pedestal and threshold studies over an expanded operating space on Alcator C-Mod”, *J Physics of Plasmas* **14** (5) 056109.

A.E. Hubbard, K. Kamiya *et al*, “Comparisons of small ELM H-Mode regimes on the Alcator C-Mod and JFT-2M tokamaks”, *Plasma Phys. Controlled Fusion* **48**, 5A, A121. (2006).

A. E. Hubbard, B. A. Carreras *et al*, “Local Threshold Conditions and Fast Transition Dynamics of the L-H Transition on Alcator C-Mod”, *Plasma Physics and Controlled Fusion* **46**(5) A95-A106 (2004).

A. E. Hubbard, B.A. Carreras *et al*, “Variation of Edge Gradients with Heat Flux across L-H and H-L Transitions in Alcator C-Mod”, *Plasma Physics and Controlled Fusion* **44**, A359-356. (2002).

A.E. Hubbard *et al*, “Pedestal profiles and fluctuations in C-Mod enhanced D-alpha H-modes”, *Physics of Plasmas* **8** (5), 2033-2040 (2001).

A. E. Hubbard, “Physics and scaling of the H-mode pedestal”, *Plasma Physics and Controlled Fusion* **42** A15-A35. (2000) (Review paper)

A.E. Hubbard *et al*, “Local variables affecting H-mode threshold on Alcator C-Mod”, *Plasma Physics & Controlled Fusion* **40** (5), 689-92 (1998)

A.E. Hubbard *et al*, “Measurements of the high confinement mode pedestal region on Alcator C-Mod”, *Physics of Plasmas* **5** (5), 1744-51. (1998)

Dr. James Irby
Principal Research Engineer

Education:

B.S. (Physics), North Carolina State University (1973)

Ph.D. (Physics), University of Maryland (1979)

Professional Experience:

At the University of Maryland Dr. Irby studied reconnection and tearing in a high voltage reversed field theta-pinch. After receiving his Ph.D. degree, he was a post-doctoral fellow for one year at the University of Maryland and was in charge of construction of the "first ever" spheromak experiment. The formation of the first laboratory spheromak plasma was documented using magnetic probe techniques that were developed by Dr. Irby during his thesis research.

Dr. Irby came to MIT in 1980 where he first performed experiments on the Constance II mirror, notably Thomson scattering and VUV spectroscopy. In 1982 he joined the new TARA mirror experiment which was being built at MIT, where in 1984 he became leader of the diagnostics group. His main physics interests on the TARA program involved the instabilities excited during ICRF and ECH heating and end plugging experiments. He carried out the first experiment identifying trapped particle modes in a tandem mirror.

Since joining the Alcator C-Mod group in 1988, he has been responsible for the development of the CO₂ laser interferometry and mm microwave reflectometry systems used on C-Mod. He has been particularly interested in the instabilities generated during pellet fueling, and using the interferometer, he has documented the mode number and amplitude of the fluctuations present during the density decay phase following pellet injection. His simulations of ordinary wave propagation are the first full-wave 2D calculations of a reflectometer system. He also did analysis of early C-Mod outer divertor current shunt data to identify the N=1 nature of disruptions.

In July of 1993, Dr. Irby became responsible for co-ordinating the C-Mod experimental activities and the interface between the physics and engineering groups. In September of 1994 he became leader of the Alcator C-Mod Operations and Engineering Group. He has since that time directed the operation of the research facility and the design and installation of major upgrades. Dr. Irby is also directing the design and fabrication of the C-Mod multichord polarimeter system which will provide crucial data needed for understanding lower hybrid current drive experiments.

Publications:

H. Lamela, P. Acedo and the Optoelectronics and Laser Technology Group, J. Irby "Laser interferometric experiments for the TJ-II stellarator electron-density measurements", *Rev. Sci. Instrum.* **72**, 96 (2001).

Y. Lin , J. H. Irby , R. Nazikian, E. S. Marmor , A. Mazurenko, "Two-dimensional full-wave simulation of microwave reflectometry on Alcator C-Mod", *Rev. Sci. Instrum.* **72**, 344 (2001).

Y. Lin, J. Irby, P. Stek, I. Hutchinson, and J. Snipes, R. Nazikian and M. McCarthy, "Upgrade of reflectometry profile and fluctuation measurements in Alcator C-Mod", *Rev. Sci. Instrum.* **70**, 1078 (1999).

J. Irby, R. Murray, P. Acedo, H. Lamela, "A two-color interferometer using a frequency doubled diode pumped laser for electron density measurements", *Rev. Sci. Instrum.* **70**, 699 (1999).

N. Bretz, F. Jobses, J. Irby, "The design of a second harmonic tangential array interferometer for C-Mod", *Rev. Sci. Instrum.* **68**, 713 (1997).

R.S. Granetz, I.H. Hutchinson, J Sorci, D.T. Garnier, J.H. Irby, B. LaBombard, E.S. Marmor, and the Alcator Group "Disruptions, halo currents and killer pellets in Alcator C-Mod", IAEA-CN-64/AP1-22 (1996).

R.S. Granetz, I.H. Hutchinson, J. Sorci, J. Irby, B. LaBombard, D. Gwinn, "Disruptions and halo currents in Alcator C-Mod", *Nuc. Fusion* **36**, 545 (1996).

J. H. Irby, S. Horne, I. H. Hutchinson, P. C. Stek, "2D full-wave simulation of ordinary mode reflectometry", *Plasma Phys. Control. Fusion* **35**, 601 (1993).

G. C. Goldenbaum, J. H. Irby, Y. P. Chong, G. W. Hart, "Formation of a spheromak plasma configuration", *Phys. Rev. Lett.* **44**, 393 (1980).

J. H. Irby, J. F. Drake, Hans R. Griem, "Observation and interpretation of magnetic-field-line reconnection and tearing in a theta pinch", *Phys. Rev. Lett.* **42**, 228 (1979).

Dr. Brian LaBombard
Principal Research Scientist

Education:

BS (Nuclear Engineering), University of Lowell (1978)
ScD (Nuclear Engineering), Massachusetts Institute of Technology (1986)

Professional Experience:

Dr. LaBombard is a Principal Research Scientist on the Alcator C-Mod tokamak at the MIT Plasma Science and Fusion Center. His research has led to fundamental insights in the area of edge plasma and divertor transport in magnetic fusion devices. In addition, he has made significant contributions in plasma diagnostic development, student training and design/engineering of first-wall and divertor components.

Dr. LaBombard began his plasma studies as an MIT doctoral student on the Alcator A and C tokamaks. Building a unique array of Langmuir probes, he investigated edge conditions with unprecedented detail and uncovered key information on poloidal transport asymmetries and MARFE phenomena. In 1986, Dr. LaBombard joined the PISCES plasma-material facility at UCLA. As co-principal investigator, he performed physics experiments on PISCES and CCT (Continuous Current Tokamak) and was project leader for construction of the PISCES-B facility. Dr. LaBombard joined Alcator C-Mod in 1988 at the start of its construction phase and, with the help of students, assembled an extensive edge diagnostics set for C-Mod, including a neutral gas injection array (NINJA), fast-scanning and fixed Langmuir probes, 'impurity plume' imaging systems and an Omegatron ion mass spectrometer. These activities spawned a number of doctoral theses investigations under Dr. LaBombard's supervision. Dr. LaBombard continues to play a key role in the engineering of the first-wall and divertor components. Most recently, he has led the physics design and implementation of a novel cryopumping system in C-Mod's upper divertor.

Turning his attention to the area of edge plasma physics, Dr. LaBombard has made a number of seminal contributions, including: (1) discovering three simultaneous parallel heat-transport regimes (sheath-limited, high-recycling, and detached) in C-Mod's 'vertical plate' divertor, depending on the location in the scrape-off layer, (2) uncovering 'main-chamber recycling' phenomenon in C-Mod's diverted plasmas and revealing intermittent, non-diffusive transport in the scrape-off layer as the underlying cause, and (3) identifying edge plasma transport and its scaling with collisionality as a key physics ingredient in the empirical tokamak density limit.

Through a series of pioneering experiments, Dr. LaBombard also demonstrated that ballooning-like transport asymmetries drive near-sonic parallel plasma flows in the plasma edge and that such transport-driven flows impose a toroidal rotation boundary condition for the confined plasma. These and other experiments have led Dr. LaBombard to advance a seminal hypothesis: transport-driven edge flows and rotation boundary condition that they impose may explain in part the sensitivity of the L-H power threshold to magnetic x-point topology.

Most recently, Dr. LaBombard has led experiments to examine the physics of cross-field transport near the last-closed flux surface. This work has uncovered clear evidence that pressure gradients are constrained at this location, clamped at a 'critical value' that scales with poloidal magnetic field squared and varies with plasma collisionality. These observations broadly connect with results from state-of-the-art numerical simulations of electromagnetic plasma turbulence,

pointing toward a first-principles understanding of the underlying transport physics, including the physics of the tokamak density limit.

Over the course of his research, Dr. LaBombard has given 12 invited oral presentations at major physics meetings (APS, EPS, PSI, Sherwood, TTF) and is the co-author on over 150 papers in refereed journals, including a recent paper [Nuclear Fusion **44** (2004) 1047] that was nominated as one of ten to be considered for the 2007 Nuclear Fusion award. He is a fellow of the American Physical Society, a key contributor to the ITER physics basis, and is presently serving as an International Program Committee member for the Plasma Surface Interactions conference series. He has served as research advisor, supervisor or external examiner for numerous graduate theses and mentor for national undergraduate fellowship students in fusion.

Publications:

LaBombard, B., Hughes, J.W., Smick, N., Graf, A., Marr, K., *et al.*, "Critical gradients and plasma flows in the edge plasma of Alcator C-Mod," Physics of Plasmas **15** (2008) 056106.

LaBombard, B., Smick, N., Greenwald, M., Hughes, J.W., Lipschultz, B., *et al.*, "The operational phase space of the edge plasma and its sensitivity to magnetic topology in Alcator C-Mod," Journal of Nuclear Materials **363-365** (2007) 517.

LaBombard, B. and Lyons, L., "Mirror Langmuir probe: A technique for real-time measurement of magnetized plasma conditions using a single Langmuir electrode," Review of Scientific Instruments **78** (2007) 073501.

LaBombard, B., Rice, J.E., Hubbard, A.E., Hughes, J.W., Greenwald, M., *et al.*, "Transport-driven scrape-off layer flows and the x-point dependence of the L-H power threshold in Alcator C-Mod," Physics of Plasmas **12** (2005) 056111.

LaBombard, B., Hughes, J.W., Mossessian, D., Greenwald, M., Lipschultz, B., *et al.*, "Evidence for electromagnetic fluid drift turbulence controlling the edge plasma state in the Alcator C-Mod tokamak," Nuclear Fusion **45** (2005) 1658.

LaBombard, B., Rice, J.E., Hubbard, A.E., Hughes, J.W., Greenwald, M., *et al.*, "Transport-Driven Scrape-off Layer Flows and the Boundary Conditions Imposed at the Magnetic Separatrix in a Tokamak Plasma," Nuclear Fusion **44** (2004) 1047.

LaBombard, B., Gangadhara, S., Lipschultz, B., and Pitcher, C.S., "Toroidal rotation as an explanation for plasma flow observations in the Alcator C-Mod scrape-off layer," Journal of Nuclear Materials **313-316** (2003) 995.

LaBombard, B., "An interpretation of fluctuation induced transport derived from electrostatic probe measurements," Physics of Plasmas **9** (2002) 1300.

LaBombard, B., Boivin, R.L., Greenwald, M., Hughes, J., Lipschultz, B., *et al.*, "Particle transport in the scrape-off layer and its relationship to discharge density limit in Alcator C-Mod," Physics of Plasmas **8** (2001) 2107.

LaBombard, B., Umansky, M.V., Boivin, R.L., Goetz, J.A., Hughes, J., *et al.*, "Cross-field plasma transport and main-chamber recycling in diverted plasmas on Alcator C-Mod," Nuclear Fusion **40** (2000) 2041.

Dr. Bruce Lipschultz
Senior Research Scientist

Education:

B.S. (Physics), University of Maryland (1975)

B.S. (Mathematics), University of Maryland (1975)

Ph.D. (Physics) University of Wisconsin (1979)

Professional Experience:

Dr. Lipschultz's primary emphasis is on the plasma physics of low-temperature (0.5 eV-100 eV), moderate density ($0.001 - 3 \times 10^{21} \text{m}^{-3}$) plasmas that exist at the edge of fusion related devices. This includes studies of ion & neutral transport, the atomic physics of the local processes (e.g. ion recombination and line radiation), ion-surface interactions and material studies. He is a Senior Scientist in the MIT Plasma Science and Fusion Center and leads the edge and divertor physics research on Alcator C-Mod. He is a Fellow of the APS. Dr. Lipschultz is co-chair the ITPA (International Tokamak Physics Activity) Divertor/edge plasma group. This group coordinates international research on a number of issues ranging from materials to materials interactions to the physics of plasma and neutral transport in the edge and divertor plasmas.

While Dr. Lipschultz's doctoral thesis led to the first experimental verification of the MHD vertical instability (now commonly called a VDE which leads to disruptions) he quickly moved on to the physics of the plasma at the edge of tokamaks upon reaching MIT. His Alcator C tokamak work included the discovery and initial model for the 'MARFE' phenomenon which is a common feature of tokamaks, playing a role in fueling and density limits. The MARFE is a unique combination of atomic and classical transport physics. He has also shown that this instability can be strongly affected by ion recombination, leading to a new, low-temperature, regime, not previously predicted for plasmas. This radiation-condensation instability is also found in solar prominences.

Dr. Lipschultz is the originator of the 'vertical-plate' divertor design which was developed for the Alcator DCT design and implemented in Alcator C-Mod. This design has been incorporated into virtually every operating divertor tokamak, as well as into the designs for next step devices such as ITER (International Thermonuclear Experimental Reactor). This advance simplified the geometry of divertors by combining the divertor plate and entrance baffle. Physics benefits include: enhanced recycling of ions as neutrals near the plate lowering electron temperatures and impurity sources; minimization of impurity neutral access to the hot core plasma (neutral impurities leave the surface directed away from the core plasma).

Continuing along these lines of research, he has led experimental campaigns to understand and develop 'dissipative divertor' operation. Dr. Lipschultz's research showed how magnetic and vessel geometry could be used to optimize the dissipation of core heat efflux through radiative losses and momentum transfer processes. He published the first experimental determination of the existence and magnitude of deuterium ion recombination in divertor plasmas (in collaboration with Dr. J. Terry).

Building on radial ion transport analysis techniques developed by Dr. B. LaBombard, he has worked with several other tokamaks to characterize the role of perpendicular transport in the edge plasma. These results show that our previous understanding of the divertor concept and radial transport were flawed and convective ion transport dominates in the Scrapeoff Layer (SOL) region outside the hot core plasma (outside the separatrix). There are important implications for plasma-wall interaction, density control, main chamber impurity sources, and possibly the density limit.

The international agreement on the ITER project has brought more focus on operational issues associated with high-Z Plasma Facing Components (PFCs) which are, at this time, the only material considered compatible with the nuclear and high heat flux environment. Dr. Lipschultz has led the C-Mod effort in identifying the role of molybdenum in affecting the core plasma, the erosion rates, mechanisms for its erosion and which erosion locations contribute most to core Mo levels. As part of that research he and C-Mod colleagues have investigated the role of boronization in control of Mo influxes and methods to more directly apply the boronization to areas where the erosion rates are highest.

A second area of emphasis in high-Z studies has been Dr. Lipschultz's role in understanding the level of fuel retention in high-Z PFCs. T retention must be low in ITER and reactors for both safety and economic reasons (bet breeding of T). Dr. Lipschultz's studies have surprisingly shown that fuel retention is much higher than would be expected from either material properties or from laboratory ion-beam studies. Understanding the processes that drive this retention and how it scales to ITER and reactors is a central focus of research for the next 5 year plan.

Publications:

B. Lipschultz, X. Bonnin, G. Counsell, A. Kallenbach, A. Kukushkin, K. Krieger, A. Leonard, A. Loarte, R. Neu, R.A. Pitts, T. Rognlien, J. Roth, C. Skinner, J.L. Terry, E. Tsitrone, D. Whyte, S. Zweben, N. Asakura, D. Coster, R. Doerner, R. Dux, G. Federici, M. Fenstermacher, W. Fundamenski, P. Ghendrih, A. Herrmann, J. Hu, S. Krasheninnikov, G. Kirnev, A. Kreter, V. Kurnaev, B. LaBombard, S. Lisgo, T. Nakano, N. Ohno, H.D. Pacher, J. Paley, Y. Pan, G. Pautasso, V. Philipps, V. Rohde, D. Rudakov, P. Stangeby, S. Takamura, T. Tanabe, Y. Yang and S. Zhu, "Plasma-surface interaction, scrape-off layer and divertor physics: implications for ITER", *Nucl. Fusion* **47** (2007) 1189.

B. Lipschultz, Y. Lin, M. L. Reinke, A. Hubbard, I. H. Hutchinson, J. Irby, B. LaBombard, E. S. Marmor, K. Marr, J. L. Terry, S. M. Wolfe, "Operation of Alcator C-Mod with high-Z plasma facing components and implications", *Phys. Plasmas* **13** (2006) 056117.

B Lipschultz, D Whyte and B LaBombard, "Comparison of particle transport in the scrape-off layer plasmas of Alcator C-Mod and DIII-D", *Plasma Phys. & Controlled Fusion* **47** (2005) 1559.

B. Lipschultz, B. LaBombard, C.S. Pitcher & R. Boivin, "Investigation of the origin of neutrals in the main chamber of Alcator C-Mod", *Plasma Phys. & Controlled Fusion* **44** (2002) 733.

B. Lipschultz, D.A. Pappas, B. LaBombard et al., "A study of molybdenum influxes and transport in Alcator C-Mod", *Nuclear Fusion* **41** (2001) 585.

B. Lipschultz, J.L. Terry, C. Boswell et al., "The role of particle sinks and sources in Alcator C-Mod detached divertor discharges", *Phys. Plasmas* **86** (1999) 1907.

B. Lipschultz, J.L. Terry, C. Boswell et al., "Ultra-high densities and volume recombination inside the separatrix of the Alcator C-Mod tokamak", *Phys. Rev. Letters* **81** (1998) 1007.

B. LaBombard, and B. Lipschultz, "Poloidal Asymmetries in the Alcator-C Edge Plasma", *Nucl. Fusion* **27** (1987) 81.

B. Lipschultz, I. Hutchinson, B. LaBombard & A. Wan, "Electric Probes in Plasmas", *J. Vac. Sci. Technology A*, **4** (1986) 1810.

B. Lipschultz, B. LaBombard, H.L. Manning et al., "Impurity Sources during lower hybrid heating on Alcator", *Nucl., Fusion* **26** (1986) 1463.

B. Lipschultz, B. LaBombard, E.S. Marmor et al., "MARFE: An Edge Plasma Phenomenon", *Nucl. Fusion* **24** (1984) 977.

Prof. Ronald R. Parker
Departments of Electrical and Nuclear Science & Engineering

Education:

B.S. (Electrical Engineering) Tufts University (1960)
S.M. MIT (1963)
Sc.D. MIT (1967)

Professional Experience:

Dr. Parker is a Professor in the Departments of Electrical Engineering and Nuclear Science & Engineering at MIT. He began his career in plasma and fusion research by investigating the excitation and propagation of ion cyclotron waves in a linear beam-plasma device, a work which formed the basis of his doctoral thesis. After completing his PhD in 1967, he joined the Electrical Engineering faculty at MIT where he taught and performed research on basic plasma physics experiments such as feedback stabilization of instabilities and parametric excitation of instabilities in beam-plasma systems.

Dr. Parker left the MIT faculty in 1973 to become head of the Alcator A experiment while it was still in the construction phase. During the operating phase, he led the international team that produced record performance in Alcator A, culminating with the world's first demonstration of confinement sufficient for fusion energy breakeven, as measured by the Lawson parameter $n\tau$. For this achievement he along with other members of the Alcator A team was awarded the first APS Award for Excellence in Plasma Physics. Under his leadership, the Alcator A team made several other important discoveries including the so-called slide away regime, methods of impurity control that resulted for the first time in tokamak operation with $Z_{\text{eff}} \sim 1$, and the concept of "Alcator Scaling". In 1977 he rejoined the MIT faculty as a Professor in the Electrical Engineering Department.

After the Alcator A experimental program was completed, Dr. Parker led the design, construction and operation of the follow-on device, Alcator C. In a notable result from this device it was found that in normal operation the confinement failed to follow the trend established by Alcator A but that Alcator Scaling could be recovered by peaking the density profile using pellet injection. This behavior was attributed to the onset and suppression of Ion Temperature Gradient modes, modes that continue to play an important role in tokamak confinement today. With pellet injection, the record confinement performance of Alcator A was surpassed and Alcator C held the record for confinement performance during the 1980's until the large tokamaks JET, TFTR and JT-60 came into operation.

In 1986, Dr. Parker became head of the physics team designing the Compact Ignition Tokamak at Princeton Plasma Physics Laboratory. He returned to MIT in 1987 and became Director of the Plasma Fusion Center, a position he held until 1995. In 1992, he took leave from MIT to become Associate Director of ITER and Head of the European ITER Design Center in Garching. There, he was responsible for the design of ITER's internal components including the vacuum vessel, divertor, first wall and blanket, and RF heating and current drive systems. Dr. Parker returned to MIT in 1998 where he resumed experimental work on Alcator C-Mod. His present responsibility is leader of the Lower Hybrid Current Drive Experiment. This new facility, constructed and operated in collaboration with PPPL is now fully operational. Over 1 MW of power at LH frequency has been coupled to C-Mod plasmas, and ~ 800 kA of current has been driven. New discoveries are being made with the use of this tool, and an upgrade that will at least double the amount of available power is in progress.

Dr. Parker has served or is serving on a number of advisory committees including the Max-Planck Institut für Plasma Physik Fachbeirat (Chair), the Helmholtz Society Review Panel for Fusion, the DIII-D Program Advisory Committee (Chair), the European Fusion Facilities Review, the CEA Conseil Scientifique du DRFC, and the NRC Burning Plasma Advisory Committee. He has received the APS Excellence in Plasma Physics Award, the ERDA (now DoE) Distinguished Associate Award and the Fusion Power Associates Leadership Award. He is a member of the National Academy of Engineering and a Fellow of the American Physical Society.

Publications:

P.T. Bonoli, J.-S. Ko, R. Parker, et. al., “Lower Hybrid Current Drive Experiments on Alcator C-Mod: Comparison with Theory and Simulation”, to be published in *Physics of Plasmas*.

V. Tang, R. Parker, et.al., “Experimental and Numerical Characterization of Ion Cyclotron Heated Protons in the Alcator C-Mod Tokamak”, *Plasma Phys. and Control. Fusion* **49** (2007) 873.

P. Bonoli, R. Parker, et. al., “Wave-Particle Studies in the Ion Cyclotron and Lower Hybrid Range of Frequencies in Alcator C-Mod”, *Fusion Science and Technology* **51**(2007)401.

V. Tang, J. Liptac, R. Parker, et. al., “A Compact Multi-Channel Neutral Particle Analyzer for Measurement of Energetic Charge-exchanged Neutrals in Alcator C-Mod”, *Review of Scientific Instruments* **77**, 083501(2006).

J. Liptac, R. Parker, et. al., “Hard X-Ray Diagnostic for Lower Hybrid Experiments on Alcator C-Mod”, *Review of Scientific Instruments* **77**,103504(2006).

V. Tang and R. Parker, “Temperature Transients of a Fusion Fission ITER Pebble Bed Reactor in Loss of Coolant Accident”, *Fusion Engineering and Design* (2002).

R. Parker, “ITER In-Vessel System Design and Performance”, *Nucl Fusion* **40**(2000) 473.

P. T. Bonoli, R. R. Parker, M. Porkolab, et. al., “Modelling of Advanced Tokamak Scenarios with LHCD in Alcator C-MOD”, *Nucl Fusion* **40**(2000)1251.

R. Parker, “Design and Issues of the ITER In-Vessel Components”, *Fusion Engineering and Design* **39-40**(1998)1.

R. Parker, G. Janeschitz, H. D. Pacher, et. al., “Plasma Wall Interactions in ITER”, *J. Nucl. Mater.* **241-243**(1997)1.

Dr. John Edward Rice
Principal Research Scientist

Education:

S.B. (Physics) Massachusetts Institute of Technology (1975)

Sc.D. (Physics) Massachusetts Institute of Technology (1979)

Professional Experience:

Dr. Rice has been working on the Alcator series of tokamaks since 1974. He is currently leader of the rotation and momentum transport task force and supervisor of the Alcator C-Mod vacuum group. He has overseen 15 undergraduate theses and 3 graduate theses over the years. He was a Visiting Scientist at Kyoto University in 1983 and at Princeton University in 1986. He served as a Visiting Associate Professor at Nagoya University in 1991 and at the National Institute of Fusion Science (Toki Japan) in 1998. He is currently an official US member of the ITPA Transport Group and on the Executive Committees of the Transport Task Force and Atomic Processes in Plasmas. He is an APS Fellow.

Dr. Rice has made significant contributions in a wide variety of research areas in plasma physics, with a common thread involving x-ray spectroscopy, from measurement of non-thermal electron distributions in Alcator A plasmas, later observed in LH heated Alcator C discharges, to the first observations of charge exchange population of very high n levels in He-like argon from excited neutral hydrogen. He has performed extensive studies of impurity transport in both tokamaks and helical devices, and was first to demonstrate the contribution of anomalous impurity diffusion to the radiative recombination population of He-like argon in the edge plasma of Alcator C. This effect led to the observation of strong up-down impurity density asymmetries in Alcator C-Mod plasmas. He was first to demonstrate the effects of the configuration interaction in the line intensities of very high n transitions in Ne-like ions. He has performed detailed observations of high n satellites to He-like ions and was involved in precision Lamb shift measurements of H-like argon. He has been a pioneer in the area of spontaneous rotation in tokamak plasmas, and has recently pointed out the role of rotation contributing to the higher H-mode power threshold with the X-point away from the grad B drift direction, a long standing mystery in tokamak research. He was instrumental in the discovery of the production and control of ITBs with off-axis ICRF heating. Recent research interest is in anomalous momentum transport.

Publications:

J.E.Rice et al., "Inter-machine Comparison of Intrinsic Toroidal Rotation in Tokamaks", *Nucl. Fusion* **47**, 1618 (2007)

J.E.Rice et al., "Spontaneous Toroidal Rotation in Alcator C-Mod Plasmas with No Momentum Input", *Fusion Sci. Technol.* **51**, 288 (2007)

J.E.Rice et al., "The Dependence of Core Rotation on Magnetic Configuration and the Relation to the H-mode Power Threshold in Alcator C-Mod Plasmas with No Momentum Input", *Nucl. Fusion* **45**, 251 (2005)

W.D.Lee, J.E.Rice, E.S.Marmor, M.J.Greenwald, I.H.Hutchinson and J.A.Snipes, "Observations of Anomalous Momentum Transport in Tokamak Plasmas with No Momentum Input", *Phys. Rev. Lett.* **91**, 205003 (2003)

J.E.Rice et al., "Double Transport Barrier Plasmas in Alcator C-Mod", *Nucl. Fusion* **42**, 510 (2002)

J.E.Rice et al., "X-ray Observations of 2l-nl' Transitions and Configuration Interaction Effects from Kr, Mo, Nb and Zr in Near Neon-like Charge States from Tokamak Plasmas", *J. Phys. B: At. Mol. Opt. Phys.* **33** 5435 (2000)

J.E.Rice et al., "Central Impurity Toroidal Rotation in ICRF Heated Alcator C-Mod Plasmas", *Nucl. Fusion* **39**, 1175 (1999)

J.E.Rice et al., "Impurity Transport in Alcator C-Mod Plasmas", *Phys. Plasmas* **4**, 1605 (1997)

J.E.Rice et al., "X-ray Observations of Up-Down Impurity Density Asymmetries in Alcator C-Mod Plasmas", *Nuc. Fusion* **37**, 241 (1997)

J.E.Rice et al., "Observation of Charge-Transfer Population of High n Levels in Ar⁺¹⁶ from Neutral Hydrogen in the Ground and Excited States in a Tokamak Plasma", *Phys. Rev. Lett.* **56**, 50 (1986)

Dr. James L. Terry
Principal Research Scientist

Education:

B.S. (Physics with Honors) Denison University (1973)

M.S. (Physics) The Johns Hopkins University (1975)

Ph.D. (Physics) The Johns Hopkins University (1978)

Professional Experience:

Dr. Terry is a Fellow of the APS, deputy Leader of the US Burning Plasma Organization's "Diagnostics" Topical Group, and a member of the "Edge Coordination Committee" (charged with US coordination of US/International efforts in edge plasma theory and modeling). He has been a member of the DIII-D Program Advisory Committee for the past 3 years, is a frequent referee for the major journals publishing work in plasma physics, and is a frequent reviewer of proposals for the Dept. of Energy's Office of Fusion Energy.

Dr. Terry has worked in the field of plasma physics for over 30 years. Over this time he has made significant contributions in a number of research areas in plasma physics, with a common thread being the use and development of diagnostics for high temperature, magnetically confined plasmas. Those research areas include: volume recombination in plasmas, plasma transport and plasma turbulence at the plasma boundary, wall-conditioning and wall-conditioning techniques for improved plasma confinement, and the study of plasma impurities. Generally, the diagnostic techniques he has employed have involved optical diagnostics, plasma spectroscopy (from the soft x-ray region to the infrared), and various particle tracers. Dr. Terry's research has for the most part been carried out on three tokamaks located at MIT: Alcator A, Alcator C, and Alcator C-Mod. He has also conducted successful experiments at the Lawrence Livermore Laboratories (2X-IIB magnetic mirror), the University of Kyoto, Japan (Heliotron E), and the Princeton Plasma Physics Laboratory (TFTR).

Publications:

Terry JL, LaBombard B, Lipschultz B, Greenwald MJ, Rice JE, Zweben SJ, "The scrape-off layer in Alcator C-Mod: transport, turbulence, and flows", *Fusion Science and Technology* **51** (2007) pp 342-56.

Terry JL, Cziegler I, Hubbard AE, Snipes JA, Hughes JW, Greenwald MJ, LaBombard B, Lin Y, Phillips P, Wukitch S, "The dynamics and structure of edge-localized-modes in Alcator C-Mod", *Journal of Nuclear Materials* **363-365** (2007) pp 994-9.

Terry JL, Zweben SJ, Hallatschek K, LaBombard B, Maqueda RJ, Bai B, Boswell CJ, Greenwald M, Kopon D, Nevins WM, Pitcher CS, Rogers BN, Stotler DP, Xu XQ, "Observations of the turbulence in the scrape-off-layer of Alcator C-Mod and comparisons with simulation", *Physics of Plasmas* **10** (2003) pp 1739-47.

Terry JL, Maqueda R, Pitcher CS, Zweben SJ, LaBombard B, Marmor ES, Pigarov AY, Wurden G, "Visible imaging of turbulence in the SOL of the Alcator C-Mod tokamak", *Journal of Nuclear Materials* **290-293** (2001) pp 757-62.

Terry JL, Lipschultz B, Pigarov AYu, Krasheninnikov SI, LaBombard B, Lumma D, Ohkawa H, Pappas D, Umansky M, “Volume recombination and opacity in Alcator C-Mod divertor plasmas”, *Physics of Plasmas* **5** (1998) pp 1759-66.

Lumma D, Terry JL, Lipschultz B, “Radiative and three-body recombination in the Alcator C-Mod divertor”, *Physics of Plasmas* **4** (1997) pp 2555-66.

Terry JL, Marmor ES, Howell RB, Bell M, Cavallo A, Fredrickson E, Ramsey A, Schmidt GL, Stratton B, Taylor G, Mauel ME, “Measurement of internal magnetic field pitch using Li pellet injection on TFTR”, *Review of Scientific Instruments* **61** (1990) pp 2908-13.

Greenwald M, Terry JL, Wolfe SM, Ejima S, Bell MG, Kaye SM, Neilson GH. “A new look at density limits in tokamaks”, *Nuclear Fusion* **28** (1988) pp 2199-207.

Terry JL, Chen KI, Moos HW, Marmor ES, “EUV impurity study of the Alcator Tokamak”, *Nuclear Fusion* **18** (1978) pp 485-91.

Terry JL, Marmor ES, Chen KI, Moos HW, “Observations of poloidal asymmetry in impurity-ion emission due to grad B drifts”, *Physical Review Letters* **39** (1977) pp 1615-18.

Dr. Dennis G. Whyte
Associate Professor, Nuclear Science and Engineering

Education

Ph.D. (Applied Physics), INRS-Energie, Université du Québec, Montréal, Canada (1992)
M.Sc. (Applied Physics), INRS-Energie, Université du Québec, Montréal, Canada (1988)
B.Eng. (Engineering Physics), University of Saskatchewan, Saskatoon, Canada (1986)

Professional Experience:

Dr. Whyte is Associate Professor with Tenure in the Nuclear Science and Engineering Department of MIT. He is the leader of the US Burning Plasma Organization Boundary Topical group, a member of the SOL/Divertor group of the ITPA and a member of the ITER Science and Technical Advisory Committee. He is presently a member of the National Academies Panel to Review the US Fusion Community Participation in ITER.

Dr. Whyte joined MIT in 2006. He has carried out research in the areas of plasma-surface interactions, tritium retention and disruption mitigation at many US and international fusion facilities, notably DIII-D, PISCES, Pilot-PSI (Netherlands), NAGDIS (Japan), TdeV (Canada) and Alcator C-Mod, with a focus towards solving the numerous issues associated with plasma-material interactions foreseen for ITER and burning plasmas. He developed the DIONISOS experiment, which features a unique combination of plasma exposure and in-situ ion beam surface analysis to understand the dynamic interactions between plasmas and materials. Dr. Whyte has extensive experience in plasma spectroscopy, ion-beam surface analysis and atomic physics. He was awarded the Department of Energy Plasma Physics Junior Faculty Development Award in 2003 and was elected Fellow of the American Physical Society – Division of Plasma Physics in 2006.

Publications:

D. G. Whyte, et al. "Mitigation of tokamak disruptions using high-pressure gas injection," *Physical Review Letters* **89** (2002) 055001.

D.G. Whyte, J.W. Davis, "Tritium recovery in ITER by radiative plasma terminations," *Journal of Nuclear Materials* **337-339** (2005) 560-564.

D.G. Whyte, et al. "The effect of detachment on divertor carbon erosion/redeposition in the DIII-D tokamak," *Nuclear Fusion* **41** (2001) 1243.

D.G. Whyte, R.C. Isler, et al. "Argon density measurements from charge-exchange spectroscopy," *Physics of Plasmas* **5** (1998) 3694.

D.G. Whyte, et al. "Measurement and verification of Z_{eff} radial profiles using charge exchange recombination spectroscopy on DIII-D," *Nuclear Fusion* **38** (1998) 387-398.

D.G. Whyte, et al. "Rapid inward impurity transport during impurity pellet injection on the DIII-D tokamak," *Physical Review Letters* **81** (1998) 4392-4396.

D.G. Whyte, D.A. Humphreys, P.L. Taylor "Measurement of plasma electron temperature and effective charge during tokamak disruptions," *Physics of Plasmas* **7** (2000) 4052-4056.

D. Whyte, et al. "Divertor retention of metallic impurities during neutralization plate biasing on TdeV," *Nuclear Fusion* **34** (1994) 203.

D.G. Whyte, B.L. Lipshultz, P.C. Stangeby, et al., "The magnitude of plasma flux to the main-wall in the DIII-D tokamak," *Plasma Physics and Controlled Fusion* **47** (2005) 1579-1607.

D.G. Whyte, G.R. Tynan, R.P. Doerner, J.N. Brooks "Carbon chemical erosion with increasing plasma flux and density," *Nuclear Fusion* **41** (2001) 47.

D.G. Whyte, et al. "Similarities in divertor erosion/redeposition and deuterium retention patterns between the tokamaks ASDEX Upgrade, DIII-D and JET," *Nuclear Fusion* **39** (1999) 1025-1030.

D.G. Whyte, "Plasma-surface interaction studies on DIII-D and their implications for next-step fusion experiments," *Fusion Science & Technology* **48** (2005) 1096-1116.

Dr. Stephen M. Wolfe
Principal Research Scientist

Education:

BS (Physics), Massachusetts Institute of Technology (1971)

PhD (Physics), Massachusetts Institute of Technology (1977)

Professional Experience:

Dr. Wolfe is the leader of the Integrated Scenarios - H-mode Baseline program at Alcator C-Mod, and also leads the Physics Operations team. Dr. Wolfe was instrumental in the development of the concept and design of the Alcator C-Mod facility, and served as Scientific Coordinator for the project during the design and construction phase. Dr. Wolfe is an experimental physicist whose technical activities have included diagnostic design and construction, MHD analysis and magnetics design, and development and use of computer codes for simulations and analysis. His present research is largely concerned with MHD and with problems of tokamak operation and control.

As leader of the Confinement Studies Group at Alcator C, Dr. Wolfe played a key role in the planning, execution, and analysis of experiments which led to the discovery of neo-Alcator scaling of energy confinement in ohmically heated tokamak plasmas, and in the pellet fueling experiments which resulted in the first attainment of confinement parameters ($n\tau_E$) in excess of the Lawson criterion required for breakeven. His work in analyzing the results of the Alcator C experiments contributed to the recognition of ion temperature gradient modes in anomalous ion thermal transport. In earlier work, he developed a novel dual-laser modulated FIR interferometer system for plasma density measurements which was adopted as a diagnostic standard at laboratories around the world.

Dr. Wolfe has also participated in a number of collaborative experiments with other laboratories, both in the U.S. and abroad, including research at the DIII-D tokamak at GA in San Diego, JFT2 in Japan, and T-10 in Moscow.

Publications:

Ferrara, M., Hutchinson, I. H., Wolfe, S. M., "Plasma inductance and stability metrics on Alcator C-Mod", to be published in Nuclear Fusion (2008).

Stillerman, J.A. Ferrara, M., Fredian, T.W., Wolfe, S.M., "Digital real-time plasma control system for Alcator C-Mod", Fusion Engineering and Design, v 81, n 15-17, July 2006, p 1905-10

Wolfe, S. M., Hutchinson, I. H., Granetz, R. S., Rice, J., Hubbard, A., Lynn, A., Phillips, P., Hender, T. C., Howell, D. F., La Haye, R. J. and Scoville, J. T., "Non-axisymmetric field effects on Alcator C-Mod", Phys. Plasmas 12, 056110 (2005)

Stambaugh, R. D., Wolfe, S. M., Hawryluk, R. J., Harris, J. H., Biglari, H., Prager, S. C., Goldston, R. J., Fonck, R. J., Ohkawa, T., Logan, B. G., Oktay, E., "Enhanced Confinement in Tokamaks", Physics of Fluids B 2, 2941 (1990)

Wolfe, S., Greenwald, M., Gandy, R., Granetz, R., Gomez, C., Gwinn, D., Lipschultz, B., McCool, S., Marmor, E., Parker, J., Parker, R., Rice, J., "Effect of Pellet Fueling on Energy Transport in Ohmically Heated Alcator-C Plasmas," Nucl. Fusion 26, 329 (1986).

Greenwald, M., Gwinn, D., Milora, S., Parker, J., Parker, R., Wolfe, S., Besen, M., Camacho, F., Fairfax, S., Fiore, C., Foord, M., Gandy, R., Gomez, C., Granetz, R., LaBombard, B., Lloyd, B.,

Marmar, E., McCool, S., Pappas, D., Petrasso, R., Pribyl, P., Rice, J., Schuresko, D., Takase, Y., Terry, J., Watterson, R., ``Energy Confinement of High-Density Pellet-Fueled Plasmas in the Alcator C Tokamak'', Phys. Rev. Lett. 53, 352 (1984).

Lipschultz, B., LaBombard, B., Marmar, E. S., Pickrell, M. M., Terry, J. L., Watterson, R., Wolfe, S. M., ``Marfe: An Edge Plasma Phenomenon'', Nuclear Fusion 24, 977 (1984).

Wolfe, S. M., Cohn, D. R., Temkin, R., Kreischer, K., ``Characteristics of Electron-Cyclotron-Resonance- Heated Tokamak Power Reactors'', Nuclear Fusion 19, 389 (1979).

Gaudreau, M., Gondhalekar, A., Hughes, M. H., Overskei, D., Pappas, D. S., Parker, R. R., Wolfe, S. M., Apgar, E., Helava, H.I., Hutchinson, I. H., Marmar, E.S., Molvig, K., ``High Density Discharges in the Alcator Tokamak'', Phys. Rev. Lett. 39, 1299 (1977).

Wolfe, S. M., Button, K. J., Waldman, J., Cohn, D. R., ``Modulated Submillimeter Laser Interferometer System for Plasma Density Measurements'', Applied Optics 15, 2645 (1976).

Dr. Steven Wukitch

Principal Research Scientist

Education:

B.S. (Nuclear Engineering), The Pennsylvania State University (1991)

M.S. (Nuclear Engineering and Engineering Physics), University of Wisconsin (1993)

Ph.D. (Nuclear Engineering and Engineering Physics), University of Wisconsin (1995)

Professional Experience:

Dr. Wukitch is a principal scientist on the Alcator C-Mod project. As ICRF group leader, he has overall responsibility for the physics program and routine operation of the 8 MW ICRF heating and current drive systems. His research interests include ICRF wave physics (wave propagation, absorption, and coupling), RF-plasma edge interactions, and antenna, transmission, and source technological challenges.

His current work is focused upon understanding RF-plasma edge interactions and the relationship between RF fields, rectified RF voltages, and impurity production associated with ICRF operation. Recent measurements of the plasma potential with RF have uncovered some unexpected features. At high power, the plasma potential increased despite insulating limiters and the plasma potential in H-mode is higher than expected. These results were reported in an invited talk at the 2007 APS-DPP annual meeting.

Dr. Wukitch has made important contributions to the understanding of ICRF mode conversion in which a wave with a long wavelength mode converts to short wave length modes. This new understanding resulted from experimental measurements using a novel phase contrast imaging diagnostic, high resolution power deposition profiles and sophisticated electromagnetic full-wave simulations of the experiment. His primary contribution was to compile an extensive experimental database of the mode conversion electron deposition profiles leading to the identification of intermediate wavelength mode in ion cyclotron range of frequencies in D(He-3) and D(H) plasmas in C-Mod. He has worked closely with modelers to understand these experiments through simple physics modes and validation of the full wave simulations against experimental data. He also showed that the mode converted wave could drive current sufficient in magnitude and localization to control the sawtooth period and this was reported in an invited talk at the 2004 APS-DPP annual meeting.

Dr. Wukitch has done extensive research on internal transport barrier experiments on C-Mod starting with the experimental observation and analysis of an ICRF-induced Enhanced Neutron mode. He also utilized a sawtooth heat pulse propagation technique to understand the transport properties of ITB modes in C-Mod that are observed with off-axis ICRF heating; these results were reported by him in an invited talk at the 2001 APS-DPP annual meeting.

Dr. Wukitch has also made important contributions to the design and utilization of ICRF antennas in C-Mod. Recent work has focused on the use of novel real time matching network to enable antenna operation over a wide range of plasma conditions while maintaining low reflected power. He has also identified the important role magnetic field and neutral pressure play in RF breakdown in antennas. He has collaborated with modelers to validate advanced electromagnetic field solvers to analyze complicated antenna structures. These contributions have led to important improvements in the antennas, allowing for higher power handling and improved reliability of the ICRF system.

Dr. Wukitch has helped to direct the thesis research of several graduate students in the RF Group as well as numerous undergraduate students through MIT's UROP program.

Publications:

S.J. Wukitch, B. Lipschultz, E. Marmor, Y. Lin, A. Parisot, M. Reinke, J. Rice, J. Terry, and the C-Mod Team, "RF Plasma Edge Interactions and their Impact on ICRF Antenna Performance in Alcator C-Mod", *J. Nucl. Mat.* **363**, 491-497 (2007).

P.T. Bonoli, R. Parker, S.J. Wukitch et al., "Wave-particle studies in the ion cyclotron and lower hybrid ranges of frequencies in Alcator C-Mod", *Fusion Sci. Tech.* **51** (3): 401-436 (2007).

A. Parisot, S.J. Wukitch et al., "Sawtooth period changes with mode conversion current drive on Alcator C-Mod", *Plasma Physics and Controlled Fusion* **49**, 219 (2007).

T. Graves, S. J. Wukitch, B. LaBombard, and I. H. Hutchinson, "The effect of multipactor discharge on Alcator C-Mod Ion Cyclotron Resonance Frequency (ICRF) heating", *J. Vac. Sci. Technol. A* **24**, 512 (2006).

S.J. Wukitch, Y. Lin, A. Parisot, J.C. Wright, P.T. Bonoli, M. Porkolab, N. Basse, E. Edlund, A. Hubbard, L. Lin, A. Lynn, E. Marmor, D. Mossessian, P. Phillips, G. Schilling, "Ion cyclotron range of frequency mode conversion physics in Alcator C-Mod: Experimental measurements and modeling", *Physics of Plasmas* **12**, 056104 (2005).

Y. Lin, S. Wukitch, A. Parisot, J.C. Wright, N. Basse, P. Bonoli, E. Edlund, L. Lin, M. Porkolab, G. Schilling, P. Phillips, "Observation and modeling of ion cyclotron range of frequencies waves in the mode conversion region of Alcator C-Mod", *Plasma Physics and Controlled Fusion* **47**, 1207 (2005).

S.J. Wukitch, R.L. Boivin, P.T. Bonoli, J.A. Goetz, J. Irby, I. Hutchinson, Y. Lin, A. Parisot, M. Porkolab, E. Marmor, G. Schilling, J.R. Wilson, "Investigation of performance limiting phenomena in a variable phase ICRF antenna in Alcator C-Mod", *Plasma Physics and Controlled Fusion* **46**, 1479 (2004).

A. Parisot, S.J. Wukitch, P. Bonoli, J.W. Hughes, B. Labombard, Y. Lin, R. Parker, M. Porkolab, A.K. Ram, "ICRF loading studies on Alcator C-Mod", *Plasma Physics and Controlled Fusion* **46**, 1781 (2004).

Y. Lin, S. Wukitch, P. Bonoli, E. Nelson-Melby, M. Porkolab, J.C. Wright, N. Basse, A.E. Hubbard, J. Irby, L. Lin, E.S. Marmor, A. Mazurenko, D. Mossessian, A. Parisot, J. Rice, S. Wolfe, C.K. Phillips, G. Schilling, J.R. Wilson, P. Phillips, A. Lynn, "Investigation of ion cyclotron range of frequencies mode conversion at the ion-ion hybrid layer in Alcator C-Mod", *Physics of Plasmas* **11**, 2466 (2004).

S. Wukitch, R. L. Boivin, P. T. Bonoli, C. L. Fiore, R. S. Granetz, M. J. Greenwald, A. E. Hubbard, I. H. Hutchinson, Y. In, J. Irby, Y. Lin, E. S. Marmor, D. Mossessian, M. Porkolab, G. Schilling, J. E. Rice, J. A. Snipes, and S. M. Wolfe, "Double transport barrier experiments on Alcator C-Mod", *Physics of Plasmas* **9**, 2149 (2002).

13.2 Alcator Publications - 2003-Present

Papers Published in Refereed Journals

2003

Antar, G.Y., LaBombard, B., et al., "Universality of intermittent convective transport in the scrape off-layer of magnetically confined devices," *Phys. Plasmas* **10** (2003) 419.

Basse, N.P., et al., "Characterization of turbulence in L- and ELM-free H-mode Wendelstein 7-AS plasmas," *Plasma Phys. Control. Fusion* **45** No. 4 (2003) 439.

Basse, N.P., et al., "Turbulence at the transition to the high density H-mode in Wendelstein 7-AS plasmas," *Nuc. Fusion* **43** No. 1 (2003) 40.

Bernabei, S., Parker, R.R., Porkolab, M., et al., "Design of a compact lower hybrid coupler for Alcator C-Mod," *Fusion Science and Technology* **43** No. 2 (2003) 145.

Boswell, C.J., LaBombard, B., Lipschultz, B., Pitcher, C.S., Terry, J.L., et al., "EIRENE neutral code modeling of the C-Mod divertor," *J. Nucl. Materials* **313-316** (2003) 1089.

Chung, T., Pitcher, C.S., LaBombard, B., Lipschultz, B., Terry, J.L., Rice, J.E., et al., "Recycling impurity compression in Alcator C-Mod divertor," *J. Nucl. Materials* **313-316** SUPPL., (2003) 990.

Gangadhara, S., LaBombard, B., "Flow measurements in the scrape-off layer of Alcator C-Mod using impurity plumes," *J. Nucl. Materials* **313-316** (2003) 1167.

Ghosh, J., Terry, J., Marmor, E., Lipschultz, B., LaBombard, B., Rice, J.E., et al., "Measurements of ion and neutral atom flows and temperatures in the inner and outer midplane scrape-off layers of the Alcator C-Mod Tokamak," *Phys. Plasmas* **11** No. 3 (2004) 1033.

Gohil, P., Rice, J., et al., "Increased Understanding of the dynamics and transport in ITB plasmas from multi-machine comparisons," *Nucl. Fusion* **43** No. 8 (2003) 708.

Greenwald, M., et al., "EU-US transport task force workshop on transport in fusion plasmas: transport near operational limits," *Plasma Phys. Control. Fusion* **45** No. 4 (2003) 445.

Greenwald, M., "Transitions of Turbulence in plasma density limits," *Phys. Plasmas* **10** (2003) 1773.

Hughes, J.W., Mossessian, D., Zhurovich, K., Hubbard, A., et al., "Thomson scattering upgrades on Alcator C-Mod," *Rev. Sci. Instrum.* **74** No. 3 (2003) 1667.

Hutchinson, I.H., "Ion Collection by a Sphere in a Flowing Plasma: 2. Non-zero Debye Length," *Plasma Phys. Control. Fusion* **45** (2003) 1477.

LaBombard, B., Gangadhara, S., Lipschultz, B., Pitcher, C.S., "Toroidal rotation as an explanation for plasma flow observations in the Alcator C-Mod scrape-off layer," *J. Nucl. Materials* **313-316** (2003) 995.

Lee, W.D., Boivin, R.L., Bonoli, P.T., Fiore, C.L., Hubbard, A., Irby, J., Porkolab, M., Wukitch, S.J., "Neutral particle analysis of ICRF heated discharges on Alcator C-Mod," *Plasma Phys. Control. Fusion* **45** No. 8 (2003) 1465.

Lee, W.D., Rice, J.E., Marmor, E.S., Greenwald, M.J., Hutchinson, I.H., Snipes, J.A., "Observation of anomalous momentum transport in Tokamak plasmas with no momentum input," *Phys. Rev. Lett.* **91** No. 20 (2003) 205003/1-4

Lin, Y., Wukitch, S.J., Bonoli, P.T., Marmor, E., Mossessian, D., Phillips, P., Porkolab, M., Schilling, G., Wolfe, S., et al., "Ion cyclotron range of frequencies mode conversion electron heating in deuterium-hydrogen plasmas in the Alcator C-Mod tokamak," *Plasma Phys. Control. Fusion* **45** No. 6 (2003) 1013.

Maqueda, R.J., Wurden, G.A., Zweben, S.J., LaBombard, B., Terry, J.L., et al., "Gas puff imaging of edge turbulence," *Rev. Sci Instrum.* **74** No. 3 (2003) 2020.

Marmor, E.S., Hutchinson, I., Parker, R., Porkolab, M., et al., "Overview of recent Alcator C-Mod research," *Nucl. Fusion* **43** No. 12 (2003) 1610-18.

Marmor, E., et al., "Thin foil Faraday collectors as a radiation hard fast lost-ion diagnostic," *Rev. Sci. Instrum.* **74** No. 3 (2003) 1747.

Mossessian, D.A., Groebner, R.J., Hughes, J.W., Greenwald, M., Hubbard, A., et al., "Edge dimensionless identity experiment on DIII-D and Alcator C-Mod," *Phys. Plasmas* **10** No. 3 (2003) 689.

Mossessian, D.A., Hubbard, A., Hughes, J.W., Greenwald, M., LaBombard, B., Snipes, J.A., Wolfe, S., et al., "High-confinement-mode edge stability of Alcator C-Mod plasmas," *Phys. Plasmas* **10** No. 5 (2003) 1720.

Nelson-Melby, E., Porkolab, M., Bonoli, P.T., Lin, Y., Wukitch, S.J., et al., "Experimental observations of mode-converted ion cyclotron waves in a tokamak plasma by phase contrast imaging," *Phys. Rev. Lett.* **90** No. 15 (2003) 1555004/1-4.

Rice, J.E., Bonoli, P.T., Fiore, C.L., Lee, W.D., Marmor, E.S., Wukitch, S.J., Granetz, R.S., Hubbard, A.E., Hughes, J.W., Irby, J.H., Lin, Y., Mossessian, D., Wolfe, S.M., Zhurovich, K., Greenwald, M.J., Hutchinson, I.H., Porkolab, M., Snipes, J.A., et al., "Pressure profile modification of internal transport barrier plasmas in Alcator C-Mod," *Nucl. Fusion* **43** No. 8 (2003) 781.

LaBombard, B., Terry, J.L., Zweben, S.J., et al., "Neutral transport simulations of gas puff imaging experiments," *J. Nucl. Mat.* **313-316** SUPPL. (2003) 1066

Terry, J.L., LaBombard, B., Bai, B., Greenwald, M., et al., "Observations of the turbulence in the scrape-off-layer of Alcator C-Mod and comparisons with simulation," *Phys. Plasmas* **10** No. 5 II (2003) 1739.

2004

Boswell, C.J. Terry, J.L., LaBombard, B., Lipschultz, B., Pitcher, C.S., "Interpretation of the D_{α} emission from the high field side of Alcator C-Mod," *Plasma Phys. and Control. Fusion* **46** No.8 (2004) 1247.

Bonnin, X., Coster, D., Schneider, R., Reiter, D., Rozhansky V., Voskoboynikov, S., "Modelling and consequences of drift effects in the edge plasma of Alcator C-Mod," *J. Nucl. Mater.* **337-339**, (2005) 301-304.

Ernst, D.R., Bonoli, P.T., Catto, P.J., Dorland, W., Fiore, C.L., Granetz, R.S., Greenwald, M., Hubbard, A.E., Porkolab, M., Redi, M.H., Rice, J.E., Zhurovich, K. "Role of trapped electron mode turbulence in internal transport barrier control in the Alcator C-Mod Tokamak," *Phys. Plasmas* **11** No. 5 (2004) 2637.

Fiore, C.L., Bonoli, P.T., Ernst, D.R., Hubbard, A.E., Greenwald, M.J., Lynn, A., Marmor, E.S., Phillips, P., Redi, M.H., Rice, J.E., Wolfe, S.M., Wukitch, S.J., Zhurovich, K., "Control of internal transport barriers on Alcator C-Mod," *Phys. Plasmas* **11** No. 5 (2004) 2480.

Fiore, C.L., Bonoli, P.T., Ernst, D.R., Greenwald, M.J., Marmor, E.S., Redi, M.H., Rice, J.E., Wukitch, S.J., Zhurovich, K., "Internal Transport Barrier Production and Control in Alcator C-Mod," *Plasma Phys. Control. Fusion* **46** No 12B (2004) B281.

Gangadhara, S., LaBombard, B., "Impurity plume experiments in the edge plasma of the Alcator C-Mod tokamak," *Plasma Phys. Control Fusion* **46** No 10 (2004) 1617.

Ghosh, J., Griem, H.R., Elton, R.C., Terry, J.L., Marmor, E., Lipschultz, B., LaBombard, B., Rice, J.E., Weaver, J.L., "Measurements of ion and neutral atom flows and temperatures in the inner and outer midplane scrape-off layers of the Alcator C-Mod Tokamak," *Phys. Plasmas* **11** No. 3 (2004) 1033.

Grulke, O., (MPI for Plasma Physics, Greifswald Branch, EURATOM Association, D-17489 Greifswald, Germany) Garcia, O. E. et al., "Dynamics of spatiotemporal fluctuation structures in the scrape-off layer of Alcator C-Mod and NSTX," *Phys. Rev. Letters* **92** (16), 2004.

Hutchinson, I.H., "Spin Stability of Asymmetrically Charged Plasma Dust," *New J. Phys.* **6** (2004) 43.

Hutchinson, I.H. "Ion Collection by a Sphere in a Flowing Plasma: 3. Floating Potential and Drag Force," *Plasma Phys. Control. Fusion* **47** No 1 (2005) 71-87.

LaBombard, B., Rice, J.E., Hubbard, A.E., Hughes, J.W., Greenwald, M., Irby, J., Lin, Y., Lipschultz, B., Marmor, E.S., Pitcher, C.S., Smick, N., Wolfe, S.M., Wukitch, S.J., "Transport-Driven Scrape-off Layer Flows and the Boundary Conditions Imposed at the Magnetic Separatrix in a Tokamak Plasma," *Nucl. Fusion* **44** No 10 (October 2004) 1047.

Lin, Y., Wukitch, S., Bonoli, P., Nelson-Melby, E., Porkolab, M., Wright, J.C., Basse, N., Hubbard, A.E., Irby, J., Lin, L., Marmor, E.S., Mazurenko, A., Mossessian, D., Parisot, A.; Rice, J., Wolfe, S., Phillips, C.K., Schilling, G., Wilson, J.R., Phillips, P., Lynn, A., "Investigation of ion cyclotron range of frequencies mode conversion at the ion-ion hybrid layer in Alcator C-Mod," *Phys. Plasmas* **11** No. 5 (2004) 2466.

Marmar, E.S., Bai, B., Boivin, R.L., Bonoli, P.T., et al., "Overview of recent Alcator C-Mod research," *Nuclear Fusion* **43** No. 12 (2003) 1610-18.

Parisot, A., Wukitch, S.J., Bonoli, P., Hughes, J.W., Labombard, B., Lin, Y., Parker, R., Porkolab, M., Ram, A.K., "ICRF loading studies on Alcator C-Mod," *Plasma Phys. Control. Fusion* **46** No 11 (2004) 1781.

Pigarov, A.Y. (MAE Center for Energy Res., California Univ., San Diego, La Jolla, CA, USA), Krasheninnikov, S.I.; Rognlien, T.D., West, W.P., LaBombard, B.L., Lipschultz, B., Maingi, R., Soukhanovskii, V., "Multi-fluid code simulations including anomalous non-diffusive transport of plasma and impurities in the tokamak SOL," *Plasma Physics* **44** No 1-3 (2004) 228-34.

Pigarov, A.Y., Krasheninnikov, S.I., Brooks, N., Hollmann, E., Maingi, R., Labombard, B., Lipschultz, B., Rognlien, T., Soukhanovskii, V., West, W. P., "Multi-ion fluid simulation of tokamak edge plasmas including non-diffusive anomalous cross-field transport," *J. of Nucl. Materials* **337-339** (2005) 371

Rice, J.E., Lee, W.D., Marmar, E.S., Bonoli, P.T., Granetz, R.S., Greenwald, M.J., Hubbard, A.E., Hutchinson, I.H., Irby, J.H., Lin, Y., Mossessian, D., Snipes, J.A., Wolfe, S.M., Wukitch, S.J., "Observations of anomalous momentum transport in Alcator C-Mod plasmas with no momentum input," *Nuc. Fusion* **44** No. 3 (2004) 379.

Rice, J.E., Lee, W.D., Marmar, E.S., Basse, N.P., Bonoli, P.T., Greenwald, M.J., Hubbard, A.E., Hughes, J.W., Hutchinson, I.H., Ince-Cushman, A., Irby, J.H., Lin, Y., Mossessian, D., Snipes, J.A., Wolfe, S.M., Wukitch, S.J., Zhurovich, K., "Toroidal rotation and momentum transport in Alcator C-Mod plasmas with no momentum input," *Phys. Plasmas* **11** No. 5 (2004) 2427.

Snipes, J.A., Schmittdiel, D., Fasoli, A., Granetz, R.S., Parker, R.R., "Initial active MHD spectroscopy experiments exciting stable Alfvén eigenmodes in Alcator C-Mod," *Plasma Phys. Control. Fusion* **46** No. 4 (2004) 611.

Terry, J.L., Zweben, S.J., Bose, B., Grulke, O., Marmar, E.S., Lowrance, J., Mastrocola, V., Renda, G., "High speed movies of turbulence in Alcator C-Mod," *Review of Scientific Instruments*, **75** No. 10 (2004) 4196-4199

Wright, J.C., Bonoli, P.T., D'Azevedo, E., Brambilla, M., "Ultrahigh Resolution Simulations of Mode Converted Ion Cyclotron Waves and Lower Hybrid Waves," *Computer Physics Communications* **164** 1-3, 1-15 (2004) 330.

Wright, J.C., Bonoli, P.T., Brambilla, M., Meo, F., D'Azevedo, E., Batchelor, D. B., Jaeger, E. F., Berry, L. A., Phillips, C. K. and Pletzer, A., "Full Wave Simulations of Fast Wave Mode Conversion and Lower Hybrid Wave Propagation in Tokamaks," *Physics of Plasmas* **11** (5) (2004) 2473.

Wukitch, S.J., Boivin, R.L.1, Bonoli, P.T., Goetz, J.A., Irby, J., Hutchinson, I.H., Lin, Y., Parisot, A., Porkolab, M., Marmar, E., Schilling, G., and Wilson, J.R., "Investigation of Performance Limiting Phenomena in a Variable Phase ICRF Antenna in Alcator C-Mod," *Plasma Phys. Control. Fusion* **46** No. 9 (2004) 1479.

Watts, C. (New Mexico Tech, Socorro, NM, USA), Yongkyoon I., Heard, J., Phillips, P., Lynn, A., Hubbard, A., Gandy, R., "Upper limit on turbulent electron temperature fluctuations in the core of Alcator C-Mod," *Nuclear Fusion* **44** No. 9 (2004) 987-91.

Lee, W.D., Rice, J.E., Marmor, E.S., Greenwald, M.J., Hutchinson, I.H., Snipes, J.A., "Observation of anomalous momentum transport in Tokamak plasmas with no momentum input," *Physical Review Letters* **91** No. 20 (2003) 205003/1-4.

2005

Basse N.P., Zoletnik S., Michelsen P.K., "Study of intermittent small-scale turbulence in Wendelstein 7-AS plasmas during controlled confinement transitions," *Phys. Plasmas* **12** (1): Art. No. 012507 Jan 2005

Basse, N.P. et al., "Small-angle scattering theory revisited: Photocurrent and spatial localization", *Physica Scripta* **71** (2005) 280-292

Basse, N.P., Edlund, E.M., Ernst, D.R. et al., "Characterization of core and edge turbulence in L- and enhanced D-alpha H-mode Alcator C-Mod plasmas", *Physics of Plasmas* **12** (2005) 052512

Basse, N.P. "Density fluctuations on mm and Mpc scales", *Physics Letters A* **340** (2005) 456-460

Batchelor, D. B., Berry, L. A., Bonoli, P. T., Carter, M. D., Choi, M., D'Azevedo, E., D'Ippolito, D. A., Gorelenkov, N., Harvey, R. W., Jaeger, E. F., Myra, J. R., Okuda, H., Phillips, C. K., Smithe, D. N., and Wright, J. C., "Electromagnetic mode conversion: understanding waves that suddenly change their nature" *Journal of Physics: Conference Series* **16** (2005) 35–39

Bonnin, X., Coster, D., Schneider, R., Reiter, D., Rozhansky V., Voskoboinikov, S., "Modelling and consequences of drift effects in the edge plasma of Alcator C-Mod," *J. Nucl. Mater.* **337-339**, 301-304 (2005).

Chung, T., Hutchinson, I.H., Lipschultz, B., LaBombard, B., and Lisgo, S., "DIVIMP modeling of impurity flows and screening in Alcator C-Mod," *J. Nucl. Mater.* **337-339** (2005) 109.

Cordey, J.G., Snipes, J.A., Greenwald, M. Sugiyama, L., et al, " Scaling of the energy confinement time with β and collisionality approaching ITER conditions ", *Nucl. Fusion* **45** (2005) 1078–1084.

Greenwald, M. et al, "Overview of Alcator C-Mod Program" *Nucl. Fusion* **45** (2005) S109–S117.

Hutchinson, I.H. "Ion Collection by a Sphere in a Flowing Plasma: 3. Floating Potential and Drag Force," *Plasma Phys. Control. Fusion* **47** No. 1 (2005) 71-87.

LaBombard, B., Rice, J.E., Hubbard, A.E., Hughes, J.W., Greenwald, M., Granetz, R.S., Irby, J.H., Lin, Y., Lipschultz, B., Marmor, E.S., Marr, K., Mossessian, D., Parker, R., Rowan, W., Smick, N., Snipes, J.A., Terry, J.L., Wolfe, S.M., Wukitch, S.J., and the Alcator C-Mod Team., "Transport-driven scrape-off layer flows and the x-point dependence of the L-H power threshold in Alcator C-Mod," *Phys. Plasmas* **12** (2005) 056111.

LaBombard, B. Hughes, J.W.; Mossessian, D.; Greenwald, M.; Lipschultz, B.; Terry, J.L. "Evidence for electromagnetic fluid drift turbulence controlling the edge plasma state in the Alcator C-Mod tokamak" *Nucl Fusion*, **45** No. 12, (2005) 1658-1675.

Lipschultz, B., Whyte, D., LaBombard, B., "Comparison of particle transport in the Scrapeoff Layer plasmas of Alcator C-Mod and DIII-D", *Plasma Phys. Control. Fusion* **47** (2005) 1559–1578.

Lipschultz B, Haasz AA, LaBombard B, et al., "Proceedings of the 16th International Conference on Plasma Surface Interactions in Controlled Fusion Devices – Preface" *J. of Nucl. Materials* **337-39** (1-3): VII-VIII (2005).

Lin, Y., Wukitch, S., et al., "Observation and modeling of ion cyclotron range of frequencies waves in the mode conversion region of Alcator C-Mod", *Plasma Physics and Controlled Fusion* **47** (2005) 1207.

Lisgo, S., Borner, P., Boswell, C., Elder, D., LaBombard, B., Lipschultz, B., Pitcher, C.S., Reiter, D., Stangeby, P.C., Terry, J.L., and Wiesen, S., "OSM-EIRENE modeling of neutral pressures in the Alcator C-Mod divertor," *J. Nucl. Mater.* **337-339** (2005) 139.

Lynch, V.E., Carreras, B.A., Sanchez, R., LaBombard, B., van Milligen, B.P., and Newman, D.E., "Determination of long-range correlations by quiet-time statistics," *Phys. Plasmas* **12** (2005) 052304.

Marr, K., Lipschultz, B., LaBombard, B, et al., "Spectroscopic measurements of plasma flow in the SOL in C-Mod," *J. of Nucl. Materials* **337-39** (1-3) (2005) 286-290.

Pigarov, A.Y., Krasheninnikov, S.I., Brooks, N., Hollmann, E., Maingi, R., Labombard, B., Lipschultz, B., et al., "Multi-ion fluid simulation of tokamak edge plasmas including non-diffusive anomalous cross-field transport," *J. of Nucl. Materials* **337–339** (2005) 371.

Redi, M. H., Dorland, W., Fiore, C. L., Baumgaertel, J. A., et al., "Microturbulent drift mode stability before internal transport barrier formation in the Alcator C-Mod radio frequency heated H-mode" *Phys. Plasmas* **12**, 072519 (2005) .

Rice, J.E., Hubbard, A.E., Hughes, J.W., Greenwald, M.J., LaBombard, B., Irby, J.H., Lin, Y., Marmor, E.S., Mossessian, D., Wolfe, S.M., Wukitch, S.J., "The dependence of core rotation on magnetic configuration and the relation to the H-mode power threshold in Alcator C-Mod plasmas with no momentum input," *Nuclear Fusion* **45**, No. 4, April (2005) 251-

Smick, N., LaBombard, B., and Pitcher, C.S., "Plasma profiles and flows in the high-field side scrape-off layer in Alcator C-Mod," *J. Nucl. Mater.* **337-339** (2005) 281.

Snipes, J. A., et al., "Active and fast particle driven Alfvén eigenmodes in Alcator C-Mod", *Physics of Plasmas* **12** (2005) 056102.

Stotler, D.P. and LaBombard, B., "Three-dimensional simulation of gas conductance measurement experiments on Alcator C-Mod," *J. Nucl. Mater.* **337-339** (2005) 510.

Terry JL, Zweben SJ, Grulke O, et al. "Velocity fields of edge/Scrape-off-layer turbulence in Alcator C-Mod" *J. of Nucl. Materials* **337-39** (1-3) (2005) 322-326.

Terry, J.L., N.P. Basse, I. Cziegler, et al "Transport Phenomena in the Edge of Alcator C-Mod Plasmas", *Nucl. Fus.* **45**, No. 11 (2005) 1321.

Van Milligen, B.P., Sanchez, R., Carreras, B.A., Lynch, V.E., LaBombard, B., Pedrosa, M.A., Hidalgo, C., Goncalves, B., Balbin, R., and Team, T.W.-A., "Additional evidence for the universality of the probability distribution of turbulent fluctuations and fluxes in the scrape-off layer region of fusion plasmas," *Phys. Plasmas* **12** (2005) 052507.

Wolfe, S. M., Hutchinson, I. H., Granetz, R. S., Rice, J., Hubbard, A., Lynn, A., Phillips, P., Hender, T. C., Howell, D. F., La Haye, R. J. and Scoville, J. T., "Non-axisymmetric field effects on Alcator C-Mod," *Phys. Plasmas* **12** (2005) 056110.

Wright, J.C., Berry, L.A., Bonoli, P.T., Batchelor, D.B., Jaeger, E.F., Carter, M.D., D'Azevedo, E., Phillips, C.K., Okuda, H., Harvey, R.W., Smithe, D.N., Myra, J.R., D'Ippolito, D.A., Brambilla, M., and Dumont, R.J., "Nonthermal particle and full-wave diffraction effects on heating and current drive in the ICRF and LHRF regimes", *Nuclear Fusion* **45** (2005) 1411.

Wukitch, S. J., Lin, Y., Parisot, A., Wright, J. C., Bonoli, et al "Ion cyclotron range of frequency mode conversion physics in Alcator C-Mod: Experimental measurements and modeling," *Phys. Plasmas* **12** (2005) 056104.

Whyte, D. G., Lipschultz, B.L., Stangeby, P.C., Boedo, J. et al, "The Magnitude of Plasma Flux to the Main-wall in the DIII-D Tokamak", *Plasma Phys. & Cont. Fusion* **47** No 10 (2005) 1579-607.

Zhurovich, K., Mossessian, D.A., Hughes, J.W., Hubbard, A.E., Irby, J.H., Marmor, E.S., "Calibration of Thomson scattering systems using electron cyclotron emission cutoff data" *Review of Scientific Instruments* **76** No. 5 (2005) 53506-1-5.

2006

Catto, P.J., Simakov, A.N. "Magnetic topology effects on Alcator C-Mod flows," *Phys. Plasmas* **13** No. 5 (2006) 52507-1-8.

Fredian, T.W., Stillerman, J.A., "Web based electronic logbook and experiment run database viewer for Alcator C-Mod," *Fusion Engineering and Design* **81** No. 15-17, (2006) 1963-7.

Graf, A. (University of California at Davis), Howard, S., Horton, R., Hwang, D., May, M., Beiersdorfer, P., Terry, J., "Visible spectrometer at the Compact Toroid Injection Experiment and the Alcator C-Mod tokamak for Doppler width and shift measurements", *Rev. Sci. Instrum.* **77** No. 10 (2006) 10F125.

Granetz, R., Whyte, D.G., Izzo, V.A., et al., "Gas jet disruption mitigation studies on Alcator C-Mod," *Nucl. Fusion* **46**, No. 12 (2006) 1001-100.

Graves, T., Wukitch S.J., Hutchinson, I.H., "The effect of multipactor discharge on Alcator C-Mod Ion Cyclotron Resonance Frequency (ICRF) heating," *J. Vac. Tech.* **24** No. 3 (2006) 512-16.

Graves, T., LaBombard, B., Wukitch, S.J., Hutchinson, I.H., "The coaxial multipactor experiment (CMX): A facility for investigating multipactor discharges," *Rev. Sci. Instrum.* **77** (2006) 014701.

Grulke, O., Terry, J. L., LaBombard, B., and Zweben, S. J., "Radially propagating fluctuation structures in the scrape-off layer of Alcator C-Mod," *Phys. Plasmas* **13** (2006) 012306.

Hutchinson, I. H., "Collisionless ion drag force on a spherical grain," *Plasma Phys. Controlled Fusion* **48** No. 2, (2006) 185-202.

Hubbard, A.E., Kamiya, K., Oyama, N., Basse, N. et al "Comparisons of small ELM H-Mode regimes on the Alcator C-Mod and JFT-2M tokamaks" *Plasma Phys. Controlled Fusion* **48** No. 5A (2006) A121.

Hughes, J.W., LaBombard, B., Mossessian, D.A., Hubbard A. E., Terry, J., Biewer, T., Alcator C-Mod Team, "Advances in measurement and modeling of the high-confinement-mode pedestal on the Alcator C-Mod tokamak," *Phys. Plasmas* **13** No. 5 (2006) 56103-1-11.

Ince-Cushman, A., Rice, J.E., Lee, S.G., Bitter, M., Reinke, M., Podpaly, Y., "Preliminary results from the soft x-ray crystal spectrometer on Alcator C-Mod," *Rev. Sci. Instrum.* **77** No. 10 (2006) 10F321.

Jaeger, E.F., Berry, L.A., Ahern, S.D., et al "Self-consistent full-wave and Fokker Planck calculations for ion cyclotron heating in non-Maxwellian plasmas," *Phys. Plasmas*, **13** (2006) 056101.

Jaeger, E.F., Harvey, R.W., Berry, L.A., et al., "Global wave solutions with self-consistent velocity distributions in ion cyclotron heated plasmas", *Nucl. Fusion* **46**, S397 (2006).

Lin, L. Edlund, E.M.; Porkolab, M.; Lin, Y.; Wukitch, S.J. "Vertical localization of phase contrast imaging diagnostic in Alcator C-Mod" *Rev. Sci. Instrum.* **77** No. 10 (2006) 10E918.

Lipschultz, B., Lin, Y., Reinke, M.L., Whyte, M.L. Hubbard, A., Hutchinson, I.H. Irby, J., LaBombard, B., Marmor, E.S., Marr, K., Terry, J.L., Wolfe S.M., and the Alcator C-Mod group, "Operation of Alcator C-Mod with high-Z plasma facing components and implications," *Phys. Plasmas* **13** No. 5 (2006) 56117-1-12.

Liptac, J., Parker, R., Tang, V., Peysson, Y., Decker, J., "Hard x-ray diagnostic for lower hybrid experiments on Alcator C-Mod," *Rev. Sci. Instrum.* **77** No. 10 (2006) 103504.

Oyama N., Gohil P., Horton L.D., Hubbard, A.E., Hughes, J.W., Kamada, Y., Kamiya, K., Leonard, A.W., Loarte, A., Maingi, R., Saibene, G., Sartori, R., Stober, J.K., Suttrop, W., Urano, H., West, W.P., and the ITPA Pedestal Topical Group, "Pedestal conditions for small ELM regimes in tokamaks," *Plasma Physics and Controlled Fusion* **48**, No. 5A (2006) A171.

Porkolab, M. et al., "Phase Contrast Imaging of Waves and Instabilities in High Temperature Magnetized Fusion Plasmas," *IEEE Transactions on Plasma Science* **34** No. 2 (2006) 229-34.

Snipes, J.A., Gorelenkov, N.N., Sears, J.A., "A comparison of measured and calculated toroidal Alfvén eigenmode damping rates in Alcator C-Mod," *Nucl. Fusion* **46** No. 12 (2006) 1036-1046.

Stillerman, J.A., Ferrara, M., Fredian, T.W., Wolfe, S.M., "Digital real-time plasma control system for Alcator C-Mod," *Fusion Engineering and Design*, **81**, No. 15-17 (2006) 1905-10.

Tang, V., Liptac, J., Parker, R.R., Bonoli, P.T., Fiore, C.L., Granetz, R.S., Irby, J.H., Lin, Y., Wukitch, S.J., Team, T.A.C.-M., Frenje, J.A., Leiter, R., Mcduffee, S., Petrasso, R.D., "Compact multichannel neutral particle analyzer for measurement of energetic charge-exchanged neutrals in Alcator C-Mod," *Rev. Sci. Instrum.* **77** No. 8 (2006) 83501-1-8.

Zweben, S.J., Maqueda, R.J., Terry, J.L., et al., "Structure and motion of edge turbulence in the national spherical torus experiment and Alcator C-Mod," *Phys. Plasmas*, **13** No. 5 (2006) 56114-118

2007

Basse, N.P., Dominguez, A., Edlund, E.M., Hutchinson, I.H., et al., "Diagnostic Systems on Alcator C-Mod", *Fusion Science and Technology*, **51**, 476 (2007).

Bonoli, P. T., Parker, R., Wukitch, S. J. *et al*, "Wave-particle studies in the ion cyclotron and lower hybrid ranges of frequencies in Alcator C-Mod", *Fusion Science and Technology*, **51** (2007) 401-436.

Bonoli, P. T., Batchelor, D. B., Berry, L. A. *et al*, "Evolution of nonthermal particle distributions in radio frequency heating of fusion plasmas", *Journal of Physics*, **78** (2007) 012006.

Callen, J. D., Anderson, J. K., ..., , Greenwald, M., et al., "Experimental tests of paleoclassical transport" *Nuclear Fusion* **47** (2007) 1449-1457.

Cohen, R.H., LaBombard, B., Ryutov, D.D., Terry, J.L., Umansky, M.V., Xu, X.Q., and Zweben, S., "Theory and fluid simulations of boundary-plasma fluctuations," *Nuclear Fusion* **47** (2007) 612.

Doyle, E. J., Houlberg, W. A., Snipes, J. A., et al., "Chapter 2: Plasma confinement and transport", *Nuclear Fusion*, **47**, (2007) S18.

Granetz, R. S., Hollmann, E. M., Whyte, et al., "Gas jet disruption mitigation studies on Alcator C-Mod and DIII-D." *Nuclear Fusion*, **47**, (2007) 1086-91.

Greenwald M, Angioni C, Hughes JW, Terry, J. , Weisen, H., "Density profile peaking in low collisionality H-modes: comparison of Alcator C-Mod data to ASDEX Upgrade/JET scalings," *Nuclear Fusion*, **47** (9): L26-L29, 2007.

Greenwald, M., Basse, N.; Bonoli, P. et al., "Confinement and transport research in Alcator C-Mod", *Fusion Science and Technology* **51** No 3 (2007) 266-87.

Guzdar, P.N.; Kleva, R.G.; Kaw, P.K.; Singh, R.; Labombard, B.; Greenwald, M., "Large transport-induced operation limits of tokamak plasmas", *Physics of Plasmas* **14**, No 2 (2007) 020701.

Hender, T. C., Wesley, J. C., Bialek, J., ..., Granetz, R. S., ..., & Mhd, D. M. C. T. G. "Chapter 3: MHD stability, operational limits and disruptions." *Nuclear Fusion*, **47** (2007) 128-202.

Hubbard, A.E, Hughes, J.W., Bespamyatnov, I.O., ..., and the Alcator C-Mod Group, "H-mode pedestal and threshold studies over an expanded operating space on Alcator C-Mod", *J. Physics of Plasmas*, **14** (5) (2007) 056109.

Hughes, J.W., LaBombard, B., Terry, J., Hubbard, A. and Lipschultz, B., "Edge profile stiffness and insensitivity of the density pedestal to neutral fuelling in Alcator C-Mod edge transport barriers", *Nuclear Fusion*, **47**, No. 8 (2007) 1057-1063.

Hughes, J.W., LaBombard, B., Terry, J., et al., , "H-Mode pedestal and L-H transition studies on Alcator C-Mod," *Fusion Science and Technology*, **51** (2007) 317.

Humphreys, D. A., Ferron, J. R., Bakhtiari, M., ..., Whyte, D. G., "Development of ITER-relevant plasma control solutions at DIII-D." *Nuclear Fusion*, **47**, (2007) 943-51.

Hutchinson, I.H., Patacchini, L., "Computation of the effect of neutral collisions on ion current to a floating sphere in a stationary plasma" *Phys. Plasmas*, **14** (2007) 013505.

Hutchinson, I.H., "Comment on Ion collection by a sphere in a flowing collisional plasma" *Phys. Plasmas* **14** (2007) 074701.

Irby, J., Gwinn, D., Beck, W., LaBombard, B., Granetz, R., and Vieira, R., "Alcator C-Mod design, engineering, and disruption research," *Fusion Science and Technology*, **51** (2007) 460.

LaBombard, B. and Lyons, L., "Mirror Langmuir probe: A technique for real-time measurement of magnetized plasma conditions using a single Langmuir electrode," *Review of Scientific Instrument*, **78** (2007) 073501.

LaBombard, B., Smick, N., Greenwald, M., Hughes, J.W., Lipschultz, B., Marr, K., and Terry, J.L., "The operational phase-space of the edge plasma and its sensitivity to magnetic topology in Alcator C-Mod," *J. of Nucl. Mat.*, **363-365** (2007) 517.

Lin, Y, Irby, J, Lipschultz, B, et al., "Hydrogen control in Alcator C-Mod walls and plasmas," *J. Nucl. Mat.*, **363** (2007) 920-924.

Lipschultz, B., LaBombard, B., Terry, J., Boswell, C., Hutchinson, I.H., "Divertor Physics Research on Alcator C-Mod", *Fusion Science and Technology*, **51** (2007) 369.

Lipschultz, B, Lin, Y., Marmor, E.S., Whyte, D.G., Wukitch, S., Hutchinson, I.H., Irby, J., LaBombard, B., Reinke, M.L., Terry, J.L., Wright, G., "Influence of boronization on operation with high-Z plasma facing components in Alcator C-Mod", *J. Nucl. Mat.*, **51**, 363 (2007) 1110-1118.

Lipschultz, B., LaBombard, B., Lisgo, S., Terry, J.L., "Neutrals studies on Alcator C-Mod", *Fusion Science & Tech.* **51** (2007) 390.

Leonard, A.W., Boedo, J.A., Groth, M., Lipschultz, B., et al., "Particle flux and radial profiles in the SOL of DIII-D during ELMing H-modes", *J. Nucl. Mat.*, **363-365** (2007) 1066-1070.

Lipschultz, B., Bonnin, X., Counsell, G., et al., "Plasma-surface interaction, scrape-off layer and divertor physics: Implications for ITER," *Nuclear Fusion* **47** (2007) 1189-1205.

Lister, J. B., Farthing, J. W., Greenwald, M., Yonekawa, I., "The ITER CODAC conceptual design", *Fusion Engineering And Design* **82** (5-14) (2007) 1167-1173.

Loarte, A., Saibene, G., Sartori, ..., Whyte, D., et al., "Transient heat loads in current fusion experiments, extrapolation to ITER and consequences for its operation." *Physica Scripta*, (2007).

Loarte, A., Lipschultz, B., Kukushkin, et al., "Chapter 4: Power and particle control," *Nuclear Fusion* **47** (2007) 203-63.

Marmor, E.S., and the Alcator C-Mod Group, "The Alcator C-Mod Program," *Fusion Science and Technology* **51**, (2007) 261.

McDonald, D.C., Cordey, J.G., Thomsen, K., ..., Snipes, J.A., Greenwald, M., et al., "Recent progress on the development and analysis of the ITPA global H-mode confinement database," *Nuclear Fusion* **47** No. 3, (2007) 147-174.

Parisot, A., Wukitch, S. J., Bonoli, P. *et al*, "Sawtooth period changes with mode conversion current drive on Alcator C-Mod", *Plasma Physics and Controlled Fusion*, **49** (2007) 219-235.

Patacchini, L., Hutchinson, I.H., "Ion-collecting sphere in a stationary, weakly magnetized plasma with finite shielding length," *Plasma Phys. Control. Fusion*, **49** (2007) 1719-1733.

Patacchini, L., Hutchinson, I.H., "Angular distribution of current to a sphere in a flowing, weakly magnetized plasma with negligible Debye length", *Plasma Phys. Control. Fusion* **49** (2007) 1208.

Patacchini, L., Hutchinson, I.H., "Electron collection by a negatively charged sphere in a collisionless magnetoplasma" *Phys. Plasmas* **14** (2007) 062111.

Pigarov, A.Y., Krasheninnikov, S.I., LaBombard, B., and Rognlien, T.D., "Simulation of large parallel plasma flows in the tokamak SOL driven by cross-field transport asymmetries," *J. of Nucl. Mat.*, **363-365** (2007) 643.

Rice, J.E., Ince-Cushman, A., deGrassie, J.S., et al., "Inter-Machine Comparison of Intrinsic Toroidal Rotation," *Nucl. Fusion*, **47** (2007) 1618.

Rice, J.E.; Marmor, E.S., Bonoli, P.T., Granetz, R.S., et al., "Spontaneous toroidal rotation in Alcator C-Mod plasmas with no momentum input," *Fusion Science and Technology*, **51** (2007) 288-302.

Rice, J.E., Terry, J.L., Marmor, E.S., Granetz, R.S., Greenwald, M.J., Hubbard, A.E., Irby, J.H., Wolfe, S.M., Sunn Pedersen, "Impurity transport in Alcator C-Mod plasmas," *Fusion Science and Technology*, **51** (2007) 357-68.

Scott, S., Bader, A., Bakhtiari, M., Basse, et al., "Overview of the Alcator C-MOD research programme," *Nuclear Fusion* **47** (2007) 598-607.

Snipes, J. A., Basse, N., Bonoli, P., Boswell, C., Edlund, E., "Energetic Particle Physics Studies on Alcator C-Mod," *Fusion Science and Technology* **51** No. 3, (2007) 437.

Tang, V., Parker, R. R., Bonoli, P.T., et.al., "Experimental and Numerical Characterization of Ion Cyclotron Heated Protons in the Alcator C-Mod Tokamak," *Plasma Phys. and Control. Fusion* **49** (2007) 873-904.

Terry, J.L., Cziegler, I., Hubbard, A.E., Snipes, J.A., Hughes, J.W., Greenwald, M.J., LaBombard, B., Lin, Y., Phillips, P., and Wukitch, S., "The dynamics and structure of edge-localized-modes in Alcator C-Mod," *J. of Nucl. Mat.*, **363-365** (2007) 994.

Terry, J.L., LaBombard, B., Lipschultz, B., Greenwald, M.J., Rice, J.E., and Zweben, S.J., "The scrape-off layer in Alcator C-Mod: transport, turbulence, and flows," *Fusion Science and Technology*, **51** (2007) 342.

Whyte, D. G., Granetz, R., Bakhtiari, M., Izzo, V., Jernigan, T., Terry, J., Reinke, M. & Lipschultz, B. "Disruption mitigation on Alcator C-Mod using high-pressure gas injection: Experiments and modeling toward ITER," *Journal of Nuclear Materials*, **363-365** (2007) 1160-7.

Wright, G. M., Whyte, D. G., Lipschultz, B., Doerner, R. P. & Kulpin, J. G. "Dynamics of hydrogenic retention in molybdenum: First results from DIONISOS," *Journal of Nuclear Materials*, **363-365**, (2007) 977-83.

Wukitch, S.J., Lipschultz, B., Marmar, E., Lin, Y., Parisot, A., Reinke, M., Rice, J., Terry, J., and the C-Mod Team, "RF Plasma Edge Interactions and their Impact on ICRF Antenna Performance in Alcator C-Mod," *J. Nucl. Mat.*, **363**, 491-497 (2007).

Zhurovich, K., Fiore, C. L., Ernst, D. R., Bonoli, P. T. *et al*, "Microturbulent drift mode suppression as a trigger mechanism for internal transport barriers on Alcator C-Mod," *Nuclear Fusion* **47** (2007) 1220-1231.

Zweben, S.J., Boedo, J.A., Grulke, O., Hidalgo, C., LaBombard, B., Maqueda, R.J., Scarin, P., and Terry, J.L., "Edge turbulence measurements in toroidal fusion devices," *Plasma Physics and Controlled Fusion*, **49** (2007) 1.

Papers Submitted for Publication:

Fasoli, A., Testa, D., Klein, A., Snipes, J. A., Sears, J., Gryaznevich, M., Martin, R., Pinches, S. D., "Active excitation and damping rate measurement of intermediate-n Toroidal Alfvén Eigenmodes in JET, C-Mod, and MAST plasmas", submitted to *Nuclear Fusion*.

Klein, A., Carfantan, H., Testa, D., Fasoli, A., Snipes, J., "A New Method for the Analysis of Magnetic Fluctuations in Unevenly-spaced Mirnov Coils", submitted to *Nuclear Fusion*.

Snipes, J. A., Parker, R. R., Schmidt, A., Wallace, G., and Phillips, P. E., "Fast Electron Driven Modes in the Current Rise in Alcator C-Mod", submitted to *Physical Review Letters*.

T. Fredian, J. Stillerman and G. Manduchi, "MDSplus extensions for long pulse experiments", *Fusion Engineering and Design* *In Press*, Corrected Proof, , Available online 24 October 2007.

J. Stillerman, D. Baron, T. Fredian, M. Greenwald and H. Schulzrinne, "Communications fabric for scientific collaboration", *Fusion Engineering and Design* In Press, Corrected Proof, , Available online 1 November 2007.

Lin, Y. Stillerman, J., Binus, A. et al. "Digital real-time control for an ICRF fast ferrite tuning system on Alcator C-Mod", accepted for publication in *Fusion Engineering and Desig.*

Terry, P.W., Greenwald, M., Leboeuf, J.N., McKee, G.R., Mikkelsen, D.R., Nevins, W.M., Newman, D.E. and Stotler, D.P., "Validation in Fusion Research: Towards Guidelines and Best Practices", accepted for publication in *Phys. Plasmas* 2008.

MIT Plasma Fusion Center Research Reports (including theses)

2003

Boswell, C.J., "Visible Imaging Spectroscopy on the Alcator C-Mod Tokamak," PSFC/RR-03-1, March 2003.

Feng, J., "Probabilistic Analysis of Fatigue Life for ITER CS Conduit," PSFC/RR-03-7, October 2003.

Gangadhara, S., "Physics and Application of Impurity Plume Dispersal as an Edge Plasma Flow Diagnostic on the Alcator C-Mod Tokamak," PSFC/RR-03-2, March 2003.

LaBombard, B., Boswell, C., "In-Situ Gas Conductance and Flow Measurements Through Alcator C-Mod Divertor Structures With and Without Plasma Present, PSFC/RR-03-6, Jan. 2003.

LaBombard, B., Lipschultz, B., "Cross-Field Particle Transport in the Edge Plasma of Tokamak Experiments and Implications for ITER Operation," PSFC/RR-03-8, Jan. 2003.

Lee, W.D., "Experimental Investigation of Toroidal Rotation Profiles in the Alcator C-Mod Tokamak, PSFC/RR-03-3, June 2003.

Schmittdiel, D., "Investigation of Alfvén Eigenmodes in Alcator C-Mod using Active MHD Spectroscopy," PSFC/RR-03-5, June 2003.

2004

Chung, T., "Study of Recycling Impurity Retention in Alcator C-Mod, PSFC/RR-04-1, September 2004.

Parisot, A., "Design of an ICRF Fast Matching System on Alcator C-Mod," PSFC/RR-04-2, September 2004.

2005

Decker, J., Peysson, Y., "DKE: a fast numerical solver for the 3-D relativistic bounce-averaged electron Drift Kinetic Equation," PSFC/RR-05-3, October 2005.

Hughes, J.W., "Edge Transport Barrier Studies on the Alcator C-Mod Tokamak," PSFC/RR-05-6, October 2005.

Lin, Y., Bonoli, P., Fiore, C., et al., "Alcator C-Mod FY2005 Level-1 OFES Science Target Completion Report: Measure Plasma Behavior with All-Metal Walls and Input Power Greater than 3.5 MW, PSFC/RR-05-11, October 2003.

Yuh, H., "The Motional Stark Effect Diagnostic on Alcator C-Mod," PSFC/RR-05-5, October 2005.

2006

Graves, T.P., "Experimental Investigation of Electron Multipactor Discharges at Very High Frequencies," PSFC/RR-06-6, May 2006.

Greenwald, M., Schissel, D.P., Alba, G., Stillerman, J., "Recommendations for Remote Conferencing for the ITER Project," PSFC/RR-06-2, January 2006.

Tang, V., "Experimental and Numerical Characterization of Ion-Cyclotron Heated Protons on the Alcator C-Mod Tokamak," PSFC/RR-06-8, March 2007.

2007

Lyons, L.A., "Construction and Operation of a Mirror Langmuir Probe Diagnostic for Alcator C-Mod Tokamak," PSFC/RR-07-8, November 2007.

Parisot, A., "Mode Conversion Current Drive Experiments on Alcator C-Mod," PSFC/RR-07-3, July 2007.

Patacchini, L., "Collisionless Ion Collection by a Sphere in a Weakly Magnetized Plasma," PSFC/RR-07-5, July 2007.

Zhurovich, K., "Investigation of Triggering Mechanism of Internal Transport Barriers on the Alcator C-Mod Tokamak Using Thomson Scattering Diagnostic," PSFC/RR-07-9, November 2007.

Invited Papers

2003

Ernst, D., "Role of Trapped Electron Mode Turbulence in Internal Transport Barrier Control in Alcator C-Mod," presented at 45th APS DPP, Albuquerque, NM, Nov. 2003.

Fiore, C., "Control of Internal Transport Barriers on Alcator C-Mod," presented at 45th APS DPP, Albuquerque, NM, Nov. 2003.

Lin, Y., "Investigation of ICRF Mode Conversion at the Ion-ion Hybrid Layer in Alcator C-Mod," presented at 45th APS DPP, Albuquerque, NM, Nov. 2003.

Rice, J., "Toroidal Rotation and Anomalous Momentum Transport in Alcator C-Mod Plasmas with No Momentum Input," presented at 45th APS DPP, Albuquerque, NM, Nov. 2003.

Wright, J., "Full Wave Simulations of Fast Wave Mode Conversion and Lower Hybrid Wave Propagation," presented at 45th APS DPP, Albuquerque, NM, Nov. 2003.

2004

Bonoli, P., "Full-wave Electromagnetic Field Simulations in the Lower Hybrid Range of Frequencies," presented at APS DPP, Savannah, GA, Nov. 2004.

Fiore, C., "Internal Transport Barrier Production and Control in Alcator C-Mod," presented at the 31st European Physical Society Conf. on Plasma Physics, Portugal, June 2004.

Fiore, C., "Internal Transport Barrier Production and Control in Alcator C-Mod," presented at the 31st European Physical Society Conf. on Plasma Physics, Portugal, June 2004.

Grulke, O., "Dynamics of spatiotemporal fluctuation structures in the scrape-off layer of the Alcator C-Mod and NSTX," presented at APS DPP, Savannah, GA, Nov. 2004.

LaBombard, B., "Transport-driven scrape-off layer flows and the x-point dependence of the L-H power threshold in Alcator C-Mod," presented at APS DPP, Savannah, GA, Nov. 2004.

Snipes, J., "Active and Fast Particle Driven Alfvén Eigenmodes in Alcator C-Mod," presented at APS DPP, Savannah, GA, Nov. 2004.

Wolfe, S., "Non-axisymmetric field effects on Alcator C-Mod," presented at APS DPP, Savannah, GA, Nov. 2004.

Wukitch, S., "ICRF Mode Conversion Physics in Alcator C-Mod: Measurements and Model Validation," presented at APS DPP, Savannah, GA, Nov. 2004.

2005

Granetz, R., "Gas Jet Disruption Mitigation Studies on Alcator C-Mod," presented at APS DPP, Denver, CO, October 2005.

Hughes, J., "Advances in Measurement and Modeling of the H-mode Pedestal on the Alcator C-Mod Tokamak," presented at APS DPP, Denver, CO, October 2005.

Jaeger, E.F., Berry, L.A., Harvey, R.W., ... Bonoli, P.T., et al, "Self-consistent Full Wave/Fokker Planck Calculations for Ion Cyclotron Heating in non-Maxwellian plasmas," presented at the 16th Topical Conference on Radio Frequency Power in Plasmas and US-Japan RF Physics Workshop: Physics Produced by Large and Steady State RF Power, April 2005.

LaBombard, B., "Transport-driven Scrape-off Layer Flows, the Role of the X-point and Connections to the L-H Power Threshold in Alcator C-Mod," presented at the 32nd European Physical Society Conference on Plasma Physics, Tarragona, Spain, June 2005.

Lipschultz, B., "Operation of Alcator C-Mod with High-Z Plasma Facing Components and Implications," presented at APS DPP, Denver, CO, October 2005.

Sweben, S., "Structure and Motion of Edge Turbulence in NSTX and Alcator C-Mod," presented at APS DPP, Denver, CO, October 2005.

Wright, J.C., Bonoli, P.T., Brambilla, M., et al., "Full-wave Electromagnetic Field Simulations of Lower Hybrid Waves in Tokamaks," presented at the 16th Topical Conference on Radio Frequency Power in Plasmas and US-Japan RF Physics Workshop: Physics Produced by Large and Steady State RF Power, April 2005.

2006

Greenwald, M., "Falling Between the Cracks: Coupling Between Transport in the SOL, Edge and Core," presented at the Transport Task Force Meeting, Myrtle Beach, SC, April 2006.

Hubbard, A., "H-mode Pedestal Threshold Studies Over an Expanded Operating Space on Alcator C-Mod," presented at APS DPP, Philadelphia, PA, Nov. 2006

LaBombard, B., "The Operational Phase Space of the Edge Plasma and its Sensitivity to Magnetic Topology in Alcator C-Mod," presented at the International Conference on Plasma Surface Interactions, Hefei, China, May 2006.

Lipschultz, B., "Operation of Alcator C-Mod with High-Z Plasma Facing Components and Implications," presented at the International Conference on Plasma Surface Interactions, Hefei, China, May 2006.

Marmor, E.S., "Alcator C-Mod: Research Highlights and Plans," Fusion Power Associates Annual Meeting, Sept. 2006

Parker, R., "Lower Hybrid Current Drive Experiments in Alcator C-Mod," presented at APS DPP, Philadelphia, 2006.

Terry, J., "Investigation of Edge Localized Modes on Alcator C-Mod," presented at APS DPP, Philadelphia, 2006

Terry, J., "Investigation of ELMs on Alcator C-Mod," presented at the International Conference on Plasma Surface Interactions, Hefei, China, May 2006.

Whyte, D., "Disruption Mitigation on Alcator C-Mod Using High-Pressure Gas Injection: Experiments and Modeling Toward ITER," presented at the International Conference on Plasma Surface Interactions, Hefei, China, May 2006.

Whyte, D., "Gas Jet Disruption Mitigation Studies," presented at the 33rd European Physical Society Conference on Plasma Physics, Rome, Italy, June 2006.

Wukitch, S.J., "RF Plasma Edge Interactions and their Impact on ICRF Antenna Performance in Alcator C-Mod," presented at the International Conference on Plasma Surface Interactions, Hefei, China, May 2006.

2007

Bonoli, P.T., Batchelor, D.B., Berry, L.A., Choi, M., D'Ippolito, D.A., Harvey, R.W., Jaeger, E.F., Myra, J.R., Phillips, C.K., Smithe, D.N., Valeo, E., Wright, J.C., Brambilla, M., Bilato, R., Lancellotti, V., Maggiora, R., "Physics Research in the SciDac Center for Wave-Plasma Interactions," presented at the 17th Topical Conf. on Radio Frequency Power in Plasmas, Clearwater, FL, May 2007.

Bonoli, P., "Lower Hybrid Current Drive Experiments on Alcator C-Mod: Comparison Between Theory and Simulation," presented at APS DPP, Orlando, FL, November 2007.

Granetz, R.S., Irby, J., LaBombard, et al., "Alcator C-Mod Status, Recent Accomplishments and Future Plans," presented at the 22nd IEEE/NPSS Symposium on Fusion Energy, Albuquerque, NM, 2007.

Hubbard, A.E., Hughes, J.W., Greenwald, M., LaBombard, B., Lin, Y., Terry, J.L. and Wukitch, S., "H-mode experiments at reduced collisionality on Alcator C-Mod", Presented at the 34th European Physical Society Conf. on Plasma Physics, Warsaw, Poland, July 2007.

Izzo, V., "MHD Simulations of Disruption Mitigation on Alcator C-Mod and DIII-D," presented at APS DPP, Orlando, FL, November 2007.

LaBombard, B., "Critical Gradients and Plasma Flows in the Edge Plasma of Alcator C-Mod," presented at APS DPP, Orlando, FL, November 2007.

Lin, Y., "Ion Cyclotron Range of Frequencies Heating and Current Drive in Tokamaks", Plasma Physics Winter School, ASIPP, Hefei, China, Jan. 11, 2008

Wukitch, S., "ICRF Performance with Metallic Plasma Facing Components: Revenge of the Sheath," presented at APS DPP, Orlando, FL, November 2007.

Porkolab, M., " RF Heating and Current Drive in Magnetically Confined Plasma: A Historical Perspective," presented at the 17th Topical Conf. on Radio Frequency Power in Plasmas, Clearwater, FL, May 2007.

Porkolab, M. "Recent Progress in Fusion Research", Hungarian Nuclear Society Annual Meeting, Budapest, Hungary, November, 2007.

Wukitch, S., Lin, Y., Lipschultz, B., Parisot, A., Reinke, M., Bonoli, P.T., Porkolab, M., Hutchinson, I.H., Marmor, E.S. and the Alcator C-Mod team, "ICRF Performance with Metallic Plasma Facing Components in Alcator C-Mod," presented at the 17th Topical Conf. on Radio Frequency Power in Plasmas, Clearwater, FL, May 2007.

Wukitch, S., "ICRF Performance with Metallic Plasma Facing Components: Revenge of the Sheath," presented at APS DPP, Orlando, FL, November 2007.

Yijun, L. “Ion Cyclotron Range of Frequencies Heating and Current Drive in Tokamaks”, Plasma Physics Winter School, ASIPP, Hefei, China, January, 2008

14 Management Capability

14.1 Overall and Project Management Capability

The Plasma Science and Fusion Center (PSFC) is MIT's largest on-campus research facility. Within PSFC, the Alcator Tokamak Program is the largest Division of the Center. Looking ahead to the next contracting period, PSFC's Director, Professor Miklos Porkolab, will continue to provide the clear direction to the PSFC. Dr. Earl Marmor, Head of the Alcator Program at PSFC, will continue to provide strong leadership and fiscal oversight to the day-to-day operations of the Alcator Program. Mr. Thomas Hrycaj, PSFC Administrative Officer, and his staff of capable accountants, will ensure dependable administrative support for the Program.

14.1.1 Massachusetts Institute of Technology (MIT)

Since MIT first opened its doors in 1865, education and related research has been its central purpose. The management of MIT's research activities, which are financed through contracts with government and industry, is supported by the Office of Sponsored Programs and carried out within MIT's academic departments as well as within many interdepartmental centers and laboratories.

The Office of the Executive Vice President and Treasurer is responsible for financial and business policies and procedures for sponsored research, including those designed to meet the requirements of grants and contracts. The Accounting Office reporting to the Vice President for Finance directs the accounting for all sponsored research projects.

The Vice President for Research and Associate Provost is the contracting officer of the Institute and is directly responsible for the negotiation and interpretation of sponsored research contracts and grants, and for negotiating the reimbursement of indirect costs and employee benefits.

The Office of Sponsored Programs (OSP) at MIT has the immediate responsibility for the business administration aspects of research projects sponsored by the government and is directly responsible for the negotiation and interpretation of terms governing sponsored research contracts and grants. OSP provides summarized terms and conditions of new and renewed research contracts to the Plasma Science and Fusion Center (PSFC) Principal Investigators and key Office of Resource Management personnel.

Other chief management systems MIT provides to its research community include the Controllers Accounting Office; Audit Division; Property Office; Travel Office; Payroll Office; Procurement Department and Accounts Payable.

14.1.2 The Plasma Science and Fusion Center

The Plasma Science and Fusion Center coordinates the fusion energy research activities located at MIT in order to provide the strong intellectual and administrative leadership required throughout these research programs. One of the Center's (and MIT's) greatest strengths is the ability to provide a forum for blending excellent research programs within

a university environment. This is important in order to train students and researchers in areas necessary for successful research on the path to the development of fusion energy.

The MIT Plasma Science and Fusion Center plays a very active and important role in both national and international fusion research efforts. It is recognized as one of the leading university laboratories in the physics and engineering aspects of magnetic confinement fusion. The PSFC's Alcator C-Mod experiment is one of three major national magnetic confinement experiments in the U.S. The administrative, technical and research staff of the PSFC work together to coordinate the communication and research efforts required to maintain this status. Currently, the funding level of the PSFC research programs is approximately \$32 Million. There are approximately 249 personnel associated with PSFC research activities. These include: 21 faculty and senior academic staff; 56 graduate students and 6 undergraduate students; 76 research scientists, engineers and post doctoral associates; 36 visiting scientists and engineers; 31 technical support staff; and 23 administrative and support staff.

Until 1977, fusion research at MIT took place under the auspices of many and various separate departments and laboratories, with most of its funding from the Department of Energy (DOE). DOE recommended that MIT pull together all of the fusion related research and organize it under one Center. The PSFC continues to work very closely with faculty, staff and graduate students from our 'affiliated departments and laboratories':

- Aeronautics & Astronautics Department.
- Chemical Engineering Department.
- Electrical Engineering & Computer Science Department.
- Mechanical Engineering Department
- Materials Science & Engineering Department.
- Nuclear Science and Engineering Department.
- Physics Department.

The PSFC is organized in the following manner:

The Director of the Center, Miklos Porkolab, oversees all PSFC research activities and provides the administrative interface between the PSFC and the Department of Energy, the MIT administration, and the national and international laboratories' administrations.

The PSFC is organized into five technical research divisions. The Alcator Division is one of these five and its relationship to the other four is shown in Fig. 14.1.

The Office of Resource Management, headed by Thomas Hrycaj, coordinates all administrative requirements for the PSFC, both within MIT and with outside agencies and laboratories. The research groups work through this office for the standardization and follow-through on their administrative requirements. The Fiscal Office (Katherine Ware, Senior Fiscal Officer), Headquarters Financial Administration (Marcia Tench-Mora, Financial Administrator), Personnel (Leslie West, Personnel Administrator) and the Library (Jason Thomas, Librarian), are all part of Headquarters. Additional elements of PSFC's operations include the Safety Office (Dr. Catherine Fiore), the Facilities Manager is Mr. Matt Fulton, and the head of the Computational Department is Dr. Martin Greenwald.

PSFC ORGANIZATION CHART

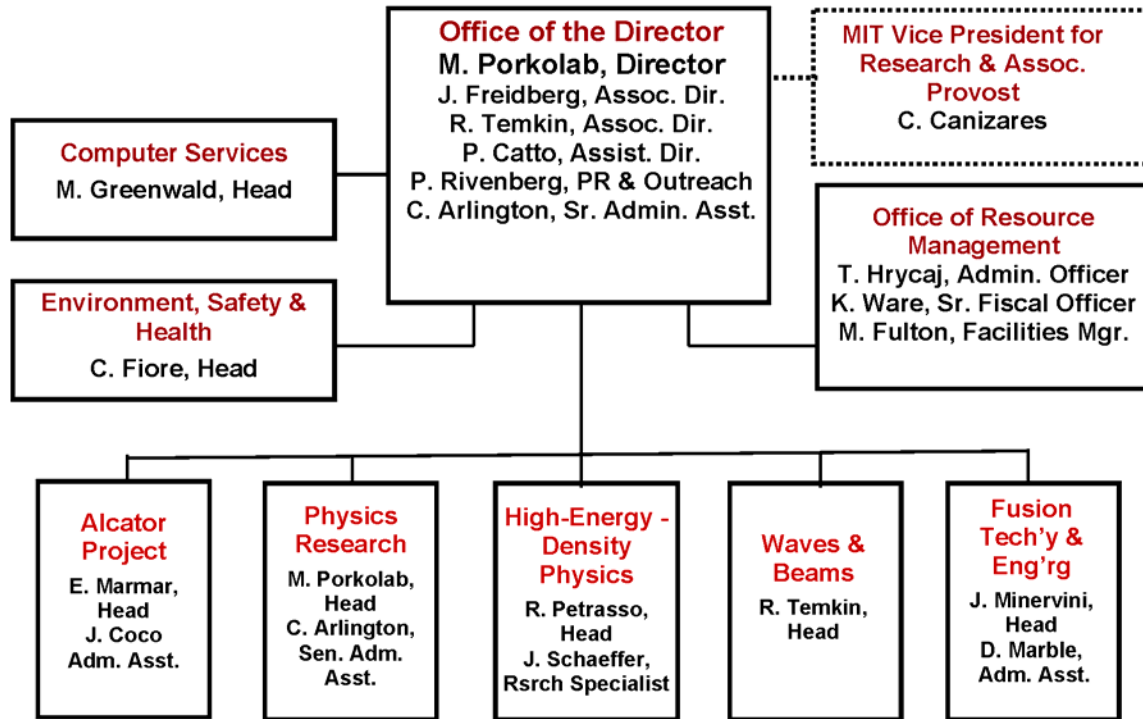


Figure 14.1: Plasma Science and Fusion Center Organization Chart

The PSFC Steering Committee, made up of the senior faculty and senior research scientists, assists the Director in establishing priorities and coordinating research activities throughout the PSFC. The PSFC Advisory Committee, made up of the heads of the affiliated MIT departments and laboratories, and the Vice President for research, assists the Director in coordinating PSFC research programs with other research activities going on at MIT and in determining promotions to senior positions within MIT. Finally, an external Visiting Committee is called in periodically to advise the Director on matters of importance as they emerge and warrant outside advice.

14.1.3 The Alcator Experimental Program

Under the leadership of Dr. Earl Marmar, the Alcator C-Mod program is focused on six basic areas of research: Core Transport, coordinated by Martin Greenwald; Ion Cyclotron RF Heating and Control, coordinated by Steve Wukitch; Lower Hybrid RF Current Drive, coordinated by Ron Parker; H-mode Pedestal Physics, coordinated by Jerry Hughes; Divertor and Plasma Boundary Physics, coordinated by Bruce Lipschultz; and Macro-stability, coordinated by Bob Granetz. These research areas support two integrated thrusts: the Advanced Scenarios thrust, coordinated by Amanda Hubbard; and the H-mode Scenarios/ITER Baseline thrust, coordinated by Steve Wolfe. On the facility side, Jim Irby heads the Operations Group.

14.1.4 Program Planning and Team Communication

Proposals for high priority research on Alcator C-Mod always outstrip the availability of run time. Program planning is organized through several specific mechanisms described here. Since C-Mod is operated as a National Facility, these planning processes are specifically designed to give contributors from all participating organizations a stake in the program.

The Project holds an annual meeting with its Program Advisory Committee (PAC), consisting of national and international experts. The PAC's purpose is to advise the Project Head and PSFC Director on technical and management aspects of the program and to ensure good integration with the rest of the US and world fusion programs. The PAC reports by letter to the Project Head and PSFC Director. The advisory committee meeting serves as a sounding board for project priorities and research strategy, and normally precedes the annual OFES budget planning meeting.

Periodically MIT hosts an Alcator Ideas Forum. This is typically held about once a year, prior to the detailed planning of the run campaign. Its objective is to encourage and draw out research ideas from across the fusion community that offer opportunities for C-Mod experiments. Far more ideas than can be accommodated with available run time are always forthcoming. All team members, including MIT staff, as well as students and collaborators, are able to put forth ideas and have them recognized, honed, and adjusted to the realities of the facility's practical constraints. The Ideas Forum is also a venue where team members, including collaborators, hear more about the strategic directions of C-Mod's plan. That helps them to understand better the project priorities, and plan their own contributions accordingly. The strategic directions are generally set forth by the Project leaders in consultation with the Experimental Program Committee, DOE leadership, and the Program Advisory Committee.

If an idea for an experiment or series of experiments is considered to warrant high enough priority, then its sponsors are encouraged to submit a detailed mini-proposal. These follow a standard format, and as far as possible specify the detailed shot sequence for the operational days being requested. The mini-proposals are written to make clear the motivation and background of the proposal, and the probable outcomes, but are only a few pages long. These proposals are published on the World Wide Web (linked from <http://www.psf.mit.edu/research/alcator/facility>). New mini-proposals are generated continually throughout each experimental campaign as opportunities are identified. The general principle is that all tokamak run time is covered by reviewed and approved mini-proposals, to help ensure the most efficient and productive use of that precious resource.

The C-Mod Experimental Program Committee consists of the leaders of key topical sections of the Project staff, and representatives of the major collaborators. Its primary purpose is to review and approve mini-proposals. The EPC also gives guidance concerning prioritization and scheduling. A member of the EPC is assigned the responsibility for establishing and publishing the week-to-week run schedule.

Weekly science meetings are held which are open to all staff, students, collaborators, OFES and other interested parties. In view of the needs of remote collaborators, these

meetings are netcast using audio/video links and web based graphical displays. Presentations are made by remote participants as well as by local attenders.

Communication among all C-Mod users is facilitated through e-mail and online bulletin boards. The `cmod_all@psfc.mit.edu` mail reflector currently (March, 2008) has 237 subscribers from all over the world.

The MDSplus data system makes it possible for anyone with authorization, anywhere in the world, to access, analyze, and display Alcator C-Mod scientific data. Authorization is provided to collaborators who sign a collaboration agreement designed to ensure that publications based on Alcator data are vetted by a leader in the C-Mod team for accuracy, consistency, and appropriate authorship. This process helps to promote exchange of information and ideas across the entire team. Many unpublished documents, including proposals, presentations to Advisory committees, and reviews are made available on the web at www.psf.mit.edu/research/alcator/program and at www.psf.mit.edu/research/alcator/pubs.

14.2 Cost Management Techniques

In research, the sponsor and MIT have a joint and continuing obligation to provide not only the contractual and administrative environment but also the financial basis for a sound program of investigation. In general, MIT's resources are such that it cannot provide this environment except on a full cost-reimbursement basis, including direct and indirect costs.

In sponsoring research at colleges and universities, the Federal Government and other sponsors reimburse the direct costs charged to specific projects as well as the indirect costs which support research projects generally, such as those incurred in personnel administration, accounting, physical plant operations and maintenance, the libraries, etc.

Since most indirect cost categories consist of "shared" costs which jointly support both instructional and sponsored research activities, they must be allocated on an equitable basis to instructional programs on the one hand and to sponsored research projects on the other.

The allocation process is governed by OMB Circular A-21, the Federal "Cost Principles Applicable to Educational Institutions," and is implemented at MIT using procedures negotiated with the Institute's cognizant Federal agencies, the Office of Naval Research (ONR), and the Defense Contract Audit Agency (DCAA). The negotiation effective July 1, 1994 removed allocation costs from allowable indirect costs. At present, therefore, the PSFC allocated costs are not charged indirect costs. The negotiation of allowable indirect costs, the direct cost base, and the applicable indirect cost rate is the direct responsibility of the Vice President for Research and Associate Provost.

The PSFC's method of cost management has a history of detailed control which ensures the highest level of responsibility and integrity in managing the way its sponsored research funds are spent.

Once a contract or grant has been approved, and OSP has assigned an account number, the supervisor receives a form requesting signatures of personnel who will be authorized

to incur charges against the account. Within the Alcator C-Mod program, all purchase requisitions must be approved by the appropriate group leader, and in some cases by the program head before being forwarded to the PSFC Fiscal Office for final approval. The Fiscal Office reviews each requisition for the necessary Alcator approvals and accounting numbers as well as any necessary backup documentation such as quotations and letters of justification. The Fiscal Office also screens for contract appropriateness as per the OMB A-21 Circular and for budget compliance. Once satisfied that all criteria have been met, the Fiscal Office approves the expenditure and forwards it on to the appropriate MIT department (i.e., Procurement, Travel, etc.). MIT's Accounts Payable Office, Travel Department, Payroll Office, and Procurement Department will not process a cost against an account unless it carries an authorized signature.

The PSFC Fiscal Office monitors all costs incurred by the various contracts. While it employs four staff account monitors, one is dedicated solely to the management of the Alcator accounts. In addition to this individual, the Fiscal Office offers the Alcator Group many varied accounting management services including the reconciliation of all account statements on a monthly basis, the maintenance of commitment logs, the processing of invoices for payment, the recording and reporting of all capital equipment procurements, the generating of monthly financial status reports and proposal budget preparation.

14.3 Management Experience and Past Performance

Since the Plasma Science and Fusion Center's inception in 1977, research groups have produced significant results on several fronts : (a) major confinement results on the Alcator C and C-Mod tokamaks, including pioneering investigations of the stability, heating and confinement properties of plasmas at high densities, temperatures and magnetic fields; (b) the basic physics of high temperature plasmas (plasma theory, RF heating, free electron lasers, development of advanced diagnostics, and experiments on the Versatile Toroidal Facility and Levitated Dipole Experiment devices); and (c) a broad program of fusion technology and engineering development that addresses problems in several critical subsystem areas (e.g., magnet systems, superconducting materials development, environmental and safety studies, advanced millimeter-wave source development, system studies of fusion reactor design, operation, and technology requirements, and plasma-aided environmental clean-up technologies). Notable in this regard is the PSFC's participation in magnetics R&D for the International Thermonuclear Experimental Reactor (ITER) Program.

The successes of the Alcator A, C, and C-Mod tokamaks have demonstrated the value of the high-field, high-density, compact tokamak approach to plasma confinement. Alcator A was operated from 1973 to 1982, and Alcator B was designed but never built. Alcator C operated from 1978 to 1987 and achieved record-breaking results in confinement quality in November, 1983, and demonstrated efficient Lower Hybrid Current Drive (LHCD) at reactor relevant densities (1984). The Alcator C tokamak was subsequently relocated to the Lawrence Livermore National Laboratory for experiments investigating electron cyclotron resonance heating using a high-power free electron laser.

The Alcator C-Mod device, which has been operating since 1993, has produced important research results in many areas, including high heat load, strongly RF auxiliary heated,

diverted modes of tokamak operation. We have entered a new phase, in which tools for active control have been implemented, including Lower Hybrid power to study current profile control, cryopumping to study active particle control, and advanced ICRF to study flow control and transport barrier manipulation. These tools are complemented by a comprehensive set of plasma diagnostics, advanced control and data acquisition, and close coupling with theory and modeling across all topical areas.

14.4 Sub-Contracting Practices

MIT adheres to Procurement policies and standard procedures which are designed to protect the interests of the Institute and the sponsors of its research. These policies comply with the provisions of Federal contracts and with the recommendations of the Institute and Federal audit and procurement review agencies.

Procurement's role is as a service activity created to assist Institute departments and laboratories in procuring their needs with the most appropriate selection and at the most advantageous price and terms. They provide counsel and advice as well as handle the mechanics of procurement.

It is the responsibility of all Procurement agents to document their procurement actions to satisfy Institute and Government audit and procurement review requirements.

MIT's policy on affirmative action requires that minority business concerns and women owned business concerns shall have the maximum practicable opportunity to participate as sources of supply for all Institute procurement, whether with Federal funds or Institute funds. Consistent with this goal, in recent years, MIT has awarded as much as 60 to 70 percent of its procurements worth as much as 50 to 60 percent of its commitments to small business concerns.

Additionally, MIT has accepted in many contracts and has agreed to the provisions of the clause entitled: "Subcontracting Plan for Small Business and Small Disadvantaged Business Concerns (Negotiated)."

15 National Budget Summary

Alcator C-Mod operates as a national tokamak research facility. The budgets developed in detail for this proposal, and provided in Volume II - Costs, cover only the MIT portion of the proposed research. However, collaborative participation in the experiments includes major joint efforts with Princeton Plasma Physics Laboratory and the University of Texas at Austin Fusion Research Center (as outlined in Chapter 12), as well as smaller-scale participation from many other universities and labs. In developing the research plans contained in this proposal, we have assumed that the total effort in the smaller collaborations remains approximately constant at the current levels; the assumptions concerning the larger collaborators are summarized in table 15.1.

Table 15.1: *Alcator National Budget Summary*
November 1, 2008 – October 31, 2013

	FY09	FY10	FY11	FY12	FY13
MIT	25,795,000	27,430,000	28,400,000	29,600,000	30,700,000
PPPL	2,700,000	3,240,000	3,400,000	3,550,000	3,720,000
U. Texas	427,000	440,000	572,000	589,000	607,000
LANL	110,000	127,000	120,000	126,000	132,000
Alcator Project Total	29,032,000	31,237,000	32,492,000	33,865,000	35,159,000

These overall national project budget levels are required to accomplish the proposed research.